

**MARINE NATURAL PRODUCTS: SYNTHESIS AND ISOLATION OF BIOACTIVE
ANALOGUES**

by

ALBAN R. PEREIRA

B.Sc., University of Costa Rica, 2000

M.Sc., University of Costa Rica, 2002

A THESIS SUBMITTED IN PARTIAL FULFILLMENT OF
THE REQUIREMENTS FOR THE DEGREE OF

DOCTOR OF PHILOSOPHY

in

THE FACULTY OF GRADUATE STUDIES

(Chemistry)

THE UNIVERSITY OF BRITISH COLUMBIA

December 2007

© Alban R. Pereira, 2007

ABSTRACT

Tauramamide (2-12), a linear acylpentapeptide recently isolated from cultures of *Brevibacillus laterosporus* (PNG-276) collected in Papua New Guinea, was synthesized in 9 steps and 29% overall yield. Besides confirming the proposed structure, synthetic (2-12) allowed the antimicrobial assessment of this novel antibiotic. Additionally, a new analogue of the surfactin depsipeptides family named dealkylsurfactin (2-48), was prepared in 10 steps and 14% overall yield. The compound was employed as a biological tool in binding studies between the mitotic regulator isomerase Pin1 and the microtubule-associated protein tau, a crucial interaction involved in Alzheimer's disease.

Chemical exploration of *Garveia annulata*, a seasonal hydroid collected in Barkley Sound, British Columbia, led to the isolation of twelve secondary metabolites including four new compounds (3-53 to 3-56). Nine of these metabolites showed inhibition of indoleamine 2,3-dioxygenase (IDO), with the annulins among the most potent *in vitro* IDO inhibitors isolated to date. IDO plays a central role in immune escape, which prevents the immunological rejection of tumors or the allogeneic fetus.

The ceratamine inspired antimitotic agent (4-142) and inactive analogue (4-157) were synthesized in no more than 8 steps, with overall yields of 20% and 15% respectively. Activity evaluation of these analogues suggested that potency improves with planarity and that the synthetically laborious imidazo[4,5,*d*]azepine core heterocycle of ceratamines is not required for activity.

Haplosamate A (5-62), isolated from the marine sponge *Dasychalina fragilis* collected in Papua New Guinea, was found to be the first member of a new family of cannabinoid-active sterols. Saturation transfer double-difference (STDD) NMR experiments confirmed that (5-62)

specifically binds the cannabinoid human receptors CB1 and CB2 via the classical cannabinoid pharmacophore.

A growing appreciation of the therapeutic potential of PI3K inhibitors has encouraged the development of new inhibitory compounds with enhanced potency, selectivity and pharmacological properties. Such substances are destined to the treatment of inflammatory and autoimmune disorders as well as cancer and cardiovascular diseases. An optimization program intended to develop more stable and isoform-selective PI3K inhibitors based on the marine-derived natural product liphagal (6-1), led to the preparation of a small library of synthetic analogues.

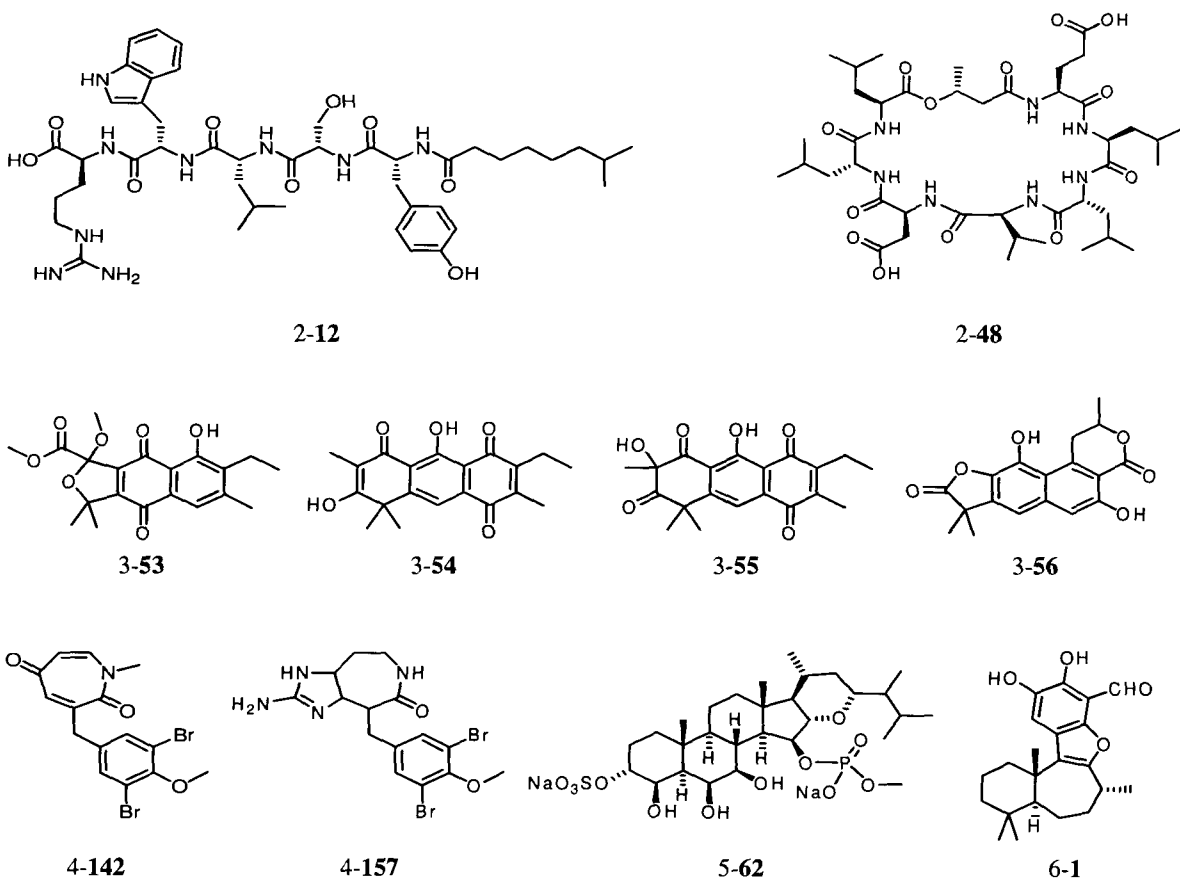


TABLE OF CONTENTS

Abstract	ii
Table of Contents	iv
List of Tables.....	vii
List of Figures	xi
List of Abbreviations.....	xvi
Acknowledgements	xix
Dedication	xx
1. Marine Natural Products Chemistry: Overview.....	1
1.1. Past and Present.....	1
1.2. Secondary metabolites?.....	2
1.3. Biological activity and current success in marine natural products research.....	5
1.4. Synthesis of marine natural products.....	9
2. Bioactive Marine Peptides: Total Synthesis of Tauramamide and Dealkylsurfactin	11
2.1. Peptides from the sea.....	11
2.2. Peptides from marine PNG bacterial isolates.....	12
2.2.1. New antibiotics from PNG-276.....	12
2.2.2. Anti-Alzheimer activity of PNG10A.....	15
2.3. Total synthesis of tauramamide.....	18
2.4. Preparation of dealkylsurfactin.....	29
2.5. Conclusions.....	41
2.6. Experimental.....	44
2.6.1. Total synthesis of tauramamide and tauramamide ethyl ester.....	48
2.6.2. Synthesis of dealkylsurfactin.....	62
3. Isolation and Structure Elucidation of new IDO Inhibitors from <i>Garveia annulata</i>.	71
3.1. IDO inhibition and <i>Garveia annulata</i>	71
3.2. IDO and the kynurenine pathway.....	72
	iv

3.3. Current IDO inhibitors and the bioassay.....	75
3.4. Secondary metabolites from hydrozoans.....	77
3.5. Minor metabolites from <i>Garveia annulata</i>	80
3.6. Isolation of IDO-active minor metabolites.....	83
3.6.1. Annulin C.....	86
3.6.2. 2-Hydroxygarveatin E.....	90
3.6.3. Garveatin E.....	93
3.6.4. Garvin C.....	96
3.7. Biological evaluation of <i>G. annulata</i> secondary metabolites.....	101
3.8. Conclusions.....	105
3.9. Experimental.....	108
4. Progress towards the Synthesis of Ceratamines.....	112
4.1. Microtubule-stabilizing agents from marine origin.....	112
4.2. Ceratamines A and B.....	114
4.2.1. Biosynthesis and similar marine metabolites.....	116
4.2.2. NMR data.....	119
4.2.3. Retrosynthetic analysis.....	121
4.3. Related syntheses and relevant synthetic methodologies: literature review.....	123
4.4. Initial synthetic proposals.....	128
4.5. Attempted preparation of ceratamines and analogues.....	130
4.5.1. Biomimetic approach to ceratamines.....	130
4.5.2. First generation approach to ceratamines.....	132
4.5.3. Second generation approach to ceratamines.....	151
4.6. Conclusions and future directions.....	169
4.7. Experimental.....	173
5. Cannabinoid activity of the Marine Sterol Haplosamate A: Direct Observation of Binding to Human Receptors by Saturation Transfer Double-Difference (STDD) NMR Spectroscopy.....	212
5.1. Brief history.....	212
5.2. Marijuana: chemistry and psychoactive effects.....	215

5.3. Phytocannabinoids.....	218
5.4. Cannabinoid receptors, endogenous cannabinoids and the endocannabinoid System.....	219
5.4.1. Cannabinoid human receptors.....	220
5.4.2. Endocannabinoids.....	222
5.4.3. The endocannabinoid system.....	223
5.5. Synthetic and patented cannabinoids.....	225
5.6. Cannabinoids and cancer.....	229
5.7. Biological evaluation of cannabinoid compounds.....	230
5.8. Isolation of haplosamate A.....	232
5.9. Haplosamate A: NMR analysis.....	234
5.10. Pharmacophoric requirements for cannabinoid activity.....	240
5.11. Evidence of haplosamate A binding to CB1 and CB2: STD NMR experiments...	246
5.12. Conclusions.....	255
5.13. Experimental.....	258
6. Synthesis of Liphagal Analogues.....	275
6.1. Liphagal, a selective PI3K α inhibitor.....	275
6.2. The phosphatidylinositol-3-kinase (PI3K) signaling pathway.....	276
6.3. First generation PI3K inhibitors.....	279
6.4. Isoform-selective second generation inhibitors.....	281
6.5. Marine natural products and the PI3K signaling pathway.....	284
6.6. Biogenesis and synthetic preparations of liphagal.....	286
6.7. Preparation of liphagal analogues.....	290
6.7.1. Variation at C14.....	290
6.7.2. Variations at C15 and C16.....	303
6.8. Biological evaluation of the new synthetic liphagane derivatives.....	312
6.9. Conclusions and future directions.....	315
6.10. Experimental.....	319
7. References.....	368

LIST OF TABLES

Table 1.1. Marine-derived compounds currently in clinical trials (Phase I and above) for the treatment of several human conditions.....	7
Table 2.1. NMR data for tauramamide (12) (recorded in DMSO- <i>d</i> ₆).....	24
Table 2.2. Antimicrobial activity (MIC's in µg/mL) of synthetic tauramamide (12) and tauramamide ethyl ester (14).....	26
Table 2.3. NMR data for dealkylsurfactin (48) (recorded in DMSO- <i>d</i> ₆).....	36
Table 2.4. Specific rotation values for natural surfactin B2 (19), synthetic analogues (19a,b), “norsurfactin” (19c), and dealkylsurfactin (48).....	39
Table 2.5. NMR data for tauramamide (12) (recorded in DMSO- <i>d</i> ₆).....	55
Table 2.6. ¹ H and ¹³ C NMR data for natural and synthetic tauramamide ethyl ester (14) (recorded in DMSO- <i>d</i> ₆).....	58
Table 2.7. NMR data for dealkylsurfactin (48) (recorded in DMSO- <i>d</i> ₆).....	67
Table 3.1. Some IDO inhibitors with high <i>in vitro</i> activity.....	76
Table 3.2. NMR data for annulin C (53) (recorded in CDCl ₃).....	88
Table 3.3. NMR data for 2-hydroxygarveatin E (55) (recorded in CDCl ₃).....	92
Table 3.4. NMR data for garveatin E (54) (recorded in CDCl ₃).....	95
Table 3.5. NMR data for garvin C (56) (recorded in CDCl ₃).....	99
Table 3.6. IDO-active secondary metabolites from <i>G. annulata</i>	102
Table 3.7. Annulin C (53) and commercially available IDO-active naphthoquinones.....	104
Table 3.8. <i>In vitro</i> inhibition of IDO by marine natural products, commercial naphthoquinones, β-carbolines, and tryptophan analogues.....	106
Table 4.1. Rearrangement of various 1,4- and 1,3-cyclohexadione derivatives.....	132
Table 4.2. NMR data for 3-benzylazepane-2,4-dione (78) (recorded in CD ₂ Cl ₂).....	135
Table 4.3. NMR data for 3-benzyl-3-chloro-1-methylazepane-2,4-dione (97) and 3-benzyl-3-bromo-1-methylazepane-2,4-dione (99) (recorded in CDCl ₃).....	140

Table 4.4. NMR data for 3-benzyl-4-(<i>tert</i> -butyldimethylsilanyloxy)-1-methyl-1,5,6,7-tetrahydroazepin-2-one (106) (recorded in CD ₂ Cl ₂).....	144
Table 4.5. NMR data for 3-[(<i>tert</i> -butyldimethylsilyl)phenylmethyl]-3-chloro-1-methylazepane-2,4-dione (107) (recorded in CD ₂ Cl ₂).....	148
Table 4.6. NMR data for 3-benzyl-1,3,6,7-tetrahydroazepin-2-one (124) (recorded in CDCl ₃).....	153
Table 4.7. NMR data for 3-(3,5-dibromo-4-methoxybenzyl)-1H-azepine-2,5-dione (141) (recorded in DMSO- <i>d</i> ₆).....	157
Table 4.8. Reaction of 126 , 141-147 with several nitrogen-based nucleophiles.....	161
Table 4.9. NMR data for 19-demethyl-1,4,5,8,9,10-hexahydroceratamine B (157) (recorded in DMSO- <i>d</i> ₆).....	166
Table 4.10. NMR data for azepane-2,4-dione (50) (recorded in CD ₂ Cl ₂).....	176
Table 4.11. NMR data for 3-benzyl-3-chloroazepane-2,4-dione (96) (recorded in CD ₂ Cl ₂).....	179
Table 4.12. NMR data for 3-benzyl-3-chloro-1-methylazepane-2,4-dione (97) (recorded in CDCl ₃).....	181
Table 4.13. NMR data for 3-[(<i>tert</i> -butyldimethylsilyl)phenylmethyl]-3-chloro-1-methylazepane-2,4-dione (107) (recorded in CD ₂ Cl ₂).....	184
Table 4.14. NMR data for 3-benzylidene-azepane-2,4-dione (120) (recorded in CD ₂ Cl ₂)...	185
Table 4.15. NMR data for 2-benzyl-8-oxa-4-aza-bicyclo[5.1.0]octan-3-one (125) (recorded in CDCl ₃).....	193
Table 4.16. NMR data for toluene-4-sulfonic acid 6-benzyl-5-hydroxy-7-oxoazepan-4-yl ester (137) (recorded in CDCl ₃).....	194
Table 4.17. NMR data for 4-bromo-3-(3,5-dibromo-4-methoxybenzyl)-azepane-2,5-dione (140) (recorded in CDCl ₃).....	198
Table 4.18. NMR data for 3-(3,5-dibromo-4-methoxy-benzyl)-6,7-dihydro-1H-azepine-2,5-dione (144) (recorded in CDCl ₃).....	200
Table 4.19. NMR data for 5-bromo-6-(3,5-dibromo-4-methoxy-benzyl)-7-oxo-azepan-4-yl-cyanamide (156) (recorded in CD ₃ OD).....	204
Table 4.20. NMR data for 4,5-dibromo-3-(3,5-dibromo-4-methoxy-benzyl)-azepan-2-one (147) (recorded in CDCl ₃).....	205
Table 4.21. NMR data for 17-Boc-1,4,5,8,9,10-hexahydroceratamine B (158) (recorded in CDCl ₃).....	208

Table 4.22. NMR data for 7,17-dipivaloyl-1,4,5,8,9,10-hexahydroceratamine B amide (159) (recorded in CDCl ₃).....	209
Table 5.1. Constituents in the resin of <i>Cannabis sativa</i> reported until 2005.....	216
Table 5.2. Pharmacological effects of smoked marijuana in humans.....	217
Table 5.3. Cannabinoid-based therapeutic agents, approved and in development.....	228
Table 5.4. Tumors exhibiting cannabinoid-induced inhibition.....	229
Table 5.5. NMR data for haplosamate A (47) (recorded in D ₂ O).....	237
Table 5.6. NMR data for haplosamate A triacetates (60) and (61) (recorded in C ₆ D ₆).....	242
Table 5.7. NMR data for haplosamate A (47) (recorded in DMSO- <i>d</i> ₆).....	263
Table 5.8. NMR data for haplosamate A (47) (recorded in DMSO- <i>d</i> ₆).....	264
Table 5.9. NMR data for haplosamate A 3,4,7-triacetate derivative (60) (recorded in C ₆ D ₆).....	267
Table 5.10. NMR data for haplosamate A 3,4,7-triacetate derivative (60) (recorded in C ₆ D ₆).....	268
Table 5.11. NMR data for haplosamate A 3,6,7-triacetate derivative (61) (recorded in C ₆ D ₆).....	269
Table 5.12. NMR data for haplosamate A 3,6,7-triacetate derivative (61) (recorded in C ₆ D ₆).....	270
Table 5.13. Group epitope mapping (GEM) analysis for CB1/CB2 and haplosamate A (relative to H18/H21 at 0.96 ppm).....	272
Table 6.1. Organization of the PI3K's family.....	277
Table 6.2. NMR data for (+)-8- <i>epi</i> -desformyl-14-bromoliphagane (46) (recorded in C ₆ D ₆).....	293
Table 6.3. NMR data for (+)-14-bromo-9,16-dihydroxylyphagane quinone (52) (recorded in C ₆ D ₆).....	295
Table 6.4. NMR data for (±)-desformyl-14-bromospiroliphagal (53) (recorded in CDCl ₃)..	298
Table 6.5. ¹³ C-NMR assignments for (+)-16-hydroxylyphagane (68), (+)-15-hydroxylyphagane (69), and (+)-14-bromo-15-hydroxylyphagane (70) (recorded in C ₆ D ₆)....	306
Table 6.6. ¹ H-NMR assignments for (+)-16-hydroxylyphagane (68), (+)-15-hydroxylyphagane (69), and (+)-14-bromo-15-hydroxylyphagane (70) (recorded in C ₆ D ₆)....	308
Table 6.7. Optical activity measurements for liphagal (1) and its synthetic analogues.....	311

Table 6.8. Inhibition of PI3K α and PI3K γ by liphagal, LY294002, wortmannin, and several new liphagane derivatives.....	312
Table 6.9. NMR data for 14-bromo-15-methoxyliphagane (67) (recorded in C ₆ D ₆).....	337
Table 6.10. NMR data for 14-bromo-15-methoxyliphagane (67) (recorded in C ₆ D ₆).....	338
Table 6.11. NMR data for (+)-8- <i>epi</i> -desformyl-14-bromoliphagal (46) (recorded in CDCl ₃).....	344
Table 6.12. NMR data for (+)-8- <i>epi</i> -desformyl-14-bromoliphagal (46) (recorded in CDCl ₃).....	345
Table 6.13. NMR data for (-)-8- <i>epi</i> -desformyl-14-bromoliphagal (46) (recorded in C ₆ D ₆)..	346
Table 6.14. NMR data for (\pm)-desformyl-14-bromospiroliphagane (53) (recorded in CDCl ₃).....	347
Table 6.15. NMR data for (-)-14-bromo-9,16-dihydroxyliphagane quinone (52) (recorded in C ₆ D ₆).....	348
Table 6.16. NMR data for (\pm)-desformylspiroliphagane A (55) (recorded in CDCl ₃).....	350
Table 6.17. NMR data for (\pm)-desformylspiroliphagane A (55) (recorded in CDCl ₃).....	351
Table 6.18. NMR data for (\pm)-desformylspiroliphagane B (56) (recorded in C ₆ D ₆).....	352
Table 6.19. NMR data for (\pm)-desformylspiroliphagane B (56) (recorded in C ₆ D ₆).....	353
Table 6.20. NMR data for (+)-14-bromo-15-hydroxyliphagane (70) (recorded in C ₆ D ₆).....	355
Table 6.21. NMR data for (+)-14-bromo-15-hydroxyliphagane (70) (recorded in C ₆ D ₆).....	356
Table 6.22. NMR data for (+)-15-hydroxyliphagane (69) (recorded in C ₆ D ₆).....	358
Table 6.23. NMR data for (+)-15-hydroxyliphagane (69) (recorded in C ₆ D ₆).....	359
Table 6.24. NMR data for (+)-16-hydroxyliphagane (68) (recorded in C ₆ D ₆).....	361
Table 6.25. NMR data for (+)-16-hydroxyliphagane (68) (recorded in C ₆ D ₆).....	362

LIST OF FIGURES

Figure 1.1. Some marine secondary metabolites with known ecological roles.....	2
Figure 1.2. Distribution of marine natural products by phylum (A) and biosynthetic origin (B), according to the MarinLit database.....	3
Figure 1.3. Distribution of biological activities evaluated in marine natural products in 2004.....	6
Figure 1.4. First marine-inspired drugs approved for human use.....	8
Figure 2.1. Prominent marine peptides currently in clinical trials.....	11
Figure 2.2. Structure of surfactin analogues.....	16
Figure 2.3. ¹ H-NMR spectrum of tauramamide (12) (recorded in DMSO- <i>d</i> ₆ at 600 MHz).	22
Figure 2.4. ¹³ C-NMR spectrum of tauramamide (12) (recorded in DMSO- <i>d</i> ₆ at 150 MHz).	23
Figure 2.5. Partial HMBC spectrum of tauramamide (12) (recorded in DMSO- <i>d</i> ₆ at 600 MHz).....	27
Figure 2.6. ¹ H-NMR spectra of bacterial-derived and synthetic tauramamide ethyl ester (14) (recorded in DMSO- <i>d</i> ₆ at 600 MHz).....	28
Figure 2.7. ¹ H-NMR spectrum of dealkylsurfactin (48) (recorded in DMSO- <i>d</i> ₆ at 600 MHz).....	34
Figure 2.8. ¹³ C-NMR spectrum of dealkylsurfactin (48) (recorded in DMSO- <i>d</i> ₆ at 150 MHz).....	35
Figure 2.9. Partial HMBC spectrum of dealkylsurfactin (48) (in DMSO- <i>d</i> ₆ at 600 MHz)...	40
Figure 2.10. ¹ H-NMR spectrum of tauramamide ethyl ester (14) (recorded in DMSO- <i>d</i> ₆ at 600 MHz).....	60
Figure 2.11. ¹³ C-NMR spectrum of tauramamide ethyl ester (14) (recorded in DMSO- <i>d</i> ₆ at 150 MHz).....	61
Figure 2.12. ¹ H-NMR spectrum of dibenzyl dealkylsurfactin (47) (recorded in DMSO- <i>d</i> ₆ at 600 MHz).....	69
Figure 2.13. ¹³ C APT-NMR spectrum of dibenzyl dealkylsurfactin (47) (recorded in DMSO- <i>d</i> ₆ at 150 MHz).....	70

Figure 3.1. Tryptophan metabolism in the kynurenine pathway.....	72
Figure 3.2. Reactions involved in the new high throughput IDO bioassay developed by Mauk and Vottero.....	77
Figure 3.3. Representative structures for secondary metabolites isolated from hydroids.....	79
Figure 3.4. Secondary metabolites isolated from <i>G. annulata</i>	80
Figure 3.5. a) A bush-like colony of <i>G. annulata</i> ; b) Map of collection site.....	84
Figure 3.6. ¹ H-NMR spectrum of a) annulin A (39) (recorded in CD ₂ Cl ₂ at 400 MHz), and b) annulin C (53) (recorded in CDCl ₃ at 400 MHz).....	87
Figure 3.7. Summary of COSY and HMBC correlations for annulin C (53).....	89
Figure 3.8. ¹ H-NMR spectrum of 2-hydroxygarveatin E (55) (recorded in CDCl ₃ at 600 MHz).....	91
Figure 3.9. Summary of HMBC correlations for 2-hydroxygarveatin E (55).....	93
Figure 3.10. Summary of HMBC correlations for garveatin E (54).....	94
Figure 3.11. ¹ H-NMR spectrum of garveatin E (54) (recorded in CDCl ₃ at 400 MHz).....	96
Figure 3.12. Summary of HMBC correlations for garvin C (56).....	97
Figure 3.13. ¹ H-NMR spectrum of garvin C (56) (recorded in CDCl ₃ at 600 MHz).....	98
Figure 3.14. Proposed pharmacophore involved in IDO inhibition.....	107
Figure 4.1. Prominent microtubule-stabilizing agents (MSA) from diverse sources.....	112
Figure 4.2. Representative pyrrole-imidazole alkaloids.....	119
Figure 4.3. ¹ H and ¹³ C-NMR spectra of ceratamine A (13) (recorded in DMSO- <i>d</i> ₆ at 500 and 125 MHz respectively).....	120
Figure 4.4. ¹ H and ¹³ C-NMR spectra of 3-benzylazepane-2,4-dione (78) (recorded in CD ₂ Cl ₂ at 400 and 100 MHz, respectively).....	136
Figure 4.5. ¹ H-NMR spectra of 3-benzyl-3-chloro-1-methylazepane-2,4-dione (97) and 3-benzyl-3-bromo-1-methylazepane-2,4-dione (99) (recorded in CDCl ₃ at 300 MHz).....	138
Figure 4.6. ¹³ C-NMR spectra of 3-benzyl-3-chloro-1-methylazepane-2,4-dione (97) and 3-benzyl-3-bromo-1-methylazepane-2,4-dione (99) (recorded in CDCl ₃ at 75 MHz).....	139
Figure 4.7. MM2 energy minimizations for enols (100) and (101).....	142
Figure 4.8. ¹ H and ¹³ C-NMR spectra of 3-benzyl-4-(<i>tert</i> -butyldimethylsilyloxy)-1-methyl-1,5,6,7-tetrahydroazepin-2-one (106) (recorded in CD ₂ Cl ₂ at 400 and 100 MHz, respectively).....	145

Figure 4.9. ^1H and ^{13}C -NMR spectra of 3-[(<i>tert</i> -butyldimethylsilyl)phenylmethyl]-3-chloro-1-methylazepane-2,4-dione (107) (recorded in CD_2Cl_2 at 400 and 100 MHz, respectively).....	147
Figure 4.10. ^1H and ^{13}C -NMR spectra of 3-benzyl-1,3,6,7-tetrahydroazepin-2-one (124) (recorded in CDCl_3 at 400 and 100 MHz, respectively).....	154
Figure 4.11. ^1H and ^{13}C -NMR spectra of 3-(3,5-dibromo-4-methoxybenzyl)-1H-azepine-2,5-dione (141) (recorded in $\text{DMSO}-d_6$ at 400 and 100 MHz, respectively).....	158
Figure 4.12. ^1H -NMR spectra of a) 3-(3,5-dibromo-4-methoxybenzyl)-1-methyl-1H-azepine-2,5-dione (142); and ceratamine A (13) (recorded in CDCl_3 and $\text{DMSO}-d_6$ at 400 MHz).....	159
Figure 4.13. Minimum energy conformations for 3-(3,5-dibromo-4-methoxybenzyl)-1-methyl-1H-azepine-2,5-dione (142), and ceratamine A (13).....	160
Figure 4.14. ^1H and ^{13}C -NMR spectra of 19-demethyl-1,4,5,8,9,10-hexahydroceratamine B (157) (recorded in $\text{DMSO}-d_6$ at 600 and 150 MHz respectively).....	165
Figure 4.15. Minimum energy conformations for 19-demethyl-1,4,5,8,9,10-hexahydroceratamine B (157); and ceratamine A (13).....	167
Figure 4.16. ^1H and ^{13}C -NMR spectra of 2-(3,5-dibromo-4-methoxybenzyl)-but-3-enoic acid but-3-enylamide (135) (recorded in CDCl_3 at 400 and 100 MHz respectively).....	210
Figure 4.17. ^1H and ^{13}C -NMR spectra of 3-(3,5-dibromo-4-methoxy-benzyl)-1,3,6,7-tetrahydroazepin-2-one (136) (recorded in CDCl_3 at 300 and 75 MHz respectively).....	211
Figure 4.18. ^1H and ^{13}C -NMR spectra of 5-bromo-6-(3,5-dibromo-4-methoxybenzyl)-7-oxo-azepan-4-yl-cyanamide (156) (recorded in CD_3OD at 400 and 100 MHz respectively).	212
Figure 5.1. a) Mature <i>C. sativa</i> crop ready for harvesting; b) trichomes.....	215
Figure 5.2. Classification of the typical cannabinoids.....	218
Figure 5.3. Serpentine-like topology of the cannabinoid receptors CB1 and CB2.....	221
Figure 5.4. Representative endocannabinoids.....	223
Figure 5.5. Endogenous cannabinoid system.....	224
Figure 5.6. Events involved in the cell-based cannabinoid bioassay.....	231
Figure 5.7. Marine natural products combining phosphorus and sulfur.....	233
Figure 5.8. Structures for the steroidal glucoside (56) and two members of the withanolides family.....	234

Figure 5.9. ^1H -NMR spectrum of haplosamate A (47) (recorded in D_2O at 600 MHz).....	235
Figure 5.10. ^{13}C -NMR spectrum of haplosamate A (47) (recorded in D_2O at 150 MHz)...	236
Figure 5.11. a) ^{31}P decoupled and b) ^{31}P coupled ^1H -NMR spectra of haplosamate A (47) (recorded in CD_3OD at 400 MHz).....	239
Figure 5.12. The classical cannabinoid pharmacophore.....	244
Figure 5.13. Minimum energy conformations for the known cannabimimetic agents (-)- 9β -hydroxyhexahydrocannabinol (62) and WIN55212-2 (23).....	245
Figure 5.14. Basic pulse sequence of a 1D STD NMR spectrum.....	247
Figure 5.15. Events involved in STD NMR spectroscopy.....	249
Figure 5.16. Sample preparation for saturation transfer double-difference (STDD) NMR...	250
Figure 5.17. STDD experiments measured for an aqueous solution of each cannabinoid receptor supported in SF21 insect cells and haplosamate A (47).....	252
Figure 5.18. Qualitative STD NMR group epitope mapping for the binding of haplosamate A (47) to the cannabinoid human receptors CB1 and CB2.....	253
Figure 5.19. STDD NMR-derived group epitope mapping for haplosamate A (47).....	256
Figure 5.20. ^1H -NMR spectrum of haplosamate A (47) (recorded in CD_3OD at 600 MHz).	261
Figure 5.21. ^{13}C -NMR spectrum of haplosamate A (47) (recorded in CD_3OD at 150 MHz).....	262
Figure 5.22. Integration of proton signals for the STD percentage measurement in a suspension of the cannabinoid human receptor CB1 supported in insect cells and haplosamate A (47) (relative to H18/H21 at 0.96 ppm).....	273
Figure 5.23. Integration of proton signals for the STD percentage measurement in a suspension of the cannabinoid human receptor CB2 supported in insect cells and haplosamate A (47) (relative to H18/H21 at 0.96 ppm).....	274
Figure 6.1. Enzymatic synthesis and degradation of PI-3,4,5-P3 (3) during the first steps of the PI3K signaling pathway.....	276
Figure 6.2. First generation PI3K inhibitors.....	280
Figure 6.3. Some PI3K-inhibitory chemotypes: A) arylmorpholine and B) non-related structures.....	282
Figure 6.4. ^1H and ^{13}C -NMR spectra of (+)-8- <i>epi</i> -desformyl-14-bromoliphagane (46) (recorded in C_6D_6 at 600 and 150 MHz respectively).....	292

Figure 6.5. ^1H and ^{13}C -NMR spectra of (+)-14-bromo-9,16-dihydroxyliphagane quinone (52) (recorded in C_6D_6 at 600 and 150 MHz respectively).....	294
Figure 6.6. Representative HMBC (H \rightarrow C) and COSY correlations for 52.....	296
Figure 6.7. ^1H and ^{13}C -NMR spectra of (\pm)-desformyl-14-bromospiroliphagal (53) (recorded in CDCl_3 at 600 and 150 MHz respectively).....	297
Figure 6.8. Representative HMBC (H \rightarrow C) and COSY correlations for 53.....	299
Figure 6.9. ^1H -NMR spectra of (\pm)-desformylspiroliphagal A (55) and B (56) (recorded in CDCl_3 and C_6D_6 respectively at 600 MHz).....	301
Figure 6.10. ^{13}C -NMR spectra of (+)-16-hydroxyliphagane (68) and (+)-15-hydroxyliphagane (69) (recorded in C_6D_6 at 150 MHz).....	307
Figure 6.11. ^1H -NMR spectra of (+)-16-hydroxyliphagane (68) and (+)-15-hydroxyliphagane (69) (recorded in C_6D_6 at 600 MHz).....	309
Figure 6.12. Key HMBC (H \rightarrow C) and COSY correlations for 68 and 69.....	310
Figure 6.13. IgE-induced calcium influx in bone marrow-derived mast cells treated with DMSO (control), liphagal (1), LY294002 (7), 68 and 69.....	314
Figure 6.14. New synthetic liphagal-based PI3K inhibitors.....	315
Figure 6.15. a) ^1H -NMR and b) ^{13}C -NMR spectra of (2-hydroxy-4-methoxyphenyl)-methyltriphenylphosphonium bromide (78) (recorded in CDCl_3 at 300 and 75 MHz respectively).....	363
Figure 6.16. ^1H and ^{13}C -NMR spectra of 2-[3-(7-bromo-6-methoxy-benzofuran-2-yl)-butyl]-1,3,3-trimethylcyclohexanol (90) (recorded in CDCl_3 at 400 and 100 MHz respectively).....	364
Figure 6.17. ^1H and ^{13}C -NMR NMR spectra of desformyl-15,16-dimethoxyliphagal (54) (recorded in C_6D_6 at 400 and 100 MHz respectively).....	365
Figure 6.18. ^{13}C -NMR spectrum of (\pm)-desformylspiroliphagane A (55) (recorded in CDCl_3 at 150 MHz).....	366
Figure 6.19. ^{13}C -NMR spectrum of (\pm)-desformylspiroliphagane B (56) (recorded in CDCl_3 at 150 MHz).....	366
Figure 6.20. ^1H and ^{13}C -NMR spectra of (+)-14-bromo-15-hydroxyliphagane (70) (recorded in C_6D_6 at 600 and 150 MHz respectively).....	367

LIST OF ABBREVIATIONS

°	- degree(s)
±	- racemic
1D	- one-dimensional
2D	- two-dimensional
$[\alpha]_D^t$	- specific rotation at wavelength of sodium D line at temperature t (°C)
Ac	- acetate
AcOH	- acetic acid
AICN	- 1,1'-azobis(cyclohexanecarbonitrile)
Arg	- arginine
Asp	- aspartic acid
b	- broad
Bn	- benzyl
Boc	- <i>t</i> -butoxycarbonyl
BOM	- butoxymethyl
Bu	- butyl
BuLi	- <i>n</i> -butyllithium
<i>t</i> BuLi	- <i>t</i> -butyllithium
bs	- broad singlet
^{13}C	- carbon-13
°C	- degrees Celsius
Calcd	- calculated
CB1	- cannabinoid receptor 1
CB2	- cannabinoid receptor 2
Cbz	- benzyloxycarbonyl
CD ₂ Cl ₂	- deuterated dichloromethane
C ₆ D ₆	- deuterated benzene
CDI	- 1,1'-carbonyldiimidazole
COSY	- two-dimensional correlation spectroscopy
δ	- chemical shift in parts per million
d	- doublet
D	- dextrorotatory
DCC	- 1,3-dicyclohexylcarbodiimide
dd	- doublet of doublets
DDQ	- 2,3-dichloro-5,6-dicyano-1,4-benzoquinone
DIEA	- diisopropylethylamine
DMAP	- 4-dimethylaminopyridine
DMF	- <i>N,N</i> -dimethylformamide
DMP	- Dess-Martin periodinane
DMSO- <i>d</i> ₆	- deuterated dimethyl sulphoxide
dt	- doublet of triplets
ε	- extinction coefficient
EDCI	- 1-(3-dimethylaminopropyl)-3-ethylcarbodiimide hydrochloride
ELISA	- enzyme linked immuno sorbant assay
eq.	- equivalent(s)
Et	- ethyl

Et ₃ N	- triethylamine
EtOAc	- ethyl acetate
EtOH	- ethanol
Fmoc	- 9-fluorenylmethoxycarbonyl
g	- gram(s)
Glu	- glutamic acid
h	- hour(s)
¹ H	- proton
HATU	- [O-(7-azabenzotriazolyl)-1,1,3,3-tetramethyluronium hexafluorophosphate]
HCl	- hydrochloric acid
HMBC	- two-dimensional heteronuclear multiple bond coherence
HMQC	- two-dimensional heteronuclear multiple quantum coherence
HPLC	- high-performance liquid chromatography
H ₂ O	- water
HOAt	- 1-hydroxy-7-azabenzotriazole
HOBt	- 1-hydroxybenzotriazole
HOSu	- N-hydroxysuccinimide
HRESIMS	- high resolution electrospray mass spectrometry
HSQC	- two-dimensional heteronuclear single quantum coherence
Hz	- hertz
IC ₅₀	- inhibitory concentration (for 50% of a biological sample)
<i>J</i>	- coupling constant in hertz
λ	- wavelength
L	- levorotatory
Leu	- leucine
LDA	- lithium diisopropylamide
LRESIMS	- low resolution electrospray mass spectrometry
m	- multiplet
M	- molar concentration
<i>m</i> -CPBA	- <i>meta</i> -chloroperbenzoic acid
Me	- methyl
MeCN	- acetonitrile
MeOH	- methanol
Mes	- mesitylene
mg	- milligram(s)
MHz	- megahertz
MIC	- minimum inhibitory concentration
min	- minute
mL	- millilitre(s)
mm	- millimetre(s)
mmol	- millimol(s)
MOM	- methoxymethyl
MRSA	- methicillin-resistant <i>Staphylococcus aureus</i>
<i>m/z</i>	- mass to charge ratio
nM	- nanomolar
NBS	- N-bromosuccinimide
NCS	- N-chlorosuccinimide

NMR	- nuclear magnetic resonance
NOE	- nuclear Overhauser enhancement
NRPS	- non-ribosomal peptide synthase
Pac	- phenacyl
pH	- $-\log_{10}[\text{H}^+]$
Ph	- phenyl
PHF	- paired helical filaments
PMB	- <i>p</i> -methylbenzoate
PNG	- Papua New Guinea
ppm	- parts per million
PPTs	- pyridinium <i>p</i> -toluenesulfonate
Pro	- proline
PyBOP	- (benzotriazol-1-yl)oxytripyrrolidinophosphonium hexafluorophosphate
Pyr	- pyridine
q	- quartet
<i>R</i>	- rectus
<i>R</i> _f	- retention factor
ROESY	- rotating frame Overhauser enhancement spectroscopy
s	- singlet
<i>S</i>	- sinister
SAR	- structure-activity relationship
SCUBA	- self-contained underwater breathing apparatus
Ser	- serine
sp.	- species
STD	- saturation transfer difference
STDD	- saturation transfer double difference
t	- triplet
TBDSCI	- <i>t</i> -butyldimethyl silyl chloride
TCA	- trichloroacetic acid
TFA	- trifluoroacetic acid
Thr	- threonine
TLC	- thin-layer chromatography
TOCSY	- total correlation spectroscopy
Tr	- trityl
Trp	- tryptophan
Ts	- tosyl, <i>p</i> -toluenesulfonyl
Tyr	- tyrosine
UV	- ultraviolet
Val	- valine
VRE	- vancomycin-resistant <i>Enterococci</i>

ACKNOWLEDGEMENTS

I would like to thank my supervisor Professor Raymond J. Andersen for giving me the opportunity to do research in marine natural products, and get actively involved in different aspects of such a gratifying scientific field. From isolation to synthesis, including diving and organization of a collecting trip to Costa Rica, his enthusiasm, support and guidance facilitated this work and allow me to grow as a chemist and above all, as a person.

Many thanks to David Williams for his advice in practical aspects of natural product isolation, and to Mike Leblanc for his assistance in both the laboratory and diving. The collaboration and guidance of Professor Nick Burlinson was fundamental during STD data acquisition and processing. The assistance of technical staff (MS and NMR facilities) in the Department of Chemistry at UBC is also gratefully acknowledged.

I am very grateful for all the biological assessments of natural and synthetic materials carried out by Eduardo Vottero and Professor Grant Mauk, as well as Professor Michel Roberge and members of his research group (Biochemistry and Molecular Biology, UBC), Tom Pfeifer and Professor Tom Grigliatti (Zoology, UBC), Professor Gerald Krystal (B.C. Cancer Agency), Dr. Ian Hollander (Wyeth) and Helen Wright (Biological Services, UBC). These rewarding collaborations have taught me that the understanding among professionals in multiple fields is crucial for the success of any drug discovery program.

To everyone in the Andersen research laboratory, my most sincere appreciation. Whether it was playing soccer with Harry and Emiliano, practicing Japanese with Kaoru and Chelsea, running reactions on Sunday mornings with Fred, Lu and Xin-Hui, sailing with Justin and Takashi, listening to heavy metal with Matt, or diving with Roger, Kelsey, Kate and Julie, all these experiences allowed me to truly enjoy my experience at UBC. In particular, thanks to Chris Gray and his wife Claire for opening the doors of their home during Christmas 2005, and to Rob Keyzers for his careful proof-reading and useful comments during the writing of this thesis.

Finally, I would like to thank all the members of my family for their support and encouragement throughout my studies.

DEDICATION

For Nancy and Helena

1. Marine Natural Products Chemistry: Overview

1.1. Past and Present

The field of marine natural products chemistry encompasses the study of chemical structures and biological activities of secondary metabolites produced by marine plants, animals and microorganisms.¹ In contrast to the study of terrestrial natural products, which started in the 1800's with the characterization of alkaloids such as morphine, strychnine and quinine, chemical exploration of marine life only began in earnest in the early 1960's.^{1,2} Pioneers like Paul Scheuer and Richard Moore in the United States, Luigi Minale and Ernesto Fattorusso in Italy, as well as Yoshiro Hashimoto and Yoshimasa Hirata in Japan, began to examine sponges, algae, and other unfamiliar marine organisms.²

Undoubtedly, the invention of SCUBA by Jacques-Yves Cousteau and Emile Gagnan in 1943³ dramatically increased accessibility of sessile marine invertebrates and algae, allowing natural products chemists to make their own field collections and establish extensive libraries of marine extracts. Today, after nearly 50 years of research, steady progress by both academic institutions and pharmaceutical industries has led to the characterization of *ca.* 17,100 new marine natural products, reported in *ca.* 6,800 publications.^{1,4-6} Another *ca.* 9,000 references deal with syntheses, biological activities, ecological studies and reviews of marine natural products.⁴ Over 300 patents have been issued on this field.^{4,6}

Secondary metabolites of marine origin range from simple achiral molecules to highly complex structures, rich in stereochemistry, concatenated rings and reactive functional groups.¹ These chemical entities are full of structural surprises and not limited by human imagination. The additional incorporation of covalently bound halogens (mainly Cl and Br) is a typical marine

variation, presumably due to the high concentration of both ions in seawater.^{1,7} Equally as diverse are the molecular modes of action by which these compounds impart their biological activity, making them an extraordinary resource for the development of new therapeutic agents.

1.2. Secondary metabolites?

In the field of marine natural products chemistry, natural products are alternatively called secondary metabolites because they are apparently not essential for the primary metabolic activities involved in the growth of the producing organism.^{1,8}

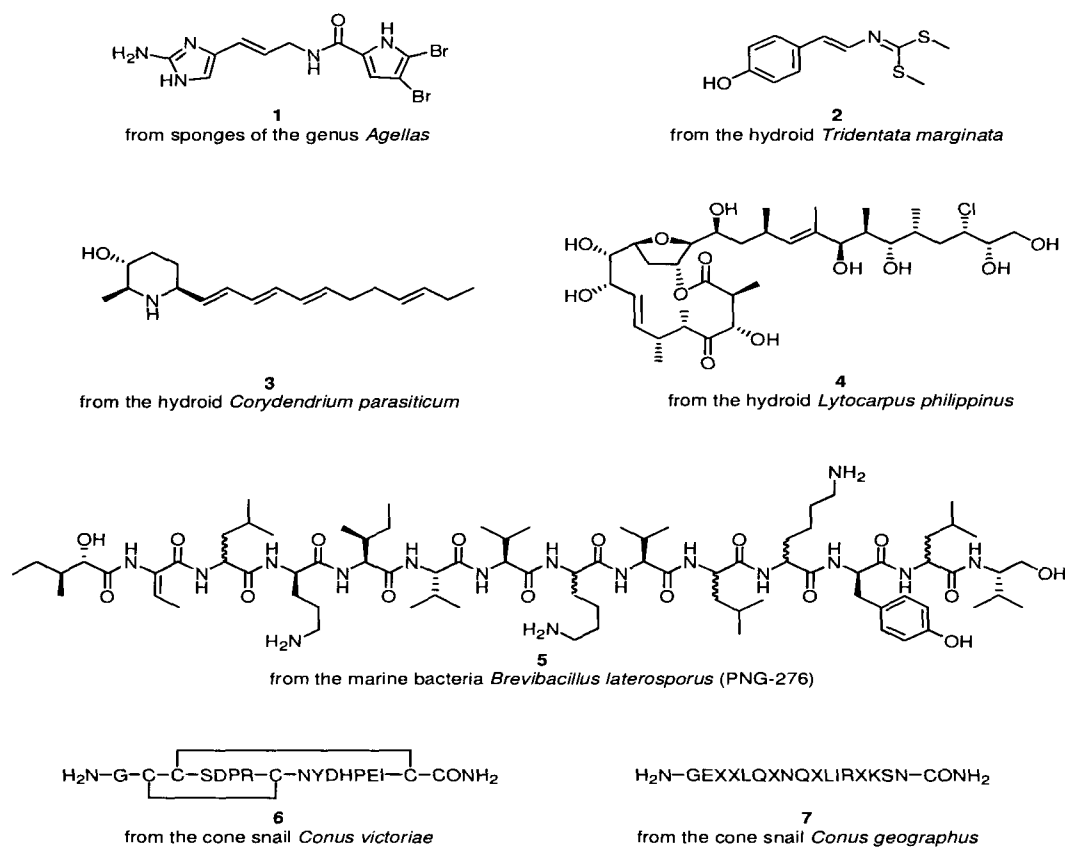


Figure 1.1. Some marine secondary metabolites with known ecological roles: oroidin (1),⁹ tridentatol A (2),^{10,11} corydendramine A (3),¹² lytophilipinne A (4),¹³ bogorol A (5),¹⁴ ACV-1 (6) and CGX-1007 (7).^{15,16}

Although in some cases there is evidence supporting antifeedant activity against predators (1-4), inhibitory effects on the growth of competitors (5, Figure 1.1),^{9-14,17} and even immobilization of motile species prior to ingestion (6, 7),^{15,16} for most secondary metabolites there is no rigorous proof of their actual ecological role. In contrast to omnipresent primary metabolites such as amino acids, fatty acids and nucleotides, the occurrence of a particular secondary metabolite is usually limited to one or a few species.⁸

Among the approximately 100,000 species of marine invertebrates described so far, most of the animals in the phyla Cnidaria, Porifera, Bryozoa, and Echinodermata are sessile, slow growing, brightly colored, and lack the physical protection of shells and spines.¹ Their intense concentration in marine habitats makes them highly competitive and biologically complex. Additionally, nutrients, light, water current, and temperature represent growth limiting components, further fueling competition.⁷ Thus, in order to ensure their survival, a high percentage of species make extensive use of biologically active secondary metabolites (Figure 1.2).

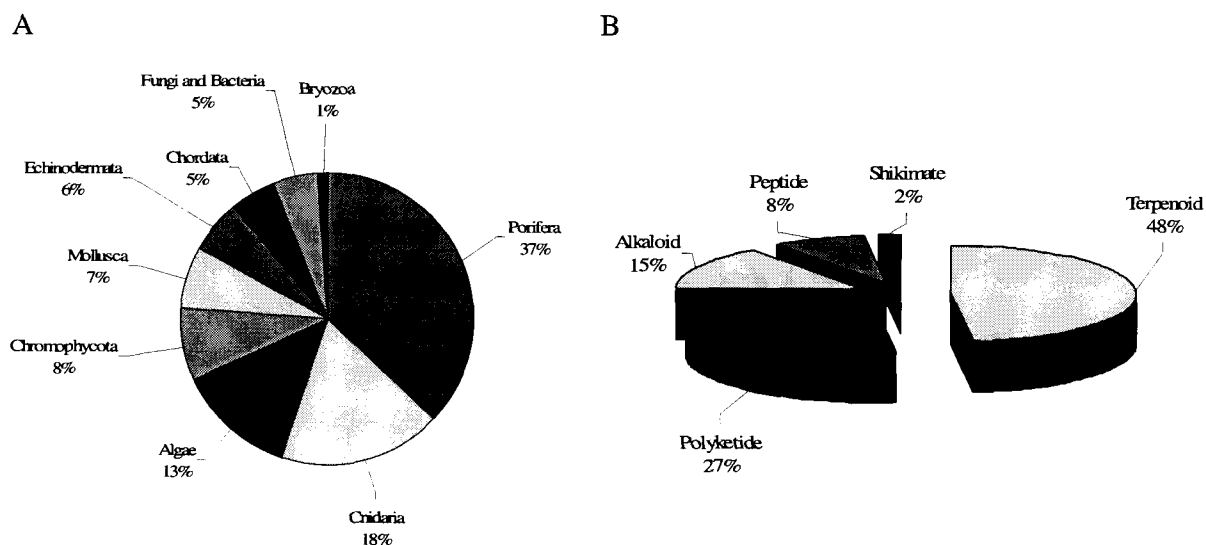


Figure 1.2. Distribution of marine natural products by phylum (A) and biosynthetic origin (B), according to the MarinLit database (Total: 17,068 structures up to 2005).⁵

Among marine invertebrates, sponges (Porifera), coelenterates (Cnidaria: soft corals and gorgonians), echinoderms, tunicates (Chordata), algae and mollusks are the most prolific sources of compounds.^{7,18} These metabolites take the form of terpenoids, polyketides, alkaloids, peptides, shikimic acid derivatives, sugars, steroids, and a large number of molecules with combined biogenetic origins (Figure 1.2B).^{5,7,19}

Drug discovery programs in both the pharmaceutical industry and academia have focused special attention on marine sponges (Figure 1.2). The broad molecular diversity and the high cytotoxic activity exhibited by sponge metabolites makes them promising anticancer drug leads.^{1,2,18,20} Approximately 5,000 living sponge species exist in the phylum Porifera, which is composed of three distinct classes: the Hexactinellida (glass sponges), the Demospongiae (siliceous sponges), and the Calcarea (calcareous sponges).²¹ As expected from their phylogenetic position, marine sponges are among the oldest known animals, with fossils dating from the late Precambrian (542 million years ago).²¹ Since 1950, over 5,600 references have reported more than 6,500 secondary metabolites including *ca.* 3,100 nitrogen-containing compounds (such as pyrrole-imidazole alkaloids, Chapter 4), unique to marine sponge species.^{6,20-23}

An increasing amount of evidence suggests that many interesting compounds isolated from marine invertebrate extracts are actually biosynthetic products of symbiotic microorganisms, including microalgae, cyanobacteria, as well as heterotrophic bacteria and fungi.^{1,7,24} However, systematic studies of invertebrate-symbiont associations are usually accompanied by serious technical challenges, such as the general resistance of symbionts to culturing attempts separately from their hosts and the complexity of many microbial consortia.^{7,24} Nevertheless, since laboratory fermentation represents a sustainable supply of an interesting metabolite,^{1,2,18} advances in genomics-based taxonomy and in new methods for

acquisition and cultivation of marine bacteria are already leading to the discovery of new classes of bacteria that produce unprecedented antibiotics and potential anticancer drugs.^{2,25} Deep ocean sediments have recently emerged as an immeasurable source (70% of Earth's surface) of actinomycete bacteria, biologically relevant since their terrestrial counterparts are responsible for producing most of the currently available antibiotics.² When microbial life is considered, the total number of species inhabiting the world's oceans may approach 1 to 2 million.⁷

1.3. Biological activity and current success in marine natural products research

Historically, the chemical exploration of oceanic invertebrate life has relied on assays to screen libraries of marine extracts in order to identify those ones capable of eliciting a desired cellular response with potential pharmaceutical applications.¹ These range from fairly simple toxicity tests such as the sea urchin egg and brine shrimp assays, to more expensive and labor intensive *in vitro* screens using purified enzymes and receptors, as well as cell-based bioassays that employ genetically engineered eukaryotic cells or microorganisms.^{1,2,7}

Recently, the combination of robotics and target-based bioassays has given birth to *high-throughput screening*, a process by which large numbers of compounds are tested in an automated fashion for activity as inhibitors or activators of a particular molecular target.^{2,7} Having as a primary directive the identification of lead chemical structures and their structure-activity optimization,^{1,2} high-throughput screening programs in major drug companies can typically handle 3,000 enzyme inhibition or 4,800 cell-based bioassays per day, allowing the biological evaluation of up to 100,000 chemical entities in a reasonable time frame.¹ With groups of academic researchers, major pharmaceutical companies and the National Cancer Institute (NCI) heavily investing resources in cancer research for decades now, it is not surprising that

such activity is a major driving force behind the discovery of new marine natural products (Figure 1.3.).²³

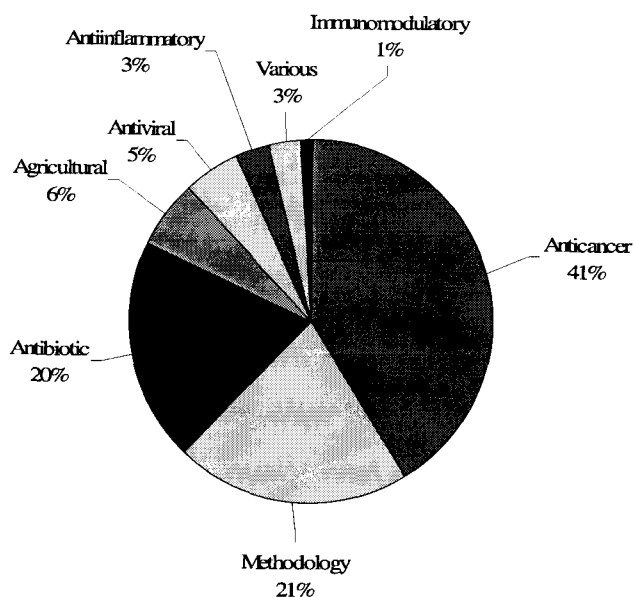


Figure 1.3. Distribution of biological activities evaluated in marine natural products in 2004.²³
Various: neurological, blood pressure, fertility, allergy-based, laxative and enzyme activation bioassays. Methodology: mechanism of action, SAR studies, radio immunoassays, as well as sea urchin egg and brine shrimp toxicity assays.

Consequently, in 2006 more than 30 marine-derived molecules were in preclinical development or clinical trials against a wide variety of cancers.² Noteworthy, a significant number of these new drug candidates were initially developed with direct or indirect NCI assistance, and later licensed to pharmaceutical partners for clinical evaluation, manufacture and sales.^{2,7} Table 1.1 summarizes 18 marine-derived compounds currently in clinical trials.

Table 1.1. Marine-derived compounds currently in clinical trials (Phase I and above) for the treatment of several human conditions.^{2,7}

Compound	Source	Chemical class	Disease	Status
Ecteinascidin 743	<i>Ecteinascidia turbinata</i> (tunicate)	Tetrahydroisoquinolone alkaloid	Cancer	II
Bryostatin 1	<i>Bugula neritina</i> (bryozoan)	Polyketide	Cancer	III
ILX651 ^a (Synthadotin)	<i>Dolabella auricularia</i> (mollusk)	Linear peptide	Cancer	I/II
Kahalalide F	<i>Elysia refescens</i> (mollusk)	Cyclic depsipeptide	Cancer	II
Squalamine	<i>Squalus acanthias</i> (shark)	Aminosteroid	Cancer	II
TYZT-1027 ^b (Soblidotin)	<i>Dolabella auricularia</i> (mollusk)	Linear peptide	Cancer	II
E7389 ^c	<i>Halichondria okadai</i> (sponge)	Macrocyclic polyether	Cancer	II
Discodermolide	<i>Discodermia dissoluta</i> (sponge)	Polyketide	Cancer	I
ES-285	<i>Mactromeris polynyma</i> (mollusk)	Alkylamino alcohol	Cancer	I
KRN-7000 ^d	<i>Agelas mauritianus</i> (sponge)	α -Galactosylceramide	Cancer	I
NVP-LAQ824 ^e	<i>Psammaphysilla</i> sp. (sponge)	Indolic cinnamyl hydroxamate	Cancer	I
Salinosporamide A	<i>Salinospora</i> sp. (bacterium)	Bicyclic γ -lactam- β lactone	Cancer	I
E-7974 ^f	<i>Cymbastella</i> sp. (sponge)	Linear peptide	Cancer	I
AE-941 (Neovastat)	<i>Scyliorhinus torazame</i> (shark)	Mixture from cartilage	Cancer	II/III
GTS-21 (DMBX)	<i>Paranemertes peregrina</i> (worm)	Pyridine alkaloid	Alzheimer's	I
Ziconotide (Prialt TM)	<i>Conus magus</i> (mollusk)	Cyclic peptide	Neuropathic pain	Appr. 2005
CGX-1160	<i>Conus geographus</i> (mollusk)	Cyclic peptide	Pain	I
ACV1	<i>Conus victoriae</i> (mollusk)	Cyclic peptide	Pain	I

Synthetic derivatives of: ^aDolastatin 15, ^bDolastatin 10, ^cHalichondrin B, ^dAgelasphin, ^ePsammaphin, ^fHemiasterlin.

As seen in Table 1.1, the first modern marine drug was ziconotide (PrialtTM), a potent calcium channel blocker used to provide relief from severe neuropathic pain.² This pharmaceutical is based on the highly toxic small peptide ω -conotoxin MVIIA (**8**) that was isolated in 1987 by Olivera and coworkers¹⁵ from the coneshell mollusk *Conus magus*. Although ziconotide is generally recognized as the first marine-derived drug, Werner Bergman, a pioneer in marine sterol chemistry, isolated two modified nucleosides (**9** and **10**) with unique antiviral activities from the sponge *Cryptotethia crypta* in the 1950's.^{18,26,27} These compounds were employed as a template that guided the development of the structurally related antiviral drugs Ara-A (**11**) and Ara-C (**12**), which have been in use since 1969 as chemotherapeutic agents for the treatment of herpes and leukemia.^{2,18}

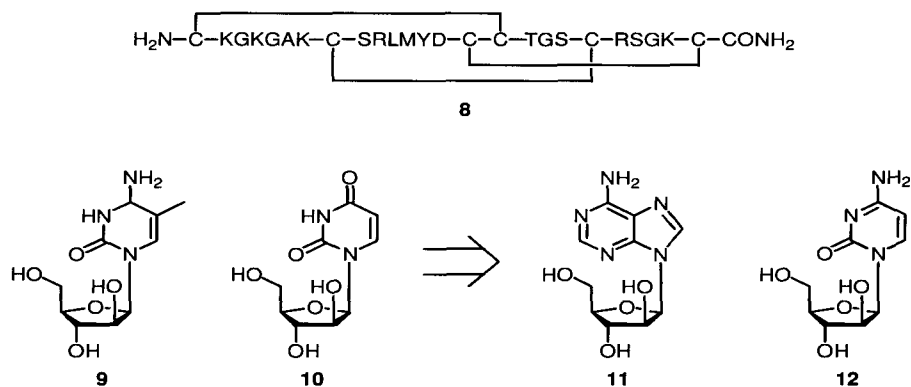


Figure 1.4. First marine-inspired drugs approved for human use.

Two of the studies described herein focus in the isolation and characterization of marine natural products based on their biological activity. Considering the major bioassay areas summarized in Figure 1.3, Chapter 3 details how secondary metabolites from the hydroid *Garveia annulata* are capable of inhibiting human indoleamine 2,3-dioxygenase (IDO), an enzyme involved in immunomodulation and the ability of tumors to evade the host immune

system. Chapter 5 features the first marine cannabinoid-active compound and provides conclusive NMR evidence about its binding mode to the cannabinoid human receptors (Methodology, Figure 1.3).

1.4. Synthesis of marine natural products

Once a bioactive marine-derived lead structure has been identified, the issues of immediate supply and eventual manufacturing-scale availability become key factors in its further progress towards pharmaceutical development.^{1,18} Evaluation of the biological activity in whole cells, *in vivo* efficacy in animal models, determination of maximum tolerated doses and minimum effective doses, as well as pharmacokinetic studies, demand large amounts of material that is in most cases unavailable from the source organism. In order for a large pharmaceutical company to invest financial and human resources in a drug development project (typically involving 12-15 years and more than US \$350 million),¹ a reliable and economical source of the target metabolite must be secured.^{1,2,7}

Organic synthesis represents one possible supply option. The wealth of structurally challenging features and potent biological activities exhibited by some marine secondary metabolites have made them attractive targets for academic synthetic programs. Besides solving supply problems, synthesis plays an increasingly important role as a method for providing solutions to structural and stereochemical questions.²⁸ Furthermore, the evaluation of biological mechanisms and targets connects synthetic organic chemistry with cell biology.²⁹ Only the combination of both allows for broadly addressing target validation with suitable potency and specificity.³⁰ Even in cases when the complexity of the natural product does not allow total synthesis on an industrial scale, a synthetic medicinal chemistry program using the marine

metabolite as a lead structure may provide simpler, synthetically accessible analogues containing the same pharmacophore.

In 2003, Blunt, Munro and coworkers³¹ pointed out the necessity of a companion review to their annual *Marine Natural Products* report in view of the rapid growth in the area of marine natural product synthesis. In response, since 2005 Nicholas and Phillips^{28,32,33} have been summarizing first and improved total syntheses of marine natural products. These and other reviews reveal significant progress in the development of efficient asymmetric reactions for building multiple stereocenters in acyclic intermediates and for construction of ring systems,^{29,34} new general strategies and methodologies for efficient coupling of highly functionalized segments,^{35,36} development of highly stereoselective routes to *E* and *Z*, di- and trisubstituted alkenes,^{9,37} reduction of functional group protection and deprotection steps,³⁸ and achieving efficient macrocyclization reactions to provide large ring sizes.^{34,39}

The selection of marine natural products covered herein provides examples where synthesis was employed to:

- Overcome shortages of supply from natural sources (Total synthesis of tauramamide, Chapter 2).
- Generate modified natural products required as biological tools for target validation (Preparation of dealkylsurfactin, Chapter 2, and synthesis of liphagal analogues, Chapter 6).
- Provide simplified analogues offering practical access to biologically active structures relevant for further drug development (Progress towards the synthesis of ceratamines, Chapter 4).

2. Bioactive Marine Peptides: Total Synthesis of tauramamide and dealkylsurfactin

2.1. Peptides from the sea

Cyclic and linear peptides isolated mainly from microorganisms and sponges represent an important class of marine-derived metabolites.⁴⁰⁻⁴² They exhibit antibacterial, antifungal, cytotoxic, antimalarial, and antitumor activities, as well as incorporating novel structural features unseen in their terrestrial counterparts, making marine peptides important lead compounds for drug development research.⁴³ For instance, over a dozen of antitumor compounds from marine origin are currently in various phases of human clinical trials.⁴⁴ Among them, the peptides aplidin (1),^{45,46} dolastatin 10 (2)^{47,48} and its synthetic congeners ILX-651⁴⁹ and cemadotin,⁵⁰ hemiasterlin analogue HTI-286 (3),⁵¹⁻⁵³ and kahalalide F (4),⁵⁴⁻⁵⁶ possess prominent inhibitory activity against different types of tumors.⁴⁴

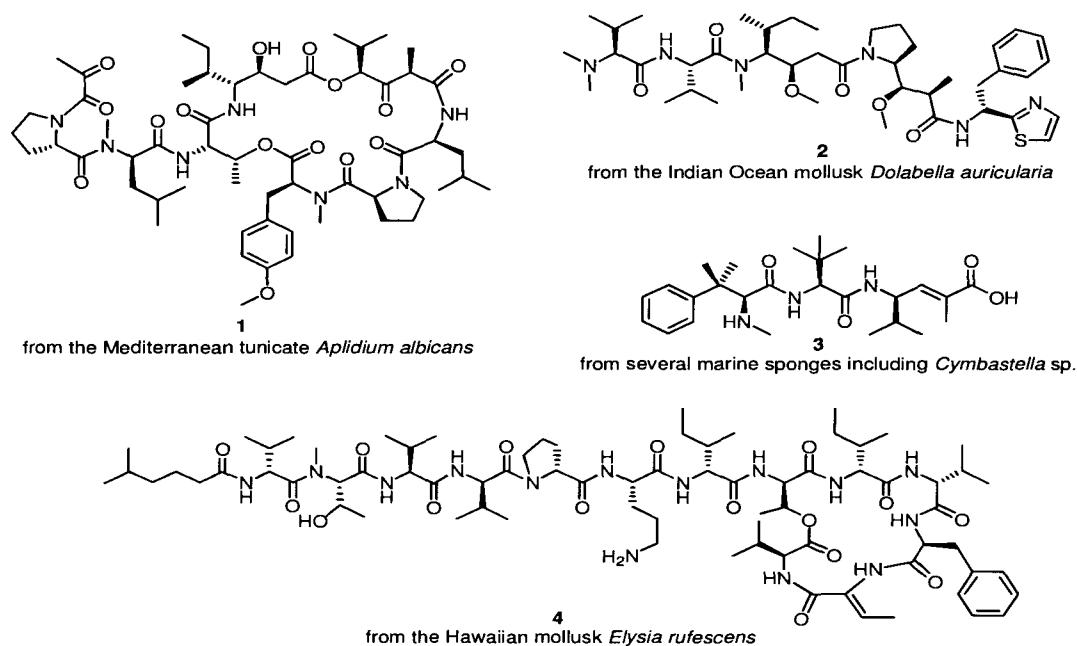
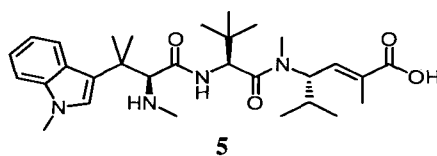


Figure 2.1. Prominent marine peptides currently in clinical trials.⁴⁴

2.2. Peptides from marine PNG bacterial isolates

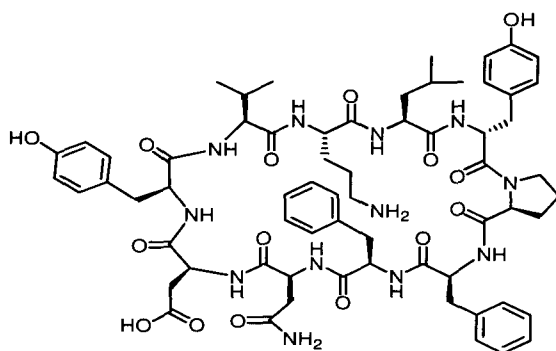
Besides having a leading role in the isolation,⁵⁷ synthesis,^{52,53} biological evaluation,⁵⁸⁻⁶⁰ and clinical development⁴⁴ of hemiasterlin (**5**) and its analogues (such as HTI-286 **3**), the Andersen research group has reported in the last decade a considerable number of other marine-derived bioactive peptides.⁶¹⁻⁶⁷ Most of these compounds have been isolated from laboratory cultures of bacterial isolates as part of an ongoing program aimed at discovering new antibiotics from the sea, which are desperately needed in the treatment of resistant strains of Gram positive human pathogens. Microorganisms isolated from marine habitats in Papua New Guinea (PNG) have proved to be an extremely rich source of new bioactive secondary metabolites.^{61,62,64,65,68}



2.2.1. New antibiotics from PNG-276

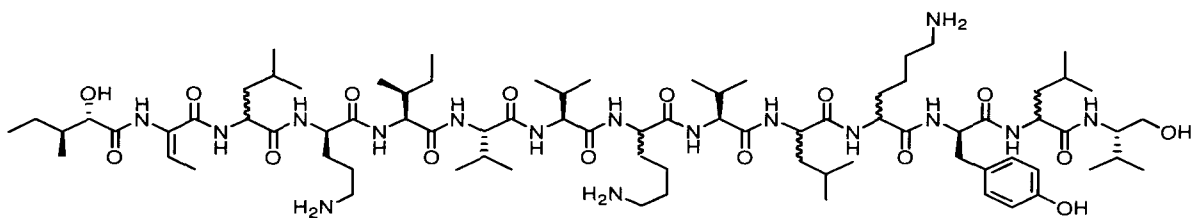
PNG-276 was initially obtained from tissues of an unidentified tube worm collected off the coast of Loloata Island, Papua New Guinea, and later identified as *Brevibacillus laterosporus* by 16S RNA analysis.⁶⁹ Crude MeOH extracts of *B. laterosporus* cells harvested from cultures grown as lawns on solid agar showed broad-spectrum antibiotic activity against several human pathogens including methicillin-resistant *Staphylococcus aureus* (MRSA), vancomycin-resistant *Enterococcus* (VRE), *Mycobacterium tuberculosis*, *Candida albicans*, and *Escherichia coli*.^{62,64,69} To date, bioassay-guided fractionation of PNG-276 cultures has yielded five structurally unrelated families of antibiotics.

The first group of PNG-276 antibacterial compounds is comprised of loloatins A-D,^{61,62} a family of cyclic decapeptides containing four aromatic amino acid residues, two of which have the unnatural D configuration. The presence of both ornithine and aspartic acid imparts zwitterionic character. Loloatins A (**6**) to C showed potent antibacterial activity against MRSA, VRE, and penicillin-resistant *Streptococcus pneumoniae* (MIC's 0.5-4.0 $\mu\text{g/mL}$).⁶²



6

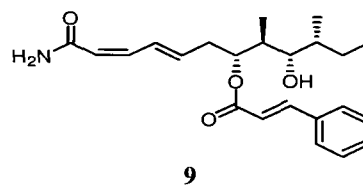
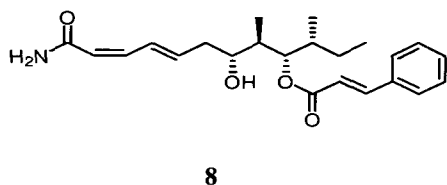
The bogorol family of linear peptides is also produced by PNG-276. At the time of its isolation, bogorol A (**7**)⁶⁴ represented a new template for cationic antibiotic peptides. Cationic peptides are widespread in nature where they play an important role in innate immune systems protecting living organisms from microbial infections.^{70,71} They seem to avoid rapid emergence of resistance by physically disrupting cell membranes, killing bacteria very quickly.⁶⁴



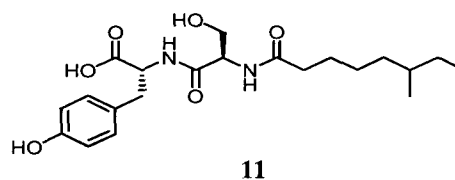
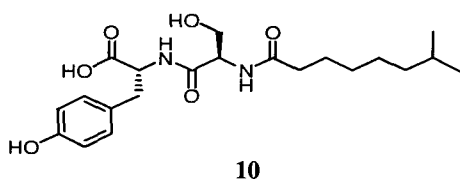
7

The bogorols contain modified C- and N-terminal residues, D amino acids and a dehydroamino acid.⁶⁸ They exhibited strong activity against MRSA and VRE (MIC's of 2.0 and 10 µg/mL, respectively).⁶⁸

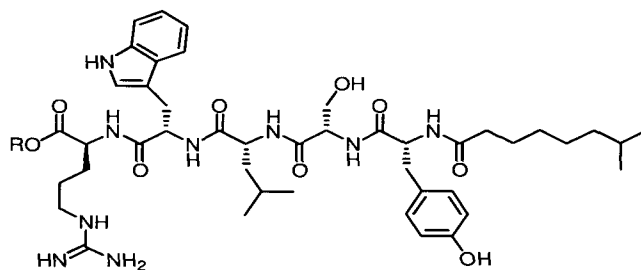
Further investigations of PNG-276 culture extract fractions exhibiting potent inhibition of *Candida albicans* led to the isolation of basiliskamides A (**8**) and B (**9**) (MIC's 1.0-3.1 µg/mL),⁶⁵ characterized by a linear $\alpha,\beta,\gamma,\delta$ -unsaturated amide backbone with a cinnamoyl substituent attached via an ester linkage.



The same report included two *Escherichia coli* active components, tupuseleiamides A (**10**) and B (**11**),⁶⁵ new acyl dipeptides in which the amino acids both have the non-proteinogenic D configuration.



The fifth and most recent family of PNG-276 derived peptide antibiotics is represented by tauramamide (**12**),⁶⁹ a linear acylpentapeptide isolated as its methyl (**13**) and ethyl ester (**14**) derivatives. As with the tupuseleiamides, **12** is acylated at the N-terminus and contains two D amino acids. Both esters showed potent (MIC's 0.1 µg/mL) and relatively selective activity against the important Gram positive human pathogen *Enterococcus* sp.



12 R=H
13 R=CH₃
14 R=CH₂CH₃

All attempts to convert the limited amounts of esters **13** and **14** obtained from *B. laterosporus* cultures to the natural product **12** failed to generate sufficient amounts for biological testing. Additional material was also necessary for an exhaustive antimicrobial assessment of **13** and **14**. Such requirements prompted the total synthesis of tauramamide (**12**) and its ethyl analogue (**14**). Furthermore, a synthetic sample of both compounds would confirm the proposed structure for this new antibiotic.

2.2.2. Anti-Alzheimer activity of PNG10A

In 1968, Arima and coworkers⁷² isolated surfactin C₁ (**20**) from *Bacillus subtilis* IAM 1213. The compound exhibited exceptional surfactant activity and its structure was elucidated as that of a cyclic depsipeptide having a hydroxyfatty acid residue.⁷³ Further studies by Nagai and Okimura⁷⁴ revealed that laboratory cultures of *Bacillus natto* KMD 2311 contained seven additional homologous lipopeptides (**15-22**), different only in the structure of their β -hydroxy side chains (Figure 2.2).

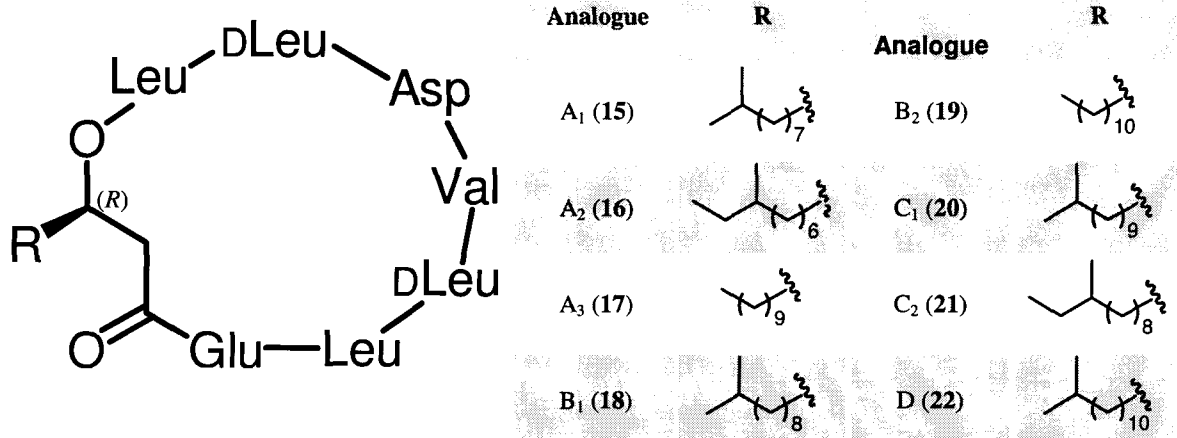
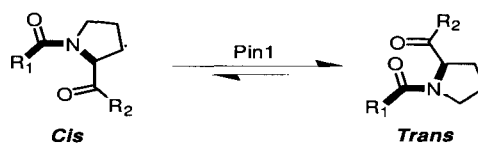


Figure 2.2. Structure of surfactin analogues.⁷⁴

Surfactin C₁ (**20**, or simply surfactin) remains the best known representative of the family,⁷⁵ although other lipopeptides have since been discovered.⁷⁵⁻⁸² Several other physiological and biochemical properties have been demonstrated for surfactin, including antibacterial,⁸³ antitumoral,⁸⁴ antiviral,^{85,86} and antimycoplasmic activities.^{87,88} Additionally, **20** has been recognized as a hypocholesterolemic agent⁸⁹ and exhibits valuable inhibition of biofilm⁹⁰ and blood clot formation.⁷² While such properties qualify surfactin for potential applications in medicine or biotechnology, they have not been subsequently exploited.^{75,91}

In our research group, surfactin C₁ (**20**) was found via bioassay-guided fractionation of cultures prepared using the marine microorganism PNG10A, also collected in Papua New Guinea. Marine organisms that have yielded similar cyclic depsipeptides, presumably through symbiotic collaborations with bacteria, include sponges, mollusks, chelicerata, crustaceans and ascidians.^{79,92-98} The screening process, developed by Dr. M. Roberge and his research group in the Department of Biochemistry at UBC, was designed to detect natural products capable of inhibiting the binding of Pin1 to the microtubule-associated protein tau. Such an interaction is believed to be crucial in the development of Alzheimer's disease symptoms.⁹⁹⁻¹⁰¹

Pin1 is a mitotic regulator essential for the G2 to M phase transition during the eukaryotic cell cycle.^{102,103} This enzyme belongs to the peptidyl-prolyl *cis-trans* isomerases, a superfamily of ubiquitous catalysts responsible for enhancing the typically slow *cis-trans* isomerization of prolyl bonds.¹⁰² Pin1 specifically isomerizes Ser/Thr-Pro bonds and regulates the function of mitotic phosphoproteins.¹⁰¹ The conformational changes induced by this enzyme play an important role in protein folding, signal transduction, trafficking, assembly and regulation of the cell cycle.^{101,102} Among others, Pin1 targets the microtubule-associated protein tau.¹⁰¹



All cases of Alzheimer's disease are characterized by the formation of neurofibrillary tangles containing paired helical filaments (PHFs), one of the neuropathological hallmarks of this human condition.⁹⁹ The main component of PHFs is hyperphosphorylated tau. In normal brains, tau stabilizes the internal microtubule structure of neurons that functions to transport proteins and other molecules through the cells. In the brains of Alzheimer's patients tau is hyperphosphorylated and unable to bind to microtubules and promote their assembly.¹⁰¹ Pin1 has a high affinity for PHFs and is sequestered by the phosphorylated tau, leading to a depletion of soluble Pin1 in the brains of Alzheimer's patients, which in turn induces mitotic arrest and apoptotic cell death. This translates to an acceleration of degenerative symptoms.⁹⁹

Several studies^{99,101,102} suggest that disrupting the interaction between Pin1 and phosphorylated tau in PHFs, might reverse the memory loss associated with the disease. Additionally, it has been shown that Pin1 can restore the ability of phosphorylated tau to bind microtubules and promote microtubule assembly *in vitro*.⁹⁹ Thus, Pin1 might be useful as a

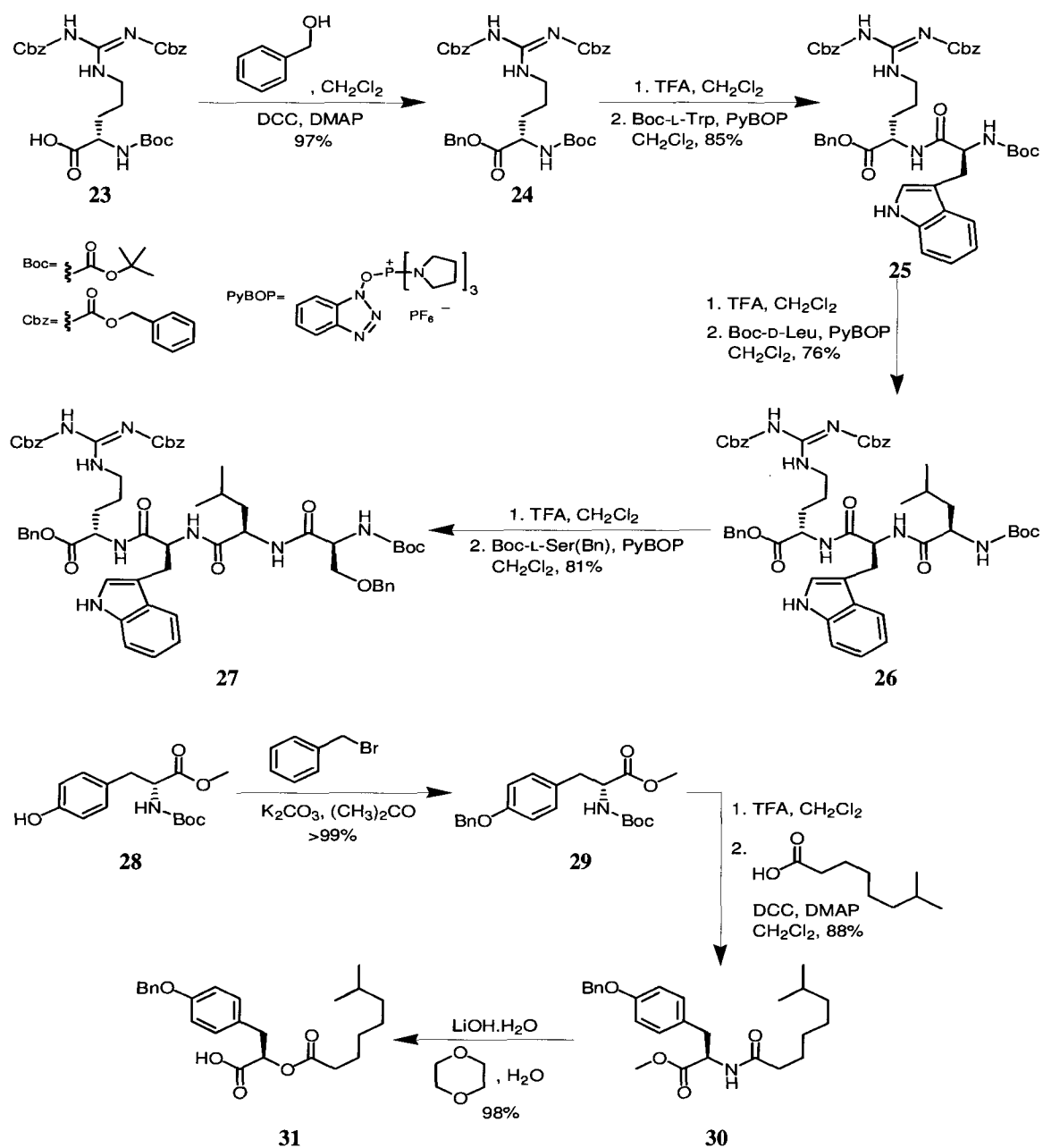
pharmacological target for the development of new therapies for Alzheimer's and related neurodegenerative diseases.

Particularly interesting as a biological tool for the study of interactions between Pin1 and phosphorylated tau, as suggested by the Roberge group, was an analogue of surfactin without its characteristic lipophilic chain. Such a compound would provide information regarding possible inhibitory mechanisms, and confirm whether the efficient surfactant capability of macrolide lipopeptides is in fact responsible for the observed disruption of Pin1/phosphorylated tau adducts. Additionally, if the macrocyclic peptide alone were active, variation of its amino acid sequence may yield more potent inhibitors attractive both as research tools and experimental drug candidates.

2.3. Total synthesis of tauramamide

To date, the only peptidic PNG-276 metabolites synthetically prepared have been the loloatins, due mainly to an increasing interest in their biological mechanism (the non-peptidic basiliskamides have also been synthesized).¹⁰⁴⁻¹⁰⁷ An Fmoc solid phase strategy for peptide elongation using (benzotriazol-1-yl)oxytripyrrolidinophosphonium hexafluorophosphate (PyBOP) and diisopropylethylamine (DIEA) as coupling reagents, followed by a generally low yielding on-resin or after-cleavage cyclization step (4-74%) employing *O*-(7-azabenzotriazolyl)-1,1,3,3-tetramethyluronium hexafluorophosphate (HATU) and 1-hydroxy-7-azabenzotriazole (HOAt), are common aspects in the three available syntheses of loloatins. The use of HOAt is reported to enhance coupling yield and suppress racemization.^{104,105}

Bogorols and tupuseleiamides have yet to be prepared. Our synthetic approach to tauramamide (**12**) was convergent, starting from both *C*- and *N*-termini simultaneously (Scheme 2.1).

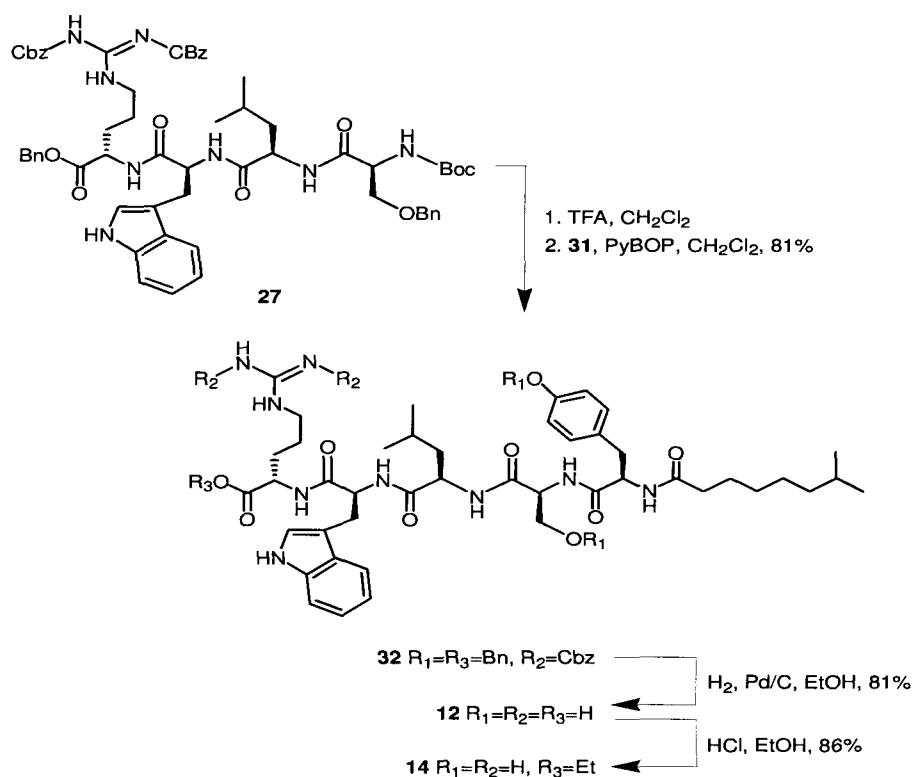


Scheme 2.1. Steps involved in the synthesis of tauramamide fragments (**27**) and (**31**).

Thus, the commercially available *N*-protected arginine derivative (**23**) was converted to its benzyl ester (**24**) by reaction with benzyl alcohol, DCC, and DMAP.¹⁰⁸ Deprotection of the α -

amino nitrogen by treatment of **24** with TFA,^{109,110} followed by three cycles of standard PyBOP¹¹¹ activated peptide coupling with Boc-L-Trp, Boc-D-Leu, and Boc-L-Ser(OBn) in sequence, generated the protected tetrapeptide (**27**).

At the same time, the phenolic hydroxyl in D-Tyr methyl ester (**28**) was protected by treatment with benzyl bromide and potassium carbonate in acetone.¹¹² Exposure of the amino group in **29** by reaction with TFA,¹¹⁰ followed by DCC mediated amide formation¹⁰⁸ with 7-methyloctanoic acid, and subsequent LiOH catalyzed ester hydrolysis¹¹³ gave acid (**31**).



Scheme 2.2. Total synthesis of tauramamide (**12**) and its ethyl ester (**14**).

Treatment of the protected tetrapeptide (**27**) with TFA followed by PyBOP¹¹¹ mediated amide coupling with acid (**31**) gave protected tauramamide (**32**) (Scheme 2.2). Hydrogenolysis

using Pd on C in EtOH removed the Bn and Cbz protecting groups to liberate tauramamide (**12**), which was purified using reversed-phase HPLC to give a pure sample.

The structure of each reaction intermediate was confirmed by $^1\text{H-NMR}$ and HRESIMS. In most steps, the products afforded did not require exhaustive purification and were directly employed in the following reaction. From all nine reaction steps leading to tauramamide (**12**), only hydrogenation of precursor **32** needed some optimization, in order to minimize the amount of mono, di- and triprotected tauramamide. Several H_2 pressures and Pd on C concentrations were tested, achieving best results when 10% Pd/C, wet Degussa type E101NE/W (~50% water, reported as an useful reagent for debenzylations),¹¹⁴ was stirred with **32** under H_2 atmosphere for one week at 20 atm.

The free acid (**12**) gave a $[\text{M}+\text{H}]^+$ ion at m/z 864.4981 in the HRESIMS, consistent with a molecular formula of $\text{C}_{44}\text{H}_{65}\text{N}_9\text{O}_9$ (calculated for $\text{C}_{44}\text{H}_{66}\text{N}_9\text{O}_9$: 864.4984). Examination of its ^1H and $^{13}\text{C-NMR}$ spectra (Figures 2.3 and 2.4, Table 2.1) revealed an evident similarity with the NMR data for both natural tauramamide esters. Detailed analysis of the COSY, HMQC and HMBC 2D spectra allowed a complete assignment of all protons and carbons in the peptide backbone and the 7-methyloctanoyl fragment (Table 2.1).

The $^1\text{H-NMR}$ spectrum (Figure 2.3) displayed a broad singlet resonance at δ_{H} 12.69 that was assigned to the OH group in the free arginine C-terminus. All $\alpha\text{-NH}$ and $\alpha\text{-H}$ resonances for the five amino acid residues in **12** can be easily recognized around δ_{H} 7.0-8.5 and δ_{H} 4.2-4.6, respectively. Five aliphatic methylene resonances between δ_{H} 1.06 and 2.00, a methine resonance at δ_{H} 1.45 (δ_{C} 27.6), and a pair of isochronous methyl doublets at δ_{H} 0.82 (δ_{C} 22.5), were assigned to the 7-methyloctanoyl alkyl chain.

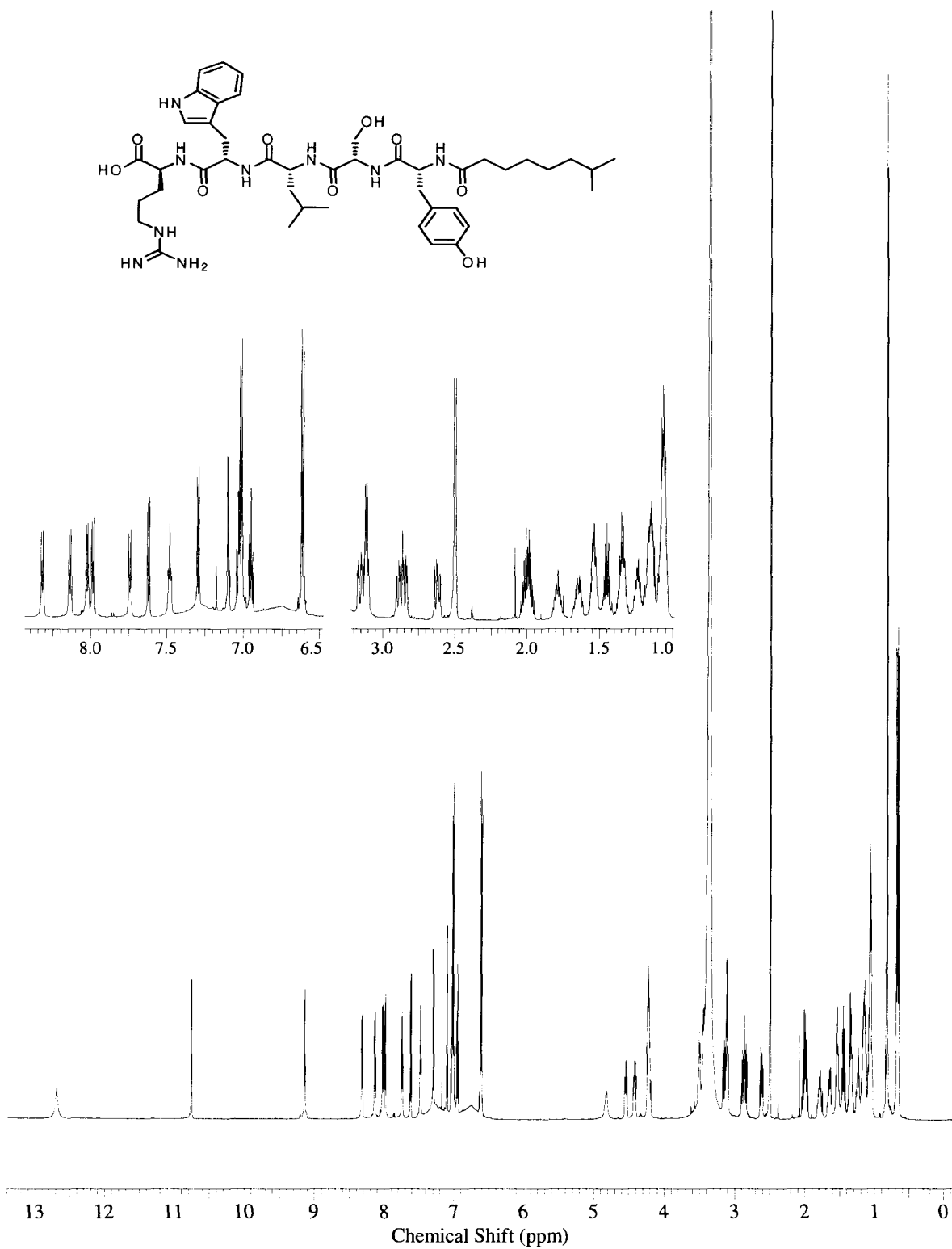


Figure 2.3. ¹H-NMR spectrum of tauramamide (12) (recorded in DMSO-*d*₆ at 600 MHz).

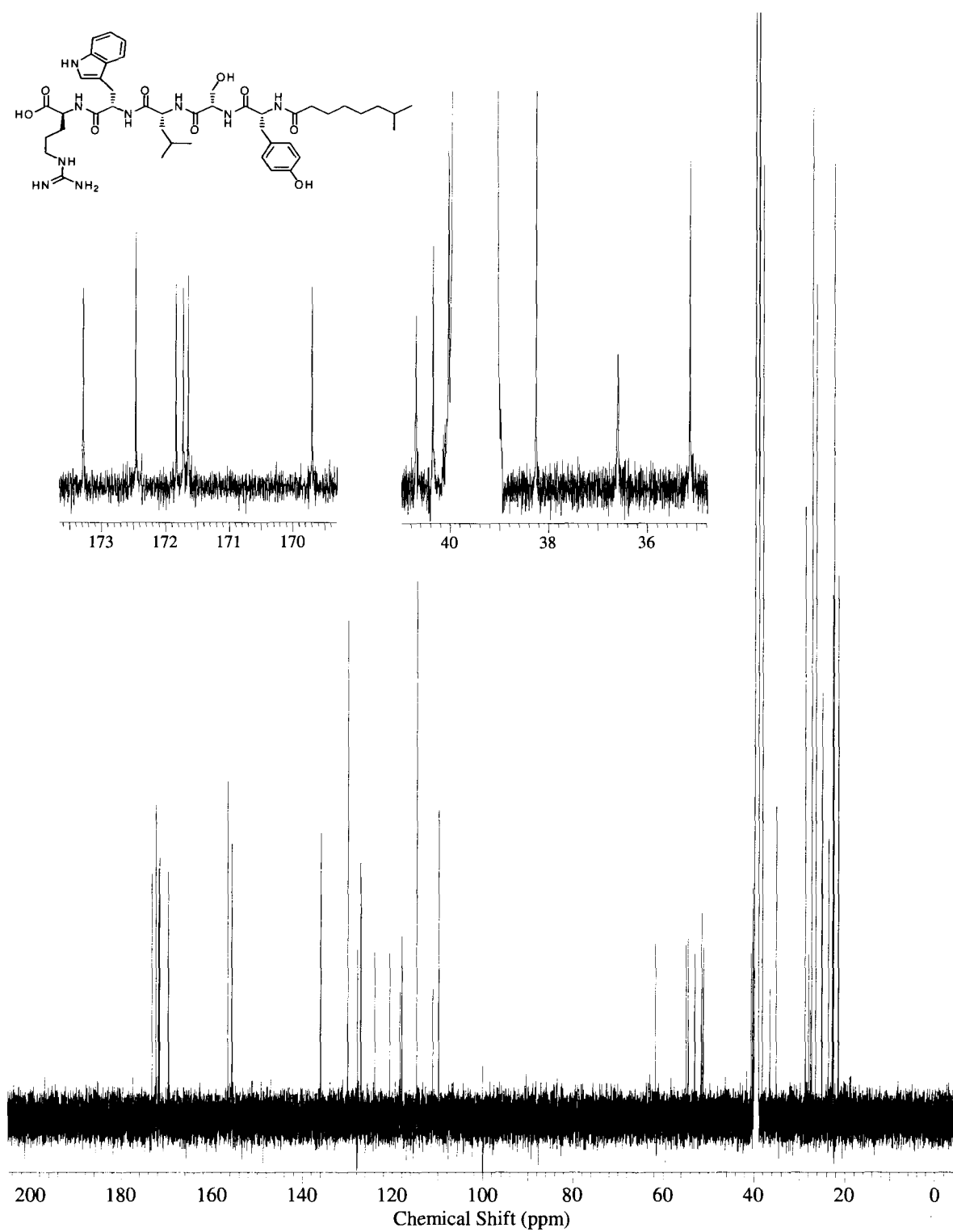
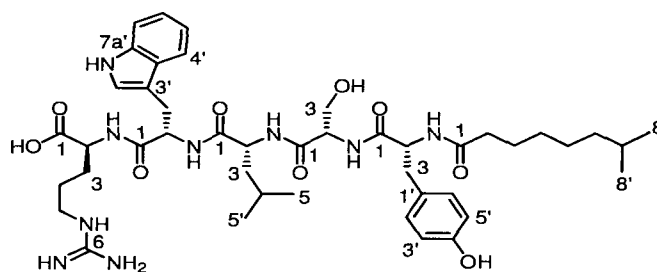
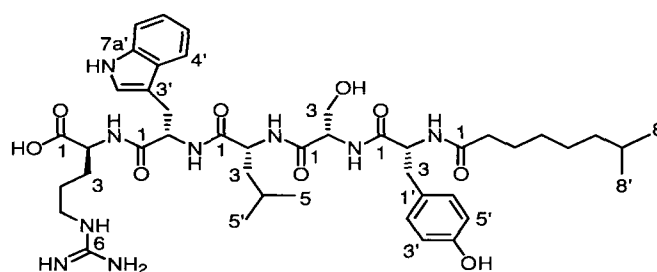


Figure 2.4. ¹³C-NMR spectrum of tauramamide (12) (recorded in DMSO-*d*₆ at 150 MHz).

Table 2.1. NMR data for tauramamide (**12**) (recorded in DMSO-*d*₆).

Amino Acid	Carbon No	¹³ C δ (ppm) ^a	¹ H δ (ppm) (mult, <i>J</i> (Hz)) ^{b,c}	HMBC ^b (H→C)
Arg	1	173.3	OH 12.69 (s, broad)	
	2	51.6	4.22 (m)	C1, C3, C4
			NH 8.32 (d, <i>J</i> = 7.8 Hz)	C2, C3, Trp C1
	3	28.0	1.64 (m), 1.79 (m)	C1, C2, C4, C5
	4	25.2	1.35 (m), 1.54 (m)	C2, C3, C5
	5	40.3	3.12 (m)	C3, C4, C6
NH 7.48 (dd, <i>J</i> = 5.8, 5.8 Hz)			C5	
Trp	6	156.6		
	1	171.8		
	2	53.1	4.54 (m)	C1, C3, C3'
			NH 8.14 (d, <i>J</i> = 8.3 Hz)	C2, C3, D-Leu C1
	3	27.4	2.88 (m), 3.16 (m)	C2, C3', C3a', C2'
	3'	109.9		
	3a'	127.1		
	4'	118.5	7.62 (d, <i>J</i> = 7.8 Hz)	C3', C3a', C6', C7a'
	5'	118.0	6.95 (dd, <i>J</i> = 7.4, 7.4 Hz)	C3a', C7'
6'	120.7	7.03 (dd, <i>J</i> = 7.1, 7.1 Hz)	C4', C7a'	
7'	111.2	7.30 (d, <i>J</i> = 8.0 Hz)	C3a', C5'	
7a'	136.0	NH 10.76 (d, <i>J</i> = 1.5 Hz)	C3, C3a', C7a', C2'	
D-Leu	2'	124.0	7.10 (d, <i>J</i> = 1.9 Hz)	C3, C3', C3a', C7a'
	1	171.6		
	2	51.2	4.21 (m)	C1, C3
			NH 7.75 (d, <i>J</i> = 7.8 Hz)	C2, C3, Ser C1
	3	40.7	1.08 (m), 1.17 (m)	C2
	4	23.7	1.24 (m)	C3, C5, C5'
5	22.8	0.68 (d, <i>J</i> = 6.8 Hz)	C3, C4, C5'	
5'	21.5	0.66 (d, <i>J</i> = 6.5 Hz)	C3, C4, C5	

^a Recorded at 150 MHz. ^b Recorded at 600 MHz. ^c According to HMQC recorded at 600 MHz.

Table 2.1. NMR data for tauramamide (**12**) (recorded in DMSO-*d*₆) (Continuation).

Amino Acid	Carbon No	¹³ C δ (ppm) ^a	¹ H δ (ppm) (mult, <i>J</i> (Hz)) ^{b,c}	HMBC ^b (H→C)
Ser	1	169.7		
	2	55.0	4.23 (m) NH 8.03 (d, <i>J</i> = 7.8 Hz)	C1, C3 C2, C3, D-Tyr C1
	3	61.7	3.44 (m), 3.51 (m) OH 4.82 (s, broad)	C1
D-Tyr	1	171.7		
	2	54.5	4.42 (m) NH 7.99 (d, <i>J</i> = 7.7 Hz)	C1, C3, C1' C2, C3, Acyl chain C1
	3	36.6	2.62 (dd, <i>J</i> = 10.2, 14.0 Hz) 2.86 (m)	C1, C2, C1', C2'
	1'	127.8		
	2'	130.0	7.02 (d, <i>J</i> = 8.3 Hz)	C3, C3', C4'
	3'	114.7	6.61 (d, <i>J</i> = 8.4 Hz)	C1', C4'
	4'	155.7	OH 9.14 (s)	C3', C4', C5'
5'	114.7	6.61 (d, <i>J</i> = 8.4 Hz)	C1', C4'	
6'	130.0	7.02 (d, <i>J</i> = 8.3 Hz)	C3, C3', C4'	
Acyl chain	1	172.5		
	2	35.1	2.00 (m)	C1, C3, C4
	3	25.2	1.35 (m)	C1, C2, C5
	4	28.7	1.06 (m), 1.14 (m)	C2, C3, C6, C7
	5	26.5	1.07 (m), 1.15 (m)	C4, C7
	6	38.2	1.09 (m)	C4, C5
	7	27.6	1.45 (m)	C6, C8, C8'
	8	22.51	0.826 (d, <i>J</i> = 6.8 Hz)	C6, C7, C8'
	8'	22.49	0.823 (d, <i>J</i> = 6.8 Hz)	C6, C7, C8

^a Recorded at 150 MHz. ^b Recorded at 600 MHz. ^c According to HMQC recorded at 600 MHz.

The second pair of methyl doublets at δ_{H} 0.67 (δ_{C} 21.5, 22.8) was attributed to the isopropyl moiety of D-Leu. Six carbonyls between δ_{C} 169.0-174.0 (Figure 2.4) account for five amide and one carboxylic acid (δ_{C} 173.3) functionalities, while the five methines bearing NH are grouped around δ_{C} 51.0-55.0.

The amino acid sequence of tauramamide (**12**) is clearly indicated by HMBC correlations (Table 2.1, Figure 2.5) observed between Arg NH (δ_{H} 8.32) and Trp C1 (δ_{C} 171.8), Trp NH (δ_{H} 8.14) and D-Leu C1 (δ_{C} 171.6), D-Leu NH (δ_{H} 7.75) and Ser C1 (δ_{C} 169.7), Ser NH (δ_{H} 8.03) and D-Tyr C1 (δ_{C} 171.7), and finally, between D-Tyr NH (δ_{H} 7.99) and carbonyl C1 (δ_{C} 172.5) of the 7-methyloctanoyl residue, at the *N*-terminus of the pentapeptide Tyr-Ser-Leu-Trp-Arg.

Esterification of **12** with EtOH and catalytic HCl yielded ethyl ester (**14**) (Scheme 2.2). This compound was in agreement by HPLC, MS, specific rotation, and NMR comparison (Figure 2.6, and Table 2.6 in Experimental section) with the material extracted from *B. laterosporus* cells using EtOH as extracting solvent, confirming the structure proposed for tauramamide (**12**).

Table 2.2. Antimicrobial activity (MIC's in $\mu\text{g/mL}$) of synthetic tauramamide (**12**) and tauramamide ethyl ester (**14**).⁶⁹

Pathogen	12	14
MRSA	200	9.4
<i>C. albicans</i>	50	75
<i>Enterococcus</i> sp.	0.1	0.1

Both **12** and **14** showed potent (MIC's 0.1 $\mu\text{g/mL}$) and relatively selective activity against the important Gram positive human pathogen *Enterococcus* sp.⁶⁹ Ethyl ester (**14**) exhibited stronger activity against MRSA, but neither compound is appreciably active against *C. albicans*.

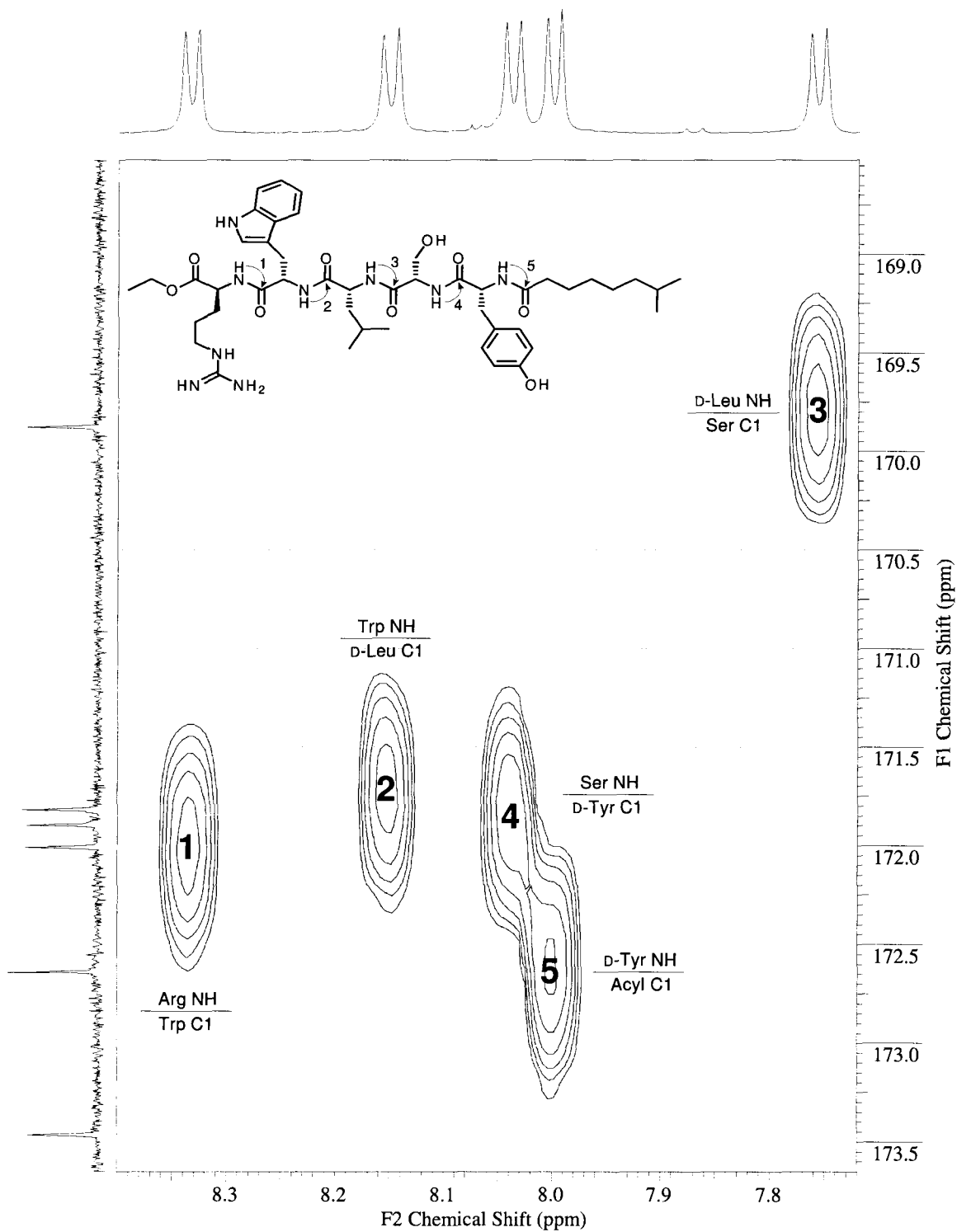


Figure 2.5. Partial HMBC spectrum of tauramamide (12) (recorded in DMSO- d_6 at 600 MHz).

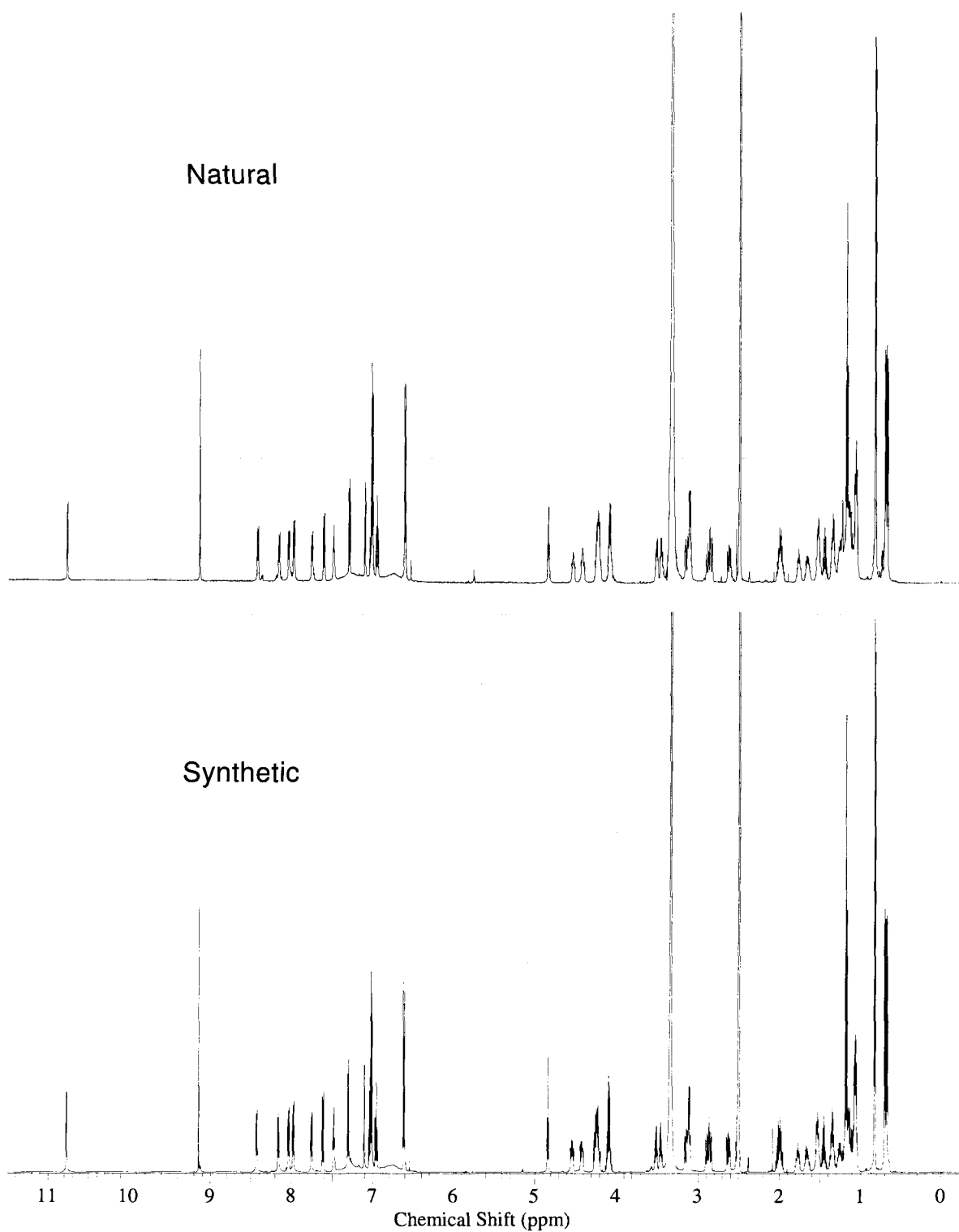


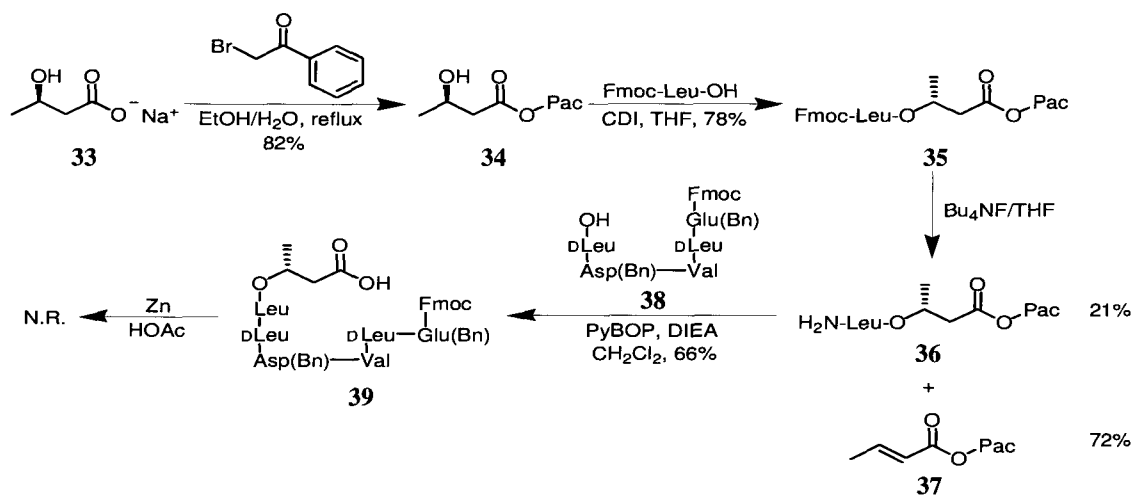
Figure 2.6. ¹H-NMR spectra of bacterial-derived and synthetic tauramamide ethyl ester (**14**) (recorded in DMSO-*d*₆ at 600 MHz).

2.4. Preparation of dealkylsurfactin

Large-scale production of surfactin is performed via fermentation,^{75,115,116} since its biosynthesis is a common feature of members of the genus *Bacillus*. From private and public collections, about 20 strains of *Bacillus subtilis* have been listed as producers.⁷⁵ Considerable resources have been directed to enhance production efficiency and recovery bioprocesses,¹¹⁶ with the surfactant market as the major consumer of surfactin and other similar lipopeptides (an industry of around US \$9.4 billion per annum).¹¹⁵ Several surfactin analogues have been obtained either by genetic engineering or by directed biosynthesis.^{75,115,117} To date however, surfactin has not been able to compete economically with petroleum-derived surfactants mainly due to poor strain productivity and the need for expensive substrates.⁷⁵

The first laboratory synthesis of a surfactin-like cyclic depsipeptide was reported in 1976 by Morrison, Ciardelli and Husman,¹¹⁸ who employed DCC-HOBt-assisted coupling of Boc- and *p*-nitrobenzyl (NB)-protected amino acids in their method. Cyclization was achieved under high dilution conditions using DCC-HOSu, and proceeded in a 41% yield. The only structural difference with the natural compound was the lack of the 13-methyl group in the β -hydroxy acid chain, but their analogue (named norsurfactin) showed comparable hemolytic and anticoagulant activities. Twenty years later, Nagai and coworkers¹¹⁹ synthesized surfactin B₂ (**19**), mainly using active ester and azide fragment condensation methods. Cyclization took place under the same conditions as reported by Morrison,¹¹⁸ but afforded the desired macrolide in 73% yield. More recently in 2002, Pagadoy, Peypoux and Wallach¹²⁰ developed a solid-phase preparation of surfactin C₁ (**20**) and four additional analogues using Fmoc protecting chemistry and HATU as coupling reagent. Once the linear depsipeptide had been constructed and cleaved from the resin, HATU-HOAt-mediated cyclization also in high dilution yielded the corresponding macrolides in 22-35% yields.

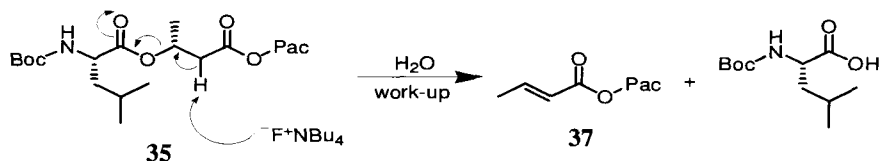
Our initial attempt to synthesize a surfactin analogue lacking the characteristic lipophilic side chain involved protection of (*R*)-(-)-3-hydroxybutyric acid sodium salt (**33**) as a phenacyl ester,^{74,121} followed by CDI mediated¹¹² coupling with Fmoc-Leu-OH (Scheme 2.3). After deprotection,¹²² intermediate (**36**) was then coupled with hexapeptide (**38**), acquired from the Peptide Synthesis Laboratory at UBC.



Scheme 2.3. Initial approach to surfactin analogues.

Two experimental factors made this approach impractical. First, the basic conditions required to remove the Fmoc group produced a substantial amount of side product (**37**), presumably via E2 elimination as outlined in Scheme 2.4. The same byproduct was obtained when piperidine was employed as deprotecting reagent.^{122,123} Secondly, the sample of hexapeptide (**38**) provided was 20 mg of a peptide mixture containing only 56% of the desired compound. Repetitive reversed-phase HPLC (80% CH₃CN/H₂O + 0.01% TFA) afforded 9 mg of **38**, which upon PyBOP¹¹¹ coupling furnished **39** (0.011 g, 0.0077 mmol). Such a small amount of linear precursor made it extremely difficult to measure and handle appropriate proportions of

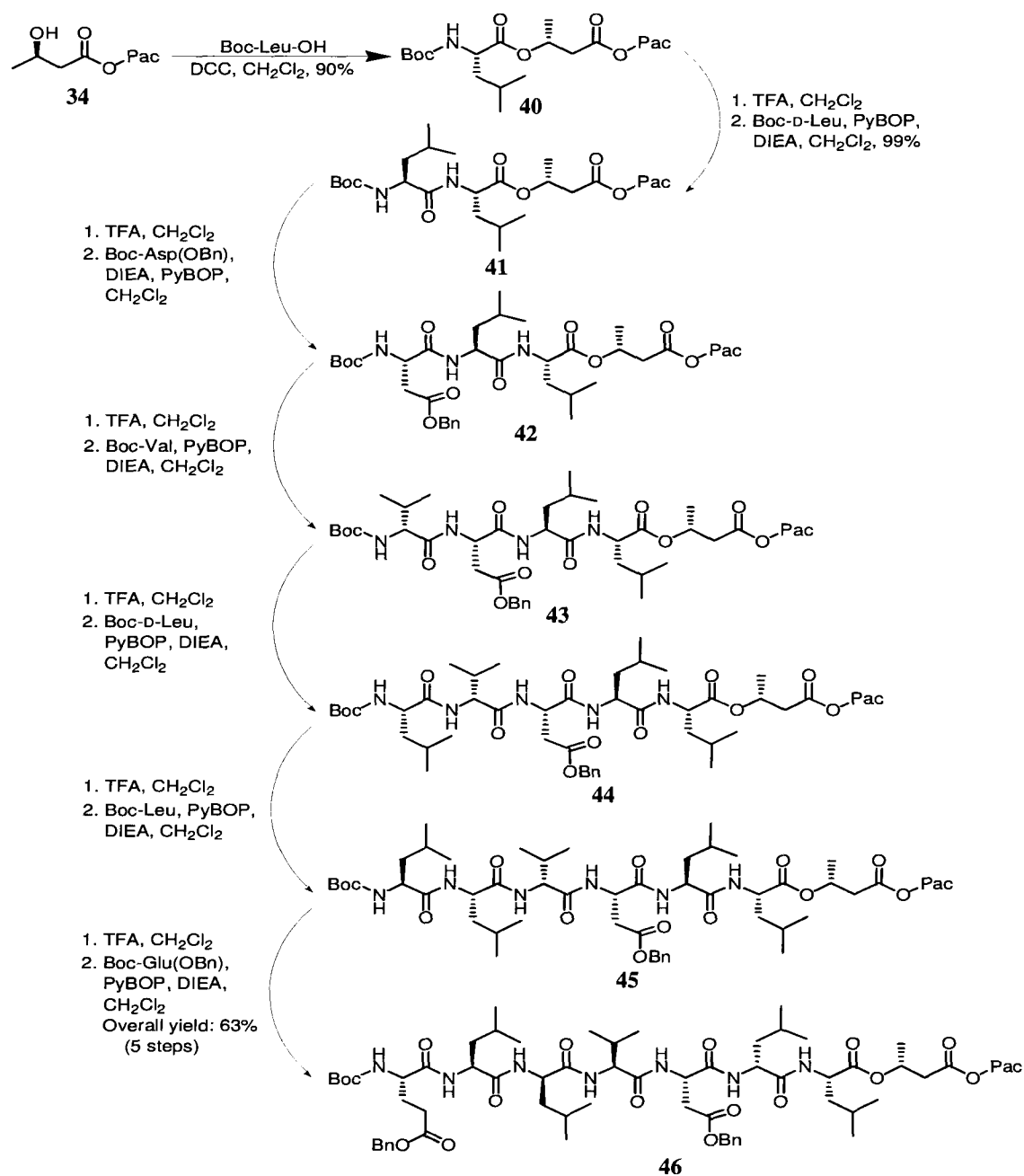
reagents in following steps, and although LRESIMS showed peaks evidencing phenacyl deprotection, the expected product was never detected by NMR.



Scheme 2.4. Proposed mechanism for the formation of **37**.

According to the Peptide Synthesis Laboratory, the presence of D-Leu in **38** was the main reason for the reduced scale in which the hexapeptide was prepared. Resin-bound D amino acids were at that moment not as commercially accessible as they are nowadays and thus, constituted a limiting factor in solid phase peptide synthesis. Furthermore, since **38** was ordered Fmoc-protected, unwanted elimination reactions were envisioned for the eventual Fmoc cleavage of the final linear precursor prior to cyclization.

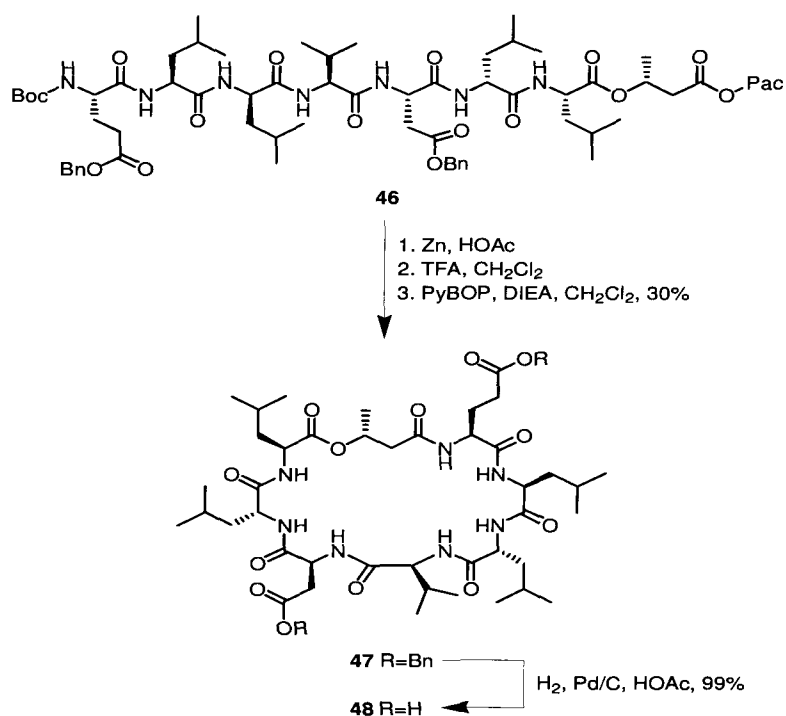
Therefore, based on the apparent incompatibility of the (*R*)-3-hydroxybutyrate fragment with basic conditions, and the impure and limited amounts of **38** provided by solid phase peptide synthesis, it was decided to change the entire synthetic proposal to Boc-based chemistry, and synthesize the required linear peptide chain by sequential coupling of amino acids starting with a Boc-protected version of **35**. This compound was obtained in good yield by DCC-mediated esterification of Boc-Leu-OH employing **34** as the alcohol component (Scheme 2.5).¹²⁴ Upon TFA deprotection^{109,110} of intermediate (**40**), six cycles of PyBOP¹¹¹ activated peptide coupling with Boc-D-Leu,¹²⁵⁻¹²⁷ Boc-Asp(OBn), Boc-Val, Boc-D-Leu, Boc-L-Leu and Boc-Glu(OBn) in sequence, afforded 0.63 g (0.49 mmol) of the desired linear precursor (**46**) in a very good overall yield (a 64-fold mol improvement compared with its Fmoc-protected counterpart).



Scheme 2.5. Preparation of the linear intermediate (46).

As with the synthesis of tauramide, each coupling step proceeded smoothly and furnished reasonably pure products, not requiring exhaustive purification. *C*- and *N*-termini

deprotections,⁷⁴ followed by a last PyBOP-assisted amide formation yielded macrolide (**47**) (Scheme 2.6). This key cyclization step was performed under dilute conditions to prevent polymerization of the linear precursor, as suggested by literature precedents.^{74,118} Still, it may account for the low isolated yield of **47**, comparable with those reported by Morrison¹¹⁸ and Pagadoy¹²⁰ in their syntheses of surfactin analogues. Quantitative removal of benzyl groups on the aspartic and glutamic residues via hydrogenolysis^{112,119} gave final product (**48**), which was named dealkylsurfactin.



Scheme 2.6. Preparation of dealkylsurfactin (**48**).

HRESIMS of **48** displayed a $[M+Na]^+$ peak at m/z 904.5015, consistent with the target molecular formula C₄₂H₇₁N₇O₁₃ (calculated for C₄₂H₇₁N₇O₁₃Na: 904.5008).

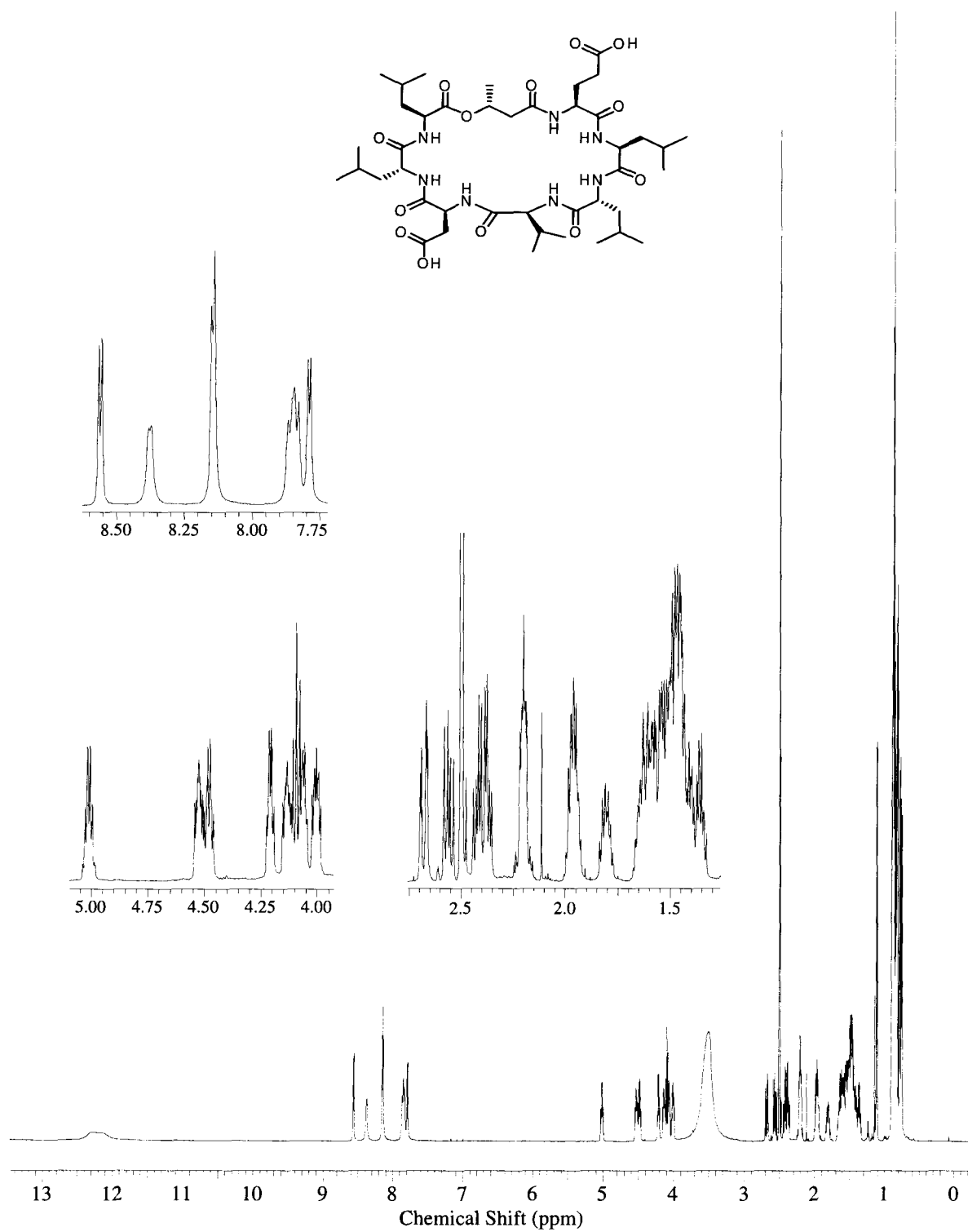


Figure 2.7. ¹H-NMR spectrum of dealkylsurfactin (**48**) (recorded in DMSO-*d*₆ at 600 MHz).

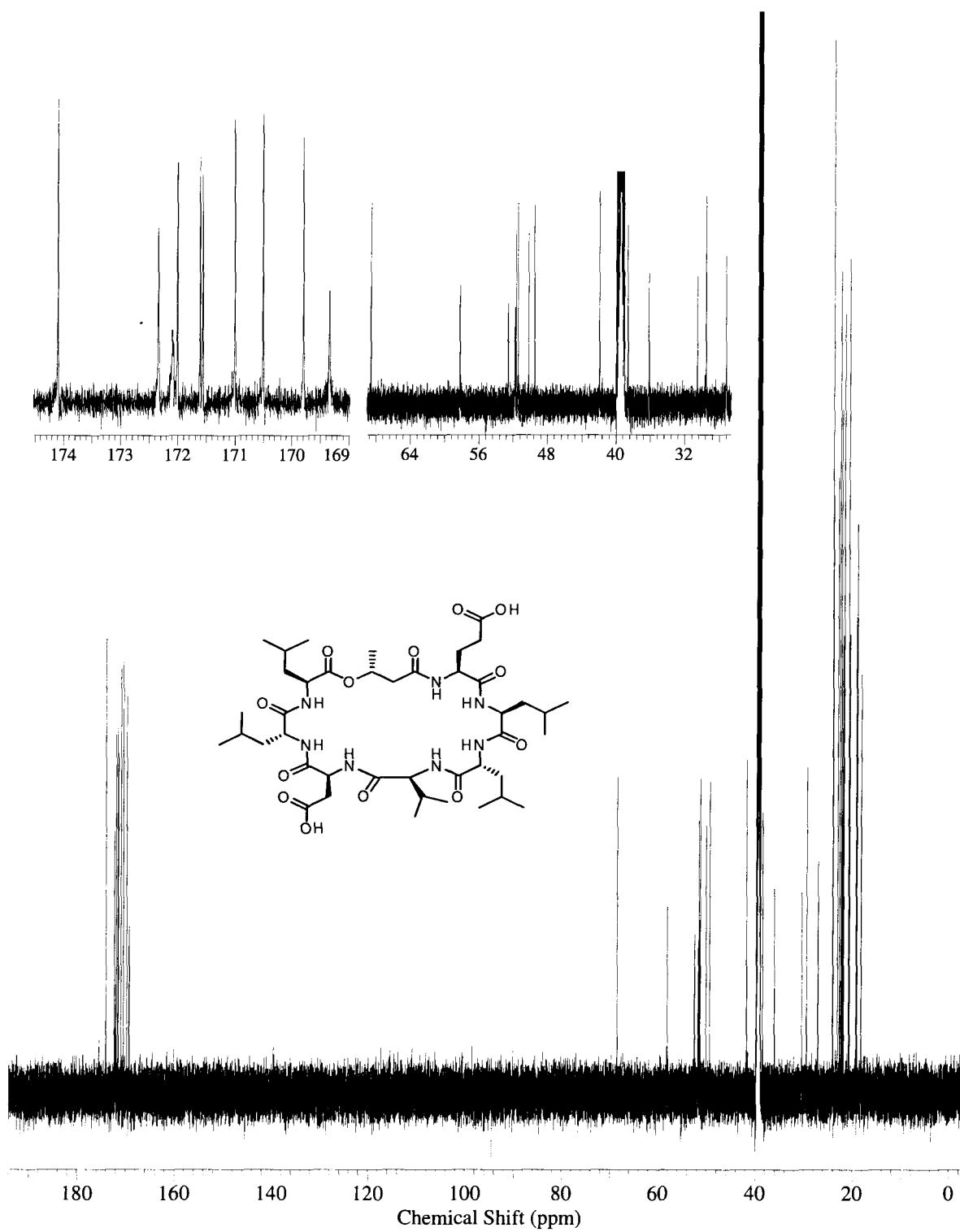
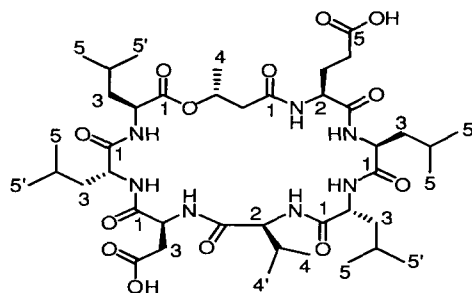
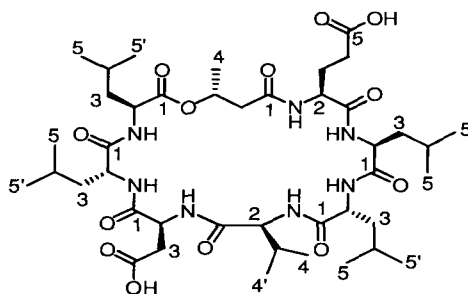


Figure 2.8. ^{13}C -NMR spectrum of dealkylsurfactin (**48**) (recorded in $\text{DMSO-}d_6$ at 150 MHz).

Table 2.3. NMR data for dealkylsurfactin (**48**) (recorded in DMSO-*d*₆).

Amino Acid	Carbon No	¹³ C δ (ppm) ^a	¹ H δ (ppm) (mult, <i>J</i> (Hz)) ^{b,c}	HMBC ^b (H→C)
<i>(R)</i> -3-HBA	1	169.4		
	2	41.9	2.37 (dd, <i>J</i> = 5.9, 13.8 Hz) 2.42 (dd, <i>J</i> = 7.9, 13.8 Hz)	C1, C3, C4,
	3	68.6	5.01 (m)	C1, C2, C4, ¹ Leu C1
	4	19.5	1.11 (d, <i>J</i> = 5.9 Hz)	C1, C2
¹ Leu	1	171.6		
	2	51.4	4.00 (m) NH 8.56 (d, <i>J</i> = 6.6 Hz)	C1, C3, C4 C2, C3, D- ¹ Leu C1
	3	38.6	1.45 (m), 1.61 (m)	C2, C4, C5, C5'
	4	24.2	1.63 (m)	C2, C3, C5, C5'
	5	21.0	0.82 (d, <i>J</i> = 6.4 Hz)	C3
	5'	23.2	0.88 (d, <i>J</i> = 6.3 Hz)	C3, C4, C5
D- ¹ Leu	1	172.0		
	2	50.2	4.48 (m) NH 7.84 (d, <i>J</i> = 9.5 Hz)	C1, C3, C4, Asp C1 C2, Asp C1
	3	41.9	1.37 (m), 1.40 (m)	C1, C2, C4
	4	24.2	1.46 (m)	C2
	5	22.8	0.87 (d, <i>J</i> = 6.9 Hz)	C3, C4, C5'
	5'	22.8	0.87 (d, <i>J</i> = 6.9 Hz)	C3, C4, C5
Asp	1	169.8		
	2	49.5	4.53 (m) NH 8.15 (d, <i>J</i> = 6.9 Hz)	C1, C3, C4 C2, C3, Val C1
	3	36.2	2.56 (dd, <i>J</i> = 9.5, 17.1 Hz) 2.68 (dd, <i>J</i> = 4.3, 16.7 Hz)	C1, C2, C4
	4	171.6	OH 12.17 ^d (s, broad)	

^a Recorded at 150 MHz. ^b Recorded at 600 MHz. ^c According to HMQC recorded at 600 MHz. ^d Interchangeable.

Table 2.3. NMR data for dealkylsurfactin (**48**) (recorded in DMSO-*d*₆) (Continuation).

Amino Acid	Carbon No	¹³ C δ (ppm) ^a	¹ H δ (ppm) (mult, <i>J</i> (Hz)) ^{b,c}	HMBC ^b (H→C)
Val	1	170.5		
	2	58.2	4.09 (dd, <i>J</i> = 8.6, 8.9 Hz) NH 7.86 (d, <i>J</i> = 9.1 Hz)	C1, C3, C4, C4', D- ² Leu C1 C2, D- ² Leu C1
	3	30.6	1.97 (m)	C2, C4'
	4	19.2	0.89 (d, <i>J</i> = 6.9 Hz)	C2, C3, C4'
	4'	18.4	0.75 (d, <i>J</i> = 6.6 Hz)	C2, C3, C4
D- ² Leu	1	172.1		
	2	51.6	4.13 (m) NH 8.38 (d, <i>J</i> = 5.6 Hz)	C1, C3, C4 C1, C2, ² Leu C1
	3	39.4	1.46 (m), 1.54 (m)	C2, C4, C5', ² Leu C1
	4	24.2	1.58 (m)	C3, C5, C5'
	5	21.9	0.82 (d, <i>J</i> = 6.6 Hz)	C4
² Leu	5'	20.8	0.78 (d, <i>J</i> = 6.2 Hz)	C4
	1	172.4		
	2	52.6	4.06 (m) NH 8.14 (d, <i>J</i> = 6.9 Hz)	C1, C3, C4
	3	39.2	1.46 (m)	C1, C2, C4
	4	24.2	1.48 (m)	C1, C5, C5'
Glu	5	22.4	0.85 (d, <i>J</i> = 6.5 Hz)	C3, C4, C5'
	5'	22.2	0.84 (d, <i>J</i> = 6.2 Hz)	C3, C4, C5
	1	171.0		
	2	51.8	4.21 (m) NH 7.79 (d, <i>J</i> = 6.3 Hz)	C1, C3, C4, 3-HBA C1 C1, C2, C3, 3-HBA C1
	3	27.2	1.81 (m), 1.96 (m)	C1, C2, C4, C5
	4	29.6	2.20 (m)	C2, C3, C5
	5	174.1	OH 12.28 ^d (s, broad)	

^a Recorded at 150 MHz. ^b Recorded at 600 MHz. ^c According to HMQC recorded at 600 MHz. ^d Interchangeable.

The ^1H -NMR spectrum of **48** (Figure 2.7, Table 2.3) showed four well defined regions typical of peptides. The most deshielded broad singlets around δ_{H} 12.20 undoubtedly corresponded to both carboxylic functionalities in the aspartic (δ_{C} 171.6) and glutamic (δ_{C} 174.1) residues. Seven multiplets (two of them isochronous), all assigned to NH groups of **48** can be located between 7.75 and 8.55 ppm. Another set of multiplets between δ_{H} 4.00-5.05 were assigned to the seven NH-bearing α -methines, plus an oxygenated stereocenter in the (*R*)-3-hydroxybutyrate fragment (δ_{H} 5.01, δ_{C} 68.6). Each of the diastereotopic methylene protons adjacent to this chiral carbon resonates as a doublet of doublets at δ_{H} 2.42 and δ_{H} 2.37 (δ_{C} 41.9), and were located in the fourth most shielded spectral region. The heavy Leu content in dealkylsurfactin is evidenced by a series of doublets close to 0.88 ppm, integrating for a total of 30 protons. This region also includes methyls for the Val residue, one of which is highly shielded and gives a doublet at δ_{H} 0.75 ppm (δ_{C} 18.4). Relevant in this area of the ^1H -NMR spectrum is a more deshielded doublet at δ_{H} 1.11 (δ_{C} 19.5), assigned to the methyl of the (*R*)-3-hydroxybutyrate fragment.

The ^{13}C -NMR spectrum (Figure 2.8, Table 2.3) revealed five clear regions. Ten completely isolated resonances at the deshielded end of the spectrum (δ_{C} 169.4-174.1) account for all the carbonyls present in **48**. These signals are followed by a group of eight methines attached to heteroatoms (δ_{C} 49.5-68.6). Obscured by the residual solvent peak and very typical in Leu-containing compounds, are the methylenes of its isobutyl side chain located between δ_{C} 38.6-41.9. A fourth assembly of signals around δ_{C} 27.2-36.2 includes a methine and three methylenes assigned to the side chains of Val, Asp and Glu residues. Finally, the most shielded cluster of peaks between 18.0 and 26.0 ppm reflects, for a second time, the high Leu content characteristic of the surfactin lipopeptide family.

As with tauramamide (**12**), the amino acid sequence of dealkylsurfactin (**48**) was determined using HMBC correlations (Figure 2.9, Table 2.3). The Glu NH and α -CH protons (δ_{H} 7.79 and 4.21 respectively) presented cross-peaks with the carbonyl of (*R*)-3-hydroxybutyrate (δ_{C} 169.4), which in turn correlated through its β -CH proton (δ_{H} 5.01) with ^1Leu C1 (δ_{C} 171.6). Likewise, ^1Leu NH (δ_{H} 8.56) exhibited HMBC cross-peaks with D- ^1Leu C1 (δ_{C} 172.0), D- ^1Leu NH (δ_{H} 7.84) with Asp C1 (δ_{C} 169.8), Asp NH (δ_{H} 8.15) with Val C1 (δ_{C} 170.5), Val NH (δ_{H} 7.86) with D- ^2Leu C1 (δ_{C} 172.1), and finally, D- ^2Leu NH (δ_{H} 8.38) as well as β -CH₂ (δ_{H} 1.46-1.54) correlated with ^2Leu C1 (δ_{C} 172.4). Cross-peaks between this last residue and carbons in the Glu fragment were not evident.

Dealkylsurfactin (**48**) was levorotatory (Table 2.4) in agreement with optical rotation values found in the products of other revised syntheses of surfactin analogues.^{118,119}

Table 2.4. Specific rotation values for natural surfactin B₂ (**19**), synthetic analogues (**19a,b**), “norsurfactin” (**19c**), and dealkylsurfactin (**48**).^{118,119}

Compound	$[\alpha]_{\text{D}}^{25}$ (<i>c</i> , MeOH) (t °C)
Surfactin B ₂ (19)	-36.5 (1)(22)
Surfactin B ₂ (19a) ^a	-37.0 (1)(9.5)
Surfactin B ₂ (19b) ^b	-19.6 (1)(12.5)
Norsurfactin (19c) ^a	-35.2 (1)(25)
Dealkylsurfactin (48)	-22.0 (3.8)(20)

^aPrepared using (+)-3-hydroxytetradecanoic acid. ^bPrepared employing (-)-3-hydroxytetradecanoic acid.

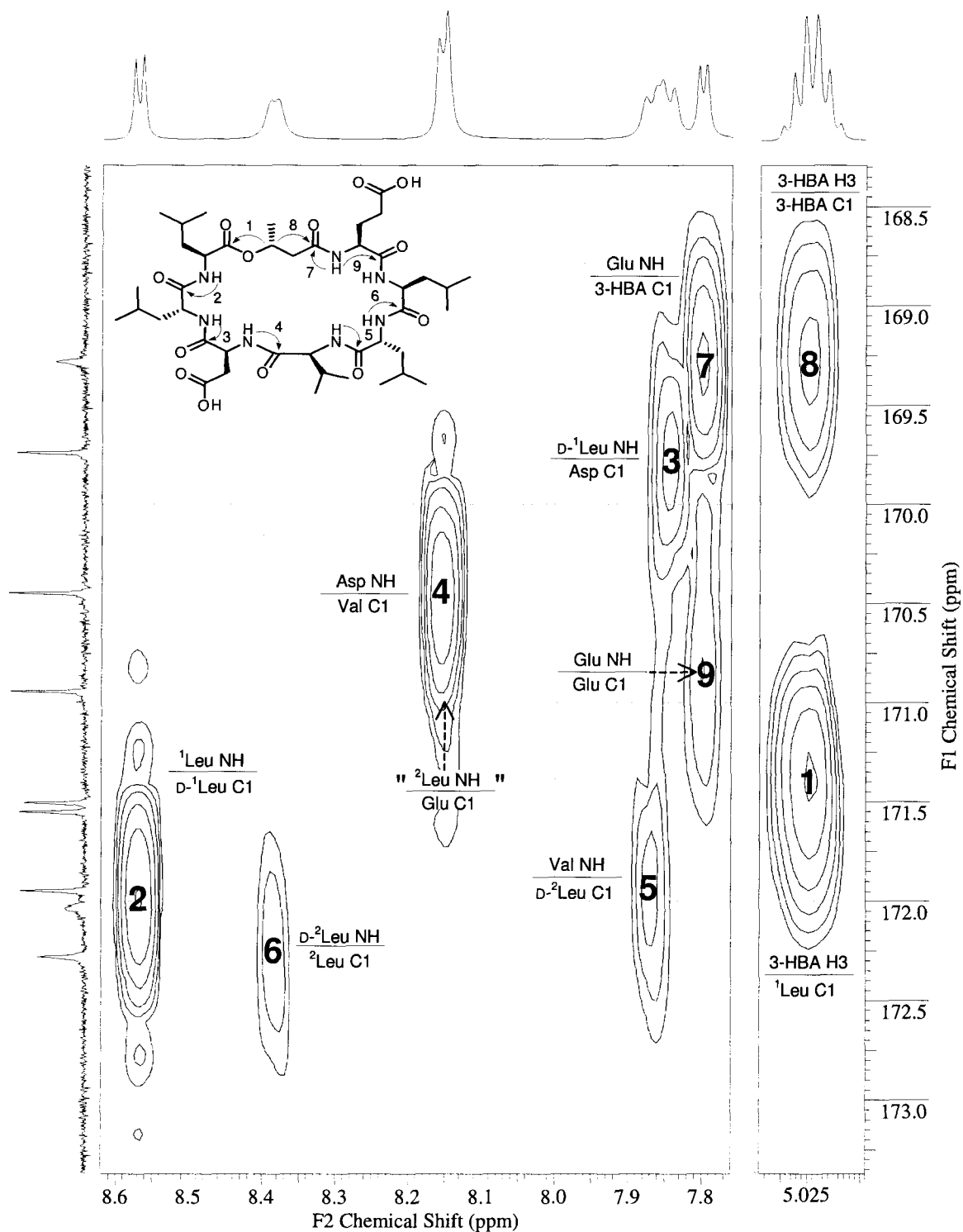
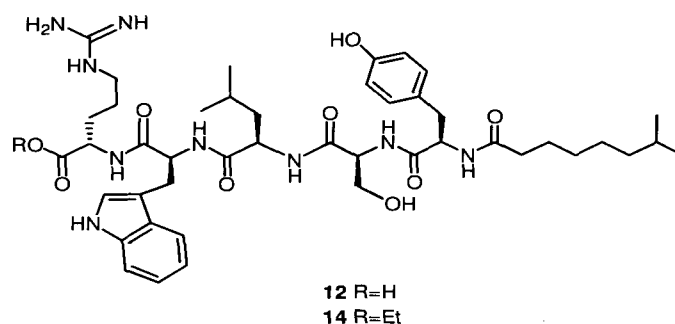


Figure 2.9. Partial HMBC spectrum of dealkylsurfactin (**48**) (in DMSO- d_6 at 600 MHz).

2.5. Conclusions

Tauramamide (**12**), a linear antibiotic acylpentapeptide recently isolated from cultures of *Brevibacillus laterosporus* (PNG-276) collected in Papua New Guinea, was synthesized in nine steps and 29% overall yield. Esterification of **12** (86%) yielded ethyl ester (**14**), which was identical by HPLC, MS, specific rotation, and NMR comparison with the material obtained from *B. laterosporus* cells using EtOH as the extracting solvent.

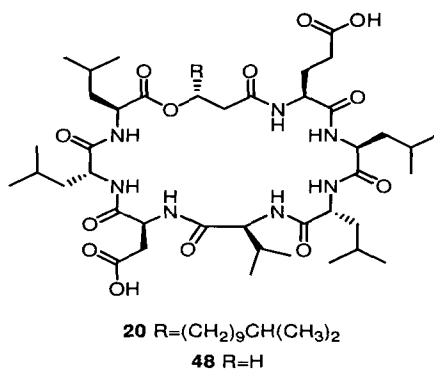


Besides confirming the structure proposed for tauramamide (**12**), the synthetic material allowed an exhaustive antimicrobial assessment for this new family of PNG-276-derived antibiotics. Both **12** and **14** showed potent (MIC's 0.1 $\mu\text{g/mL}$) and relatively selective activity against the important Gram positive human pathogen *Enterococcus* sp.⁶⁹ Ethyl ester (**14**) exhibited stronger activity against MRSA, but neither compound is appreciably active against *C. albicans*.

Our convergent synthetic approach to tauramamide (**12**) (Schemes 2.1 and 2.2) started simultaneously from both ends of the molecule. Most reactions afforded relatively pure intermediates, which were used directly in the following reaction without any further

purification. Only the final deprotection leading to **12** required optimization in order to minimize amounts of partially benzylated tauramamide derivatives obtained as byproducts.

A new analogue of the surfactin depsipeptide family, named dealkylsurfactin (**48**), has been prepared in 10 steps and 14% overall yield. The compound was employed as a biological tool in binding studies between the mitotic regulator isomerase Pin1 and the microtubule-associated protein tau, a crucial interaction involved in the development of Alzheimer's disease symptoms.⁹⁹⁻¹⁰¹ The parent compound surfactin C₁ (**20**) had been previously isolated via bioassay-guided fractionation from cultures prepared using the microorganism PNG10A (also collected in Papua New Guinea).



Our synthetic pathway to dealkylsurfactin (**48**) (Schemes 2.5 and 2.6) began with protection of the C-terminus, followed by sequential standard peptide elongation in solution using Boc-protecting chemistry and PyBOP as the coupling reagent for all amide bond formation steps. Such methodology furnished the desired linear precursor in a 64-fold yield improvement, when compared with a previously attempted preparation employing Fmoc solid phase synthesis. The key cyclization step was run under dilute conditions and proceeded in 30% yield, in

concordance with similar reported syntheses.^{105,106,118,120} Polymerization of the linear precursor may have been the main contributor to the low isolated yield.

Biological evaluation of dealkylsurfactin (**48**) showed that the compound does not inhibit binding of Pin1 to phosphorylated tau. Thus, the macrocyclic peptide fragment in surfactin C₁ (**20**) does not play any role in activity, and more likely its efficient surfactant properties were responsible for the observed inhibition during assay-guided isolation. Such unspecific interaction is not ideal in the development of potential pharmaceuticals, since unwanted side effects are very likely to arise.

In order to minimize the possibility of amino acid racemization in both syntheses, the amounts of base used were carefully controlled. This aspect was particularly important during the preparation to dealkylsurfactin (**48**), given the apparent susceptibility towards basic conditions shown by the (*R*)-3-hydroxybutyrate fragment. Diisopropylethylamine (DIEA) was the only base employed, limited to assisting PyBOP during amide bond formation and is not strong enough (¹Pr₃NH *pK_a*~11) to abstract α-protons in amino acids (*pK_a*~15).^{128,129} The use of a urethane-based protecting strategy, with *t*-butyloxycarbonyl (Boc) amino acids as building blocks, as well as the fast and efficient coupling reagent PyBOP, is reported to be advantageous in avoiding racemization and dehydration side reactions.^{111,112,130} Noteworthy, the levorotatory nature of the corresponding parent molecules was retained in both **14** and **48**.

Although the present status of linear peptide synthesis has reached a high degree of enantiomeric purity, macrocyclization of linear peptides still poses problems, such as low yields (as evidenced in the present work) and epimerization.¹³⁰ After all, the process is entropically unfavored since it involves the loss of rotational freedom.^{105,131} Selection of a suitable cyclization point and the necessity of dilute conditions in order to inhibit intermolecular processes, are key aspects that must be considered when planning the synthesis of macrocyclic peptides.

2.6. Experimental

General experimental procedures

All reactions described in this thesis were performed under dry nitrogen or argon using glassware previously oven dried (150°C), unless otherwise specified. Glassware was allowed to reach room temperature under a flow of inert gas. Likewise, glass syringes and stainless steel needles, used to handle anhydrous reagents and solvents, were oven dried, cooled in a desiccator, and flushed with inert gas prior to use.

With the exception of THF and CH₂Cl₂, which were distilled from sodium/benzophenone and CaH₂ respectively, MeOH, benzene, toluene, DMF and pyridine were purchased anhydrous quality and used without further purification. HPLC grade solvents (MeCN, acetone, hexanes, CCl₄, EtOAc and CH₂Cl₂) were used without further purification. EtOH reagent grade was treated with activated molecular sieves prior to use. All chemical reagents were purchased in an analytical or higher grade from Aldrich or Fluka.

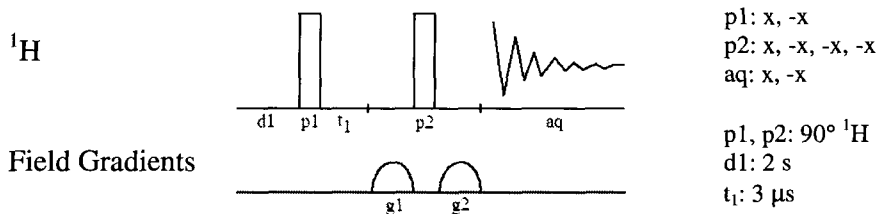
Cold baths were prepared using ice/water, ice/NaCl/water, MeCN/dry ice and acetone/dry ice, for 0, -10, -40 and -78 °C respectively. Liquid nitrogen was employed for condensing ammonia.

Flash chromatography was carried out with 70-230 and 230-400 mesh silica gel (Silicycle). For reverse phase column chromatography, Sep Pak[®] C18 columns (Waters) were used. Size exclusion chromatography was performed using lipophilic Sephadex[®] LH-20 (Sigma, bead size 25-100μ). Precoated silica gel plates (Merck, Kieselgel 60 F₂₅₄, 0.25 mm and Whatman, MKC18F 60 A) were employed in normal and reversed-phase thin layer chromatography (TLC). TLC visualization was accomplished using ultraviolet light (254 nm),

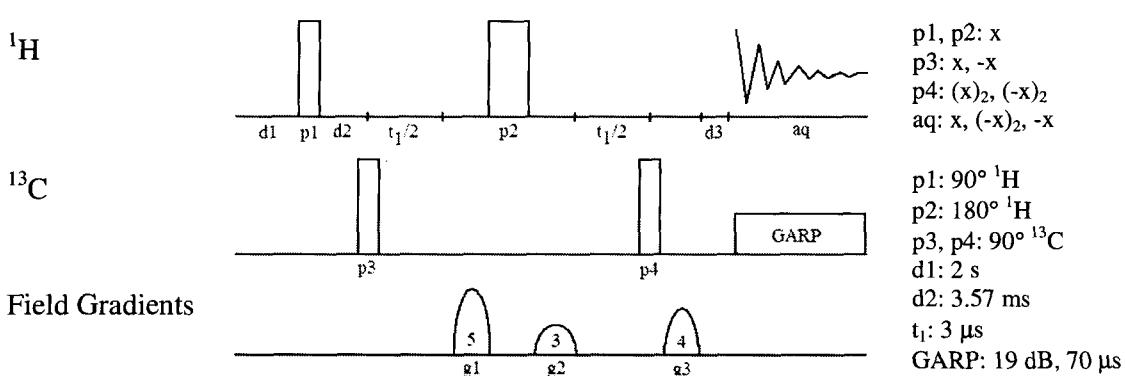
followed by heating the plate after staining with vanillin in H₂SO₄/EtOH (6% vanillin w/v, 4% H₂SO₄ v/v, and 10% H₂O v/v in EtOH), *p*-anisaldehyde in H₂SO₄/EtOH (5% *p*-anisaldehyde v/v and 5% H₂SO₄ v/v in EtOH) or 20% KMnO₄ w/v in H₂O. High performance liquid chromatography (HPLC) was carried out using a Waters 1500 Series pump system, equipped with Waters 2487 dual λ absorbance detector and either a CSC-Inertsil 150A/ODS2 column, or an Alltech Econosil Silica 5u column.

NMR spectra were recorded using chloroform-*d* (CDCl₃), methylene chloride-*d*₂ (CD₂Cl₂), dimethylsulfoxide-*d*₆ (DMSO-*d*₆), methanol-*d*₄ (CD₃OD), benzene-*d*₆ (C₆D₆), deuterium oxide (D₂O), acetonitrile-*d*₃ (CD₃CN) or acetone-*d*₆ (CD₃COCD₃). Chemical shifts (δ) are given in parts per million (ppm) relative to tetramethylsilane (δ 0) and were calibrated internally to the signal of the solvent in which the sample was dissolved (CDCl₃: δ 7.24 ¹H-NMR; δ 77.0 ¹³C NMR; CD₂Cl₂ δ 5.32 ¹H-NMR; δ 54.0 ¹³C NMR; DMSO-*d*₆: δ 2.50 ¹H-NMR; δ 39.51 ¹³C NMR; CD₄OD: δ 3.31 ¹H-NMR; δ 49.15 ¹³C NMR; C₆D₆: δ 7.16 ¹H-NMR; δ 128.39 ¹³C NMR; D₂O: δ 4.80 ¹H-NMR; CD₃CN: δ 1.94 ¹H-NMR; δ 118.69 ¹³C NMR; CD₃COCD₃: δ 2.05 ¹H-NMR; δ 29.92 ¹³C NMR). ¹H-NMR spectral data are tabulated in the order: multiplicity (s, singlet; d, doublet; dd, doublet of doublets; t, triplet; q, quartet; m, multiplet), coupling constant, number of protons and proton assignment where applicable. ¹H-NMR data was acquired using Bruker spectrometers WH400 (400 MHz), Avance 300 (300 MHz), Avance 400 (400 MHz), or Avance 600 (600 MHz) equipped with a CRYOPROBE[®]. ¹³C-NMR spectra were recorded on Avance 300 (75 MHz), Avance 400 (100 MHz), or Avance 600 (150 MHz). ³¹P-NMR data was collected using the Avance 400 (100 MHz) spectrometer. 2D-NMR data was acquired using the following pulse sequences and parameters.

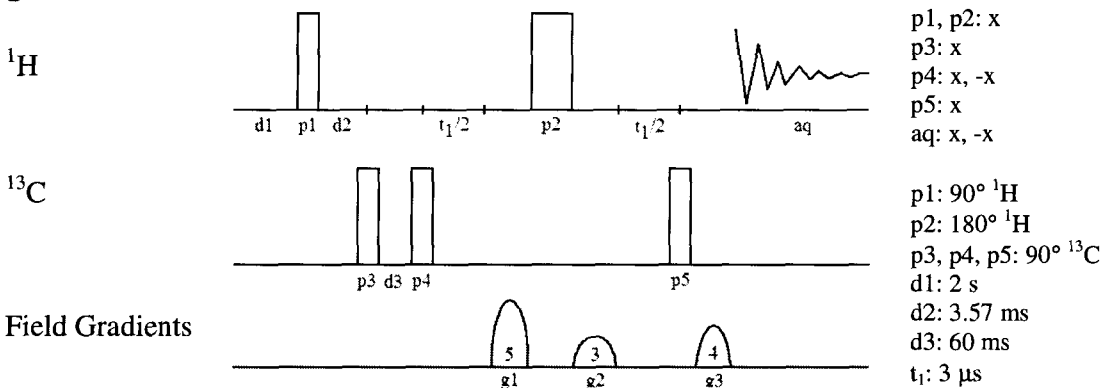
gs-COSY



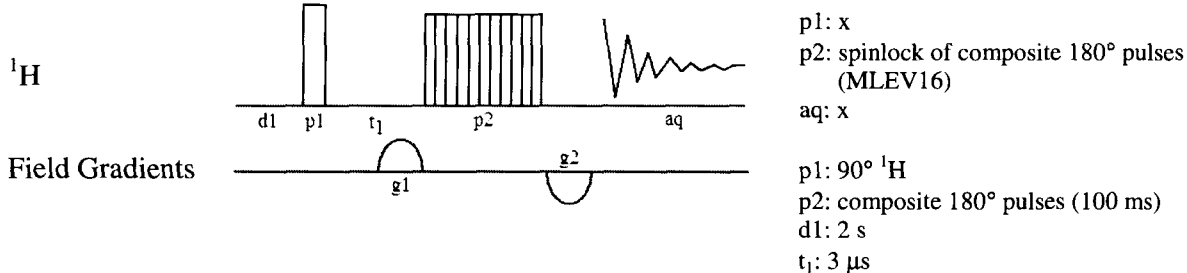
gs-HMQC



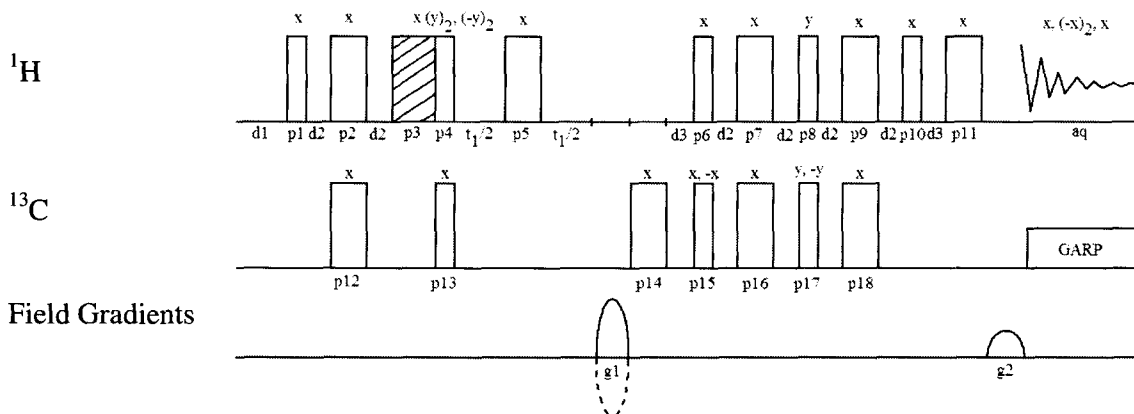
gs-HMBC



gs-TOCSY

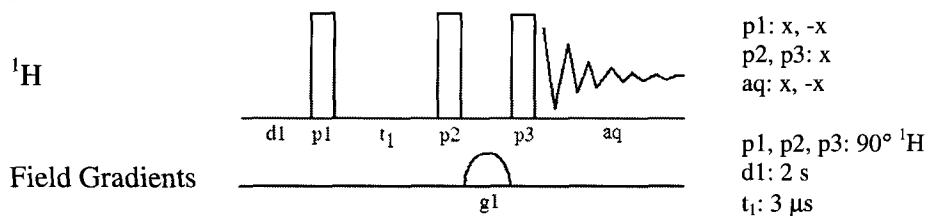


gs-HSQC



p1, p4, p6, p8, p10: 90° ^1H p2, p5, p7, p9, p11: 180° ^1H p3: 2 ms ^1H
 p13, p15, p17: 90° ^{13}C p12, p14, p16, p18: 180° ^{13}C d1: 2 s
 d2: 1.8 ms d3: 1.6 ms t₁: 3 μs
 GARP: 19 dB, 70 μs

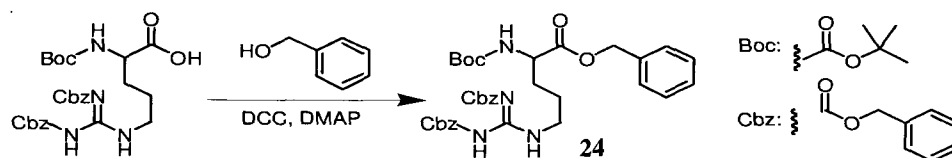
gs-NOESY



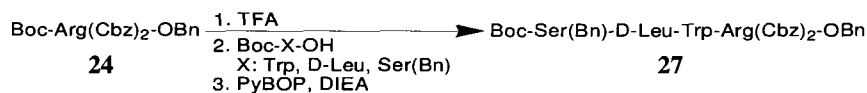
Low and high resolution electron impact (EI) mass spectra were recorded on Kratos MS50 or MS80 mass spectrometers at 70 eV. Low and high resolution electrospray (ESI) mass spectra were obtained with Bruker Esquire-LC and Micromass LCT mass spectrometers.

Circular dichroism (CD) data was recorded with a JASCO J-810 CD spectrometer at 20.0°C, using a 2.0 mm micro cell. Optical rotations were measured with a JASCO P-1010 polarimeter at 20°C and 589 nm (sodium D line). UV spectra were acquired with a Waters 2487 Dual λ Absorbance Detector, using a 1 cm cell.

2.6.1. Total synthesis of tauramamide and tauramamide ethyl ester

Preparation of N_{α} -Boc- N_{δ} - N_{ω} -di-Z-arginine benzyl ester (**24**)

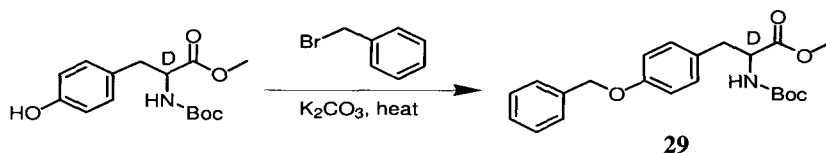
To a solution of Boc-Arg(Cbz)₂-OH (2.5 g, 4.6 mmol) and benzyl alcohol (0.71 mL, 6.9 mmol) in CH₂Cl₂ (50 mL) at 0°C, DCC (1.04 g, 5.06 mmol) and DMAP (0.06 g, 0.46 mmol) were added and the resulting mixture was stirred overnight. The solution was poured into water and extracted with CH₂Cl₂ (30 mL x 3). The organic extracts were dried (Na₂SO₄) and concentrated *in vacuo*. Purification by Sephadex LH20 column chromatography (100% MeOH) afforded (**24**) as a colorless solid (2.91 g, 97%). ¹H NMR (CDCl₃, 600 MHz) δ 9.36 (1H, s), 9.12 (1H, s), 7.30-7.10 (15H, m), 5.30 (1H, d, *J* = 8.3 Hz), 5.10-4.90 (6H, m), 4.24 (1H, m), 3.83 (2H, m), 1.85-1.70 (4H, m), 1.31 (9H, s). ¹³C NMR (CDCl₃, 100 MHz) δ 171.9 (C), 163.3 (C), 159.9 (C), 155.2 (C), 155.0 (C), 136.5 (C), 135.0 (C), 134.3 (C), 128.3 (3CH), 128.0 (2CH), 127.9 (4CH), 127.8 (3CH), 127.7 (CH), 127.4 (CH), 127.3 (CH), 79.1 (C), 68.3 (CH₂), 66.4 (2CH₂), 52.9 (CH), 43.6 (CH₂), 28.7 (CH₂), 27.8 (3CH₃), 24.4 (CH₂). HRESIMS calcd for C₃₄H₄₀N₄O₈Na ([M+Na]⁺): 655.2744; found 655.2743.

Preparation of Boc-Ser(Bn)-DLeu-Trp-Arg(Cbz)₂-OBn (27)

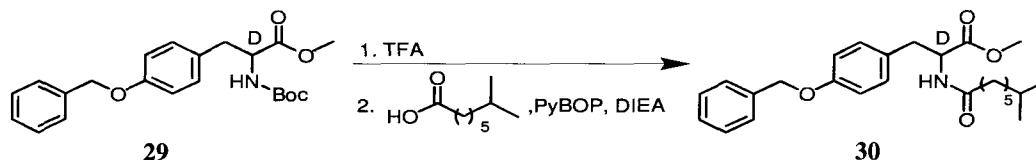
A solution of Boc-Arg(Cbz)₂-OBn (**24**) (1.87 g, 2.9 mmol, 1 eq) in CH₂Cl₂ (25 mL) was treated with TFA (3 mL, 40.3 mmol, 14 eq) and stirred for 4 h, whereupon it was concentrated *in vacuo* to a pale red oil. This oil was dissolved in CH₂Cl₂ (20 mL) and added to a solution of Boc-Trp-OH (0.82 g, 2.7 mmol, 0.90 eq) and PyBOP (1.69 g, 3.24 mmol, 1.10 eq) in CH₂Cl₂ (10 mL); followed by addition of DIEA (1.55 mL, 8.90 mmol, 3 eq). After overnight stirring at 25 °C, NH₄Cl sat. was added and CH₂Cl₂ (3x20 mL) extractions performed. The organic extracts were combined and dried (Na₂SO₄), to be then concentrated *in vacuo*. Column chromatography on silica (80% EtOAc/Hexanes) afforded (**25**) as a white amorphous solid (1.87 g, 85%). The procedure above was repeated successively with Boc-DLeu-OH (0.48 g, 2.07 mmol), and Boc-Ser(Bn)-OH (0.46 g, 1.57 mmol); to afford Boc-DLeu-Trp-Arg(Cbz)₂-OBn (1.93 g, 76%) and Boc-Ser(Bn)-DLeu-Trp-Arg(Cbz)₂-OBn (**27**) (1.75 g, 81%), respectively. ¹H NMR (CDCl₃, 400 MHz) δ 9.40 (1H, s), 9.28 (1H, s), 9.00 (1H, s), 7.26-6.90 (30H, m), 5.65 (1H, m), 5.20-4.90 (6H, m), 4.80 (1H, dd, *J* = 6.3, 7.4 Hz), 4.55-4.40 (2H, m), 4.40-4.25 (2H, m), 3.95-3.80 (2H, m), 3.67 (1H, m), 3.50 (1H, dd, *J* = 6.1, 2.8 Hz), 3.31 (1H, dd, *J* = 6.3, 8.7 Hz), 3.15 (1H, dd, *J* = 5.7, 8.7 Hz), 1.85-1.75 (1H, m), 1.75-1.60 (2H, m), 1.60-1.35 (4H, m), 1.41 (9H, s), 0.80 (6H, m); ¹³C NMR (CDCl₃, 100 MHz) δ 171.4 (C), 171.2 (C), 170.9 (C), 170.8 (C), 170.5 (C), 163.4 (C), 160.2 (C), 155.4 (C), 137.1 (C), 136.4 (C), 135.9 (C), 135.0 (C), 134.3 (C), 128.4 (4CH), 128.2 (4CH), 128.0 (3CH), 128.0 (3CH), 127.9 (3CH), 127.8 (CH), 127.8 (CH), 127.6 (CH), 127.4 (C), 123.4 (CH), 121.5 (CH), 119.0 (CH), 118.2 (CH), 111.1 (CH), 109.3 (C), 79.7 (C), 72.8 (CH₂), 69.4 (CH₂), 68.5 (CH₂), 66.7 (CH₂), 66.6 (CH₂), 66.5 (CH₂), 60.0 (CH₂), 54.0 (CH), 53.6 (CH),

52.2 (CH), 51.9 (CH), 43.7 (CH₂), 40.2 (CH₂), 27.9 (3CH₃), 24.1 (CH), 22.5 (CH₂), 21.4 (CH₃), 20.7 (CH₃). HRESIMS calcd for C₆₁H₇₂N₈O₁₂Na ([M+Na]⁺): 1131.5167; found 1131.5162.

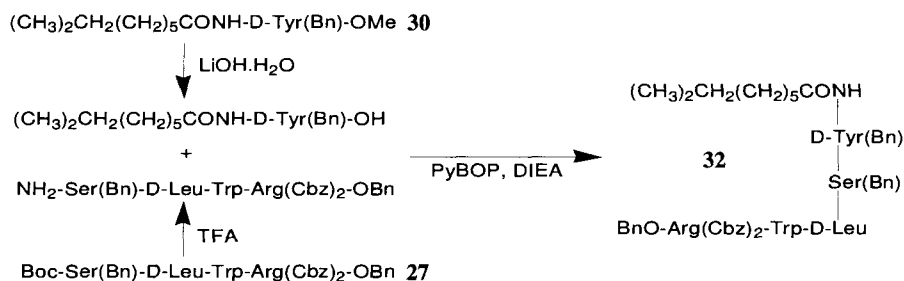
Preparation of Boc-DTyr(Bn)-OMe (**29**)



A solution of Boc-DTyr-OMe (2.0 g, 6.8 mmol), K₂CO₃ (1.4 g, 10.1 eq) and BnBr (1 mL, 8.1 mmol) in acetone was refluxed for 3 h and stirred overnight at 25 °C. After solid filtration and solvent evaporation, column chromatography on silica (30% EtOAc/Hexanes) afforded (**29**) as an amorphous white solid (2.60 g, 99%). ¹H NMR (CDCl₃, 400 MHz) δ 7.35-7.20 (5H, m), 6.94 (2H, d, *J* = 5.6), 6.81 (2H, d, *J* = 5.7), 4.94 (2H, s), 4.89 (1H, d, *J* = 5.0 Hz), 4.45 (1H, dd, *J* = 4.4 Hz), 3.61 (3H, s), 2.95 (1H, dd, *J* = 3.64, 9.2 Hz), 2.91 (1H, dd, *J* = 3.6, 9.0 Hz), 1.33 (9H, s); ¹³C NMR (CDCl₃, 100 MHz) δ 172.3 (C), 157.8 (C), 155.0 (C), 136.5 (C), 130.2 (2CH), 128.5 (2CH), 128.2 (C), 127.9 (CH), 127.4 (2CH), 114.2 (2CH), 79.8 (C), 69.9 (CH₂), 54.5 (CH₃), 52.1 (CH), 37.4 (CH₂), 28.2 (3CH₃). HRESIMS calcd for C₂₂H₂₇NO₅Na ([M+Na]⁺): 408.1787; found 408.1790.

Preparation of $(\text{CH}_3)_2\text{CH}_2(\text{CH}_2)_5\text{CONH-DTyr(Bn)-OMe}$ (**30**)

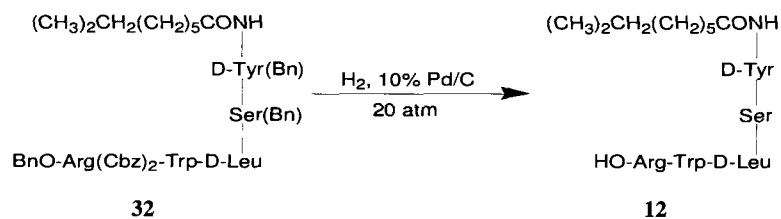
A solution of Boc-DTyr(Bn)-OMe (**29**) (1.50 g, 3.9 mmol) in CH_2Cl_2 (35 mL) was treated with TFA (2 mL, 27 mmol) and stirred for 4 h, whereupon it was concentrated *in vacuo* to a colorless oil. This oil was dissolved in CH_2Cl_2 (10 mL) and added to a solution of 7-methyloctanoic acid (0.62 g, 3.9 mmol) and PyBOP (2.0 g, 3.8 mmol) in CH_2Cl_2 (40 mL); followed by addition of DIEA (2.0 mL, 12 mmol). After overnight stirring at 25 °C, NH_4Cl sat. was added and CH_2Cl_2 (3x20 mL) extractions performed. The organic extracts were combined and dried (Na_2SO_4), to be then concentrated *in vacuo*. Column chromatography on silica (80% EtOAc/Hexanes) afforded (**30**) as a yellowish powder (1.67 g, 88%). ^1H NMR (CDCl_3 , 400 MHz) δ 7.35-7.15 (5H, m), 6.98 (2H, d, $J = 8.5$), 6.80 (2H, d, $J = 8.5$), 6.71 (1H, d, $J = 8.0$), 4.87 (2H, s), 4.79 (1H, dd, $J = 6.8, 7.2$ Hz), 3.57 (3H, s), 3.01 (1H, dd, $J = 5.6, 14.0$ Hz), 2.89 (1H, dd, $J = 7.0, 14.0$ Hz), 2.10 (2H, t, $J = 7.6$ Hz), 1.51 (2H, quintet, $J = 7.96$ Hz), 1.43 (1H, septet, $J = 6.5$ Hz), 1.18 (4H, m), 1.08 (2H, quintet, $J = 6.8$ Hz), 0.80 (6H, d, $J = 6.5$ Hz); ^{13}C NMR (CDCl_3 , 100 MHz) δ 172.6 (C), 171.8 (C), 157.3 (C), 136.5 (C), 129.7 (2CH), 128.0 (C), 127.9 (2CH), 127.3 (CH), 126.8 (2CH), 114.2 (2CH), 69.2 (CH_2), 52.8 (CH), 51.5 (CH_3), 38.3 (CH_2), 36.4 (CH_2), 35.7 (CH_2), 28.9 (CH_2), 27.4 (CH), 26.6 (CH_2), 25.1 (CH_2), 22.1 (2 CH_3). HRESIMS calcd for $\text{C}_{26}\text{H}_{36}\text{NO}_4$ ($[\text{M}+\text{H}]^+$): 426.2644; found 426.2645.

Preparation of $(\text{CH}_3)_2\text{CH}_2(\text{CH}_2)_5\text{CONH-D-Tyr(Bn)-Ser(Bn)-D-Leu-Trp-Arg(Cbz)}_2\text{-OBn}$ (**32**)

A solution of $(\text{CH}_3)_2\text{CH}_2(\text{CH}_2)_5\text{CONH-D-Tyr(Bn)-OMe}$ (**30**) (0.717 g, 1.68 mmol) and LiOH.H₂O (0.705 g, 16.8 mmol) in 1,4-dioxane/H₂O (150 mL, 2:1) was stirred at 25 °C. After 1 h, TLC (80% EtOAc/Hexanes) showed absence of starting material. Solvents were evaporated off and the resulting residue was dissolved in H₂O, acidified and extracted with EtOAc (3x30 mL). Combined organic extracts were dried (Na₂SO₄) and concentrated to obtain a white solid (free acid, 0.68 g, 98%). In a separate reaction, Boc-Ser(Bn)-D-Leu-Trp-Arg(Cbz)₂-OBn (**27**) (1.42 g, 1.3 mmol) in CH₂Cl₂ (50 mL) was treated with TFA (3 mL, 40.3 mmol) and stirred for 5 h, whereupon it was concentrated *in vacuo* to a red oil. This oil was dissolved in CH₂Cl₂ (20 mL) and added to a solution of free acid (0.58 g, 1.41 mmol) and PyBOP (0.73 g, 1.41 mmol) in CH₂Cl₂ (30 mL); followed by addition of DIEA (0.66 mL, 3.84 mmol). After stirring 16 h at 25 °C, reaction was quenched with NH₄Cl sat. and 1 M HCl used to neutralize aqueous layer. CH₂Cl₂ (3x30 mL) extractions were performed; the organic extracts were combined and dried (Na₂SO₄), to be then concentrated *in vacuo*. Column chromatography on silica (80% EtOAc/Hexanes) afforded (**32**) as pale yellow leaves (1.45 g, 81%). ¹H NMR (DMSO, 600 MHz) δ 10.74 (1H, s), 9.16 (1H, s, broad), 8.52, (1H, d, *J* = 6.9 Hz), 8.15, (1H, d, *J* = 8.0 Hz), 8.13, (1H, d, *J* = 8.6 Hz), 8.00 (2H, d, *J* = 6.9 Hz), 7.58 (1H, d, *J* = 7.7 Hz), 7.60-6.80 (25H, m), 7.13 (3H, m), 7.09 (1H, d, *J* = 2.0 Hz), 7.03 (1H, dd, *J* = 7.1, 7.1 Hz), 6.93 (1H, dd, *J* = 7.4, 7.4),

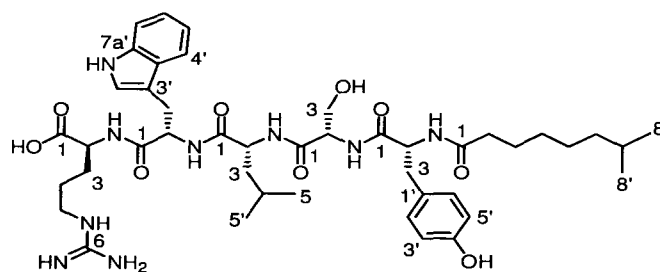
6.85 (3H, m), 5.20 (2H, m), 5.05-5.00 (6H, m), 4.55 (3H, m), 4.29 (2H, m), 3.90 (1H, m), 3.85 (1H, m), 3.61-3.45 (4H, m), 3.07 (1H, m), 2.85 (1H, m), 2.65 (1H, m), 1.98 (2H, m), 1.70 (1H, m), 1.43 (3H, m), 1.32 (4H, m), 1.25-1.00 (10H, m), 0.79 (3H, d, $J = 6.2$ Hz), 0.78 (3H, d, $J = 6.3$ Hz), 0.62 (6H, d, $J = 5.5$ Hz); ^{13}C NMR (CDCl_3 , 150 MHz) δ 172.3 (C), 172.2 (C), 171.9 (C), 171.6 (C), 171.4 (C), 168.9 (C), 162.9 (C), 159.7 (C), 156.8 (C), 154.9 (C), 138.1 (C), 137.15 (C), 137.04 (C), 135.9 (C), 135.8 (C), 135.2 (C), 130.1 (CH), 130.0 (CH), 128.5 (2CH), 128.4 (4CH), 128.3 (2CH), 128.2 (4CH), 128.2 (2CH), 129.1 (2CH), 128.0 (2CH), 127.93 (CH), 127.9 (CH), 127.8 (CH), 127.7 (CH), 127.65 (CH), 127.64 (CH), 127.62 (CH), 127.5 (CH), 127.4 (C), 127.3 (C), 123.8 (CH), 120.6 (CH), 117.9 (CH), 114.18 (CH), 114.15 (CH), 111.1 (CH), 109.9 (C), 72.0 (CH_2), 69.0 (CH_2), 68.2 (CH_2), 66.0 (CH_2), 65.8 (CH_2), 59.7 (CH_2), 54.2 (CH), 53.8 (CH), 52.9 (CH), 52.1 (CH), 51.1 (CH), 44.0 (CH_2), 40.2 (CH_2), 38.2 (CH_2), 36.7 (CH_2), 35.1 (CH_2), 28.8 (CH_2), 28.7 (CH_2), 27.7 (CH), 27.3 (CH_2), 26.5 (CH_2), 25.1 (CH_2), 25.0 (CH_2), 23.7 (CH), 22.8 (CH_3), 22.4 (2 CH_3), 21.4 (CH_3). HRESIMS calcd for $\text{C}_{81}\text{H}_{96}\text{N}_9\text{O}_{13}$ ($[\text{M}+\text{H}]^+$): 1402.7128; found 1402.7125.

Synthesis of tauramamide (**12**)



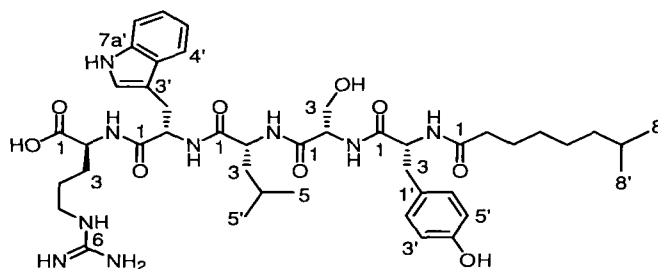
A solution of $(\text{CH}_3)_2\text{CH}_2(\text{CH}_2)_5\text{CONH-D-Tyr(Bn)-Ser(Bn)-D-Leu-Trp-Arg(Cbz)}_2\text{-OBn}$ (**32**) (0.21 g, 0.15 mmol) and 10 % Pd/C, wet Degussa type E101NE/W; was stirred in the presence H_2 at 25 °C and 20 atm, until TLC (RP, 90% $\text{CH}_3\text{CN}/\text{H}_2\text{O}$) showed the absence of starting material (around 1 week). Catalyst filtration, followed by solvent evaporation and

reverse phase column chromatography (90% CH₃CN/H₂O); afforded a colorless solid residue. Further purification by reverse phase HPLC (50% CH₃CN/H₂O, 0.1% TFA) yielded pure tauramamide (**12**) (0.132 g, 81%). $[\alpha]_D^{25} -52$ (*c* 0.9, MeOH). For a summary of ¹H and ¹³C NMR assignments, see Tables 2.1 and 2.5. ¹H NMR (DMSO, 600 MHz) δ 12.69 (1H, s, broad), 10.76 (1H, d, *J* = 1.5 Hz), 9.14 (1H, s), 8.32 (1H, d, *J* = 7.8 Hz), 8.14 (1H, d, *J* = 8.3 Hz), 8.03 (1H, d, *J* = 7.8 Hz), 7.99 (1H, d, *J* = 7.7 Hz), 7.75 (1H, d, *J* = 7.8 Hz), 7.62 (1H, d, *J* = 7.8 Hz), 7.48 (1H, dd, *J* = 5.8, 5.8 Hz), 7.30 (1H, d, *J* = 8.0 Hz), 7.10 (1H, d, *J* = 1.9 Hz), 7.03 (1H, dd, *J* = 7.1, 7.1 Hz), 7.02 (1H, d, *J* = 8.3 Hz), 7.02 (1H, d, *J* = 8.3 Hz), 6.95 (1H, dd, *J* = 7.4, 7.4 Hz), 6.61 (1H, d, *J* = 8.4 Hz), 6.61 (1H, d, *J* = 8.4 Hz), 4.82 (1H, s, broad), 4.54 (1H, m), 4.42 (1H, m), 4.23 (1H, m), 4.22 (1H, m), 4.21 (1H, m), 3.51 (1H, m), 3.44 (1H, m), 3.16 (1H, m), 3.12 (2H, m), 2.88 (1H, m), 2.86 (1H, m), 2.62 (1H, dd, *J* = 10.2, 14.0 Hz), 2.00 (2H, m), 1.79 (1H, m), 1.64 (1H, m), 1.54 (1H, m), 1.45 (1H, m), 1.35 (2H, m), 1.35 (1H, m), 1.24 (1H, m), 1.17 (1H, m), 1.15 (1H, m), 1.14 (1H, m), 1.09 (2H, m), 1.08 (1H, m), 1.07 (1H, m), 1.06 (1H, m), 0.826 (3H, d, *J* = 6.8 Hz), 0.823 (3H, d, *J* = 6.8 Hz), 0.68 (3H, d, *J* = 6.8 Hz), 0.66 (3H, d, *J* = 6.5 Hz); ¹³C NMR (CDCl₃, 150 MHz) δ 173.3 (C), 172.5 (C), 171.8 (C), 171.7 (C), 171.6 (C), 169.7 (C), 156.7 (C), 155.7 (C), 136.0 (C), 130.0 (2CH), 127.8 (C), 127.1 (C), 124.0 (CH), 120.7 (CH), 118.5 (CH), 118.0 (CH), 114.7 (2CH), 111.2 (CH), 109.9 (C), 61.7 (CH₂), 55.0 (CH), 54.5 (CH), 53.1 (CH), 51.6 (CH), 51.2 (CH), 40.7 (CH₂), 40.3 (CH₂), 38.2 (CH₂), 36.6 (CH), 35.1 (CH₂), 28.7 (CH₂), 28.0 (CH₂), 27.6 (CH₂), 27.4 (CH₂), 26.5 (CH₂), 25.2 (CH₂), 25.1 (CH₂), 23.7 (CH), 22.8 (CH₃), 22.51 (CH₃), 22.49 (CH₃), 21.5 (CH₃). HRESIMS calcd for C₄₄H₆₆N₉O₉ ([M+Na]⁺): 864.4984; found 864.4981.

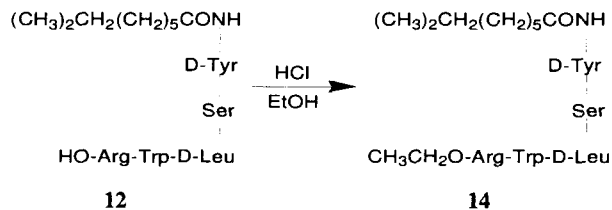
Table 2.5. NMR data for tauramamide (**12**) (recorded in DMSO-*d*₆).

Amino Acid	Proton No	¹ H δ (ppm) (mult, <i>J</i> (Hz)) ^{b,c}	COSY ^a (H→H)
Arg	1OH	12.69 (s, broad)	
	2	4.22 (m)	2NH, H3
	2NH	8.32 (d, <i>J</i> = 7.8 Hz)	H2
	3	1.64 (m), 1.79 (m)	H2, H4
	4	1.35 (m), 1.54 (m)	H3, H5
	5	3.12 (m)	4H, 5NH
	5NH	7.48 (dd, <i>J</i> = 5.8, 5.8 Hz)	H5
Trp	2	4.54 (m)	2NH, H3
	2NH	8.14 (d, <i>J</i> = 8.3 Hz)	H2
	3	2.88 (m), 3.16 (m)	H2
	4'	7.62 (d, <i>J</i> = 7.8 Hz)	H5'
	5'	6.95 (dd, <i>J</i> = 7.4, 7.4 Hz)	H4'
	6'	7.03 (dd, <i>J</i> = 7.1, 7.1 Hz)	H7'
	7'	7.30 (d, <i>J</i> = 8.0 Hz)	H6'
	7a'NH	10.76 (d, <i>J</i> = 1.5 Hz)	H2'
D-Leu	2'	7.10 (d, <i>J</i> = 1.9 Hz)	7a'NH
	2	4.21 (m)	2NH, H3
	2NH	7.75 (d, <i>J</i> = 7.8 Hz)	H2
	3	1.08 (m), 1.17 (m)	H2
	4	1.24 (m)	H5, H5'
	5	0.68 (d, <i>J</i> = 6.8 Hz)	H4
Ser	5'	0.66 (d, <i>J</i> = 6.5 Hz)	H4
	2	4.23 (m)	2NH, H3
	2NH	8.03 (d, <i>J</i> = 7.8 Hz)	H2
	3	3.44 (m), 3.51 (m)	H2, 3OH
	3OH	4.82 (s, broad)	H3

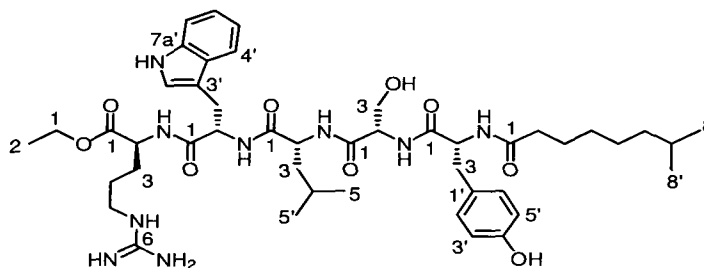
^aRecorded at 600 MHz.

Table 2.5. NMR data for tauramamide (**12**) (recorded in DMSO-*d*₆) (Continuation).

Amino Acid	Proton No	¹ H δ (ppm) (mult, <i>J</i> (Hz)) ^{b,c}	COSY ^a (H→H)	
D-Tyr	2	4.42 (m)	2NH, H3	
	2NH	7.99 (d, <i>J</i> = 7.7 Hz)	H2	
	3	2.62 (dd, <i>J</i> = 10.2, 14.0 Hz), 2.86 (m)	H2	
	2'	7.02 (d, <i>J</i> = 8.3 Hz)	H3'	
	3'	6.61 (d, <i>J</i> = 8.4 Hz)	H2'	
	4'OH	9.14 (s)		
	5'	6.61 (d, <i>J</i> = 8.4 Hz)	H6'	
	6'	7.02 (d, <i>J</i> = 8.3 Hz)	H5'	
	Acyl chain	2	2.00 (m)	H3
		3	1.35 (m)	H2, H4
4		1.06 (m), 1.14 (m)	H3	
5		1.07 (m), 1.15 (m)		
6		1.09 (m)	H7	
7		1.45 (m)	H6, H8, H8'	
8		0.826 (d, <i>J</i> = 6.8 Hz)	H7	
8'		0.823 (d, <i>J</i> = 6.8 Hz)	H7	

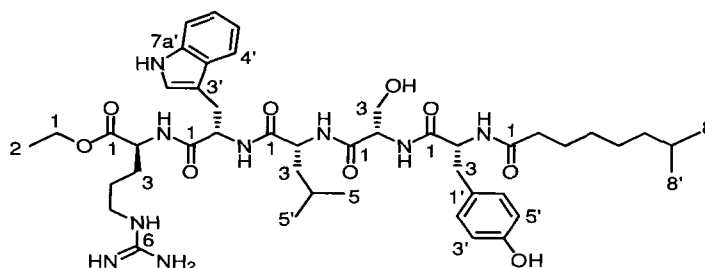
^aRecorded at 600 MHz.**Preparation of tauramamide ethyl ester (**14**)**

A solution of tauramamide (**12**) (0.0628 g, 0.073 mmol) and HCl (1 mL HCl 2M in diethyl ether, 2 mmol) in ethanol was stirred at 25 °C until the TLC spot for starting material (RP, 90% CH₃CN/H₂O) disappeared (around 5 days). Solvent evaporation, followed by reverse phase HPLC (50% CH₃CN/H₂O, 0.1% TFA) yielded pure tauramamide ethyl ester (**14**) (0.0559 g, 86%). $[\alpha]_D^{25} -4.7$ (*c* 1.8, MeOH). For a summary of ¹H and ¹³C NMR assignments, see Table 2.6. ¹H NMR (DMSO, 600 MHz) δ 10.77 (1H, d, *J* = 1.6 Hz), 9.14 (1H, s), 8.43 (1H, d, *J* = 7.4 Hz), 8.16 (1H, d, *J* = 8.3 Hz), 8.04 (1H, d, *J* = 7.7 Hz), 7.98 (1H, d, *J* = 7.7 Hz), 7.75 (1H, d, *J* = 7.7 Hz), 7.62 (1H, d, *J* = 7.7 Hz), 7.48 (1H, dd, *J* = 5.5, 5.6 Hz), 7.30 (1H, d, *J* = 8.0 Hz), 7.10 (1H, d, *J* = 2.2 Hz), 7.04 (1H, dd, *J* = 7.2, 7.5 Hz), 7.02 (1H, d, *J* = 8.6 Hz), 7.02 (1H, d, *J* = 8.6 Hz), 6.96 (1H, dd, *J* = 7.2, 7.5 Hz), 6.61 (1H, d, *J* = 8.6 Hz), 6.61 (1H, d, *J* = 8.6 Hz), 4.84 (1H, dd, *J* = 5.2, 5.5 Hz), 4.54 (1H, m), 4.42 (1H, m), 4.25 (1H, m), 4.24 (1H, m), 4.23 (1H, m), 4.09 (2H, m), 3.51 (1H, m), 3.45 (1H, m), 3.15 (1H, dd, *J* = 3.8, 14.6 Hz), 3.11 (2H, m), 2.88 (1H, m), 2.84 (1H, m), 2.62 (1H, dd, *J* = 10.0, 13.8 Hz), 2.00 (2H, m), 1.77 (1H, m), 1.66 (1H, m), 1.53 (2H, m), 1.45 (1H, m), 1.35 (2H, m), 1.26 (1H, m), 1.18 (3H, t, *J* = 7.2 Hz), 1.14 (2H, m), 1.08 (2H, m), 1.08 (2H, m), 1.06 (2H, m), 0.824 (3H, d, *J* = 6.7 Hz), 0.822 (3H, d, *J* = 6.6 Hz), 0.70 (3H, d, *J* = 6.6 Hz), 0.67 (3H, d, *J* = 6.6 Hz); ¹³C NMR (CDCl₃, 150 MHz) δ 172.4 (C), 172.0 (C), 171.72 (C), 171.66 (C), 171.64 (C), 169.7 (C), 156.6 (C), 155.7 (C), 136.0 (C), 130.0 (2CH), 127.8 (C), 127.1 (C), 123.9 (CH), 120.7 (CH), 118.4 (CH), 118.0 (CH), 114.7 (2CH), 111.2 (CH), 109.8 (C), 61.7 (CH₂), 60.5 (CH₂), 55.0 (CH), 54.5 (CH), 53.1 (CH), 51.8 (CH), 51.2 (CH), 40.7 (CH₂), 40.3 (CH₂), 38.2 (CH₂), 36.6 (CH), 35.1 (CH₂), 28.8 (CH₂), 27.8 (CH₂), 27.6 (CH₂), 27.4 (CH₂), 26.5 (CH₂), 25.15 (CH₂), 25.08 (CH₂), 23.7 (CH), 22.8 (CH₃), 22.50 (CH₃), 22.49 (CH₃), 21.5 (CH₃), 14.0 (CH₃). HRESIMS calcd for C₄₆H₇₀N₉O₉ ([M+Na]⁺): 892.5297; found 892.5295.

Table 2.6. ^1H and ^{13}C NMR data for natural⁶⁹ and synthetic tauramamide ethyl ester (**14**) (recorded in $\text{DMSO-}d_6$).

Amino Acid	No	Natural		Synthetic	
		^{13}C δ (ppm) ^a	^1H δ (ppm) (mult, J (Hz)) ^a	^{13}C δ (ppm) ^a	^1H δ (ppm) (mult, J (Hz)) ^a
Ethyl	1	60.5	4.09 (m)	60.5	4.09 (m)
	2	14.1	1.18 (t, $J = 7.2$ Hz)	14.0	1.18 (t, $J = 7.2$ Hz)
Arg	1	172.0		172.0	
	2	51.8	4.25 (s, broad)	51.8	4.25 (m)
	2NH		8.43 (d, $J = 7.7$ Hz)		8.43 (d, $J = 7.4$ Hz)
	3	27.8	1.67 (m) 1.77 (m)	27.8	1.66 (m) 1.77 (m)
	4	25.1	1.53 (m)	25.08	1.53 (m)
	5	40.3	3.11 (m)	40.3	3.11 (m)
	5NH		7.49 (1H, m)		7.48 (dd, $J = 5.5, 5.6$ Hz)
Trp	1	156.6		156.6	
	1	-		171.72	
	2	53.1	4.54 (s, broad)	53.1	4.54 (m)
	2NH		8.17 (d, $J = 8.2$ Hz)		8.16 (d, $J = 8.3$ Hz)
	3	27.6	2.88 (m) 3.16 (m)	27.6	2.88 (m) 3.15 (dd, $J = 3.8, 14.6$ Hz)
	3'	109.9		109.8	
	3a'	127.1		127.1	
	4'	118.4	7.62 (d, $J = 7.7$ Hz)	118.4	7.62 (d, $J = 7.7$ Hz)
	5'	118.1	6.96 (dd, $J = 7.2, 7.7$ Hz)	118.0	6.96 (dd, $J = 7.2, 7.5$ Hz)
	6'	120.7	7.04 (m)	120.7	7.04 (dd, $J = 7.2, 7.5$ Hz)
	7'	111.2	7.30 (d, $J = 8.2$ Hz)	111.2	7.30 (d, $J = 8.0$ Hz)
7a'	136.0		136.0		
7a'NH		10.77 (s)		10.77 (d, $J = 1.6$ Hz)	
2'	123.9	7.11 (d, $J = 1.5$ Hz)	123.9	7.10 (d, $J = 2.2$ Hz)	
D-Leu	1	-		171.64	
	2	51.2	4.23 (s, broad)	51.2	4.23 (m)
	2NH		7.76 (d, $J = 8.2$ Hz)		7.75 (d, $J = 7.7$ Hz)
	3	40.5	1.08 (m)	40.7	1.08 (m)
4	23.7	1.23 (m)	23.7	1.26 (m)	

^aRecorded at 150 MHz. ^bRecorded at 600 MHz.

Table 2.6. ^1H and ^{13}C NMR data for natural⁶⁹ and synthetic tauramamide ethyl ester (**14**) (recorded in $\text{DMSO-}d_6$) (Continuation).

Amino Acid	No	Natural		Synthetic	
		^{13}C δ (ppm) ^a	^1H δ (ppm) (mult, J (Hz)) ^a	^{13}C δ (ppm) ^a	^1H δ (ppm) (mult, J (Hz)) ^a
D-Leu	5	22.8	0.70 (d, $J = 6.6$ Hz)	22.8	0.70 (d, $J = 6.6$ Hz)
	5'	21.5	0.67 (d, $J = 6.7$ Hz)	21.5	0.67 (d, $J = 6.6$ Hz)
Ser	1	169.7		169.7	
	2	55.0	4.24 (s, broad)	55.0	4.24 (m)
	2NH		8.05 (d, $J = 7.7$ Hz)		8.04 (d, $J = 7.7$ Hz)
	3	61.7	3.46 (m) 3.51 (m)	61.7	3.45 (m) 3.51 (m)
	3OH		4.84 (t, $J = 5.4$ Hz)		4.84 (dd, $J = 5.2, 5.5$ Hz)
D-Tyr	1	-		171.67	
	2	54.5	4.42 (s, broad)	54.5	4.42 (m)
	2NH		7.99 (d, $J = 7.7$ Hz)		7.98 (d, $J = 7.7$ Hz)
	3	36.6	2.63 (m) 2.84 (m)	36.6	2.62 (dd, $J = 10.0, 13.8$ Hz) 2.84 (m)
	1'	127.9		127.8	
	2'	130.0	7.02 (d, $J = 8.2$ Hz)	130.0	7.02 (d, $J = 8.6$ Hz)
	3'	114.7	6.61 (d, $J = 8.2$ Hz)	114.7	6.61 (d, $J = 8.6$ Hz)
	4'	155.7		155.7	
	4'OH		9.14 (s)		9.14 (s)
	5'	114.7	6.61 (d, $J = 8.2$ Hz)	114.7	6.61 (d, $J = 8.6$ Hz)
6'	130.0	7.02 (d, $J = 8.2$ Hz)	130.0	7.02 (d, $J = 8.6$ Hz)	
Acyl chain	1	-		172.4	
	2	35.1	2.00 (m)	35.1	2.00 (m)
	3	25.2	1.35 (m)	25.15	1.35 (m)
	4	28.8	1.06 (m)	28.8	1.06 (m)
	5	26.5	1.14 (m)	26.5	1.14 (m)
	6	38.3	1.08 (m)	38.2	1.08 (m)
	7	27.4	1.45 (m)	27.4	1.45 (m)
	8	22.5	0.83 (d, $J = 6.7$ Hz)	22.49	0.822 (d, $J = 6.6$ Hz)
	8'	22.5	0.83 (d, $J = 6.7$ Hz)	22.50	0.824 (d, $J = 6.7$ Hz)

^a Recorded at 150 MHz. ^b Recorded at 600 MHz.

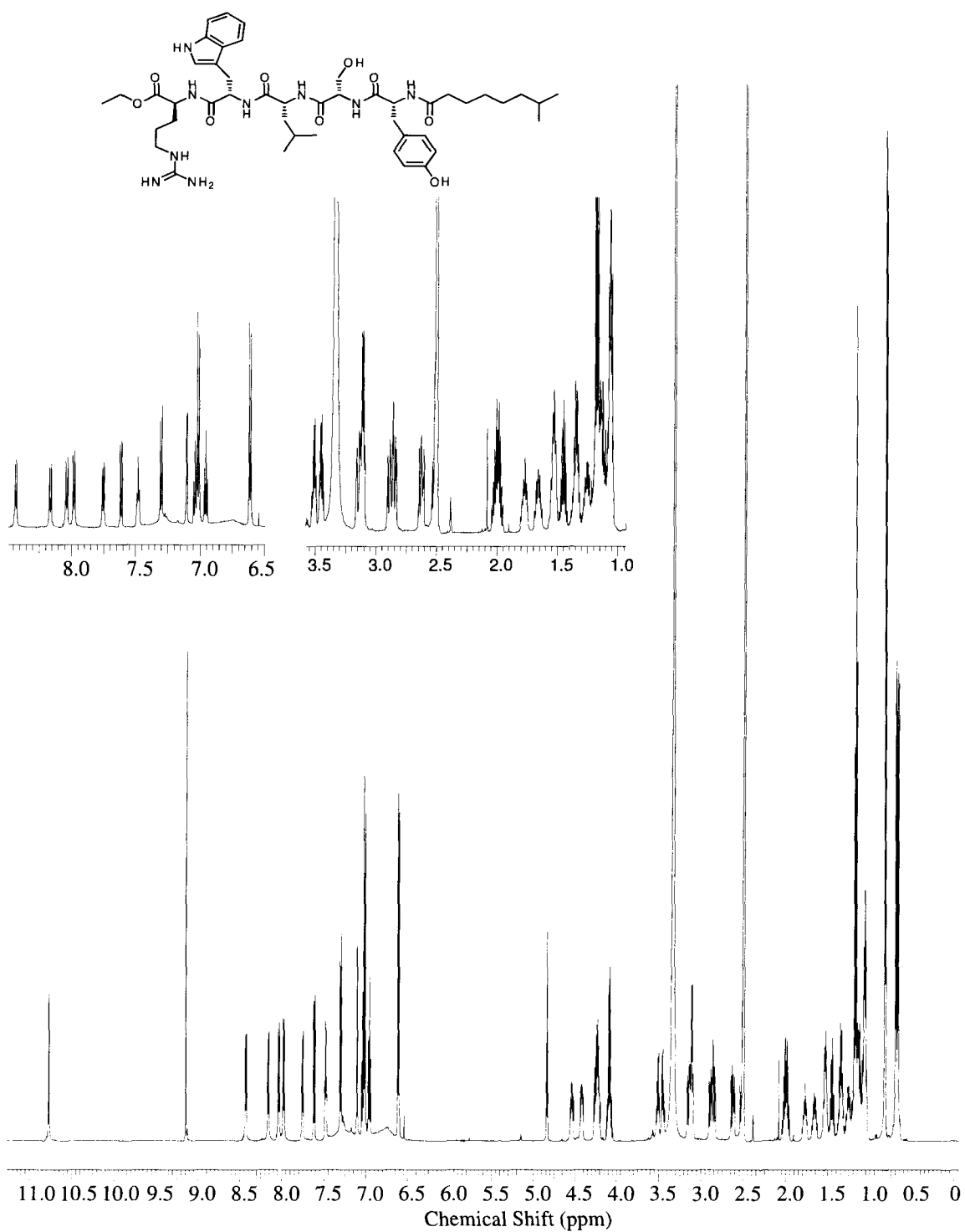


Figure 2.10. ¹H-NMR spectrum of tauramamide ethyl ester (**14**) (recorded in DMSO-*d*₆ at 600 MHz).

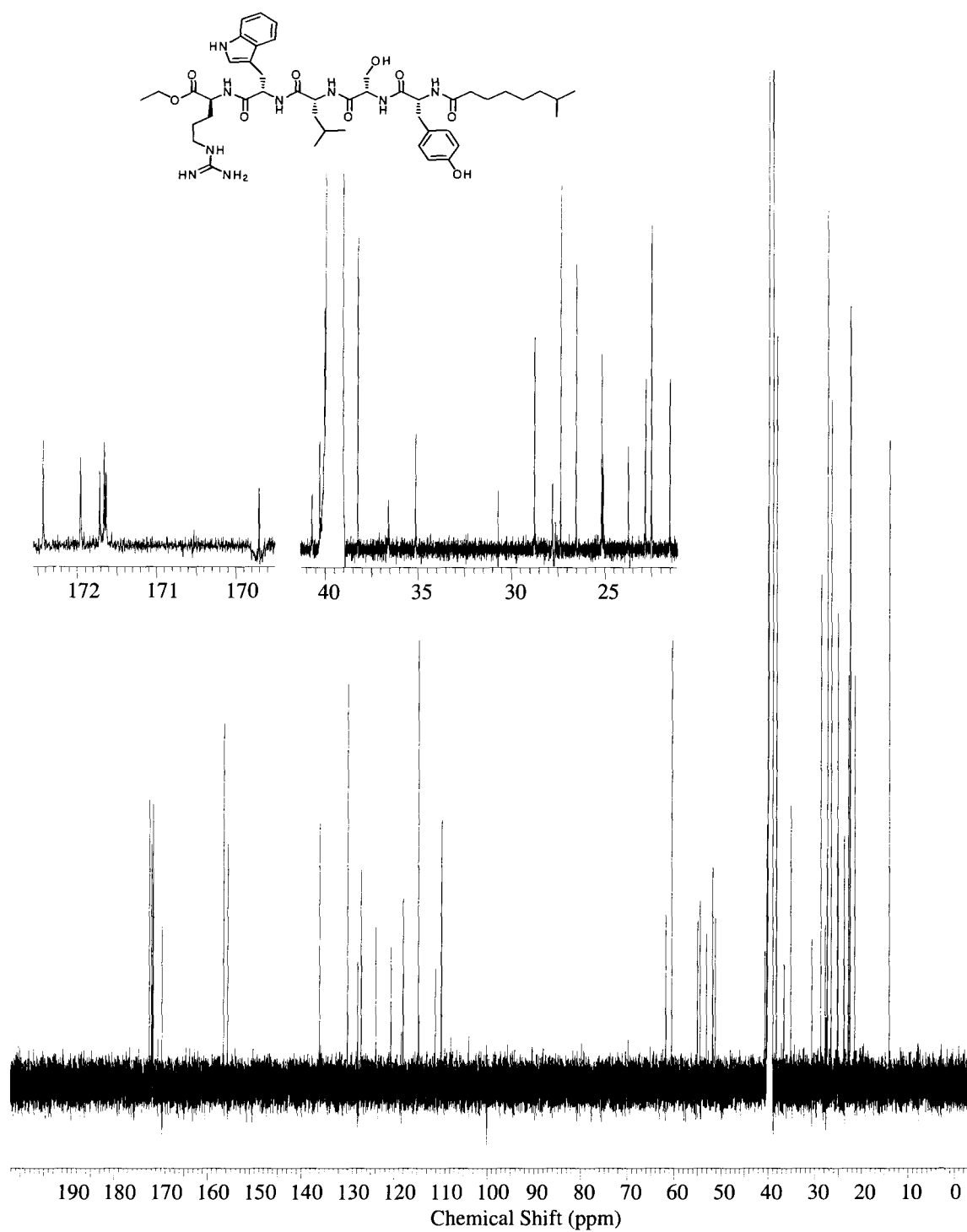
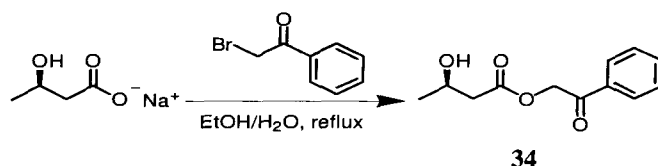


Figure 2.11. ¹³C-NMR spectrum of tauramide ethyl ester (**14**) (recorded in DMSO-*d*₆ at 150 MHz).

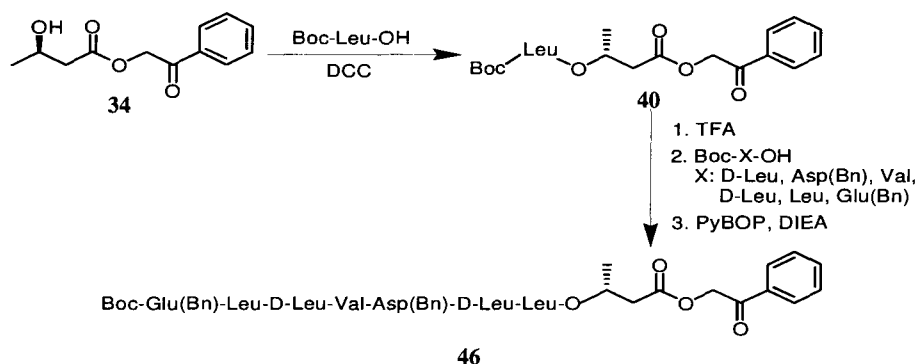
2.6.2. Synthesis of dealkylsurfactin

Preparation of (*R*)-(-)-3-hydroxybutyric phenacyl ester (**34**)



To a solution of (*R*)-(-)-3-hydroxybutyric acid sodium salt (0.76 g, 6.0 mmol) in EtOH/H₂O (H₂O added drop by drop until complete solubility was achieved, total volume: 18 mL), was added phenacyl bromide (1.20 g, 6.0 mmol) and the mixture refluxed for 4 h. The reaction crude was concentrated *in vacuo* and the resulting residue purified by silica gel column chromatography (50% EtOAc/hexanes), to afford (**34**) as a yellowish solid (1.10 g, 82%). ¹H NMR (CD₃OD, 400 MHz) δ 7.97 (2H, d, *J* = 7.3 Hz), 7.65 (1H, dd, *J* = 7.3, 7.6 Hz), 7.52 (2H, dd, *J* = 7.9, 7.6 Hz), 5.45 (2H, m), 4.23 (1H, m), 2.60 (2H, m), 1.26 (3H, d, *J* = 6.1 Hz); ¹³C NMR (CD₃OD, 100 MHz) δ 194.6 (C), 172.5 (C), 135.5 (C), 135.1 (CH), 130.0 (2CH), 128.9 (2CH), 67.4 (CH₂), 65.6 (CH), 44.5 (CH₂), 23.2 (CH₃). HRESIMS calcd for C₁₂H₁₄O₄Na ([M+Na]⁺): 245.0790; found 245.0784.

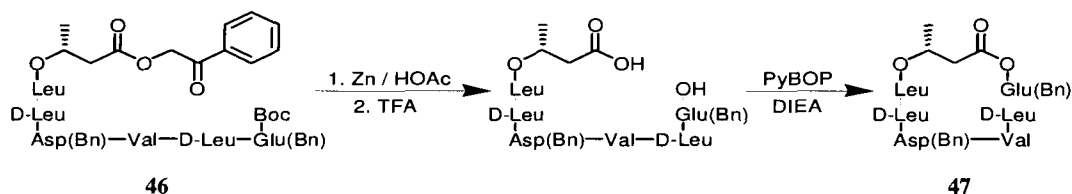
Preparation of
Boc-Glu(Bn)-Leu-DLeu-Val-Asp(Bn)-DLeu-Leu-OCH(CH₃)CH₂COOCH₂COPh (46)



To a mixture of Boc-Leu-OH (0.91 g, 3.9 mmol, 1 eq) and (*R*)-(-)-3-hydroxybutyric phenacyl ester (**34**) (0.79 g, 3.6 mmol) in CH₂Cl₂ (25 mL) at 0 °C, was added DCC (0.80 g, 3.9 mmol) dissolved in CH₂Cl₂ (5 mL). The cooling bath was removed and the mixture was stirred overnight. Purification by silica gel column chromatography (50% EtOAc/hexanes) afforded (**40**) as a crystalline amorphous powder (1.39 g, 90%). Intermediate (**40**) (0.39 g, 0.89 mmol) was treated with TFA (1 mL, 12.5 mmol, 14 eq) and stirred for 5 h, whereupon it was concentrated *in vacuo* to a pale red oil. This oil was dissolved in CH₂Cl₂ (10 mL) and added to a solution of Boc-DLeu-OH (0.19 g, 0.81 mmol, 0.90 eq) and PyBOP (0.51 g, 0.98 mmol, 1.10 eq) in CH₂Cl₂ (20 mL); followed by addition of DIEA (0.46 mL, 2.70 mmol, 3 eq). After overnight stirring at 25 °C, NH₄Cl sat. was added and CH₂Cl₂ (3x20 mL) extractions performed. The organic extracts were combined and dried (Na₂SO₄), to be then concentrated *in vacuo*. Column chromatography on silica (70% EtOAc/Hexanes) afforded desired product as a white amorphous solid (0.45 g, 99%). The procedure above was repeated successively with Boc-Asp(Bn)-OH (0.25 g, 0.77 mmol), Boc-Val-OH (0.16 g, 0.70 mmol), Boc-D-Leu-OH (0.15 g, 0.62 mmol), Boc-Leu-OH (0.16 g, 0.70 mmol) and Boc-Glu-OH (0.16 g, 0.49 mmol); to afford product (**46**) (0.63 g, overall yield for 5 steps: 63%). ¹H NMR (CDCl₃, 400 MHz) δ 8.36 (1H, d, *J* = 8.0 Hz),

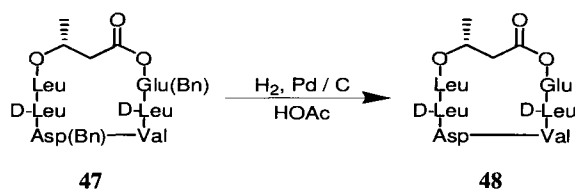
7.82 (2H, d, $J = 7.3$ Hz), 7.57 (1H, d, $J = 9.5$ Hz), 7.53 (1H, dd, $J = 7.3, 7.6$ Hz), 7.39 (2H, dd, $J = 7.6, 7.9$ Hz), 7.32-7.21 (10H, m), 7.07 (1H, d, $J = 7.9$ Hz), 6.99 (1H, s), 5.97 (1H, d, $J = 7.3$ Hz), 5.37 (1H, d, $J = 16.8$ Hz), 5.27 (1H, d, $J = 16.5$ Hz), 5.23 (1H, s), 5.07 (1H, d, $J = 12.5$ Hz), 5.04 (3H, m), 4.89 (1H, d, $J = 12.5$ Hz), 4.54 (1H, m), 4.46 (1H, m), 4.42 (1H, m), 4.19 (1H, m), 3.97 (1H, m), 3.81 (1H, dd, $J = 5.2, 6.4$ Hz), 3.08 (1H, dd, $J = 3.7, 15.3$ Hz), 2.93 (1H, dd, $J = 10.1, 15.3$ Hz), 2.86 (1H, dd, $J = 7.3, 15.6$ Hz), 2.57 (1H, dd, $J = 6.1, 15.6$ Hz), 2.54 (1H, m), 2.46 (1H, m), 1.90 (2H, m), 1.78 (2H, m), 1.70-1.45 (13H, m), 1.30 (9H, s), 1.23 (3H, d, $J = 6.1$ Hz), 0.95-0.75 (30H, m); ^{13}C NMR (CDCl_3 , 100 MHz) δ 192.2 (C), 173.7 (C), 173.5 (C), 173.2 (C), 173.1 (C), 172.3 (C), 172.1 (C), 171.7 (C), 171.3 (C), 170.2 (C), 169.4 (C), 155.5 (C), 135.5 (C), 135.2 (C), 134.0 (CH), 133.8 (C), 128.8 (2CH), 128.4 (2CH), 128.3 (2CH), 128.2 (CH), 128.1 (2CH), 128.0 (CH), 127.9 (2CH), 127.6 (2CH), 79.5 (C), 68.4 (CH), 66.4 (CH_2), 66.4 (CH_2), 66.1 (CH_2), 61.8 (CH), 53.2 (CH), 52.8 (CH), 52.0 (CH), 50.7 (CH), 50.1 (CH), 49.2 (CH), 41.0 (CH_2), 40.4 (CH_2), 40.1 (CH_2), 40.0 (CH_2), 37.3 (CH_2), 35.7 (CH_2), 30.2 (CH_2), 29.1 (CH_2), 28.1 (3 CH_3), 24.6 (CH), 24.6 (CH), 24.5 (CH), 24.4 (CH), 22.9 (CH_3), 22.8 (CH_3), 22.7 (CH_3), 22.6 (CH_3), 22.0 (CH_3), 21.7 (CH_3), 21.5 (CH_3), 21.3 (CH_3), 19.3 (CH_3), 19.2 (CH_3), 18.5 (CH_3). HRESIMS calcd for $\text{C}_{69}\text{H}_{99}\text{N}_7\text{O}_{17}\text{Na}$ ($[\text{M}+\text{Na}]^+$): 1320.6995; found 1320.6971.

Preparation of dibenzyl dealkylsurfactin (**47**)



To a solution of (**46**) (0.30 g, 0.23 mmol) in HOAc (8 mL), was added Zn (2 g, 30 mmol) and the mixture was stirred overnight. After filtration through a reverse phase Sep Pak[®] (2 g) and

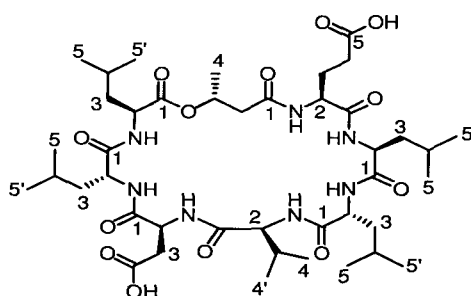
solvent evaporation, resulting residue was dissolved in EtOAc and washed with water, followed by a second wash with NaCl sat. The organic extracts were dried (Na_2SO_4) and concentrated *in vacuo*. The resulting residue was dissolved in CH_2Cl_2 (10 mL) and stirred in the presence of TFA (1 mL) for 24 h. A second Sep Pak[®] filtration and solvent evaporation allowed to isolate the desired deprotected intermediate, which was dissolved in CH_2Cl_2 (20 mL) and reacted with PyBOP (0.056 g, 1.1 mmol) in the presence of DIEA (0.05 mL, 0.29 mmol). Overnight stirring followed by LH-20 (70% EtOAc/hexanes) and silica gel (gradient from 70% EtOAc/hexanes to 10% MeOH/EtOAc) column chromatography afforded (**47**) as a colorless solid (0.074 g, 30%). $[\alpha]_{\text{D}}^{20}$ -18 (*c* 1.9, MeOH); UV (MeOH) λ_{max} (log ϵ) 226 nm (2.80). ^1H NMR (DMSO, 600 MHz) δ 8.54 (1H, d, $J = 6.5$ Hz), 8.34 (1H, d, $J = 7.0$ Hz), 8.17 (1H, d, $J = 7.5$ Hz), 8.11 (1H, d, $J = 4.8$ Hz), 7.90 (1H, d, $J = 8.9$ Hz), 7.82 (1H, d, $J = 8.7$ Hz), 7.78 (1H, d, $J = 6.3$ Hz), 7.40-7.29 (10H, m), 5.08 (4H, m), 5.02 (1H, dd, $J = 6.3, 7.0$ Hz), 4.63 (1H, m), 4.48 (1H, dd, $J = 6.5, 8.6$ Hz), 4.23 (1H, dd, $J = 5.9, 6.4$ Hz), 4.14 (1H, dd, $J = 10.9, 14.9$ Hz), 4.10 (1H, dd, $J = 12.6, 12.8$ Hz), 4.08 (1H, m), 4.01 (1H, m), 2.84 (1H, dd, $J = 4.3, 16.7$ Hz), 2.72 (1H, dd, $J = 9.8, 16.7$ Hz), 2.38 (4H, m), 2.08-1.82 (3H, m), 1.68-1.32 (12H, m), 1.11 (3H, d, $J = 6.2$ Hz), 0.90-0.80 (24H, m), 0.78 (3H, d, $J = 5.9$ Hz), 0.74 (3H, d, $J = 6.8$ Hz); ^{13}C NMR (DMSO, 150 MHz) δ 172.4 (C), 172.3 (C), 172.1 (C), 171.9 (C), 171.5 (C), 170.8 (C), 170.5 (C), 169.9 (C), 169.4 (C), 169.3 (C), 136.1 (C), 135.9 (C), 128.4 (2CH), 128.3 (2CH), 128.0 (CH), 127.9 (CH), 127.8 (2CH), 127.7 (2CH), 68.5 (CH), 65.6 (CH₂), 65.4 (CH₂), 58.2 (CH), 52.5 (CH), 51.7 (2CH), 51.4 (CH), 50.2 (CH), 49.3 (CH), 41.9 (CH₂), 38.6 (CH₂), 36.0 (CH₂), 30.5 (CH), 29.5 (CH₂), 26.9 (CH₂), 24.2 (CH), 24.1 (3CH), 23.1 (CH₃), 22.8 (CH₃), 22.7 (CH₃), 22.4 (CH₃), 22.1 (CH₃), 21.9 (CH₃), 21.0 (CH₃), 20.8 (CH₃), 19.5 (CH₃), 19.1 (CH₃), 18.3 (CH₃). HRESIMS calcd for $\text{C}_{56}\text{H}_{83}\text{N}_7\text{O}_{13}\text{Na}$ ($[\text{M}+\text{Na}]^+$): 1084.5947; found 1084.5957.

Synthesis of dealkylsurfactin (**48**)

Dibenzyl dealkylsurfactin (**47**) (0.030 g, 0.028 mmol) was dissolved in HOAc (5 mL), and stirred overnight in the presence of Pd/C under H₂ atmosphere using a balloon. Filtration followed by solvent evaporation afforded a dark residue, which was purified by size exclusion column chromatography (100% EtOAc). A colorless residue, identified as dealkylsurfactin (0.025 g, 99%) was obtained. $[\alpha]_D^{20}$ -22 (*c* 3.8, MeOH); UV (MeOH) λ_{max} (log ϵ) 222 nm (2.85). For a summary of ¹H and ¹³C NMR assignments, see Tables 2.3 and 2.7. ¹H NMR (DMSO, 600 MHz) δ 12.28 (1H, s, broad), 12.17 (1H, s, broad), 8.56 (1H, d, *J* = 6.6 Hz), 8.38 (1H, d, *J* = 5.6 Hz), 8.15 (1H, d, *J* = 6.9 Hz), 8.14 (1H, d, *J* = 6.9 Hz), 7.86 (1H, d, *J* = 9.1 Hz), 7.84 (1H, d, *J* = 9.5 Hz), 7.79 (1H, d, *J* = 6.3 Hz), 5.01 (1H, m), 4.53 (1H, m), 4.48 (1H, m), 4.21 (1H, m), 4.13 (1H, m), 4.09 (1H, dd, *J* = 8.6, 8.9 Hz), 4.06 (1H, m), 4.00 (1H, m), 2.68 (1H, dd, *J* = 4.3, 16.7 Hz), 2.56 (1H, dd, *J* = 9.5, 17.1 Hz), 2.42 (1H, dd, *J* = 7.9, 13.8 Hz), 2.37 (1H, dd, *J* = 5.9, 13.8 Hz), 2.20 (2H, m), 1.97 (1H, m), 1.96 (1H, m), 1.81 (1H, m), 1.63 (1H, m), 1.61 (1H, m), 1.58 (1H, m), 1.54 (1H, m), 1.48 (1H, m), 1.46 (2H, m), 1.46 (1H, m), 1.46 (1H, m), 1.45 (1H, m), 1.40 (1H, m), 1.37 (1H, m), 1.11 (3H, d, *J* = 5.9 Hz), 0.89 (3H, d, *J* = 6.9 Hz), 0.88 (3H, d, *J* = 6.3 Hz), 0.87 (3H, d, *J* = 6.9 Hz), 0.87 (3H, d, *J* = 6.9 Hz), 0.85 (3H, d, *J* = 6.5 Hz), 0.84 (3H, d, *J* = 6.2 Hz), 0.82 (3H, d, *J* = 6.6 Hz), 0.82 (3H, d, *J* = 6.5 Hz), 0.78 (3H, d, *J* = 6.2 Hz), 0.75 (3H, d, *J* = 6.6 Hz); ¹³C NMR (DMSO, 150 MHz) δ 174.1 (C), 172.4 (C), 172.1 (C), 172.0 (C), 171.6 (C), 171.6 (C), 171.0 (C), 170.5 (C), 169.8 (C), 169.4 (C), 68.6 (CH), 58.2 (CH), 52.6 (CH), 51.8 (CH), 51.6 (CH), 51.4 (CH), 50.2 (CH), 49.5 (CH), 41.9 (CH₂), 41.9 (CH₂), 39.4

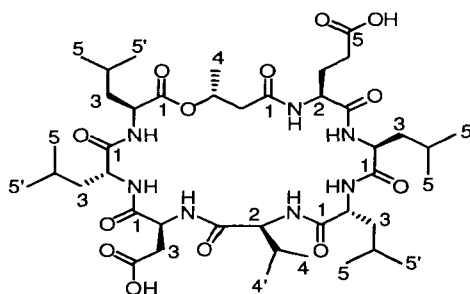
(CH₂), 39.2 (CH₂), 38.6 (CH₂), 36.2 (CH₂), 30.6 (CH), 29.6 (CH₂), 27.2 (CH₂), 24.2 (CH), 24.2 (CH), 24.2 (CH), 23.2 (CH₃), 22.8 (CH₃), 22.8 (CH₃), 22.4 (CH₃), 22.2 (CH₃), 21.9 (CH₃), 21.0 (CH₃), 20.8 (CH₃), 19.5 (CH₃), 19.2 (CH₃), 18.4 (CH₃). HRESIMS calcd for C₄₂H₇₁N₇O₁₃Na ([M+Na]⁺): 904.5008; found 904.5015.

Table 2.7. NMR data for dealkylsurfactin (**48**) (recorded in DMSO-*d*₆).



Amino Acid	Proton No	¹ H δ (ppm) (mult, J (Hz)) ^a	TOCSY ^a (H→H)
<i>(R)</i> -3-HBA	2	2.37 (dd, <i>J</i> = 5.9, 13.8 Hz) 2.42 (dd, <i>J</i> = 7.9, 13.8 Hz)	H3, H4
	3	5.01 (m)	H2, H4
	4	1.11 (d, <i>J</i> = 5.9 Hz)	H2, H3
	2NH	8.56 (d, <i>J</i> = 6.6 Hz)	H2, H3
Leu	2	4.00 (m)	H3, H5, 2NH
	3	1.45 (m), 1.61 (m)	H2, 2NH
	4	1.63 (m)	H5, H5'
	5	0.82 (d, <i>J</i> = 6.4 Hz)	H2, H4
	5'	0.88 (d, <i>J</i> = 6.3 Hz)	H4
D-Leu	2	4.48 (m)	H3, H4, 2NH
	2NH	7.84 (d, <i>J</i> = 9.5 Hz)	H2, H3
	3	1.37 (m), 1.40 (m)	H2, 2NH
	4	1.46 (m)	H2, H5, H5'
	5	0.87 (d, <i>J</i> = 6.9 Hz)	H4
	5'	0.87 (d, <i>J</i> = 6.9 Hz)	H4
Asp	2	4.53 (m)	H3, 2NH
	2NH	8.15 (d, <i>J</i> = 6.9 Hz)	H2, H3
	3	2.56 (dd, <i>J</i> = 9.5, 17.1 Hz) 2.68 (dd, <i>J</i> = 4.3, 16.7 Hz)	H2, 2NH

^a Recorded at 600 MHz.

Table 2.7. NMR data for dealkylsurfactin (**48**) (recorded in DMSO-*d*₆) (Continuation).

Amino Acid	Proton No	¹ H δ (ppm) (mult, <i>J</i> (Hz)) ^a	TOCSY ^a (H→H)
Val	2	4.09 (dd, <i>J</i> = 8.6, 8.9 Hz)	H3, H4, H4', 2NH
	2NH	7.86 (d, <i>J</i> = 9.1 Hz)	H2, H3, H4, H4'
	3	1.97 (m)	H2, H4, H4', 2NH
	4	0.89 (d, <i>J</i> = 6.9 Hz)	H2, H3, 2NH
	4'	0.75 (d, <i>J</i> = 6.6 Hz)	H2, H3, 2NH
D-Leu	2	4.13 (m)	H3, 2NH
	2NH	8.38 (d, <i>J</i> = 5.6 Hz)	H2, H3
	3	1.46 (m), 1.54 (m)	H2, 2NH
	4	1.58 (m)	H5, H5'
	5	0.82 (d, <i>J</i> = 6.6 Hz)	H4
	5'	0.78 (d, <i>J</i> = 6.2 Hz)	H4
Leu	2	4.06 (m)	H4, 2NH
	2NH	8.14 (d, <i>J</i> = 6.9 Hz)	H2, H3
	3	1.46 (m)	2NH
	4	1.48 (m)	H2, H5, H5'
	5	0.85 (d, <i>J</i> = 6.5 Hz)	H4
	5'	0.84 (d, <i>J</i> = 6.2 Hz)	H4
Glu	2	4.21 (m)	H3, H4, 2NH
	2NH	7.79 (d, <i>J</i> = 6.3 Hz)	H2, H3, H4
	3	1.81 (m), 1.96 (m)	H2, H4, 2NH
	4	2.20 (m)	H2, H3, 2NH

^a Recorded at 600 MHz.

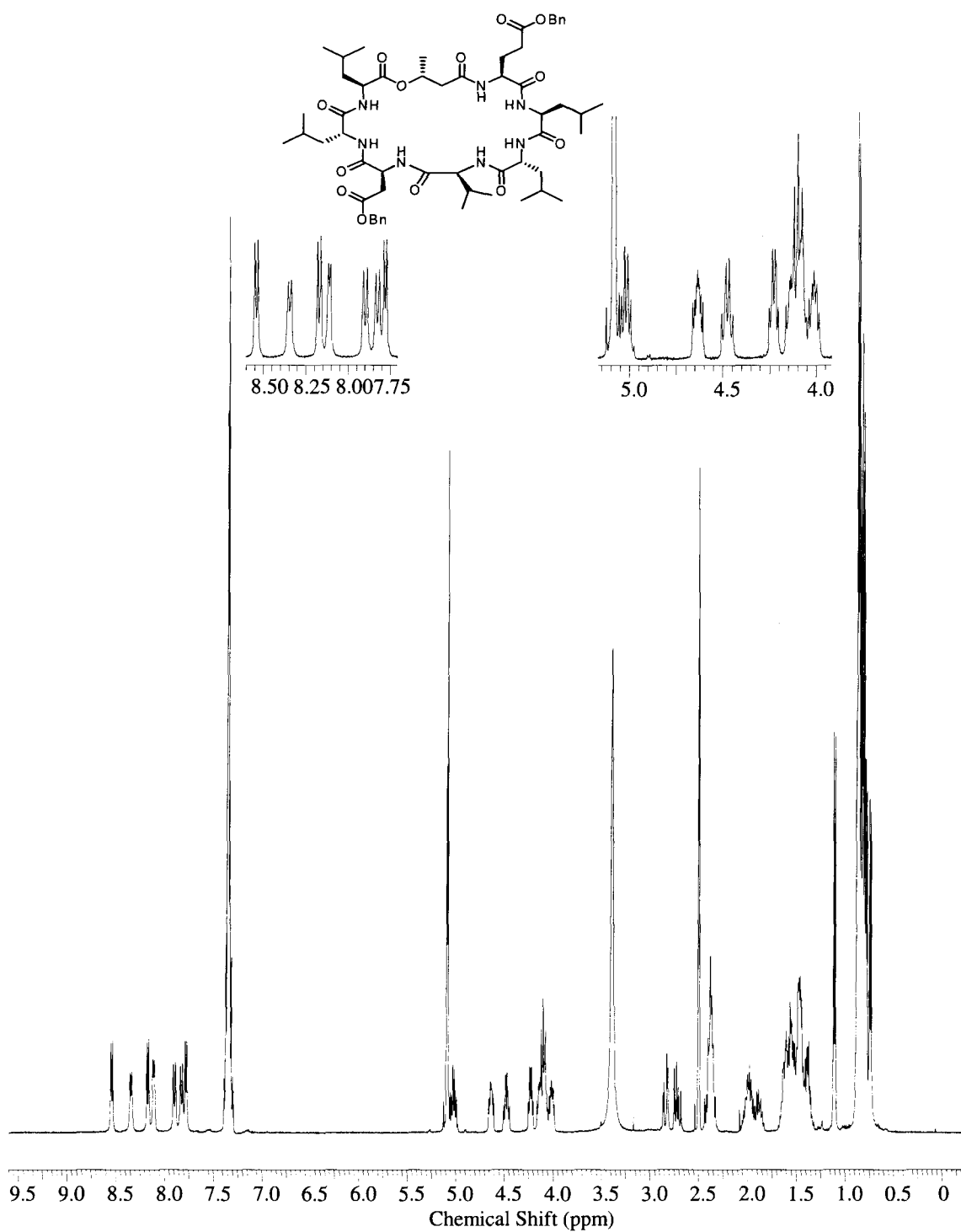


Figure 2.12. ¹H-NMR spectrum of dibenzyl dealkylsurfactin (**47**) (recorded in DMSO-*d*₆ at 600 MHz).

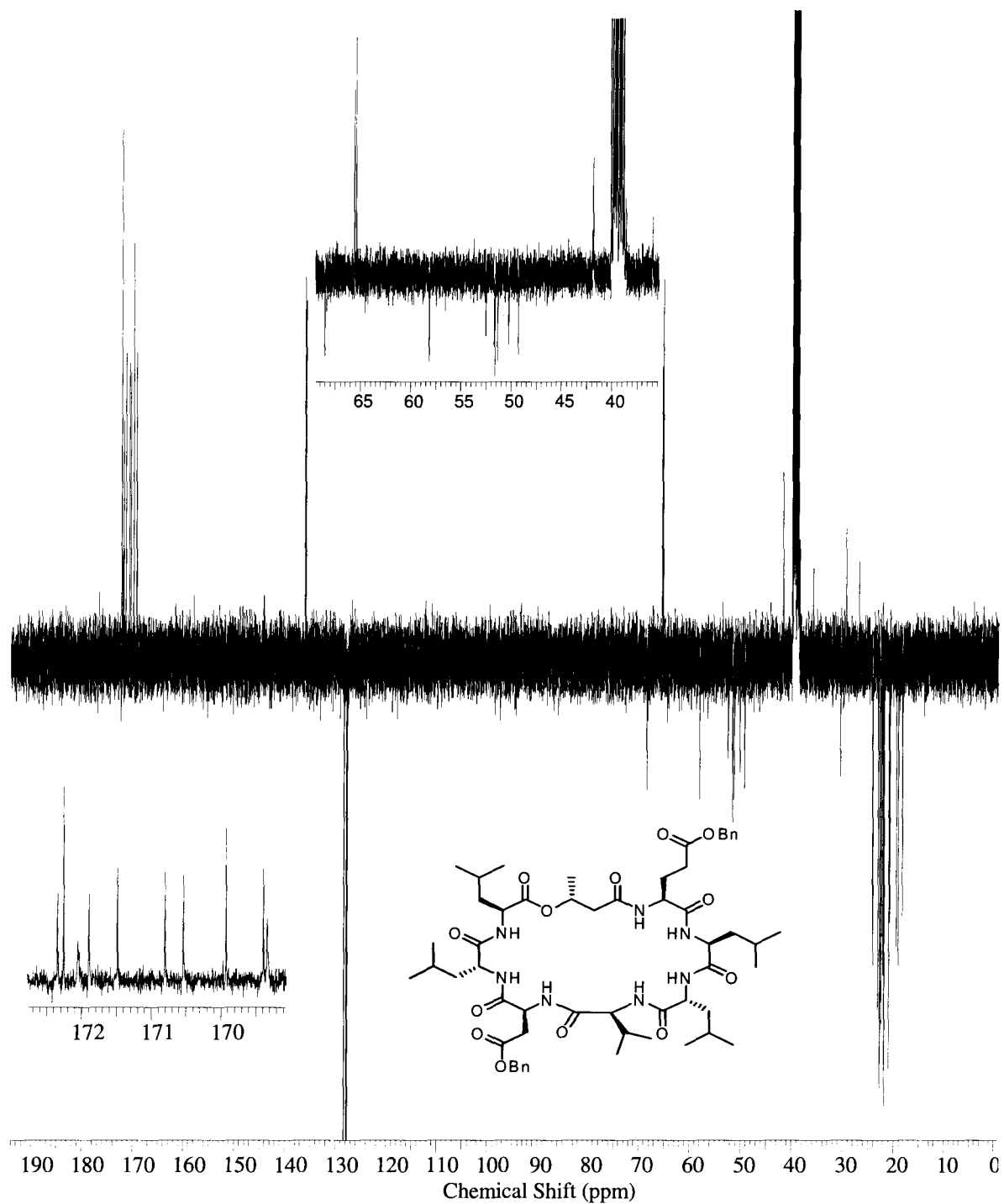


Figure 2.13. ^{13}C APT-NMR spectrum of dibenzyl dealkylsurfactin (**47**) (recorded in $\text{DMSO-}d_6$ at 150 MHz).

3. Isolation and Structure Elucidation of new IDO Inhibitors from *Garveia annulata*

3.1. IDO inhibition and *Garveia annulata*

Immune escape plays an important role in cancer progression¹³²⁻¹³⁵ and fetal development.¹³⁶ Although the mechanism is still not completely understood, it has been proposed that indoleamine 2,3-dioxygenase (IDO) contributes to evasion of T-cell-mediated immune rejection.¹³⁵ IDO catalyzes the oxidative cleavage of the 2,3 bond of tryptophan.^{137,138} T-cell lymphocytes are extremely sensitive to tryptophan shortage, which causes them to undergo cell cycle arrest in G1. Degradation of tryptophan via IDO expressed by tumors or by the placenta inhibits T-cell proliferation and, as a result, prevents immunological rejection of the tumor or fetus.^{134,137,138} In addition, IDO present in the ocular lens has been implicated as a key factor in the development of senile cataracts.^{139,140}

Most of the known IDO inhibitors are tryptophan analogues active only at micromolar concentrations, making them marginal drug candidates.¹³⁷ As part of an ongoing program designed to find potent IDO inhibitors belonging to new structural classes, a library of marine invertebrate extracts was screened for their ability to inhibit purified recombinant human IDO *in vitro*. A MeOH extract of the Northeastern Pacific hydroid *Garveia annulata* was among the first hits exhibiting potent enough IDO inhibitory activity to justify further investigation. Details of the isolation and structure elucidation of *G. annulata* metabolites along with a discussion of their biological activity are described below.

3.2. IDO and the kynurenine pathway

Indoleamine 2,3-dioxygenase (IDO; EC 1.13.11.42) is a heme-containing intracellular enzyme that catalyses the initial and rate-limiting step in the metabolism of tryptophan, oxidation of tryptophan to *N*-formylkynurenine (1), along the kynurenine pathway in mammalian cells (Figure 3.1).^{141,142}

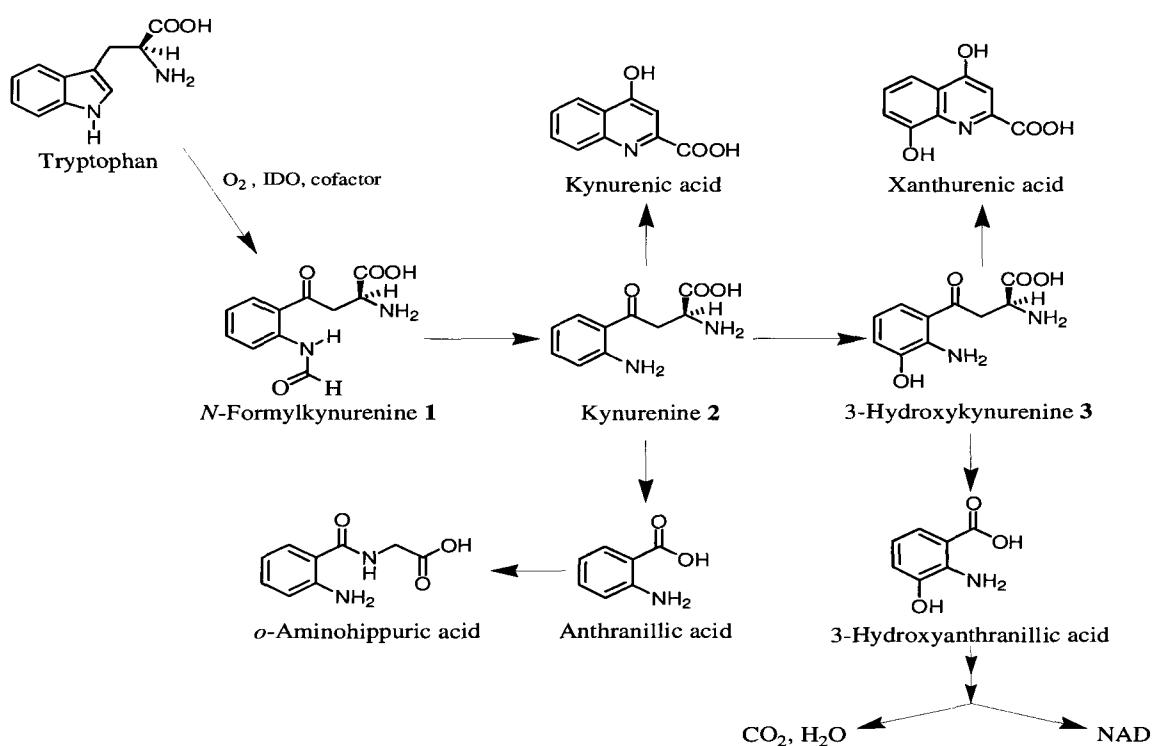
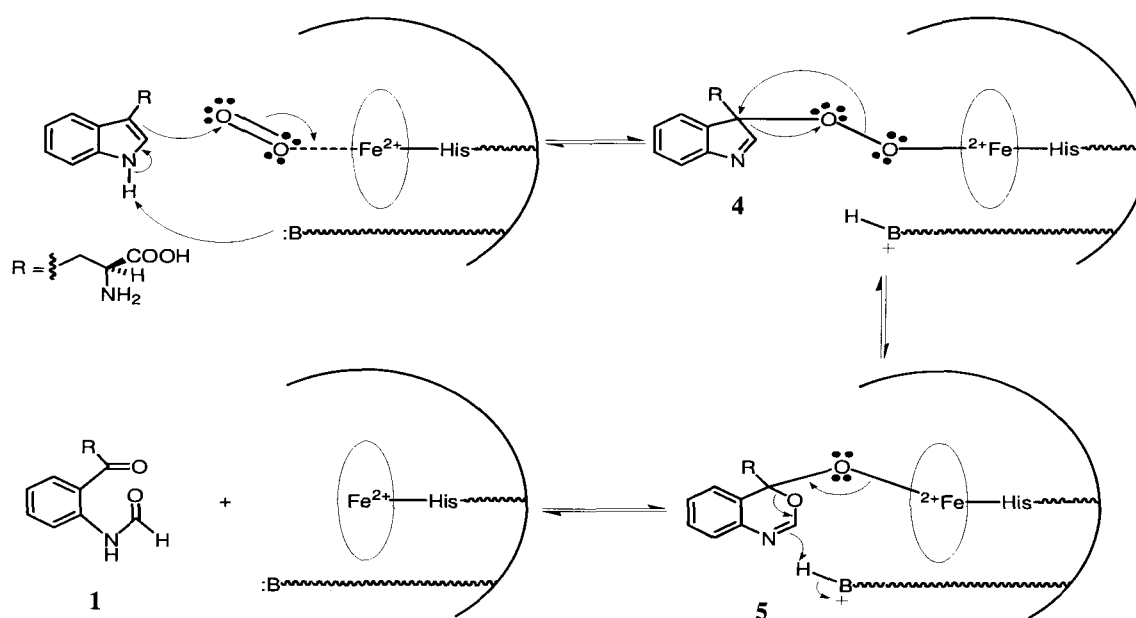


Figure 3.1. Tryptophan metabolism in the kynurenine pathway.^{141,143}

All proposed mechanisms for this reaction initiate with O₂ and tryptophan binding (the order is unknown) at the active site (Scheme 3.1).¹⁴³ The active form of IDO has the heme iron in the ferrous (Fe²⁺) oxidation state and, although the enzyme is prone to auto-oxidation, the primary catalytic effect does not involve changes in oxidation state (the ferric form Fe³⁺ is inactive). Formation of intermediate (4) may occur via ionic (shown), pericyclic or radical

processes. The following step most likely proceeds through a concerted Criegee-type rearrangement to yield a labile cyclic hemiacetal (**5**), which is released to generate *N*-formylkynurenine (**1**).¹⁴³



Scheme 3.1. Possible mechanism for the IDO-catalyzed formation of *N*-formylkynurenine (**1**).¹⁴³

IDO was originally discovered in 1967 in the rabbit intestine.¹⁴⁴ It is found under basal conditions in the epididymis, thymus, gut, lung, placenta, and some subsets of dendritic cells.¹⁴⁵⁻¹⁴⁷ Recent studies indicate that IDO plays an important immunosuppressive function.¹⁴⁸ T lymphocytes must divide to be activated, but this process is particularly sensitive to availability of tryptophan. Cells expressing IDO can deplete their microenvironment of tryptophan, promoting T lymphocyte arrest in the G1 phase of the cell cycle. Additionally, tryptophan metabolites from the kynurenine pathway have a strong T cell inhibitory action.¹⁴⁵

IDO is highly expressed in the placenta where it plays a significant role in the immunosuppressive and tolerogenic mechanism contributing to maternal tolerance towards the

allogeneic fetus during pregnancy.^{145,149} It has also been implicated in regulation of autoimmune disorders and suppression of transplant rejection.¹⁴⁶ Furthermore, IDO was associated with depression as well as other neurological and psychiatric diseases through interference with serotonin production and accumulation of neurotoxic kynurenine metabolites.¹⁴⁸

The immunosuppressive function of IDO can be exploited by tumor cells to escape immune detection and achieve tolerance, a hallmark in carcinogenesis and cancer progression.¹⁴⁵ IDO has been found in cancer cells in a variety of human malignancies.^{133,148} IDO is also expressed by host antigen-presenting cells (APC's) at the periphery of tumors, and draining lymph nodes of breast cancer and melanoma, where appropriate T lymphocytes would otherwise be activated.^{149,150} In patients with malignant melanoma, the presence of these IDO-expressing cells (APC's) in sentinel lymph node biopsies was correlated with a significantly worse clinical outcome.¹⁴⁶ In murine models, transfection of immunogenic tumor cell lines with recombinant IDO renders them immunosuppressive and lethally progressive *in vivo*.¹⁴⁶ Expression of IDO by ovarian,¹⁵¹ endometrial¹⁴² and colorectal cancer¹⁵² cells has been found to be a significant predictor of poor prognosis. Thus, expression of IDO, either by host cells or by tumor cells, seems associated with poor outcome in a number of clinical settings.

In addition, IDO is expressed in the ocular lens where it participates in the UV filter synthetic pathway.¹⁵³ In 2001, Takikawa and coworkers demonstrated that IDO is the first enzyme in the UV filter biosynthesis.¹⁴⁰ Some of the tryptophan degradation products (Scheme 3.1) bind to the lens major protein, crystalline, and accumulate with time in a process linked to the formation of age-related nuclear cataracts.^{139,154} It is also known that 3-hydroxykynurenine (**3**) is readily oxidized in the presence of just trace amounts of oxygen, generating mostly orange, red, brown or black pigments.¹³⁹ Thus, oxidation of the protein-bound UV filters could possibly

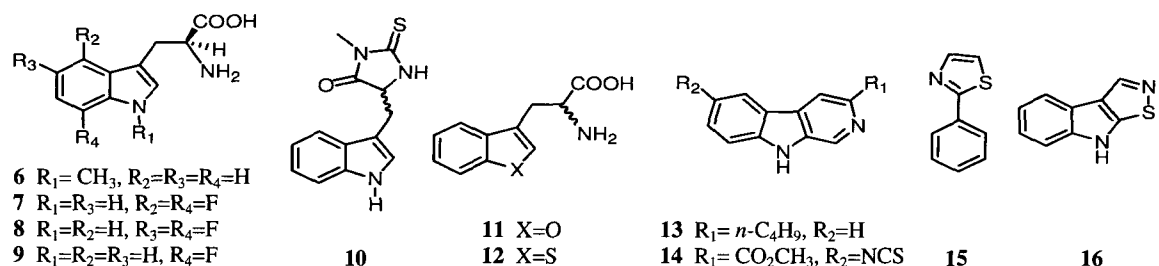
lead to the range of lens colors that are characteristic of age-related nuclear cataracts. This opacification may be preventable by drug-induced suppression of lens IDO activity.¹⁴⁰

From a therapeutic standpoint, drugs that inhibit IDO potentially represent a novel class of immunomodulatory agents, targeting a pathway that might be involved mechanistically in the ability of tumors to evade the host immune system. Their initial application is likely to be as adjuvants, used in combination with existing vaccination, conventional chemotherapy and radiation strategies.¹⁴⁹

3.3. Current IDO inhibitors and the bioassay

To date, the most potent competitive IDO inhibitors known are tryptophan analogues, active only at concentrations of ~10 μM and greater (Table 3.1).¹³⁴ Clearly, more potent and effective IDO inhibitors are required as lead compounds for drug therapy. The most widely studied IDO inhibitor is 1-methyltryptophan (**6**),¹³² which has been used to demonstrate proof-of-principle in cancer therapy.¹⁴⁸ Recently, it was shown that administration of either **6** or thiohydantointryptophan (**10**) potentiates the efficacy of DNA-damaging chemotherapeutic agents in the inhibition of tumor growth in mouse models.^{132,135} However, **6** is poorly water-soluble and difficult to administer to animals,^{137,148} and even though **10** is more potent and water-soluble than **6**, its availability in plasma is low.¹⁴⁸

In 1984, a group of β -carboline (e.g. **13** and **14**) were reported to exhibit IDO inhibition.¹⁵⁵ They were classified as noncompetitive inhibitors upon evidence of direct interaction with the heme iron as an electron donor ligand (instead of O_2),¹⁵⁶ and remain as the most common structures for this type of IDO-active compounds.¹⁴³ β -Carboline derivatives, however, possess neuroactivity as benzodiazepine receptor ligands, which could cause problematic side effects in cancer therapy.¹⁵⁷

Table 3.1. Some IDO inhibitors with high *in vitro* activity.^{143,148}

Type	Compound	K _i (μM)
Competitive	(<i>S</i>)-Methyltryptophan (6)	34
	(<i>S</i>)-4,7-Difluorotryptophan (7)	40
	(<i>S</i>)-5,7-Difluorotryptophan (8)	24
	(<i>S</i>)-7-Difluorotryptophan (9)	37
	(<i>R,S</i>)-Thiohydantointryptophan (10)	11.4
	(<i>R,S</i>)-2-Amino-3-benzofuran-3-yl-propionic acid (11)	25
	(<i>R,S</i>)-2-Amino-3-benzo[<i>b</i>]thiophen-3-yl-propionic acid (12)	70
Noncompetitive	3-Butyl-9 <i>H</i> -β-carboline (13)	3.3
	6-Isothiocyanato-9 <i>H</i> -β-carboline-3-carboxylic acid methyl ester (14)	8.5
	4-Phenylimidazole (15)	4.4
	Brassilexin (16)	5.4

Recognizing the need for new IDO inhibitors belonging to different structural classes, the Mauk research group in the Department of Molecular Biology at UBC modified and adapted an IDO-activity assay published by Takikawa and colleagues in 1988,^{138,158} in order to develop a high-throughput bioassay capable of screening libraries of marine invertebrate extracts in a multiwell plate format. A mixture containing phosphate buffer (pH 6.5), ascorbic acid, catalase, methylene blue, L-tryptophan and recombinant IDO, was added to a solution of the invertebrate extract and the resulting reaction crude was allowed to react at 37°C for 30 min (Figure 3.2). The process was stopped by addition of trichloroacetic acid, followed by heating at 65°C to afford kynurenine (2). Treatment of 2 with *p*-dimethylaminobenzaldehyde in acetic acid generates the yellow adduct *p*-(*N*-dimethylaminobenzylidene)kynurenine (17). The amount of this product

formed was monitored at 480 nm as a measure of IDO activity. As shown in Figure 3.2, extracts with inhibitory activity displayed uncolored wells, since the enzyme cannot oxidize tryptophan to *N*-formylkynurenine (1), the precursor of 2 and 17. In total, approximately 4500 extracts from a marine invertebrate extract library were screened.

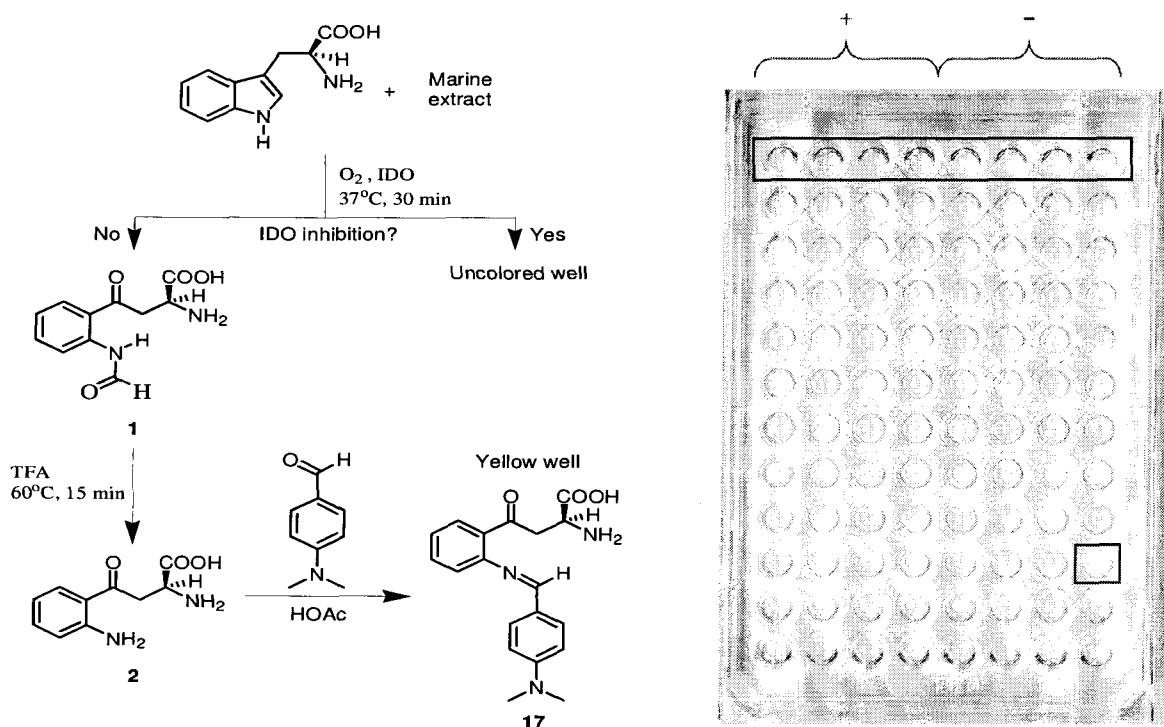


Figure 3.1. Reactions involved in the new high throughput IDO bioassay developed by Mauk and Vottero.¹⁵⁶ Control column: (+), wells with IDO; (-), wells without IDO.¹⁵⁶

3.4. Secondary metabolites from hydrozoans

The phylum *Cnidaria* encompasses a diverse collection of marine invertebrates that include hard and soft corals, gorgonians, sea pens, jellyfish, and sea anemones. Hydroids, a large class of cnidarians (around 3000 species), are generally small and somewhat inconspicuous.¹⁵⁹ In the last three decades, marine natural products researchers have successfully isolated a large number of secondary metabolites from soft corals, sea pens and zooanthids,¹⁶⁰⁻¹⁶³ but hydroids

have received very little attention.^{159,164} According to MarinLit,^{137,165} from a total of 2281 structures reported for cnidarians, only 60 were found from hydroids.¹³⁷

The polyhydroxylated steroid (**18**, Figure 3.3), isolated by Cimino¹⁶⁶ in 1980 from *Eudendrium* sp. collected in the Bay of Naples, was the first publication on a natural compound from a hydroid. In the following years, Fattorusso and coworkers¹⁶⁷⁻¹⁶⁹ reported the distribution of mono and polyhydroxylated sterols such as (**19**), in four Mediterranean hydroids. The same source yielded three brominated β -carboline derivatives similar to (**20**).¹⁷⁰ Fusetani¹⁷¹ reported in 1986 one of the first phosphate-containing marine natural products (**21**) along with two more phosphorylglycerylethers exhibiting hemolytic activity, from the hydroid *Solanderia secunda* collected in the Gulf of Sagami, Japan. Around a decade later in 1996, the same hydroid was collected offshore of Jaeju Island (Korea), and its DCM/MeOH extract was purified by Shin and coworkers¹⁷² to give solandelactones A (**22**) to I, nine lactonized oxylipins exhibiting moderate inhibitory activity against Farnesyl Protein Transferase.

A study¹⁷³ focused on predator-prey interactions in animals of the pelagic *Sargassum* communities of the western Atlantic Ocean, found that among four common hydroids growing on the *Sargassum*, only *Tridentata marginata* was not eaten by the most abundant predator, the Planehead fish. Bioassay-guided fractionation led Lindquist, Lobkovski and Clardy, to isolate tridentatols A (**23**) to C in 1996,¹⁷⁴ and tridentatols D-H in 2002.¹⁷⁵ Given the UV-absorbing characteristics and their high tissue concentrations, these compounds were also proposed to function as sunscreens, protecting *T. marginata* from intense levels of solar radiation typical of near-surface oceanic habitats.¹⁷⁴ Potent antioxidant activity against human low density lipoprotein (LDL) was later reported for tridentatol A (**23**).¹⁷⁶ Corydendramines A (**24**) and B, two piperidinol metabolites isolated from *Corydendrium parasiticum* L. by Lindquist, Shigematsu and Pannel,¹⁷⁷ showed similar predator deterrence activity.

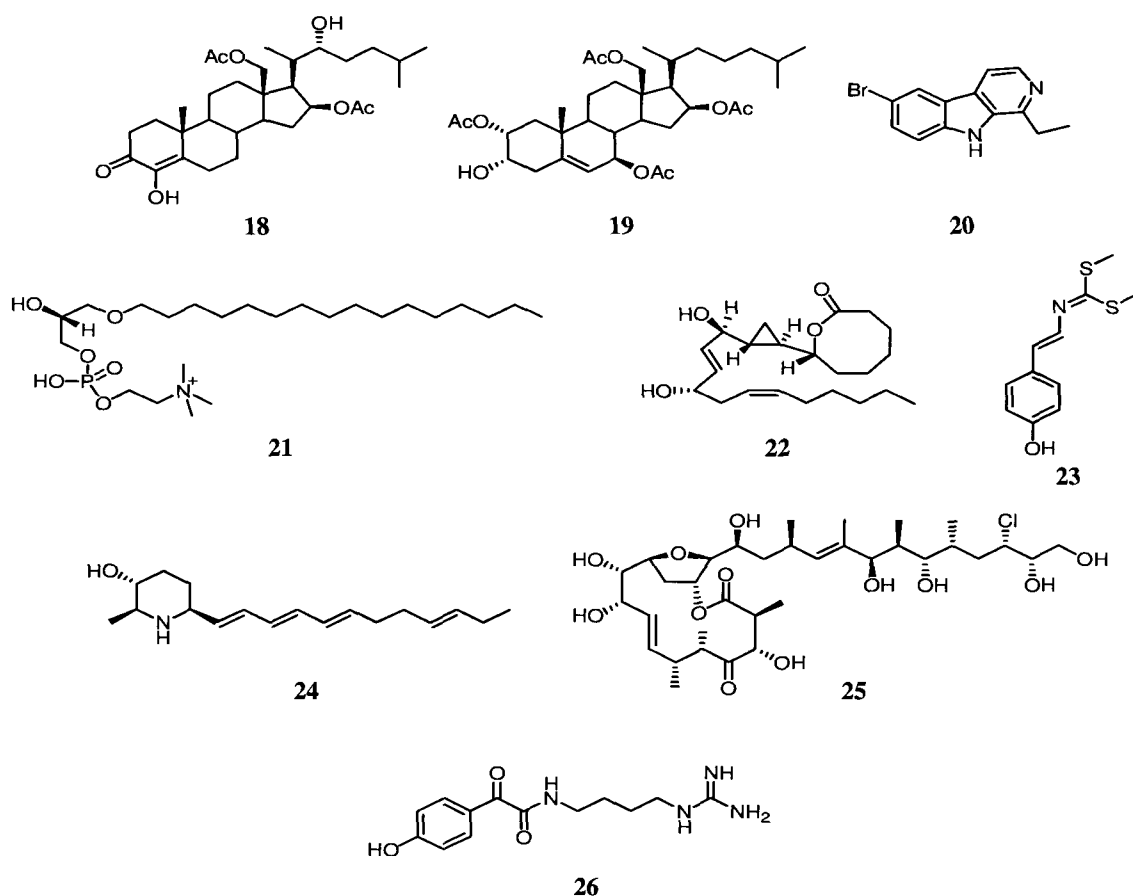


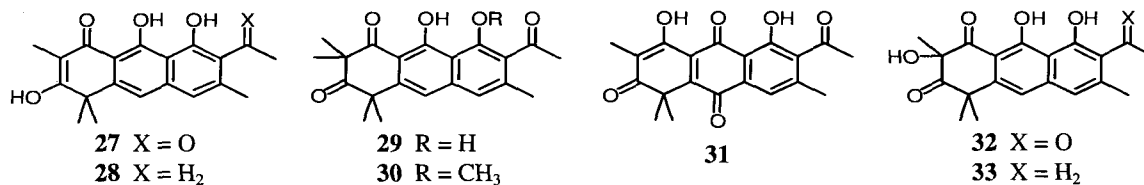
Figure 3.3. Representative structures for secondary metabolites isolated from hydroids: cholest-4-en-4,16 β ,18,22*R*-tetrol-3-one 16,18-diacetate (**18**),¹⁶⁶ cholest-5-en-2 α ,3 α ,7 β ,15 β ,18-pentol 2,7,15,18-tetraacetate (**19**),¹⁶⁸ 6-bromo-1-ethyl- β -carboline (**20**),¹⁷⁰ 1-hexadecyl-*sn*-glycerol-3-phosphorylcholine (**21**),¹⁷¹ solandelactone A (**22**),¹⁷² tridentatol A (**23**),¹⁷⁴ corydendramine A (**24**),¹⁷⁷ lytophilippine A (**25**),¹⁷⁸ and *Campanularia* sp. metabolite (**26**).¹⁷⁹

Recently, lytophilippines A (**25**) to C, three new chloro-containing macrolides, were found by Rezanka, Hanus and Dembitsky,¹⁷⁸ in the Red Sea hydroid *Lytocarpus philippinus*. The compounds exhibited moderate antibacterial activity, as well as crown gall tumor inhibition and potent toxicity against *Artemia salina* (brine shrimp toxicity assay), suggesting a role in the hydroid's defense. Finally, Houssen and Jaspars¹⁷⁹ examined the hydroid *Campanularia* sp. collected from New Zealand and isolated (**26**), with no relevant activity.

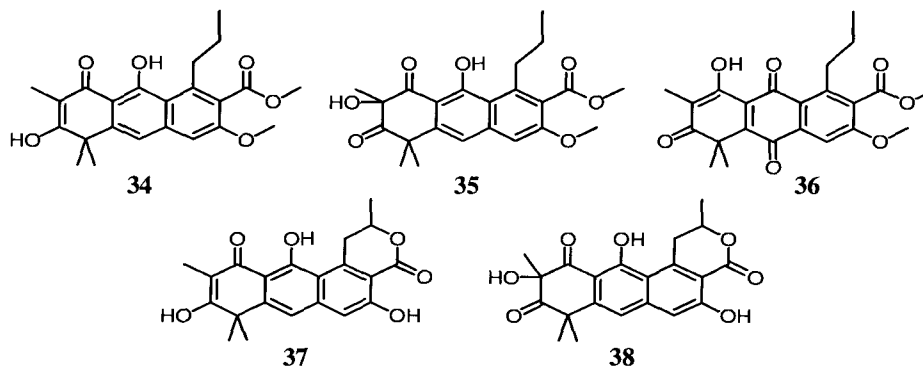
3.5. Minor metabolites from *Garveia annulata*

One more representative family of metabolites isolated from hydroids must be added to those ones depicted in Figure 3.3.

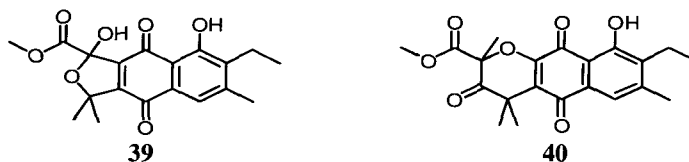
Garveatins



Garvins



Annulins



Garvalones

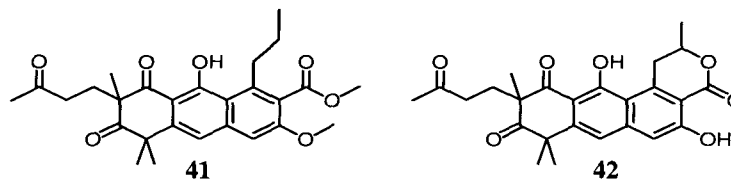
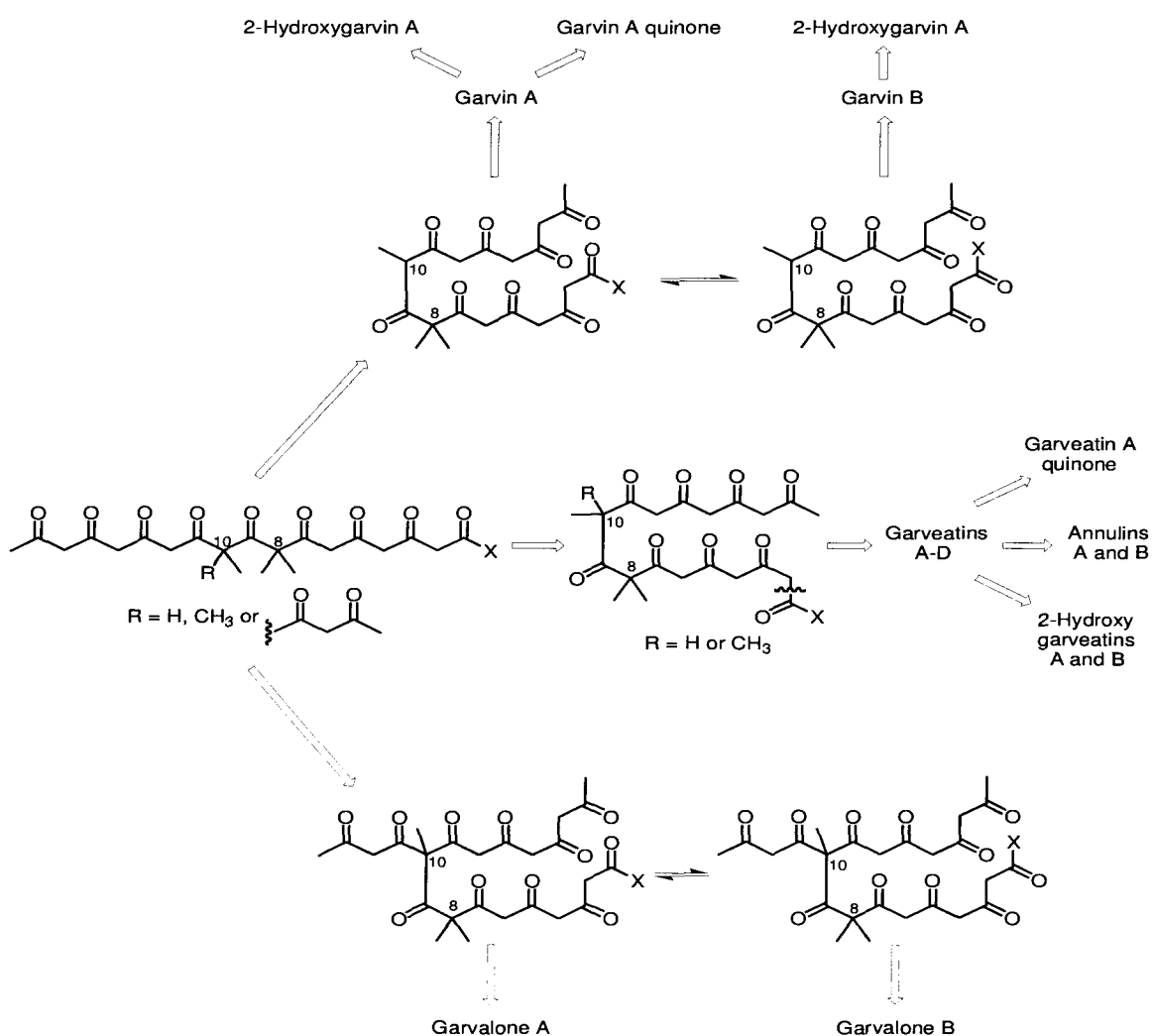


Figure 3.4. Secondary metabolites isolated from *G. annulata*: garveatins A (27),¹⁵⁹ B (28), C (29),¹⁶⁴ and D (30),¹⁸⁰ garveatin A quinone (31), and 2-hydroxygarveatins A (32) and B (33); garvin A (34), 2-hydroxygarvin A (35), garvin A quinone (36),¹⁶⁴ garvin B (37), and 2-hydroxygarvin B (38),¹⁸⁰ annulins A (39) and B (40);¹⁸¹ garvalones A (41) and B (42).¹⁸⁰

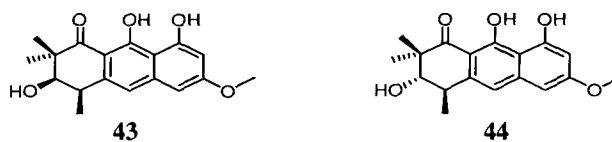
In 1985, Fahy and Andersen¹⁵⁹ reported garveatin A (**27**, Figure 3.4), the first compound isolated from *G. annulata*. Metabolite (**27**), which exhibited mild antimicrobial activity, was obtained as orange needles via bioassay-guided fractionation of methanolic extracts. In the following months, additional reports on 16 new *G. annulata* polyketide secondary metabolites^{164,180,181} would follow. They can be organized into four families according to the number of carbons in the putative polyketide precursor and other structural similarities (Figure 3.4).



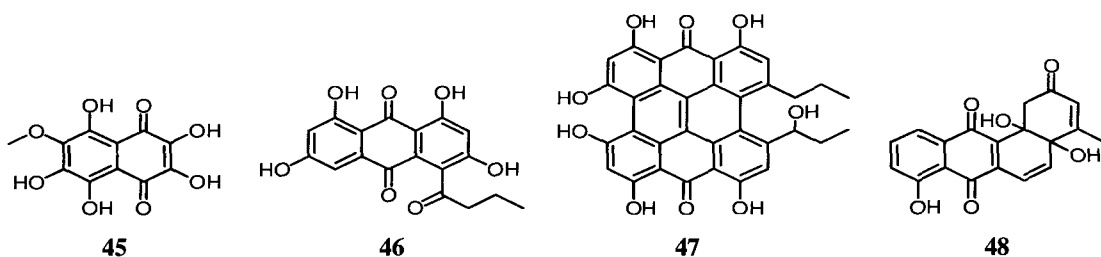
Scheme 3.2. Proposed biogenesis of *G. annulata* secondary metabolites.

Garveatins, garvins, annulins and garvalones, are classical examples of polyketide derived secondary metabolites. At the time of their isolation, they represented the first examples of polyketide metabolism from coelenterates.¹⁶⁴ All of them are proposed to be biosynthesized from similar nonaketide precursors exhibiting the same methylation pattern at C8 and C10. Additional variability is introduced at C10, limited to three substituents: a proton, a methyl, or a diketobutyl branch (Scheme 3.2). Decarboxylation at C1 generates the only methyl substituent for the aromatic system in the garveatins. Different folding patterns give rise to an ethyl substituent or a δ -lactone in garvins and garvalones. Secondary biogenetic transformations, such as hydroxylation at C10 and oxidation of the central ring to a quinone,¹⁸⁰ may be responsible for the formation of 2-hydroxygarveatin A (**32**), B (**33**) and 2-hydroxygarvin A (**35**), as well as garveatin A and garvin A quinones (**31** and **36**). 2-Hydroxygarveatin B (**33**) is possibly an intermediate in the biogenesis of annulins A (**39**) and B (**40**), considered to be degradation products of the garveatins.¹⁸¹

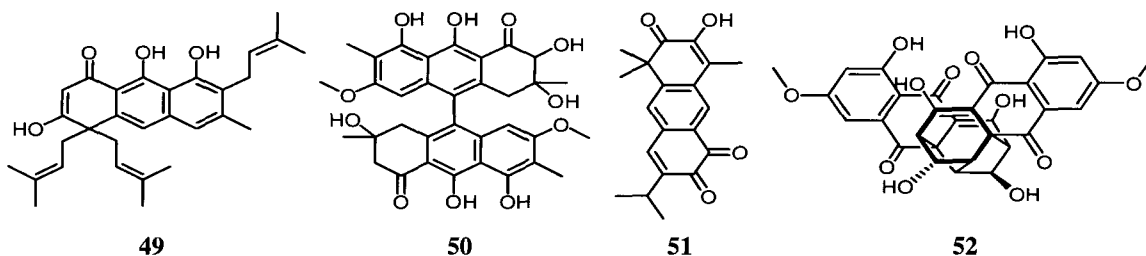
G. annulata metabolites are closely related to the cytotoxic abietinarins A (**43**) and B (**44**), also isolated by the Andersen research group shortly after the garveatin publications.¹⁸² *Abietinaria* sp., collected off the southern coast of Vancouver Island, became the second hydroid reported to produce 1-[4*H*]-anthracenone-based polyketide-derived metabolites. Abietinarin A (**43**) exhibited significant *in vitro* cytotoxicity.



Additional marine-derived naphthoquinone and anthraquinone compounds include a series of pigments (e.g. **45–47**), presumably polyketide-derived and isolated from echinoderms,^{183,184} as well as a benz[*a*]anthraquinone antibiotic (**48**) from a marine actinomycete *Chania* sp.¹⁸⁵



Condensed polycyclic aromatic systems are more common in terrestrial species of plants and fungi. Berries, leaves, bark and root bark in specimens of the genera *Vismia*,^{186,187} *Cassia*^{188,189} and *Gasteria*,¹⁹⁰ have afforded a series of mono and dimeric anthranoids similar to 49 and 50. Rare diterpene *ortho*-quinones such as pygmaeocine E (51), were found in the roots of several medicinal plants used as a folk remedy in China to reduce inflammation and cure malaria.¹⁹¹ Cytoskyrin A (52), a bisanthraquinone highly active in an anticancer bioassay¹⁹² was isolated from an endophytic fungus collected in Costa Rica.



3.6. Isolation of IDO-active minor metabolites

Garveia annulata is a small orange hydroid encountered in rocky subtidal habitats from Alaska to Southern California during the winter and spring months.¹⁹³ It is reasonably abundant in Barkley Sound, British Columbia, especially in winter.¹⁸¹ In its polyp stage, it possesses small tentacles supported by a hydrostatic skeleton that allows the different colonies to stay together in bush-like structures, and keep their shape in the moving tides (Figure 3.5). As a colonial hydrozoan, it is composed of a number of specialized polyps with feeding, reproductive and protective functions. Its medusa stage is sexually active, but has a limited lifespan.¹⁹⁴

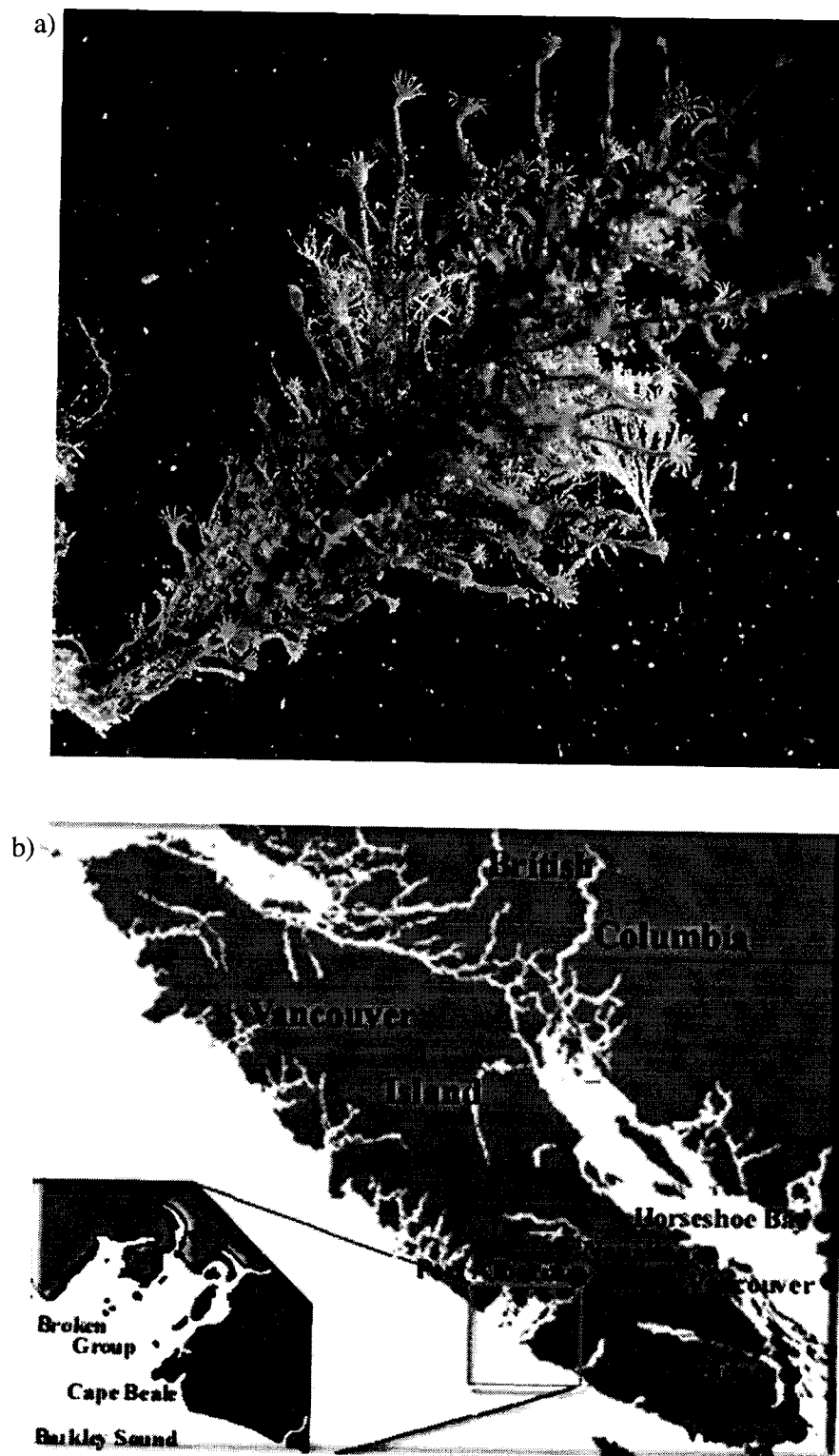


Figure 3.5. a) A bush-like colony of *G. annulata*; b) Map of collection site.

Bioassay-guided fractionation of a *G. annulata* methanolic extract (0.35 g) as detailed in the Experimental section, led to the purification and structure elucidation of two of the most potent IDO inhibitors known to date; the new metabolite annulin C (0.3 mg, 0.0006% wet wt) obtained as a yellow oil, and the known annulin B (**40**) (0.6 mg, 0.001% wet wt). Such promising results prompted the recollection and examination of additional *Garveia* specimens.

Samples of *G. annulata* (424 g wet wt) were collected by hand using SCUBA at depths of 10-15 m off the coast surrounding the Broken Islands, Barkley Sound, on June 2003 (Figure 3.5). Specimens were frozen immediately upon collection and transported back to UBC in coolers packed with dry ice, where they were immediately extracted using MeOH.

Repetitive extraction and solvent concentration for a week yielded an IDO-active brown gum (2.5 g), which was fractionated as described in the Experimental section. This second batch of specimens afforded the new metabolite garveatin E (0.5 mg, 0.0001%, wet wt) as a pale yellow oil, and the previously reported 2-hydroxygarveatin B (**33**) (1.1 mg, 0.0002%, wet wt), annulin A (**39**) (0.5 mg, 0.0001%, wet wt), garveatins A (**27**) (34.0 mg, 0.008%, wet wt) and C (**29**) (0.5 mg, 0.0001%, wet wt), 2-hydroxygarvin A (**35**) (3.7 mg, 0.0009, wet wt), and garvin A quinone (**36**) (0.4 mg, 0.00009%, wet wt).

Once all IDO-active fractions were elucidated, it was decided to attempt isolating *G. annulata* metabolites with reduced or zero inhibition, in order to show that activity resides preferentially in the annulin naphthoquinone substructure, and confirm that garveatins, garvins and garvalones are less potent. Thus, exploration of the inactive fractions yielded the new compounds 2-hydroxygarveatin E (0.4 mg, 0.00009%, wet wt) and garvin C (0.3 mg, 0.00007%, wet wt) as pale yellow oils. Due to limited amounts of all the new *G. annulata* compounds, the ¹³C-NMR data was derived from HMQC and HMBC spectra (sections 3.6.1-3.6.4, and Experimental), and some quaternary carbons were not assigned.

3.6.1. Annulin C

Annulin C (**53**) was isolated as a yellow oil that gave an $[M]^+$ ion at m/z 374.1367 in the HREIMS, appropriate for a molecular formula of $C_{20}H_{22}O_7$. The 1D and 2D NMR data obtained for **53** showed a strong resemblance to the data reported for annulin A (**39**),¹¹ indicating that the molecules were closely related (Figure 3.6). The major difference in the 1H NMR spectra of the two compounds was the absence in the spectrum of annulin C (**53**) (Figure 3.6b, Table 3.2) of a singlet that could be assigned to the hemiketal C8-OH present in the spectrum of **39** (δ 4.85), and its replacement by a methyl singlet at 3.45 ppm (H18). Through HMQC, this new methyl resonance was shown to belong to a carbon at 51.7 ppm, whereas the HMBC spectrum showed a correlation (Table 3.2, Figure 3.7) from H18 to a carbon resonance at δ 106.8 (C8), typical of a ketal functionality. Therefore, it was evident that the hemiketal at C8 in annulin A (**39**) had been replaced by a methyl ketal in annulin C (**53**).

The remaining HMBC correlations established two main fragments for the structure of annulin C:

- I. Ketal-*gem* dimethyl fragment: with methyl H10 (s, δ_H 3.82, δ_C 52.5) correlating to the carbonyl C9 at 167.2 ppm; and both methyl singlets H19/H20 showing cross peaks with quaternary carbons C11 (δ_C 88.3) adjacent to an oxygen atom, and C12 (δ_C 154.3) in an aromatic system (Figure 3.7).
- II. Branched phenol fragment: displaying very informative correlations from methylene H2 (δ_H 2.75, q, $J = 7.5$ Hz, δ_C 19.4) and methyl H17 (s, δ_H 2.41, δ_C 19.7), that allowed assignment of their position in an aromatic ring and the relative location of methine H15 (s, δ_H 7.44, δ_C 121.5) and sp^2 carbon C4 (δ_C 160.3), attached to a hydroxyl group (s, δ_H 12.2) (Figure 3.7).

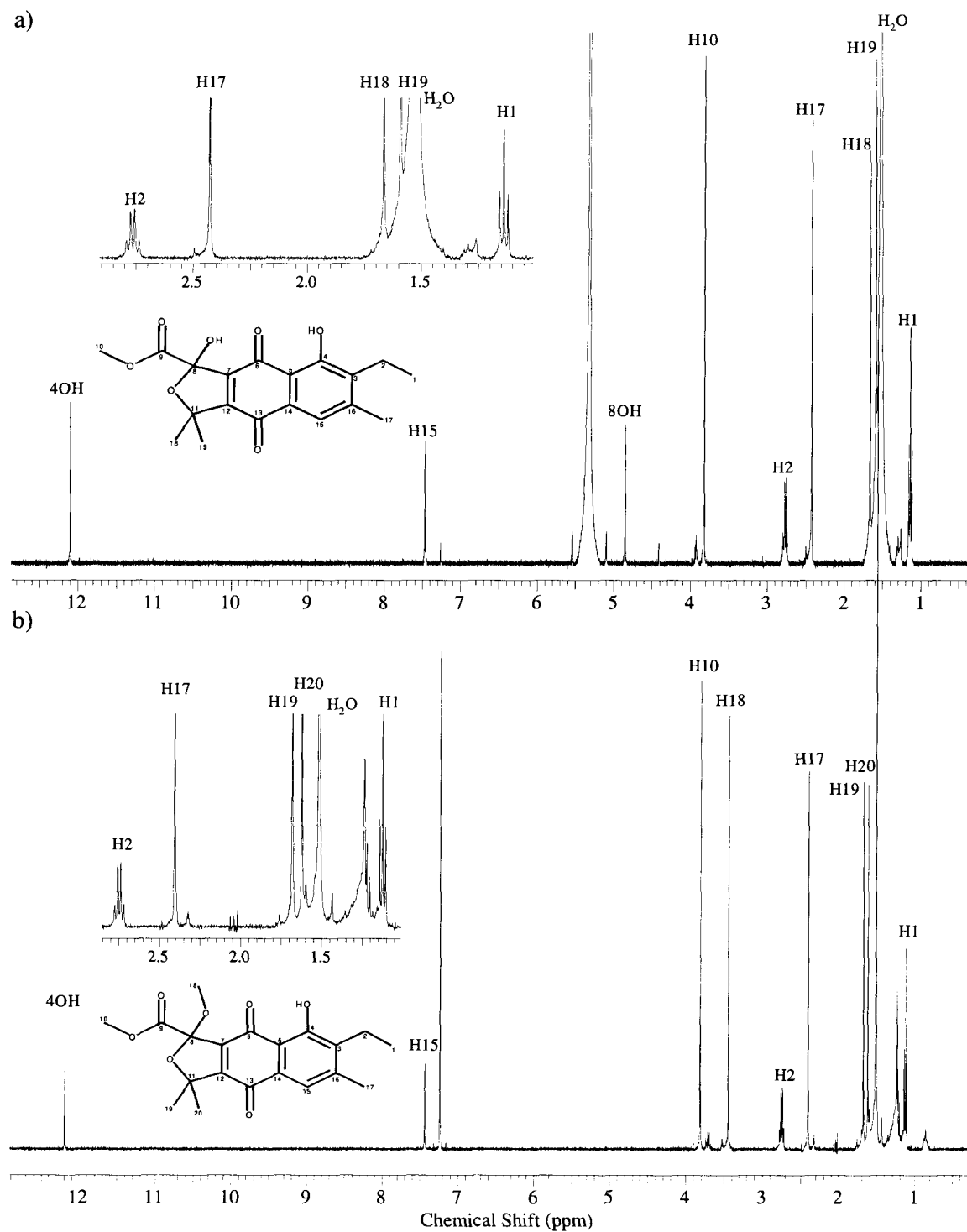
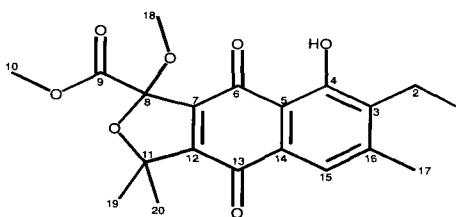


Figure 3.6. $^1\text{H-NMR}$ spectrum of a) annulin A (**39**) (recorded in CD_2Cl_2 at 400 MHz), and b) annulin C (**53**) (recorded in CDCl_3 at 400 MHz).

Table 3.2. NMR data for annulin C (**53**) (recorded in CDCl₃).

Carbon No	¹³ C δ (ppm) ^a	¹ H δ (ppm) (mult, J (Hz)) ^a	HMBC ^a (H→C)	COSY ^a (H→H)
1	12.8	1.12 (t, J = 7.5 Hz)	C2, C3	H2
2	19.4	2.75 (2q, J = 7.5 Hz)	C1, C3, C4, C16	H1
3	140.0			
4	160.3	OH 12.2 (s)	C4	
5 ^b				
6 ^b				
7 ^b				
8	106.8			
9	167.2			
10	52.5	3.82 (s)	C9	
11	88.3			
12	154.3			
13 ^b				
14 ^b				
15	121.5	7.44 (s)		
16	145.3			
17	19.7	2.41 (s)	C3, C15, C16	
18	51.7	3.45 (s)	C8	
19	26.4	1.68 (s)	C11, C12, C20	
20	26.4	1.62 (s)	C11, C12, C19	

^a According to HMQC and HMBC recorded at 400 MHz. ^b Not assigned.

After accounting for the atoms already assigned from the NMR data of substructures I and II, a C₅O₂ fragment remained to be allocated. Based on these atoms, and by comparing the chemical shift of C12 with NMR data for annulin A (**39**), it was evident that a *para*-quinone was connecting I and II.

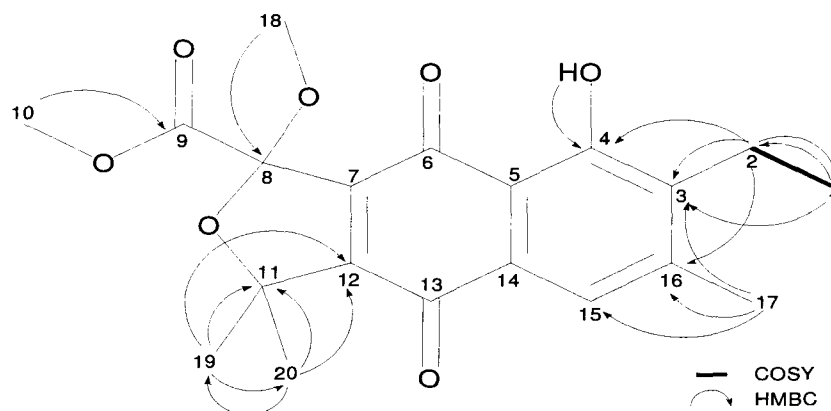
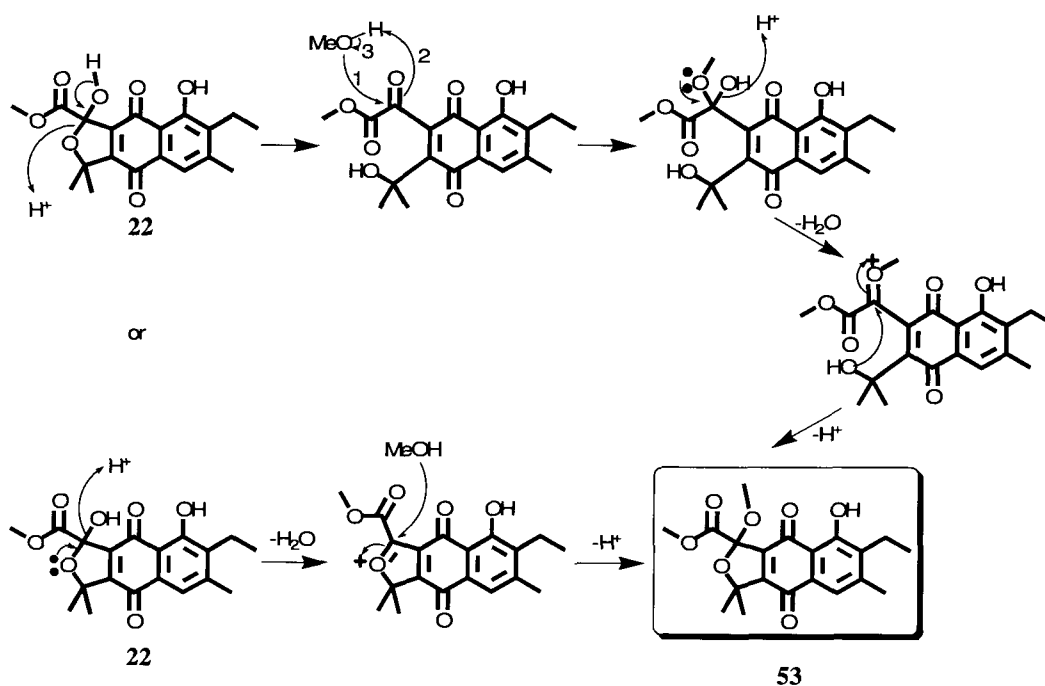


Figure 3.7. Summary of COSY and HMBC correlations for annulin C (**53**).

It is important to point out that annulin C (**53**) may be an isolation artifact in which the C8 methyl ketal has been formed by reaction of the co-occurring metabolite annulin A (**39**) with MeOH, according to Scheme 3.3.



Scheme 3.3. Proposal for the formation of annulin C (**53**) from annulin A (**22**).

3.6.2. 2-Hydroxygarveatin E

2-Hydroxygarveatin E (**55**), isolated as a yellow oil, gave a $[M+Na]^+$ ion at m/z 379.1160 in the positive ion HRESIMS, consistent with a molecular formula of $C_{20}H_{20}O_6$ (calculated for $C_{20}H_{20}O_6Na$: 379.1158), requiring 11 sites of unsaturation. The 1H -NMR spectrum of **55** (Figure 3.8, Table 3.3) contained resonances that could be assigned to an ethyl fragment (δ_H 1.12, t, $J = 7.7$ Hz, H1; δ_H 2.67, q, $J = 7.7$ Hz, H2/H2'), four methyl groups (all singlets, δ_H 1.44, H19; δ_H 1.56, H18; δ_H 1.76, H20; δ_H 2.21, H17), an aromatic methine (δ_H 7.72, s, H13), and a phenol OH (δ_H 13.37, s, 6OH), accounting for 19 of a total of 20 protons in the molecule.

HMBC correlations (Table 3.3, Figure 3.9) observed between methyl H1 and a carbon resonance at 149.2 ppm (C3), between methylene H2 and quaternary sp^2 carbon resonances at δ_C 144.3 (C16), 149.2 (C3) and 188.6 (C4), and between H17 and carbon resonances at δ_C 144.3 (C16), 149.2 (C3), and 183.5 (C15), suggested that the methyl and ethyl residues were vicinal substituents on a *para*-quinone substructure. The aromatic methine H13 showed an HMBC correlation to a quinone carbonyl resonance at 183.5 ppm (C15), which situated C13 (δ_C 115.2) two bonds away from the carbonyl. Additional HMBC correlations between H13 and sp^2 carbons at δ_C 114.5 (C5) and δ_C 122.3 (C14), and between 6OH (δ_H 13.27) and carbons at δ_C 114.5 (C5), δ_C 122.3 (C7), and δ_C 160.4 (C6) were consistent with placement of the phenol-bearing carbon C6 two bonds away from the second quinone carbonyl C4.

The two methyl resonances H19 and H20 displayed HMBC correlations to each other as well as to carbon resonances at δ_C 48.4 (C11), 154.5 (C12), and 207.0 (C10), which demonstrated the methyls were geminal substituents on a quaternary carbon (C11) attached on one side to an aromatic ring and on the other side to a saturated ketone.

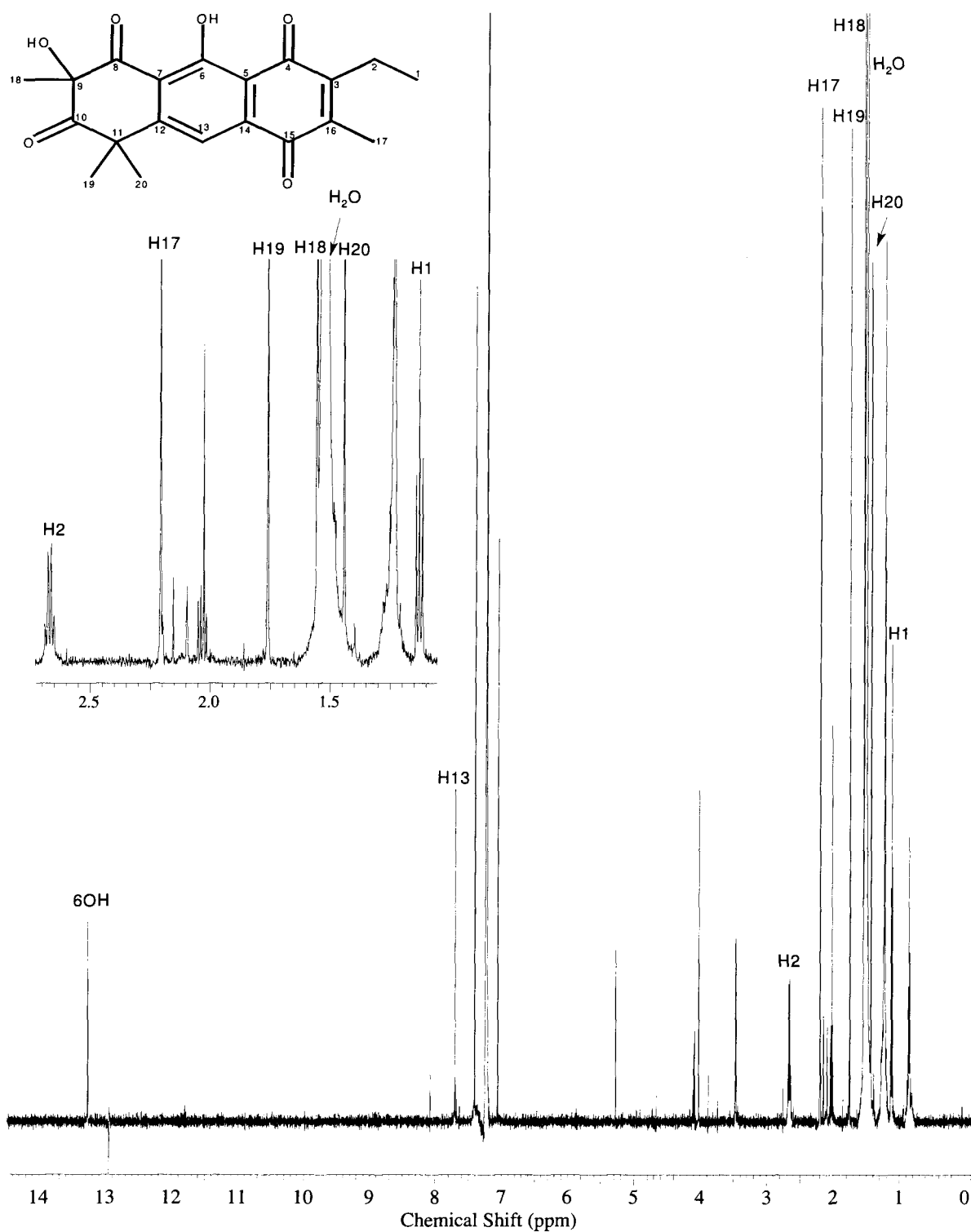
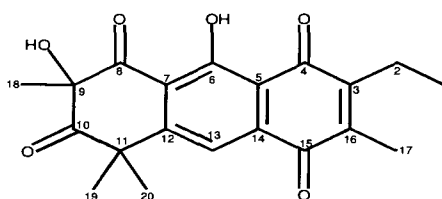


Figure 3.8. ¹H-NMR spectrum of 2-hydroxygarveatin E (55) (recorded in CDCl₃ at 600 MHz).

Table 3.3. NMR data for 2-hydroxygarveatin E (**55**) (recorded in CDCl₃).

Carbon No	¹³ C δ (ppm) ^a	¹ H δ (ppm) (mult, J (Hz)) ^a	HMBC ^a (H→C)
1	12.7	1.12 (t, J = 7.7 Hz)	C2, C3
2	19.8	2.67 (q, J = 7.7 Hz)	C1, C3, C4, C16
3	149.2		
4	188.6		
5	114.5		
6	160.4	OH 13.3 (s)	C5, C6, C7
7	122.2		
8	194.3		
9	83.9		
10	207.0		
11	48.4		
12	154.5		
13	115.2	7.72 (s)	C5, C14, C15
14	122.3		
15	183.5		
16	144.3		
17	12.3	2.21 (s)	C3, C15, C16
18	26.4	1.56 (s)	C8, C9, C10
19	26.2	1.76 (s)	C10, C11, C12, C20
20	30.0	1.44 (s)	C10, C11, C12, C19

^a According to HMQC and HMBC recorded at 600 MHz. ^b Not assigned.

HMBC cross peaks from methyl H18 to carbon resonances at δ_c 83.9 (C9), 194.3 (C8), and 207.0 (C10) showed that H18 was attached to a quaternary oxygenated carbon (C9), which was in turn flanked by two ketones. The oxygen atom on C9 had to be part of a hydroxyl functionality to account for the molecular formula of **55**.

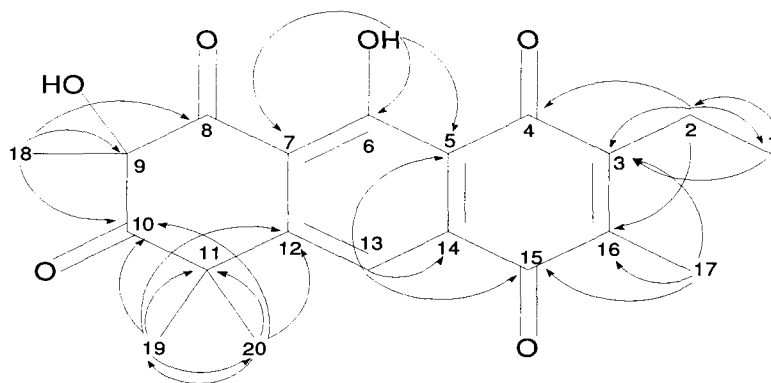


Figure 3.9. Summary of HMBC correlations for 2-hydroxygarveatin E (**55**).

There are two possible ways to attach the *gem*-dimethyl-bearing C11 and ketone termini C8 of the aliphatic fragment, to the unsatisfied valences of the naphthoquinone fragment (C7 and C12). The HMBC data showed that the *gem*-dimethyl-bearing carbon is linked to a carbon with a chemical shift of 154.5 ppm. This deshielded carbon (C12) could only be *meta* to the phenol (C6), leading to the structure **55** for 2-hydroxygarveatin E. Compound (**55**) is a C4/C15 *para*-quinone, analogue of the previously described metabolite 2-hydroxygarveatin B (**33**).

3.6.3. Garveatin E

Garveatin E (**54**), a very minor component of the extract, was obtained as a pale yellow oil that gave an $[M+Na]^+$ ion at m/z 363.1200 in the HRESIMS, consistent with a molecular formula of $C_{20}H_{20}O_5$ (calculated for $C_{20}H_{20}O_5Na$: 363.1208), which differed from the molecular formula of 2-hydroxygarveatin E (**55**) simply by loss of one oxygen atom. Analysis of the NMR data obtained for **54** indicated that it differed from 2-hydroxygarveatin E (**55**) simply by loss of the hydroxyl functionality at C9.

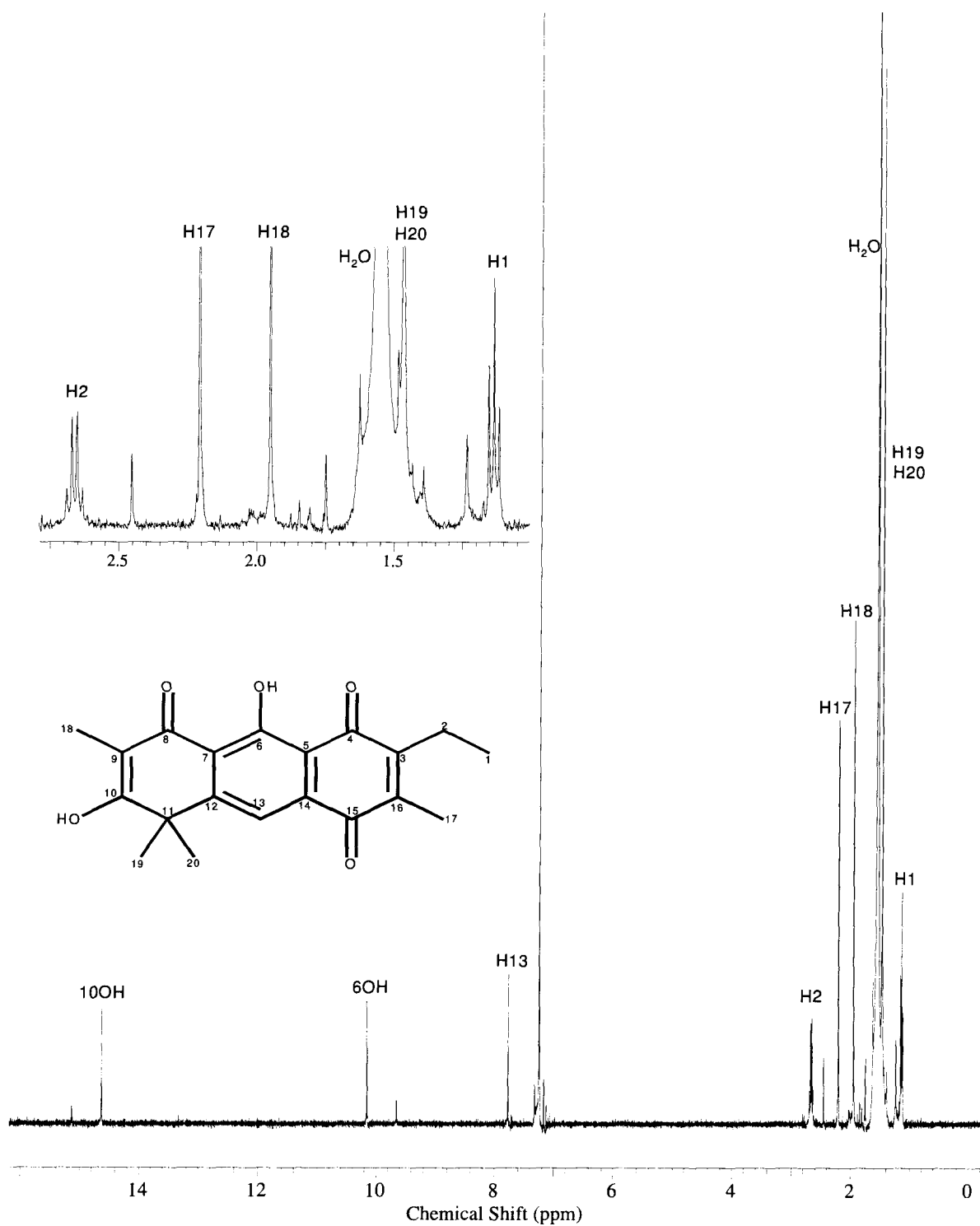
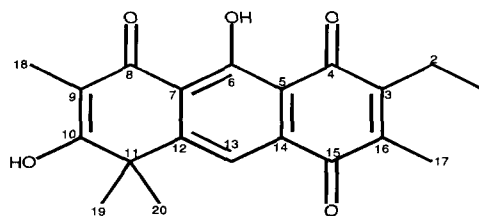


Figure 3.10. ¹H-NMR spectrum of garveatin E (54) (recorded in CDCl₃ at 400 MHz).

Table 3.4. NMR data for garveatin E (**54**) (recorded in CDCl₃).

Carbon No	¹³ C δ (ppm) ^a	¹ H δ (ppm) (mult, <i>J</i> (Hz)) ^a	HMBC ^a (H→C)
1	12.5	1.14 (t, <i>J</i> = 7.6 Hz)	C2, C3
2	19.5	2.66 (q, <i>J</i> = 7.6 Hz)	C1, C3, C4, C16
3	148.9		
4	188.9		
5 ^b			
6 ^b		OH 10.15 (s)	
7 ^b			
8	200.0		
9	113.3		
10	160.6	OH 14.6 (s)	
11	48.3		
12	114.4		
13	117.5	7.76 (s)	C11, C12, C14
14	122.2		
15	183.3		
16	145.3		
17	12.2	2.21 (s)	C3, C15, C16
18	7.18	1.95 (s)	C8, C9, C10
19	30.0	1.46 (s)	C11
20	27.7	1.46 (s)	C11

^a According to HMQC and HMBC recorded at 400 MHz. ^b Not assigned.

The ¹H NMR spectrum of (**54**) (Figure 3.11, Table 3.4) contained resonances that could be assigned to an ethyl (δ_{H} 1.14, t, *J* = 7.6 Hz, H1; 2.66, q, *J* = 7.6 Hz; H2/H2') and two olefinic methyl (δ_{H} 2.21, s, H17; 1.95, s, H18) groups, an aromatic methine (δ_{H} 7.76, s, H13), and a pair of geminal methyls (δ_{H} 1.46, s, H19/H20). HMBC correlations (Figure 3.10, Table 3.4) between methylene H2 and a carbonyl resonance at 188.9 (C4) ppm, and between methyl H17 and a

second carbonyl resonance at 183.3 (C15) ppm, confirmed that the ethyl and one of the methyl residues in **54** were also vicinal substituents on a *para*-quinone, as in **55**.

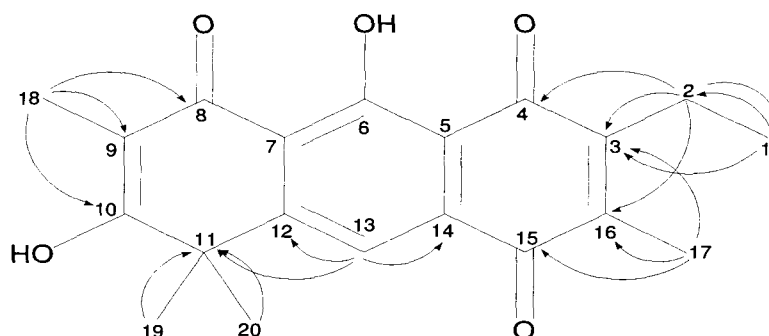


Figure 3.11. Summary of HMBC correlations for garveatin E (**54**).

The olefinic methyl H18 displayed HMBC correlations to carbon resonances at δ_C 200.0 (C8), 113.3 (C9), and 160.6 (C10), which were assigned to an α,β -unsaturated ketone, a quaternary olefinic methine and an oxygenated olefinic carbon, respectively. Furthermore, the aromatic methine H13 showed an HMBC cross peak with the quaternary carbon C11 (48.3 ppm), all in agreement with the proposed structure **54**. Fortuitously, attachment of the *gem*-dimethyl-bearing C11 and ketone termini C8 of the aliphatic fragment, to the naphthoquinone fragment at C12 is completely unambiguous, as evidenced by HMBC correlations from H13 to C12 and C11.

3.6.4. Garvin C

Garvin C (**56**) was isolated as a pale yellow solid that gave a $[M-H]^-$ ion at m/z 327.0866 in the negative ion HRESIMS, appropriate for a molecular formula of $C_{18}H_{16}O_6$ (calculated for $C_{18}H_{15}O_6$: 327.0869), requiring 11 sites of unsaturation. Detailed analysis of the NMR data collected for **56** showed that it was closely related to the known metabolite garvin B (**37**). In

particular, HMQC and HMBC (Figure 3.12) data confirmed the presence of a δ -lactone (C1 to C4, C15, and C16) and dihydroxy naphthalene (C4 to C6 and C11 to C15) substructures in **56** that were identical to the corresponding substructures in **37**.

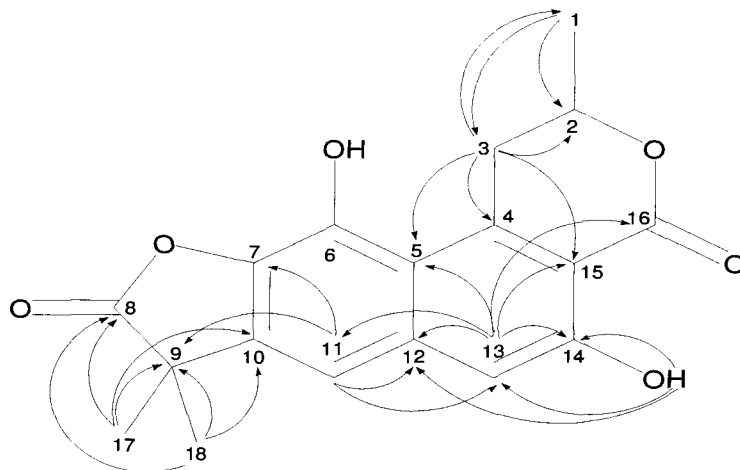


Figure 3.12. Summary of HMBC correlations for garvin C (**56**).

The $^1\text{H-NMR}$ spectrum of **56** (Figure 3.13, Table 3.5) contained resonances suitable for a methyl (H1, δ_{H} 1.59, d, $J = 6.4$ Hz), an oxygenated methine (H2, δ_{H} 4.75, m), and a benzylic methylene (H3, δ_{H} 4.31, dd, $J = 4.3, 17.9$ Hz, δ_{H} 3.39, dd, $J = 3.4, 18.2$ Hz) in the δ -lactone. For the dihydroxy naphthalene fragment, a singlet for 14OH at 10.9 ppm is evident, whereas the aromatic region exhibits methines H11 (δ_{H} 7.06, m) and H13 (δ_{H} 7.15, m). Finally, the characteristic geminal methyls H17 and H18 present singlets at 1.576 and 1.582 ppm, respectively. Although $^1\text{H-NMR}$ resonances for impurities can be observed in compounds (**53**) to (**55**), metabolite (**56**) in particular possesses an important number of additional peaks exhibiting integration values well below those measured for its constituting protons. Clearly, the chemical complexity of the invertebrate extract and the reduced amounts of material available limited the degree of purity of these new *Garveia* compounds.

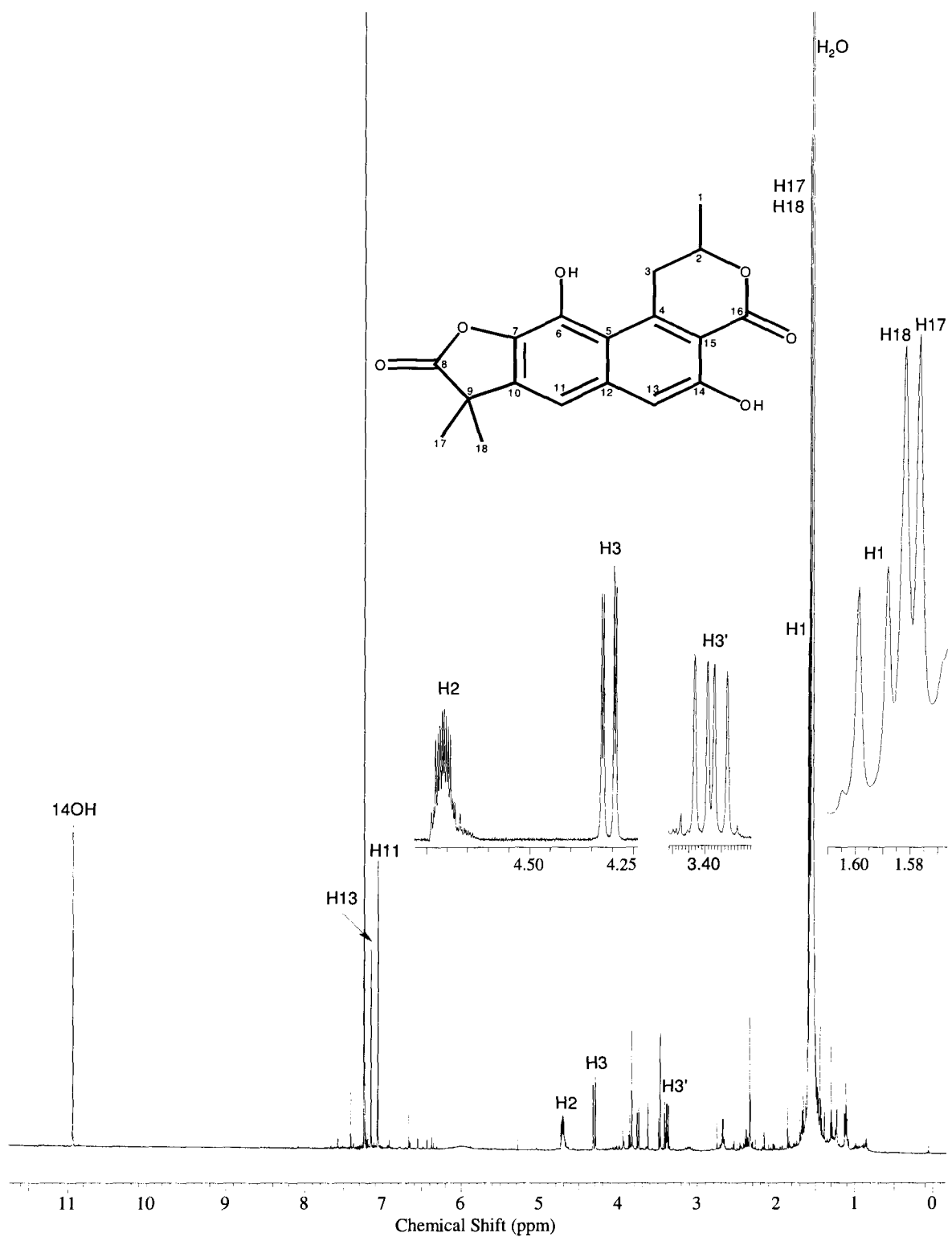
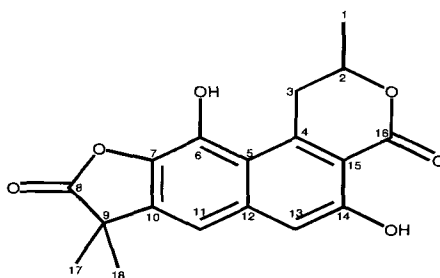


Figure 3.13. ¹H-NMR spectrum of garvin C (56) (recorded in CDCl₃ at 600 MHz).

Table 3.5. NMR data for garvin C (**56**) (recorded in CDCl₃).

Carbon No	¹³ C δ (ppm) ^a	¹ H δ (ppm) (mult, J (Hz)) ^a	HMBC ^a (H→C)
1	20.6	1.59 (d, J = 6.4 Hz)	C2, C3
2	75.4	4.71 (m)	
3	33.7	3.39 (dd, J = 3.4, 18.2 Hz), 4.31 (dd, J = 4.3, 17.9 Hz)	C1, C2, C4, C5, C15
4	140.3		
5	110.5		
6 ^b			
7	134.1		
8	178.5		
9	43.9		
10	137.8		
11	112.6	7.06 (s)	C7, C9, C12, C13
12	136.8		
13	111.2	7.15 (s)	C5, C11, C12, C14, C15, C16
14	155.7	OH 10.9 (s)	C12, C13, C14
15	116.1		
16	169.9		
17	25.1	1.576 (s)	C8, C9, C10
18	25.1	1.582 (s)	C8, C9, C10

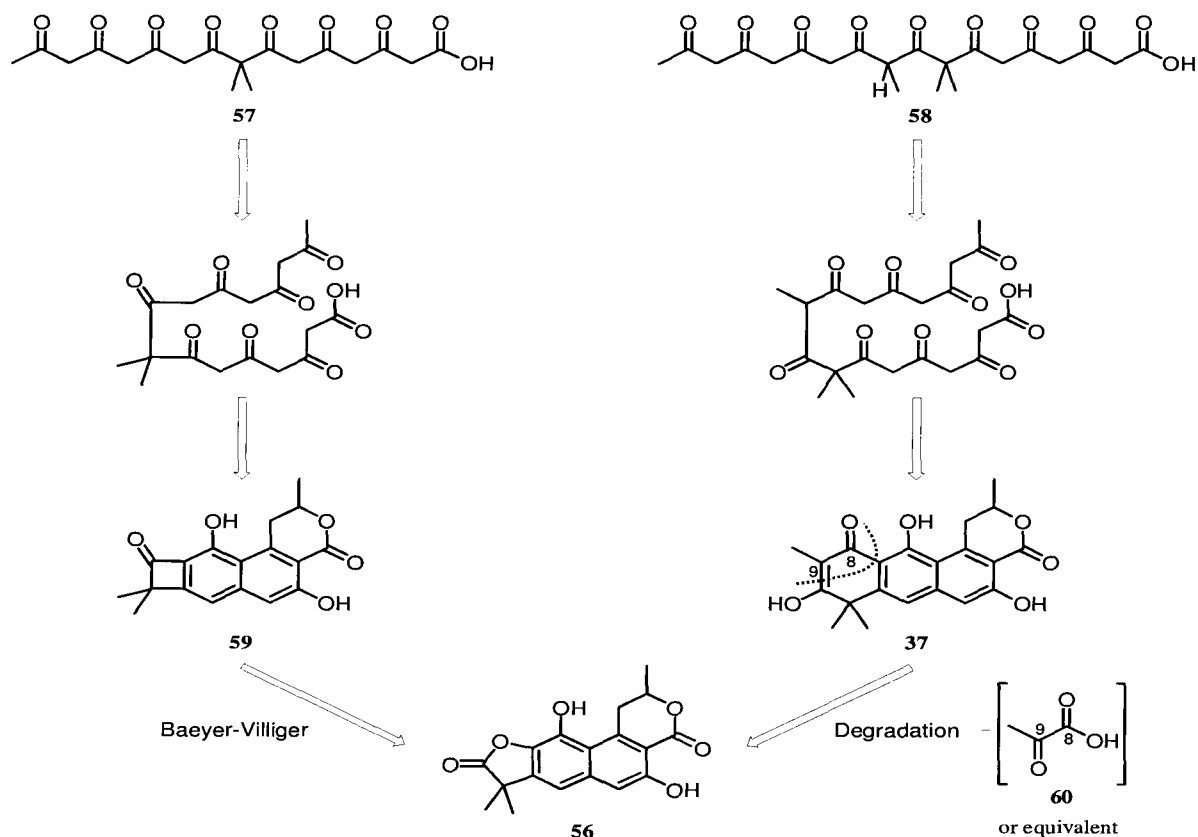
^a According to HMQC and HMBC recorded at 600 MHz. ^b Not assigned.

Long-range HMBC correlations (Table 3.5, Figure 3.12) between the aromatic methine H13 and the ester carbonyl resonance at δ_H 169.9 (C16), and between 14OH and the aromatic carbon C12 (136.8 ppm), both attributed to *W* coupling pathways, provided additional support for the substitution pattern on the naphthalenic substructure. HMBC correlations observed

between methyl singlets H17/H18, and carbon resonances at δ_C 43.9 (C9), 137.8 (C10), and 178.5 (C8), identified a quaternary carbon bearing a pair of geminal methyl groups, linked to an ester/acid carbonyl as one of the two remaining substituents at C7 or C10 of the naphthalenic fragment in **56**.

In order to account for the molecular formula of **56**, the carbonyl functionality had to be part of a γ -lactone fused to the naphthalenic fragment. An HMBC correlation between the aromatic methine H11 and the quaternary carbon C9 demonstrated that C9 was *ortho* to H11, as shown in (**56**). Such positioning was consistent with the relatively shielded chemical shift observed for the oxygenated aromatic carbon C7 (134.1 ppm), which forms part of the γ -lactone.

The new metabolites annulin C (**53**), garveatin E (**54**) and 2-hydroxygarveatin E (**55**), represent minor structural variations of the known compounds annulin A (**39**) and garveatin B (**28**). Garvin C (**56**) on the other hand, while obviously related to garvin B (**37**), has a new carbon framework not previously found among *G. annulata* polyketides. The garvin C skeleton might arise from degradation of garvin B (**37**), which requires excision of the equivalent of one polyketide residue comprising C8/C9 (**60**) along with the associated substituents (Scheme 3.4). Alternatively, garvin C (**56**) might arise from a dimethylated octaketide (**57**) instead of the putative nonaketide precursor (**58**) to garvin B (**37**). Cyclization of the octaketide (**57**) to give a naphthalenic core fused to a δ -lactone on one end and a cyclobutanone on the other (compound **59**), followed by a biological Baeyer-Villiger reaction on the cyclobutanone, would lead directly to garvin C (**56**).

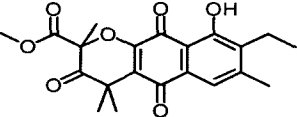
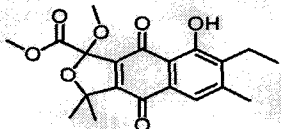
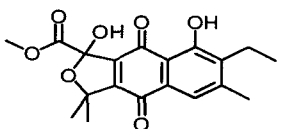
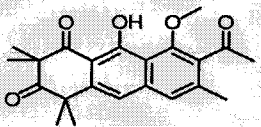
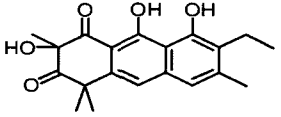
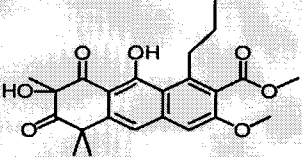
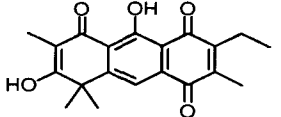
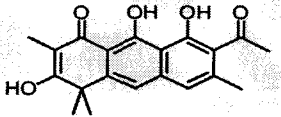
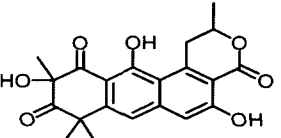


Scheme 3.4. Possible biogenesis of garvin C (56).

3.7. Biological evaluation of *G. annulata* secondary metabolites

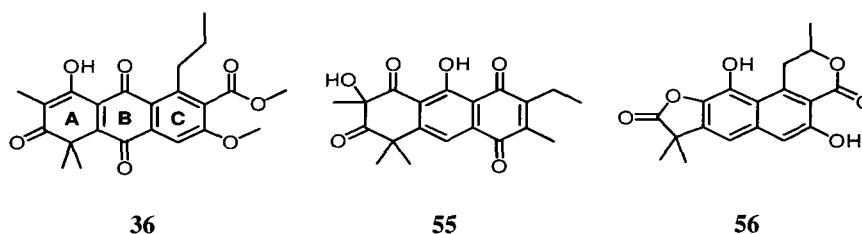
Table 3.6 summarizes all the chemical components isolated from *Garveia annulata* that exhibit IDO inhibition ordered by their potency. Compared with those listed in Table 3.1, annulins B and C are 100 and 30 times more potent than (*R,S*)-thiohydantointryptophan (**10**) and 3-butyl-9*H*- β -carboline (**13**), two IDO inhibitors (competitive and noncompetitive) exhibiting the highest activity to date. All *Garveia* compounds showed noncompetitive inhibition against tryptophan,¹⁵⁶ suggesting that they may bind IDO at a site other than the tryptophan active site.

Table 3.6. IDO-active secondary metabolites from *G. annulata*.

Entry	Name	Structure	K_i (μM) ¹	Remarks
1	Annulin B (40)		0.12	Known ¹⁸¹
2	Annulin C (53)		0.14	New
3	Annulin A (39)		0.69	Known ¹⁸¹
4	Garveatin C (29)		1.2	Known ¹⁶⁴
5	2-Hydroxygarveatin B (33)		1.4	Known ¹⁸⁰
6	2-Hydroxygarvin A (35)		2.3	Known ¹⁶⁴
7	Garveatin E (54)		3.1	New
8	Garveatin A (27)		3.2	Known ¹⁵⁹
9	2-Hydroxygarvin B (38)		>10	Known ¹⁸⁰

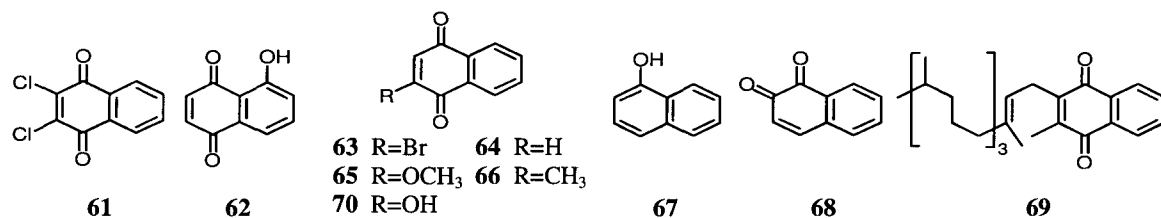
$$^1 [\text{EI}] \xrightleftharpoons{K_i} [\text{Enzyme}][\text{Inhibitor}].$$

Missing in Table 3.6 are garvin A quinone (36), and the new 2-hydroxygarveatin E (55) and garvin C (56), isolated from *G. annulata* fractions exhibiting low IDO inhibition.



A sharp decay in inhibitory activity (more than 10 times) is observed when the naphthoquinone substructure of the annulins is replaced by the anthracenoid skeleton of the remaining metabolites (garveatins, garvins, garvalones), with the exception of garveatin E (**54**). Additionally, large substituents in the C ring, such as *n*-propyl in 2-hydroxygarvin A (**35**) and garvin A quinone (**36**), or a γ -lactone in 2-hydroxygarvin B (**38**) and garvin C (**56**), decrease inhibition. The relative position of a *para*-quinone within the polycyclic ring system seems to be crucial for potency, since activity falls as the quinone moves from ring B in annulins, to ring C in garveatin E (**54**) and 2-hydroxygarveatin E (**55**). This trend is overshadowed by large substituents in ring C, which explains the inactivity shown by garvin A quinone (**36**).

The high inhibitory activity of *G. annulata* compounds exhibiting a naphthoquinone core, and its dependence to the position of the quinone, led Mauk and Vottero¹⁵⁶ to evaluate IDO inhibition in a small library of commercially available naphthoquinones (Table 3.7). Among them, a water-soluble analogue of vitamin K₁ (**69**) called menadione (**66**), exhibited nanomolar inhibition making it a candidate for *in vivo* examination, and further drug development. Annulins A (**39**), B (**40**), and C (**53**) were all inactive in a recently developed yeast-based IDO inhibition assay,¹⁴⁸ suggesting that they may not cross the yeast cell wall. Conversely, menadione (**66**) and 2-bromo-2,4-naphthoquinone (**63**) are able to cross the yeast membrane and inhibit human IDO expressed in the yeast cytoplasm.¹⁵⁶

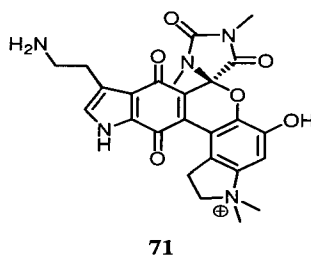
Table 3.7. Annulin C (**53**) and commercially available IDO-active naphthoquinones.¹⁵⁶

Entry	Name	K_i (nM) ¹
1	Dichlone (61)	45
2	Juglone (62)	48
2	Annulin C (53)	144
4	2-Bromo-1,4-naphthoquinone (63)	215
5	1,4-Naphthoquinone (64)	334
6	2- Methoxynaphthoquinone (65)	530
7	Vitamin K ₃ (Menadione, 66)	580
8	1-Naphthol (67)	1800
9	1,2-Naphthoquinone (68)	3400
10	Vitamin K ₁ (69)	>40000
11	Lawsone (70)	>100000

$$^1 [EI] \xrightleftharpoons{K_i} [\text{Enzyme}][\text{Inhibitor}].$$

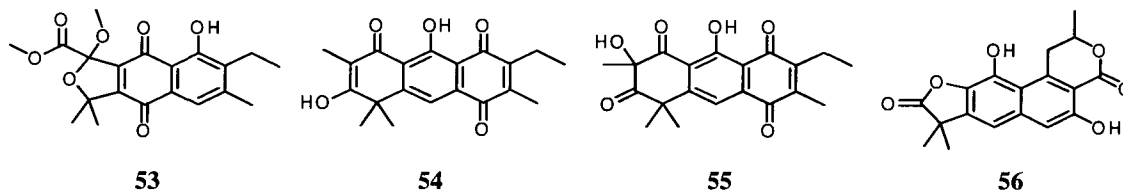
Besides their mild antimicrobial and high IDO inhibitory activities, no additional biological roles have been reported for the secondary metabolites of *G. annulata*. Menadione (**66**) causes oxidative stress due to the formation of reactive oxygen species such as H₂O₂, \bar{O}_2 , and $\bullet\text{OH}$ during metabolism,¹⁹⁵⁻¹⁹⁷ and has been shown to induce lung¹⁹⁸ and liver¹⁹⁹ cancer cell death by either apoptosis or necrosis. Computer-assisted docking studies and kinetic experiments indicate that interaction of menadione (**66**) with IDO occurs primarily through hydrophobic contacts above the distal side of the heme in the binding site.¹⁵⁶ The high potential of **66** to become a drug was recognized by NewLink Genetics Corporation, a biopharmaceutical company in Iowa that recently acquired patent rights for the IDO technology from UBC.²⁰⁰

Recently, the same IDO bioassay detailed in Section 3.3 led to the isolation of exiguamine A (**71**) from *Neopetrosia exigua*, a sponge collected in Papua New Guinea.¹³⁴ This new potent IDO inhibitor ($K_i = 210$ nM) exhibited a complex hexacyclic alkaloid skeleton, without precedent among known natural products. Noteworthy, the novel carbon backbone combines elements from tryptophan and naphthoquinones in one structure.



3.8. Conclusions

Bioassay-guided fractionation of MeOH extracts obtained from *Garveia annulata*, a seasonal hydroid collected in Barkley Sound, British Columbia, led to the isolation of twelve secondary metabolites including four new compounds: annulin C (**53**), garveatin E (**54**), 2-hydroxygarveatin E (**55**), and garvin C (**56**).



Annulin C (**53**), garveatin E (**54**), and 2-hydroxygarveatin E (**55**), are analogues of the previously reported annulin A (**39**) and garveatin B (**28**),^{164,181} while garvin C (**56**) has a new carbon framework not previously found among *G. annulata* polyketides. Nine of these

metabolites showed inhibition of indoleamine 2,3-dioxygenase (IDO), with the annulins among the most potent *in vitro* IDO inhibitors isolated to date (Table 3.8).

Table 3.8. *In vitro* inhibition of IDO by marine natural products, commercial naphthoquinones, β -carbolines, and tryptophan analogues.

Entry	Name	K_i (nM) ¹
1	Annulin B (40)	120
2	Annulin C (53)	144
3	Exiguamine A (71)	210
4	Menadione (66)	580
5	Annulin A (39)	690
6	3-Butyl-9H- β -carboline (13)	3300
7	(<i>R,S</i>)-Thiohydantointryptophan (10)	11400
8	(<i>S</i>)-Methyltryptophan (6)	34000

¹ $[E] \xrightleftharpoons{K_i} [Enzyme][Inhibitor]$.

The term pharmacophore refers to the ensemble of steric and electronic features required to ensure optimal interactions with a specific biological target structure and to trigger (or to block) its biological response.²⁰¹ The annulin family of *Garveia* metabolites share a common 5-hydroxy-6-ethyl-7-methyl-1,4-naphthoquinone core substructure, which by comparison with other inhibitors, seems to be a requisite for potent IDO inhibition. Based on the initial inhibitory activity shown by tryptophan derivatives (Table 3.1), and the high potency exhibited by annulins and similar naphthoquinones (Tables 3.6 and 3.7), a possible pharmacophore for human IDO can be proposed (Figure 3.14).

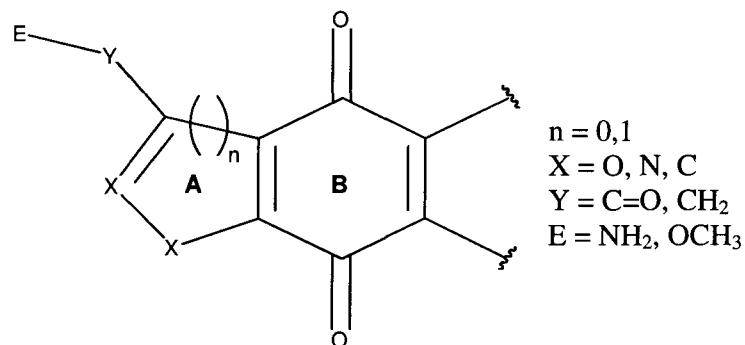


Figure 3.14. Proposed pharmacophore involved in IDO inhibition.

The core for this proposal is the quinone ring B. Some flexibility is seen for size and heteroatom positioning within ring A, as well as for length and substituents in its side arm. An additional third ring, or substituents on quinone B are not required for activity. IDO inhibition improves as planarity in the A/B ring system decreases from an indole in tryptophan derivatives, to dihydroheteronuclear five or six-membered A rings fused to *ortho*-quinones as in the annulins.

3.9. Experimental

General Experimental Procedures

For general experimental procedures see Section 2.6.

Isolation Procedure

The screening of a library of marine invertebrates for their ability to inhibit human IDO *in vitro*, revealed very promising activity in crude extracts of the Northeastern Pacific hydroid *Garveia annulata*.

Samples of the red/orange hydroid *Garveia annulata* (200 g wet wt) were collected from Barkley Sound, British Columbia, on April of 1999, by hand using SCUBA at depths of 10-15 m (48° 0.50' N, 125° 12.50' W). The collected material was frozen immediately upon collection and transported back to the University of British Columbia in coolers packed with dry ice. A portion of the frozen material (~50 g) was extracted in MeOH (3 x 200 mL) and the combined extracts concentrated to dryness *in vacuo* to give a brownish solid (0.35 g). This residue was dissolved in H₂O to obtain a light brown colored solution, and extracted sequentially with hexanes (3 x 50 mL), CH₂Cl₂ (3 x 50 mL) and EtOAc (3 x 50 mL), followed by concentration *in vacuo* of each partition. The CH₂Cl₂ bioactive fraction (0.1275 g) was subjected to silica gel column chromatography (20% EtOAc/Hexanes), followed by normal phase HPLC (15% EtOAc/Hexanes), to afford the new analogue annulin C (**53**) (0.0003 g, 0.80 μmol, 0.0006% wet wt) as a yellow oil, and the known annulin B (**40**) (0.0006 g, 1.5 μmol, 0.001% wet wt).

A second batch of specimens (424 g wet wt), collected on June of 2003, was processed as above to generate 2.50 g of active CH₂Cl₂ extract. Silica gel gradient column chromatography, followed by gradient (20% CH₃CN/H₂O to 83% CH₃CN/H₂O) or isocratic (70% CH₃CN/H₂O) reversed phase HPLC, yielded the new garveatin E (**54**) (0.0005 g, 1.5 μmol, 0.0001%, wet wt) as a pale yellow oil, and the previously reported 2-hydroxygarveatin B (**33**) (0.0011 g, 3.2 μmol, 0.0002%, wet wt), annulin A (**39**) (0.0005 g, 1.4 μmol, 0.0001%, wet wt), garveatins A (**27**) (0.034 g, 0.1 mmol, 0.008%, wet wt) and C (**29**) (0.0005 g, 1.3 μmol, 0.0001%, wet wt), 2-hydroxygarvin A (**35**) (0.0037 g, 8.9 μmol, 0.0009, wet wt), and garvin A quinone (**36**) (0.0004 g, 0.97 μmol, 0.00009%, wet wt). Additional purification of IDO inactive fractions by reverse phase HPLC (70% CH₃OH/H₂O) allowed the identification of the new compounds 2-hydroxygarveatin E (**55**) (0.0004 g, 0.1 μmol, 0.00009%, wet wt) as a yellow oil, and garvin C (**56**) (0.0003 g, 0.91 μmol, 0.00007%, wet wt) as a pale yellow oil. Due to limited amounts of all *G. annulata* compounds, the ¹³C-NMR data was derived from HMQC and HMBC spectra. Therefore, some quaternary carbons were not assigned.

Annulin B (**40**): spectral data was in accord with that previously reported for the natural product.¹⁸¹

Annulin C (**53**): for a summary of ¹H and ¹³C NMR assignments based on HMQC and HMBC data, see Table 3.2. Yellow oil; ¹H NMR (CDCl₃, 400 MHz) δ 12.2 (1H, s), 7.44 (1H, s), 3.82 (3H, s), 3.45 (3H, s), 2.75 (2H, q, *J* = 7.5 Hz), 2.41 (3H, s), 1.68 (3H, s), 1.62 (3H, s), 1.12 (3H, t, *J* = 7.5 Hz); ¹³C NMR (CDCl₃, 100 MHz) δ 167.2 (C), 160.3 (C), 154.3 (C), 145.3 (C), 140.0 (C), 121.5 (CH), 106.8 (C), 88.3 (C), 52.5 (CH₃), 51.7 (CH₃), 26.4 (CH₃), 26.4 (CH₃), 19.7 (CH₃), 19.4 (CH₂), 12.8 (CH₃); HREIMS calcd for C₂₀H₂₂O₇ (M⁺): 374.13655; found 374.13670.

Garveatin E (**54**): for a summary of ^1H and ^{13}C NMR assignments based on HMQC and HMBC data, see Table 3.4. Pale yellow oil; ^1H NMR (CDCl_3 , 400 MHz) δ 14.6 (1H, s), 10.15 (1H, s), 7.76 (1H, s), 2.66 (2H, q, $J = 7.6$ Hz), 2.21 (3H, s), 1.95 (3H, s), 1.46 (3H, s), 1.46 (3H, s), 1.14 (3H, t, $J = 7.6$ Hz); ^{13}C NMR (CDCl_3 , 100 MHz) δ 200.0 (C), 188.9 (C), 183.3 (C), 160.6 (C), 148.9 (C), 145.3 (C), 122.2 (C), 117.5 (CH), 114.4 (C), 113.3 (C), 48.3 (C), 30.0 (CH_3), 27.7 (CH_3), 19.5 (CH_2), 12.5 (CH_3), 12.2 (CH_3), 7.18 (C); HRESIMS calcd for $\text{C}_{20}\text{H}_{20}\text{O}_5\text{Na}$ ($[\text{M}+\text{Na}]^+$): 363.1208; found 363.1200.

2-Hydroxygarveatin B (**33**): spectral data was in accord with that previously reported for the natural product.¹⁸⁰

Annulin A (**39**): spectral data was in accord with that previously reported for the natural product.¹⁸¹

Garveatin A (**27**): spectral data was in accord with that previously reported for the natural product.¹⁵⁹

Garveatin C (**29**): spectral data was in accord with that previously reported for the natural product.¹⁶⁴

2-Hydroxygarvin A (**35**): spectral data was in accord with that previously reported for the natural product.¹⁶⁴

Garvin A quinone (**36**): spectral data was in accord with that previously reported for the natural product.¹⁶⁴

2-Hydroxygarveatin E (**55**): for a summary of ^1H and ^{13}C NMR assignments based on HMQC and HMBC data, see Table 3.3. Yellow oil; ^1H NMR (CDCl_3 , 600 MHz) δ 13.3 (1H, s), 7.72 (1H, s), 2.67 (2H, q, $J = 7.7$ Hz), 2.21 (3H, s), 1.76 (3H, s), 1.56 (3H, s), 1.44 (3H, s), 1.12 (3H, t, $J = 7.7$ Hz); ^{13}C NMR (CDCl_3 , 150 MHz) δ 207.0 (C), 194.3 (C), 188.6 (C), 183.5 (C), 160.4 (C), 154.5 (C), 149.2 (C), 144.3 (C), 122.3 (C), 122.2 (C), 115.2 (CH), 114.5 (C), 83.9 (C), 48.4 (C), 30.0 (CH_3), 26.4 (CH_3), 26.2 (CH_3), 19.8 (CH_2), 12.7 (CH_3), 12.3 (CH_3); HRESIMS calcd for $\text{C}_{20}\text{H}_{20}\text{O}_6\text{Na}$ ($[\text{M}+\text{Na}]^+$): 379.1158; found 379.1160.

Garvin C (**56**): for a summary of ^1H and ^{13}C NMR assignments based on HMQC and HMBC data, see Table 3.5. Pale yellow oil; ^1H NMR (CDCl_3 , 600 MHz) δ 10.9 (1H, s), 7.15 (1H, s), 7.06 (1H, s), 4.71 (1H, m), 4.31 (1H, dd, $J = 4.3, 17.9$ Hz), 3.39 (1H, dd, $J = 3.4, 18.2$ Hz), 1.59 (3H, d, $J = 6.4$ Hz), 1.582 (3H, s), 1.576 (3H, s); ^{13}C NMR (CDCl_3 , 150 MHz) δ 178.5 (C), 169.9 (C), 155.7 (C), 140.3 (C), 137.8 (C), 136.8 (C), 134.1 (C), 116.1 (C), 112.6 (CH), 111.2 (CH), 110.5 (C), 75.4 (C), 43.9 (C), 33.7 (C), 25.1 (CH_3), 25.1 (CH_3), 20.6 (CH_3); HRESIMS calcd for $\text{C}_{18}\text{H}_{15}\text{O}_6$ ($[\text{M}-\text{H}]^-$): 327.0869; found 327.0866.

4. Progress towards the Synthesis of Ceratamines

4.1. Microtubule-stabilizing agents from marine origin

The microtubule-stabilizing properties of taxol (**1**) were first reported in 1979,²⁰² and for the next 16 years **1** and its analogues were the only compounds known to exhibit such activity.²⁰³ However, since 1995 a variety of natural products from plant (**2**, **3**), bacterial (**4-5**) and marine (**6-12**) origins have been recognized as microtubule-stabilizing agents (MSA).²⁰³⁻²⁰⁹

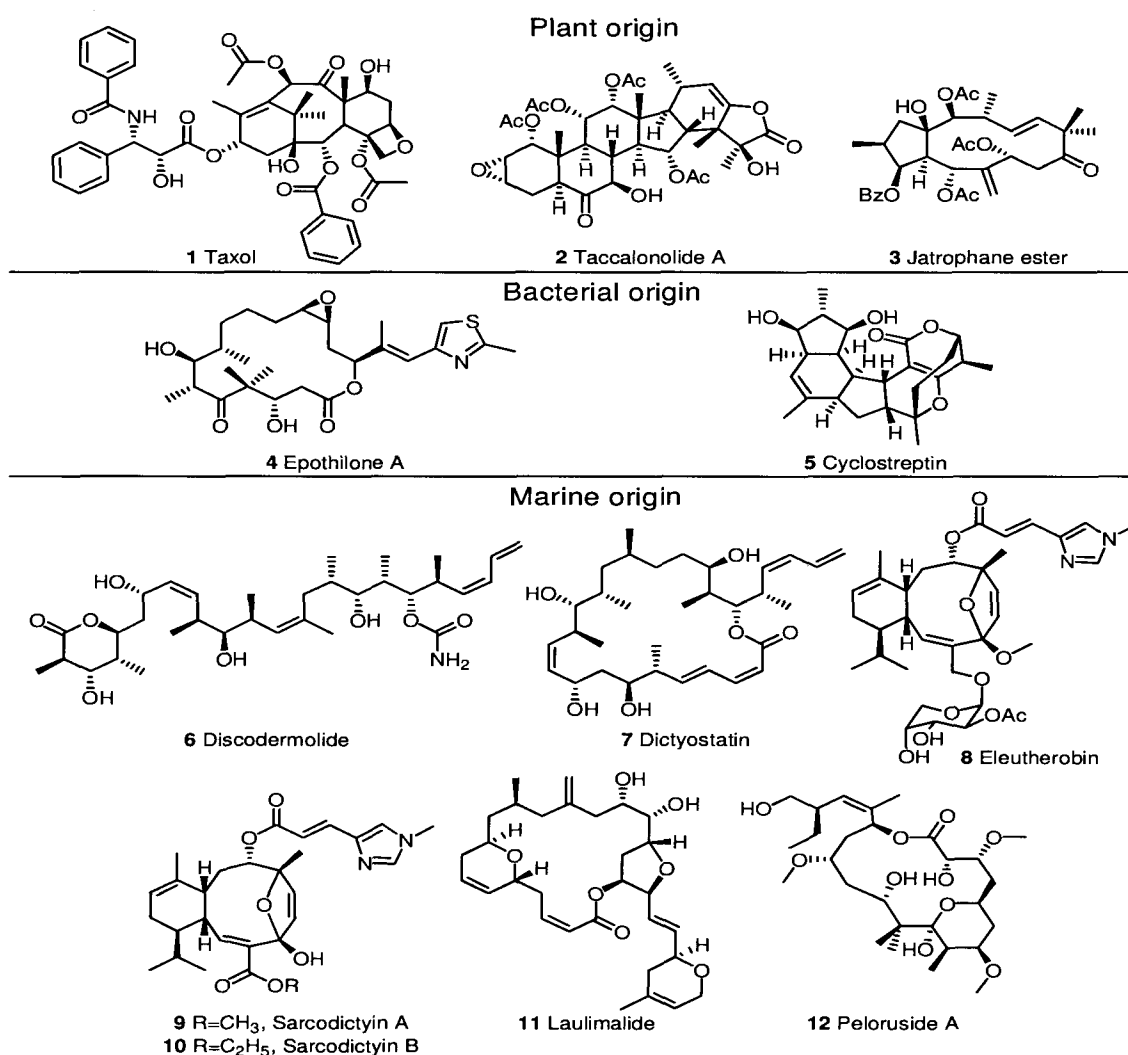


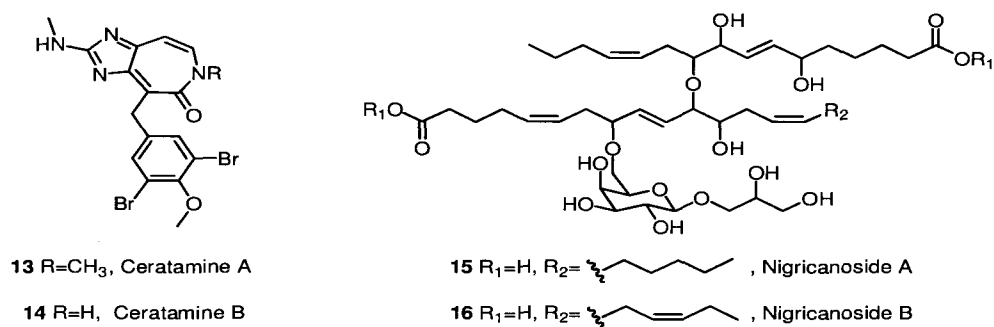
Figure 4.1. Prominent microtubule-stabilizing agents (MSA) from diverse sources.^{203,210}

It is noteworthy that all potent microtubule stabilizers known to date are either natural products, or derived from natural products leads.²⁰³ Furthermore, the majority of these prominent compounds are marine-derived. Discodermolide (**6**), a polyhydroxy- δ -lactone of polypropionate origin exhibiting immunosuppressive activity, was isolated from the sponge *Discodermia dissoluta* in 1990 by Gunasekera.^{211,212} The polyketide-derived macrolide dictyostatin-1 (**7**), was first reported by Pettit and coworkers²¹³ in 1988 from a marine sponge of the genus *Spongia* sp. collected in the Republic of Maldives. The compound showed potent growth inhibition of lymphocytic leukemia cells. The soft coral *Eleutherobia* sp. found in waters of Western Australia yielded in 1997 a tricyclic triterpene christened eleutherobin (**8**) by Lindel and colleagues.²¹⁴ This compound was re-isolated in 2000 by Andersen and coworkers^{215,216} from the octocoral *Erythropodium caribaeorum*, along with several analogues. *E. caribaeorum* is more abundant and represents a better source of **8** than *Eleutherobia* sp. Its potent tubulin polymerization activity was recognized shortly after the first isolation.²¹⁷

The discovery of microtubule-stabilizing properties of eleutherobin (**8**) triggered a more serious and intense search for non-taxane-based MSA's, which eventually led to sarcodictyins A (**9**) and B (**10**). Both metabolites had been isolated 10 years before **8**, in 1987 from the Mediterranean stolonifer *Sarcodictyon roseum* by Pietra and coworkers.²¹⁸ As in the case of sarcodictyins, it would take several years (even decades) before the initially reported biological activities of discodermolide (**6**) and dictyostatin-1 (**7**) could be traced to their interaction with the tubulin-microtubule system.^{219,220} The last member of this group of rediscovered secondary metabolites is laulimalide (**11**), reported in 1988 by two research groups working independently. Crews²²¹ isolated **11** from the sponge *Spongia mycofijiensis* collected in Vanuatu, whereas Moore and Scheuer²²² found it in extracts of the Indonesian sponge *Hyatella* sp. The compound was reported as a potent antiproliferative agent, and in 1999 confirmed as a MSA by Mooberry

and colleagues.²²³ Laulimalide (**11**) was found unable to displace radiolabeled taxol, and therefore does not bind to the taxol site on β -tubulin.²²⁴

More recently, another polyketide-based macrolide, peloruside A (**12**), was isolated by Northcote and colleagues²²⁵ from the New Zealand sponge *Mycale* sp. Miller and coworkers reported that **12** promotes tubulin polymerization *in vitro* with essentially the same activity as taxol (**1**).²²⁶ It is the second MSA, after laulimalide (**11**), demonstrated to bind at a site different from taxol (**1**).²²⁷



The latest additions to the expanding group of potent MSA's from marine organisms are metabolites (**13**)-(16), discovered in the Andersen research laboratory. The heterocyclic alkaloids ceratamines A (**13**) and B (**14**) were isolated in 2003 from the sponge *Pseudoceratina* sp. collected in Papua New Guinea.^{203,210} Similarly, specimens of the green algae *Avrainvillea nigricans* harvested from reef flats near Portsmouth, Dominica, yielded in 2007 the antimetabolic glycosylated polyketides nigricanosides A (**15**) and B (**16**) as the corresponding dimethyl esters.²²⁸ Herein, details regarding several attempts to synthesize ceratamines will be described.

4.2. Ceratamines A and B

The heterocyclic alkaloids ceratamines A (**13**) and B (**14**) are the first examples of a new family of MSA's for which tubulin-polymerizing activity has been firmly established.^{203,210,229}

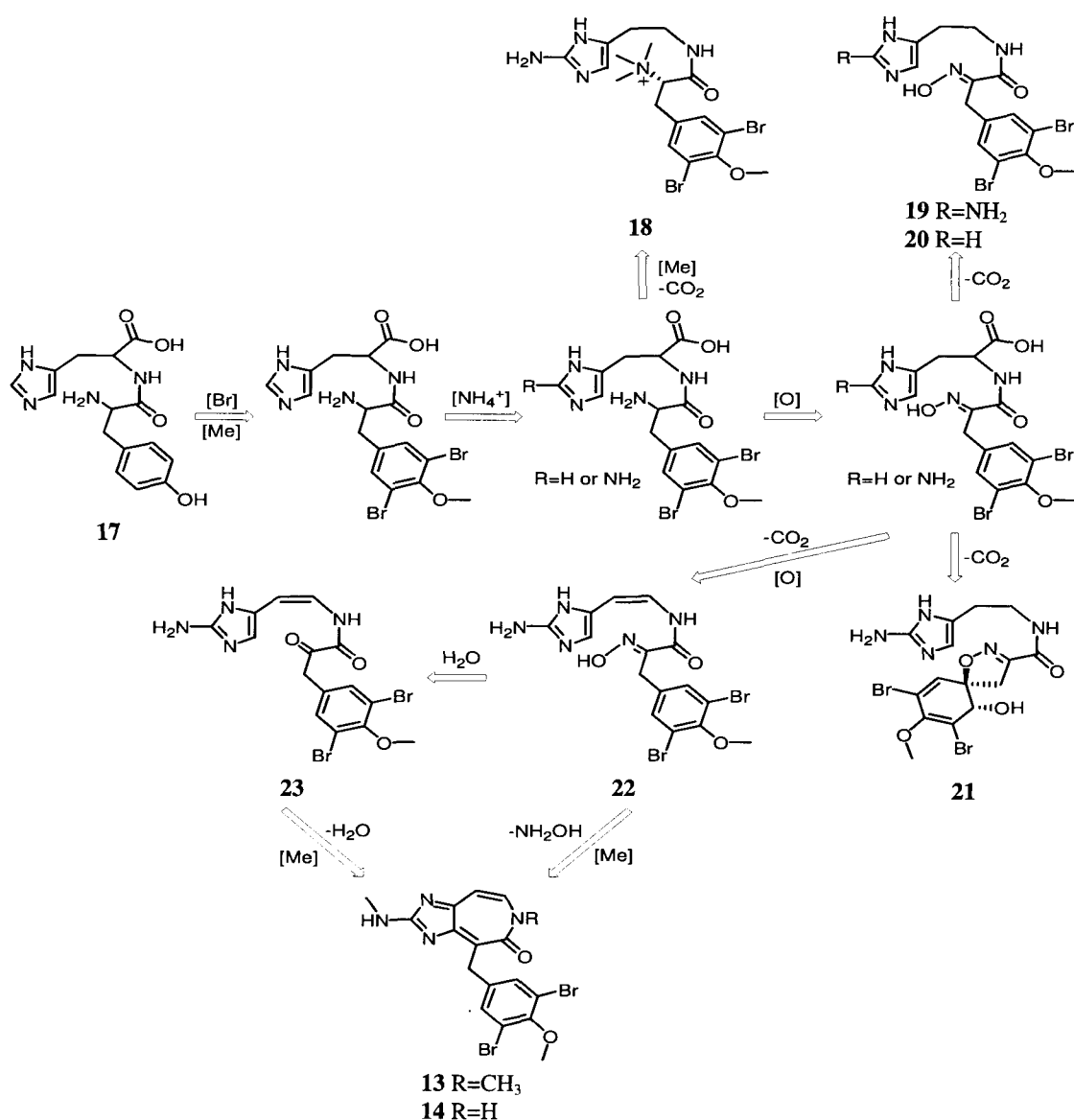
Both compounds are achiral and present significantly less elaborate structures than other polyketide and terpenoid-based marine MSA's (Figure 4.1). In addition, the imidazo[4,5,*d*]azepine core heterocycle of the ceratamines has no precedent among known natural and synthetic compounds to date.²¹⁰

The metabolites were discovered in a cell-based screen for mitosis inhibitors that uses human breast carcinoma MCF-7 cells. In the assay, arrested cells are detected by ELISA using the monoclonal antibody TG-3.²³⁰ Treatment of MCF-7 cells with a 20 μ M concentration of **13** caused readily detectable changes in the interphase microtubule network, leading to accumulation of microtubules around the nucleus.²³⁰ The same dose also led to cell cycle arrest in mitosis, where arrested cells displayed pillar-like tubulin structures extending vertically from the basal surface of the cells. These observations are qualitatively different from those described for taxol (**1**), and confirmed ceratamines as microtubule-stabilizers that target microtubules directly.²²⁹ The polymerizing power of ceratamine A (**13**), the most active analogue, is around 10-fold lower than taxol (**1**).^{203,229} Additionally, **13** was found not to compete with **1** for binding to microtubules, suggesting a different binding site.²²⁹ Such unusual characteristics make ceratamines attractive as research tools and experimental drug candidates. They might act differently on normal and cancer cells than other MSA's, and show a distinctive spectrum of toxicity and antitumor activity.

A limiting factor in the further development of ceratamines A (**13**) and B (**14**) as leads for new anticancer drugs is their availability, since only 8 and 14 mg were isolated, respectively, from a relatively rare sponge. Clearly, total synthesis of the natural product and preparation of analogues is imperative to solve the supply issue.

4.2.1. Biosynthesis and similar marine metabolites

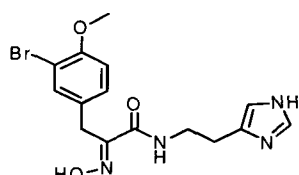
The biosynthesis of ceratamines may involve bromination and methylation of a histidine-tyrosine dipeptide (**17**), followed by amination and oxidation to generate common precursors in the biogenesis of pseudoceratinine B (**18**),²³¹ ianthelline (**19**),²³² 5-bromoverongamide (**20**),²³³ and pseudoceratinine A (**21**),²³¹ also isolated from *Pseudoceratina* sp. sponges collected off New Caledonia, Bahamas and Curacao.



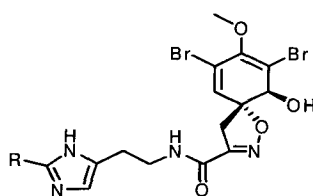
Scheme 4.1. Proposed biogenesis of *Pseudoceratina* sp. secondary metabolites.

Oxidative decarboxylation and oxime hydrolysis lead to intermediates **22** and **23**, which may eliminate H₂O or NH₂OH via nucleophilic addition to a carbonyl (or oxime) in an aldol-like fashion (Scheme 4.1). The driving force for this last reaction is a complete aromatization of the core heterocycle in the final product.

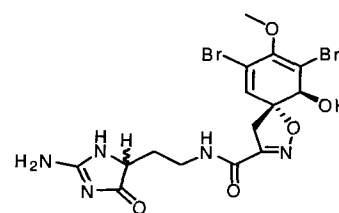
Besides **18-21**, the ceratamines share a biogenetic relationship with at least 30 bromotyrosine/histidine-derived metabolites isolated from marine sponges belonging to the order Verongida, which include among others, the genera *Aplysina*, *Ianthella*, *Psammaplysilla*, *Pseudoceratina*, and *Verongula*.^{234,235} These compounds are associated with the large number of chemical variations possible within the aromatic ring systems and side chains of the tyrosine and histidine moieties.



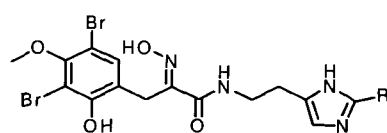
24 verongamine



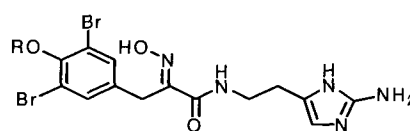
25 R=NH₂, purealidin J
26 R=H, aerophobin-1



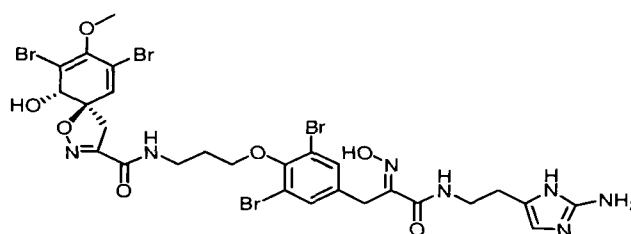
27 purealidin K



28 R=NH₂, purealidin M
29 R=H, purealidin N



30 R=H, lipopurealidin H
31 R=(CH₂)₃NHCO(CH₂)₁₂CH₃, lipopurealidin A
32 R=(CH₂)₃NH₂, purealidin A
33 R=(CH₂)₃C₅H₅N⁺, purealidin D
34 R=(CH₂)₃N⁺(CH₃)₃, purealidin E



35 purealin

The aromatic system can be either oxygenated (**28**, **29**),²³⁶ monobrominated (**24**)²³⁷ or dibrominated. The bromotyrosine moiety can undergo rearrangement to a spirohexadienylisoxazole system (**25-27**, **35**),²³⁸⁻²⁴¹ or link to form linear chains through ether bonds (**31-35**).^{236,239-243} The imidazole ring in histidine may be left unchanged (**24**),²³⁷ but amination is commonly observed (**25**, **28**, **30-35**)^{240,242,243} and oxidation is also possible (**27**).²³⁶

Bromotyrosine-derived metabolites have long been noted as distinct markers for marine sponges belonging to the order Verongida, which are rather variable in color, shape, consistency, and skeletal arrangement.²³⁴ These compounds exhibit a wide range of interesting biological activities including antiviral, antibiotic, Na⁺/K⁺ ATPase inhibition, anti-HIV, antifouling, anti-inflammatory, and anticancer.^{234,235,238,244}

The 2-aminoimidazole moiety in ceratamines is also a characteristic structural element of the pyrrole-imidazole alkaloids in the oroidin family, some of the most common metabolites isolated from marine sponges (Figure 4.2).²⁴⁵ They range in complexity from the chlorohydrin derivative girolline (**36**)²⁴⁶ to the tetrameric stylissadine A (**40**).^{247,248} The non-cyclized precursors for this small (approximately 100 members) but highly diverse family of sponge alkaloids are oroidin (**37**) and congeners (hymenidin **38**, clathrodine **39**).²⁴⁹

In addition to their ornate structures, these molecules also possess a broad range of biological activities. Oroidin (**37**) is the major fish feeding deterrent agent of sponges of the genus *Agellas*, and thus, secures their survival.²⁴⁹ Scepttrin (**41**) is a potent antibacterial, as well as an antiviral, antihistaminic, and antimuscarinic agent.²⁵⁰ Ageliferin (**43**) also possesses antibiotic and antiviral activities, and is an useful compound for the study of actin-myosin contractile systems.²⁵⁰ Palau'amine (**42**) exhibits potent immunosuppressive activity,²⁴⁹ while grossularines A (**44**) and B (**45**) possess pronounced effects against solid human tumor cell lines.²⁵¹

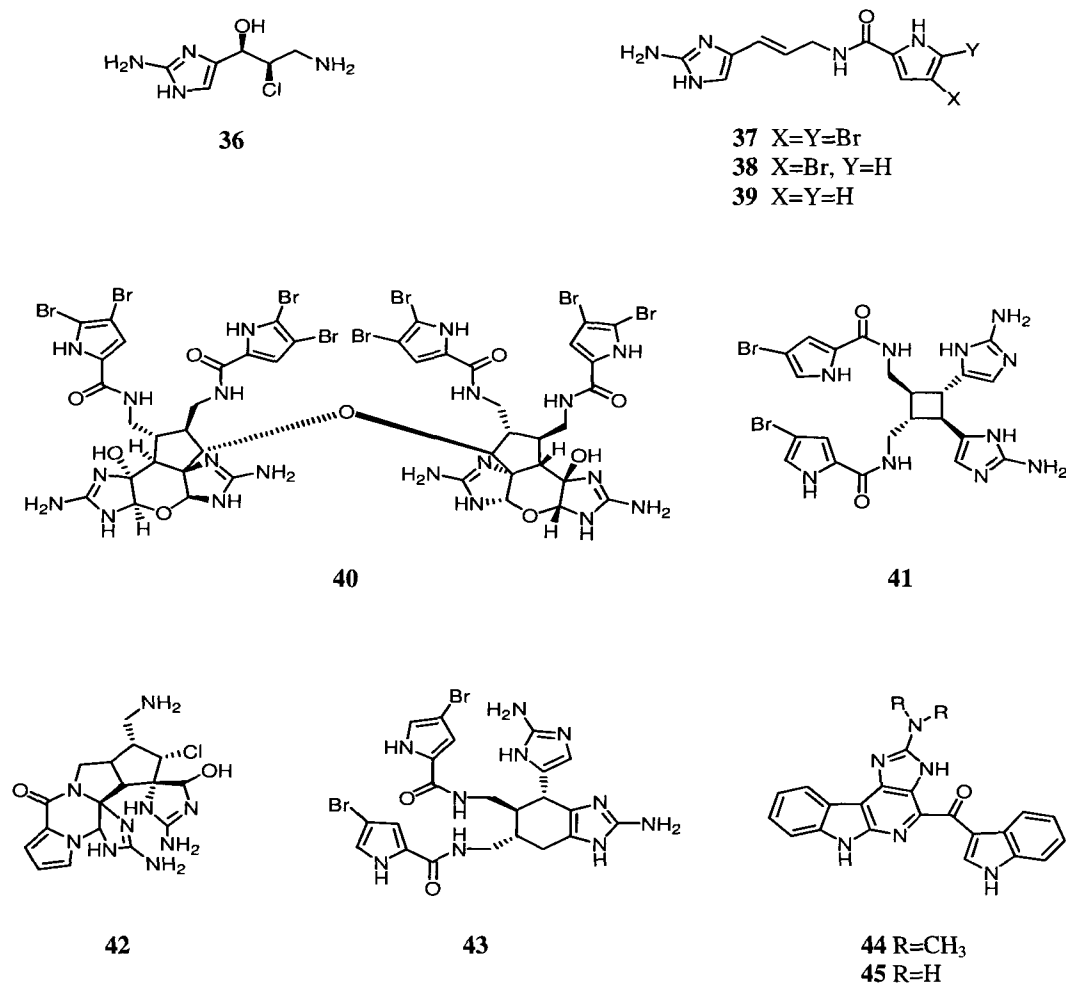


Figure 4.2. Representative pyrrole-imidazole alkaloids.

4.2.2. NMR data

The NMR data in Figure 4.3 shows evidence of two conformers for ceratamine A (**13**). This is particularly apparent for the resonances assigned to H13/H17 (δ_{H} 7.67, δ_{C} 133.2), H9 (δ_{H} 6.42, d, $J = 10.0$ Hz, δ_{C} 100.4), and H8 (δ_{H} 7.73, d, $J = 10.0$ Hz, δ_{C} 142.9), all in a peak ratio of 4:1. Scalar coupling between 18NH (δ_{H} 8.69) and H19 (δ_{H} 3.07, δ_{C} 29.2) can be appreciated in both rotational isomers.

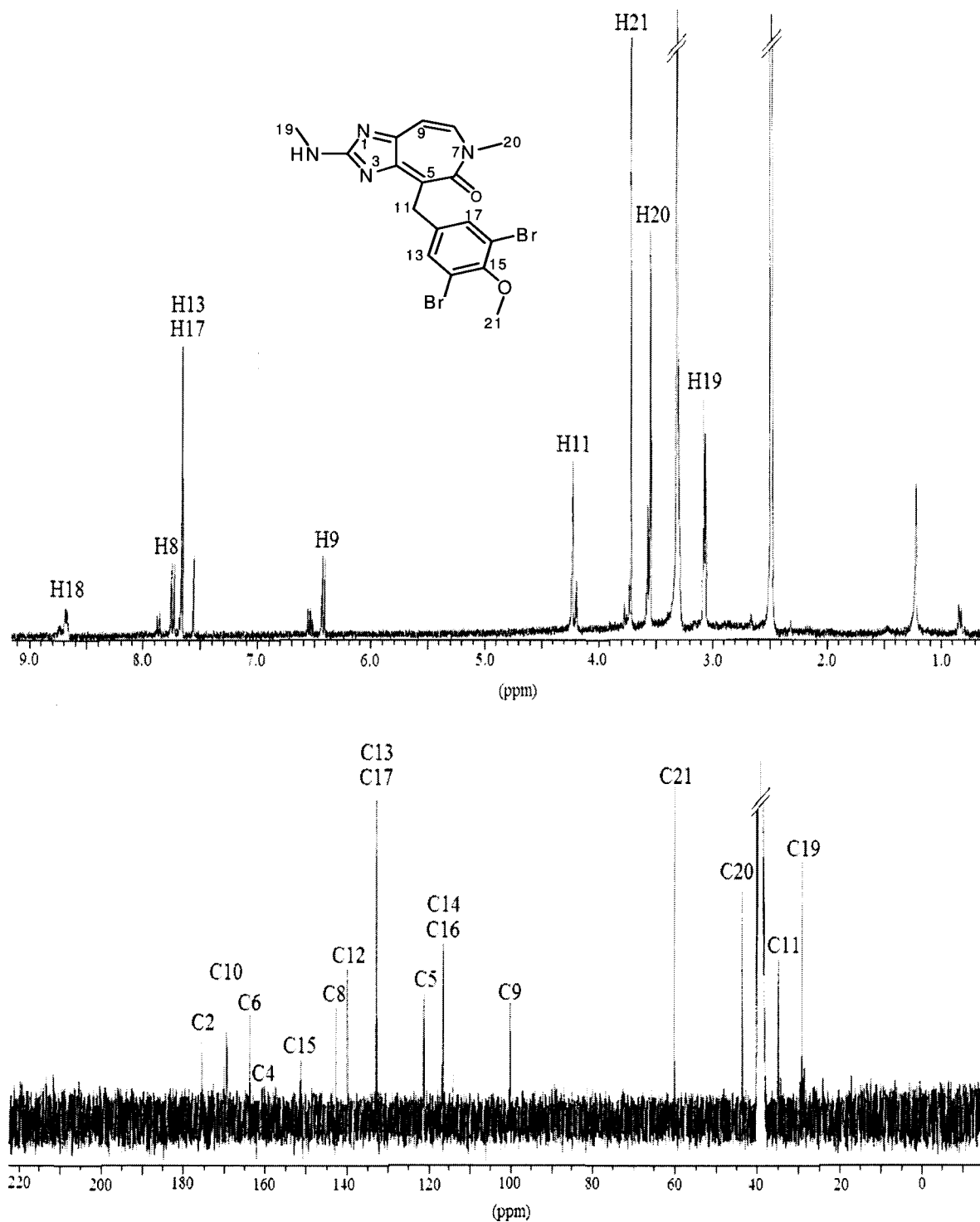
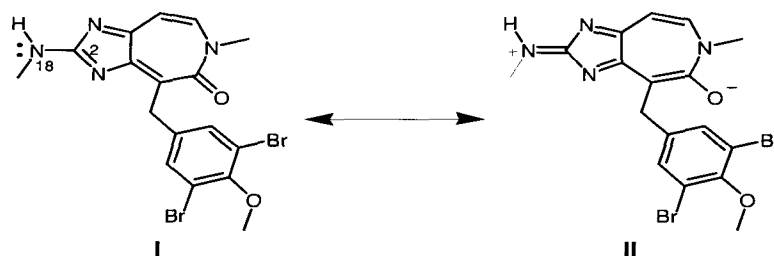


Figure 4.3. ¹H and ¹³C-NMR spectra of ceratamine A (**13**) (recorded in DMSO-*d*₆ at 500 and 125 MHz respectively).²¹⁰

Evidently, the C2-N18 imine bond possesses a high double bond character which gives rise to restricted rotation around this bond (Scheme 4.2). The case is comparable to a vinylogous amide.

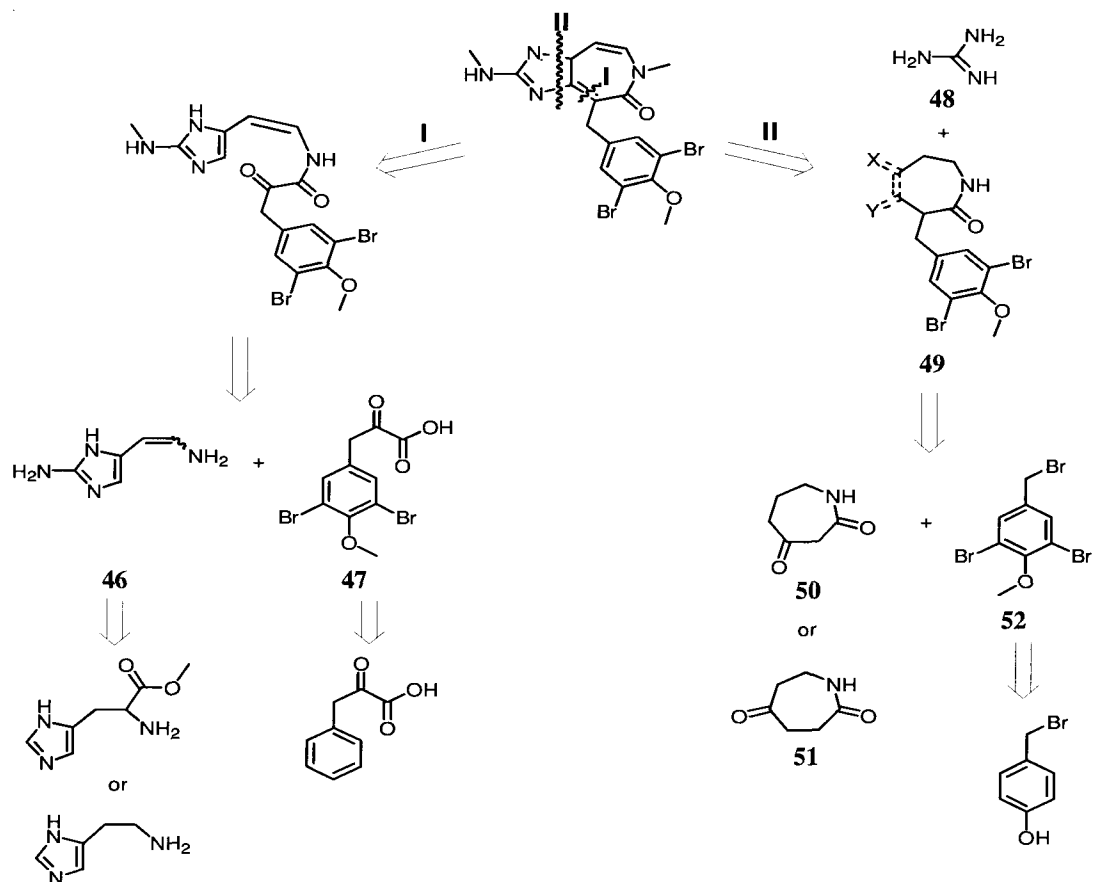


Scheme 4.2. Double bond character of the C2-N18 imine bond of ceratamine A (**13**).²¹⁰

The NMR data for ceratamine B (**14**) also presents two sets of NMR resonances in the same ratio as **13**.²¹⁰ When methyl H19 is removed as in recent synthetic analogues, only one set of NMR peaks can be observed. Nevertheless, both amine protons are distinct in such derivatives, suggesting again restriction in the free rotation of this functionality.

4.2.3. Retrosynthetic analysis

Considering the proposed biogenetic origin of ceratamines (Section 4.2.1), disconnection **I** (Scheme 4.3) seemed a logical starting point. Synthones (**46**) and (**47**) may be prepared from phenylpyruvic acid and either histidine or histamine. Disconnection **II** leads to guanidine (**48**) and synthon (**49**), which may be obtained via alkylation of azepanediones (**50**) or (**51**) with a benzyl bromide derivative (**52**). Preparation of azepanediones (**50**) and (**51**) may be possible via Beckmann rearrangement of a suitable cyclic diketone.

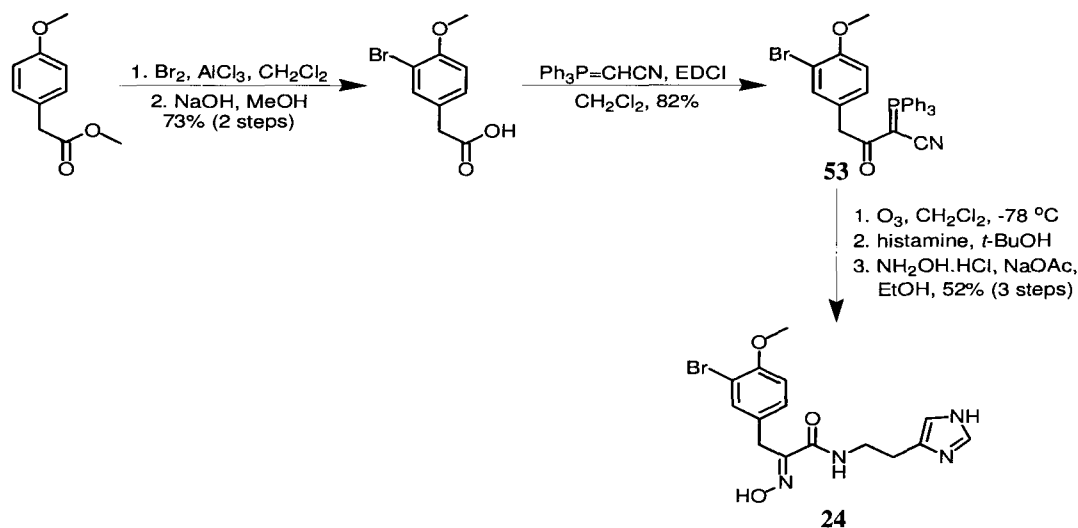


Scheme 4.3. Retrosynthetic analysis of ceratamine A (13).

Clearly, synthetic methodologies leading to the preparation of 2-aminoimidazoles, either from guanidine or starting with a preformed imidazole ring, will determine the viability of any proposal for the preparation of ceratamines. Besides possessing the common aspects of an efficient synthetic pathway (minimum amount of steps, good yields, commercially accessible starting materials, inexpensive), the synthesis of ceratamines should be designed to allow generation of analogues required for structure-activity relationship studies.

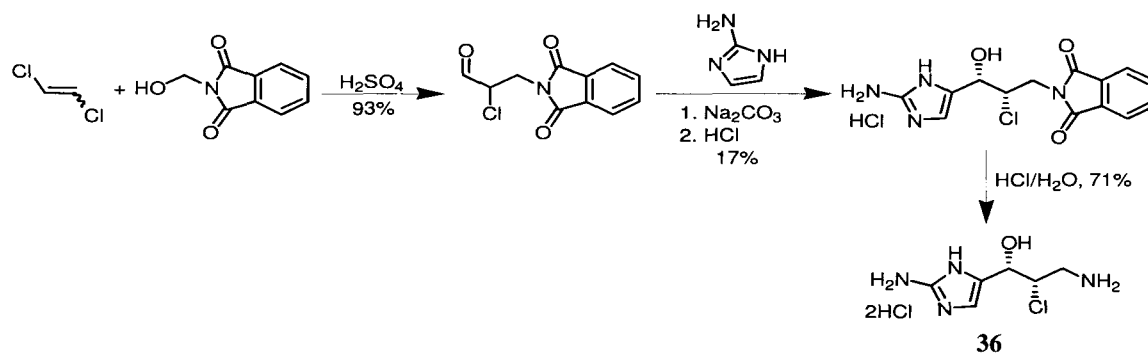
4.3. Related syntheses and relevant synthetic methodologies: literature review

Among the bromotyrosine/histidine-derived metabolites biogenetically related to the ceratamines (Scheme 4.1), only verongamine (**24**) has been synthesized. In 1988, Wasserman and Wang²⁴⁴ developed an efficient method for producing α -keto amido residues, precursors of the α -oximido units common in these compounds (Scheme 4.4). The procedure involves conversion of a carboxylic acid to an acyl cyano phosphorane (**53**) which may be oxidized to a α,β -diketonitrile, and afforded **24** in 6 steps with an overall yield of 31%.



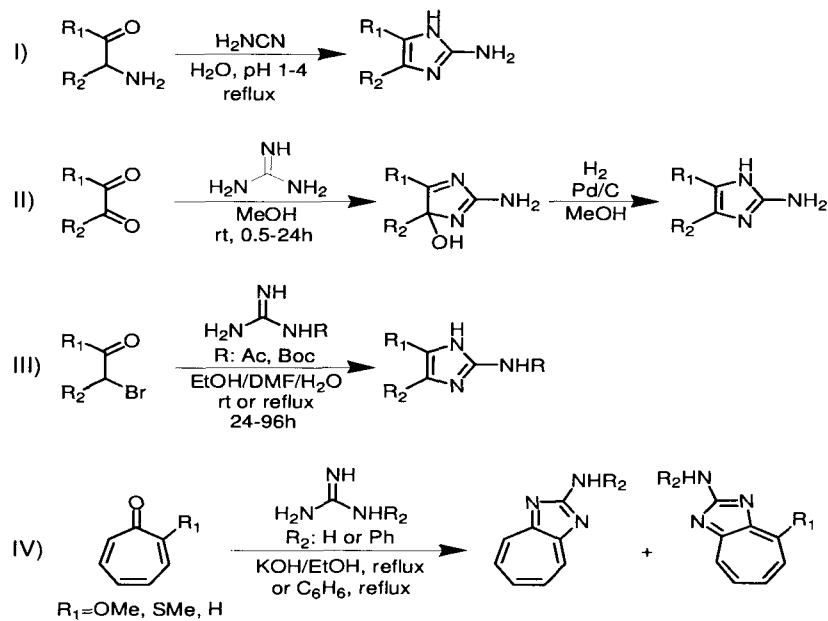
Scheme 4.4. Total synthesis of verongamine (**24**).²⁴⁴

Several syntheses of the 1,4-disubstituted imidazole alkaloid girolline (**36**) have been reported.²⁵²⁻²⁵⁴ Although **36** is structurally simple, the density of functionalities and rapid decomposition of intermediates provided an additional challenge during its preparation. In one of these methodologies, Al-Mourabit and coworkers²⁵⁵ exploited the fact that 2-aminoimidazoles can undergo nucleophilic addition in reactions analogous to those of enamides with aldehydes (Scheme 4.5).²⁵⁶



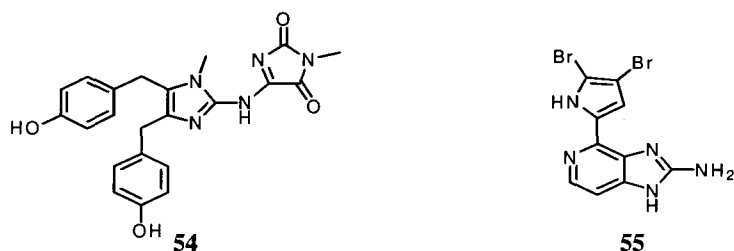
Scheme 4.5. Synthesis of girolline (**36**) by Al-Mourabit and coworkers.²⁵⁵

Synthetic transformations directed to the preparation of the 2-aminoimidazole motif can be divided in two categories, *de novo* imidazole construction and imidazole elaboration. In the first category, classical approaches include the condensation of α -aminocarbonyl compounds with cyanamide (**I**),²⁵⁷⁻²⁶⁰ combination of α -diketones with guanidine followed by reduction (**II**),^{261,262} and reaction of α -haloketones (**III**)²⁶³ and cycloheptatrienones (**IV**) with guanidine derivatives.²⁶⁴⁻²⁶⁶

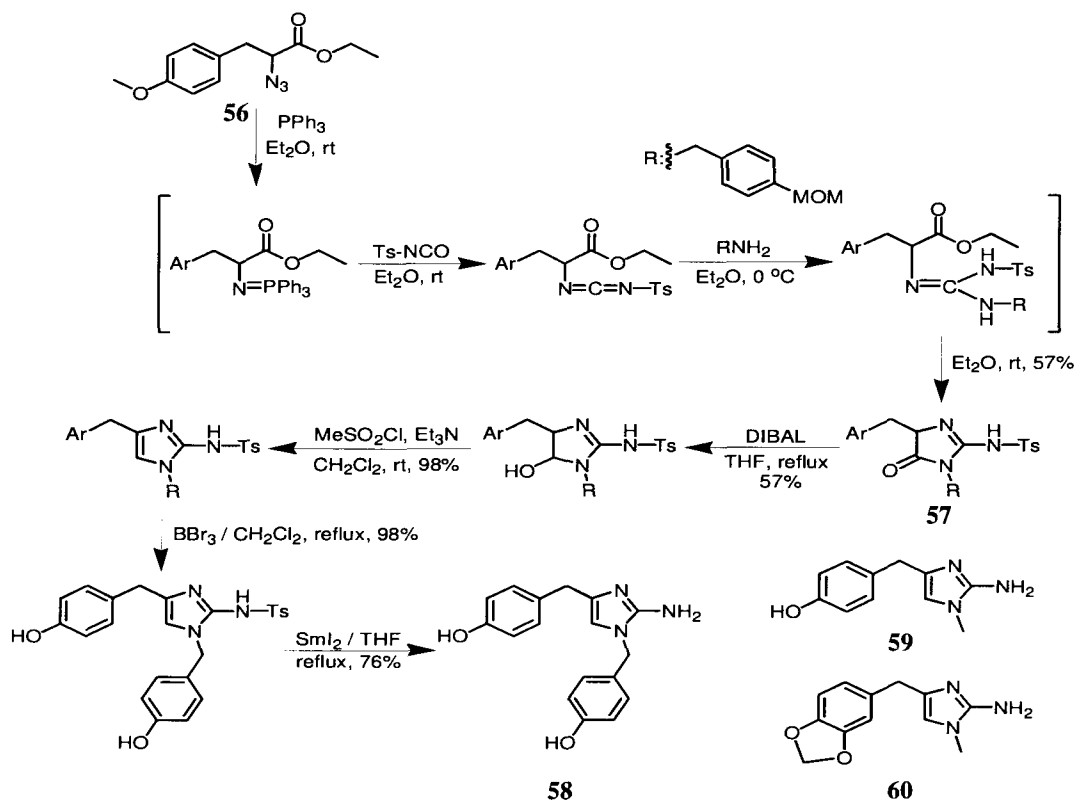


Scheme 4.6. Classical *de novo* preparation of 2-aminoimidazoles.

Recently, methodologies **I** and **III** have been successfully applied in the total synthesis of sceptrin (**41**),^{250,267} ageliferin (**43**),²⁶⁸ grossularines A (**44**) and B (**45**),²⁵¹ naamidine A (**54**),²⁶⁹ ageladine A (**55**),²⁷⁰ and other similar marine metabolites.²⁷¹⁻²⁷⁷

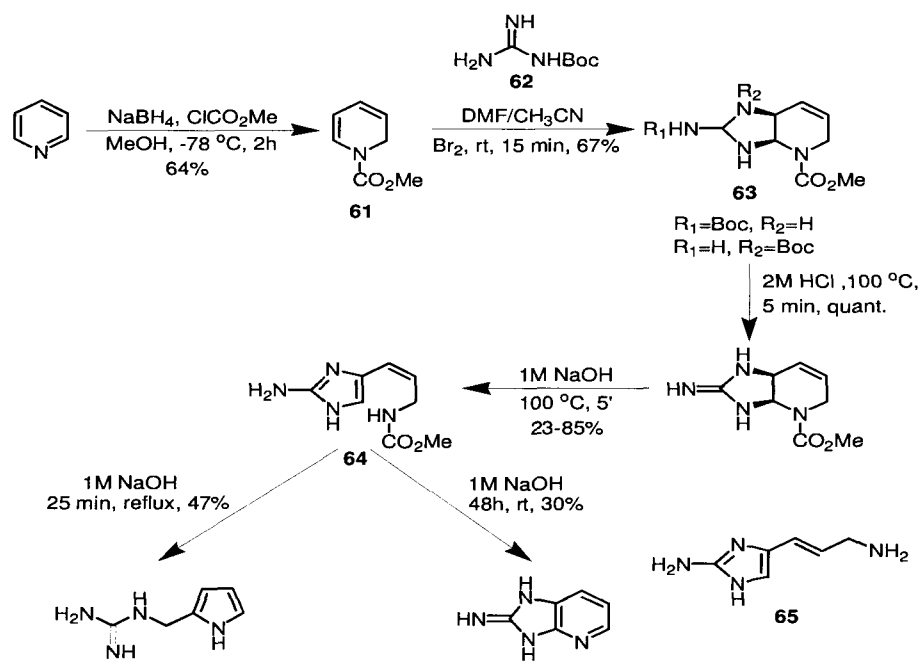


A different approach was developed by Molina, Fresneda and Sanz,²⁷⁸ who synthesized isonaamine A (**58**), dorimidazole A (**59**), and preclathridine A (**60**), via a Staudinger/aza-Wittig/carbodiimide-mediated cyclization process (Scheme 4.7). The one-pot conversion of α -azido ester (**56**) to imidazolone (**57**) proceeded in a 50-60% yield.



Scheme 4.7. Construction of 2-aminoimidazoles according to Molina, Fresneda and Sanz.²⁷⁸

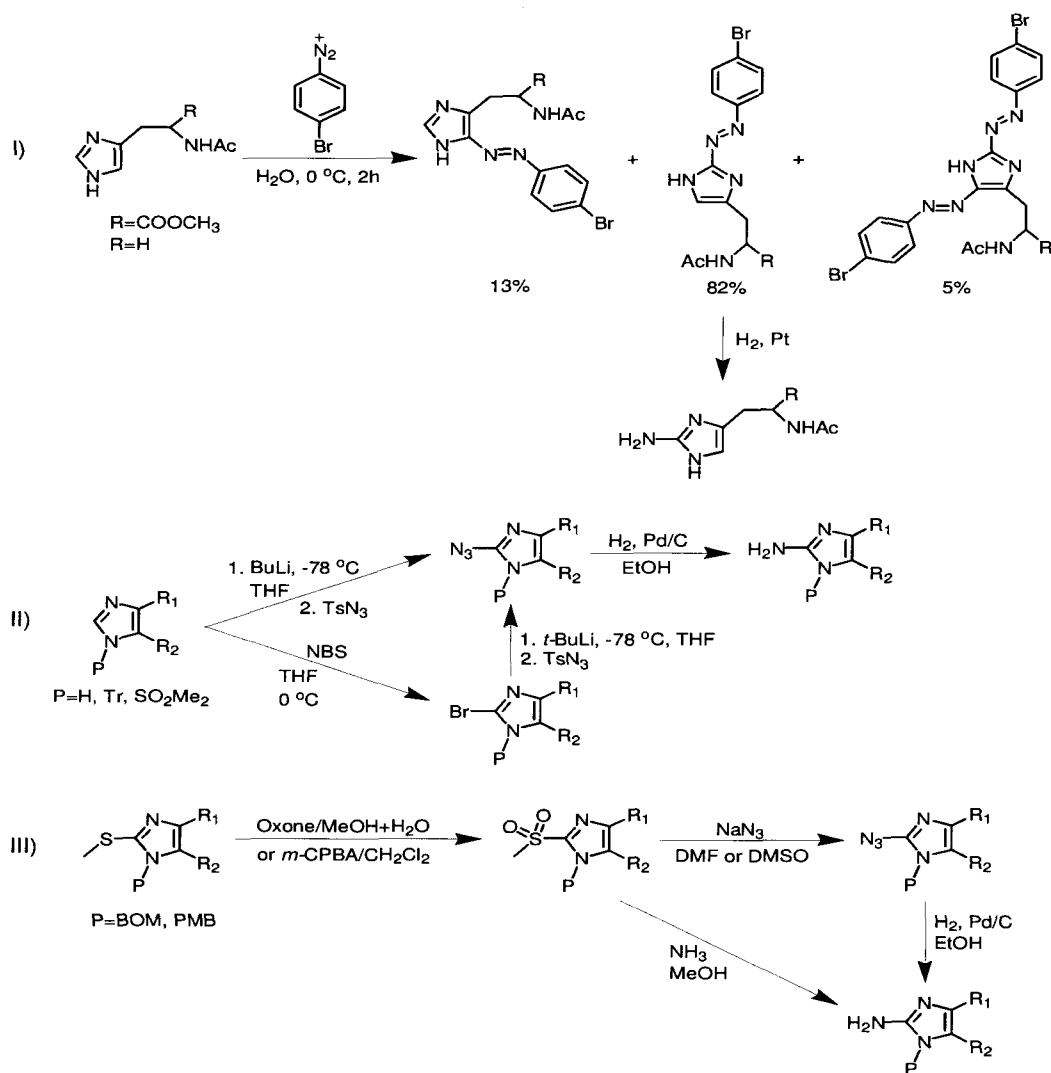
Another procedure was reported by Al-Mourabit and colleagues²⁷⁹ in their synthesis of (*Z*)-3-amino-1-(2-aminoimidazol-4-yl)prop-1-ene methyl carbamate (**64**), closely related to metabolite (**65**) isolated in 1991 from *Axinellidae* sponges.²⁸⁰ Addition of Boc-guanidine (**62**) to *N*-carbomethoxy-1,2-dihydropyridine (**61**) in the presence of Br₂ afforded aminal (**63**), which upon deprotection was cleaved under basic conditions to afford **64**. The yield for this last step is dramatically time and temperature dependant, and the instability exhibited by **64** under basic conditions limits its preparation in large quantities. Recently, an improved version of this method was applied in the synthesis of hymenidin (**38**).²⁸¹



Scheme 4.8. Synthesis of (*Z*)-3-amino-1-(2-aminoimidazol-4-yl)prop-1-ene methyl carbamate (**64**) according to Al-Mourabit and colleagues.²⁷⁹

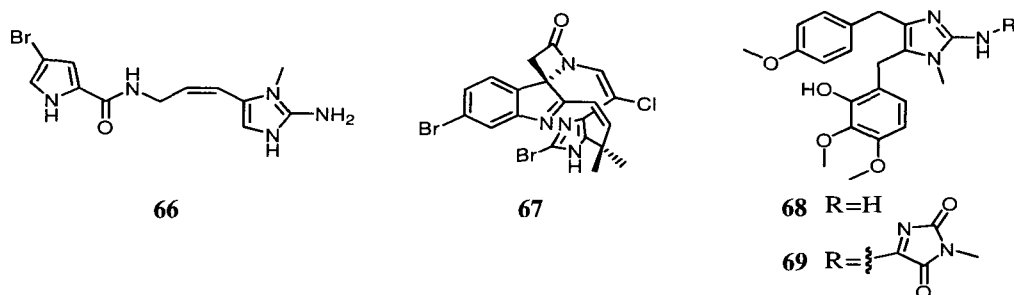
Only three methods, starting from preformed imidazole rings, have been reported for the direct introduction of an amino functionality at position 2: coupling with arene diazonium salts and further reduction (**I**, Scheme 4.9),²⁸² bromide-mediated or direct metalation followed by

sequential treatment with aryl azide, acid or hydrogenation (**II**),²⁸³⁻²⁸⁶ and oxidation of a sulfur substituent at position 2 followed by treatment with ammonia (**III**), or azidation-hydrogenation sequence as in **II**.²⁸⁷



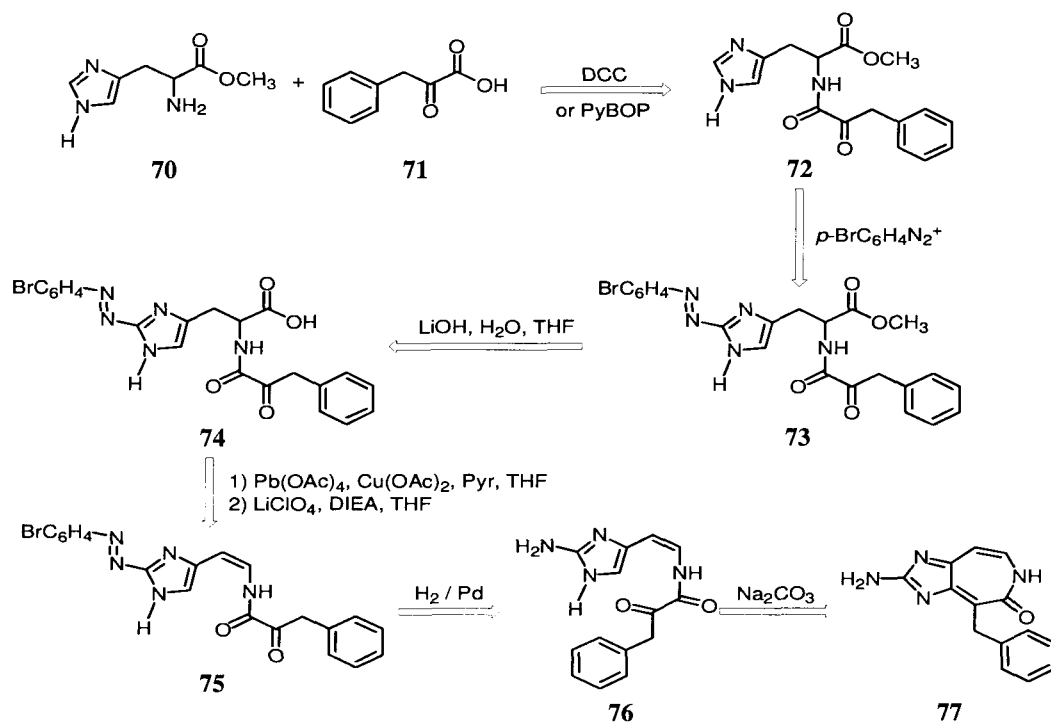
Scheme 4.9. Synthesis of 2-aminoimidazoles via elaboration of a preexisting imidazole ring.

The initial preparations of oroidin (**37**)^{288,289} and its methyl analogue keramidine (**66**),²⁸⁹ as well as the more recent total syntheses of naamidine A (**54**),²⁹⁰ ageladine A (**55**),^{291,292} chartelline C (**67**),²⁹³ naamine C (**68**), and pyronaamidine (**69**),²⁹⁴ were executed using methods **II** and **III**.



4.4. Initial synthetic proposals

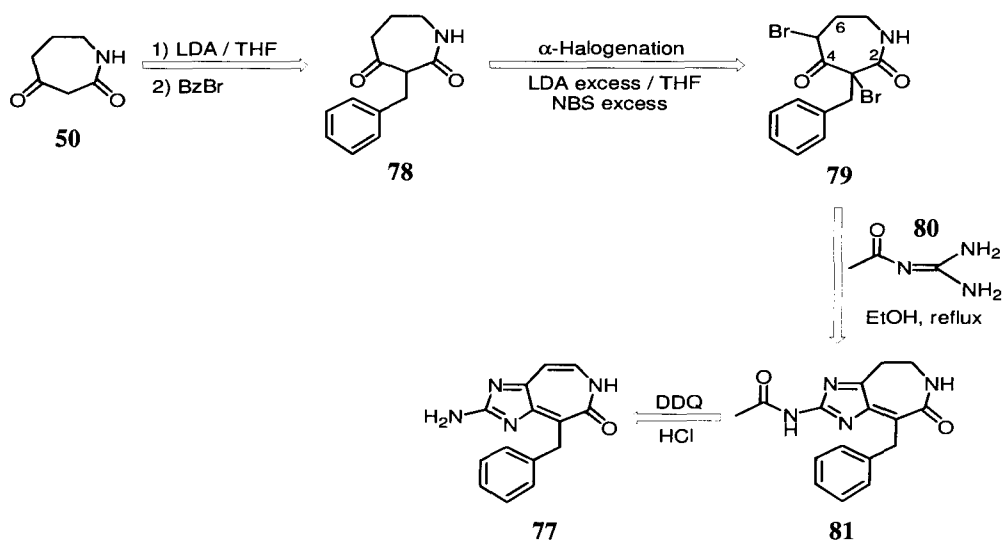
The first route envisioned to build the new imidazo[4,5,*d*]azepine core of ceratamines follows very closely their proposed biogenesis (Scheme 4.1), and employs L-histidine methyl ester (**70**) and phenylpyruvic acid (**71**) as starting materials (Scheme 4.10).



Scheme 4.10. Biomimetic synthetic pathway for the preparation of ceratamine analogue (**77**).

Thus, standard peptide coupling between starting materials (**70**) and (**71**) was expected to afford intermediate (**72**), which under treatment with an aryldiazonium salt,²⁸² would form **73**. Ester hydrolysis and $\text{Pb}(\text{OAc})_4/\text{Cu}(\text{OAc})_2$ mediated oxidative decarboxylation²⁹⁵ lead to **75**, while hydrogenation conditions cleaves the diazo linkage to afford a 4-substituted 2-aminoimidazole ring.²⁸² In the last step, an intramolecular base-promoted condensation as in the synthesis of girolline (**36**) by Marchais and coworkers,²⁵⁵ would afford ceratamine analogue (**77**). As mentioned in Section 4.2.1, the driving force for the formation of **77** is achievement of aromaticity.

Parallel to the biomimetic route above, a more classical pathway was also implemented (Scheme 4.11). Lithiation of azepane-2,4-dione (**50**) and treatment with benzyl bromide was expected to form **78**, which upon α -halogenation with excess of base and NBS would afford dibrominated intermediate (**79**). The bromine in C5 sets the stage for condensation with *N*-acetylguanidine (**80**) according to Little and Weber,²⁶³ whereas bromine at C3 will serve as a leaving group assisting the DDQ-mediated aromatization of the entire carbon backbone.



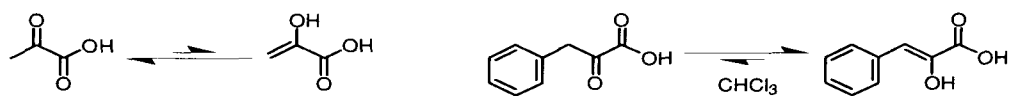
Scheme 4.11. A more classical first generation approach to analogue **77**.

Both synthetic sequences can be applied in the preparation of analogues with several substitution patterns in the benzylic side arm, or even completely different alkyl groups at C3, by employing other commercially available pyruvic acids (Scheme 4.10) or alkyl halides (Scheme 4.11). The second route is more flexible if ring size or heteroatom content is to be varied. For example, the use of a six-membered analogue of **50** can be easily implemented. Replacement of *N*-acetylguanidine with acetamide (CH_3CONH_2) and thioacetamide (CH_3CSNH_2) should incorporate oxygen and sulfur into the bicyclic system.

4.5. Attempted preparation of ceratamines and analogues

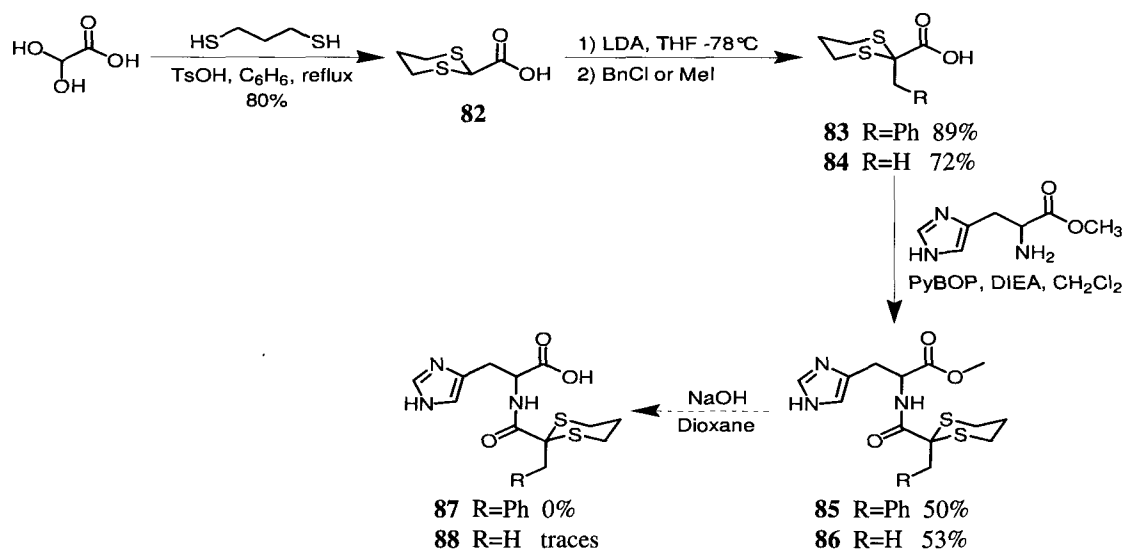
4.5.1. Biomimetic approach to ceratamines

Initial DCC, CDI and PyBOP-mediated coupling reactions between L-histidine methyl ester and phenylpyruvic acid (Scheme 4.10) were fruitless. Examination of NMR data revealed in all reaction crudes the presence of an enolized phenylpyruvic acid, also detected as the major constituent in the starting material. Unlike pyruvic acid, enolization of phenylpyruvic acid leads to a stable conjugated system, which seems to prevail over the ketone form depending on the solvent.²⁹⁶⁻²⁹⁹



Such conjugation decreases reactivity of the carboxylic group, which cannot be activated by standard peptide coupling reagents. Additionally, the presence of a β -hydroxyl group may not be compatible with their action. It was thus necessary to build a carbonyl-protected version of phenylpyruvic acid, capable of coupling with L-histidine methyl ester. Bates and Ramaswamy³⁰⁰

prepared several protected α -keto acids, by alkylating the lithium dianion derived from glyoxilic thioketal (**82**) with various alkyl halides (Scheme 4.12). This methodology afforded analogues (**83**) and (**84**) with high purity, in a simple, fast and high yielding fashion. Furthermore, it added flexibility in the future preparation of ceratamine variants via the biomimetic approach. The carbonyl can later be deprotected by acid hydrolysis.^{300,301}



Scheme 4.12. Reactions involved in the biomimetic approach to ceratamine analogues.

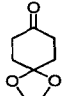
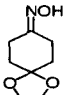
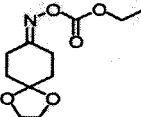
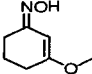
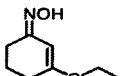
PyBOP-mediated coupling³⁰² of L-histidine methyl ester with **83** or **84** afforded the desired adducts in 50% and 53% yields, respectively, which were confirmed by HRESIMS and NMR analysis. The thioketal motif as a protecting group would be incompatible with the strong acidic conditions involved in preparing 2-aminoimidazoles via arene diazonium salts (I, Scheme 4.9.),²⁸² hence it was decided to proceed with the decarboxylation step. However, basic hydrolysis of the methyl ester in the histidine component also cleaved the amide bond, apparently weakened by steric as well as electronic effects from both sulfurs and the six-membered ring constituting the thioketal functionality (Scheme 4.12). Such surprising events,

together with several failed attempts to separately functionalize the imidazole of L-histidine methyl ester, prompted immediate implementation of an alternative route to ceratamines.

4.5.2. First generation approach to ceratamines

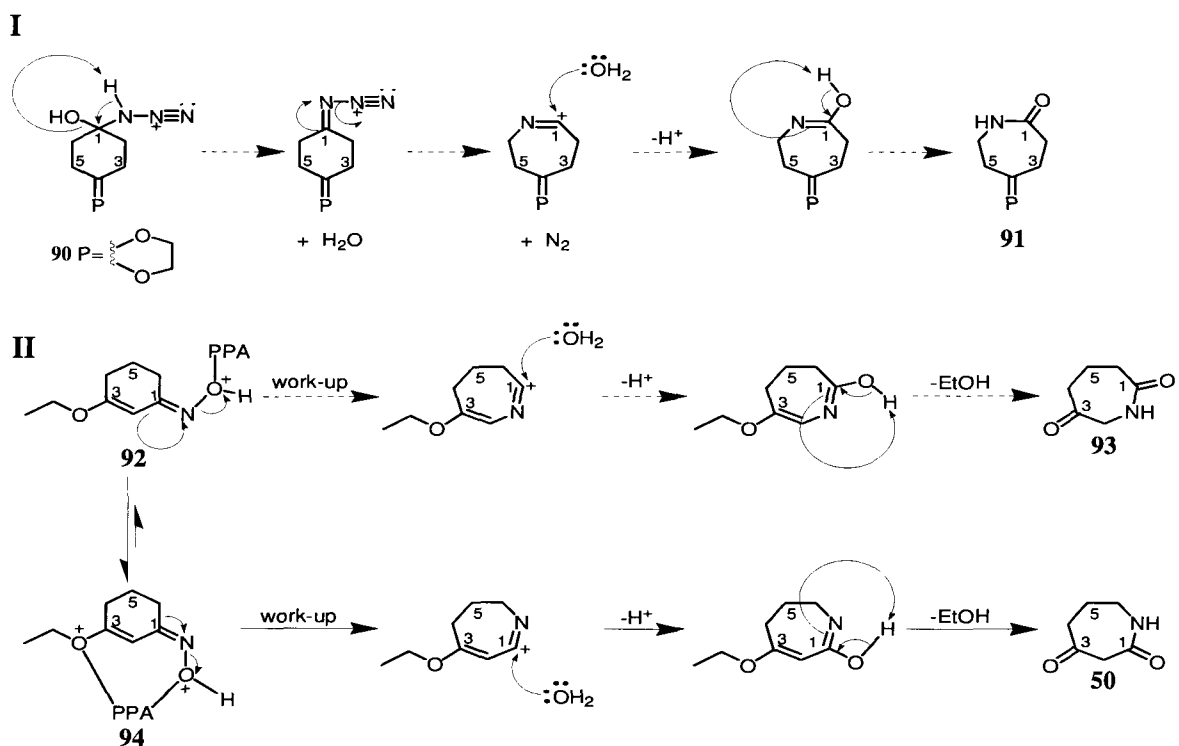
According to Scheme 4.11, access to an azepanedione similar to **50** was the first task that needed to be achieved. As mentioned in Section 4.2.3, Beckmann rearrangement of an appropriate oxime may be a viable method to generate **50**. Several starting materials and reaction conditions were therefore tested and are summarized in Table 4.1. In principle, azepane-2,4-dione (**50**) and azepane-1,4-dione (**51**) can both act as a suitable precursor for constructing 2-aminoimidazoles.

Table 4.1. Rearrangement of various 1,4- and 1,3-cyclohexadione derivatives.

No	S. M. ^a	Reagents and conditions	Observations ^c
1		CH ₃ SO ₃ H, NaN ₃ , 25°C, 3 h. ³⁰³⁻³⁰⁶ NH ₂ OH.HCl, (COOH) ₂ , 80°C, 12 h. ^{303,304,307}	Multiple byproducts Multiple byproducts
2		PCl ₅ , 25°C, 16 h. ^{308,309} AlCl ₃ , 60°C, 30 min. ^{309,310} PPA, ^b 100°C, 4 h. ³⁰⁹ 0.5 eq. BF ₃ .Et ₂ O, 25°C, 12 h. ³¹¹	Traces (51) 1,4-cyclohexadione Traces (51) S. M.
3		1 eq. BF ₃ .Et ₂ O, 25°C, 12 h. ³¹¹ 1 eq. BF ₃ .Et ₂ O, 25°C, 48 h. ³¹¹ 1.5 eq. BF ₃ .Et ₂ O, 25°C, 12 h. ³¹¹ 2 eq. BF ₃ .Et ₂ O, 25°C, 12 h. ³¹¹ 3 eq. BF ₃ .Et ₂ O, 25°C, 12 h. ³¹¹ 4 eq. BF ₃ .Et ₂ O, 25°C, 12 h. ³¹¹	S. M. S. M. Deprotection S. M., deprotection Multiple byproducts S. M., deprotection
4		32 mmol, 120 g PPA 115°C, 1 h, CH ₂ Cl ₂ extractions. ^{312,313}	17% yield (50)
5		6.6 mmol, 30 g PPA, 115°C, 1 h, CH ₂ Cl ₂ extractions. ^{312,313} 37.0 mmol, 100 g PPA, 115°C, 1 h, EtOAc extractions. ^{312,313} 24.5 mmol, 100 g PPA, 115°C, 1 h, BuOH extractions. ^{312,313}	21% yield (50) 60% yield (50) 89% yield (50)

^aS. M.: starting material. ^bPPA: polyphosphoric acid. ^cAccording to NMR and MS data, or isolated yield.

Entry 1 (Table 4.1) actually corresponds to Schmidt^{305,306} rearrangement conditions (I, Scheme 4.13), which employ NaN_3 and $\text{CH}_3\text{SO}_3\text{H}$ to generate hydrazoic acid (HN_3) *in situ*. Entries 2-5 represent several reaction conditions for Beckmann rearrangement (II).³⁰⁷⁻³¹³ The best results were obtained when polyphosphoric acid (PPA) was used to catalyze the process. Clearly, azepane-2,4-dione (**50**) is quite water-soluble and must be extracted from the neutralized aqueous layer during work-up with very polar organic solvents, in order to minimize losses. All NMR and MS data were in accord with that previously reported for **50**.³¹³



Scheme 4.13. Mechanisms for Schmidt (I) and Beckmann (II) rearrangements.

Noteworthy, only one rearrangement product was obtained when cyclohexan-1,3-dione was employed as starting material (II). According to the classical Beckmann mechanism, any of the alkyl groups flanking the carbonyl can migrate (Scheme 4.13). Moreover, Tamura and coworkers³¹³ reported that the migratory aptitude of both alkyl substituents during the Beckmann

rearrangement of α,β -unsaturated ketones is difficult to predict confidently. The symmetric cyclohexan-1,4-dione derivative (**90**) was expected to furnish only one rearrangement product (**I**). A possible explanation for the observed regioselectivity leading to **50** may involve the coordination of both the oxime's oxygen and the methoxy substituent at C3 with PPA, which acts as an anchor favoring the oxime's *syn*-isomer (**94**) over the *anti*-isomer (**92**). The former possesses an appropriate alignment between the acting nucleophile C6 and the leaving group attached to the nitrogen atom, for an intramolecular S_N2 -like process. Lewis acids assist in the departure of the leaving group.

Lithiation of azepane-2,4-dione (**50**) and treatment with benzyl chloride yielded the key intermediate 3-benzylazepane-2,4-dione (**78**) in 35% yield. The C3-dibenzylated byproduct (**95**) was also detected in the reaction crude, and accounts for the low yields obtained in this alkylation. When benzyl bromide was used as electrophile, the amount of dibenzyl byproduct increased. Evidently, after monobenzylation takes place, proton H3 of the newly formed 3-benzylazepane-2,4-dione (**78**) ($pK_a \sim 11$) is almost as acidic as the corresponding H3 of azepane-2,4-dione (**50**) ($pK_a \sim 10$)^{298,299}, and reacts easily with LDA giving rise to dibenzylation. When a more reactive electrophile such as BnBr is employed, the process is accelerated and the consumption of **78** increases.

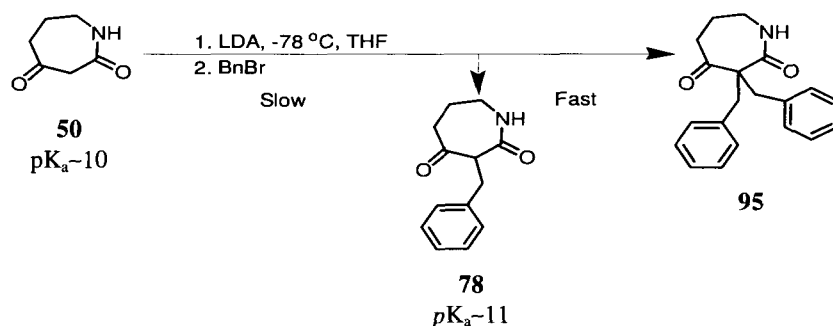
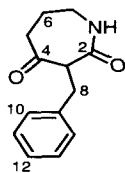


Table 4.2. NMR data for 3-benzylazepane-2,4-dione (**78**) (recorded in CD₂Cl₂).

Carbon No	¹³ C δ (ppm) ^a	¹ H δ (ppm) (mult, J (Hz)) ^{b,c}	HMBC ^b (H→C)
N1		6.11 (s, broad)	
2	169.5		
3	59.4	4.24 (dd, J = 6.7, 6.8 Hz)	C2, C4, C8, C9
4	204.2		
5	46.3	2.60 (m)	C3, C4, C7
6	30.7	1.92 (m), 2.10 (m)	C4, C5
7	41.9	3.31 (m), 3.75 (m)	C2, C5
8	31.8	3.15 (m)	C2, C3, C4, C9, C10
9	140.5		
10	129.6	7.16	C8, C12
11	128.8	7.24	C9
12	126.7	7.22	C10

^aRecorded at 100 MHz. ^bRecorded at 400 MHz. ^cAccording to HMQC recorded at 400 MHz.

Positive HRESIMS provided a [M+Na]⁺ ion at m/z 240.0996 consistent with a molecular formula of C₁₃H₁₅NO₂ (calculated for C₁₃H₁₅NO₂Na: 240.1000). NMR data (Table 4.2, Figure 4.4) shows the same coupled spin system H5/H6/H7/NH as in the starting material (**50**), and a new methine H3 (δ_H 4.24, dd, J = 6.7, 6.8 Hz, δ_C 59.4) coupled to the benzylic methylene H8 (δ_H 3.15, m, δ_C 31.8). The new stereocenter makes methylenes H5/H6/H7 diastereotopic, with protons in H6 (δ_H 1.92/2.10, δ_C 30.7) and H7 (δ_H 3.31/3.75, δ_C 41.9) showing important differences in chemical shifts. H3 displays HMBC correlations with both carbonyls C2 (δ_C 169.5) and C4 (δ_C 204.2), as well as C8 and the aromatic quaternary carbon C9 (δ_C 140.5). H8 in turn showed HMBC cross-peaks with neighboring carbons C3 and C9 (δ_C 140.5), carbonyls C2 and C4, as well as aromatic C10 (δ_C 129.6).

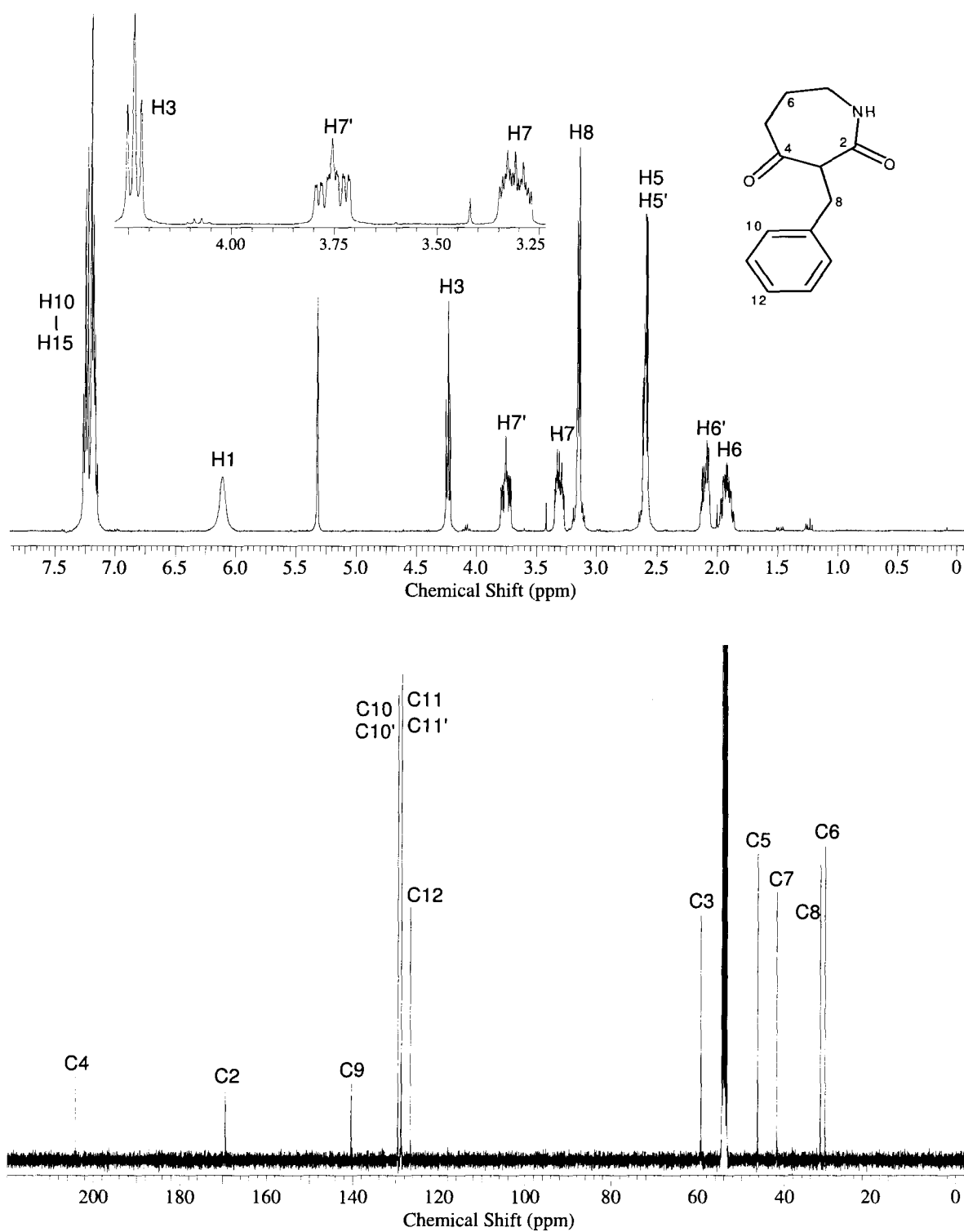
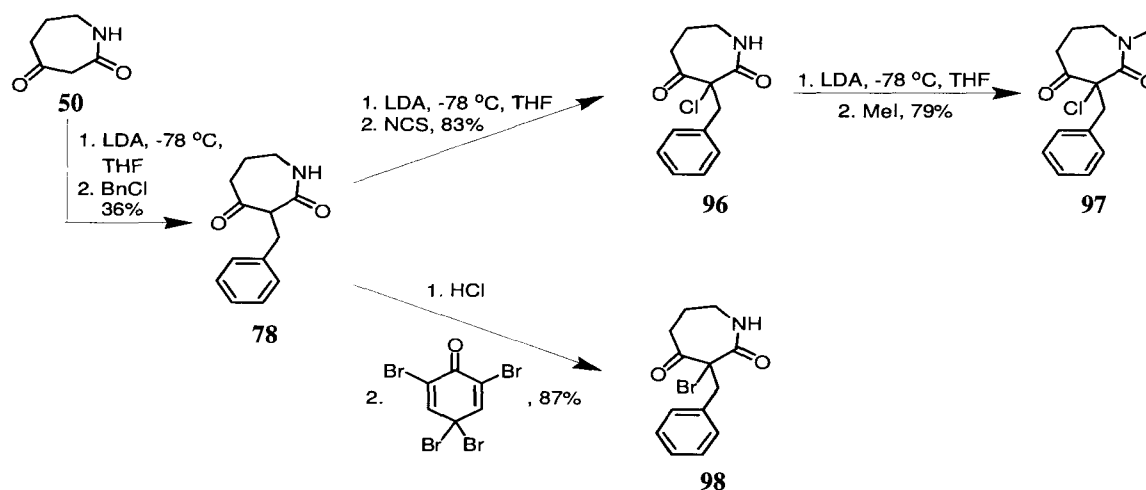


Figure 4.4. ^1H and ^{13}C -NMR spectra of 3-benzylazepane-2,4-dione (78) (recorded in CD_2Cl_2 at 400 and 100 MHz, respectively).

The next chemical modifications aimed to sequentially eliminate acidic protons and install halogens at C3 and C5, having in mind the procedure reported by Little and Weber²⁶³ for building 2-aminoimidazoles (Scheme 4.6). α -Bromination at C3 was achieved by treatment of **78** with 2,4,4,6-tetrabromoquinone in acidic media.^{314,315} Likewise, lithiation using LDA and addition of NCS^{316,317} furnished the chlorinated intermediate **96** (Scheme 4.14), which was then methylated under standard conditions³¹⁸ to afford 3-benzyl-3-chloro-1-methylazepane-2,4-dione (**97**).



Scheme 4.14. Synthesis of intermediates **97** and **98**.

The ¹H-NMR data for **97** shows absence of the amide proton resonance (around 6 ppm), which was replaced by a new singlet for methyl H13 (δ_{H} 3.00, δ_{C} 36.5) (Figures 4.5 and 4.6). More importantly, the now isolated methylene H8 (δ_{C} 44.0) displays two doublet resonances at δ_{H} 3.29 ($J = 12.8$ Hz) and δ_{H} 3.83 ($J = 12.8$ Hz), typical for diastereotopic benzylic protons.

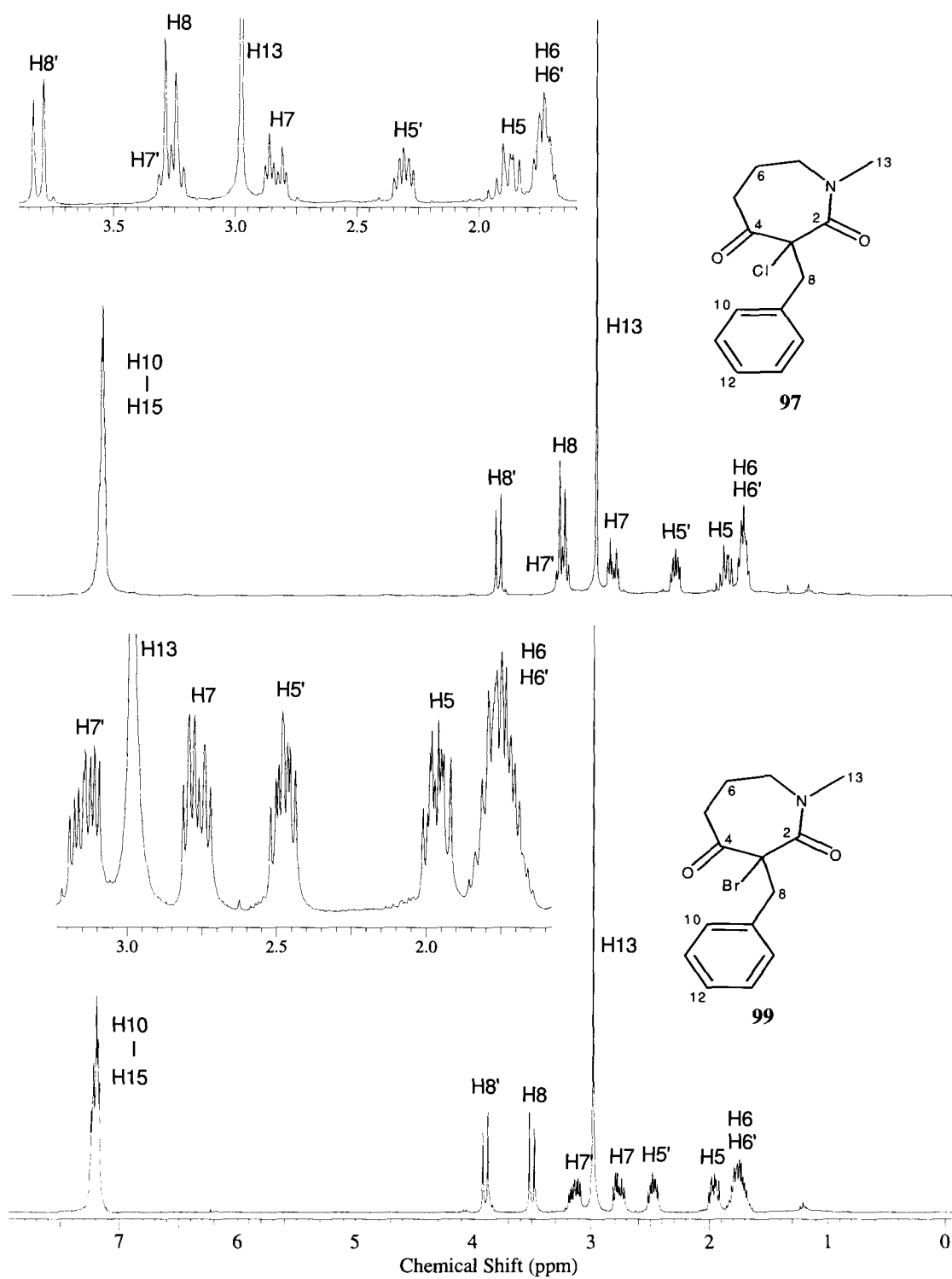


Figure 4.5. $^1\text{H-NMR}$ spectra of 3-benzyl-3-chloro-1-methylazepane-2,4-dione (**97**) and 3-benzyl-3-bromo-1-methylazepane-2,4-dione (**99**) (recorded in CDCl_3 at 300 MHz).

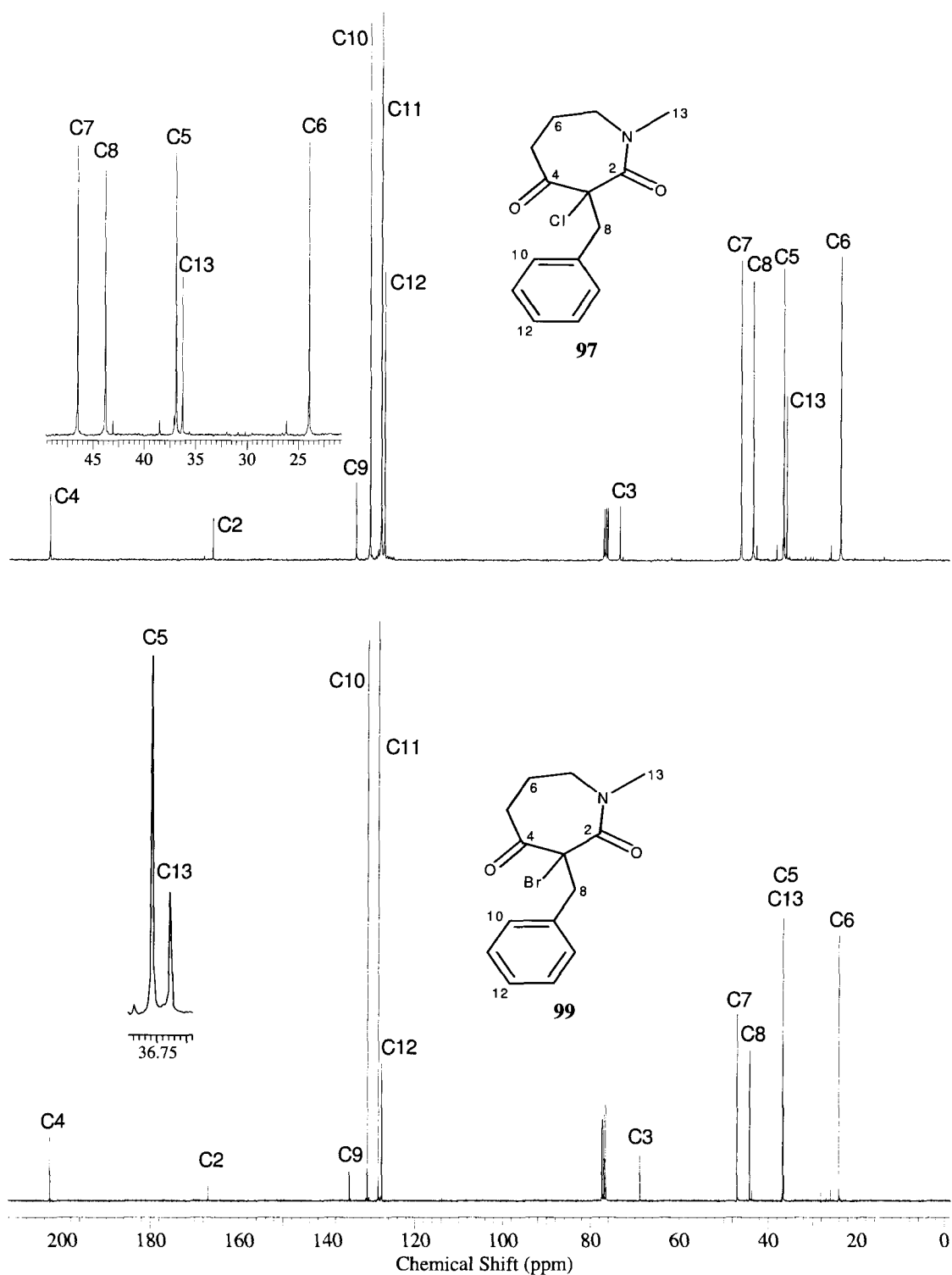
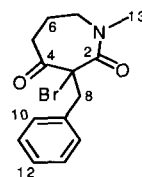
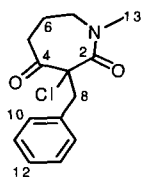


Figure 4.6. ^{13}C -NMR spectra of 3-benzyl-3-chloro-1-methylazepane-2,4-dione (**97**) and 3-benzyl-3-bromo-1-methylazepane-2,4-dione (**99**) (recorded in CDCl_3 at 75 MHz).

Methylenes H5 (δ_{H} 1.90, 2.33; δ_{C} 37.8), H6 (δ_{H} 1.75, δ_{C} 24.2), and H7 (δ_{H} 2.85, 3.28; δ_{C} 46.7) are also diastereotopic, but the difference in chemical shifts is less pronounced for H6 (flanked by methylenes, similar chemical and magnetic environments for both protons). Table 4.3 summarizes all the NMR assignments for 3-benzyl-3-chloro-1-methylazepane-2,4-dione (**97**). Methylation and chlorination was also confirmed by positive HRESIMS, which produced a $[\text{M}+\text{H}]^+$ ion at m/z 288.0764, in agreement with the molecular formula $\text{C}_{14}\text{H}_{16}\text{NO}_2\text{Cl}$ (calculated for $\text{C}_{14}\text{H}_{16}\text{NO}_2\text{Na}^{35}\text{Cl}$: 288.0767).

Table 4.3. NMR data for 3-benzyl-3-chloro-1-methylazepane-2,4-dione (**97**) and 3-benzyl-3-bromo-1-methylazepane-2,4-dione (**99**) (recorded in CDCl_3).

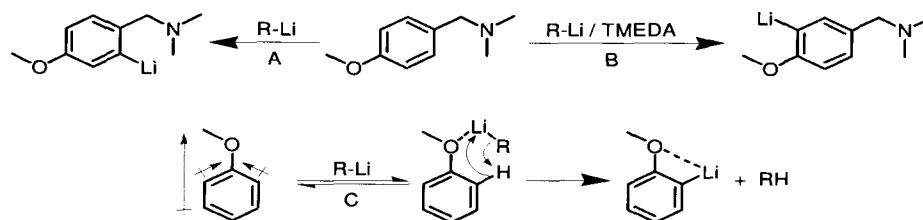


Carbon No	97		99	
	^{13}C δ (ppm) ^a	^1H δ (ppm) (mult, J (Hz)) ^{b,c}	^{13}C δ (ppm) ^a	^1H δ (ppm) (mult, J (Hz)) ^{b,c}
2	166.7		167.2	
3	74.1		69.1	
4	203.6		203.1	
5	37.8	1.90 (m), 2.33 (m)	37.0	1.95 (m), 2.48 (m)
6	24.2	1.75 (m)	24.3	1.75 (m)
7	46.7	2.85 (dt, $J = 5.2, 15.7$ Hz), 3.28 (m)	47.3	2.76 (m), 3.14 (m)
8	44.0	3.29 (d, $J = 12.8$ Hz), 3.83 (d, $J = 12.8$ Hz)	44.4	3.50 (d, $J = 12.7$ Hz), 3.90 (d, $J = 12.7$ Hz)
9	134.2		135.2	
10	131.0	7.21 (m)	131.1	7.25
11	128.4	7.19 (m)	128.6	7.19
12	127.6	7.17 (m)	127.8	7.18
13	36.5	3.00 (s)	36.9	2.99 (s)

^aRecorded at 75 MHz. ^bRecorded at 400 MHz. ^cAccording to HMQC recorded at 400 MHz.

Unfortunately, intermediates **97** and **98** proved remarkably intransigent, since attempts to functionalize C5 all failed. When **97** was treated with LDA and NCS a second time, only starting material was recovered. Replacing NCS by NBS furnished 3-benzyl-3-bromo-1-methylazepane-2,4-dione (**99**) in 79% yield, easily identified by comparing its NMR data with that previously obtained for **97** (Figures 4.5 and 4.6, Table 4.3). Additionally, positive HRESIMS afforded a $[M+H]^+$ peak at 310.0439, suitable for the molecular formula $C_{14}H_{16}NO_2Br$ (calculated for $C_{14}H_{17}NO_2^{79}Br$: 310.0443). Reaction of this compound with *t*-BuLi (2 eq.) and NCS yielded back the initial chlorinated starting material (**97**).

These last reactions showed that instead of proton abstraction at C5, **97** was undergoing lithium-halogen exchange at C3, and revealed the particular affinity of any lithium-based reagent towards this center. It is widely known that heteroatoms are able to direct the attack of lithium bases and promote regioselective deprotonation. They can coordinate with the organolithium reagent and increase kinetic basicity (**A**), or simply make nearby protons more acidic via inductive and/or resonance effects (**B**). A combination of both mechanisms is also possible (**C**).³¹⁹⁻³²¹



Upon LDA treatment, it is therefore reasonable to assume that the influence of both oxygen atoms at C2 and C4 leads preferentially to halogen-lithium exchange at C3, than the expected H5 abstraction. Furthermore, formation of an intermediate similar to enol (**101**) seems to be greatly disfavored in comparison with the conjugated and more stable enol (**100**), due to an

increment in eclipsed interactions ($H5 \leftrightarrow H6 \leftrightarrow H7$, $Cl \leftrightarrow O$) and ring tension, product of the additional induced planarity (Figure 4.7).

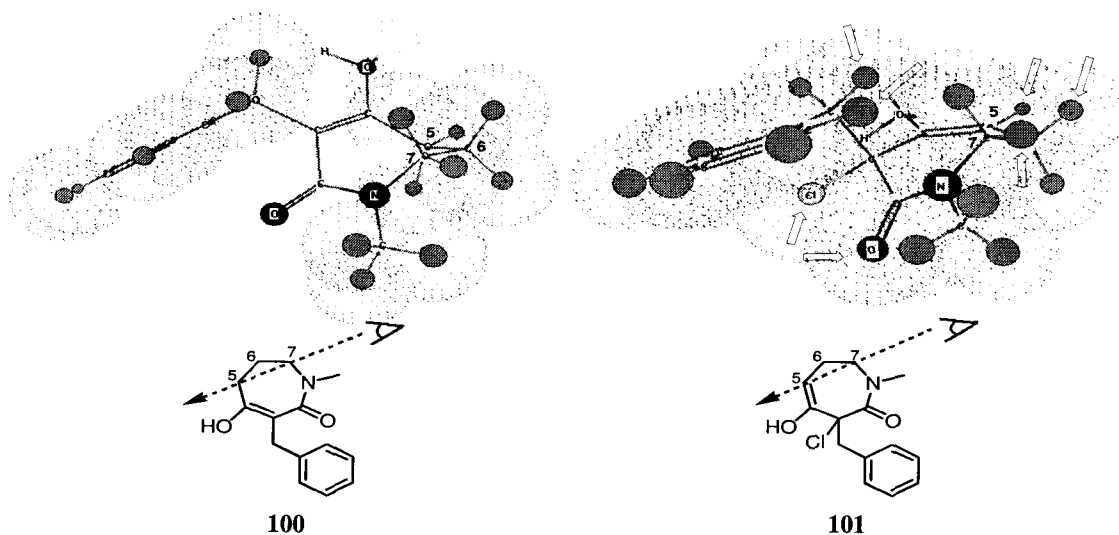
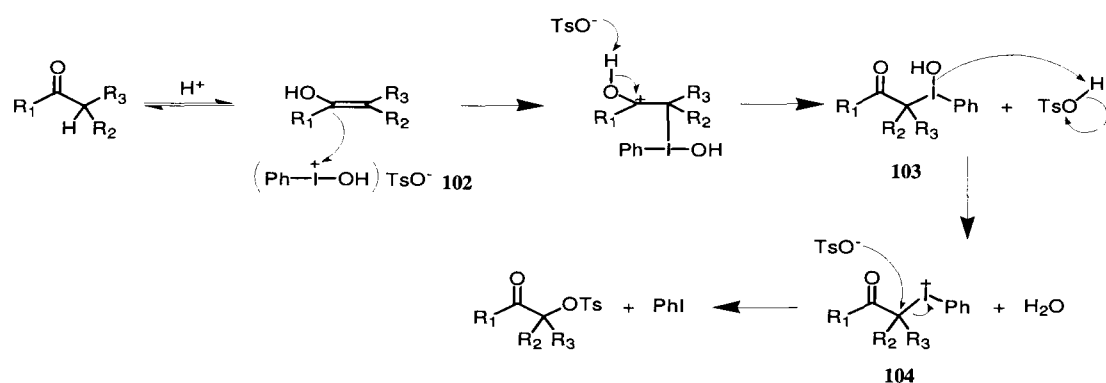


Figure 4.7. MM2 energy minimizations for enols (**100**) and (**101**). Arrows indicate eclipsed atoms (CS Chem3D Ultra 7.0, minimum RMS gradient 0.100).

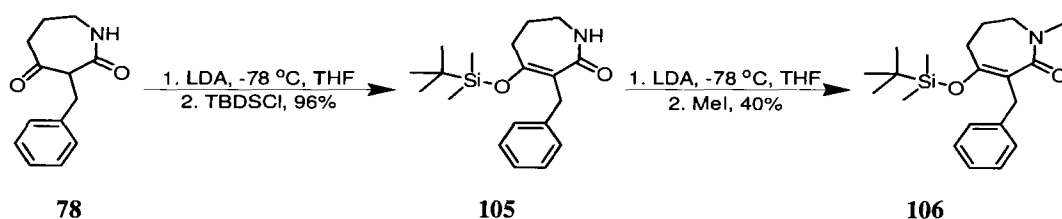
A bulkier bromine at C3 would provoke even more strain in the putative reaction intermediate (**101**), favoring again halogen-lithium exchange. In order to avoid this effect, an alternative route to functionalize C5 was evaluated. Several publications^{277,322-326} suggest the use of hypervalent iodine-based reagents to modify asymmetric ketones at their α -carbon. Particularly, Koser and coworkers,³²² as well as Nicolaou and his group,²⁷⁷ achieved α -tosylation of ketones using the commercially available [hydroxyl(tosyloxy)iodo]benzene (**102**) and iodobenzene diacetate $PhI(OAc)_2$, respectively. Presumably, reaction is initiated by electrophilic addition of $(PhIOH)^+OTs^-$ (**102**) (Scheme 4.15) to the enol tautomer yielding α -phenyliodonio ketones (**104**) as intermediates, which undergo nucleophilic displacement of iodobenzene by the tosylate ion, yielding the desired product.³²²



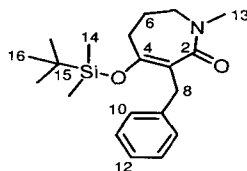
Scheme 4.15. α -Tosylation of ketones with hypervalent iodine reagent (**102**).^{322,325}

However, neither **97** nor **99** underwent tosylation at C5 using the previous methodologies. It was then decided to trap enol (**100**) and use a strong base to removed H5 in the enolate itself. In principle, *t*-BuLi ($pK_a \sim 53$ for 2-methylpropane) would be a good candidate for proton abstraction at C5 ($pK_a \sim 43$ for propene).²⁹⁹ However, from the intermediate viewpoint and as seen previously, two more sp^2 centers (five in total for the new enolate) in a seven-membered ring may not be viable. Nevertheless, the existence in nature of the ceratamine core itself was the main argument supporting such a forceful measure.

After several failed attempts to produce enolate (**100**) from intermediate (**97**) using various methodologies,³²⁷⁻³³⁰ the target compound was synthesized from 3-benzylazepane-2,4-dione (**78**) using TBDSCl, according to Scheme 4.16. Table 4.4 outlines all the NMR data collected for compound (**106**).



Scheme 4.16. Preparation of 3-benzyl-4-(*tert*-butyldimethylsilanyloxy)-1-methyl-1,5,6,7-tetrahydroazepin-2-one (**106**).

Table 4.4. NMR data for 3-benzyl-4-(*tert*-butyldimethylsilyloxy)-1-methyl-1,5,6,7-tetrahydroazepin-2-one (**106**) (recorded in CD₂Cl₂).

Carbon No	¹³ C δ (ppm) ^a	¹ H δ (ppm) (mult, J (Hz)) ^{b,c}	HMBC ^b (H→C)
2	172.6		
3	117.2		
4	154.1		
5	30.8	2.36 (t, J = 7.2 Hz)	C3, C4, C6, C7
6	29.0	2.00 (m)	C4, C5, C7
7	48.4	3.24 (m)	C2, C5, C13
8	32.9	3.67 (s)	C2, C3, C4, C9, C10, C11
9	142.0		
10	128.9	7.25-7.15 (m)	C8
11	128.7	7.25-7.15 (m)	C8
12	126.0	7.12 (m)	
13	34.5	2.94 (s)	C2, C7
14	-3.23	0.22 (s)	C15
15	18.6		
16	26.0	0.96 (s)	C15

^aRecorded at 100 MHz. ^bRecorded at 400 MHz. ^cAccording to HMQC recorded at 400 MHz.

In comparison with Figures 4.5 and 4.6, NMR data for **106** was significantly simplified when planarity was induced in the molecule. The ¹H-NMR spectrum (Figure 4.8, Table 4.4) displayed four singlet resonances, two of them typical for methyls H14 (δ_H 0.22, δ_C -3.23) and H16 (δ_H 0.96, δ_C 26.0) in the *t*-butyldimethylsilyloxy moiety. The remaining ones can be assigned to methyl H13 (δ_H 2.94, δ_C 34.5) and methylene H8 (δ_H 3.67, δ_C 32.9). H13 presented HMBC correlations with amide carbonyl C2 (δ_C 172.6) and methylene H7 (δ_H 3.24, δ_C 48.4), whereas H8 correlates with carbons in the aromatic and seven-membered rings, among them the vinylic C3 (δ_C 117.2) and C4 (δ_C 154.1), attached to an oxygen.

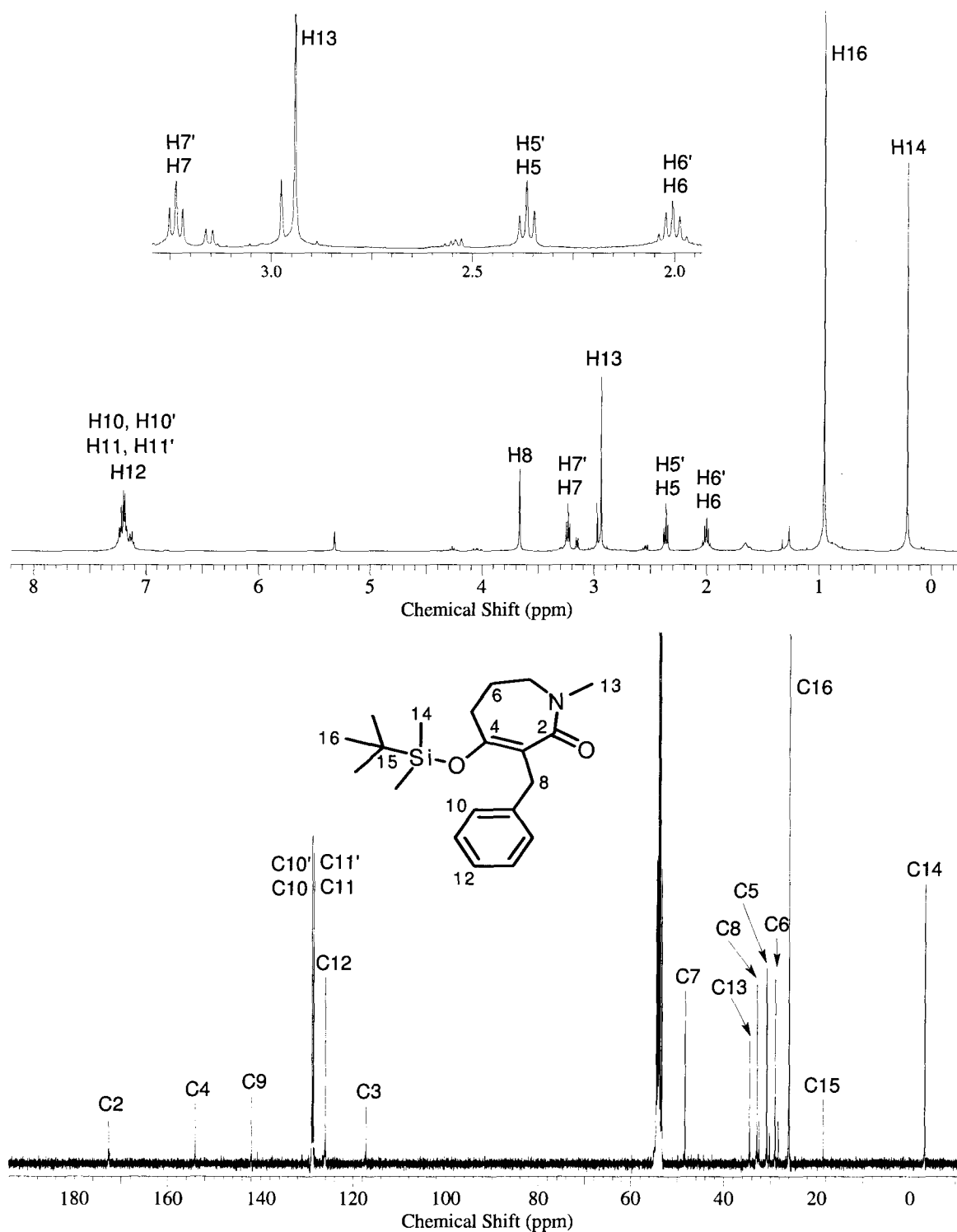


Figure 4.8. ^1H and ^{13}C -NMR spectra of 3-benzyl-4-(*tert*-butyldimethylsilyloxy)-1-methyl-1,5,6,7-tetrahydroazepin-2-one (**106**) (recorded in CD_2Cl_2 at 400 and 100 MHz, respectively).

Finally, HRESIMS displayed a $[M+Na]^+$ ion at m/z 368.2028, which was assigned the molecular formula $C_{20}H_{31}NO_2Si$ (calculated for $C_{20}H_{31}NO_2NaSi$: 368.2022).

Interestingly enough, treatment of **106** with LDA at low temperature followed by NCS addition furnished only one main reaction product displaying a $[M+Na]^+$ ion at m/z 402.1633, which was in agreement with a molecular formula of $C_{20}H_{30}NO_2SiCl$ (calculated for $C_{20}H_{30}NO_2NaSi^{35}Cl$: 402.1632). Clearly, a proton had been replaced by chlorine as expected, but not with the desired regiochemistry. Examination of the apparently simple 1H -NMR spectrum for this reaction product (Figure 4.9) showed a new singlet H8 (δ_H 3.02, δ_C 45.6) and a more disperse aromatic region (δ_H 7.75-6.75 ppm) than the starting material (Figure 4.8). HMQC correlations (Table 4.5) allow assignment of protons for methylenes H5 (δ_H 1.63/1.80, δ_C 39.2), H6 (δ_H 1.60/1.66, δ_C 24.2) and H7 (δ_H 3.11/3.79, δ_C 47.8) in the seven-membered ring, the now disperse aromatic proton resonances, especially H10 (δ_H 7.58, δ_C 132.5) and H14 (δ_H 6.37, δ_C 134.7), as well as methyls H16 (δ_H 0.14, δ_C -2.89), H17 (δ_H 0.33, δ_C -1.41) and H19 (δ_H 0.80, δ_C 27.8) in the *t*-butyldimethylsilyl group. The remaining carbons had chemical shifts typical for a ketone (C4, δ_C 206.4), an amide (C2, δ_C 168.1), a chlorinated quaternary carbon (C3, δ_C 77.6) as in **96** (Figure 4.6, Table 4.3), a quaternary sp^2 (C9, δ_C 138.6) and a quaternary sp^3 (C18, δ_C 19.4).

Thus, the *t*-butyldimethylsilyl motif was linked to neither the seven-membered nor the aromatic ring, leaving methine C8 as the only possible option. This was confirmed by HMBC correlations between H8 and carbons C16/C18, as well as between methyls H16/H17 and C8 (Table 4.5). H8 also gave HMBC cross peaks with numerous carbons in both rings, including carbonyls C2 and C4, as well as the *ortho* C10 and C14. The proximity between benzyl and *t*-butyldimethylsilyl moieties in **107** explains the newly acquired differences in chemical shifts for methyls H16 and H17 usually indistinguishable by NMR, as well as the pronounced dispersion of the aromatic resonances.

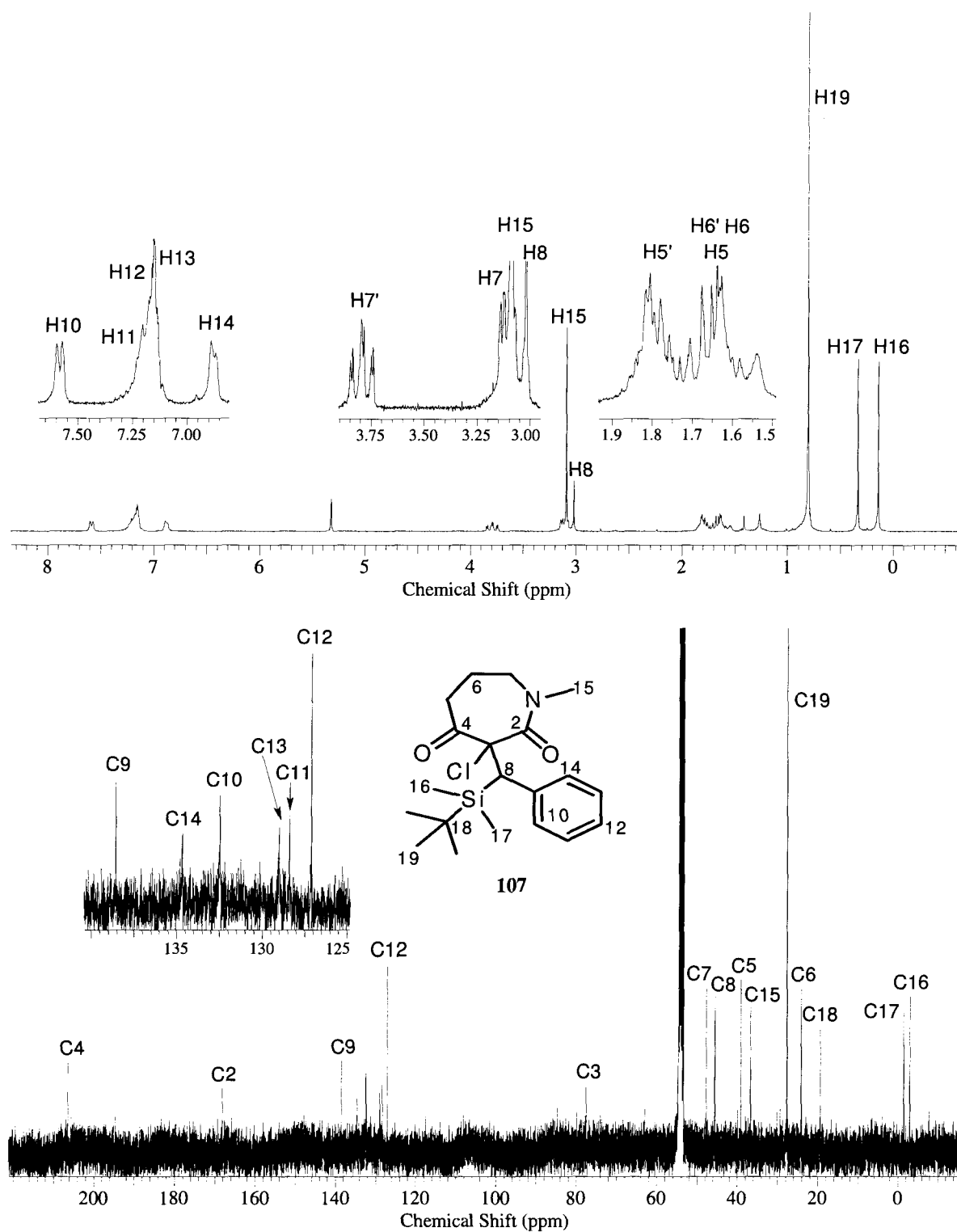
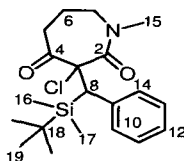


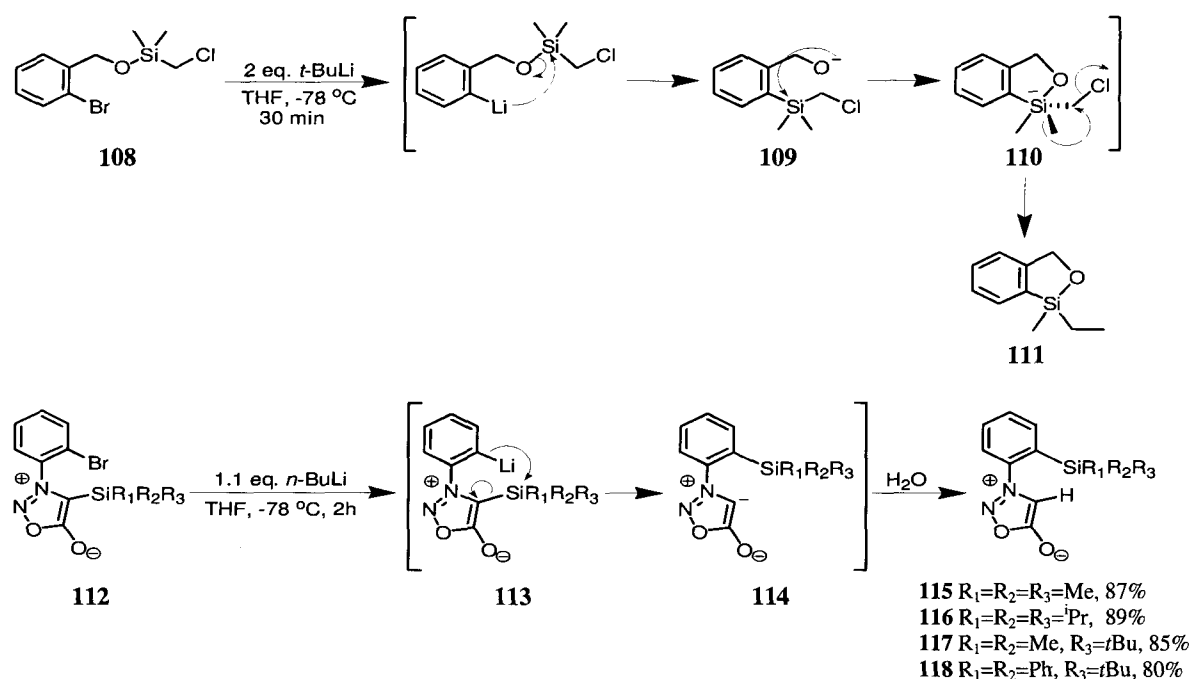
Figure 4.9. ^1H and ^{13}C -NMR spectra of 3-[(*tert*-butyldimethylsilyl)phenylmethyl]-3-chloro-1-methylazepane-2,4-dione (**107**) (recorded in CD_2Cl_2 at 400 and 100 MHz, respectively).

Table 4.5. NMR data for 3-[(*tert*-butyldimethylsilyl)phenylmethyl]-3-chloro-1-methylazepane-2,4-dione (**107**) (recorded in CD₂Cl₂).

Carbon No	¹³ C δ (ppm) ^a	¹ H δ (ppm) (mult, <i>J</i> (Hz)) ^{b,c}	HMBC ^b (H→C)
2	168.1		
3	77.6		
4	206.4		
5	39.2	1.63 (m), 1.80 (m)	C3, C4, C6, C7
6	24.2	1.60 (m), 1.66 (m)	C4, C5
7	47.8	3.11 (m), 3.79 (m)	C2, C5, C6, C15
8	45.6	3.02 (s)	C2, C3, C4, C9, C10, C14, C16, C18
9	138.6		
10	132.5	7.58 (d, <i>J</i> = 7.6 Hz)	C12, C14
11	128.4	7.18 (m)	C9, C13
12	127.0	7.14 (m)	C9, C10, C14
13	129.0	7.12 (m)	C14
14	134.7	6.87 (d, <i>J</i> = 6.7 Hz)	C10, C12
15	36.8	3.08 (s)	C2, C7
16	-2.89	0.14 (s)	C8, C17, C18
17	-1.41	0.33 (s)	C8, C16, C18
18	19.4		
19	27.8	0.80 (s)	C18

^aRecorded at 100 MHz. ^bRecorded at 400 MHz. ^cAccording to HMQC recorded at 400 MHz.

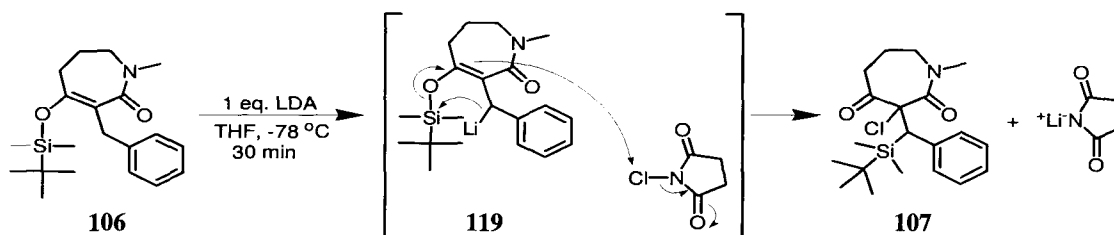
Rearrangements of organosilanes have been found to take place under acidic,^{331,332} basic^{331,333-336} or thermal^{331,337} conditions. During their studies about the stereochemistry of such rearrangements, Hijji, Hudrlik and Hudrlik³³⁸ treated silyl ether (**108**) with *t*BuLi at low temperature, to isolate after work-up, oxasilacyclopentane (**111**) as the only reaction product (Scheme 4.17). It was proposed that **111** arises via rearrangement to γ -oxidosilane (**109**), followed by methyl migration (presumably through intermediate **110**).



Scheme 4.17. Some examples for the rearrangement of organosilanes induced by alkyl-lithium reagents.^{338,339}

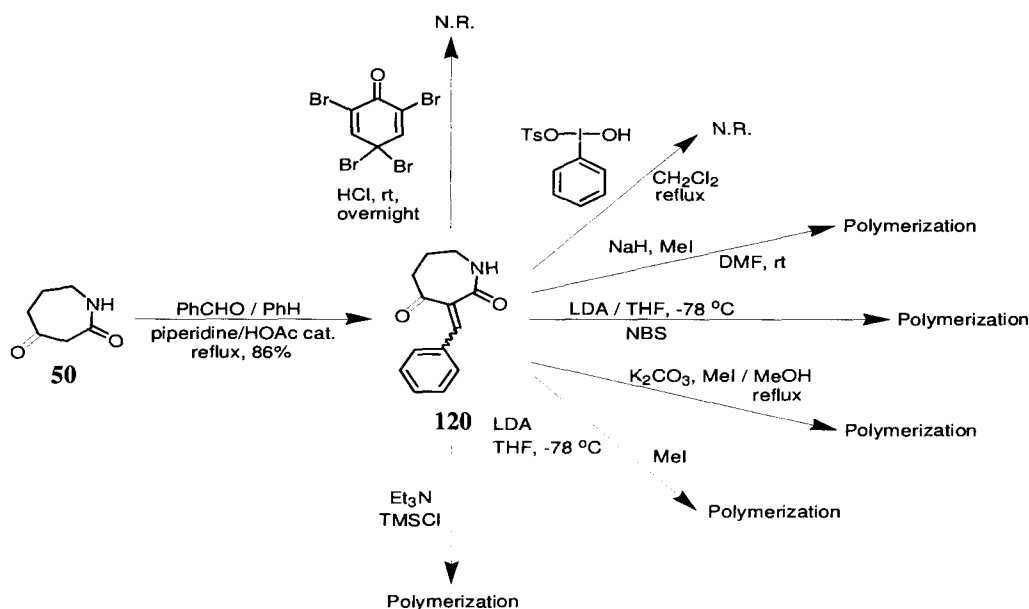
In another example, Turnbull and Krein³³⁹ synthesized in excellent yields (80-89%) a series of new sydnones (**115-118**) upon treatment of **112** with *n*-butyllithium in the absence of electrophiles. They suggested a very facile rearrangement of **113** to **114**, unaffected by steric hindrance around the silicon atom, with the greater thermodynamic stability of the sydnone anion (**114**) as the driving force for the whole process.

Based on these reports, a similar mechanism can be proposed for the formation of **107** (Scheme 4.18). Thus, upon exposure to alkyl-lithium, starting material **106** undergoes deprotonation at C8 to form a stable benzyl/allyl anion (**119**) which attacks the 4-silyl moiety and liberates the trapped enol. Ketone regeneration leads to a nucleophilic attack on *N*-chlorosuccinimide, giving rise to chlorination at C3. Preferential deprotonation at C8 correlates with relative acidities exhibited by methylene protons of 3-benzylpropan-2-one ($pK_a \sim 20$) and propene ($pK_a \sim 43$),²⁹⁹ as well as with the formation of a stable benzyl/allyl anion.



Scheme 4.18. Proposed mechanism for the rearrangement of **106** to **107**.

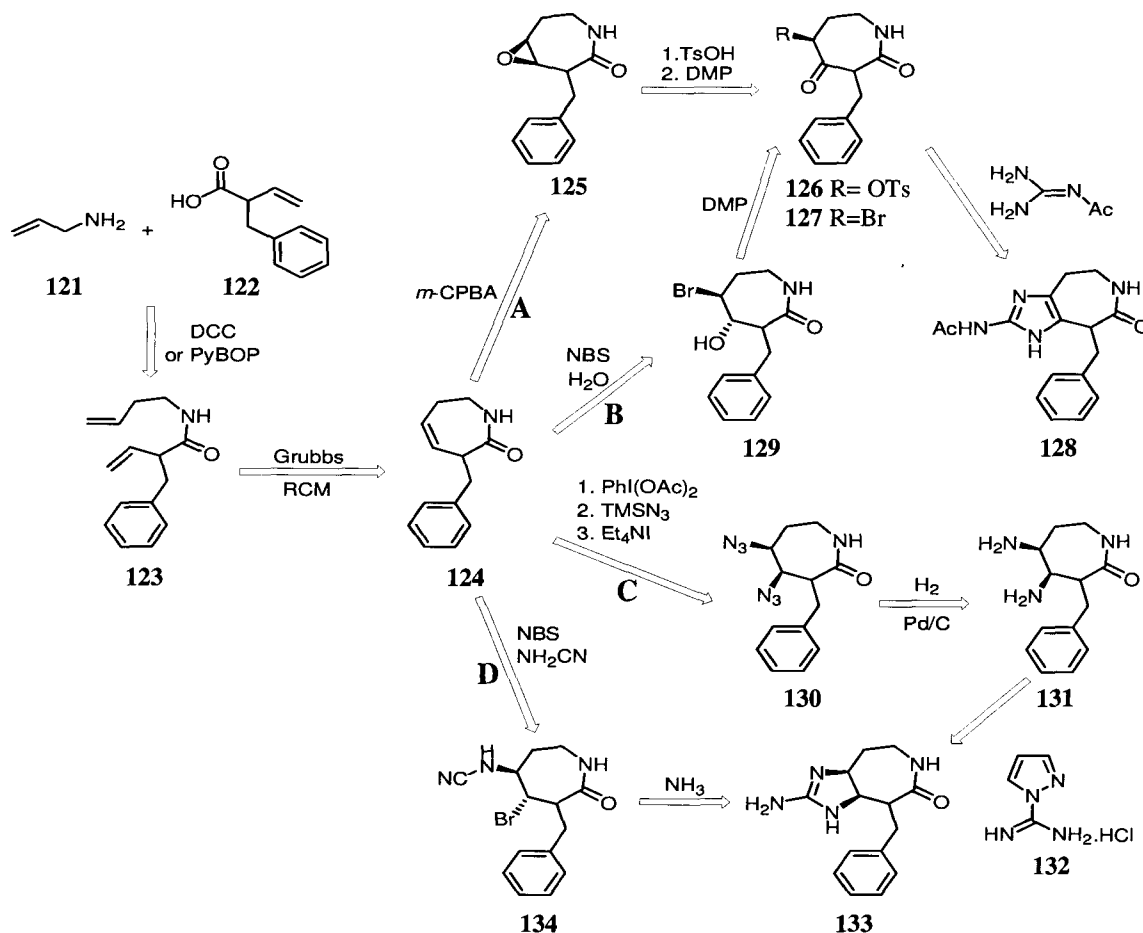
As a last resort, 3-benzylideneazepane-2,4-dione (**120**) (Scheme 4.19) was synthesized via a classical aldol condensation,^{340,341} with the hope of facilitating the deprotonation of C5 given the highly conjugated character of the molecule. Furthermore, absence of acidic protons at C3 makes 1NH and H5 the most likely targets for non-nucleophilic bases such as LDA. However, **120** proved to be non-reactive under either acidic or neutral conditions, as well as highly prone to polymerization under basic conditions, generating bakelite-like solids completely insoluble in non-polar or polar solvents, including water. At this point, it became apparent that a completely new strategy was required.



Scheme 4.19. Preparation of 3-benzylideneazepane-2,4-dione (**120**).

4.5.3. Second generation approach to ceratamines

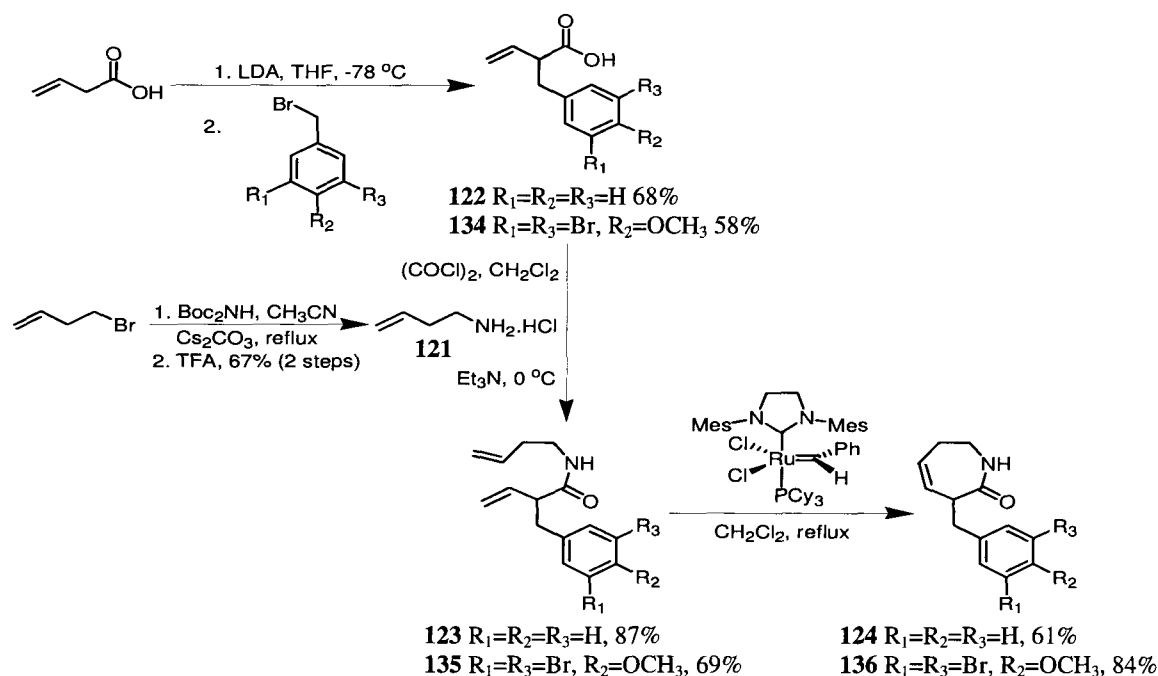
A new strategy was devised with 3-(3,5-dibromo-4-methoxybenzyl)-1,3,6,7-tetrahydroazepin-2-one (**124**) as the key intermediate (Scheme 4.20). From **124**, at least four logical pathways could lead to reduced ceratamine analogues.



Scheme 4.20. Second generation approach to ceratamine analogues **128** and **133**.

Once again, routes A and B aim to prepare a 2-aminoimidazole ring by condensation of α -functionalized ketones with *N*-acetylguanidine (Scheme 4.6).²⁶³ As starting material, **124** was considered more suitable than **78** (Scheme 4.11) for the preparation of intermediates **126** or **127**, either by epoxidation, TsOH-mediated ring opening and oxidation (Route A), or through

oxidation of halohydrin (**129**) (Route B). The remaining pathways make use of available methodologies to form vicinal *syn* diamines³⁴²⁻³⁴⁶ as intermediates to facilitate the construction of a dihydro-2-aminoimidazole moiety. Route C was encouraged by the commercially accessible guanilating reagent (**132**),³⁴⁷ and involves a hypervalent iodine-mediated vicinal diazidation recently employed by Austin and coworkers³⁴⁸ in their synthesis of (\pm)-dibromophakellstatin. Route D introduces the use of cyanamide (NH₂CN) to build 2-aminoimidazoles (Scheme 4.6) and is based on a method used by Jung and Kohn^{349,350} to prepare vicinal diamines, combined with the Pinner synthesis of amidines through imidoesters.³⁵¹⁻³⁵³ A final dehydrogenation/aromatization step³⁵⁴⁻³⁵⁶ on either **128** or **133** would afford the imidazo[4,5,*d*]azepine core of ceratamines.

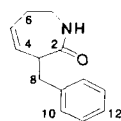


Scheme 4.21. Preparation of key intermediates **124** and **136**.

Thus, coupling of but-3-enylamine (**121**)³⁵⁷ hydrochloride salt and 2-benzylbut-3-enoic acid (**122**),^{358,359} or the more elaborate 2-(3,5-dibromo-4-methoxybenzyl)-but-3-enoic acid

(**134**),³⁶⁰⁻³⁶² was best accomplished by activating both carboxylic acids as their respective acyl chlorides (Scheme 4.21).³⁵⁸ Ring closing metathesis of **123** to produce the desired seven-membered cyclolactam (**124**) was carried out in good yields using second generation Grubbs catalyst.³⁶³⁻³⁶⁸

Table 4.6. NMR data for 3-benzyl-1,3,6,7-tetrahydroazepin-2-one (**124**) (recorded in CDCl₃).



Carbon No	¹³ C δ (ppm) ^a	¹ H δ (ppm) (mult, J (Hz)) ^{b,c}	HMBC ^b (H→C)
N1		6.44 (s, broad)	
2	176.8		
3	42.8	3.85 (m)	C2, C4, C8
4	126.4	5.32 (m)	C2, C3, C6
5	128.9	5.56 (m)	C3, C6
6	30.1	2.24 (m)	C5, C7
7	38.8	3.16 (m), 3.71 (m)	C2, C5
8	36.5	2.73 (dd, J = 9.4, 14.2 Hz), 3.29 (dd, J = 5.8, 14.2 Hz)	C2, C3, C9, C10
9	139.9		
10	129.2	7.28 (m)	C8, C12
11	128.4	7.25 (m)	C9
12	126.1	7.18 (m)	C10

^aRecorded at 100 MHz. ^bRecorded at 400 MHz. ^cAccording to HMQC recorded at 400 MHz.

The NMR data for **124** (Table 4.6, Figure 4.10) shows both vinylic methines H4 (δ_{H} 5.32, δ_{C} 127.1) and H5 (δ_{H} 5.56, δ_{C} 129.6) as multiplets due to coupling with H3 (δ_{H} 3.85, δ_{C} 42.8) and methylene H6 (δ_{H} 2.24, δ_{C} 30.1), respectively. As previously seen with similar intermediates (**96** and **98** Table 4.3), the strategic bridge position of methylene H8 (δ_{H} 2.73/3.29, δ_{C} 36.5) allows it to display HMBC correlations with carbons in both the seven-membered (C2, δ_{C} 176.8; C3, δ_{C} 42.8) and the aromatic rings (C9, δ_{C} 139.9; C10, δ_{C} 129.2). The amide proton resonance is found as a broad singlet at 6.44 ppm. HRESIMS gave an $[\text{M}+\text{Na}]^+$ peak at m/z 224.1050, in accordance with the molecular formula C₁₃H₁₅NO (mass calculated for C₁₃H₁₅NONa: 224.1051).

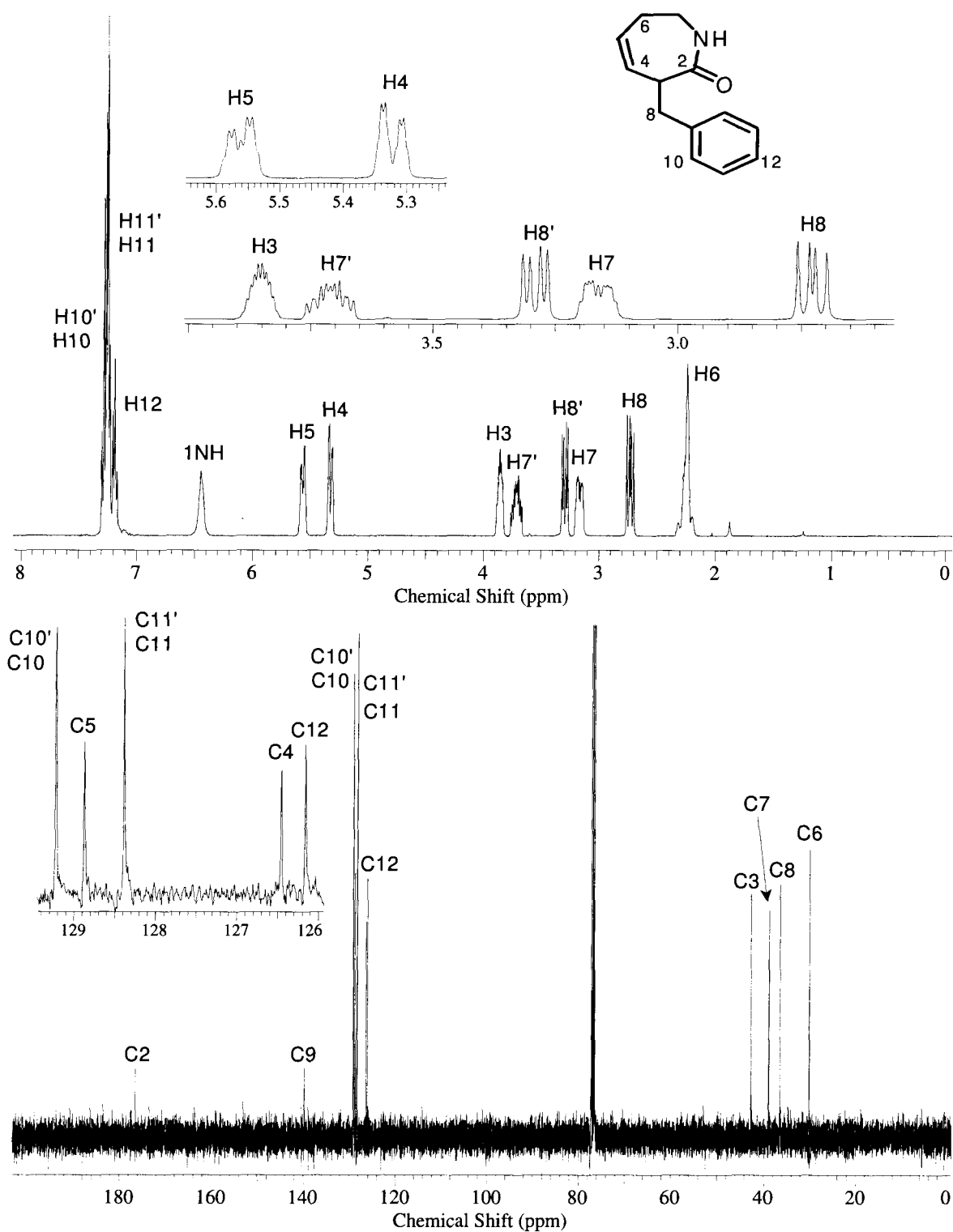
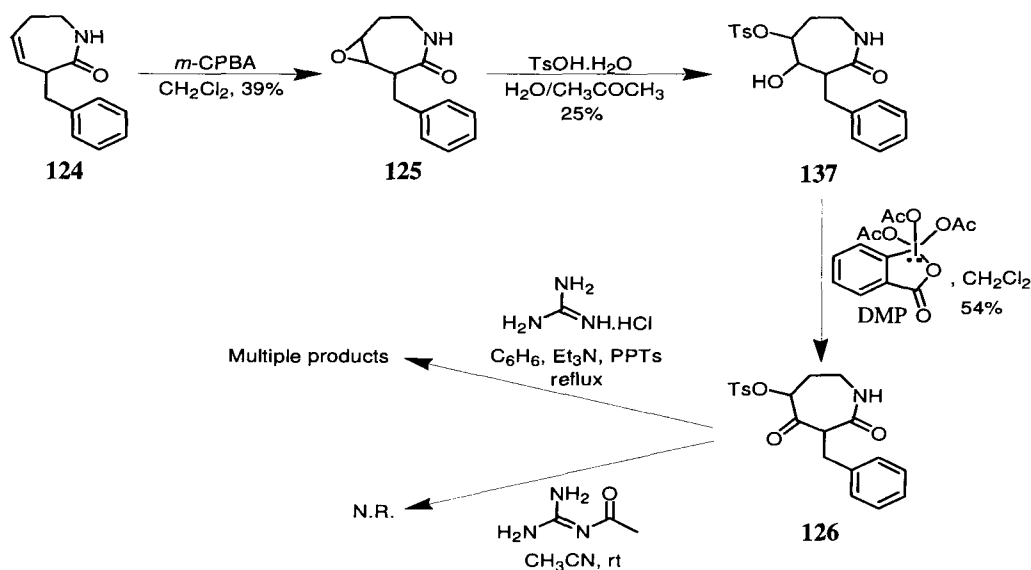


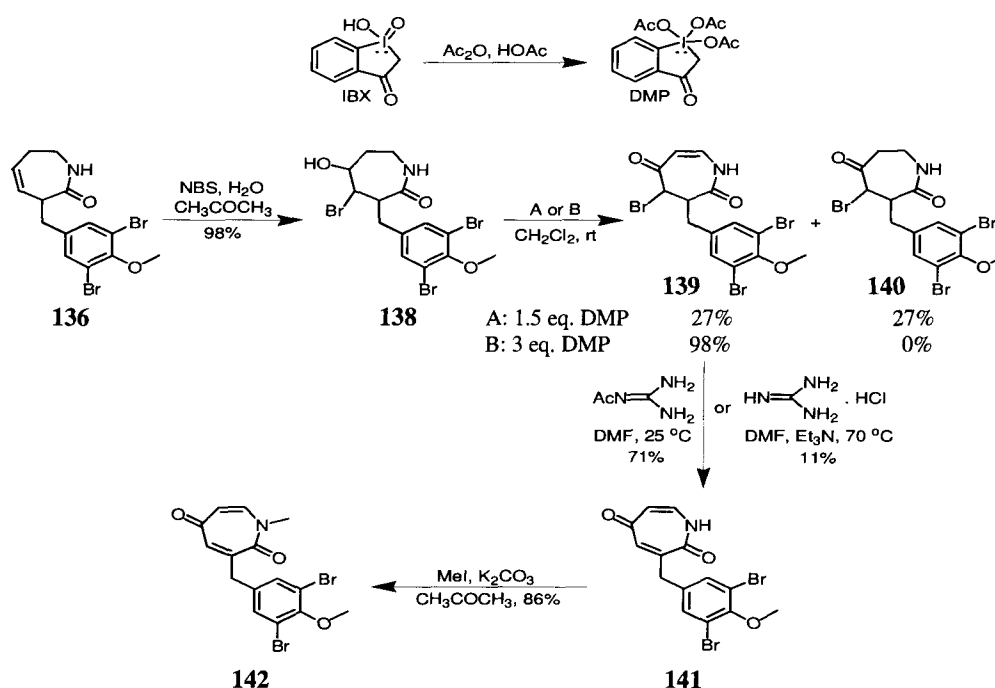
Figure 4.10. ^1H and ^{13}C -NMR spectra of 3-benzyl-1,3,6,7-tetrahydroazepin-2-one (**124**) (recorded in CDCl_3 at 400 and 100 MHz, respectively).

Extensive effort was spent in developing streamlined conditions to facilitate the large scale synthesis of key intermediates (**124**) and (**136**). Epoxidation,³⁶⁹ tosylation^{369,370} and oxidation methodologies³⁷¹⁻³⁷³ starting from **124** according to route A (Scheme 4.20), required small scales and exhausting column chromatography after each step, in order to eliminate excess reagents and expected byproducts (benzoic, iodobenzoic and *p*-toluenesulfonic acids exhibited similar TLC R_f values with the corresponding reaction products). Normally, aqueous NaHCO_3 extractions provide good separation, but products (**125**) and (**137**) proved to be quite water-soluble. The low yields obtained during this sequence reflect a combination of these experimental factors and a generalized low efficiency (Scheme 4.22). Furthermore, attempts to produce a 2-aminoimidazole ring from **126**^{263,270,275} were fruitless and afforded very complicated mixtures. Neither NMR nor LRESIMS were able to confirm the presence of the desired addition products.



Scheme 4.22. Preparation of toluene-4-sulfonic acid 6-benzyl-5,7-dioxoazepan-4-yl ester (**126**) and its reaction with guanidine derivatives.

Execution of pathway B (Scheme 4.20) led to the preparation of halohydrin (**138**) in good yields, whereas its oxidation using Dess-Martin periodinane (1.5 eq.) yielded a 1:1 mixture of products (Scheme 4.23). When 3 eq. of DMP were employed, only 4-bromo-3-(3,5-dibromo-4-methoxybenzyl)-3,4-dihydro-1H-azepine-2,5-dione (**139**) was obtained. The surprising formation of this compound was initially considered very positive since it already has a C6-C7 double bond, required at some point to produce the imidazo[4,5,*d*]azepine core of ceratamines. Nicolaou, Zhong and Baran³⁵⁴ had proposed the use of another hypervalent iodine-based reagent, iodoxybenzoic acid (IBX), in an efficient method for the one-pot conversion of alcohols, ketones and aldehydes to α,β -unsaturated carbonyl compounds. Thus, it is reasonable for DMP to yield **139** when used in excess.



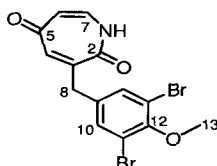
Scheme 4.23. Chemical transformations involved in the synthesis of **141** and **142**.

Interestingly, the conditions used to react **139** with guanidine derivatives^{263,267,275} afforded compound (**141**) as the main product. Clearly, bromide elimination to constitute a stable

conjugated heterocycle was favored over addition of guanidine to the non-reactive carbonyl in **139**. Furthermore, guanidine is one of the best organic bases, with strength comparable to NaOH (pK_a of guanidinium salt in water at 25°C: 13.6).³⁵²

The NMR spectrum of **141** (Table 4.7, Figure 4.11) showed a coupled spin system comprised of H4 (δ_H 6.94, δ_C 141.9), H6 (δ_H 5.67, δ_C 111.5), and H7 (δ_H 6.81, δ_C 136.1). The remaining resonances in the 1H -NMR are all singlets. Methylene H8 (δ_H 3.76, δ_C 38.5) and the broad 1NH signal (δ_H 11.10), H4, H8 and H10 (δ_H 7.58, δ_C 133.33) all showed HMBC correlations with all possible carbons located two and three bonds apart, evidencing the highly conjugated character of **141**. HRESIMS gave a $[M+H]^+$ peak at m/z 399.9189, corresponding to a molecular formula of $C_{14}H_{11}NO_3Br_2$ (calculated for $C_{14}H_{12}NO_3^{79}Br_2$: 399.9184).

Table 4.7. NMR data for 3-(3,5-dibromo-4-methoxybenzyl)-1H-azepine-2,5-dione (**141**) (recorded in DMSO- d_6).



Carbon No	^{13}C δ (ppm) ^a	1H δ (ppm) (mult, J (Hz)) ^{b,c}	HMBC ^b (H→C)
N1		11.10 (s, broad)	
2	165.1		
3	142.7		
4	141.9	6.94 (d, $J = 2.2$ Hz)	C2, C3, C5, C6, C8
5	185.4		
6	111.5	5.67 (dd, $J = 2.2, 10.0$ Hz)	C4, C5, C7
7	136.1	6.81 (d, $J = 10.0$ Hz)	C2, C5, C6
8	38.5	3.76 (s)	C2, C3, C4, C9, C10
9	138.0		
10	133.3	7.58 (s)	C3, C8, C9, C11, C12
11	117.2		
12	152.0		
13	60.3	3.76 (s)	C12

^aRecorded at 100 MHz. ^bRecorded at 400 MHz. ^cAccording to HMQC recorded at 400 MHz.

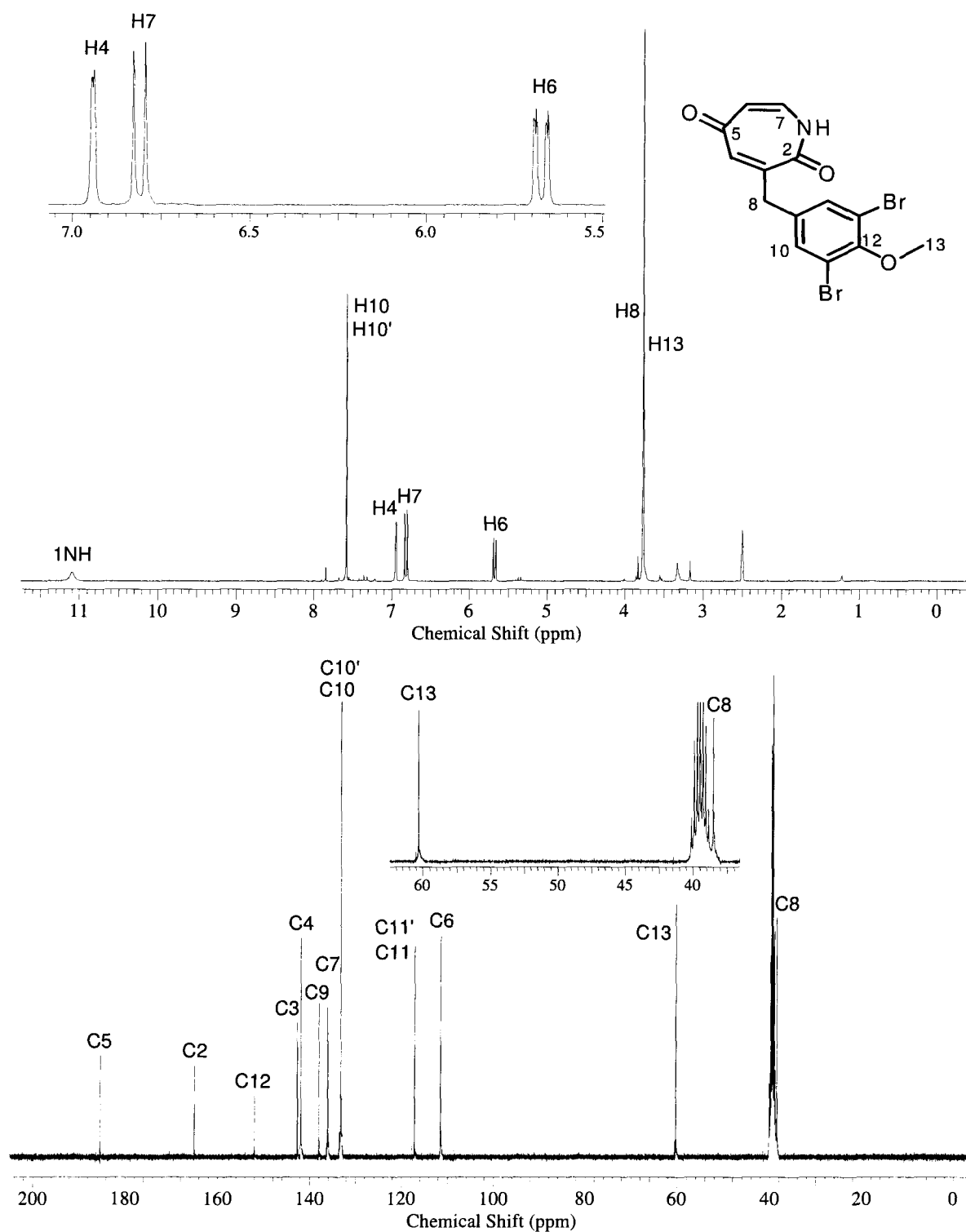


Figure 4.11. ^1H and ^{13}C -NMR spectra of 3-(3,5-dibromo-4-methoxybenzyl)-1H-azepine-2,5-dione (**141**) (recorded in DMSO- d_6 at 400 and 100 MHz, respectively).

Methylation of **141** furnished 3-(3,5-dibromo-4-methoxybenzyl)-1-methyl-1H-azepine-2,5-dione (**142**) in good yield. Noteworthy, analysis of the $^1\text{H-NMR}$ spectra for **142** and ceratamine A (**13**) (Figure 4.12) generates quite similar structural information.

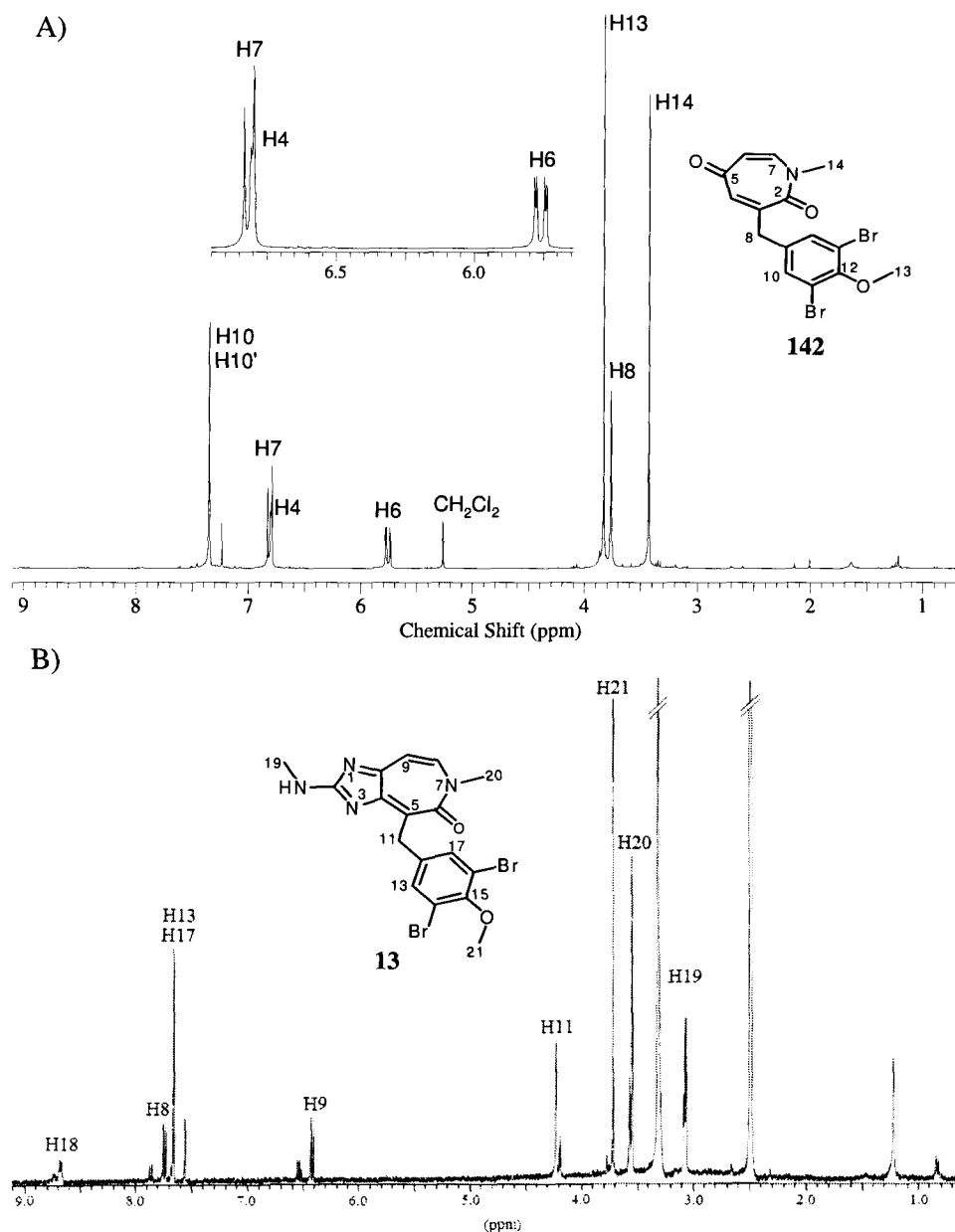


Figure 4.12. $^1\text{H-NMR}$ spectra of a) 3-(3,5-dibromo-4-methoxybenzyl)-1-methyl-1H-azepine-2,5-dione (**142**); and ceratamine A (**13**) (recorded in CDCl_3 and $\text{DMSO-}d_6$ at 400 MHz).

Lacking only a 2-aminoimidazole motif, compound (**142**) possesses instead a carbonyl group that can establish hydrogen bond interactions in a similar fashion as N1 in ceratamines A (**13**) or B (**14**). Some planarity in the seven-membered ring is also shared, particularly for the area surrounding carbonyl C5, but carbonyl C2 may project outside the plane outlined by carbons C3 to C7. Evidently, the absence of a fused five-membered aromatic ring concedes additional flexibility to the amide bond (Figure 4.13).

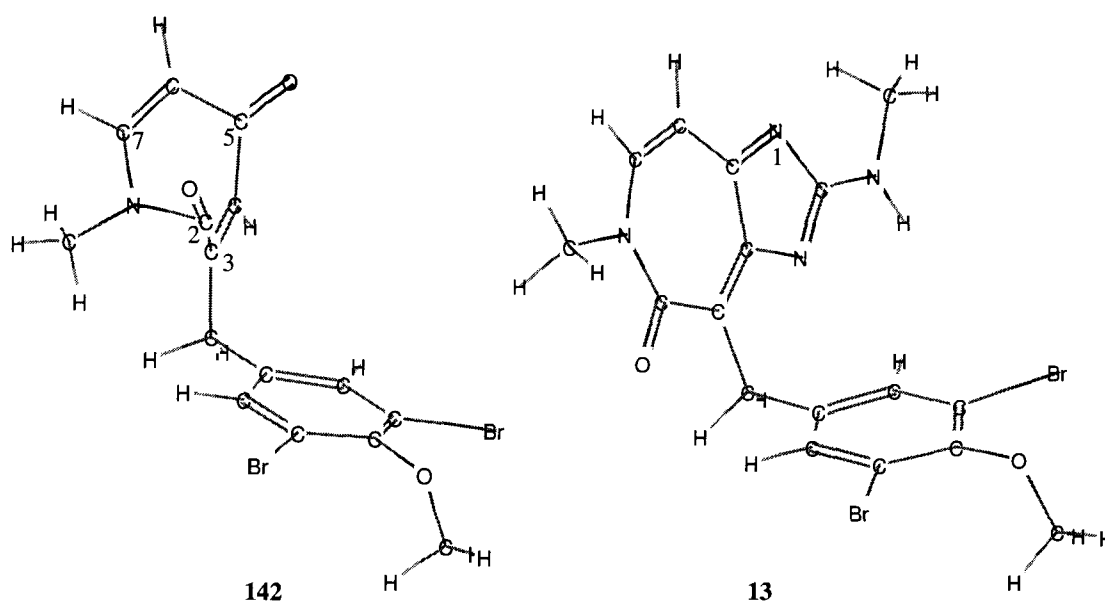
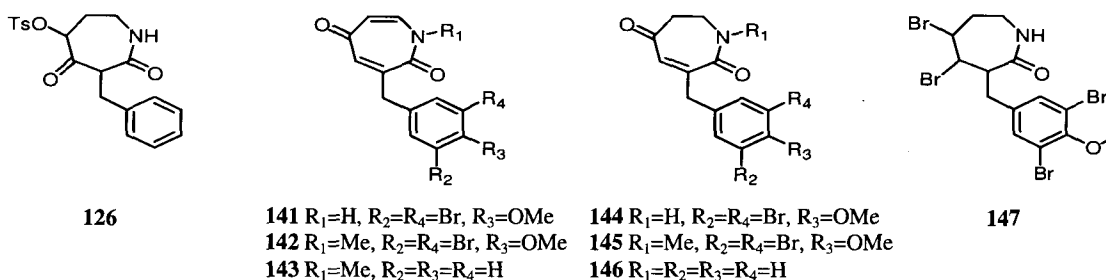


Figure 4.13. Minimum energy conformations for 3-(3,5-dibromo-4-methoxybenzyl)-1-methyl-1H-azepine-2,5-dione (**142**), and ceratamine A (**13**). 2C=O in 142 points out of the page (MM2, CS Chem3D Ultra 7.0, minimum RMS gradient 0.100).

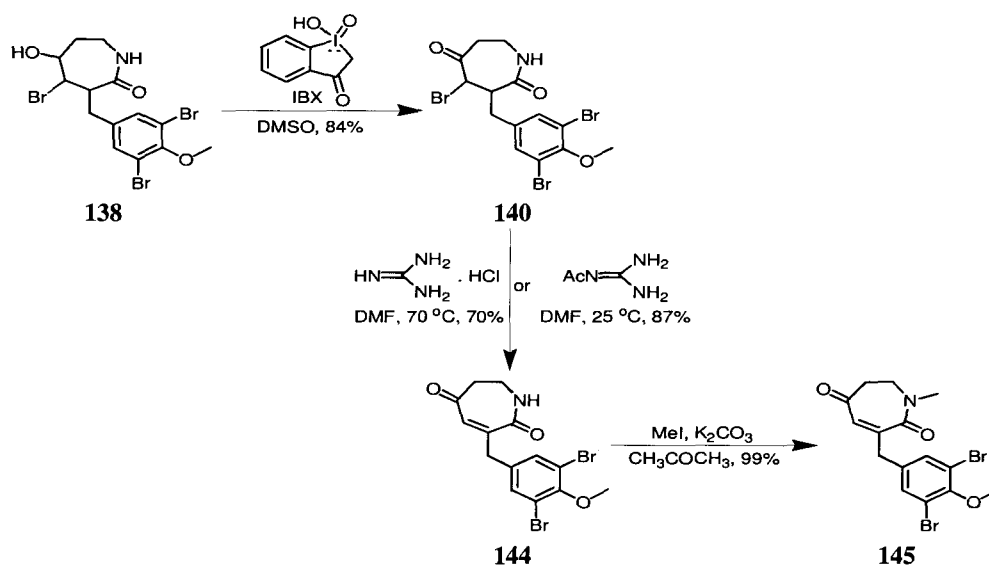
Such structural resemblance may explain the activity exhibited by **142** in the same bioassay used to test ceratamines, clearly showing cell arrest in mitosis at a starting concentration of 33 $\mu\text{g/mL}$ (IC_{50} for ceratamines A and B: 10 $\mu\text{g/mL}$).^{229,230} However, some of the unusual features observed for the natural product concerning microtubule arrangements around the cell nucleus were not observed with this analogue.

Table 4.1. Reaction of **126**, **141-147** with several nitrogen-based nucleophiles.

N	SM ^a	Nucleophile	Conditions ^{263,267,275,349,350,374}	Outcome ^b
1		Guanidine.HCl	Et ₃ N, PPTs, C ₆ H ₆ , reflux, 18 h	Complex mixture
2	126	Guanidine.HCl	Et ₃ N, C ₆ H ₆ , reflux, 16 h	Product not found
3		<i>N</i> -Acetylguanidine	CH ₃ CN, rt, 96 h	S. M.
4		<i>N</i> -Methylguanidine	Et ₃ N, DMF, 70 °C, 24 h	Complex mixture
5		141	Guanidine.HCl	EtONa, EtOH, reflux 2 h
6	Guanidine.HCl		EtONa, EtOH, reflux 12 h	Product not found
7		Guanidine.HCl	EtONa, EtOH, rt, 48 h	Complex mixture
8		Guanidine.HCl	DMF, 70 °C, 48 h	S. M.
9	142	<i>N</i> -Methylguanidine	Et ₃ N, DMF, 70 °C, 24 h	S. M.
10		NH ₃	CH ₃ OH, 80 °C, sealed tube, 5 h	Addition?
11		NH ₃	CH ₃ OH, 80 °C, sealed tube, 18 h	Addition?
12		NH ₃	1,4-Dioxane, 80 °C, sealed tube, 5 h	S. M.
13		NH ₂ CN	1,4-Dioxane, 80 °C, sealed tube, 18 h	S. M.
14		Guanidine.HCl	CH ₃ CN, reflux, 24 h	S. M.
15		<i>N</i> -Methylguanidine	DMF, reflux, 48 h	Addition?
16	143	Guanidine.HCl	CH ₃ CN, reflux, 24 h	S. M.
17		Guanidine.HCl	DMF, reflux, 24 h	S. M.
18		<i>N</i> -Boc-guanidine	DMF, rt, 4 days	S. M.
19	144	Guanidine.HCl	DMF, rt, 3 days	S. M.
20		Guanidine.HCl	Et ₃ N, DMF, 70 °C, 18 h	S. M.
21	145	<i>N</i> -Methylguanidine	Et ₃ N, DMF, 70 °C, 24 h	S. M.
22		Guanidine.HCl	DMF, 70 °C, 5 days	S. M.
23	146	<i>N</i> -Boc-guanidine	DMF, rt, 4 days	S. M.
24		<i>N</i> -Boc-guanidine	EtONa, EtOH, rt, 3 h	Complex mixture
25		Guanidine.HCl	DMF, 70 °C, 2 days	Br ⁻ elimination
26	147	<i>N</i> -Boc-guanidine	DMF, 70 °C, 2 days	Br ⁻ elimination
27		<i>N</i> -Boc-guanidine	THF, Et ₃ N, reflux, 24 h	S. M.
28		<i>N</i> -Boc-guanidine	THF, NaOMe, 60 °C, 24 h	Product not found

^aS.M.: starting material. ^bAccording to ¹H-NMR and LRESIMS.

Compounds **141-143** showed an extraordinary stability towards condensation with guanidine derivatives (Table 4.8, entries 5-9 and 14-18). Therefore, in order to avoid forming a C6-C7 double bond in precursor (**139**) that eventually leads to elimination and complete conjugation in **141**, starting material (**138**) was oxidized exclusively to 4-bromo-3-(3,5-dibromo-4-methoxybenzyl)-azepane-2,5-dione (**140**) employing IBX (Scheme 4.24).^{354,374-378} Nevertheless, condensation attempts of **140** with guanidine produced only elimination product (**144**), which in turn also proved to be inert (Table 4.8, entries 19-24).

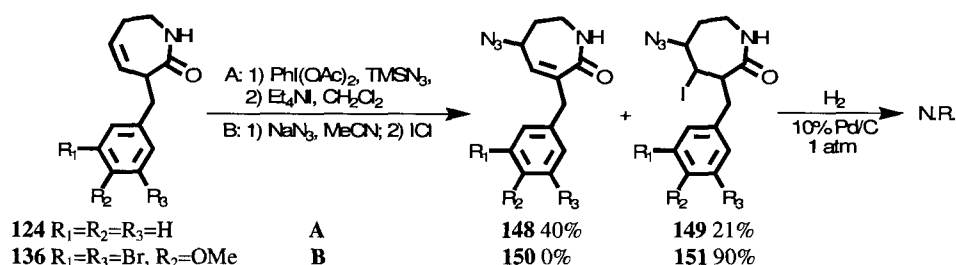


Scheme 4.24. Reactions leading to the synthesis of 3-(3,5-dibromo-4-methoxybenzyl)-1-methyl-6,7-dihydro-1H-azepine-2,5-dione (**145**).

According to Table 4.8, only strong basic media and heating seemed to produce changes in the starting materials, sometimes accompanied by minimum amounts of products usually detected in the ¹H-NMR baseline, exhibiting a new coupling pattern for H4, H6 and H7 in the seven-membered ring (entries 10, 11 and 15). However, scarce amounts made it impossible to verify nucleophile addition in these compounds. Starting material **147** (entries 25-28) was always isolated as a minor byproduct in reactions involving NBS, or directly prepared by bromination of **136** in 99% yield. Even small nucleophiles like NH₃ required extreme reaction conditions to only

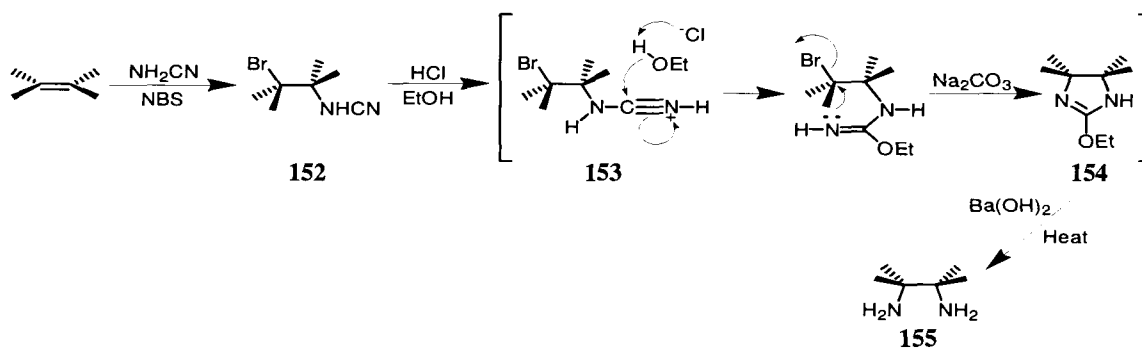
give a faint indication of addition (entries 10-14). In general, all the data in Table 4.8 reflects the high stability of the different starting materials, and poor performance of guanidine and its derivatives as nucleophiles.

Route C (Scheme 4.20) rapidly led to another dead end when, upon reaction with IN_3 ^{348,379} or $\text{I}(\text{N}_3)_2$,^{348,380} only byproducts were isolated. Additionally, hydrogenation conditions^{250,348,381} intended to form a primary amine at C5 were not successful (Scheme 4.25).



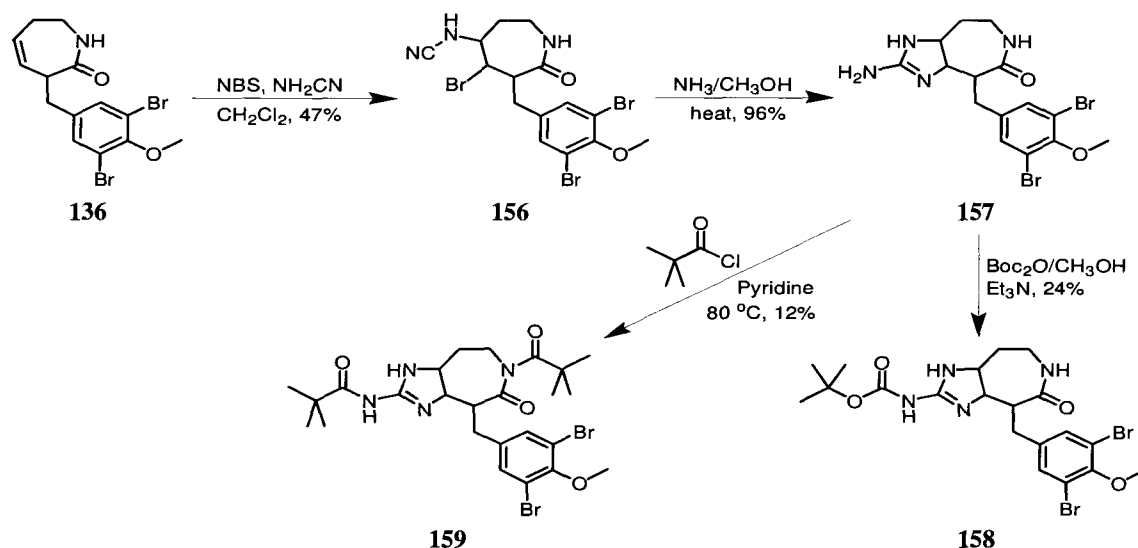
Scheme 4.25. Chemical transformations of **124** and **136** involved in route C.

Contrary to the guanidine case, cyanamide (NH_2CN) is highly nucleophilic and can be added to double bonds through a bromonium ion.³⁸² In their methodology to stereoselectively prepare vicinal diamines, Jung and Kohn^{349,350,374} generated a stable cyclic imido ester (**154**) by reaction of a β -bromoalkyl cyanamide (**152**) with ethanol in acidic media (Scheme 4.26), as the precursor for the final product **155**.



Scheme 4.26. Synthesis of vicinal diamines by Jung and Kohn.³⁷⁴

In analogy to this process, it was envisioned that a similar five-membered cyclic compound might be formed by treatment of β -bromoalkyl cyanamide (**156**) with ammonia, giving rise to a reduced version of the targeted imidazo[4,5,*d*]azepine core of ceratamines (Scheme 4.27). Addition of amines to cyanamide derivatives is just one of the common methods to synthesize substituted guanidines,³⁵² whereas the preparation of imido esters followed by addition of primary amines (including NH_3) is known as the Pinner method for synthesis of amidines $[\text{RC}(=\text{NH})\text{NH}_2]$.³⁵¹ Thus, heating a sealed pyrex tube containing intermediate (**156**) and NH_3 in CH_3OH , yielded the reduced ceratamine B analogue (**157**) in good yield.



Scheme 4.27. Synthesis of 19-demethyl-1,4,5,8,9,10-hexahydroceratamine B (**157**).

The ^1H and ^{13}C -NMR data for **157** (Figure 4.14, Table 4.9) shows resonances for NH protons at 7.66, 7.90 and 8.20 ppm, whereas signals for the vinylic protons of **136** were substituted by methines H4 (δ_{H} 3.80, δ_{C} 60.7) and H10 (δ_{H} 3.82, δ_{C} 58.5). Diastereotopic methylenes H8 (δ_{H} 3.10/3.42, δ_{C} 38.3), H9 (δ_{H} 1.57/2.15, δ_{C} 31.7) and H11 (δ_{H} 2.92, δ_{C} 29.0) do not exhibit important changes in their chemical shifts, when compared with **156** (Experimental).

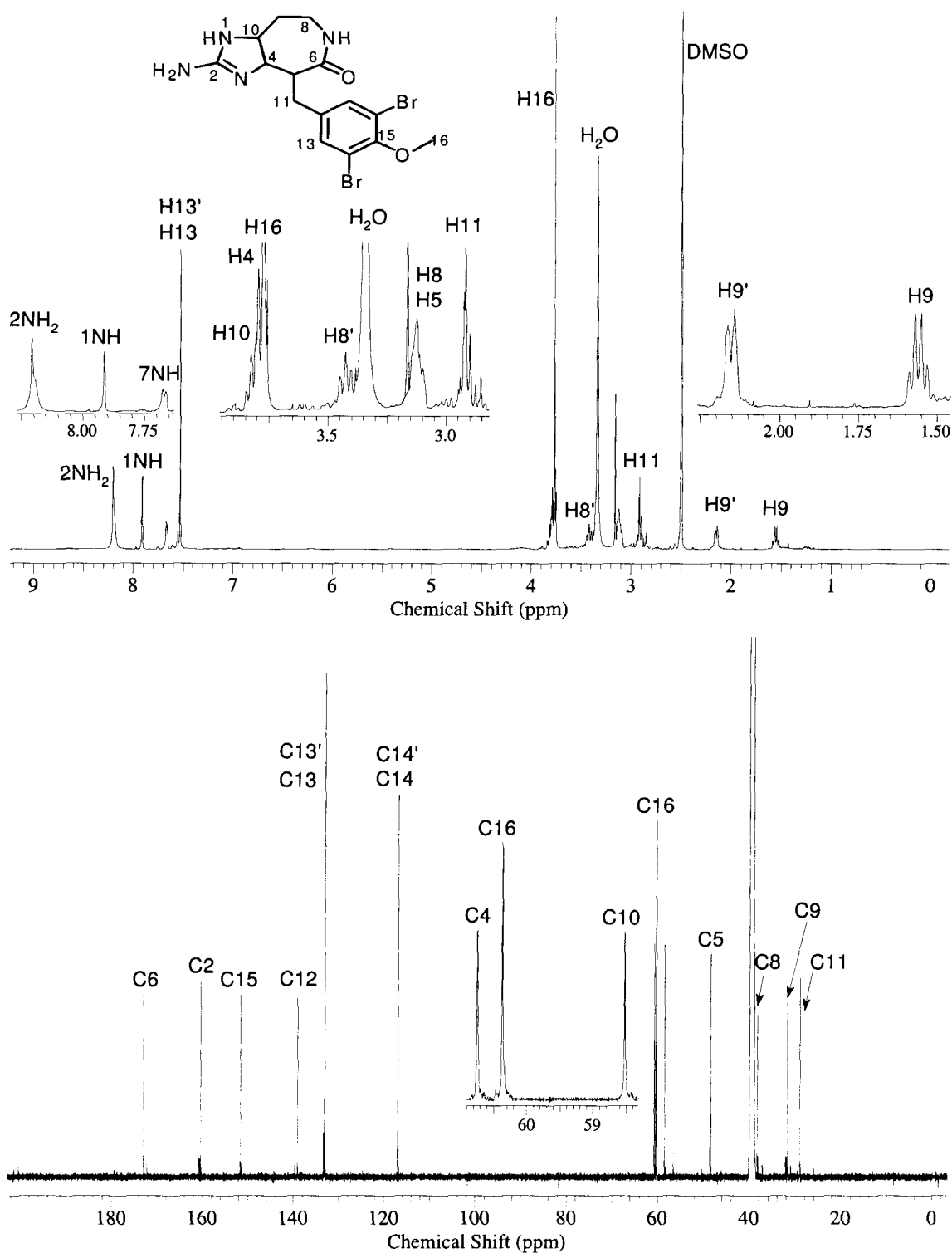
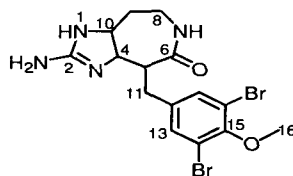


Figure 4.14. ^1H and ^{13}C -NMR spectra of 19-demethyl-1,4,5,8,9,10-hexahydroceratamine B (157) (recorded in $\text{DMSO-}d_6$ at 600 and 150 MHz respectively).

Table 4.9. NMR data for 19-demethyl-1,4,5,8,9,10-hexahydroceratamine B (**157**) (recorded in DMSO-*d*₆).

Carbon No	¹³ C δ (ppm) ^a	¹ H δ (ppm) (mult, <i>J</i> (Hz)) ^{b,c}	HMBC ^b (H→C)
N1		7.90 (s, broad)	C2, C4, C10
2	160.4	NH ₂ 8.20 (s, broad)	C2, C4, C10
N3			
4	60.7	3.80 (m)	C6, C9, C10, C11
5	48.5	3.12 (m)	C6, C11, C12
6	172.9		
N7		7.66 (d, <i>J</i> = 7.4 Hz)	C5, C6, C9
8	38.3	3.10 (m), 3.42 (m)	C9, C10
9	31.7	1.57 (m), 2.15 (m)	C4, C8, C10
10	58.5	3.82 (m)	C4
11	29.0	2.92 (m)	C5, C6, C12, C13
12	139.1		
13	133.1	7.53 (s)	C11, C14, C15
14	117.0		
15	151.6		
16	60.4	3.77 (s)	C15

^aRecorded at 150 Hz. ^bRecorded at 600 MHz. ^cAccording to HMQC recorded at 600 MHz.

More evidence for the presence of a fused five-membered ring was given by HMBC correlations from the primary amine at C2 to carbons C4 and C10. The secondary amine 1NH also correlates with these carbons, whereas 7NH does it with methine C5 (δ_C 48.5), carbonyl C6 (δ_C 172.9) and methylene C9 (δ_C 31.7), allowing an unambiguous assignment of these groups to the dihydro-2-aminoguanidine and amide motifs, respectively. As usual, the linking methylene H11 displayed HMBC cross-peaks with carbons in both rings. HRESIMS provided a $[M+H]^+$ peak at m/z 444.9871, suggesting a molecular formula C₁₅H₁₈N₄O₂Br₂ (calculated for

$C_{15}H_{19}N_4O_2^{79}Br_2$: 444.9875), and confirmed that upon ammonia addition, displacement of bromide by guanidine installed the new ring.

Compared with active analogue (**142**), compound (**157**) is completely non-planar and its low-energy conformation presents folding of the seven-membered ring in a boat-like conformation (Figure 4.15). The lack of antimitotic activity exhibited by **157** is undoubtedly due to this factor. Additionally, in the case of inactive compounds (**158**) and (**159**), the presence of bulky groups must interfere with binding and generation of hydrogen bond interactions with the active site.

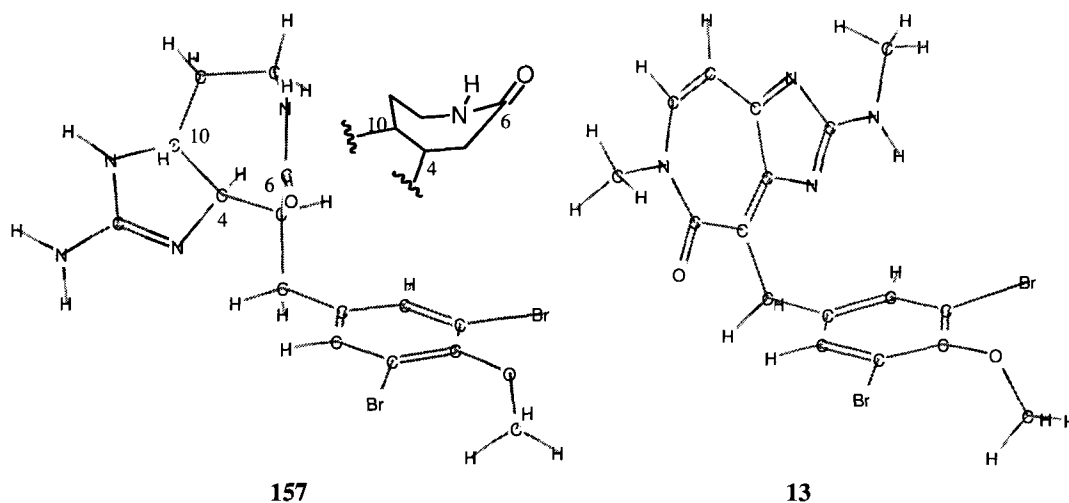
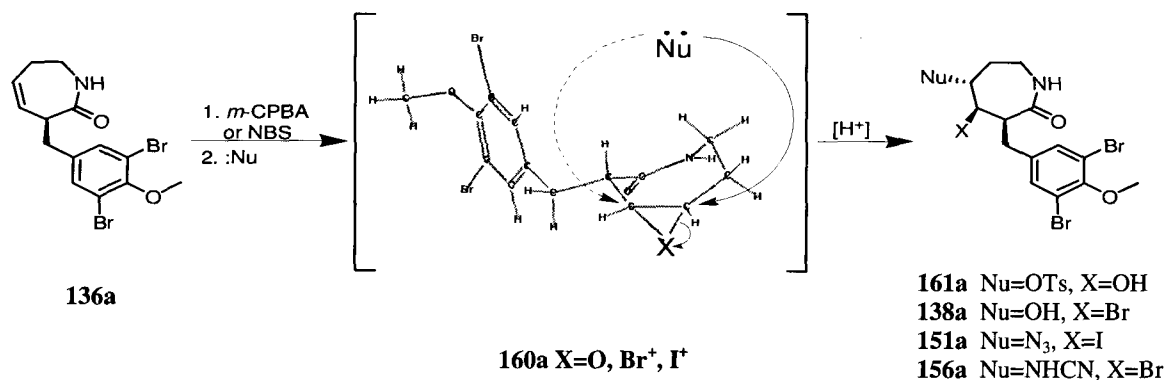


Figure 4.15. Minimum energy conformations for 19-demethyl-1,4,5,8,9,10-hexahydroceratamine B (**157**); and ceratamine A (**13**). 6C=O in **157** is pointing out of the page (MM2, CS Chem3D Ultra 7.0, minimum RMS gradient 0.100).

So far, a noticeable regioselectivity has been obtained regarding addition of nucleophiles to the double bond in **136**. Whether the electrophilic species was an epoxide or a halonium cation, TsOH, H₂O, Br⁻ and NH₂CN all attacked the same carbon C5 in the tricyclic intermediate (**160**) (Scheme 4.28). An important steric effect from the benzyl substituent at C3, which blocks

access to C4 and consequently favors nucleophile attack at C5, may be the main reason behind this tendency.

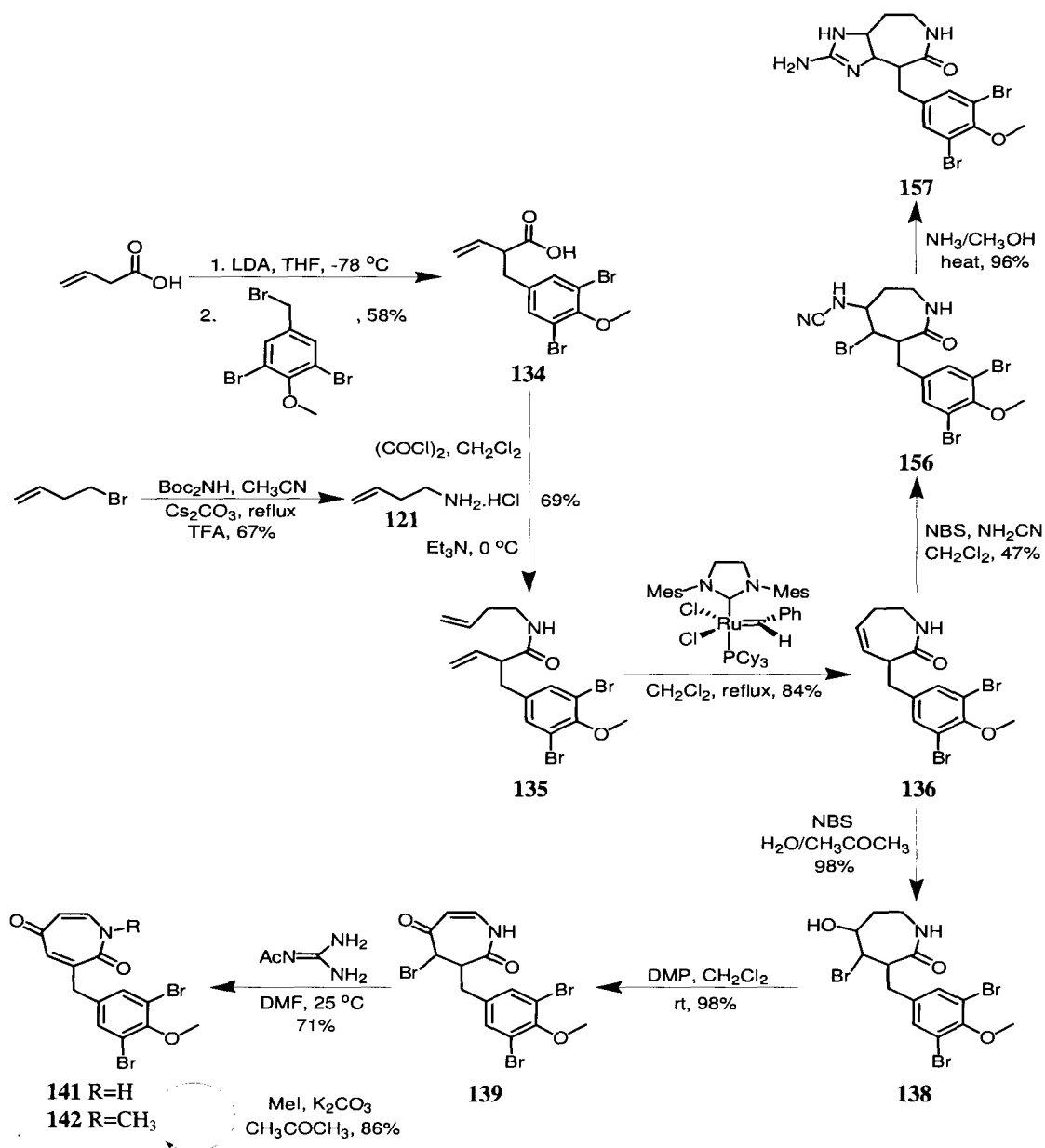


Scheme 4.28. Preferential nucleophile attack at C5 observed during addition reactions to (**136**). Only one stereoisomer is shown (MM2, CS Chem3D Ultra 7.0, minimum RMS gradient 0.100).

Attempts to manipulate **157** revealed the intractable nature of 2-aminoimidazole containing compounds. The analogue does not react with common staining reagents and is immovable on normal phase silica gel. The dihydro-2-aminoimidazole motif is quite labile, and exhibited ring opening during reversed-phase chromatography. Such effect was more evident with the imido ester version (**154**) (Scheme 4.26), only detectable in traces by LRESIMS. Likewise, when methylamine and benzylamine replaced ammonia in the reaction with α -bromoalkyl cyanamide (**156**), the corresponding methyl and benzyl analogues were obtained in minimum amounts. Reactions of **157**, as well as protected derivatives (**158**) and (**159**), were characterized by opening of the five-membered ring and total loss of the resulting substituted guanidine group, as evidenced by LRESIMS. Normal procedures intended to remove protons and assist with aromatization of the carbocyclic skeleton, including treatment with DDQ,³⁸³⁻³⁸⁶ IBX,³⁵⁴⁻³⁵⁶ chloranil²⁷⁰ or Pd/C,³⁸⁷⁻³⁹⁰ were all fruitless.

4.6. Conclusions and future directions

The ceratamine inspired antimitotic agent (**142**) and inactive analogue (**157**) were synthesized in no more than 8 steps, with overall yields of 20% and 15% respectively (Scheme 4.29).



Scheme 4.29. Syntheses of 19-demethyl-1,4,5,8,9,10-hexahydroceratamine B (**157**) and 3-(3,5-dibromo-4-methoxy-benzyl)-1-methyl-1H-azepine-2,5-dione (**142**).

Preparation of key intermediate **136** was achieved in only four steps, via standard peptide coupling of **121** and **134**, followed by ring closing metathesis using second generation Grubbs catalyst. This efficient and condensed synthetic sequence proceeded with acceptable yields and in scale large enough to ensure an appropriate stock of material for further reactions. The double bond in **136** is quite versatile, and exhibited high regioselectivity towards nucleophilic addition. NBS mediated addition of cyanamide and condensation of the resulting precursor with ammonia yielded the reduced ceratamine B analogue (**157**), in a total of six steps. Alternatively, preparation of bromohydrin (**138**), followed by Dess-Martin periodinane oxidative dehydrogenation afforded intermediate (**139**) in excellent yields. The azepine core of **141** was best furnished by basic treatment with *N*-acetylguanidine, initially intended as a methodology to produce 2-aminoimidazole motifs. Lastly, a simple methylation procedure provided **142** in a total of eight steps.

In general, the chemistry involved preparing **142** and **157** proved to be quite robust and repeatable. Some aspects that may be considered as shortcomings include the high costs of second generation Grubbs catalysts, and dangers associated with ammonia reactions in closed systems. Furthermore, addition of cyanamide to **136** through a bromonium cation was always accompanied by a considerable amount of dibrominated product. Thus, variation of reaction conditions to optimize this step may be in order.

The incredible stability exhibited by **142** and its demethyl analogue **141** made attempts to elaborate both compounds fruitless. On the other hand, the dihydro-2-aminoimidazole motif in **157** turned out to be very labile, and efforts intended to aromatize its bicyclic carbon skeleton were characterized by ring opening and loss of the resulting guanidine moiety.

When antimetabolic activity^{229,230} was evaluated for these compounds, **142** exhibited cell arrest in mitosis at a starting concentration of 33 $\mu\text{g/mL}$ and thus, it is significantly less potent

than both natural ceratamines A and B, sharing an IC_{50} value of $10 \mu\text{g/mL}$.²¹⁰ Furthermore, some of the attractive unusual effects in microtubule polymerization described for ceratamine A that suggest its binding to a different active site than taxol,²²⁹ were not observed for **142**.

Insights about the ceratamines pharmacophore earned with the preparation and activity evaluation of both **142** and **157**, include:

- I. Requirement for flat carbon backbones: both **142** and ceratamine A share some planarity, and while the natural product is completely flat, absence of a fused imidazole ring in **142** concedes additional mobility to the azepine core, which folds to project the amide carbonyl outside the plane outlined by other ring components (Figure 4.13). Analogue (**157**) on the other hand is non-planar and completely inactive.
- II. The unique imidazo[4,5,*d*]azepine core heterocycle proper of ceratamines is not required for activity. A 2-aminoimidazole ring improves potency and efficiency, but it is not crucial for cell cycle arrest. Replacement by just a carbonyl as in **142** provided a biologically active compound.

This second statement is very important for future synthetic attempts, since modification or replacement of the 2-aminoimidazole substructure in ceratamine analogues may increase their antimitotic power. Additionally, the reported^{250,270,292} intractable nature of compounds containing this functionality suggests the use of more synthetically accessible heteroatomic arrangements, capable of structurally emulating substituted imidazole rings. For this purpose, availability of active analogues for structure-activity relationship studies is clearly vital. The preparation of tetrahydroazepin-2-one (**136**) provides a good starting point to synthesize such compounds.

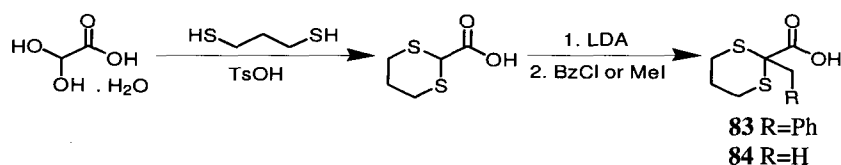
In case of a total synthesis of ceratamines, deferring installation of the 2-aminoimidazole ring until the final stages of synthesis is definitely advantageous. Most of the recently published total syntheses of compounds bearing this substructure, including scep trin (**41**),^{250,267} ageliferin (**43**),²⁶⁸ naamidine A (**54**),²⁶⁹ and ageladine A (**55**)²⁷⁰ prepare it in the last reaction step via condensation of α -haloketones with guanidine derivatives as proposed by Little and Weber²⁶³ in 1994. According to observations made during the first and second generation approaches implemented in the present work, available methods to prepare 2-substituted imidazoles and their compatibility with acidic protons, steric constraints of seven-membered rings, and the presence of other functionalities such as amides, will determine the outcome of future ceratamine synthetic proposals.

A thorough exploration of biomimetic approaches, using a preformed imidazole ring as starting material is also suggested. Literature procedures to sequentially functionalize imidazoles are readily available,³⁹¹⁻³⁹⁵ and as evidenced when handling **157**, the additional aromatic stability of imidazole derivatives is essential to successfully elaborate synthetic intermediates without ring opening or decomposition. Contrary to the 7+5 approach followed in the present work, a 5+7-membered ring construction may give better results in installing both the amide and the primary amine moieties in imidazole. Above all, the aromatic element present in the imidazole ring provides a solid ground that may facilitate dehydrogenation steps down the road.

4.7. Experimental

General experimental procedures

For general experimental procedures see Section 2.6.

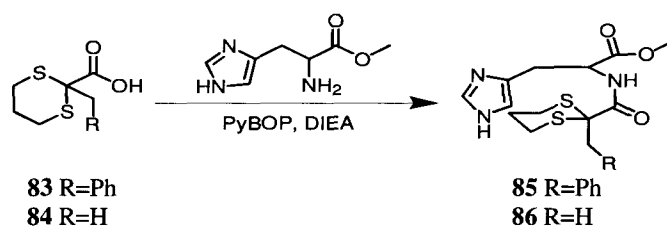
Preparation of 2-benzyl-[1,3]dithiane-2-carboxylic (**83**) and 2-methyl-[1,3]dithiane-2-carboxylic (**84**) acids

A mixture of dihydroxyacetic acid monohydrate (9.2 g, 100 mmol), 1,3-propanedithiol (11.0 mL, 110 mmol) and *p*-toluenesulfonic acid (1.9 g, 10 mmol), in benzene (250 mL), was refluxed for 1 h. Once at 25 °C, the crude was extracted with NaHCO₃ sat. (3 x 100 mL), acidified with HCl conc., and extracted again with EtOAc (4 x 100 mL). The organic layer was dried (Na₂SO₄) and concentrated *in vacuo*, to afford desired [1,3]dithiane-2-carboxylic acid intermediate as a yellowish solid (13.15 g, 80%). Without further purification, this intermediate (1.64 g, 10 mmol) was dissolved in THF (75 mL) and treated with LDA (12 mL, 21.6 mmol, 1.8 M) at 0 °C. After stirring for 30 min at the same temperature, benzyl chloride (1.27 mL, 11 mmol) was added and the resulting mixture stirred overnight. Aqueous hydrolysis, followed by HCl acidification and Et₂O extractions, provided after solvent evaporation a pale yellow amorphous solid identified as (**83**) (2.54 g, 89%). When MeI (0.70 mL, 11 mmol) was used to quench the dianion intermediate under the same conditions, 2-methyl-[1,3]dithiane-2-carboxylic acid (**84**) was obtained (1.78 g, 72%).

2-Benzyl-[1,3]dithiane-2-carboxylic acid (**83**): ^1H NMR (CDCl_3 , 400 MHz) δ 7.36-7.08 (5H, m), 3.37 (2H, s), 3.25 (2H, ddd, $J = 2.8, 12.2, 13.7$ Hz), 2.68 (2H, ddd, $J = 3.7, 4.0, 13.7$ Hz), 2.12 (1H, m), 1.83 (1H, m); ^{13}C NMR (CDCl_3 , 100 MHz) δ 176.3 (C), 134.0 (C), 130.8 (2CH), 128.1 (2CH), 127.6 (CH), 46.5 (C), 44.3 (CH_2), 28.1 (2CH_2), 24.1 (CH_2). HRESIMS calcd for $\text{C}_{12}\text{H}_{14}\text{O}_2\text{S}_2\text{Na}$ ($[\text{M}+\text{Na}]^+$): 277.0333; found 277.0328.

2-Methyl-[1,3]dithiane-2-carboxylic (**84**): ^1H NMR (CDCl_3 , 400 MHz) δ 3.39 (2H, ddd, $J = 2.8, 13.6, 14.4$ Hz), 2.63 (2H, ddd, $J = 3.8, 4.3, 13.4$ Hz), 2.16 (1H, m), 1.82 (1H, m), 1.67 (3H, s); ^{13}C NMR (CDCl_3 , 100 MHz) δ 176.2 (C), 45.9 (C), 28.0 (2CH_2), 25.4 (CH_2), 23.8 (CH_3). HREIMS calcd for $\text{C}_6\text{H}_{10}\text{O}_2\text{S}_2$ (M^+): 178.01222; found 178.01228.

Coupling of 2-benzyl-[1,3]dithiane-2-carboxylic (**83**) and 2-methyl-[1,3]dithiane-2-carboxylic (**84**) acids with histidine methyl ester

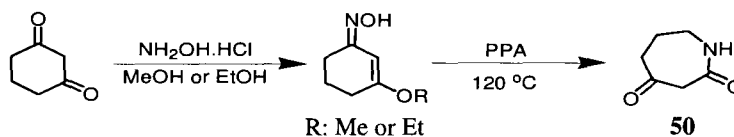


To a solution of (**83**) (0.25 g, 1 mmol) in CH_2Cl_2 (10 mL), was added PyBOP (0.54 g, 1 mmol), histidine methyl ester (0.27 g, 1.1 mmol) and DIEA (0.50 mL, 2.8 mmol). After overnight stirring at 25 °C, NaCl sat. was added and CH_2Cl_2 extractions performed. The organic extracts were dried (Na_2SO_4), concentrated *in vacuo*, and the resulting residue was purified by a gradient silica gel column chromatography (50% EtOAc/hexanes to 20% MeOH/EtOAc), to afford (**85**) as a colorless powder (0.20 g, 50%). When compound (**84**) (0.18 g, 1 mmol) was used as starting material, the procedure above provided desired product (**86**) also as a colorless solid (0.18 g, 53%).

2-Benzyl-[1,3]dithiane-2-carboxylic acid-histidine methyl ester adduct (**85**): ^1H NMR (CD_2Cl_2 , 300 MHz) δ 8.34 (1H, d, $J = 7.4$ Hz), 7.58 (1H, s), 7.20-7.14 (5H, m), 6.70 (1H, s), 4.68 (1H, ddd, $J = 5.5, 6.6, 6.6$ Hz), 3.63 (3H, s), 3.17 (2H, m), 3.05 (1H, dd, $J = 9.9, 14.9$ Hz), 2.94 (1H, dd, $J = 9.4, 14.9$ Hz), 2.91 (1H, m), 2.79 (1H, m), 2.57 (2H, m), 1.98 (1H, m), 1.83 (1H, m); ^{13}C NMR (CD_2Cl_2 , 75 MHz) δ 171.4 (C), 169.5 (C), 134.7 (C), 134.4 (CH), 133.5 (C), 130.5 (2CH), 127.7 (2CH), 127.2 (CH), 115.4 (CH), 59.9 (CH), 52.1 (CH_3), 49.5 (C), 42.2 (CH_2), 28.6 (CH_2), 28.15 (CH_2), 28.07 (CH_2), 24.4 (CH_2). HRESIMS calcd for $\text{C}_{19}\text{H}_{24}\text{N}_3\text{O}_3\text{S}_2$ ($[\text{M}+\text{H}]^+$): 406.1259; found 406.1251.

2-Methyl-[1,3]dithiane-2-carboxylic acid-histidine methyl ester adduct (**86**): ^1H NMR (CD_2Cl_2 , 300 MHz) δ 8.53 (1H, d, $J = 7.6$ Hz), 7.57 (1H, s), 6.80 (1H, s), 4.67 (1H, ddd, $J = 5.7, 6.2, 6.9$ Hz), 3.64 (3H, s), 3.15 (1H, m), 3.07 (1H, m), 3.00 (1H, m), 2.86 (1H, m), 2.57 (2H, m), 2.00 (1H, m), 1.80 (1H, m), 1.55 (3H, s); ^{13}C NMR (CD_2Cl_2 , 75 MHz) δ 172.0 (C), 171.4 (C), 135.2 (CH), 134.6 (C), 115.6 (CH), 53.9 (CH), 52.5 (CH_3), 42.7 (C), 29.0 (2 CH_2), 28.9 (CH_2), 27.7 (CH_2), 24.7 (CH_3). HRESIMS calcd for $\text{C}_{13}\text{H}_{20}\text{N}_3\text{O}_3\text{S}_2$ ($[\text{M}+\text{H}]^+$): 330.0946; found 330.0954.

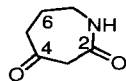
Preparation of azepane-2,4-dione (**50**) via Beckmann rearrangement



A mixture of 1,3-cyclohexadione (22.4 g, 200 mmol) and hydroxylamine hydrochloride (14.0 g, 200 mmol) in EtOH (200 mL) was refluxed for 1.5 h. Once at room temperature, the crude was neutralized using 10% K_2CO_3 , extracted with CH_2Cl_2 and dried (Na_2SO_4). Solvent evaporation provided the corresponding 3-ethoxy-2-cyclohexen-1-one oxime quantitatively. This intermediate (7.6 g, 49 mmol) was heated under mechanical stirring and solvent less conditions

in the presence of polyphosphoric acid (PPA, 100 g), for 3 h at 110-120 °C. Upon reaction time completion, the viscous final crude was added to ice/H₂O (100 mL), neutralized with NaOH pellets and extracted with BuOH. Solvent concentration *in vacuo*, followed by silica gel column chromatography (100 EtOAc), afforded azepane-2,4-dione (**50**) as a reddish amorphous solid (5.26 g, 85%). For a summary of ¹H and ¹³C NMR assignments, see Table 4.10. ¹H NMR (CD₂Cl₂, 400 MHz) δ 7.37 (1H, s, broad), 3.50 (2H, s), 3.45 (2H, m), 2.62 (2H, t, *J* = 6.9 Hz), 1.98 (2H, m); ¹³C NMR (CD₂Cl₂, 100 MHz) δ 203.1 (C), 169.8 (C), 52.6 (CH₂), 44.3 (CH₂), 41.6 (CH₂), 28.6 (CH₂). HRESIMS calcd for C₆H₁₀NO₂ ([M+H]⁺): 128.0712; found 128.0710.

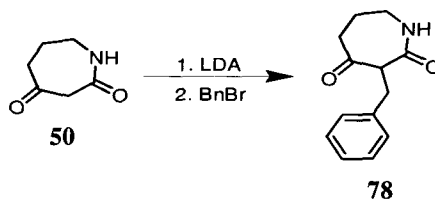
Table 4.10. NMR data for azepane-2,4-dione (**50**) (recorded in CD₂Cl₂).



Carbon No	¹³ C δ (ppm) ^a	¹ H δ (ppm) (mult, <i>J</i> (Hz)) ^{b,c}	HMBC ^b (H→C)
N1		7.37 (s, broad)	
2	169.8		
3	52.6	3.50 (2H, s)	C2, C4, C5
4	203.1		
5	44.3	2.62 (t, <i>J</i> = 6.9 Hz)	C3, C4, C6, C7
6	28.6	1.98 (m)	C3, C5, C7
7	41.6	3.45 (m)	C2, C5, C6

^a Recorded at 100 MHz. ^b Recorded at 400 MHz. ^c According to HMQC recorded at 400 MHz.

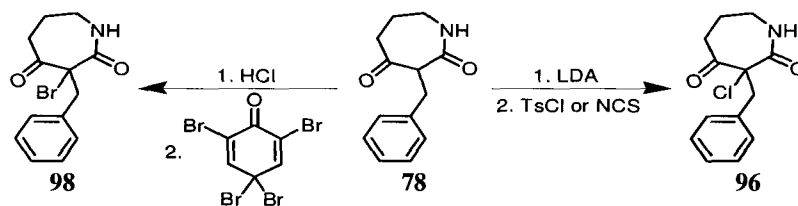
Preparation of 3-benzylazepane-2,4-dione (**78**)



Azepane-2,4-dione (**50**) (0.70 g, 5.5 mmol) was dissolved in THF (25 mL) and cool down to -78°C. After 15 min, LDA (3.7 mL, 6.6 mmol, 1.8 M) was added and the crude allowed to gradually warmed up to -30°C for 1h. Once at this temperature, benzyl bromide (0.90 mL, 7.5

mmol) was added and stirring continued overnight. The reaction crude was treated with NH_4Cl sat., extracted with EtOAc and dried (Na_2SO_4). Solvent concentration, followed by gradient silica gel column chromatography (80% EtOAc/hexanes to 10% MeOH/EtOAc), provided desired 3-benzylazepane-2,4-dione (**78**) (0.43 g, 36%) as a white solid. For a summary of ^1H and ^{13}C NMR assignments, see Table 4.2. ^1H NMR (CD_2Cl_2 , 400 MHz) δ 7.29-7.13 (5H, m), 6.11 (1H, s, broad), 4.24 (1H, dd, $J = 6.7, 6.8$ Hz), 3.75 (1H, m), 3.31 (1H, m), 3.15 (2H, m), 2.60 (2H, m), 2.10 (1H, m), 1.92 (1H, m); ^{13}C NMR (CD_2Cl_2 , 100 MHz) δ 204.2 (C), 169.5 (C), 140.5 (C), 129.6 (2CH), 128.8 (2CH), 126.7 (CH), 59.4 (CH), 46.3 (CH_2), 41.9 (CH_2), 31.8 (CH_2), 30.7 (CH_2). HRESIMS calcd for $\text{C}_{13}\text{H}_{15}\text{NO}_2\text{Na}$ ($[\text{M}+\text{Na}]^+$): 240.1000; found 240.0996.

Halogenation of 3-benzylazepane-2,4-dione (**78**)



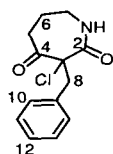
To a solution of 3-benzylazepane-2,4-dione (**78**) (0.040 g, 0.18 mmol) in Et_2O (5 mL), was added HCl in Et_2O (0.4 mL, 0.4 mmol, 1M) and 2,4,4,6-tetrabromoquinone (0.30 g, 0.73 mmol) diluted also in Et_2O (15 mL). The resulting mixture was stirred at 25 °C for 45 h refluxing periodically, whereupon 10% Na_2CO_3 was added and THF extractions performed. The organic fractions were dried with Na_2SO_4 and concentrated *in vacuo* to give a yellowish residue, which was additionally purified by silica gel column chromatography (80% EtOAc/hexanes) to afford 3-benzyl-3-bromoazepane-2,4-dione (**98**) as a white amorphous powder (0.047 g, 87%).

On the other hand, a solution of starting material (**78**) (0.13 g, 0.6 mmol) in THF (5 mL) at -78 °C was treated with LDA (0.36 mL, 0.66 mmol, 1.8 M), following shortly after the

addition of *N*-chlorosuccinimide (0.12 g, 0.9 mmol) in THF (5 mL), and overnight stirring at 25 °C. Crude work-up and further purification was done following the same procedure as above, to obtain desired 3-benzyl-3-chloro-azepane-2,4-dione (**96**) (0.12 g, 83%).

3-Benzyl-3-bromoazepane-2,4-dione (**98**): ^1H NMR (CD_2Cl_2 , 300 MHz) δ 7.25 (5H, m), 6.65 (1H, s, broad), 3.84 (1H, d, $J = 13.1$ Hz), 3.50 (1H, d, $J = 13.1$ Hz), 3.12 (1H, m), 2.84 (1H, m), 2.56 (1H, m), 2.12 (1H, m), 1.80 (2H, m); ^{13}C NMR (CD_2Cl_2 , 75 MHz) δ 203.2 (C), 169.8 (C), 135.4 (C), 131.5 (2CH), 129.0 (2CH), 128.1 (CH), 68.6 (C), 44.2 (CH_2), 39.6 (CH_2), 37.6 (CH_2), 26.7 (CH_2). HRESIMS calcd for $\text{C}_{13}\text{H}_{14}\text{NO}_2\text{Na}^{79}\text{Br}$ ($[\text{M}+\text{Na}]^+$): 318.0106; found 318.0099.

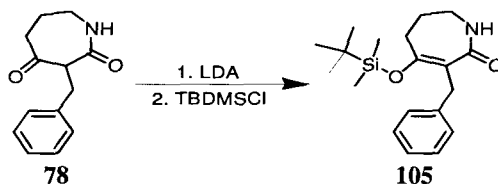
3-Benzyl-3-chloroazepane-2,4-dione (**96**): for a summary of ^1H and ^{13}C NMR assignments, see Table 4.11. ^1H NMR (CD_2Cl_2 , 300 MHz) δ 7.25 (5H, m), 6.69 (1H, s, broad), 3.78 (1H, d, $J = 13.1$ Hz), 3.33 (1H, d, $J = 13.1$ Hz), 3.23 (1H, m), 2.95 (1H, m), 2.50 (1H, m), 2.13 (1H, m), 1.83 (2H, m); ^{13}C NMR (CD_2Cl_2 , 75 MHz) δ 203.8 (C), 169.3 (C), 134.6 (C), 131.6 (2CH), 128.9 (2CH), 128.1 (CH), 74.1 (C), 43.6 (CH_2), 39.3 (CH_2), 37.8 (CH_2), 27.0 (CH_2). HRESIMS calcd for $\text{C}_{13}\text{H}_{14}\text{NO}_2\text{NaCl}$ ($[\text{M}+\text{Na}]^+$): 274.0611; found 274.0609.

Table 4.2. NMR data for 3-benzyl-3-chloroazepane-2,4-dione (**96**) (recorded in CD₂Cl₂).

Carbon No	¹³ C δ (ppm) ^a	¹ H δ (ppm) (mult, J (Hz)) ^{b,c}	HMBC ^b (H→C)
N1		6.69 (s, broad)	
2	169.3		
3	74.1		
4	203.8		
5	37.8	2.13 (m), 2.50 (m)	C3, C4, C6, C7
6	27.0	1.83 (m)	C4, C5, C7
7	39.3	2.95 (m), 3.23 (m)	C2, C5
8	43.6	3.33 (d, J = 13.1 Hz), 3.78 (d, J = 13.1 Hz)	C2, C3, C4, C5, C9, C10
9	134.6		
10	131.6	7.25 (m)	C8, C12
11	128.9	7.25 (m)	C9
12	128.1	7.25 (m)	C10

^aRecorded at 75 MHz. ^bRecorded at 300 MHz. ^cAccording to HMQC recorded at 300 MHz.

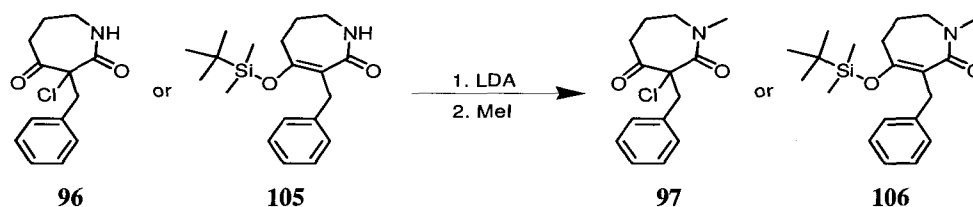
Preparation of 3-benzyl-4-(*tert*-butyldimethylsilyloxy)-1,5,6,7-tetrahydroazepin-2-one (**105**)



To a solution of 3-benzylazepane-2,4-dione (**78**) (0.13 g, 0.58 mmol) in THF (3 mL) at -78°C, was added LDA (0.32 mL, 0.58 mmol, 1.8 M). After stirring for 30 min., *tert*-butyldimethylsilyl chloride (TBDMSCl) (0.13 g, 0.87 mmol) was added and the mixture stirred overnight. The reaction was quenched with NH₄Cl sat., extracted with EtOAc and dried (Na₂SO₄). Solvent concentration *in vacuo* provided a colorless solid identified as pure (**105**) (0.18 g, 96%). No further purification was required according to TLC (100% EtOAc) and ¹H NMR. ¹H NMR (CD₂Cl₂, 400 MHz) δ 7.28-7.19 (5H, m), 6.92 (1H, s, broad), 3.69 (2H, s), 3.10

(2H, m), 2.48 (2H, t, $J = 7.2$ Hz), 1.96 (2H, m), 0.97 (9H, s), 0.24 (6H, s); ^{13}C NMR (CD_2Cl_2 , 100 MHz) δ 175.7 (C), 157.0 (C), 141.9 (C), 128.8 (2CH), 128.6 (2CH), 126.1 (CH), 116.4 (C), 40.0 (CH_2), 32.7 (CH_2), 31.5 (CH_2), 30.5 (CH_2), 26.0 (3 CH_3), 18.6 (C), -3.19 (2 CH_3). HRESIMS calcd for a $\text{C}_{19}\text{H}_{29}\text{NO}_2\text{Na}^{28}\text{Si}$ ($[\text{M}+\text{Na}]^+$): 354.1865; found 354.1859.

Preparation of 3-benzyl-3-chloro-1-methylazepane-2,4-dione (97) and 3-benzyl-4-(*tert*-butyldimethylsilyloxy)-1-methyl-1,5,6,7-tetrahydroazepin-2-one (106)



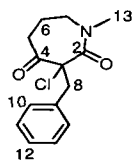
To a solution of 3-benzyl-3-chloroazepane-2,4-dione (**96**) (0.26 g, 1.0 mmol) in THF (5 mL) at -78°C , was added LDA (0.57 mL, 1.0 mmol, 1.8 M). After stirring for 30 min., methyl iodide (0.10 mL, 1.5 mmol) was added and the mixture stirred overnight. The reaction was quenched with NH_4Cl sat., extracted with EtOAc and dried (Na_2SO_4). Solvent concentration *in vacuo* and silica gel column chromatography (100% EtOAc), provided (**97**) as a white powder (0.22 g, 79%). When 3-benzyl-4-(*tert*-butyldimethylsilyloxy)-1,5,6,7-tetrahydroazepin-2-one (**105**) (0.051 g, 0.15 mmol), LDA (0.22 mL, 0.4 mmol, 1.8 M) and MeI (0.071 g, 0.5 mmol), were used following the same procedure as above (column chromatography with 80% EtOAc/hexanes as eluent), a colorless solid identified as desired (**106**) (0.021 g, 40%) was obtained.

3-Benzyl-3-chloro-1-methylazepane-2,4-dione (**97**): for a summary of ^1H and ^{13}C NMR assignments, see Tables 4.3 and 4.12. ^1H NMR (CDCl_3 , 400 MHz) δ 7.24-7.16 (5H, m), 3.83 (1H, d, $J = 12.8$ Hz), 3.29 (1H, d, $J = 12.8$ Hz), 3.28 (1H, m), 3.00 (3H, s), 2.85 (1H, ddd, J

= 5.2, 5.2, 15.7 Hz), 2.33 (1H, m), 1.90 (1H, m), 1.75 (2H, m); ^{13}C NMR (CDCl_3 , 75 MHz) δ 203.6 (C), 166.7 (C), 134.2 (C), 131.0 (2CH), 128.4 (2CH), 127.6 (CH), 74.1 (C), 46.7 (CH_2), 44.0 (CH_2), 37.1 (CH_2), 36.5 (CH_3), 24.2 (CH_2). HRESIMS calcd for $\text{C}_{14}\text{H}_{16}\text{NO}_2\text{Na}^{35}\text{Cl}$ ($[\text{M}+\text{Na}]^+$): 288.0767; found 288.0764.

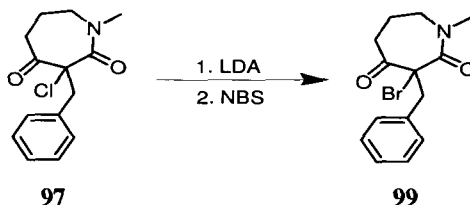
3-Benzyl-4-(*tert*-butyldimethylsilanyloxy)-1-methyl-1,5,6,7-tetrahydroazepin-2-one (**106**): for a summary of ^1H and ^{13}C NMR assignments, see Table 4.4. ^1H NMR (CD_2Cl_2 , 400 MHz) δ 7.25-7.15 (5H, m), 3.67 (2H, s), 3.24 (2H, m), 2.94 (3H, s), 2.36 (2H, t, $J = 7.2$ Hz), 2.00 (2H, m), 0.96 (9H, s), 0.22 (6H, s); ^{13}C NMR (CD_2Cl_2 , 100 MHz) δ 172.6 (C), 154.1 (C), 142.0 (C), 128.9 (2CH), 128.7 (2CH), 126.0 (CH), 117.2 (C), 48.4 (CH_2), 34.5 (CH_3), 32.9 (CH_2), 30.8 (CH_2), 29.0 (CH_2), 26.0 (3 CH_3), 18.6 (C), -3.23 (2 CH_3). HRESIMS calcd for $\text{C}_{20}\text{H}_{31}\text{NO}_2\text{NaSi}$ ($[\text{M}+\text{Na}]^+$): 368.2022; found 368.2028.

Table 4.12. NMR data for 3-benzyl-3-chloro-1-methylazepane-2,4-dione (**97**) (recorded in CDCl_3).



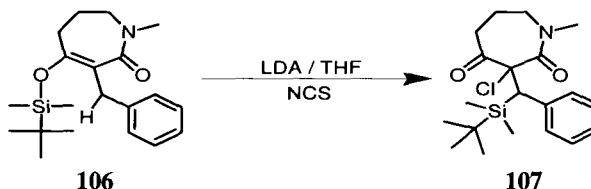
Carbon No	^{13}C δ (ppm) ^a	^1H δ (ppm) (mult, J (Hz)) ^{b,c}	HMBC ^b (H→C)
2	166.7		
3	74.1		
4	203.6		
5	37.8	1.90 (m), 2.33 (m)	C3, C4, C6, C7
6	24.2	1.75 (m)	C5, C4, C7
7	46.7	2.85 (ddd, $J = 5.2, 5.2, 15.7$ Hz), 3.28 (m)	C2, C5, C6
8	44.0	3.29 (d, $J = 12.8$ Hz), 3.83 (d, $J = 12.8$ Hz)	C2, C3, C4, C9, C10
9	134.2		
10	131.0	7.21 (m)	C8, C12
11	128.4	7.19 (m)	C9
12	127.6	7.17 (m)	C10
13	36.5	3.00 (s)	C2, C7

^aRecorded at 75 MHz. ^bRecorded at 400 MHz. ^cAccording to HMQC recorded at 400 MHz.

Bromination of 3-benzyl-3-chloro-1-methylazepane-2,4-dione (97)

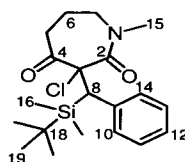
A solution of 3-benzyl-3-chloro-1-methyl-azepane-2,4-dione (**97**) (0.061 g, 0.2 mmol) in THF (5 mL) at -78 °C was treated with LDA (0.27 mL, 0.50 mmol, 1.8 M), following shortly after the addition of *N*-bromosuccinimide (0.13 g, 0.74 mmol) in THF (5 mL), and overnight stirring at 25 °C. NH₄Cl was added and EtOAc extractions performed. The organic fractions were dried with Na₂SO₄ and concentrated *in vacuo* to give a white powder, which was additionally purified by silica gel column chromatography (80% EtOAc/hexanes) to afford 3-benzyl-3-bromo-1-methyl-azepane-2,4-dione (**99**) as a white amorphous powder (0.056 g, 79%).

¹H NMR (CDCl₃, 300 MHz) δ 7.28-7.15 (5H, m), 3.90 (1H, d, *J* = 12.7 Hz), 3.50 (1H, d, *J* = 12.7 Hz), 3.14 (1H, m), 2.99 (3H, s), 2.76 (1H, m), 2.48 (1H, m), 1.95 (1H, m), 1.75 (2H, m); ¹³C NMR (CDCl₃, 75 MHz) δ 203.1 (C), 167.2 (C), 135.2 (C), 131.1 (2CH), 128.6 (2CH), 127.8 (CH), 69.1 (C), 47.3 (CH₂), 44.4 (CH₂), 37.0 (CH₂), 36.9 (CH₃), 24.3 (CH₂). HRESIMS calcd for C₁₄H₁₇NO₂⁷⁹Br ([M+H]⁺): 310.0443; found 310.0439.

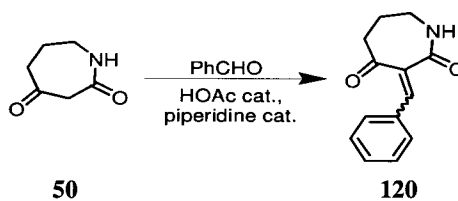
Chlorination of 3-benzyl-4-(*tert*-butyldimethylsilyloxy)-1-methyl-1,5,6,7-tetrahydroazepin-2-one (106)

A solution of 3-benzyl-4-(*tert*-butyldimethylsilyloxy)-1-methyl-1,5,6,7-tetrahydroazepin-2-one (**106**) (0.013 g, 0.038 mmol) in THF (5 mL) at -78 °C was treated with

LDA (0.023 mL, 0.041 mmol, 1.8 M), following shortly after the addition of *N*-chlorosuccinimide (0.0076 g, 0.057 mmol) in THF (5 mL), and overnight stirring at 25 °C. NH₄Cl was added and EtOAc extractions performed. The organic fractions were dried with Na₂SO₄ and concentrated *in vacuo* to give a colorless solid, which was additionally purified by silica gel column chromatography (100% EtOAc) to afford rearranged product (**107**) as a colorless solid (0.0065 g, 45%). For a summary of ¹H and ¹³C NMR assignments, see Tables 4.5 and 4.13. ¹H NMR (CD₂Cl₂, 400 MHz) δ 7.58 (1H, d, *J* = 7.6 Hz), 7.18 (1H, m), 7.14 (1H, m), 7.12 (1H, m), 6.87 (1H, d, *J* = 6.7 Hz), 3.79 (1H, m), 3.11 (1H, m), 3.08 (3H, s), 3.02 (1H, s), 1.80 (1H, m), 1.66 (1H, m), 1.63 (1H, m), 1.60 (1H, m), 0.80 (9H, s), 0.33 (3H, s), 0.14 (3H, s); ¹³C NMR (CD₂Cl₂, 100 MHz) δ 206.4 (C), 168.1 (C), 138.6 (C), 134.7 (CH), 132.5 (CH), 129.0 (CH), 128.4 (CH), 127.0 (CH), 77.6 (C), 47.8 (CH₂), 45.6 (CH), 39.2 (CH₂), 36.8 (CH₃), 27.8 (3CH₃), 24.2 (CH₂), 19.4 (C), -1.41 (CH₃), -2.89 (CH₃). HRESIMS calcd for C₂₀H₃₀NO₂NaSi³⁵Cl ([M+Na]⁺): 402.1632; found 402.1633.

Table 4.13. NMR data for 3-[(*tert*-butyldimethylsilyl)phenylmethyl]-3-chloro-1-methylazepane-2,4-dione (**107**) (recorded in CD₂Cl₂).

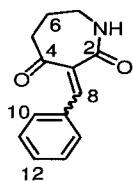
Proton No	¹ H δ (ppm) (mult, J (Hz)) ^a	COSY ^a (H→H)
H5	1.63 (m)	H7, H7'
H5'	1.80 (m)	H6, H6', H7, H7'
H6	1.60 (m)	H5', H7, H7'
H6'	1.66 (m)	H5', H7, H7'
H7	3.11 (m)	H5, H5', H6, H6', H7'
H7'	3.79 (m)	H5, H5', H6, H6', H7
8	3.02 (s)	
10	7.58 (d, J = 7.6 Hz)	H11, H14
11	7.18 (m)	H10, H12
12	7.14 (m)	H11, H13
13	7.12 (m)	H12, H14
14	6.87 (d, J = 6.7 Hz)	H10, H13
15	3.08 (s)	
16	0.14 (s)	
17	0.33 (s)	
19	0.80 (s)	

^aRecorded at 400 MHz.Preparation of 3-benzylidene-azepane-2,4-dione (**120**)

A mixture of azepane-2,4-dione (**50**) (1.27 g, 10 mmol) and benzaldehyde (1.01 mL, 10 mmol) in benzene (50 mL), was refluxed for 3 h in the presence of catalytic amounts of HOAc and piperidine. Once at 25 °C, H₂O (25 mL) was added and Et₂O extractions performed. The organic extracts were combined and washed with H₂O, HCl 1M and NaHCO₃ sat., to be then

dried (Na_2SO_4) and concentrated *in vacuo*. The resulting yellow solid was additionally purified by washing with petroleum ether, and later identified as pure (**120**) (1.85 g, 86%). For a summary of ^1H and ^{13}C NMR assignments, see Table 4.14. ^1H NMR (CD_2Cl_2 , 400 MHz) δ 7.78 (1H, s), 7.66 (2H, m), 7.45-7.30 (4H, m), 6.45 (1H, s, broad), 3.38 (2H, m), 2.75 (2H, m), 2.01 (2H, m); ^{13}C NMR (CD_2Cl_2 , 100 MHz) δ 195.7 (C), 171.9 (C), 143.2 (CH), 134.2 (C), 133.8 (C), 131.4 (2CH), 131.3 (CH), 129.1 (2CH), 39.8 (CH_2), 38.8 (CH_2), 27.4 (CH_2). HRESIMS calcd for $\text{C}_{13}\text{H}_{13}\text{NO}_2\text{Na}$ ($[\text{M}+\text{Na}]^+$): 238.0844; found 238.0844.

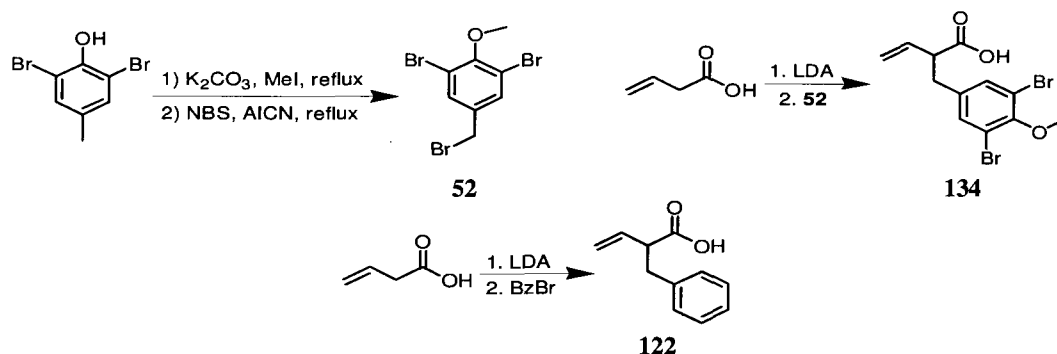
Table 4.14. NMR data for 3-benzylidene-azepane-2,4-dione (**120**) (recorded in CD_2Cl_2).



Carbon No	^{13}C δ (ppm) ^a	^1H δ (ppm) (mult, <i>J</i> (Hz)) ^{b,c}	HMBC ^b (H→C)
N1		6.45 (s, broad)	
2	171.9		
3	133.8		
4	195.7		
5	38.8	2.75 (m)	C3, C4, C6, C7
6	27.4	2.01 (m)	C4, C5, C7
7	39.8	3.38 (m)	C2, C5, C6
8	143.2	7.78 (s)	C2, C3, C4, C10
9	134.2		
10	131.4	7.66 (m)	C8, C12
11	129.1	7.45-7.30 (m)	C12
12	131.3	7.45-7.30 (m)	C11

^aRecorded at 100 MHz. ^bRecorded at 400 MHz. ^cAccording to HMQC recorded at 400 MHz.

Preparation of 2-(3,5-dibromo-4-methoxy-benzyl)-but-3-enoic (134) and 2-benzylbut-3-enoic (122) acids



A mixture of 2,6-dibromo-4-methylphenol (15 g, 56 mmol) and K_2CO_3 (11.6 g, 84 mmol) was stirred at 25 °C for 30 min, whereupon MeI (5.2 mL, 84 mmol) was added and the resulting slurry refluxed for 3 h. Once at room temperature, the excess K_2CO_3 was filtrated off and the crude concentrated *in vacuo*, to give a white solid. This solid was dissolved in CCl_4 , and NBS (10 g, 56 mmol) followed by 1,1'-azobis(cyanocyclohexane) (AICN) (0.5 g, 2 mmol) were added to the solution. The resulting mixture was refluxed for 12 h, to be then separated from an insoluble precipitate (*N*-succinimide) by filtration and concentrated. The obtained crystalline white solid (19.8 g, 98%) was pure by TLC and identified by 1H -NMR as 1,3-dibromo-5-bromomethyl-2-methoxybenzene (52).

In a second reaction, a mixture of diisopropylamine (21.8 mL, 154 mmol) and BuLi (96 mL, 154 mmol, 1.6 M) in THF (150 mL) was stirred at 0 °C for 10 min, to be then treated with vinylacetic acid (6.4 mL, 75 mmol). After stirring for 45 min at 0 °C, 1,3-dibromo-5-bromomethyl-2-methoxybenzene (52) (27 g, 75 mmol) was added and the solution stirred for 30 min at 0 °C and 2 h at 25 °C. H_2O was slowly added to the reaction crude and the pH for the aqueous layer was adjusted to 2.5 using HCl 0.1 M. After EtOAc extractions, the organic extracts were combined, dried (Na_2SO_4) and concentrated *in vacuo*. The resulting residue was

poured into a silica gel column and eluted using a gradient of EtOAc/hexanes mixtures (from 30% to 100%), to afford after solvent evaporation a white amorphous solid (16.0 g, 58%) of desired product (**134**).

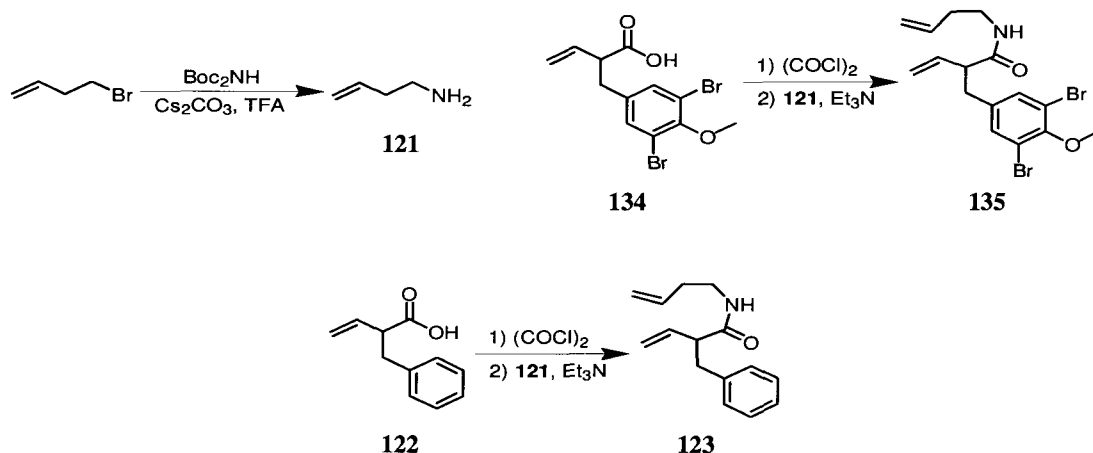
When the previous procedure was followed using LDA (13.4 mL, 24.1 mmol, 1.8 M), vinylacetic acid (1.0 mL, 11.8 mmol) in THF (10 mL), and benzyl bromide (1.43 mL, 12.0 mmol), 2-benzyl-but-3-enoic acid (**122**) was obtained as a colorless liquid (1.4 g, 68%).

1,3-Dibromo-5-bromomethyl-2-methoxybenzene (**52**): ^1H NMR (CDCl_3 , 300 MHz) δ 7.51 (2H, s), 4.34 (2H, s), 3.86 (3H, s); ^{13}C NMR (CDCl_3 , 75 MHz) δ 155.7 (C), 137.6 (C), 134.6 (2CH), 119.6 (2C), 62.1 (CH_3), 32.0 (CH_2).

2-(3,5-Dibromo-4-methoxy-benzyl)-but-3-enoic acid (**134**): ^1H NMR (CDCl_3 , 300 MHz) δ 10.84 (1H, s, broad), 7.30 (2H, s), 5.79 (1H, m), 5.15 (2H, m), 3.83 (3H, s), 3.27 (1H, ddd, $J = 7.3, 7.7, 8.1$ Hz), 3.00 (1H, dd, $J = 7.3, 13.9$ Hz), 2.74 (1H, dd, $J = 7.3, 13.9$ Hz); ^{13}C NMR (CDCl_3 , 75 MHz) δ 180.0 (C), 154.2 (C), 138.5 (C), 135.3 (CH), 134.6 (2CH), 120.5 (CH_2), 119.3 (2C), 62.0 (CH_3), 52.7 (CH_2), 37.9 (CH). HRESIMS calcd for $\text{C}_{12}\text{H}_{11}\text{O}_3^{79}\text{Br}_2$ ($[\text{M}+\text{H}]^+$): 360.9075; found 360.9071.

2-Benzylbut-3-enoic acid (**122**): ^1H NMR (CDCl_3 , 400 MHz) δ 7.36-7.12 (5H, m), 5.87 (1H, m), 5.15 (2H, m), 3.36 (1H, ddd, $J = 7.6, 7.7, 7.8$ Hz), 3.14 (1H, dd, $J = 7.3, 13.7$ Hz), 2.88 (1H, dd, $J = 7.5, 13.7$ Hz); ^{13}C NMR (CDCl_3 , 100 MHz) δ 179.9 (C), 138.2 (C), 134.6 (CH), 129.0 (2CH), 128.3 (2CH), 126.5 (CH), 118.3 (CH_2), 51.7 (CH), 38.0 (CH_2). HRESIMS calcd for $\text{C}_{11}\text{H}_{11}\text{O}_2$ ($[\text{M}+\text{H}]^+$): 175.0759; found 175.0758.

Preparation of 2-(3,5-dibromo-4-methoxybenzyl)-but-3-enoic acid but-3-enylamide (**135**) and 2-benzylbut-3-enoic acid but-3-enylamide (**123**)



A solution of di-*t*-butyl iminodicarboxylate (44.0 g, 202 mmol) in CH_3CN (200 mL) was treated with Cs_2CO_3 (65 g, 200 mmol), followed by addition of 4-bromobutene (26 mL, 256 mmol) while stirring. The resulting slurry was refluxed for 18 h, whereupon the insoluble salts were removed by filtration and the crude concentrated *in vacuo*. Dilution of the obtained residue in CH_2Cl_2 and addition of TFA (60 mL, 300 mmol) with stirring for 4 h at 25 °C provided the trifluoroacetic salt of but-3-enylamine, which was precipitated as a gray powder by addition of $\text{HCl}/\text{Et}_2\text{O}$ (120 mL, 240 mmol). This precipitate was characterized by NMR and MS as but-3-enylamine (**121**) hydrochloric salt (14.5 g, 67%).

To a solution of 2-(3,5-dibromo-4-methoxybenzyl)-but-3-enoic acid (**134**) (32.3 g, 88 mmol) in CH_2Cl_2 (150 mL) at 0 °C, was added oxalic chloride (8.38 mL, 97 mmol) and ten drops of DMF. The mixture was stirred for 16 h at 25 °C, to be then concentrated *in vacuo* under N_2 atmosphere. The resulting red and oily residue was diluted in CH_2Cl_2 (30 mL) and added at 0 °C to a slurry of but-3-enylamine (**121**) hydrochloric salt (14.2 g, 132 mmol) and triethylamine (37 mL, 264 mmol), with the consequent formation of HCl gas. After stirring at 25 °C for 12 h, a H_2O partition was made and EtOAc extractions performed. Drying (Na_2SO_4) and concentration

of the organic extracts provided a reddish residue, which was purified by gradient silica gel column chromatography (40% to 100% EtOAc/hexanes) to afford 2-(3,5-dibromo-4-methoxybenzyl)-but-3-enoic acid but-3-enylamide (**135**) as a gray powder (25.5 g, 69%).

Following the second procedure above, 2-benzylbut-3-enoic acid but-3-enylamide (**123**) (3.6 g, 87%) was prepared using the following amounts of reagents: 2-benzylbut-3-enoic acid (**122**) (3.1 g, 17.9 mmol), oxalic chloride (5.53 mL, 63.4 mmol), but-3-enylamine.HCl (**121**) (4.55 g, 42.3 mmol) and triethylamine (8.84 mL, 63.4 mmol).

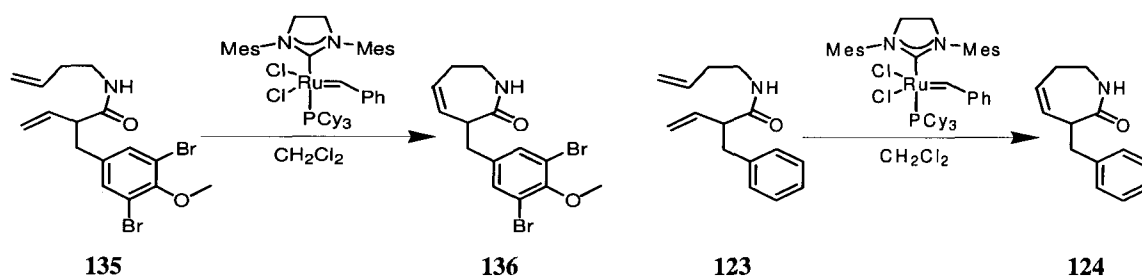
But-3-enylamine.HCl (**121**): ^1H NMR (CD_3OD , 300 MHz) δ 5.81 (1H, m), 5.18 (2H, m), 4.87 (2H, s, broad), 3.00 (2H, t, $J = 7.4$ Hz), 2.42 (2H, q, $J = 7.1$ Hz); ^{13}C NMR (CD_3OD , 75 MHz) δ 134.3 (CH), 119.3 (CH_2), 40.1 (CH_2), 32.8 (CH_2). HRESIMS calcd for $\text{C}_4\text{H}_{10}\text{N}$ ($[\text{M}+\text{H}]^+$): 72.0813; found 72.0812.

2-(3,5-Dibromo-4-methoxybenzyl)-but-3-enoic acid but-3-enylamide (**135**): ^1H NMR (CDCl_3 , 400 MHz) δ 7.29 (2H, s), 5.79 (1H, m), 5.64 (1H, m), 5.49 (1H, s, broad), 5.12 (2H, m), 4.99 (2H, m), 3.83 (3H, s), 3.26 (2H, m), 3.09 (1H, dd, $J = 7.4, 13.5$ Hz), 2.94 (1H, ddd, $J = 7.4, 7.5, 8.0$ Hz), 2.69 (1H, dd, $J = 6.7, 13.5$ Hz), 2.16 (2H, m); ^{13}C NMR (CDCl_3 , 100 MHz) δ 171.9 (C), 152.2 (C), 138.1 (C), 136.0 (CH), 134.9 (CH), 133.1 (2CH), 118.0 (CH_2), 117.6 (2C), 116.9 (CH_2), 60.4 (CH_3), 53.0 (CH), 38.5 (CH_2), 36.7 (CH_2), 33.6 (CH_2). HRESIMS calcd for $\text{C}_{16}\text{H}_{19}\text{NO}_2\text{Na}^{79}\text{Br}^{81}\text{Br}$ ($[\text{M}+\text{Na}]^+$): 439.9660; found 439.9651.

2-Benzylbut-3-enoic acid but-3-enylamide (**123**): ^1H NMR (CDCl_3 , 400 MHz) δ 7.29-7.11 (5H, m), 5.85 (1H, m), 5.62 (1H, m), 5.46 (1H, s, broad), 5.10 (2H, m), 4.96 (2H, m), 3.24 (2H, m), 3.16 (1H, dd, $J = 7.4, 13.6$ Hz), 3.01 (1H, ddd, $J = 7.5, 7.6, 7.8$ Hz), 2.79 (2H, dd, $J = 7.0, 13.4$

Hz), 2.09 (2H, m); ^{13}C NMR (CDCl_3 , 100 MHz) δ 172.2 (C), 139.2 (C), 136.6 (CH), 135.0 (CH), 129.0 (2CH), 128.2 (2CH), 126.2 (CH), 117.8 (CH_2), 117.1 (CH_2), 54.0 (CH), 38.20 (CH_2), 38.17 (CH_2), 33.5 (CH_2). HRESIMS calcd for $\text{C}_{15}\text{H}_{19}\text{NONa}$ ($[\text{M}+\text{Na}]^+$): 252.1364; found 252.1368.

Preparation of 3-(3,5-dibromo-4-methoxy-benzyl)-1,3,6,7-tetrahydroazepin-2-one (136) and 3-benzyl-1,3,6,7-tetrahydroazepin-2-one (124)



A solution of 2-(3,5-dibromo-4-methoxybenzyl)-but-3-enoic acid but-3-enylamide (**135**) (0.70 g, 1.68 mmol) in degassed CH_2Cl_2 (110 mL), was treated with Grubbs catalyst 2nd generation (0.1 g, 0.12 mmol) and refluxed for 18 h. Once at room temperature, the crude was concentrated and poured into a silica gel column (70% EtOAc/hexanes) followed by TLC. Concentration of the fractions containing product afforded (**136**) as white amorphous powder (0.69 g, 84%).

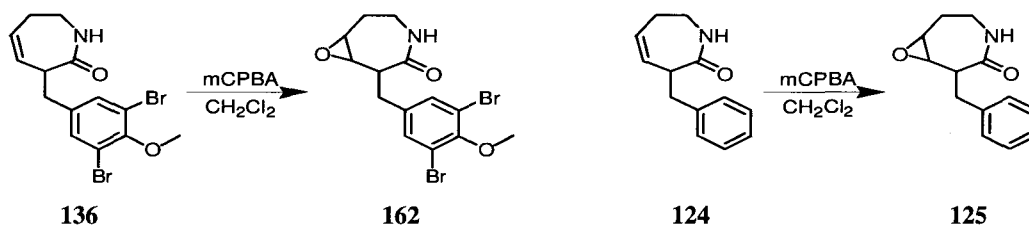
This same procedure, using 2-benzylbut-3-enoic acid but-3-enylamide (**123**) (0.33 g, 1.45 mmol) together with Grubbs catalyst (0.050 g, 0.06 mmol), provided 3-benzyl-1,3,6,7-tetrahydro-azepin-2-one (**124**) (0.13 g, 61%) as a colorless solid.

3-(3,5-Dibromo-4-methoxy-benzyl)-1,3,6,7-tetrahydroazepin-2-one (**136**): ^1H NMR (CDCl_3 , 300 MHz) δ 7.33 (2H, s), 7.19 (1H, dd, $J = 5.8, 6.5$ Hz), 5.51 (1H, m), 5.16 (1H, m), 3.75 (3H, s),

3.73 (1H, m), 3.60 (1H, m), 3.11 (1H, dd, $J = 6.9, 14.2$ Hz), 3.10 (1H, m), 2.54 (1H, dd, $J = 7.7, 14.5$ Hz), 2.16 (2H, m); ^{13}C NMR (CDCl_3 , 75 MHz) δ 177.8 (C), 153.7 (C), 140.5 (C), 134.8 (2CH), 131.1 (CH), 127.2 (CH), 119.1 (2C), 62.0 (CH_3), 44.0 (CH_2), 40.1 (CH), 36.9 (CH_2), 31.5 (CH_2). HRESIMS calcd for $\text{C}_{14}\text{H}_{15}\text{NO}_2\text{Na}^{79}\text{Br}^{81}\text{Br}$ ($[\text{M}+\text{Na}]^+$): 411.9347; found 411.9343.

3-Benzyl-1,3,6,7-tetrahydroazepin-2-one (**124**): for a summary of ^1H and ^{13}C NMR assignments, see Table 4.6. ^1H NMR (CDCl_3 , 400 MHz) δ 7.33-7.15 (5H, m), 6.44 (1H, s, broad), 5.56 (1H, m), 5.32 (1H, m), 3.85 (1H, m), 3.71 (1H, m), 3.29 (1H, dd, $J = 5.8, 14.2$ Hz), 3.16 (1H, m), 2.73 (1H, dd, $J = 9.4, 14.2$ Hz), 2.24 (2H, m); ^{13}C NMR (CDCl_3 , 100 MHz) δ 176.8 (C), 139.9 (C), 129.6 (CH), 129.2 (2CH), 128.4 (2CH), 127.1 (CH), 126.1 (CH), 42.8 (CH), 38.8 (CH_2), 36.5 (CH_2), 30.1 (CH_2). HRESIMS calcd for $\text{C}_{13}\text{H}_{15}\text{NONa}$ ($[\text{M}+\text{Na}]^+$): 224.1051; found 224.1050.

Preparation of 2-(3,5-dibromo-4-methoxybenzyl)-8-oxa-4-aza-bicyclo[5.1.0]octan-3-one (**162**) and 2-benzyl-8-oxa-4-aza-bicyclo[5.1.0]octan-3-one (**125**)

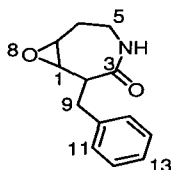


A solution of 3-(3,5-dibromo-4-methoxybenzyl)-1,3,6,7-tetrahydro-azepin-2-one (**136**) (0.1 g, 0.26 mmol) in CH_2Cl_2 (10 mL) was stirred in the presence of *m*-chloroperbenzoic acid (0.11 g, 0.51 mmol, 77%), until TLC analysis showed the absence of starting material (12-72 h). Water partition and EtOAc extraction gave a crystalline solid after solvent evaporation, which was purified by silica gel column chromatography (70% EtOAc/hexanes) to obtain desired product (**162**) (0.043 g, 42%) as a white powder. With 3-benzyl-1,3,6,7-tetrahydroazepin-2-one

(**124**) (0.95 g, 4.7 mmol) and *m*-CPBA (2.0 g, 9.5 mmol) as starting materials, 2-benzyl-8-oxa-4-aza-bicyclo[5.1.0]octan-3-one (**125**) (0.36 g, 39%) was successfully prepared.

2-(3,5-Dibromo-4-methoxybenzyl)-8-oxa-4-aza-bicyclo[5.1.0]octan-3-one (**162**): ^1H NMR (CDCl_3 , 400 MHz) δ 7.44 (2H, s), 6.50 (1H, m, broad), 3.83 (3H, s), 3.44 (1H, m), 3.30 (1H, m), 3.18 (1H, m), 3.11 (1H, m), 3.00 (1H, m), 2.95 (1H, m), 2.91 (1H, m), 2.20 (1H, m), 1.96 (1H, m); ^{13}C NMR (CDCl_3 , 100 MHz) δ 172.8 (C), 152.6 (C), 137.9 (C), 133.3 (2CH), 117.8 (2C), 60.5 (CH₃), 55.7 (CH), 53.6 (CH), 43.8 (CH), 36.1 (CH₂), 34.5 (CH₂), 28.2 (CH₂). HRESIMS calcd for C₁₄H₁₅NO₃Na⁷⁹Br₂ ([M+Na]⁺): 425.9316; found 425.9315.

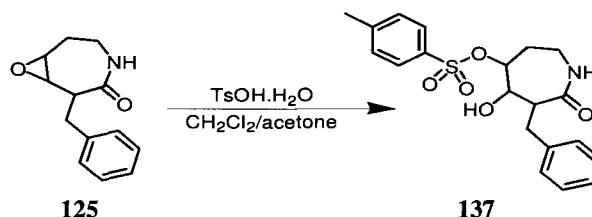
2-Benzyl-8-oxa-4-aza-bicyclo[5.1.0]octan-3-one (**125**): for a summary of ^1H and ^{13}C NMR assignments, see Table 4.15. ^1H NMR (CDCl_3 , 400 MHz) δ 7.29 (5H, m), 6.42 (1H, m, broad), 3.38 (1H, m), 3.35 (1H, m), 3.18 (1H, m), 3.08 (1H, m), 3.01 (1H, m), 2.98 (1H, m), 2.93 (1H, m), 2.17 (1H, m), 1.94 (1H, m); ^{13}C NMR (CDCl_3 , 100 MHz) δ 173.7 (C), 138.9 (C), 129.0 (2CH), 128.4 (2CH), 126.3 (CH), 55.8 (CH), 53.5 (CH), 43.8 (CH), 36.1 (CH₂), 35.6 (CH₂), 28.2 (CH₂). HRESIMS calcd for C₁₃H₁₅NO₂Na ([M+Na]⁺): 240.1000; found 240.1001.

Table 4.15. NMR data for 2-benzyl-8-oxa-4-aza-bicyclo[5.1.0]octan-3-one (**125**) (recorded in CDCl₃).

Carbon No	¹³ C δ (ppm) ^a	¹ H δ (ppm) (mult, J (Hz)) ^{b,c}	HMBC ^b (H→C)
1	55.8	2.93 (m)	C7
2	43.8	3.08 (m)	
3	173.7		
N4		6.42 (s, broad)	C2
5	36.1	2.98 (m), 3.35 (m)	C7
6	28.2	1.94 (m), 2.17 (m)	C1, C7
7	53.5	3.18 (m)	C6
O8			
9	35.6	3.01 (m), 3.38 (m)	C1, C2, C3, C10, C11
10	138.9		
11	129.0	7.28 (m)	C10, C13
12	128.4	7.29 (m)	C10, C13
13	126.3	7.20 (m)	C11

^a Recorded at 100 MHz. ^b Recorded at 400 MHz. ^c According to HMQC recorded at 400 MHz.

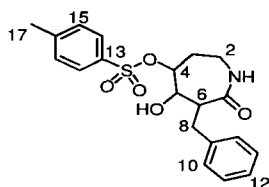
Preparation of toluene-4-sulfonic acid 6-benzyl-5-hydroxy-7-oxoazepan-4-yl ester (**137**)



2-Benzyl-8-oxa-4-aza-bicyclo[5.1.0]octan-3-one (**125**) (0.55 g, 2.5 mmol) was diluted in CH₂Cl₂/acetone 1:4 (40 mL), and stirred at room temperature in the presence of *p*-toluenesulfonic acid monohydrate (2.7 g, 14.2 mmol), until TLC analysis (100% EtOAc) indicated the absence of starting material (48 h). Silica gel column chromatography (100% EtOAc) provided (**137**) as a white solid (0.24 g, 25%). For a summary of ¹H and ¹³C NMR assignments, see Table 4.16. ¹H NMR (CDCl₃, 300 MHz) δ 7.77 (2H, m), 7.33 (2H, m), 7.20 (2H, m), 7.20 (2H, m), 7.13 (1H,

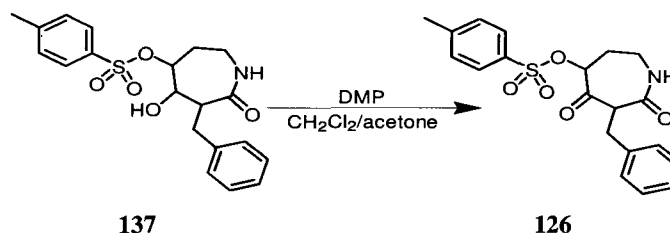
m), 6.69 (1H, s, broad), 2.43 (3H, s), 4.47 (1H, m), 4.20 (1H, m), 3.55 (1H, m), 3.20 (2H, m), 3.18 (1H, m), 3.11 (1H, m), 3.00 (1H, m), 2.43 (1H, m); ^{13}C NMR (CDCl_3 , 100 MHz) δ 173.9 (C), 145.2 (C), 138.9 (C), 133.4 (C), 129.9 (2CH), 129.1 (2CH), 128.3 (2CH), 127.7 (2CH), 126.2 (CH), 78.6 (CH), 67.4 (CH), 41.4 (CH), 36.3 (CH_2), 33.7 (CH_2), 31.5 (CH_2), 21.6 (CH_3). HRESIMS calcd for $\text{C}_{20}\text{H}_{24}\text{NO}_5^{32}\text{S}$ ($[\text{M}+\text{H}]^+$): 390.1375; found 390.1372.

Table 4.16. NMR data for toluene-4-sulfonic acid 6-benzyl-5-hydroxy-7-oxoazepan-4-yl ester (**137**) (recorded in CDCl_3).

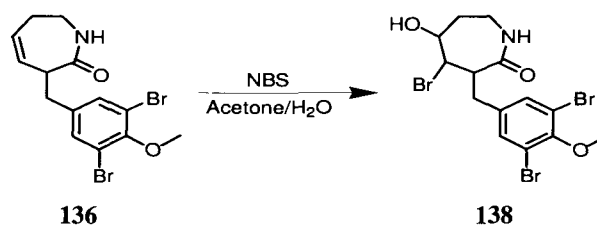


Carbon No	^{13}C δ (ppm) ^a	^1H δ (ppm) (mult, J (Hz)) ^{b,c}	HMBC ^b (H \rightarrow C)
N1		6.69 (s, broad)	
2	36.3	3.20 (m)	C7
3	31.5	3.11 (m), 3.18 (m)	
4	67.4	4.20 (m)	
5	78.6	4.47 (m)	C3, C4, C7, C8
6	41.4	3.55 (m)	C7, C8
7	173.9		
8	33.7	2.43 (m), 3.00 (m)	C5, C6, C7, C9
9	138.9		
10	128.3	7.20 (m)	C8
11	129.1	7.20 (m)	C9, C10, C12
12	126.2	7.13 (m)	C11
13	133.4		
14	127.7	7.77 (m)	C13, C15
15	129.9	7.33 (m)	C13, C14, C16, C17
16	145.2		
17	21.6	2.43 (s)	C15, C16

^a Recorded at 100 MHz. ^b Recorded at 300 MHz. ^c According to HMQC recorded at 400 MHz.

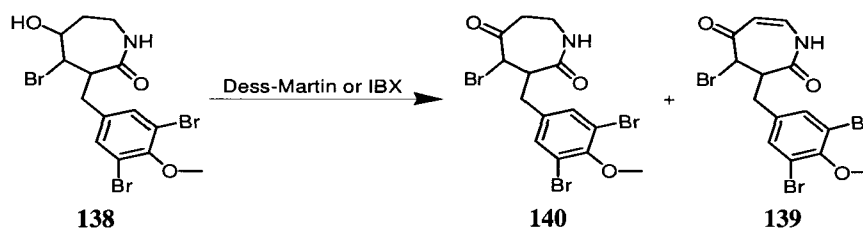
Preparation of toluene-4-sulfonic acid 6-benzyl-5,7-dioxoazepan-4-yl ester (126)

Toluene-4-sulfonic acid 6-benzyl-5-hydroxy-7-oxoazepan-4-yl ester (**137**) (0.088 g, 0.22 mmol) was diluted in CH₂Cl₂/acetone 1:1 (4 mL), and stirred at room temperature in the presence of Dess-Martin periodinane (0.19 g, 0.45 mmol), until TLC analysis (100% EtOAc) indicated the absence of starting material (2 h). Silica gel column chromatography (80% EtOAc/hexanes) provided toluene-4-sulfonic acid 6-benzyl-5,7-dioxo-azepan-4-yl ester (**126**) as a colorless solid (0.047 g, 54%). ¹H NMR (CDCl₃, 300 MHz) δ 7.76 (2H, m), 7.48 (1H, m), 7.38-7.15 (4H, m), 7.07 (2H, m), 6.35 (1H, s, broad), 5.12 (1H, dd, $J = 7.0, 11.4$ Hz), 3.99 (1H, dd, $J = 6.7, 6.9$ Hz), 3.71 (1H, m), 3.30 (1H, dd, $J = 6.7, 14.0$ Hz), 2.94 (1H, dd, $J = 6.6, 14.2$ Hz), 2.45 (2H, m), 2.43 (3H, s), 2.05 (1H, m); ¹³C NMR (CDCl₃, 100 MHz) δ 198.7 (C), 167.7 (C), 145.7 (C), 139.0 (C), 131.7 (C), 130.2 (2CH), 129.3 (2CH), 128.4 (2CH), 128.0 (2CH), 126.3 (CH), 82.5 (CH), 54.0 (CH), 36.7 (CH₂), 35.6 (CH₂), 30.9 (CH₂), 21.7 (CH₃). HRESIMS calcd for C₂₀H₂₁NO₅Na³²S ([M+Na]⁺): 410.1038; found 410.1033.

Preparation of 4-bromo-3-(3,5-dibromo-4-methoxybenzyl)-5-hydroxyazepan-2-one (138)

3-(3,5-Dibromo-4-methoxybenzyl)-1,3,6,7-tetrahydroazepin-2-one (**136**) (0.19 g, 0.5 mmol) was dissolved in a mixture acetone/H₂O (3:1, 2 mL) and stirred in the presence of NBS (0.12 g, 0.65 mmol), until TLC analysis (70% EtOAc/hexanes) showed the absence of starting material (72 h). The crude was concentrated *in vacuo* and purified by silica gel column chromatography (50, then 70% EtOAc/hexanes) to afford a white crystalline solid (0.24 g, 98%) identified as desired halohydrine (**138**). ¹H NMR (CDCl₃, 300 MHz) δ 7.33 (2H, s), 6.84 (1H, dd, *J* = 5.4, 6.5 Hz), 4.14 (1H, m), 3.83 (1H, m), 3.76 (3H, s), 3.70 (1H, m), 3.60 (1H, dd, *J* = 5.8, 9.2 Hz), 3.08 (1H, dd, *J* = 5.4, 14.6 Hz), 2.90 (1H, m), 2.63 (1H, dd, *J* = 5.4, 14.6 Hz), 2.15 (1H, m), 1.72 (1H, m); ¹³C NMR (CDCl₃, 100 MHz) δ 174.3 (C), 152.6 (C), 138.1 (C), 133.4 (2CH), 118.0 (2C), 70.8 (CH), 60.6 (CH₃), 51.0 (CH), 42.6 (CH), 34.8 (CH₂), 33.9 (CH₂), 30.6 (CH₂). HRESIMS calcd for C₁₄H₁₆NO₃Na⁷⁹Br₃ ([M+Na]⁺): 505.8578; found 505.8577.

Preparation of 4-bromo-3-(3,5-dibromo-4-methoxybenzyl)-azepane-2,5-dione (**140**) and 4-bromo-3-(3,5-dibromo-4-methoxybenzyl)-3,4-dihydro-1H-azepine-2,5-dione (**139**)

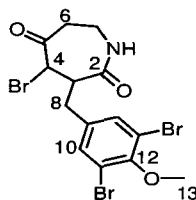


Dess-Martin periodinane (0.2 g, 0.47 mmol) was added to a solution of 4-bromo-3-(3,5-dibromo-4-methoxybenzyl)-5-hydroxyazepan-2-one (**138**) (0.13, 0.28 mmol) in CH₂Cl₂ (5 mL), and the mixture stirred at 25 °C until TLC revealed the absence of starting material (24 h). After solvent removal, the residue was purified by silica gel column chromatography (70% EtOAc/hexanes) to provide a 1:1 mixture (0.13 g, 54%) of desired (**140**) and byproduct (**139**), as a white powder.

4-Bromo-3-(3,5-dibromo-4-methoxybenzyl)-azepane-2,5-dione (**140**) was more efficiently prepared by adding IBX (0.12 g, 0.42 mmol) to a solution of starting material (**138**) (0.16 g, 0.3 mmol) in DMSO (3 mL), and stirring for 5 h at 25 °C. The solvent was removed using high vacuum, and the resulting residue purified as above, to afford (**140**) (0.13 g, 84%) as a colorless powder.

4-Bromo-3-(3,5-dibromo-4-methoxy-benzyl)-azepane-2,5-dione (**140**): for a summary of ^1H and ^{13}C NMR assignments, see Table 4.17. ^1H NMR (CDCl_3 , 300 MHz) δ 7.35 (1H, s, broad), 7.34 (2H, s), 4.11 (1H, m), 3.82 (3H, s), 3.45 (1H, m), 3.37 (1H, m), 3.32 (1H, m), 3.23 (1H, m), 3.11 (1H, m), 2.71 (1H, dd, $J = 8.1, 10.9$ Hz), 2.50 (1H, m); ^{13}C NMR (CDCl_3 , 75 MHz) δ 200.6 (C), 172.3 (C), 153.0 (C), 136.7 (C), 133.4 (2CH), 118.2 (2C), 60.5 (CH_3), 52.0 (CH), 44.5 (CH), 40.1 (CH_2), 36.8 (CH_2), 33.4 (CH_2). HRESIMS calcd for $\text{C}_{14}\text{H}_{15}\text{NO}_3^{79}\text{Br}_3$ ($[\text{M}+\text{H}]^+$): 481.8602; found 481.8607.

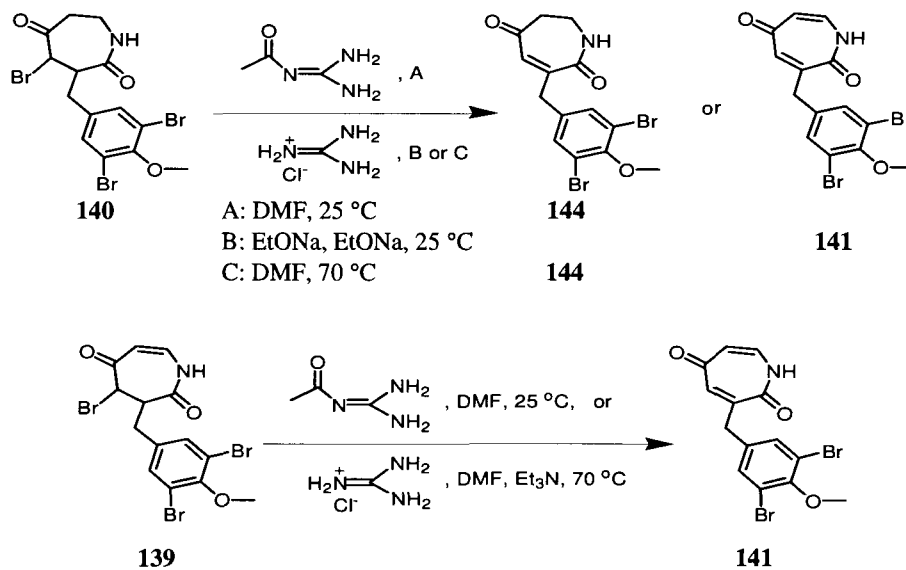
4-Bromo-3-(3,5-dibromo-4-methoxy-benzyl)-3,4-dihydro-1H-azepine-2,5-dione (**139**): ^1H NMR (CDCl_3 , 300 MHz) δ 8.91 (1H, d, $J = 6.9$ Hz), 7.34 (2H, s), 6.58 (1H, dd, $J = 6.9, 10.4$ Hz), 5.53 (1H, d, $J = 10.0$ Hz), 4.19 (1H, m), 3.84 (3H, s), 3.33 (1H, dd, $J = 4.6, 11.5$ Hz), 3.22 (1H, m), 2.74 (1H, dd, $J = 6.5, 11.6$ Hz); ^{13}C NMR (CDCl_3 , 75 MHz) δ 199.2 (C), 170.2 (C), 154.7 (C), 136.67 (C), 134.7 (2CH), 136.58 (CH), 120.0 (2C), 110.0 (CH), 62.1 (CH_3), 53.5 (CH), 44.7 (CH), 34.8 (CH_2). HRESIMS calcd for $\text{C}_{14}\text{H}_{12}\text{NO}_3\text{Na}^{79}\text{Br}_2^{81}\text{Br}$ ($[\text{M}+\text{Na}]^+$): 503.8245; found 503.8243.

Table 4.17. NMR data for 4-bromo-3-(3,5-dibromo-4-methoxybenzyl)-azepane-2,5-dione (**140**) (recorded in CDCl₃).

Carbon No	¹³ C δ (ppm) ^a	¹ H δ (ppm) (mult, J (Hz)) ^{b,c}	HMBC ^b (H→C)
N1		7.35 (s, broad)	C7
2	172.3		
3	44.5	3.11 (m)	C2, C5, C8, C9
4	52.0	4.11 (m)	C2, C3, C5, C6, C8
5	200.6		
6	40.1	2.50 (m), 3.32 (m)	C4, C5, C8
7	36.8	3.45 (m), 3.37 (m)	C2, C5, C6
8	33.4	2.71 (dd, J = 8.1, 10.9 Hz), 3.23 (m)	C2, C3, C4, C9, C10
9	136.7		
10	133.4	7.34 (s)	C3, C8, C11, C12
11	118.2		
12	153.0		
13	60.5	3.82 (s)	C12

^a Recorded at 75 MHz. ^b Recorded at 300 MHz. ^c According to HMQC recorded at 300 MHz.

Reaction of 4-bromo-3-(3,5-dibromo-4-methoxybenzyl)-azepane-2,5-dione (**140**) and 4-bromo-3-(3,5-dibromo-4-methoxybenzyl)-3,4-dihydro-1H-azepine-2,5-dione (**139**) with guanidine reagents



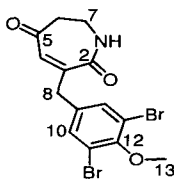
4-Bromo-3-(3,5-dibromo-4-methoxybenzyl)-azepane-2,5-dione (**140**) (0.058 g, 0.12 mmol) and acetylguanidine (0.36 mmol) were stirred in DMF at 25 °C, until TLC analysis showed total consumption of starting material (5 days). After solvent removal, the residue was purified by silica gel chromatography (70% EtOAc/hexanes), to afford 3-(3,5-dibromo-4-methoxybenzyl)-6,7-dihydro-1H-azepine-2,5-dione (**144**) as a colorless solid (0.042 g, 87%). This product was also obtained by reacting (**140**) (0.075 g, 0.15 mmol) with guanidine hydrochloride (0.1 g, 1 mmol) in DMF at 70 °C (0.044 g, 70%). When the same starting material (0.010 g, 0.021 mmol) was diluted in dry EtOH and added to a mixture of EtONa/EtOH (0.11 g of Na in 5 mL EtOH) and guanidine hydrochloride (0.5 g, 5 mmol), the procedure above afforded 3-(3,5-dibromo-4-methoxybenzyl)-1H-azepine-2,5-dione (**141**) (0.0016 g, 18%) also as a colorless solid.

In another reaction, byproduct (**139**) (0.10 g, 0.22 mmol) was diluted in DMF (5 mL) and stirred in the presence of acetylguanidine (0.082 g, 0.81 mmol) at 25 °C. The previous work-up and isolation procedure provided more 3-(3,5-dibromo-4-methoxybenzyl)-1H-azepine-2,5-dione (**141**) (0.062 g, 71%). When byproduct (**139**) (0.34 g, 0.7 mmol) was reacted with guanidine hydrochloride (0.20 g, 2.1 mmol) in DMF at 70 °C for 18 h, the only product isolated was also (**141**) (0.032 g, 11%).

3-(3,5-Dibromo-4-methoxybenzyl)-6,7-dihydro-1H-azepine-2,5-dione (**144**): for a summary of ^1H and ^{13}C NMR assignments, see Table 4.18. ^1H NMR (CDCl_3 , 300 MHz) δ 7.33 (2H, s), 7.30 (1H, s, broad), 6.17 (1H, s), 3.84 (3H, s), 3.71 (2H, s), 3.44 (2H, m), 2.73 (2H, m); ^{13}C NMR (CDCl_3 , 75 MHz) δ 200.2 (C), 168.2 (C), 153.1 (C), 145.1 (C), 135.7 (C), 133.3 (2CH), 132.6 (CH), 118.3 (2C), 60.6 (CH_3), 45.0 (CH_2), 39.2 (CH_2), 36.8 (CH_2). HRESIMS calcd for $\text{C}_{14}\text{H}_{13}\text{NO}_3\text{Na}^{79}\text{Br}_2$ ($[\text{M}+\text{Na}]^+$): 423.9160; found 423.9164.

3-(3,5-Dibromo-4-methoxybenzyl)-1H-azepine-2,5-dione (**141**): for a summary of ^1H and ^{13}C NMR assignments, see Table 4.7. ^1H NMR (DMSO, 400 MHz) δ 11.10 (1H, s, broad), 7.58 (2H, s), 6.94 (1H, d, $J = 2.2$ Hz), 6.81 (1H, d, $J = 10.0$ Hz), 5.67 (1H, dd, $J = 2.2, 10.0$ Hz), 3.76 (2H, s), 3.76 (3H, s); ^{13}C NMR (DMSO, 100 MHz) δ 185.4 (C), 165.1 (C), 152.0 (C), 142.7 (C), 141.9 (CH), 138.0 (C), 136.1 (CH), 133.3 (2CH), 117.2 (2C), 111.5 (CH), 60.3 (CH₃), 38.5 (CH₂). HRESIMS calcd for C₁₄H₁₂NO₃⁷⁹Br₂ ([M+H]⁺): 399.9184; found 399.9189.

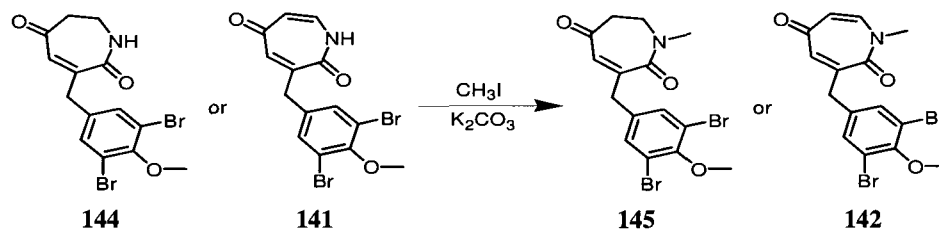
Table 4.18. NMR data for 3-(3,5-dibromo-4-methoxy-benzyl)-6,7-dihydro-1H-azepine-2,5-dione (**144**) (recorded in CDCl₃).



Carbon No	^{13}C δ (ppm) ^a	^1H δ (ppm) (mult, J (Hz)) ^{b,c}	HMBC ^b (H→C)
N1		7.30 (s, broad)	
2	168.2		
3	145.1		
4	132.6	6.17 (s)	C2, C3, C8
5	200.2		
6	45.0	2.73 (m)	C2, C5
7	36.8	3.44 (m)	C2, C5, C6
8	39.2	3.71 (s)	C2, C3, C4, C10
9	135.7		
10	133.3	7.33 (s)	C8, C11, C12
11	118.3		
12	153.1		
13	60.6	3.84 (s)	C12

^aRecorded at 75 MHz. ^bRecorded at 300 MHz. ^cAccording to HMQC recorded at 300 MHz.

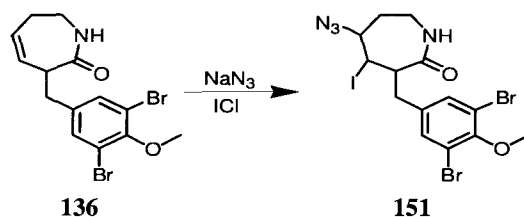
Synthesis of 3-(3,5-dibromo-4-methoxybenzyl)-1-methyl-6,7-dihydro-1H-azepine-2,5-dione (145) and 3-(3,5-dibromo-4-methoxybenzyl)-1-methyl-1H-azepine-2,5-dione (142)



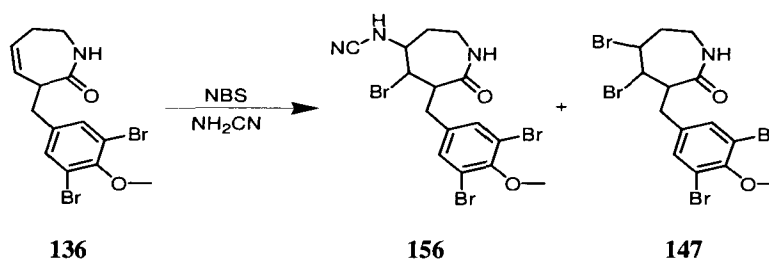
The reflux of starting materials (**144**) (0.044 g, 0.10 mmol) and (**141**) (0.025 g, 0.063 mmol), with K_2CO_3 (0.026 g, 0.19 mmol) and iodomethane (0.020 mL, 0.31 mmol) in acetone (10 mL) for 1 h, afforded after silica gel column chromatography (70% EtOAc/hexanes) desired products (**145**) (0.045 g, 99%) and (**142**) (0.023 g, 86%) as colorless solids.

3-(3,5-Dibromo-4-methoxybenzyl)-1-methyl-6,7-dihydro-1H-azepine-2,5-dione (**145**): 1H NMR ($CDCl_3$, 400 MHz) δ 7.33 (2H, s), 7.19 (1H, s, broad), 6.16 (1H, s), 3.83 (3H, s), 3.70 (2H, s), 3.44 (2H, m), 2.95 (3H, s), 2.71 (2H, m); ^{13}C NMR ($CDCl_3$, 100 MHz) δ 200.1 (C), 167.9 (C), 153.1 (C), 145.1 (C), 135.7 (C), 133.2 (2CH), 132.5 (CH), 118.2 (2C), 60.6 (CH₃), 45.0 (CH₂), 39.3 (CH₂), 36.8 (CH₂), 24.7 (CH₃).

3-(3,5-Dibromo-4-methoxybenzyl)-1-methyl-1H-azepine-2,5-dione (**142**): 1H NMR ($CDCl_3$, 300 MHz) δ 7.35 (2H, s), 6.815 (1H, d, $J = 10.4$ Hz), 6.806 (1H, d, $J = 2.7$ Hz), 5.76 (1H, dd, $J = 2.7$, 10.8 Hz), 3.83 (3H, s), 3.77 (2H, s), 3.43 (3H, s); ^{13}C NMR ($CDCl_3$, 75 MHz) δ 185.4 (C), 164.8 (C), 153.0 (C), 143.2 (C), 140.9 (CH), 139.7 (C), 136.3 (CH), 133.2 (2CH), 118.2 (2C), 112.4 (CH), 60.6 (CH₃), 42.2 (CH₂), 41.0 (CH₃). HRESIMS calcd for $C_{15}H_{14}NO_3^{79}Br_2$ ($[M+H]^+$): 413.9340; found 413.9335.

Preparation of 5-azido-3-(3,5-dibromo-4-methoxybenzyl)-4-iodoazepan-2-one (151)

To a slurry of NaN_3 (0.15 g, 2.3 mmol) in CH_3CN (5 mL) at 0 °C, was added ICl (2 mL, 2 mmol, 1 M) over a period of 20 min, and the mixture was stirred for 10 additional min, to be then treated drop by drop with 3-(3,5-dibromo-4-methoxybenzyl)-1,3,6,7-tetrahydro-azepin-2-one (**136**) (0.19 g, 0.5 mmol) in CH_3CN and stirred overnight. NH_4Cl sat. was added and EtOAc extractions performed. The combined organic extracts were washed with $\text{Na}_2\text{S}_2\text{O}_3$, H_2O and NaCl sat, followed by Na_2SO_4 treatment and solvent concentration. The residue was purified by silica gel column chromatography (70% EtOAc /hexanes), to afford white crystals (0.50 g, 90%) of desired product (**151**). ^1H NMR (CDCl_3 , 400 MHz) δ 7.34 (2H, s), 4.11 (1H, m), 3.97 (1H, m), 3.76 (3H, s), 3.50 (1H, m), 3.00 (3H, m), 2.48 (1H, m), 2.29 (1H, m), 1.76 (1H, m); ^{13}C NMR (CDCl_3 , 100 MHz) δ 174.3 (C), 152.6 (C), 137.2 (C), 132.9 (2CH), 118.1 (2C), 65.0 (CH), 60.3 (CH_3), 43.4 (CH), 35.2 (CH_2), 34.4 (CH_2), 29.4 (CH_2), 28.0 (CH_2). HRESIMS calcd for $\text{C}_{14}\text{H}_{16}\text{N}_4\text{O}_2\text{Na}^{79}\text{Br}_2\text{I}$ ($[\text{M}+\text{Na}]^+$): 556.8685; found 556.8683.

Preparation of 5-bromo-6-(3,5-dibromo-4-methoxybenzyl)-7-oxo-azepan-4-yl-cyanamide (156) and 4,5-dibromo-3-(3,5-dibromo-4-methoxybenzyl)-azepan-2-one (147)

To a solution of 3-(3,5-dibromo-4-methoxybenzyl)-1,3,6,7-tetrahydroazepin-2-one (**136**) (1.0 g, 2.6 mmol) in CH₂Cl₂ (20 mL) at 0 °C, was added NBS (0.50 g, 2.8 mmol) followed by cyanamide (0.43 g, 10.3 mmol), until TLC analysis (70% EtOAc/hexanes) showed the absence of starting material (72 h). The crude was concentrated *in vacuo* and purified by silica gel column chromatography (100% EtOAc) to afford first 4,5-dibromo-3-(3,5-dibromo-4-methoxybenzyl)-azepan-2-one (**147**) (0.69 g) as white crystals, and then desired 5-bromo-6-(3,5-dibromo-4-methoxybenzyl)-7-oxo-azepan-4-yl-cyanamide (**157**) (0.62 g, 47%) as a colorless powder.

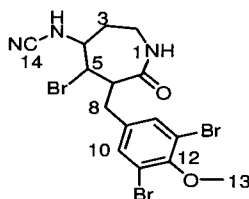
Compound (**147**) was also prepared by Br₂ (0.2 mL, 3.9 mmol) addition at -78 °C, to a solution of 3-(3,5-dibromo-4-methoxybenzyl)-1,3,6,7-tetrahydro-azepin-2-one (**136**) (0.31 g, 0.80 mmol) in CH₂Cl₂ (5 mL). After stirring for 3 h, the crude was added to Na₂S₂O₃ sat. and extracted with CH₂Cl₂, to be then dried (Na₂SO₄) and concentrated *in vacuo*. This procedure provided (**147**) as a foamy white solid (0.44 g, 99%).

5-Bromo-6-(3,5-dibromo-4-methoxybenzyl)-7-oxo-azepan-4-yl-cyanamide (**156**): for a summary of ¹H and ¹³C NMR assignments, see Table 4.19. ¹H NMR (CD₃OD, 400 MHz) δ 7.48 (2H, s), 4.00 (1H, m), 3.81 (1H, m), 3.80 (3H, s), 3.53 (1H, m), 3.52 (1H, m), 3.16 (1H, dd, *J* = 6.1, 14.4 Hz), 3.01 (1H, m), 2.64 (1H, dd, *J* = 8.7, 14.2 Hz), 2.25 (1H, m), 1.85 (1H, m); ¹³C NMR (CD₃OD, 100 MHz) δ 175.4 (C), 154.4 (C), 139.5 (C), 134.8 (2CH), 119.3 (2C), 116.0 (C), 61.2 (CH₃), 60.0 (CH), 50.2 (CH), 45.0 (CH), 35.9 (CH₂), 35.4 (CH₂), 29.3 (CH₂). HRESIMS calcd for C₁₅H₁₇N₃O₂⁷⁹Br₃ ([M+H]⁺): 507.8871; found 507.8874.

4,5-Dibromo-3-(3,5-dibromo-4-methoxybenzyl)-azepan-2-one (**147**): for a summary of ¹H and ¹³C NMR assignments, see Table 4.20. ¹H NMR (CDCl₃, 400 MHz) δ 7.39 (2H, s), 6.21 (1H, s,

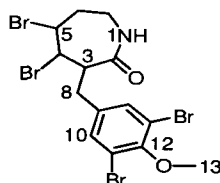
broad), 4.77 (1H, m), 4.15 (1H, m), 3.85 (3H, s), 3.84 (1H, m), 3.72 (1H, m), 3.21 (1H, dd, $J = 5.4, 14.6$ Hz), 3.13 (1H, m), 2.69 (1H, dd, $J = 9.4, 14.6$ Hz), 2.61 (1H, m), 2.08 (1H, m); ^{13}C NMR (CDCl_3 , 75 MHz) δ 173.0 (C), 152.9 (C), 136.9 (C), 133.4 (2CH), 118.1 (2C), 60.6 (CH_3), 55.6 (CH), 50.0 (CH), 43.9 (CH), 36.6 (CH_2), 34.0 (CH_2), 32.1 (CH_2). HRESIMS calcd for $\text{C}_{14}\text{H}_{15}\text{NO}_2\text{Na}^{79}\text{Br}_3^{81}\text{Br}$ ($[\text{M}+\text{Na}]^+$): 569.7713; found 569.7709.

Table 4.19. NMR data for 5-bromo-6-(3,5-dibromo-4-methoxy-benzyl)-7-oxo-azepan-4-yl-cyanamide (**156**) (recorded in CD_3OD).



Carbon No	^{13}C δ (ppm) ^a	^1H δ (ppm) (mult, J (Hz)) ^{b,c}	HMBC ^b (H→C)
1N			
2	35.9	3.01 (m), 3.52 (m)	C4
3	29.3	1.85 (m), 2.25 (m)	C4, C5
4	60.0	3.81 (m)	C2, C3, C5, C6, C14
5	50.2	4.00 (m)	C3, C4, C6, C7, C8
6	45.0	3.53 (m)	C4, C7, C8, C9
7	175.4		
8	35.4	3.16 (dd, $J = 6.1, 14.4$ Hz), 2.64 (dd, $J = 8.7, 14.2$ Hz)	C5, C6, C7, C9, C10
9	139.5		
10	134.8	7.48 (s)	C8, C11, C12
11	119.3		
12	154.4		
13	61.2	3.80 (s)	C12
14	116.0		

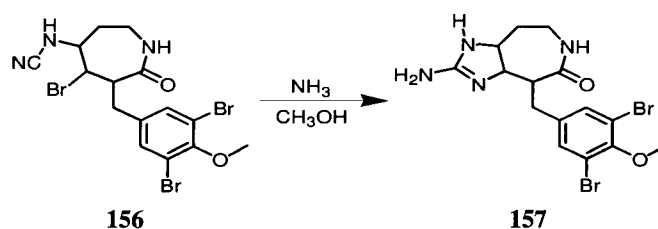
^a Recorded at 100 MHz. ^b Recorded at 400 MHz. ^c According to HMQC recorded at 400 MHz.

Table 4.20. NMR data for 4,5-dibromo-3-(3,5-dibromo-4-methoxy-benzyl)-azepan-2-one (**147**) (recorded in CDCl₃).

Carbon No	¹³ C δ (ppm) ^a	¹ H δ (ppm) (mult, J (Hz)) ^{b,c}	HMBC ^b (H→C)
N1		6.21 (s, broad)	
2	173.0		
3	43.9	3.72 (m)	C2, C4, C5, C8
4	50.0	4.15 (m)	C2, C6, C5, C8
5	55.6	4.77 (m)	
6	32.1	2.08 (m), 2.61 (m)	C7
7	36.6	3.13 (m), 3.84 (m)	C2, C5
8	34.0	2.69 (dd, J = 9.4, 14.6 Hz), 3.21 (dd, J = 5.4, 14.6 Hz)	C2, C3, C4, C9, C10
9	136.9		
10	133.4	7.39 (s)	C8, C11, C12
11	118.1		
12	152.9		
13	60.6	3.85 (s)	C12

^a Recorded at 75 MHz. ^b Recorded at 400 MHz. ^c According to HMQC recorded at 400 MHz.

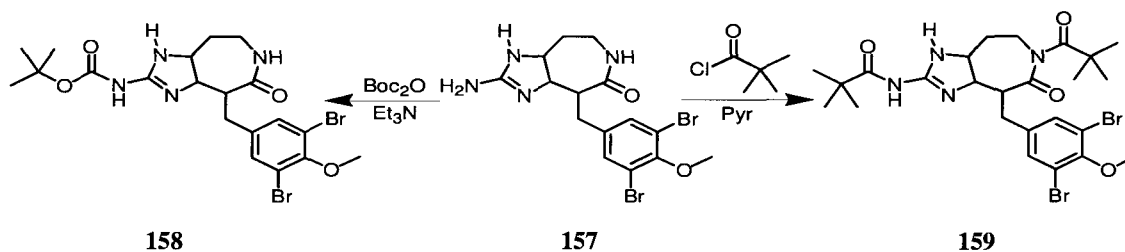
Synthesis of 19-demethyl-1,4,5,8,9,10-hexahydroceratamine B (**157**)



5-Bromo-6-(3,5-dibromo-4-methoxybenzyl)-7-oxo-azepan-4-yl-cyanamide (**156**) (0.23 g, 0.45 mmol) was dissolved in NH₃/MeOH (2 mL, 4 mmol, 2 M), and heated to 80 °C for 5 h in a sealed tube. Once at room temperature, the reaction crude was concentrated *in vacuo*, to give desired 19-demethyl-1,4,5,8,9,10-hexahydroceratamine B (**157**) (0.19 g, 96%) as a pale yellow powder. For a summary of ¹H and ¹³C NMR assignments, see Table 4.9. ¹H NMR (DMSO, 600

MHz) δ 8.20 (2H, s, broad), 7.90 (1H, s, broad), 7.66 (1H, d, $J = 7.4$ Hz), 7.53 (2H, s), 3.82 (1H, m), 3.80 (1H, m), 3.77 (3H, s), 3.42 (1H, m), 3.12 (1H, m), 3.10 (1H, m), 2.92 (2H, m), 2.15 (1H, m), 1.57 (1H, m); ^{13}C NMR (DMSO, 150 MHz) δ 172.9 (C), 160.4 (C), 151.6 (C), 139.1 (C), 133.1 (2CH), 117.0 (2C), 60.7 (CH), 60.4 (CH₃), 58.5 (CH), 48.5 (CH), 38.3 (CH₂), 31.7 (CH₂), 29.0 (CH₂). HRESIMS calcd for C₁₅H₁₉N₄O₂⁷⁹Br₂ ([M+H]⁺): 444.9875; found 444.9871.

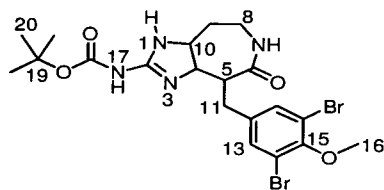
Protection 19-demethyl-1,4,5,8,9,10-hexahydroceratamine B (157)



To a solution of 19-demethyl-1,4,5,8,9,10-hexahydroceratamine B (**157**) (0.14 g, 0.32 mmol) in MeOH (10 mL), was added triethylamine (0.13 mL, 0.96 mmol) and di-*tert*-butyldicarbonate (0.14 g, 0.64 mmol). After stirring for 30 min. at 50 °C and then at room temperature, H₂O partition followed by EtOAc extractions, Na₂SO₄ treatment, and solvent concentration, provided a colorless residue. This crude was purified by gradient silica gel column chromatography (30% EtOAc/hexanes to 100% EtOAc), to afford (**158**) (0.043 g, 24%) as a colorless solid. In another reaction, the same starting material (**157**) (0.2 g, 0.45 mmol) was dissolved in pyridine (15 mL) and stirred in the presence of 2,2-dimethylpropanoic acid chloride (5 mL, 40 mmol), first at 80 °C for 2 h, and then at room temperature overnight. Silica gel column chromatography (10%MeOH/EtOAc) provided diprotected product (**159**) (0.033 g, 12%) as a colorless solid.

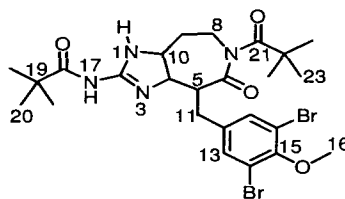
18-Boc-1,4,5,8,9,10-hexahydroceratamine B (**158**): for a summary of ^1H and ^{13}C NMR assignments, see Table 4.21. ^1H NMR (CDCl_3 , 400 MHz) δ 7.44 (2H, s), 7.04 (1H, m, broad), 3.88 (1H, m), 3.81 (3H, s), 3.73 (1H, m), 3.29 (1H, dd, $J = 2.8, 13.7$ Hz), 3.04 (1H, dd, $J = 6.1, 13.7$ Hz), 2.94 (1H, m), 2.83 (1H, m), 2.80 (1H, m), 2.75 (1H, m), 2.61 (1H, m), 1.48 (9H, s); ^{13}C NMR (CDCl_3 , 100 MHz) δ 174.6 (C), 156.7 (C), 152.8 (C), 151.7 (C), 137.9 (C), 133.8 (2CH), 117.9 (2C), 85.0 (C), 61.7 (CH), 60.6 (CH_3), 58.4 (CH), 53.2 (CH), 36.6 (CH_2), 34.2 (CH_2), 31.5 (CH_2), 28.0 (3 CH_3). HRESIMS calcd for $\text{C}_{20}\text{H}_{27}\text{N}_4\text{O}_4$ $^{79}\text{Br}_2$ ($[\text{M}+\text{H}]^+$): 545.0399; found 545.0397.

7,17-Dipivaloyl-1,4,5,8,9,10-hexahydroceratamine B amide (**159**): for a summary of ^1H and ^{13}C NMR assignments, see Table 4.22. ^1H NMR (CDCl_3 , 600 MHz) δ 7.43 (2H, s), 3.84 (3H, s), 3.74 (1H, m), 3.56 (1H, m), 3.52 (2H, m), 3.15 (1H, m), 3.00 (2H, m), 2.28 (1H, m), 1.75 (1H, m), 1.19 (9H, s), 1.18 (9H, s); ^{13}C NMR (CDCl_3 , 150 MHz) δ 190.2 (C), 189.0 (C), 173.9 (C), 162.9 (C), 153.0 (C), 137.4 (C), 133.4 (2CH), 118.2 (2C), 63.1 (CH), 60.6 (CH_3), 60.5 (CH), 51.6 (CH), 44.2 (C), 42.5 (CH_2), 40.8 (C), 33.3 (CH_2), 30.9 (CH_2), 27.9 (3 CH_3), 27.4 (3 CH_3). HRESIMS calcd for $\text{C}_{25}\text{H}_{35}\text{N}_4\text{O}_4$ $^{79}\text{Br}_2$ ($[\text{M}+\text{H}]^+$): 613.1025; found 613.1024.

Table 4.21. NMR data for 17-Boc-1,4,5,8,9,10-hexahydroceratamine B (**158**) (recorded in CDCl₃).

Carbon No	¹³ C δ (ppm) ^a	¹ H δ (ppm) (mult, J (Hz)) ^{b,c}	HMBC ^b (H→C)
N1			
2	156.7		
N3			
4	61.7	3.88 (m)	C5, C10
5	53.2	2.83 (m)	C11
6	174.6		
N7		7.04 (m, broad)	
8	36.6	2.80 (m), 2.94 (m)	
9	31.5	2.61 (m), 2.75 (m)	
10	58.4	3.73 (m)	C4, C9
11	34.2	3.04 (dd, J = 6.1, 13.7 Hz), 3.29 (dd, J = 2.8, 13.7 Hz)	C5, C6, C12, C13
12	137.9		
13	133.8	7.44 (s)	C11, C14, C15
14	117.9		
15	152.8		
16	60.6	3.81 (s)	C15
N17			
18	151.7		
19	85.0		
20	28.0	1.48 (s)	C19

^aRecorded at 100 Hz. ^bRecorded at 400 MHz. ^cAccording to HMQC recorded at 400 MHz.

Table 4.22. NMR data for 7,17-dipivaloyl-1,4,5,8,9,10-hexahydroceratamine B amide (**159**) (recorded in CDCl₃).

Carbon No	¹³ C δ (ppm) ^a	¹ H δ (ppm) (mult, J (Hz)) ^{b,c}	HMBC ^b (H→C)
N1			
2	162.9		
N3			
4	60.5	3.56 (m)	C6, C9
5	51.6	3.15 (m)	C4, C6, C12
6	173.9		
N7			
8	42.5	3.52 (m)	C6, C10, C21
9	30.9	1.75 (m), 2.28 (m)	C8, C10
10	63.1	3.74 (m)	C4, C5
11	33.3	3.00 (m)	C4, C6, C12, C13
12	137.4		
13	133.4	7.43 (s)	C12, C14, C15
14	118.2		
15	153.0		
16	60.6	3.84 (s)	C15
N17			
18	189.0		
19	44.2		
20	27.4	1.18 (s)	C18, C19
21	190.2		
22	40.8		
23	27.9	1.19 (s)	C21, C22

^a Recorded at 150 Hz. ^b Recorded at 600 MHz. ^c According to HMQC recorded at 600 MHz.

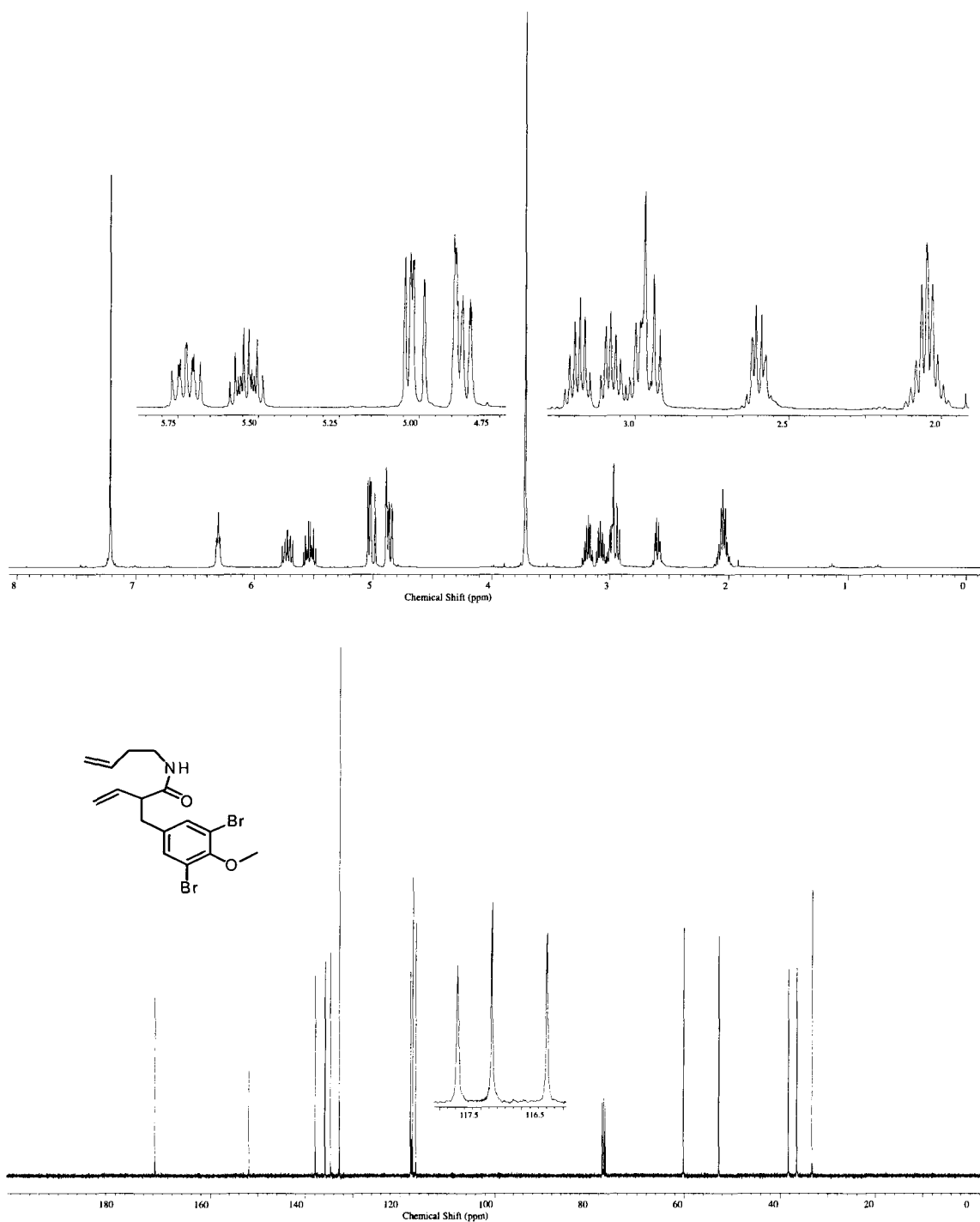


Figure 4.16. ^1H and ^{13}C -NMR spectra of 2-(3,5-dibromo-4-methoxybenzyl)-but-3-enoic acid but-3-enylamide (**135**) (recorded in CDCl_3 at 400 and 100 MHz respectively).

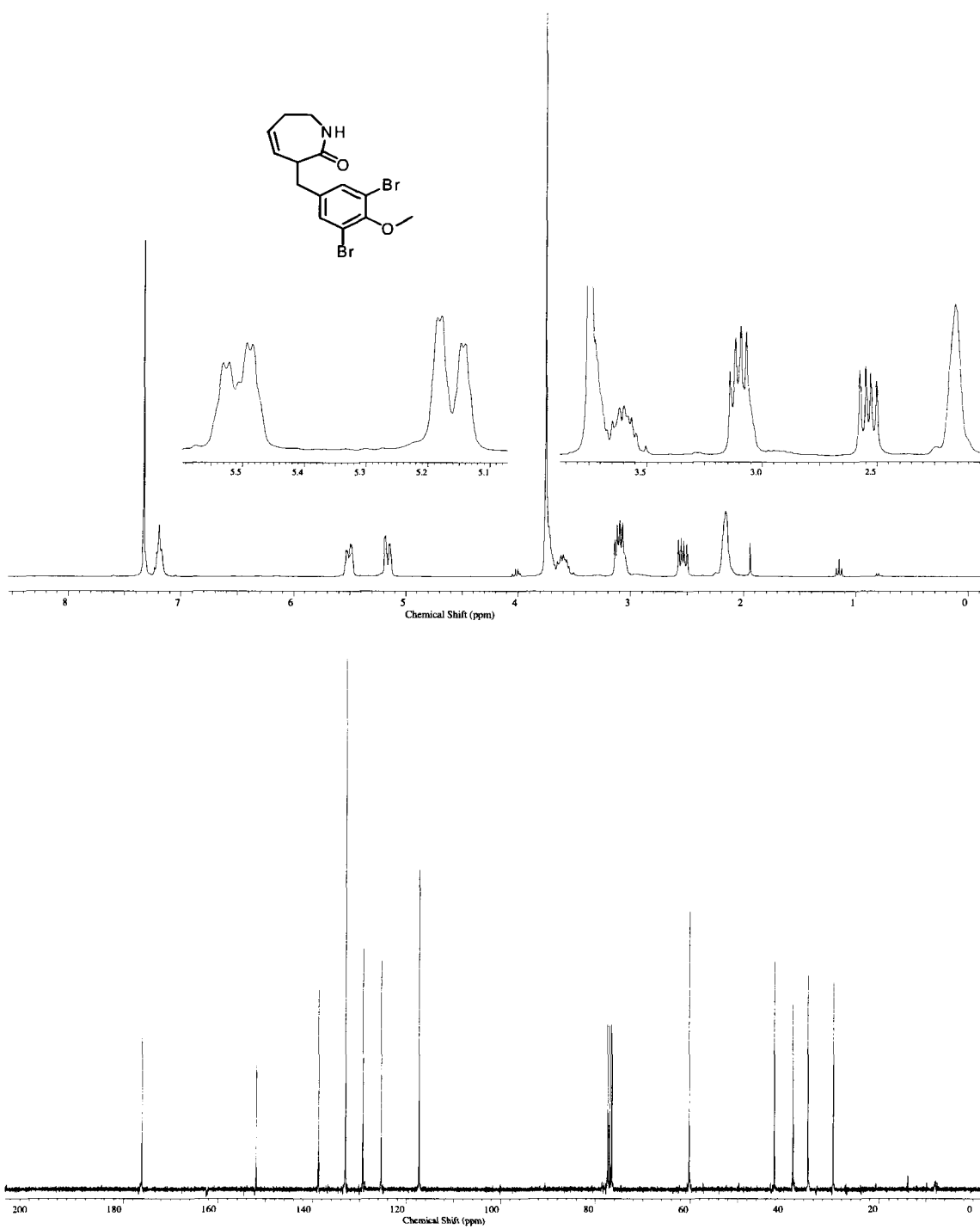


Figure 4.17. ^1H and ^{13}C -NMR spectra of 3-(3,5-dibromo-4-methoxy-benzyl)-1,3,6,7-tetrahydroazepin-2-one (**136**) (recorded in CDCl_3 at 300 and 75 MHz respectively).

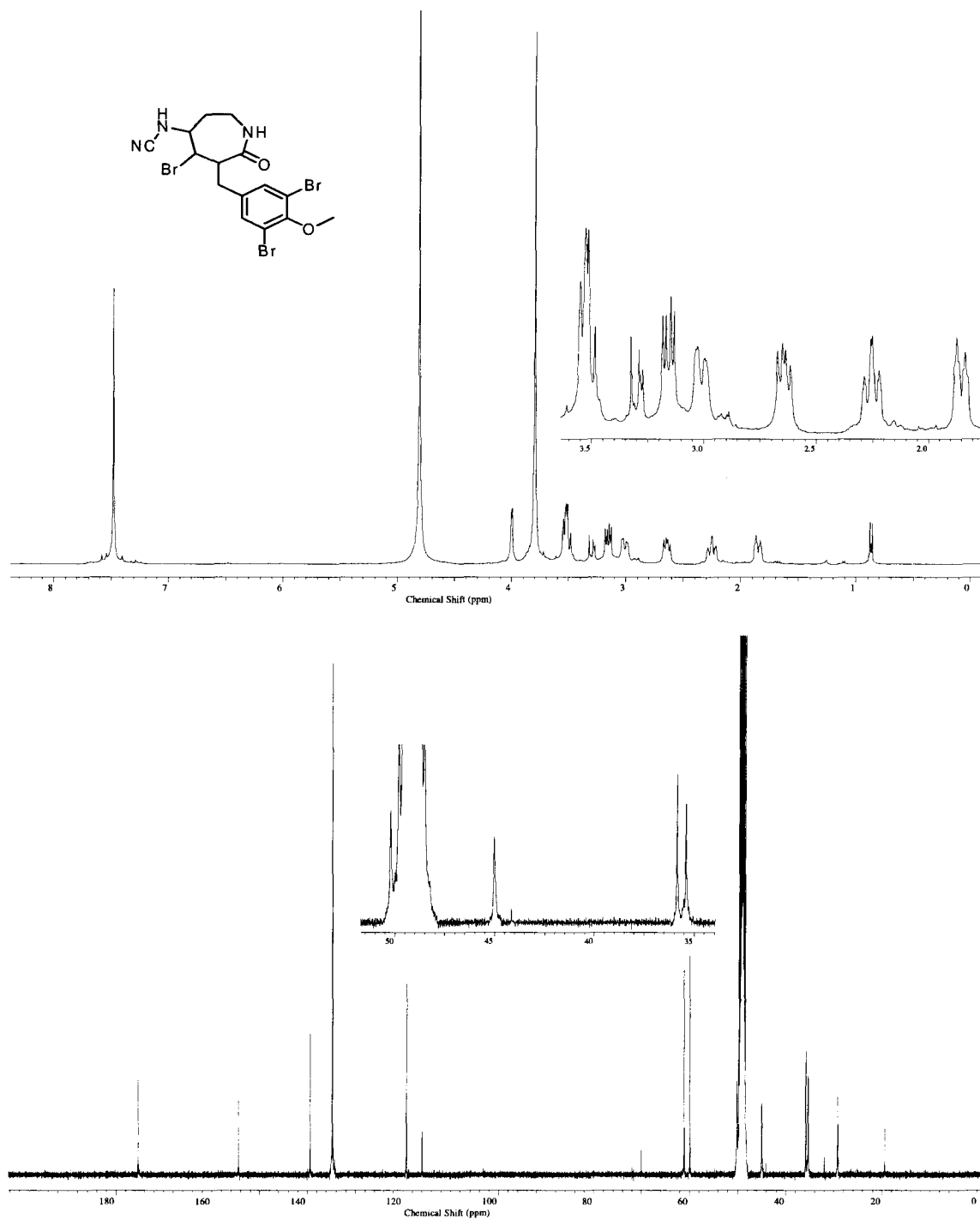


Figure 4.18. ^1H and ^{13}C -NMR spectra of 5-bromo-6-(3,5-dibromo-4-methoxybenzyl)-7-oxoazepan-4-yl-cyanamide (**156**) (recorded in CD_3OD at 400 and 100 MHz respectively).

5. Cannabinoid activity of the Marine Sterol Haplosamate A: Direct Observation of Binding to Human Receptors by Saturation Transfer Double-Difference (STDD) NMR Spectroscopy

5.1. Brief history

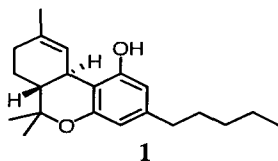
Hemp, *Cannabis sativa* L., and its derivatives (such as marijuana, hashish and hash oil) have a long history of use for therapeutic, ritual and recreational purposes. The therapeutic potential of ginseng, ephedra and cannabis was documented in Chinese medicine as early as 3000 B.C. when, during the rule of Emperor Shen Nung, the Chinese used marijuana for the treatment of malaria, constipation, rheumatic pains, absentmindedness, and gynecological disorders.³⁹⁶⁻³⁹⁹ The use of cannabis would spread west from early China to ancient India, where the anxiety relieving effect of bhang (the Indian term for marijuana ingested as food) was recorded more than 3000 years ago.³⁹⁹ Other civilizations used cannabis to treat pain, nausea, fever, infections, and to stimulate appetite.⁴⁰⁰

The use of cannabis as a psychoactive substance reached Europe and the Americas through the Arab world at the end of the 18th century, where anecdotal information about its health benefits was finally put to scientific scrutiny.³⁹⁹ Early in the 19th century, the therapeutic value of cannabis was recognized by British physicians. Sir John Russell Reynolds, one of Queen Victoria's physicians, was a proponent of the use of cannabis in medicine.³⁹⁷ In 1839 W. B. O'Shaughnessy at the Medical College of Calcutta observed its use in the indigenous treatment of various disorders and found that tincture of hemp was an effective analgesic, anticonvulsant, and muscle relaxant.^{400,401}

Over the next several decades, many papers on cannabis appeared in European medical literature.³⁹⁸ Marijuana extracts were widely used for medicinal purposes in the first decades of

the 20th century until 1937, when concern about the dangers of abuse led to the banning of marijuana for further medicinal use in United States (Marijuana Tax Act).³⁹⁹ Canada had made it illegal more than a decade before, in 1923, under the Opium and Drug Narcotic Act.⁴⁰²

A major breakthrough in the esoteric field of cannabis research was the isolation and elucidation in 1964, by Gaoni and Mechoulam,⁴⁰³ of the main psychoactive ingredient of marijuana, Δ^9 -tetrahydrocannabinol (**1**), and the following demonstration that bioactivity resides in its (-)-enantiomer.^{404,405} This discovery stimulated the generation of a structurally diverse range of synthetic compounds in the 1970's (classical and non-classical cannabinoids, aminoalkylindoles). More potent and selective new cannabinoids constituted the key for a second milestone in cannabis research, the discovery in 1988 and 1991 of specific cannabinoid receptors.^{397,398} Soon, reports on the first endogenous cannabinoids would follow.³⁹⁹



Over the last few years there has been an active debate regarding the medicinal aspects of cannabis. Currently cannabis products are classified as Schedule I drugs under the U. S. Drug Enforcement Administration (DEA) Controlled Substances Act, which means that the drug is only available for research purposes.⁴⁰⁶ In 1999, the Court of Appeal for Ontario ruled it unconstitutional to enforce the rule of law with respect to cannabis.⁴⁰⁷ Since 2001, the Marijuana Medical Access Regulations (MMAR) have made cannabis possession legal for authorized patients in Canada. Herbal cannabis, cultivated by Prairie Plant Systems Inc., licensee to Health Canada, is distributed to patients for CAN \$5/g.⁴⁰⁸

5.2. Marijuana: chemistry and psychoactive effects

The popular term marijuana refers to the dried material of the *Cannabis sativa* L. plant (*Cannabaceae*), a hemp which grows throughout temperate and tropical climates in almost any soil condition.⁴⁰⁰ Dried flowering tops and leaves are commonly smoked in hand-rolled cigarettes. All the different cannabinoids are concentrated in a viscous resin produced in glandular structures known as trichomes (Figure 5.1).⁴⁰⁶ The content ranges from 5% to 16% m/m, depending on latitude, weather, and soil conditions.⁴⁰⁰

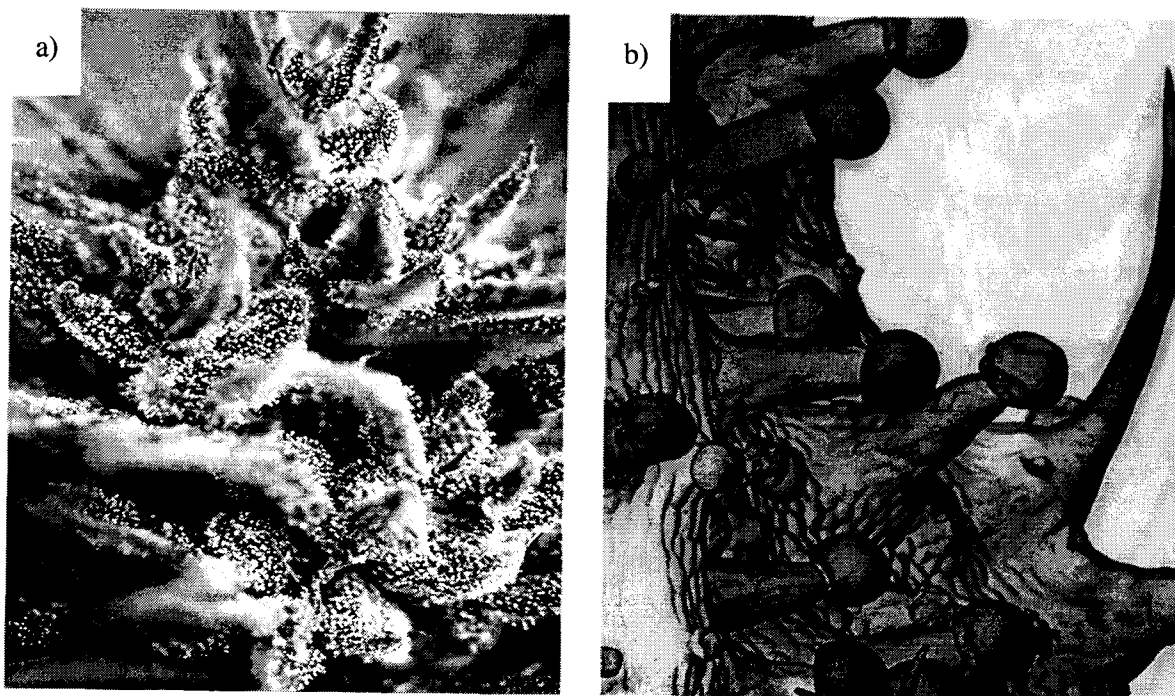


Figure 5.1. a) Mature *C. sativa* crop ready for harvesting; b) trichomes.⁴⁰⁶

Cannabis constituents represent almost all kinds of chemical compounds, including mono- and sesquiterpenes, sugars, hydrocarbons, steroids, flavonoids, nitrogenous compounds

and amino acids (Table 5.1),⁴⁰⁶ with Δ^9 -tetrahydrocannabinol (1) and similar terpenophenolic components as the most psychoactive.^{403,405}

Table 5.1. Constituents in the resin of *Cannabis sativa* reported until 2005.⁴⁰⁶

General Class	Amount
Cannabinoids	70
Nitrogenous compounds	27
Amino acids	18
Proteins, enzymes and glycoproteins	11
Sugars and related compounds	34
Hydrocarbons	50
Alcohols	7
Aldehydes	12
Ketones	13
Carboxylic acids	20
Fatty acids	23
Esters and lactones	13
Steroids	11
Terpenes	120
Non-cannabinoid phenols	25
Flavonoids	23
Vitamins	1
Pigments	2
Elements	9
Total	489

Table 5.2 summarizes the most typical effects of cannabis in humans. Many of them are described as biphasic,⁴⁰⁹ showing increased activity with acute or smaller doses and decreased response with larger doses or chronic use. They also vary greatly among individuals and may be more severe in ill and elderly patients.

Table 5.2. Pharmacological effects of smoked marijuana in humans.⁴⁰⁹

Body System	Effect	Description
Nervous (CNS)	Psychological	Euphoria (high), dysphoria, anxiety, precipitation or aggravation of psychosis, depersonalization.
	Perception	Heightened sensory perception, distortion of space and time, sense, hallucinations, misperceptions.
	Sedative	Generalized CNS depression, drowsiness, somnolence; additive with other CNS depressants.
	Cognition, psychomotor performance	Fragmentation of thoughts, mental clouding, memory impairment, global impairment of performance especially in complex demanding tasks.
	Motor function	Increased motor activity followed by inertia and in coordination, ataxia, dysarthria, tremulousness, weakness, muscle twitching.
	Analgesic	Currently available oral cannabinoids are similar in potency to codeine.
	Anti-emetic, increased appetite	With acute doses; the effect is reversed with larger doses or chronic use (tolerance).
	Tolerance	To most behavioral and somatic effects, including the "high".
Cardiovascular	Dependence, abstinence syndrome	Produced experimentally following prolonged intoxication: symptoms include disturbed sleep, decreased appetite, restlessness, irritability and sweating.
	Heart rate	Tachycardia with acute dosage, bradycardia with chronic use.
	Peripheral circulation	Vasodilation, conjunctival redness, postural hypotension.
	Cardiac output	Increased output and myocardial oxygen demand.
Respiratory	Cerebral blood flow	Increased with acute dose, decreased with chronic use.
	Ventilation	Small doses stimulate; larger doses depress.
	Bronchodilation	Coughing, but tolerance develops.
Eyes	Airways obstruction	From chronic smoking.
	Decreased intraocular pressure.	
Immune	Chronic use: impaired bactericidal activity of macrophages in lung and spleen.	
	Males	Anti-androgenic, decreased sperm count and sperm motility (chronic use, but tolerance may develop).
Reproductive	Females	Suppression of ovulation, complex effects on prolactin secretion; chronic use: increased obstetric risk.

Currently, there are three general types of cannabinoids: *herbal cannabinoids* or *phytocannabinoids*, which occur only in the cannabis plant; *endogenous cannabinoids*, produced in humans and other animals; and *synthetic cannabinoids*.

5.3. Phytocannabinoids

Introduced in the late 1990's, the term phytocannabinoids is used to describe the natural and most psychoactive terpenophenolic components of *Cannabis sativa*.^{397,406} There are around 70 known phytocannabinoids (Table 5.1), which are in turn grouped into 11 different classes according to common carbon backbones.⁴⁰⁶ Figure 5.2 shows the most representative member for each type.

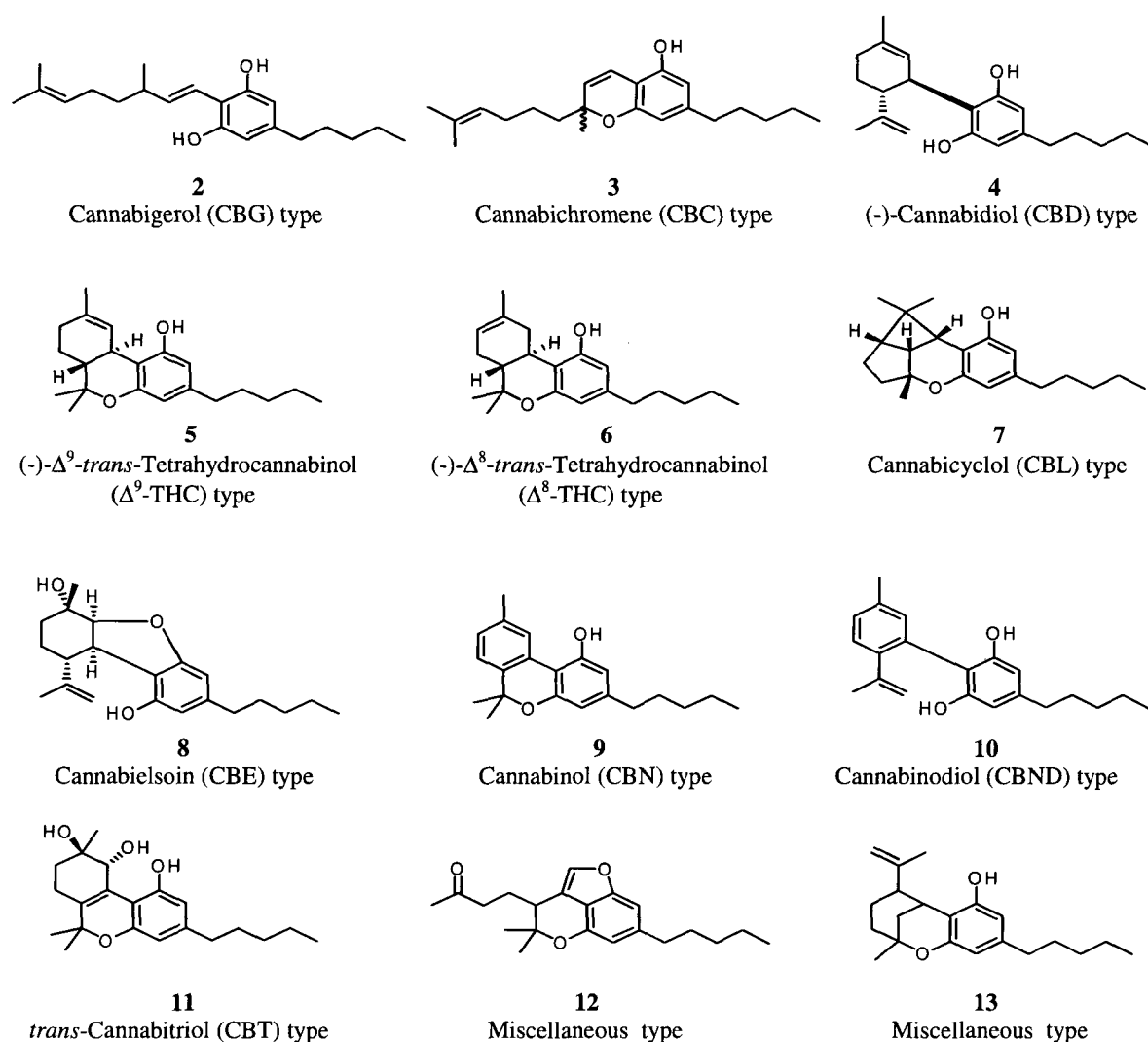


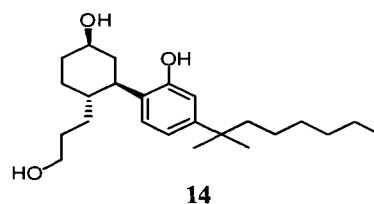
Figure 5.2. Classification of the typical cannabinoids.⁴⁰⁶

Cannabigerol (**2**) was the first compound isolated from the *C. sativa* resin.⁴⁰⁴ Although psychologically inactive when compared with Δ^9 -THC compounds, CBG-type cannabinoids exhibit antibacterial activity.⁴⁰⁶ The absolute configuration for (-)-cannabidiol (**4**) was assigned as (-)-*trans*-(1*R*,6*R*) by synthesis, being the first compound synthetically prepared.⁴¹⁰ There is no clear evidence for the natural origin of cannabielsoin (**8**)-type compounds, since they can be considered as oxidation products of naturally occurring CBD metabolites. Likewise, the fully aromatized CBN and CBND compounds are also thought to be artifacts, since their concentration increases during storage and exposure to light and air, with a subsequent decrease in the amount of Δ^9 -THC and CBD cannabinoids respectively.⁴⁰⁶ In fresh plants, the amount of CBE, CBN and CBND is usually minimal.⁴⁰⁰

5.4. Cannabinoid receptors, endogenous cannabinoids and the endocannabinoid system

In the 1980s, scientific research on cannabis became significantly more interdisciplinary, attracting the attention of more chemists, biochemists and pharmacologists. Before then, it was often speculated that cannabinoids produced their physiological and behavioral effects via nonspecific interaction with cell membranes, instead of interacting with specific membrane-bound receptors.³⁹⁷

The synthesis of less lipophilic and more potent cannabinoid ligands than Δ^9 -THC (**1**) improved the observations obtained from traditional receptor binding techniques, making possible the discovery of authentic cannabinoid binding sites.^{396,397} In 1988 the Pfizer compound CP-55,940 (**14**), a more potent and polar agonist, was used as the first probe of cannabinoid receptors.³⁹⁷⁻³⁹⁹ Autoradiography and competitive radioligand binding assays using [³H]CP-55,940, confirmed the presence of cannabinoid binding sites in the brain.^{396,397}



In 1990, the CB1 receptor was cloned from rats, and later from humans and mice.⁴¹¹ Its distribution has been well characterized in rat and human brain.^{396,397} Three years later, a second receptor subtype CB2 was found by sequence homology.⁴⁰⁰ Exhibiting a low overall homology with the CB1 receptor (44%, with 68% in the helical regions),³⁹⁶ CB2 was cloned from humans, mice and rats, and found to be restricted to the immune system, including macrophages from the spleen.^{397,399,411}

5.4.1. Cannabinoid human receptors

CB1 receptors exhibit a widespread distribution in the brain that correlates well with the known effects of cannabinoids on memory, perception, and the control of movement.⁴¹² Specifically, they are found in the basal ganglia and the cerebellum (involved in motor activity), in the limbic system, including the cortex and hippocampus (related with memory and cognition), amygdala (emotion), thalamus (sensory perception), hypothalamus, pons and medulla (regulation of the autonomic and endocrine functions).^{397,398} The CB1 receptor is also expressed in peripheral nerve terminals and various extraneural sites such as the reproductive systems (both male and female), eyes, vascular endothelium and spleen.³⁹⁹ In addition, CB1 receptor mRNA has been described in the adrenal gland, heart, lung, prostate, bone marrow, thymus, and tonsils.^{398,411}

In contrast, CB1 receptors are essentially absent in the medulla oblongata, the part of the brain stem responsible for respiratory and cardiovascular functions. This might explain the general lack of serious acute effects, including respiratory or cardiovascular failure, associated

with cannabis abuse when compared with other drugs.³⁹⁶ Both central and many of the peripheral effects of cannabinoids depend on the activation of CB1 receptors. In humans, CB1 is responsible for the “high” and anticonvulsive effects produced by smoked marijuana.⁴¹¹

CB2 receptors are almost exclusively found in the immune system, with the greatest density in the spleen.³⁹⁸ They are expressed by cells, including B and T lymphocytes, macrophages, and by tissues, like tonsils and lymph nodes besides the spleen.⁴¹¹ CB2 receptors appear to be responsible for the anti-inflammatory and possibly other therapeutic effects of cannabis. Thus, compared to CB1, CB2 represents a more attractive pharmacological target in developing cannabinoid-based therapeutic agents.³⁹⁹

Both CB1 and CB2 have amino acid sequences characteristic of G-protein-coupled receptors (GPCR's), in which a single polypeptide structure spans the plasma membrane seven times in a serpentine-like topology (Figure 5.3).^{397,411} They are common in animals, and have been found in mammals, birds, fish, and reptiles. The term cannabinoid has been extended to any molecule that binds to one of the cannabinoid receptors.³⁹⁷

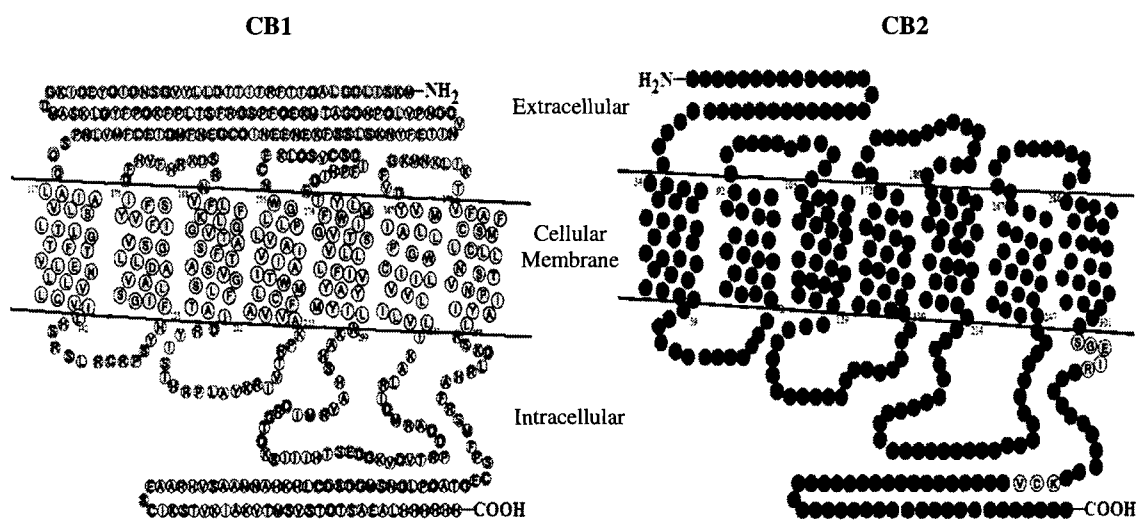


Figure 5.3. Serpentine-like topology of the cannabinoid receptors CB1 and CB2. CB1 is 126 amino acids longer and thus, possesses more units outside the cellular membrane.⁴¹¹

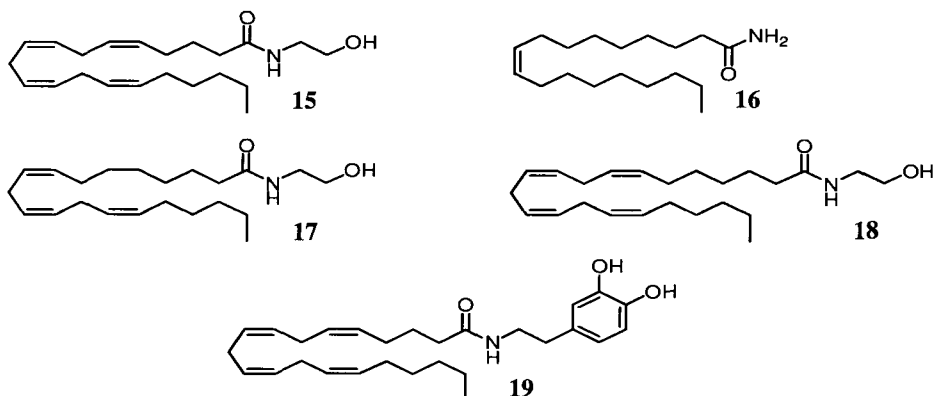
Recent studies have demonstrated a number of biological activities that are not considered to be mediated via CB1 or CB2 receptors. These include endothelium-dependent vasodilator effects of certain cannabinoids, and presynaptic inhibition of glutamatergic neurotransmission in the hippocampus.^{411,413,414} However, to date the NC-IUPHAR (International Union of Pharmacology Committee on Receptor Nomenclature and Drug Classification) has not designated additional cannabinoid receptors.³⁹⁷

5.4.2. Endocannabinoids

The discovery of specific cannabinoid receptors launched the quest for their corresponding endogenous ligands. Assuming that the endogenous agonist would have hydrophobic properties similar to those of current cannabinoid agonists, Devane, Mechoulam, and coworkers⁴¹⁵ isolated in 1992 the lipid derivative anandamide (**15**, from the Sanskrit *ananda* meaning “bliss and tranquility”),^{397,411} from organic solvent extracts of porcine brain. It is about as potent as Δ^9 -THC (**1**), binds to both CB1 and CB2 receptors, and is found in nearly all tissues in a wide range of animals.³⁹⁷

Besides anandamide (**15**), numerous endogenous polyunsaturated compounds capable of binding one or both cannabinoid receptors have been reported (Figure 5.4).^{399,416} Oleamide (**16**) shares with **15** some pharmacological properties, including sleep induction, anticonvulsant effects and modulation of appetite.³⁹⁷ Arachidonoyldopamine (**19**) presented high selectivity as a CB1 agonist and inhibited the proliferation of human breast cancer cells.^{397,399} 2-Arachidonoylglycerol (**20**) is more abundant and potent than **15**,^{399,417} but as a monoglyceride, it takes part in several pathways of lipid metabolism which minimize its availability in endocannabinoid signaling. This metabolite inhibited the proliferation of breast and prostate cancer cells, and was found to induce hypotension, contractile action on colon muscles, and neuroprotection after brain injury.³⁹⁷

Endocannabinoid Amides



Endocannabinoid Esters



Endocannabinoid Ether

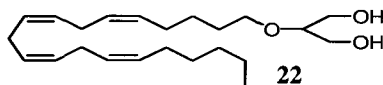


Figure 5.4. Representative endocannabinoids: anandamide (**15**), oleamide (**16**), homo- γ -linolenylethanolamide (**17**), docosatetraenylethanolamide (**18**), arachidonoyldopamine (**19**), 2-arachidonoylglycerol (**20**), *O*-arachidonylethanolamine (**21**), and 2-arachidonylethanolamine ether (noladin ether **22**).³⁹⁷

5.4.3. The endocannabinoid system

Phytocannabinoids, as well as their synthetic analogues, act in the organism by activating CB1 and/or CB2, normally engaged by the endogenous cannabinoids.^{397,399} The cannabinoid receptors, endocannabinoid ligands, and specific processes of synthesis, uptake and degradation, constitute the endogenous cannabinoid system (Figure 5.5), essential in brain modulation and therefore, almost every major life function in the human body.^{396,399,418}

After neurotransmitters bind their receptors (iR, mR) in a postsynaptic neuron, they synthesize membrane-bound endocannabinoid precursors and cleave them to release active

endocannabinoids following an increase of cytosolic free Ca^{2+} concentrations. Endocannabinoids subsequently act as *retrograde messengers*, traveling backwards against the synaptic flow to bind presynaptic CB1 cannabinoid receptors, which downregulate voltage-sensitive Ca^{2+} channels and activate K^+ channels.⁴¹⁸ This blunts membrane depolarization and exocytosis, which in turn inhibits the release of neurotransmitters such as glutamate, dopamine and γ -aminobutyric acid (GABA), involved in learning, movement and memory processes, respectively.^{399,418} The endocannabinoid neuromodulatory signaling is terminated by a membrane-transport system⁴¹⁹ (T) and a family of intracellular degradative enzymes. The most studied member of this family is a fatty acid amide hydrolase (FAAH), in charge of degrading anandamide (**15**) to ethanolamine and arachidonic acid.^{396,397,418,420}

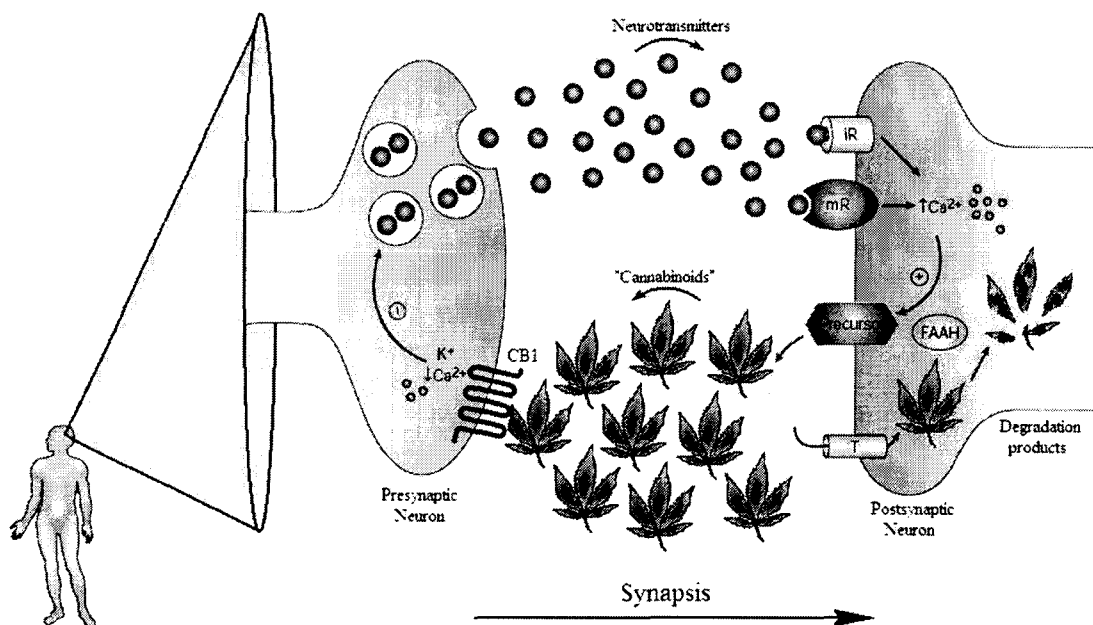


Figure 5.5. Endogenous cannabinoid system. Presynaptic and postsynaptic designate the sending and receiving sides of a synapse, respectively. iR: ionotropic receptors, channel-like receptors opened by agonist binding, and through which ions (Na^+ , K^+ and Ca^{2+}) can pass. mR: metabotropic receptors: seven-transmembrane heptahelical receptors coupled to G proteins.^{397,399,418}

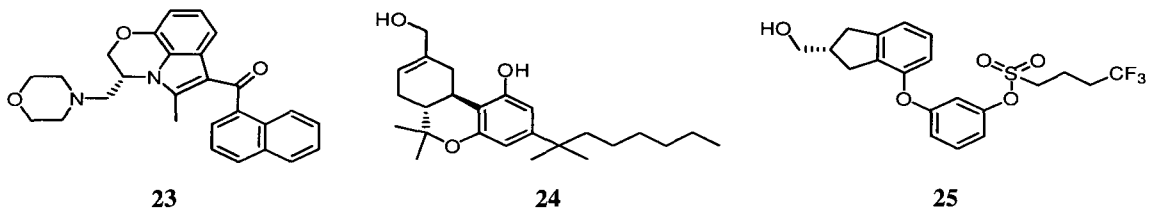
The endogenous cannabinoid system might also exert modulatory functions outside the brain, both in the peripheral nervous system and in extraneural sites, controlling processes such as peripheral pain, vascular tone, intraocular pressure and immune function.^{399,419} Although they share an intercellular signaling role with traditional water-soluble neurotransmitters, endocannabinoids are hydrophobic molecules with restricted mobility in the aqueous media surrounding cells and, therefore, act locally on nearby cells.³⁹⁷

5.5. Synthetic and patented cannabinoids

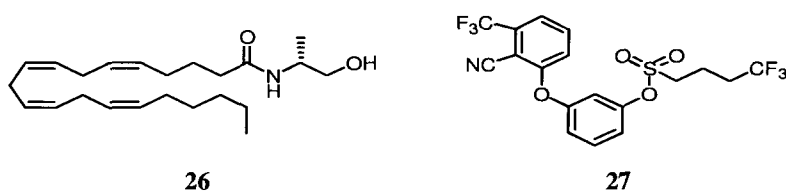
Historically, synthetic cannabinoids were often based on the structure of phytocannabinoids and a large number of analogues have been produced and tested.⁴²¹⁻⁴²⁶ The first total synthesis of Δ^9 -THC (**1**) was reported in 1965 by Gaoni and Mecholaun,⁴²⁷ the same researchers who had elucidated and reported its structure just one year before. As mentioned earlier, more potent and selective synthetic cannabinoids were the key for the discovery of both cannabinoid receptors currently known.

Newer synthetic compounds are no longer related to natural cannabinoids or based on the structure of the endogenous cannabinoids. The massive and growing spectrum of cannabinoid-active synthetic compounds is organized according to their efficacy and affinity for the CB1 and CB2 receptors, as follows:^{397,399,411}

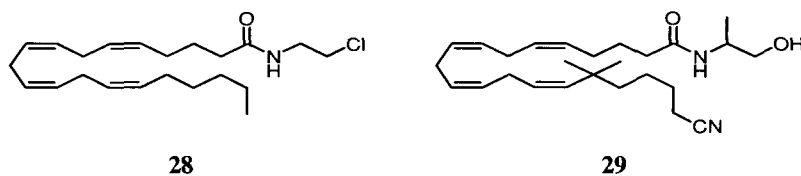
- a) High efficacy compounds without remarkable selectivity between CB receptors: including 2-arachidonoylglycerol (**20**), CP-55,940 (**14**), (*R*)-WIN 55,212-2 (**23**), HU-210 (**24**) and BAY 38-7271 (**25**).



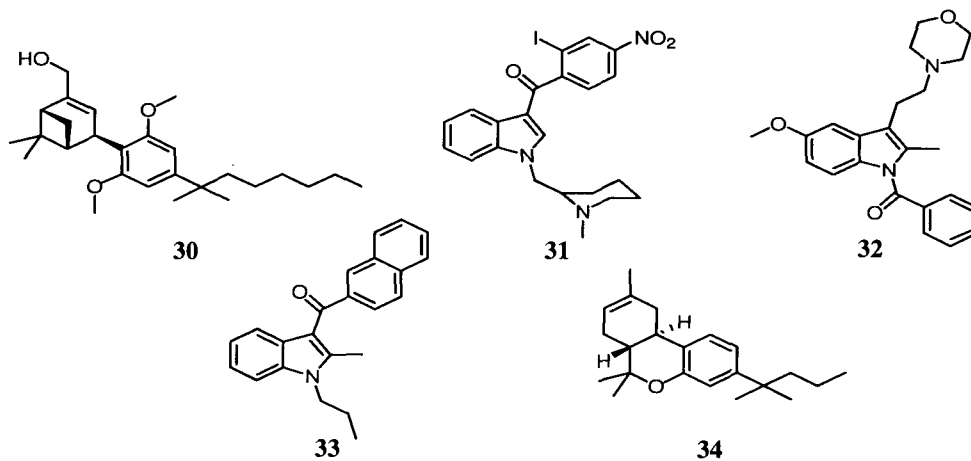
- b) Partial agonists without remarkable selectivity between CB receptors: for example Δ^9 -tetrahydrocannabinol (1), anandamide (15), (*R*)-methanandamide (26) and BAY 59-3074 (27).



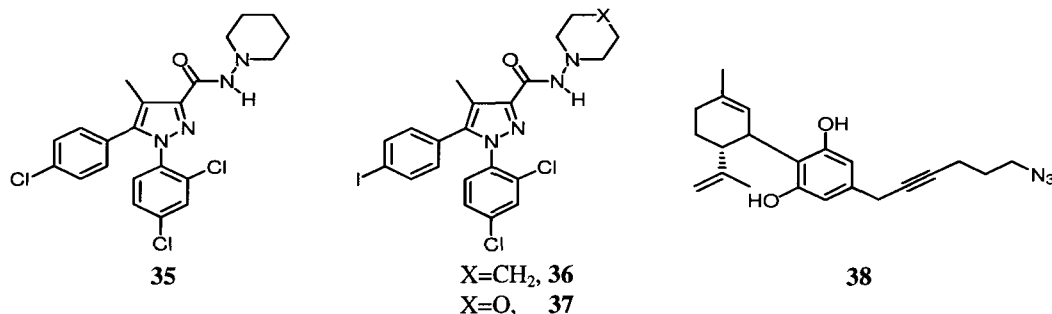
- c) Selective CB1 agonists: like ACEA (28) and O-1812 (29).



- d) Selective CB2 agonists: HU308 (30), AM1241 (31), GW405833 (32), JWH015 (33) and JWH133 (34), among others.⁴²⁶



- e) Selective CB1 antagonists/inverse agonists: including SR141716A (**35**, rimonabant)⁴²⁸, AM251 (**36**), AM281 (**37**) and O-2654 (**38**).



- f) Selective CB2 antagonists/inverse agonists: with JTE907 (**39**), SR144528 (**40**) and AM630 (**41**) as main representatives.⁴²⁹

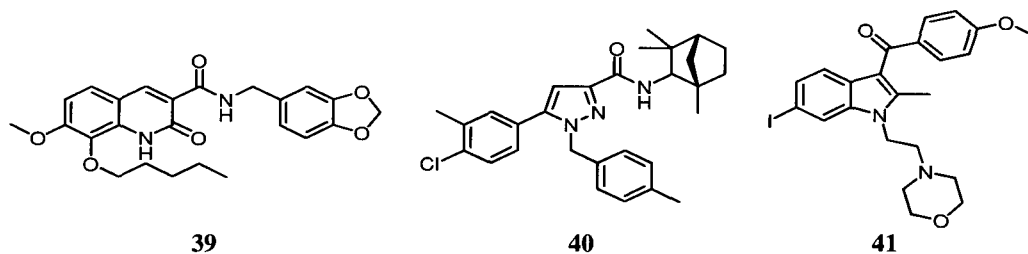
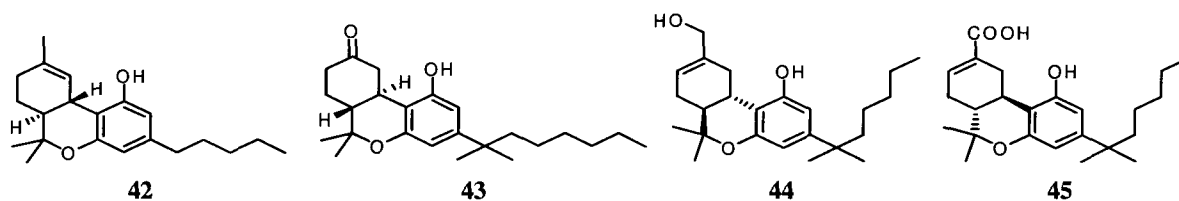


Table 5.3 presents commercial cannabinoid-based therapeutic agents currently available or in development.^{412,428,430} Marinol[®] was the first cannabinoid with approval for marketing in the United States.^{396,398} Manufactured as a capsule containing dronabinol (**42**) in sesame oil, it is taken orally. It was approved by the FDA in 1985 for the treatment of nausea and vomiting associated with cancer chemotherapy, and anorexia associated with weight loss in AIDS patients.^{396,400} Annual sales of Marinol[®] are estimated at US \$20 million.^{412,430} Cesamet[®] was also endorsed in 1985 under the same therapeutic applications as Marinol[®], but only became marketed in 2006.^{400,412,430} Sativex[®] was accepted by Health Canada for prescription use in 2005.^{398,412} It is an oromucosal (mouth) spray developed by the British GW Pharmaceuticals for

multiple sclerosis patients, to alleviate neuropathic pain and spasticity.^{399,400} It is also the only cannabinoid preparation currently available produced from botanical material, rather than organic synthesis.⁴¹² Rimonabant (**35**) is the first CB1 antagonist to be approved worldwide as an anorectic anti-obesity drug.⁴¹²

Table 5.3. Cannabinoid-based therapeutic agents, approved and in development.^{398,412,428,430}



Name	Company	Active Ingredient	Use	Approved in:
Marinol [®]	Unimed	Dronabinol (42)	Anti-emetic, appetite stimulant ¹	USA, CAN
Cesamet [®]	Valeant	Nabilone (43)	Anti-emetic ¹	USA, CAN, UK
Acomplia [®]	Sanofi-Aventis	Rimonabant (35)	Anti-obesity	Worldwide
Sativex [®]	GW	Δ^9 -THC (1), cannabidiol (4)	Neuropathic pain (MS)	CAN, Spain, CT III USA
None	Pharmos Corp.	HU-211 (44)	Neuroprotection ²	CT II Israel
None	Atlantic	CT-3 (45)	Anti-inflammatory, analgesic	Preclinical USA
None	Unimed	Δ^9 -THC (1)	Neuropathic pain (MS)	CT I USA
Marijuana	Prairie Plant Systems Inc., Health Canada	Phyto-cannabinoids	Numerous	CAN
<i>Cannabis sativa</i>	HortaPharm, GW	Phyto-cannabinoids	Development of new strains	Clinical UK
	Donald Abrams, MD Ethan Russo, MD		Appetite stimulant Migraine	CT I USA

¹Chemotherapy relief. ²Neurotrauma, stroke, Parkinson's, Alzheimer's. MS: multiple sclerosis. CT: clinical trials.

Some cannabinoids are being developed for new therapeutic applications like neuroprotection, since they are able to rescue neurons from cell death associated with trauma, ischemia, and neurological diseases. The synthetic HU-211 (dexanabinol, **44**) is an antioxidant which protects neurons from neurotoxicity induced by excess glutamate concentrations.³⁹⁹ This compound is employed in the treatment of severe head trauma.⁴³⁰

5.6. Cannabinoids and cancer

The palliative effects of cannabinoids in cancer patients have been well known since the 1970's, and include appetite stimulation, inhibition of nausea and emesis associated with chemo- or radiotherapy, pain relief, mood elevation, and relief from insomnia.^{398,418} As shown in Table 5.3, both dronabinol (**42**) and nabilone (**43**) are being currently prescribed to cancer patients.

In addition, numerous studies have suggested that cannabinoids might directly inhibit cancer growth through several mechanisms, including induction of apoptosis in tumor cells, antiproliferative action, and an antimetastatic effect by inhibiting angiogenesis and tumor cell migration.^{399,418} Table 5.4 shows the cannabinoid-induced inhibition of several tumors treated with Δ^9 -tetrahydrocannabinol (**1**), cannabidiol (**4**), WIN-55,212-2 (**23**), HU-210 (**24**), anandamide (**15**) and 2-arachidonoylglycerol (**20**), members of the three basic cannabinoid types.⁴¹⁸

Table 5.4. Tumors exhibiting cannabinoid-induced inhibition.^{399,418}

Type	System	Effect	Receptor
Lung carcinoma	<i>In vivo</i> (mouse), <i>in vitro</i>	Decreased tumor size, cell-growth inhibition	N.D.
Glioma	<i>In vivo</i> (mouse, rat), <i>in vitro</i>	Decreased tumor size, apoptosis	CB1/CB2
Thyroid epithelioma	<i>In vivo</i> (mouse), <i>in vitro</i>	Decreased tumor size, cell cycle arrest	CB1
Lymphoma, leukemia	<i>In vivo</i> (mouse), <i>in vitro</i>	Decreased tumor size, apoptosis	CB2
Skin carcinoma	<i>In vivo</i> (mouse), <i>in vitro</i>	Decreased tumor size, apoptosis	CB1/CB2
Uterus carcinoma	<i>In vitro</i>	Cell-growth inhibition	N.D.
Breast carcinoma	<i>In vitro</i>	Cell-cycle arrest	CB1
Prostate carcinoma	<i>In vitro</i>	Apoptosis	CB1
Neuroblastoma	<i>In vitro</i>	Apoptosis	VR1
Colon carcinoma	<i>In vitro</i>	Apoptosis	CB1/CB2/VR1
Lymphoid tumors	<i>In vitro</i>	Apoptosis	CB1/CB2/VR1

N.D.: not determined. VR1: type 1 vanilloid receptor.

5.7. Biological evaluation of cannabinoid compounds

Before the identification of cannabinoid receptors, *in vivo* screening assays for cannabinoid activity were largely behavioral in nature.⁴¹¹ Among them, the *cannabinoid tetrad test*^{397,431} is still used to provide valuable quantitative information on the central cannabimimetic activity of test compounds. This assay comprises four different behavioral tests performed mostly in mice, evaluating hypothermia, reduction of locomotion, analgesia, and catalepsy.^{411,431}

Modern *in vitro* bioassays include displacement assays of [³H]CP-55,940 by new unlabeled ligands, inhibition of cyclic AMP (adenosine-3',5'-monophosphate) production, inhibition of electrically evoked contractions of isolated smooth muscle preparations (high sensitivity), and [³⁵S]guanosine-5'-O-(3-thiophosphate) binding assays, which exploits the coupling of CB1 and CB2 to G proteins.⁴¹¹

In contrast to biochemical binding assays, functional cell-based bioassays directly identify ligands that activate receptors, and not simply bind them.^{432,433} They detect and quantify the interactions between G-protein-coupled receptors (GPCR's) and ligands in a faster, nonradioactive, convenient and more efficient way, due to its adaptability to multiwell plate formats.^{432,433} Cell-based bioassays clearly depend on the nature of the host cells, in which GPCR's are expressed.⁴³³ To date, expression of CB1 and CB2 (two GPCR's, Section 5.4.1) has been reported in mammalian cells, *Escherichia coli*, yeast, and insect cells.⁴³⁴ Mammalian and amphibian cells possess a high amount of endogenous GPCR's which can lead to false positives, while yeast cells in turn can fail to express traffic receptors properly, and generate false negative results.^{432,435} Insect cells fall in the middle, combining many of the best features of mammalian and yeast cells as host systems for any GPCR assay.^{432,433} This last host was used by the Grigliatti research group (Department of Zoology, UBC) to design a cell-based bioassay⁴³² capable of detecting CB1 and CB2 ligands selectively, according to their binding affinity.

Lepidopteran cell lines, specifically SF21 cells from pupal ovaries of the army fallworm *Spodoptera frugiperda*, were engineered to express high levels of both cannabinoid receptors, using the Ca^{+2} -sensitive luminescent protein aequorin as a reporter. Obtained from the jellyfish *Aequoria victoria*, aequorin forms a bioluminescent complex when linked to the chromophore coelenterazine and O_2 . When the agonist binds CB1 or CB2, the signal is channeled to the insect phospholipase ($\text{PLC}\beta$, Figure 5.6), which generates inositol triphosphate (IP_3). In the next step, Ca^{+2} is released from intercellular stores via IP_3 receptor-mediated response. Upon Ca^{+2} binding to aequorin, a conformational change takes place, resulting in the oxidation of bound coelenterazine to coelenteramide, with subsequent CO_2 and blue light (λ_{max} 470 nm) production. Since cells do not spontaneously produce light, background noise is extremely low and the emitted blue light is easily detectable with a luminometer.⁴³²

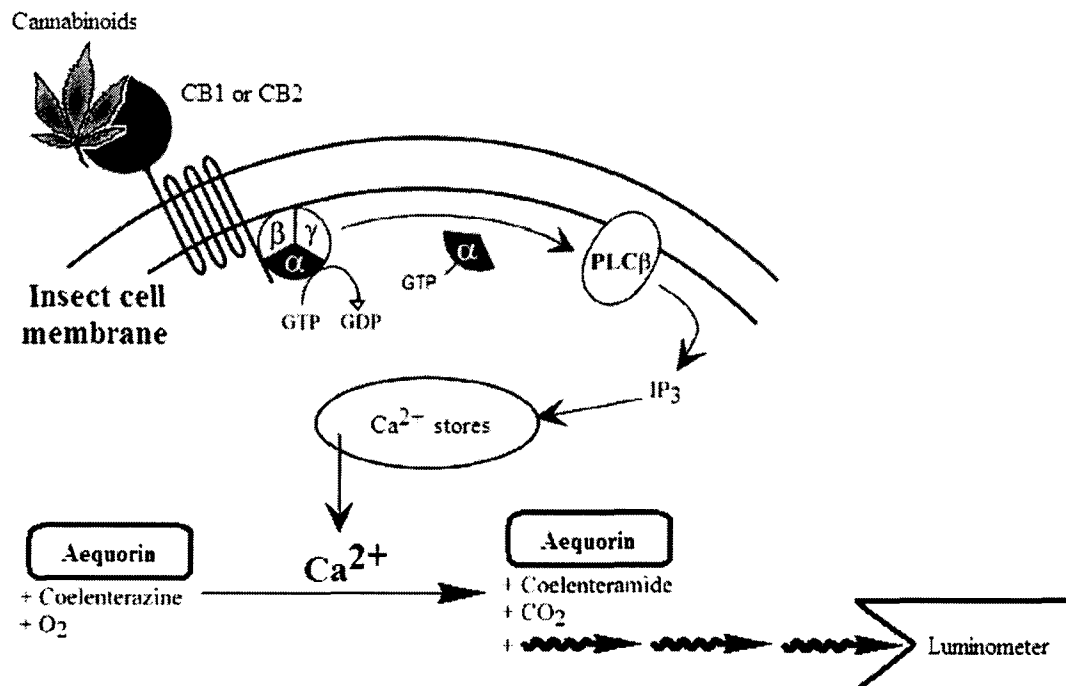
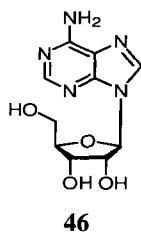


Figure 5.6. Events involved in the cell-based cannabinoid bioassay.⁴³²

5.8. Isolation of haplosamate A

As part of an ongoing program designed to isolate new biologically active secondary metabolites from marine sources, a series of methanolic extracts of marine invertebrates were evaluated for cannabinoid activity in the bioassay previously described. These extracts resulted inactive in other bioassays run by different collaborators at UBC, including antimetabolic, angiogenesis inhibition, anti-invasion, antibacterial, IDO and PI3K inhibition assays.

Screening afforded just a few hits, among them the methanolic extract of the marine sponge *Dasychalina fragilis* (Ridley & Dendy, 1886), collected from Keviang in Papua New Guinea. Previous reports on isolation of secondary metabolites from members of the *Dasychalina* genus include only adenosine (**46**) (*D. cyathina*), exhibiting cardiovascular activity.⁴³⁶ Similar nucleosides inspired the first marine-derived drugs, as mentioned in Chapter 1.



Bioassay-guided fractionation of the *D. fragilis* extract led to the isolation of the known phosphorylated sterol sulfate haplosamate A (**47**), as a white amorphous powder. This compound was initially isolated together with haplosamate B (**48**) by Qureshi and Faulkner⁴³⁷ in 1999, from two sponges collected in the Philippines, one a *Xestospongia* sp. and the other an unidentified haplosclerid sponge. Reported as sulfamate esters (Figure 5.7), haplosamates A and B were shown to inhibit HIV-1 integrase with IC₅₀'s of 50 and 15 μg/mL, respectively.

In 2001, Fusetani and coworkers⁴³⁸ isolated two inhibitors of membrane-type metalloproteinase (MT1-MMP, a key enzyme in tumor metastasis), from a marine sponge

Cribrochalina sp., collected in western Japan. The NMR data for the major metabolite was almost identical to the one acquired for haplosamate A two years before, leading to a revision and correction of the haplosamate structures, as shown in Figure 5.7. Both compounds exhibited moderate inhibition, with IC_{50} 's of 150 $\mu\text{g/mL}$ for haplosamate A (**47**) and 160 $\mu\text{g/mL}$ for the minor metabolite (**48**).

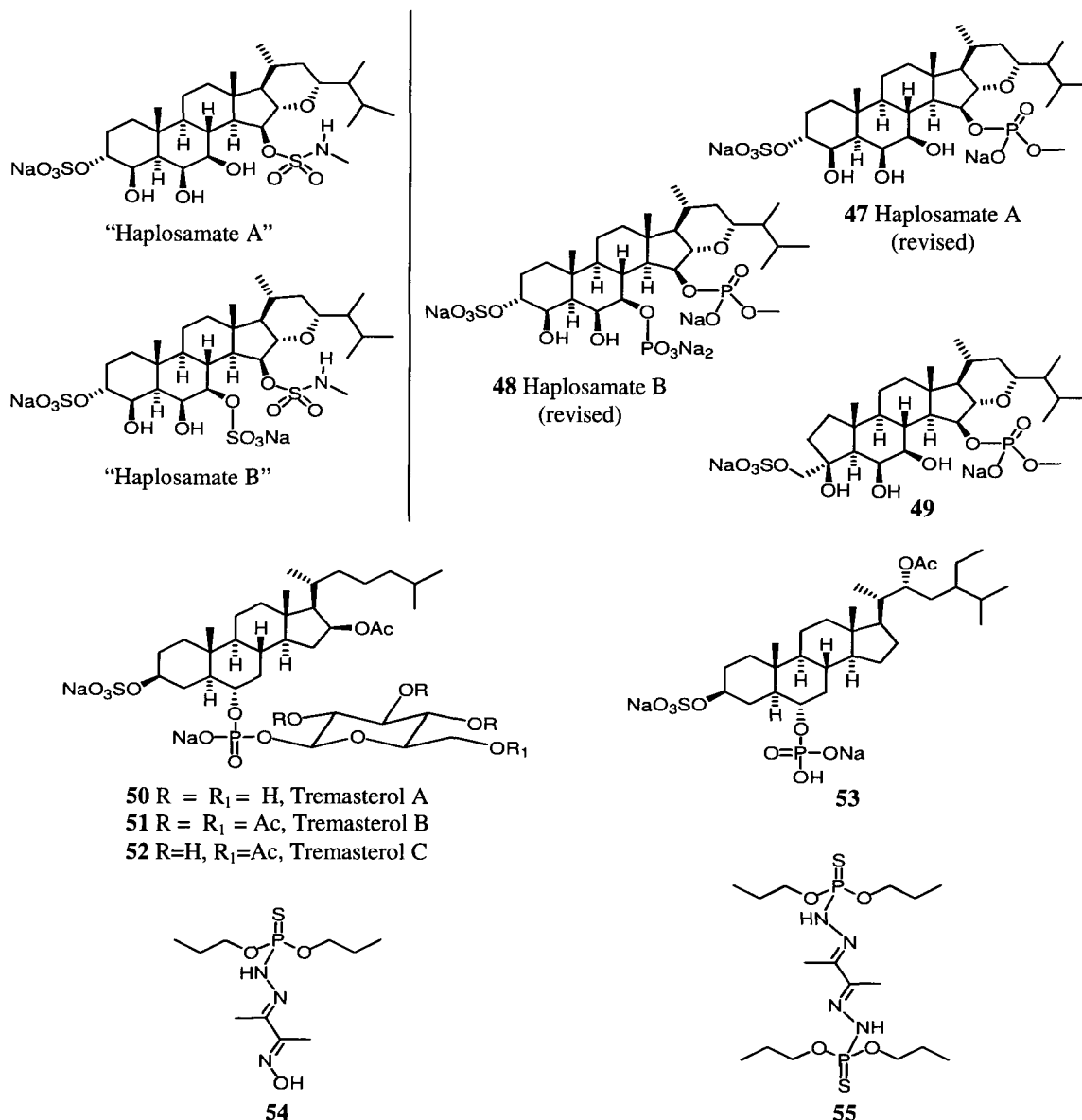


Figure 5.7. Marine natural products combining phosphorus and sulfur.

Although steroidal sulfates are widely distributed in marine sponges,⁴³⁹ steroids containing both sulfate and phosphate groups have only been reported from marine sources once before, by De Riccardis and coworkers⁴⁴⁰ in 1992. Christened as tremasterols A (**50**), B (**51**) and C (**52**), they were isolated from the starfish *Tremaster novaecaledoniae* (Jangoux, 1982) collected at a depth of 530 m off New Caledonia. A year later, the same authors added compound (**53**).⁴⁴¹ Figure 5.7 also shows one more relevant P-S combination found in marine organisms: (*E*)-2-(1-methyl-2-oxopropylidene)phosphorohydrazidothioate (*E*) oxime (**54**), an ichthyotoxic metabolite from the dinoflagellate *Gymnodinium breve* (implicated in the production of toxic red tides in Florida),⁴⁴² and a minor cytotoxic metabolite (**55**) from the fungus *Lignincol laevis*.⁴⁴³

Furthermore, an additional heteroatomic 6-membered ring in the basic sterol structure sets haplosamates A (**47**), B (**48**) as well as the minor metabolite (**49**), apart from other marine and terrestrial sterol sulfates. Such a feature has been reported before only in three steroids isolated from aerial parts of plants (Figure 5.8).⁴⁴⁴⁻⁴⁴⁷

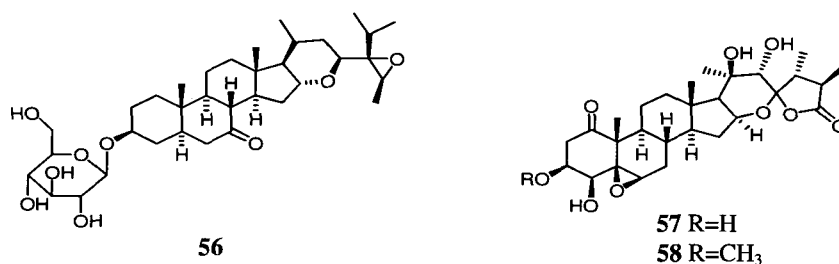


Figure 5.8. Structures for the steroidal glucoside (**56**) (from *Vernonia hindii* S. Moore, Asteraceae),^{444,445} and two members of the withanolides family (from *Physalis philadelphica* Lam, Solanaceae).^{446,447}

5.9. Haplosamate A: NMR analysis

Figures 5.9, 5.10 and Table 5.5 show the NMR data for haplosamate A (**47**) in D₂O (see Experimental section for NMR spectra in CD₃OD as in the original report,⁴³⁷ and DMSO-*d*₆).

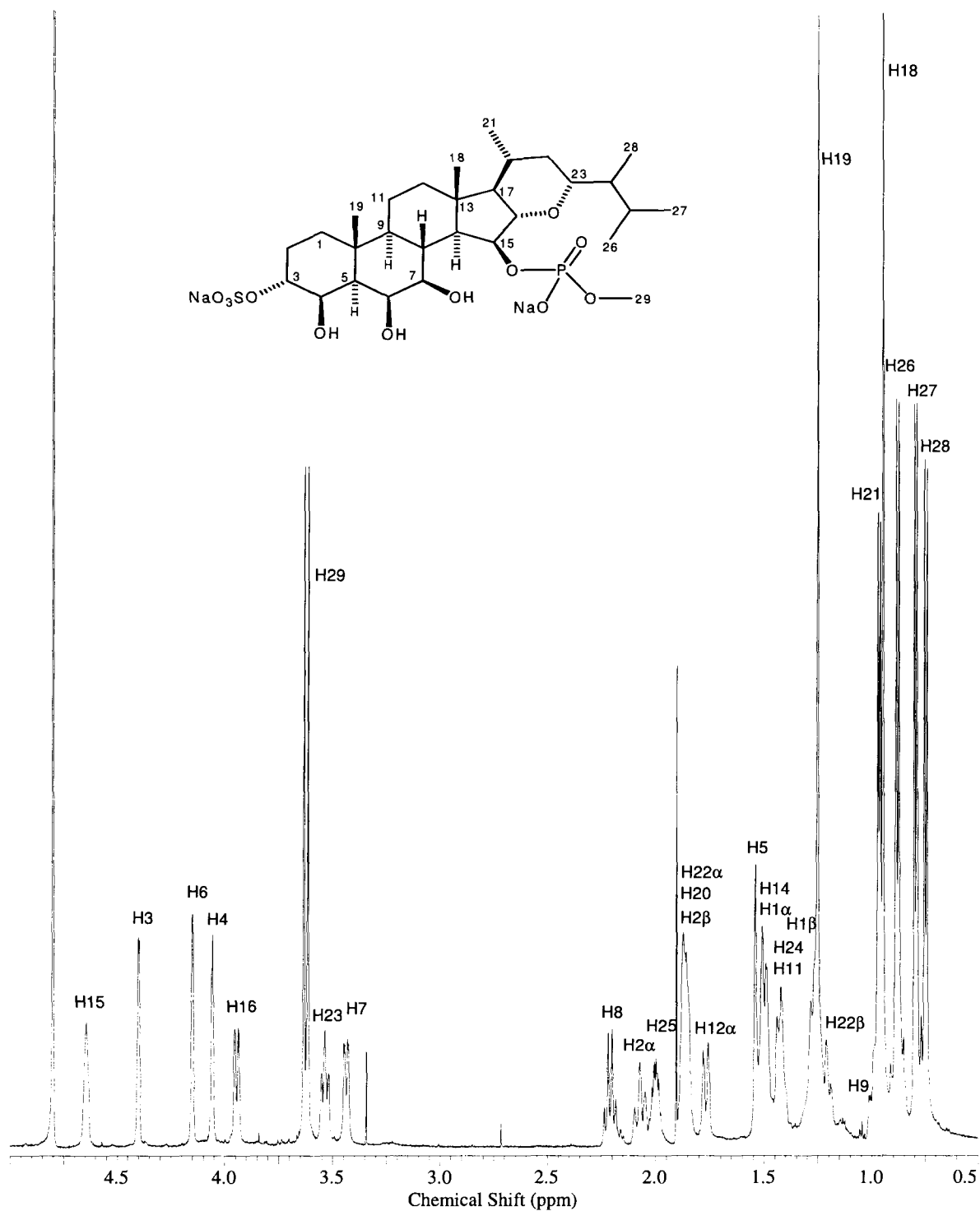


Figure 5.9. ¹H-NMR spectrum of haplosamate A (47) (recorded in D₂O at 600 MHz).

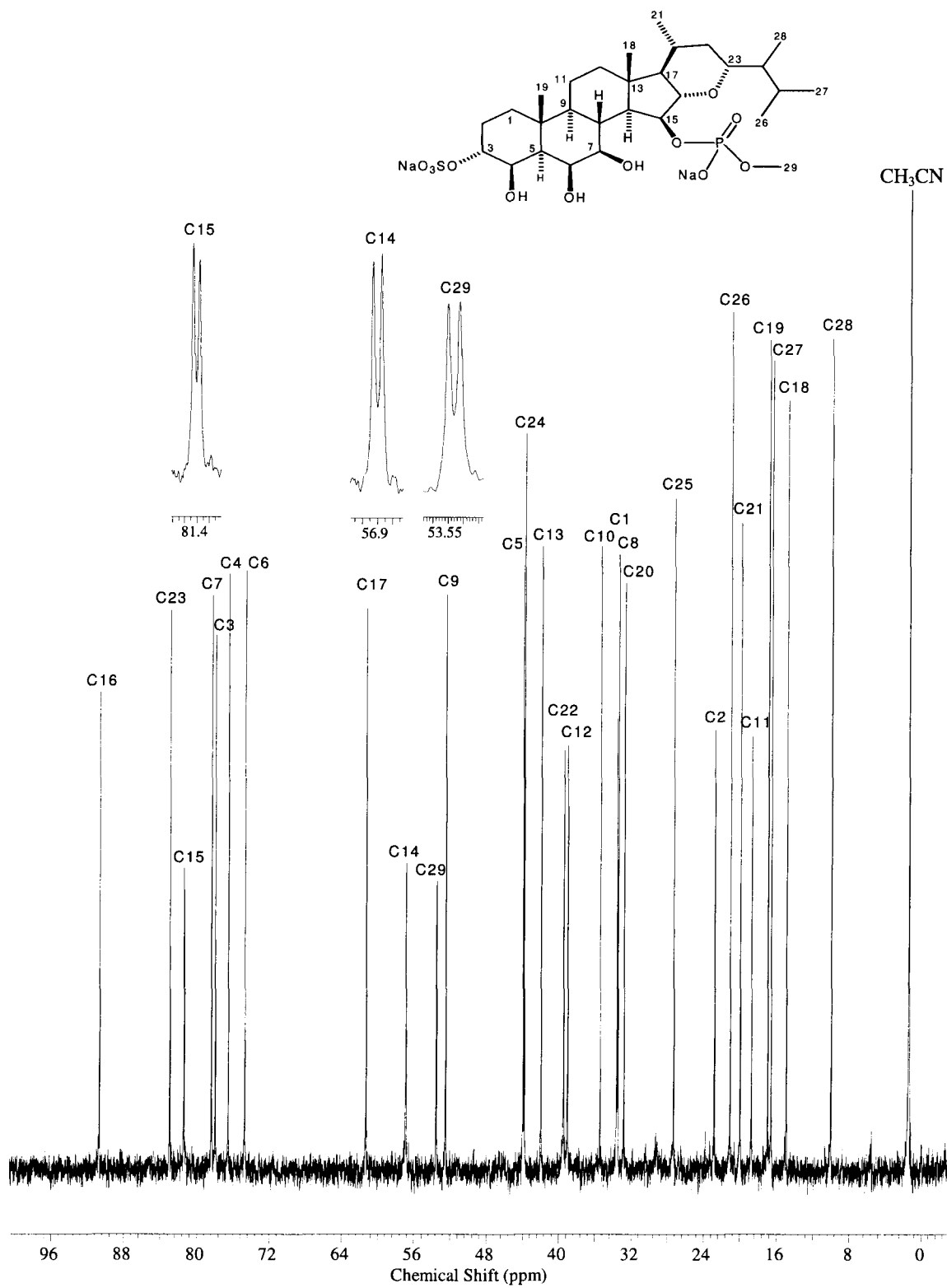
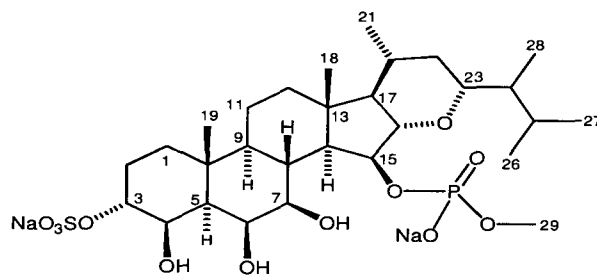


Figure 5.10. ^{13}C -NMR spectrum of haplosamate A (47) (recorded in D_2O at 150 MHz).

Table 5.5. NMR data for haplosamate A (**47**) (recorded in D₂O).

Carbon No	¹³ C δ (ppm) ^a	¹ H δ (ppm) (mult, <i>J</i> (Hz)) ^{b,c}	HMBC ^b (H→C)
1	34.2	Hβ 1.27 (m), Hα 1.51 (m)	
2	23.4	Hα 2.07 (dd, <i>J</i> = 14.2, 14.3 Hz) Hβ 1.86 (m)	
3	78.5	4.40 (d, <i>J</i> = 2.6 Hz)	C1
4	77.1	4.06 (s, broad)	C1, C3, C10
5	44.6	1.54 (m)	C4, C6, C10, C19
6	75.3	4.15 (s, broad)	C7, C10
7	79.0	3.45 (dd, <i>J</i> = 3.8, 10.6 Hz)	C8
8	34.1	2.21 (ddd, <i>J</i> = 10.6, 10.6, 10.7 Hz)	C7, C9, C14
9	53.1	0.99 (m)	
10	36.5		
11	19.4	1.42 (m), 1.54 (m)	
12	39.6	Hα 1.77 (d, <i>J</i> = 13.4 Hz) Hβ 0.88 (m)	
13	42.6		
14	57.6	1.49 (m)	C7, C8, C9, C13, C17, C18
15	82.0	4.64 (s, broad)	C13, C16
16	91.2	3.95 (dd, <i>J</i> = 4.0, 10.1 Hz)	C15, C20
17	61.9	0.79 (m)	C13, C16, C18, C20, C22
18	15.4	0.95 (s)	C12, C13, C14, C17
19	17.5	1.25 (s)	C1, C5, C9, C10
20	33.4	1.88 (m)	
21	20.5	0.97 (d, <i>J</i> = 6.3 Hz)	C17, C20, C22
22	40.1	Hα 1.87 (m) Hβ 1.21 (dd, <i>J</i> = 4.1, 12.7 Hz)	
23	83.5	3.54 (dd, <i>J</i> = 8.9, 9.1 Hz)	
24	44.4	1.42 (m)	C23
25	27.9	2.00 (m)	C24, C26, C27, C28
26	21.7	0.88 (d, <i>J</i> = 6.9 Hz)	C23, C24, C25, C27
27	17.2	0.80 (d, <i>J</i> = 6.9 Hz)	C24, C25, C26
28	10.6	0.75 (d, <i>J</i> = 6.9 Hz)	C23, C24, C25
29	54.0	3.62 (d, <i>J</i> = 10.9 Hz)	P

^a Recorded at 150 MHz. ^b Recorded at 600 MHz. ^c According to HMQC recorded at 600 MHz.

A number of shielded methyl doublets H28 (δ_{H} 0.75, δ_{C} 10.6), H27 (δ_{H} 0.80, δ_{C} 17.2), H26 (δ_{H} 0.88, δ_{C} 21.7) and H21 (δ_{H} 0.97, δ_{C} 20.5), as well as singlets H18 (δ_{H} 0.95, δ_{C} 15.4) and H19 (δ_{H} 1.25, δ_{C} 17.5), are very characteristic of a basic sterol structure. The most striking feature is the additional methyl doublet H29 (δ_{H} 3.62, δ_{C} 54.0), assigned to the *O*-methylphosphate functionality. Flanking this resonance are methines H23 (δ_{H} 3.54, δ_{C} 83.5) and H16 (δ_{H} 3.95, δ_{C} 91.2), connected through an oxygen atom. The remaining methines in this area of the ^1H -NMR spectrum are either hydroxylated, as in H7 (δ_{H} 3.45, δ_{C} 79.0), H4 (δ_{H} 4.06, δ_{C} 77.1) and H6 (δ_{H} 4.15, δ_{C} 75.3), sulfated as H3 (δ_{H} 4.40, δ_{C} 78.5), or phosphorylated as H15 (δ_{H} 4.64, δ_{C} 82.0).

The presence of a phosphate group also generates splitting in neighboring carbon resonances (Figure 5.10), particularly C29 (δ_{C} 54.0, $^2J_{\text{C,P}} = 6.0$ Hz), C14 (δ_{C} 57.6, $^3J_{\text{C,P}} = 9.0$ Hz) and C15 (δ_{C} 82.0, $^2J_{\text{C,P}} = 7.5$ Hz). Figure 5.11 presents the dramatic change in multiplicity observed when the ^1H -NMR spectrum is acquired while decoupling ^{31}P . The presence of one phosphorous atom was also confirmed by a singlet at 0.84 ppm in the ^{31}P -NMR spectrum. HRESIMS gave a $[\text{M}+\text{Na}]^+$ peak at m/z 721.2377, consistent with the elemental composition $\text{C}_{29}\text{H}_{49}\text{O}_{12}\text{Na}_2\text{PS}$ (calculated for $\text{C}_{29}\text{H}_{49}\text{O}_{12}\text{Na}_3\text{PS}$: 721.2375).

In general, bioassaying cannabinoids both *in vivo* and *in vitro* has always faced water solubility problems, due to the high lipophilic character of these ligands.⁴¹¹ Therefore, water-miscible vehicles (such as EtOH, DMSO, bovine serum albumin) have been used for the administration and test of cannabinoids, requiring additional control experiments to evaluate any possible pharmacological change produced by the vehicle itself. The present cell-based bioassay was also run in aqueous media, but haplosamate A (**47**) is completely water-soluble, eliminating the use of additional solvents.

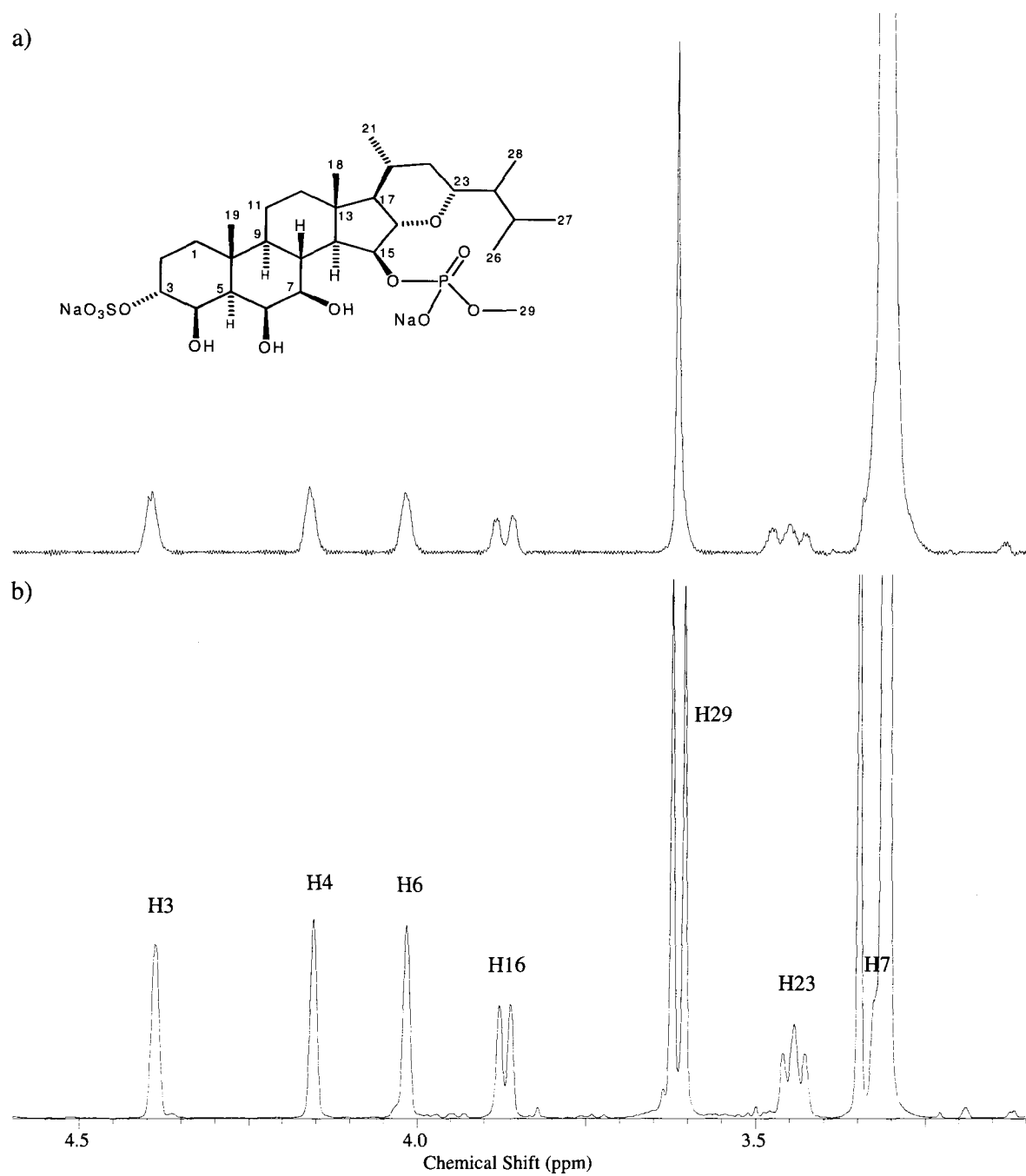
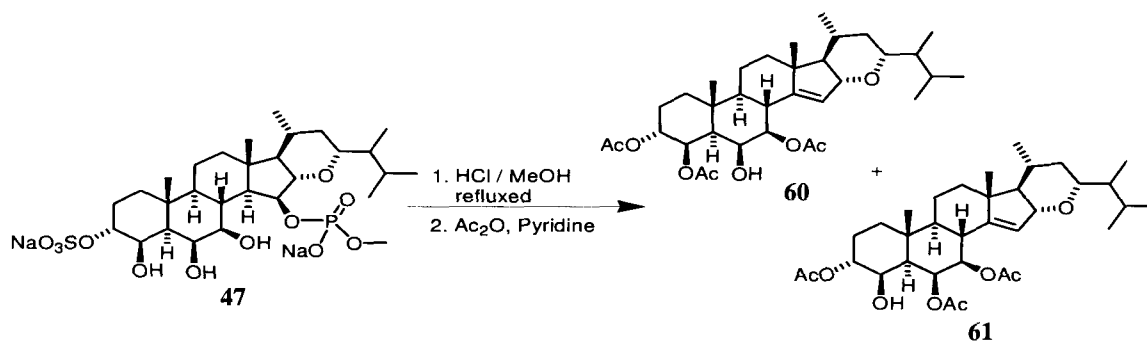


Figure 5.11. a) ^{31}P decoupled and b) ^{31}P coupled ^1H -NMR spectra of haplosamate A (**47**) (recorded in CD_3OD at 400 MHz).

Sulfur is the fourth more abundant element in sea-water, after chlorine, sodium and magnesium. Its sulfate ion follows chloride in importance and is the most stable sulfur combination in sea-water.⁴³⁹ This correlates with the fact that, according to MarinLit,⁴⁴⁸ there are approximately 1838 marine-derived sulfated compounds mostly isolated from Porifera and Echinodermata phyla, whereas reports on organophosphorus are close to 97 structures.

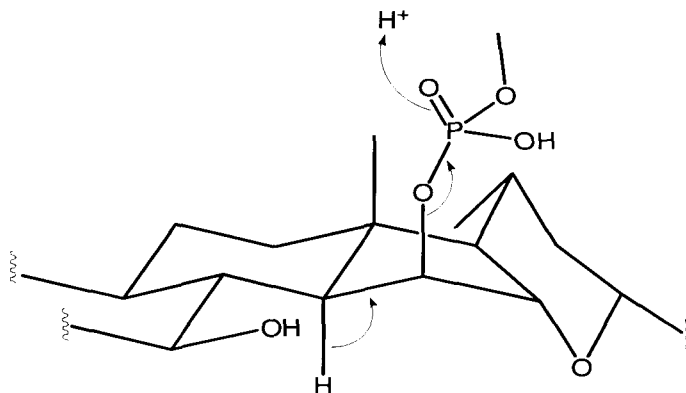
5.10. Pharmacophoric requirements for cannabinoid activity

A general trend for most steroidal sulfates isolated via bioassay-guided fractionation, as evidenced by Qureshi and Faulkner,⁴³⁷ is the loss of activity after the natural product is desulfated. In general, sulfated compounds are known to irreversibly bind proteins, since the sulfate functionality is able to establish multiple hydrogen bonds with amino acids in the binding sites, or simply adhere to phospholipids in cell membranes.⁴⁴⁹ In most cases, such interactions are completely unspecific and the usually displayed high activity disappears upon sulfate removal. When haplosamate A (**47**) was refluxed in acidic media and acetylated using standard conditions, the triacetyl-derivatives (**60**) and (**61**) were obtained. Surprisingly, the cannabinoid activity was retained in both triacetates, suggesting that the phosphate and sulfate groups in haplosamate A (**47**) are not required for activity, and possibly do not even interact with CB1 or CB2.

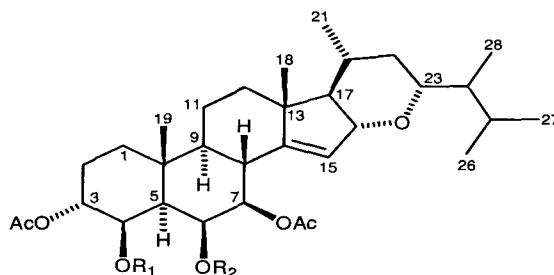


NMR data for both triacetates (Table 5.6) showed an absence of the methylphosphate group, and the presence of two new alkene carbons C14 ($\delta_C \sim 151$) and C15 ($\delta_C \sim 124$). HMQC data assigned only a proton (H15, δ_H 5.64) to the second carbon. For derivative (**60**), HMBC correlations between H3 (δ_H 5.12) and C29 (δ_C 169.2), H4 (δ_H 5.47) and C31 (δ_C 169.9), as well as H7 (δ_H 4.93) and C33 (δ_C 169.9), allow unambiguous assignment of three acetate groups (see Experimental section). HMBC data for compound (**61**) does not show cross peaks between H3 (δ_H 4.77) or H4 (δ_H 3.51) and acetate carbons, but the deshielding effect commonly observed in oxygenated methines when attached to an acetate suggested that H3 (δ_H 4.77) was also acetylated. Water loss and the presence of only three acetates were additionally confirmed by HRESIMS, which yielded $[M+Na]^+$ ions at m/z 611.3558 for **60** and 611.3564 for **61**, in concordance with the molecular formula $C_{34}H_{52}O_8$ (calculated for $C_{34}H_{52}O_8Na$: 611.3560).

Given the right geometry in the starting material, as well as bulkiness and high stability in the leaving group, it is not surprising for an E1 elimination to occur under hot acidic conditions (Scheme 5.1).

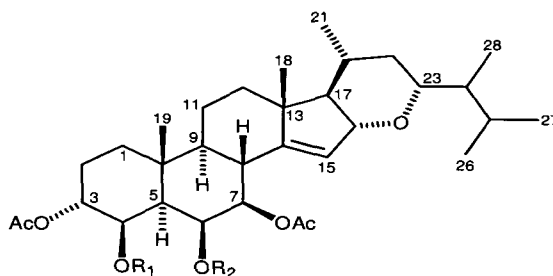


Scheme 5.1. E1 elimination in haplosamate A (**47**).

Table 5.6. NMR data for haplosamate A triacetates (**60**) and (**61**) (recorded in C₆D₆).**60** R₁= OAc, R₂=H**61** R₁= H, R₂=OAc

C No	60		61	
	¹³ C δ (ppm) ^a	¹ H δ (ppm) (mult, J (Hz)) ^{b,c}	¹³ C δ (ppm) ^a	¹ H δ (ppm) (mult, J (Hz)) ^{b,c}
1	34.8	Hβ 1.13 (td, 3.3, 13.6) Hα 1.34 (m)	35.1	Hα 1.11 (td, 3.3, 13.8) Hβ 1.31 (m)
2	23.1	Hα 1.94 (ddt, 3.0, 14.4, 14.6) Hβ 1.72 (m)	22.5	Hα 1.96 (ddt, 3.3, 14.3, 14.4) Hβ 1.54 (m)
3	70.5	5.12 (d, 2.8)	72.8	4.77 (d, 2.5)
4	73.2	5.47 (s, broad)	73.3	3.51 (m)
5	44.0	1.54 (m)	43.3	1.42 (m)
6	72.0	4.43 (s, broad)	72.6	5.83 (d, 2.4)
7	76.3	4.93 (dd, 3.3, 10.8)	73.8	5.06 (dd, 3.8, 11.0)
8	36.5	2.63 (t, 11.3)	36.2	2.65 (t, 11.3)
9	53.3	0.65 (td, 2.5, 11.9)	53.3	0.68 (td, 2.2, 11.6)
10	36.0		37.2	
11	22.0	1.31 (m)	21.8	1.40 (m), 1.31 (m)
12	42.3	Hα 1.74 (m) Hβ 1.16 (td, 3.9, 14.1)	42.3	Hα 1.73 (dd, 3.1, 3.6) Hβ 1.17 (td, 3.3, 13.3)
13	46.3		46.3	
14	151.0		150.9	
15	123.9	5.64 (s, broad)	124.3	5.72 (s, broad)
16	86.6	4.13 (dd, 2.2, 7.1)	86.5	4.12 (dd, 2.5, 9.4)
17	65.9	1.23 (dd, 8.0, 9.4)	65.8	1.23 (dd, 9.7, 10.8)
18	17.1	0.90 (s)	17.1	0.90 (s)
19	18.0	1.38 (s)	18.0	1.33 (s)
20	32.0	1.63 (m)	32.0	1.62 (m)
21	20.8	0.90 (d, 6.9)	20.8	0.89 (d, 6.4)
22	39.3	Hα 1.54 (m) Hβ 0.99 (dd, 11.2, 11.6)	39.4	Hα 1.54 (m) Hβ 0.98 (dd, 11.6, 12.0 Hz)

^aRecorded at 150 MHz. ^bRecorded at 600 MHz. ^cAccording to HMQC recorded at 600 MHz. ^dInterchangeable for 73.

Table 5.6. NMR data for haplosamate A triacetates (**60**) and (**61**) (recorded in C₆D₆)(Cont.)**60** R₁ = OAc, R₂ = H**61** R₁ = H, R₂ = OAc

C No	60		61	
	¹³ C δ (ppm) ^a	¹ H δ (ppm) (mult, <i>J</i> (Hz)) ^{b,c}	¹³ C δ (ppm) ^a	¹ H δ (ppm) (mult, <i>J</i> (Hz)) ^{b,c}
23	80.7	3.38 (ddd, <i>J</i> = 2.2, 7.2, 9.7 Hz)	80.7	3.37 (ddd, <i>J</i> = 2.2, 7.2, 9.3 Hz)
24	44.7	1.66 (m)	44.7	1.66 (m)
25	28.2	2.16 (m)	28.2	2.17 (m)
26	18.4	0.87 (d, <i>J</i> = 6.6 Hz)	18.3	0.87 (d, <i>J</i> = 6.4 Hz)
27	22.1	0.94 (d, <i>J</i> = 6.9 Hz)	22.1	0.95 (d, <i>J</i> = 6.7 Hz)
28	11.3	0.88 (d, <i>J</i> = 7.2 Hz)	11.3	0.88 (d, <i>J</i> = 6.4 Hz)
29	169.2		169.4	
30	21.0	1.66 (s)	21.2	1.72 (s)
31	169.9		170.6	
32 ^d	21.5	1.76 (s)	21.4	1.76 (s)
33	169.9		170.2	
34 ^d	20.9	1.42 (s)	21.0	1.67 (s)

^aRecorded at 150 MHz. ^bRecorded at 600 MHz. ^cAccording to HMQC recorded at 600 MHz. ^dInterchangeable for **73**.

Retention of the cannabinoid activity in triacetates (**60**) and (**61**) led to an extensive examination of the structural requirements for their cannabinoid activity. Traditional cannabinoid structure-activity relationships (SAR)^{411,450-454} indicate three general molecular requirements for activity (Figure 5.12):

- I. Bonding availability (**A**) at one end (H bridge, π electron interactions).
- II. An appropriately oriented carbocyclic ring system (**B**) in the central part of the ligand.
- III. A lipophilic alkyl side chain (**C**) at the opposite end.

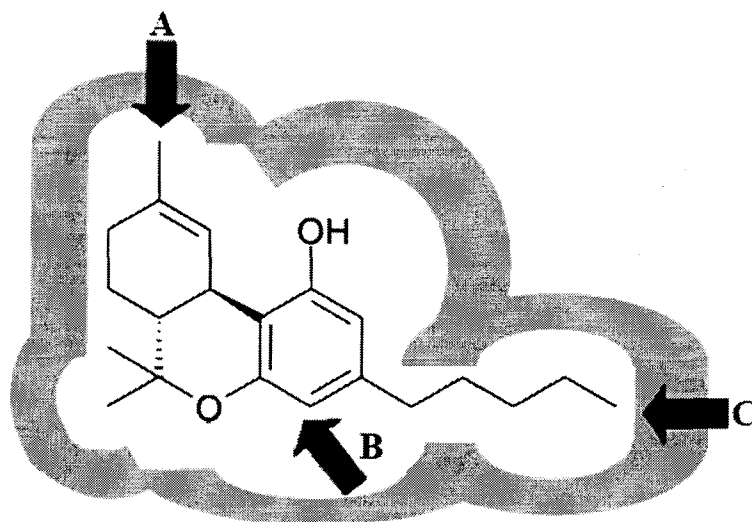


Figure 5.12. The classical cannabinoid pharmacophore.⁴⁵³

In addition, multiple computer-assisted studies have shown superimposition of electronegative regions (associated with carbonyl or hydroxyl oxygen atoms), linear hydrocarbon side chains, and π -electron rich areas, between low-energy conformations for Δ^9 -tetrahydrocannabinol (**1**) and anandamide (**15**),⁴⁵⁴ as well as (-)-9 β -hydroxyhexahydrocannabinol (**62**) and (*R*)-WIN55212-2 (**23**).⁴⁵⁵ This suggests common pharmacophoric elements among phytocannabinoids, endocannabinoids and aminoalkylindoles.

When the minimum energy conformation of haplosamate A (**47**) was estimated through molecular mechanics (RMS = 0.100, CS Chem3D Pro[®] 9.0) following Xie, Eissenstat and Makriyannis publication,⁴⁵⁵ the 1,2-dimethylpropyl side chain and the pentacyclic ring system show acceptable alignment with similar features in (-)-9 β -hydroxyhexahydrocannabinol (**62**) and (*R*)-WIN55212-2 (**23**). Due to its polyhydroxylated character, haplosamate A (**47**) possesses several possibilities for hydrogen bonding interactions (Figure 5.13).

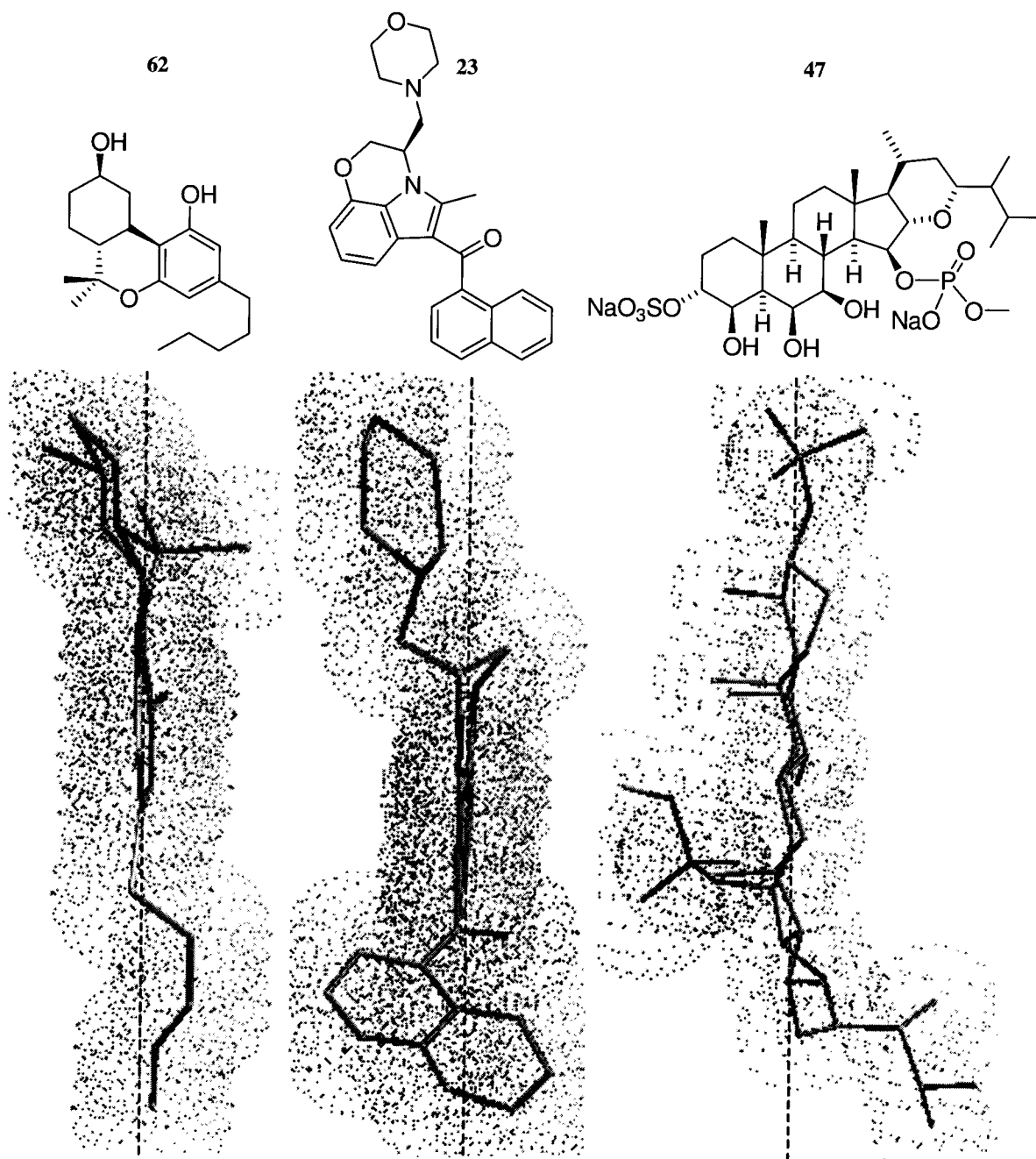


Figure 5.13. Minimum energy conformations for the known cannabimimetic agents (-)-9β-hydroxyhexahydrocannabinol (**62**) and WIN55212-2 (**23**).¹⁸ Properly oriented, haplosamate A (**47**) shows acceptable alignment.

In summary, Figure 5.13 predicts that haplosamate A (**47**) may interact with CB1 and CB2 in the same fashion as classical and synthetic cannabinoids, and not unspecifically via sulfate or phosphate functionalities. This observation correlates with the cannabinoid activity observed for triacetate derivatives (**60**) and (**61**), suggesting that neither sulfate nor phosphate groups are required for receptor binding.

5.11. Evidence of haplosamate A binding to CB1 and CB2: STDD NMR experiments

Because the cannabinoid receptor's structure and shape are still being characterized and no crystallographic data is available showing receptor-bound ligands, knowledge regarding the nature of ligand/receptor interactions is limited. Specific characterization of those parts of a ligand in direct contact with a protein is mostly left to X-ray analyses of cocrystallized ligand-receptor complexes,⁴⁵⁶ but crystallization of membrane receptor proteins is extremely difficult, and even if a truncated form is available, its binding affinity or specificity may differ from the native receptor embedded into a membrane.⁴⁵⁷

In 1999, Mayer and Meyer⁴⁵⁸ introduced saturation transfer difference (STD) NMR, developed to characterize binding interactions at an atom level, or group epitope mapping (GEM). Several NMR methods such as transferred nuclear Overhauser effect (trNOE),⁴⁵⁹ SAR by NMR,⁴⁶⁰ NOE pumping,⁴⁶¹ and competitive binding spectroscopy,⁴⁶² are also employed to screen and study binding processes, but these techniques do not allow the observation of binding ligands to membrane proteins in their natural environment.^{456,458} STD NMR has been used in the last seven years as an efficient tool to study protein-ligand recognition events in a variety of systems.⁴⁶³⁻⁴⁶⁷ Advantages include high sensitivity, requiring small amounts of both protein and ligand. The methodology enables mapping of the ligand's binding epitope, since those parts of the ligand having the strongest contact to the protein exhibit the most intense NMR signals, and

the binding component can be identified even from mixtures, allowing it to be used as a screening method for ligands with dissociation constants ranging 10^{-3} - 10^{-8} M.^{456,468} Very valuable and related to this last advantage is that the STD pulse sequence (Figure 5.14) can be applied to most 1D or nD NMR experiments already in use, to generate STD versions of TOCSY, COSY, NOESY and inversely detected ^{13}C or ^{15}N spectra, for example.⁴⁵⁸ This makes structure elucidation conceivable even before the binding ligand has been purified.⁴⁶⁸

The basis for STD NMR is the transfer of saturation from the protein to the ligand.^{456,458,469} Selective saturation of a protein is possible because its resonances are often anisotropically shifted as well as broadened, and can be irradiated outside the spectral window of low-molecular-weight ligands (usually 0-10 ppm).⁴⁵⁶ In practice, this is done using the pulse sequence detailed in Figure 5.14.

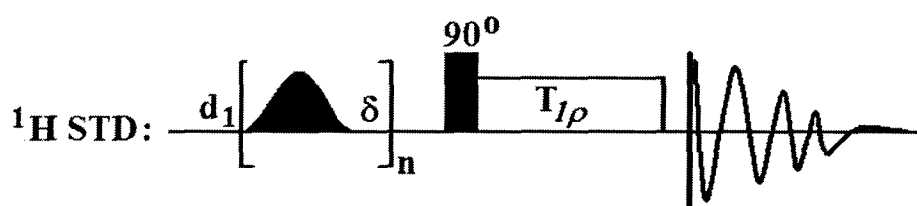


Figure 5.14. Basic pulse sequence of a 1D STD NMR spectrum. d_1 : relaxation time; δ : delay between hard pulses (usually 1 ms); n : number of pulses (around 40 is recommended); $T_{1\rho}$: filter, consisting of a spin-lock pulse, to eliminate broad resonances of the protein.^{456,458}

The 1D STD NMR corresponds to a modified 1D NOE difference pulse sequence. The experiment is performed by selectively saturating the protein with a train of Gauss-shaped pulses separated by δ .⁴⁵⁶ In the first scan, these hard pulses are centered on a region of the ^1H NMR that contains only resonances for the protein envelop: any frequency ranging -0.4 to -5 ppm, or 8 to 15 ppm if no aromatic or acid moieties are present in the ligands is usually chosen (*on-resonance* irradiation).⁴⁶⁹

Once the protein is saturated, the remainder of the pulse sequence corresponds to a 1D NOE experiment. The saturated protein will transfer its magnetization to the bound ligand through spin diffusion. Then, the experiment is repeated aiming the train of hard pulses this time to another region of the ^1H NMR where no protein signals are present: anywhere between 30-100 ppm (*off-resonance* irradiation).⁴⁵⁷

Subtraction of the spectrum without saturation (*off-resonance*) from the spectrum with saturation of the protein (*on-resonance*), yields the final STD NMR spectrum that cancels all resonances, except those from species with binding affinity. The difference between STD spectra is obtained by internal alternated subtraction with appropriate phase cycling using a frequency list for *on-resonance* and *off-resonance* irradiations.^{457,468}

From a macromolecular viewpoint, proteins are constituted by a large system of proton spins tightly coupled by dipole-dipole interactions due to restricted mobility (slow tumbling rates).⁴⁵⁸ Thus, selective saturation of a single protein resonance (See Figure 5.15, **I**) will result in a rapid spread of magnetization over the entire molecule via spin diffusion (**II**). Intermolecular transfer of magnetization from protein to ligand (also by spin diffusion) leads to progressive saturation of the bound ligands (**III**). This saturation is then transferred into solution through fast exchange of ligand molecules from the bound to the free state (**IV**), where the saturation-transfer effect is detected. The difference mode ensures that only nuclei of molecules that were at one time bound to the receptor contribute to the STD spectrum.^{456,468} Resonances of non-binding compounds are canceled out, since they do not become saturated.

Additionally, the ligand's binding epitope can be determined from the STD spectra because protons in close proximity to the protein surface carry a much larger saturation (**V**, Figure 5.15), and therefore more STD signal intensity than other nuclei situated far away from

the binding site, which obtain saturation (if any) only through spin diffusion within the ligand.^{456,457}

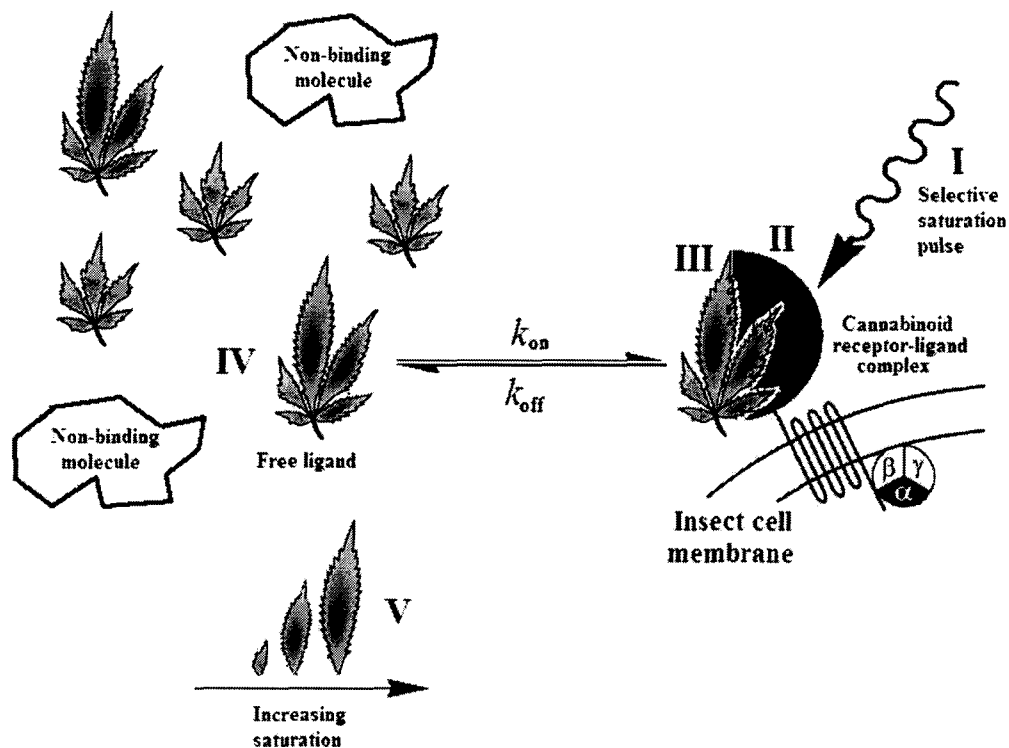


Figure 5.2. Events involved in STD NMR spectroscopy: I) selective protein saturation; II) magnetization transfer within the protein and, III) to the bound ligand via spin diffusion; IV) receptor-ligand complex dissociation that carries saturation into solution; V) differential saturation degree in protons of the ligand correlates to their proximity to the protein.^{456,458}

The intensity of the STD signal increases as a function of ligand excess, provided that ligand molecules with zero or little saturation bind to the receptor.^{458,468} Since the method relies on transferred saturation from protein to ligand, the larger the number of ligands that pick up magnetization, the greater the build-up in STD signal intensity. Therefore, faster turnover rates at high ligand excess results in a larger STD effect.⁴⁵⁷

The application of a $T_{1\rho}$ -filter in the STD pulse sequence (Figure 5.14) is a common procedure to suppress NMR signals of large molecules. However, sometimes even such a spin

lock field is not enough to eliminate signals originating from the biological components in the system (buffers, glucose, host cells), which produce hump regions with extreme proton overlap. To eliminate these disturbing background resonances, Meyer and coworkers⁴⁶⁹ introduced in their last update an additional filter, or STDD-filter (Figure 5.16).

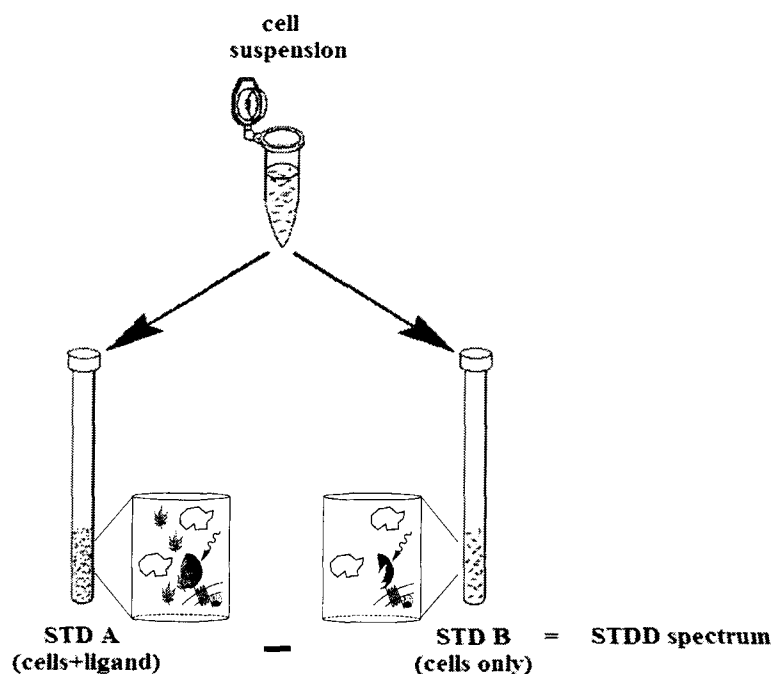


Figure 5.16. Sample preparation for saturation transfer double-difference (STDD) NMR.⁴⁶⁹

The idea behind the STDD-filter is to divide the cell suspension into two NMR tubes, one of which has been preloaded with ligand. This tube will provide a STD spectrum containing signals generated by binding of the ligand to the receptor. The second NMR tube, prepared under the same conditions but without ligand, affords another STD spectrum with background resonances. A further subtraction of these two STD's yields the new saturation transfer double-difference spectrum, showing only signals of the binding ligand. As a result, acquisition times of STDD spectra are shorter, and spin lock pulses ($T_{1\rho}$) which often result in loss of saturation from the ligand due to T_1 and T_2 relaxation processes, are not required (better S/N ratio).⁴⁶⁹

Figure 5.17 displays STDD spectra obtained for buffered aqueous solutions of each cannabinoid receptor embedded in insect cells, and haplosamate A (**47**) in an approximate 24000-fold excess of ligand/receptor. In order to detect unspecific interactions that may take place between ligand and host cells, two negative controls were prepared by adding haplosamate A (**47**) to SF21 insect cells incubated in absence of receptors, and to F8 (coagulation factor VIII) cells. As shown in Figure 5.17 (Controls 1 and 2), no STD effects were observed for these control samples, indicating that haplosamate A (**47**) does not bind unspecifically to the cell membranes.

The STD spectra prove that haplosamate A (**47**) specifically binds to the cannabinoid receptors CB1 and CB2, since signals of the ligand can be observed. Sucrose resonances between 3.25–4.25 ppm in the reference spectra, are evidenced by a series of dispersion peaks in both STDD spectra, which obscure any STD effect given by methine protons in this region. The high concentration of sucrose in the media (0.080 mM) generates very intense NMR signals that cannot be completely subtracted in the STDD spectrum. Another practical aspect that contributes to deficient signal subtraction is the use of two NMR tubes for each sample (Figure 5.16), which introduces shimming differences. Fortunately, some of the shielded protons between 0.50 and 2.25 ppm can be observed without any interference.

Signal broadening is a common issue in STD experiments and it results from ligand-receptor exchange processes or fast T_1 relaxation in the protein.⁴⁵⁶ The protein envelope is basically absent in the reference spectra, which show a flat baseline. Although early references^{456,458} show broad hump regions reaching negative chemical shift values, this is not always the case.^{464,465,469} *On-* and *off-*resonances were chosen as -1.1 and 114 ppm as suggested by Mayer and Meyer.^{456,469}

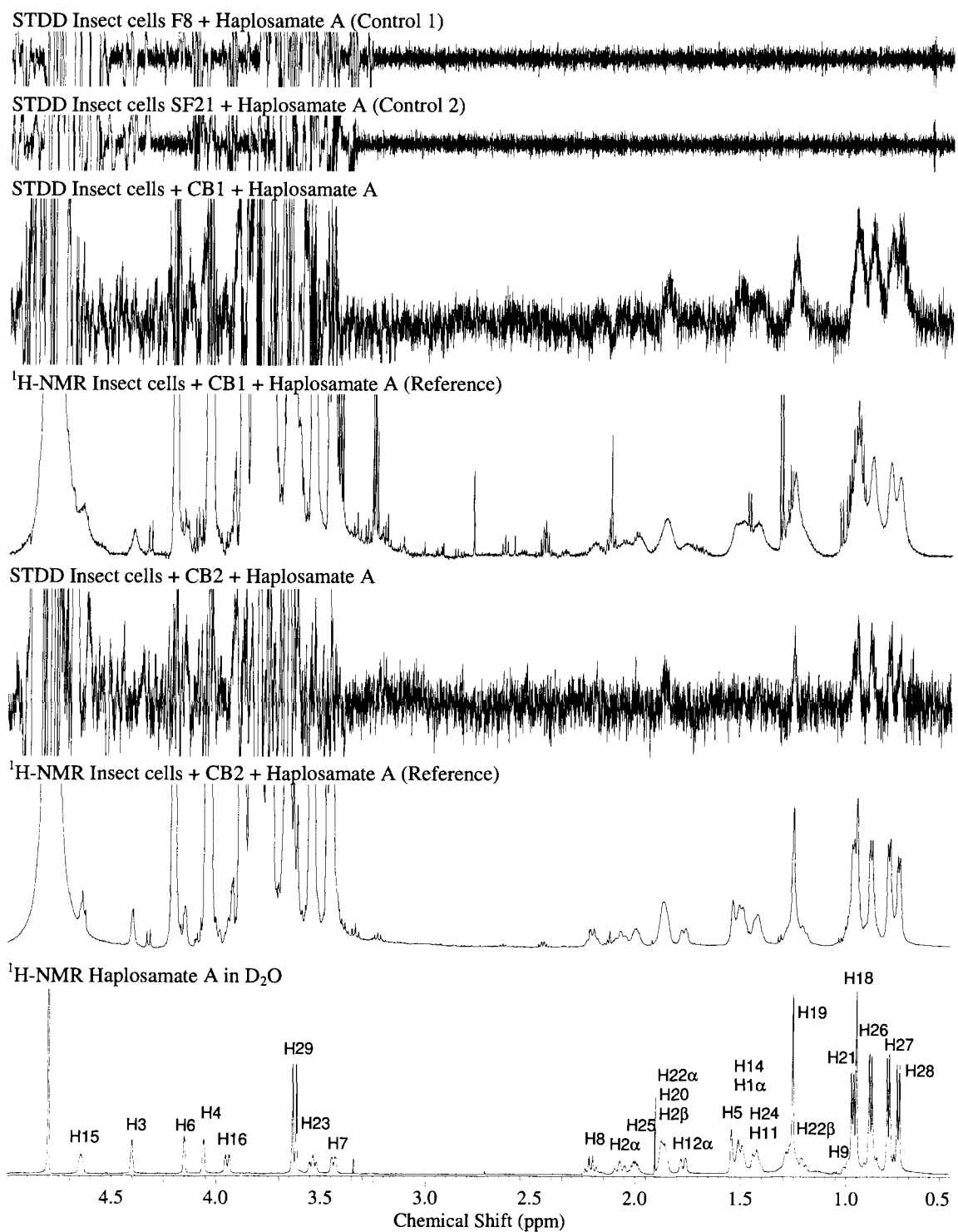


Figure 5.17. STDD experiments measured for an aqueous solution of each cannabinoid receptor supported in SF21 insect cells and haplosamate A (47).

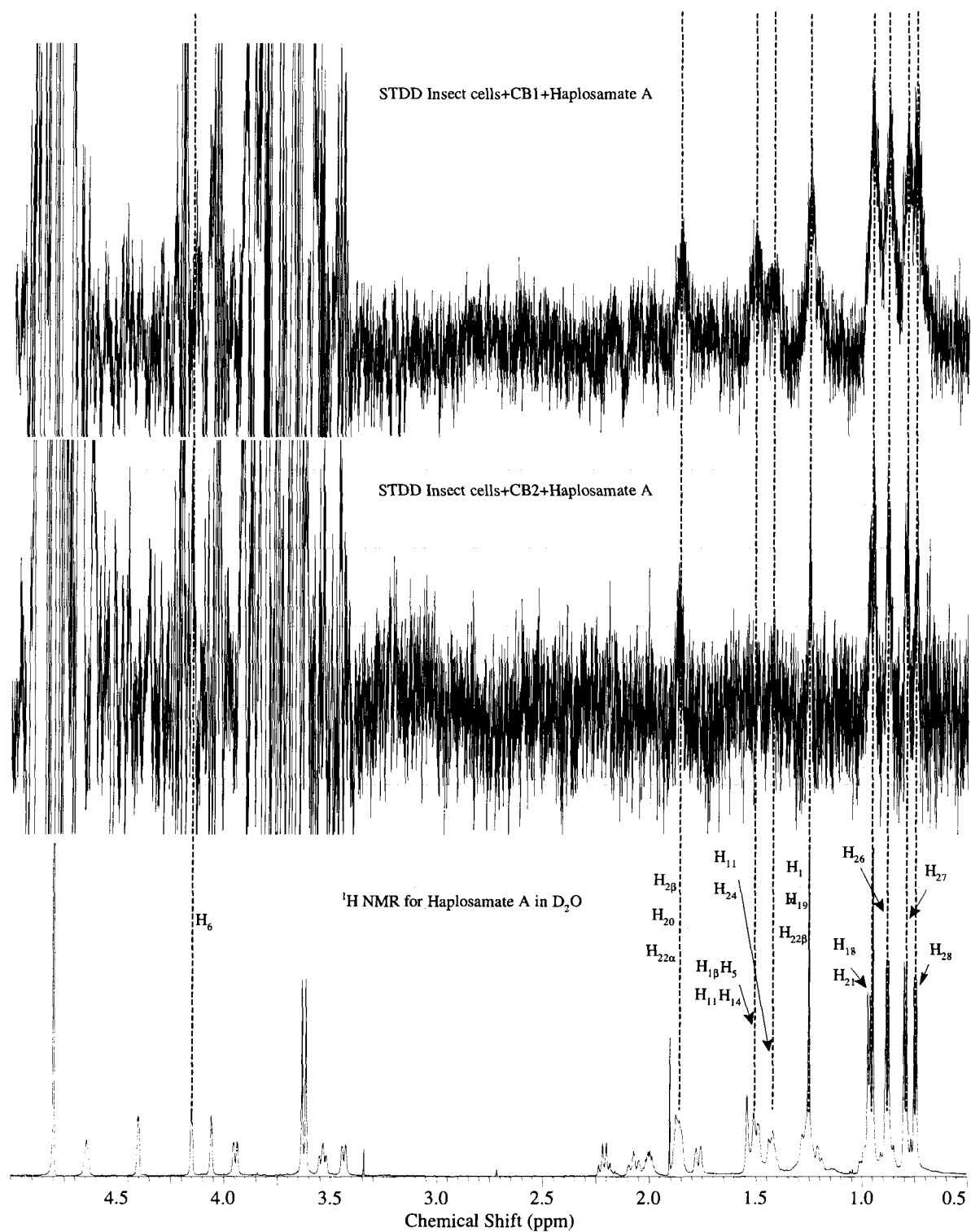


Figure 5.18. Qualitative STD NMR group epitope mapping for the binding of haplosamate A (47) to the cannabinoid human receptors CB1 and CB2.

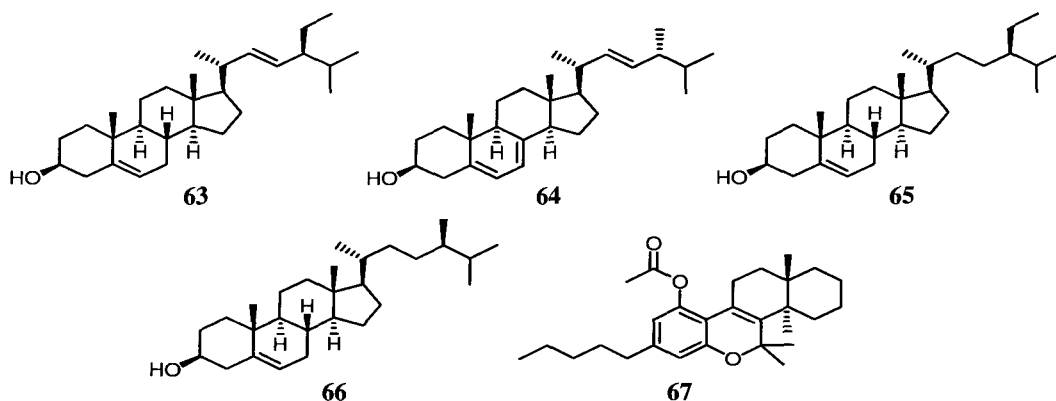
Only those protons of the ligand which are nearest to the binding site of the protein can easily be identified from STDD spectra, since they are saturated to the highest degree. Hence, if both STDD and the $^1\text{H-NMR}$ of **47** are compared (Figures 5.17, 5.18), some resonances are missing in the STDD spectra.

The different signal intensities are best analyzed by integrating the broad proton resonances and referencing them to the most intense signal.^{456,458} However, the reduced S/N ratio obtained for the STDD spectra makes peak integration impractical. Additionally, just a few NMR signals are dispersed enough to be separately integrated. Therefore, only those STD resonances of significant intensity were considered for group epitope mapping (Figure 5.18). Clearly, the strongest STD effect is localized in the (1,2-dimethyl)propyl side chain (H26-H28) and protons of methyls H18/H21 as well as methine H6 of the ring system. The latter indicates a possible hydrogen bond between C6-OH and amino acids in the receptor.

The STD NMR data points out the same binding epitope in **47** for both cannabinoid receptors. These results match and confirm the prediction established in Section 5.10, where through molecular mechanics the low energy conformation of **47** was estimated. Therefore, haplosamate A (**47**) binds CB1 and CB2 in the same fashion as some phytocannabinols, endocannabinols, and synthetic analogues. Since the sulfate and phosphate bulky groups are not required for activity and protons nearby do not exhibit strong STD effects, it is reasonable to assume that they are not in close proximity to the binding site.

5.12. Conclusions

Haplosamate A (**47**) constitutes the first member of a new family of cannabinoid-active compounds. Structurally different than phytocannabinoids, endocannabinoids and synthetic analogues known to date, it is the only marine-derived sterol that exhibits such activity. Natural occurring steroids in *Cannabis sativa*, such as stigmasterol (**63**), ergosterol (**64**), β -sitosterol (**65**) and campesterol (**66**), are not psychoactive (Table 5.1, Section 5.2).^{406,470} The only active steroid-like compound reported so far is the synthetic analogue (**67**), prepared by Razdan, Pars and Granchelli⁴²³ in 1968.



The presence of sulfate, phosphate and several hydroxyl groups bestow haplosamate A (**47**) with high water solubility, a very desirable characteristic when studying cannabinoid receptor inhibition *in vivo* or *in vitro*. Historically, lack of water solubility has always presented a challenge during bioassay due to the lipophilic character of typical cannabinoid ligands. Based on the activity of **47**, it is reasonable to propose the use of phosphate and sulfate groups to modify traditional inhibitors and improve their solubility in water without interference in activity, since as proven by STDD NMR and chemical degradation, they do not play any crucial role in the binding process.

Saturation transfer double-difference (STDD) NMR spectroscopy is a fast and versatile methodology to screen and characterize binding processes. Selective saturation of CB1 and CB2 yielded difference spectra where only those protons of haplosamate A (**47**) close enough to the binding site in the protein were visible, confirming that **47** specifically binds to these receptors. Additionally, STDD-derived group epitope mapping correlates with computer-assisted predictions about the binding mode of **47** to the cannabinoid receptors. For both CB1 and CB2, this natural ligand interacts via the classical cannabinoid pharmacophore, which suggests that the (1,2-dimethyl)propyl side chain, the ring system, and hydrogen-bonding groups, are required for activity (Figure 5.19).

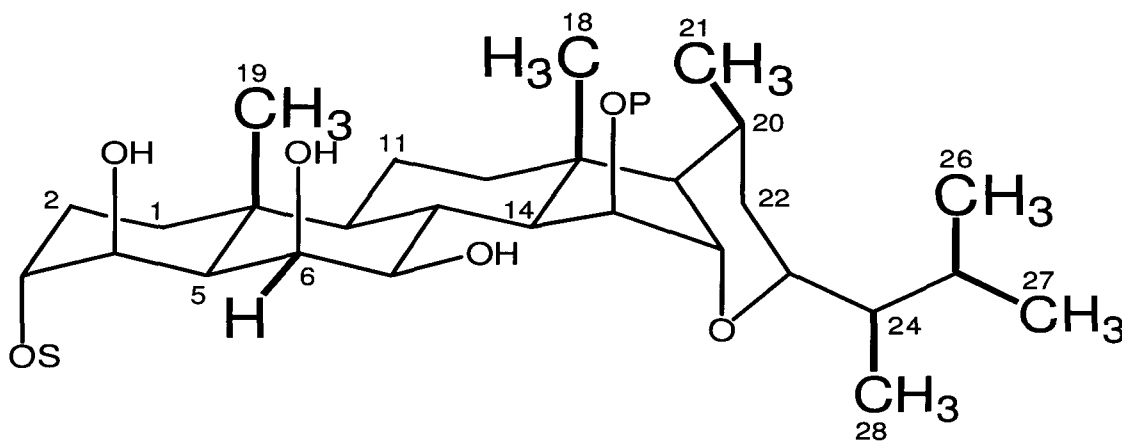


Figure 5.19. STDD NMR-derived group epitope mapping for haplosamate A (**47**). Only protons displaying STD effects are numbered. OS: sulfate; OP: methylphosphate.

Although group epitope mapping characterization used to be left mostly to X-ray crystal analyses, the present investigation proves that STDD NMR can also provide binding epitope information in a short amount of time. On ligands, the only limitation imposed is that they must not be affected by the selective saturation pulse.⁴⁵⁸ On the biological system, this must be fully operational during the whole acquisition time. In our case, since CB1 and CB2 are integrated

into the insect cell membranes, efficient protein saturation was not a limiting factor. Moreover, the use of STDD NMR allowed a complete data acquisition within the life span of the host cells.

From the biomedical viewpoint, most relevant proteins in drug discovery are membrane-bound, with about 7% of the human genome coding for seven helix GPCR's,⁴⁵⁷ such as CB1 and CB2. Since their binding specificity and affinity is very susceptible to parameters including ionic strength, ion composition, and electric field strength, it is desirable to study membrane proteins in living cells, avoiding the use of truncated receptor forms. STDD NMR has made it possible to investigate both cannabinoid receptors and their binding events directly in a cell-based bioassay, which provides the closest conditions to a natural environment.

5.13. Experimental

General experimental procedures

For general experimental procedures see Section 2.6.

Isolation procedure

Samples of a red/purple irregular tube sponge (350 g wet wt) were collected from Keviang in Papua New Guinea on September of 2003, by hand using SCUBA at depths of 15 m (2° 45.33' S, 150° 41.23' E). The sponge was later identified as *Dasychalina fragilis* (Ridley & Dendy, 1886) by Dr. R. van Soest (University of Amsterdam), and a voucher specimen was deposited at the Zoologisch Museum, Amsterdam (ref. no. ZMA POR 19111). The collected material was frozen immediately upon collection and transported back to the University of British Columbia in coolers packed with dry ice. A portion of the frozen material (100 g) was extracted in MeOH (3 x 200 mL) and the combined extracts concentrated to dryness *in vacuo* to give a brown solid (0.60 g). This residue was treated with H₂O to obtain a light yellow colored solution and an insoluble precipitate. The aqueous layer was extracted sequentially with hexanes (3 x 50 mL), CH₂Cl₂ (3 x 50 mL) and EtOAc (3 x 50 mL), followed by concentration *in vacuo* of each partition.

The water insoluble brown gum (major fraction, 0.38 g) was placed on a small reversed-phase column (20 g) and eluted with MeOH/H₂O (7:3, 200 mL), to afford three major fractions: 183Me1 (0.250 g), 183Me2 (0.032 g) and 183Me3 (0.056 g). 1D and 2D NMR data confirmed the presence of the known compound haplosamate A in fraction 183Me2, in high purity. Further

purification by reversed-phase HPLC using CH₃CN/H₂O (7:3), afforded haplosamate A (47) (0.030 g, 0.043 mmol, 0.008% wet wt) as a white amorphous powder. $[\alpha]_D^{20}$ -5.8 (*c* 0.8, MeOH); UV (MeOH) λ_{\max} (log ϵ) 206 nm (2.98). For a summary of ¹H and ¹³C NMR assignments based on HMQC and HMBC data, see Tables 5.5, 5.7-5.8. ¹H NMR (CD₃OD, 600 MHz) δ 4.73 (1H, m, broad), 4.39 (1H, d, *J* = 2.6 Hz), 4.15 (1H, s, broad), 4.01 (1H, s, broad), 3.88 (1H, d, *J* = 9.8 Hz), 3.61 (3H, d, *J* = 11.0 Hz), 3.44 (1H, m), 3.34 (1H, m), 2.30 (1H, dt, *J* = 10.5, 10.6 Hz), 2.09 (1H, m), 2.07 (1H, m), 1.89 (1H, d, *J* = 14.2 Hz), 1.85 (1H, d, *J* = 12.5 Hz), 1.83 (1H, m), 1.64 (1H, d, *J* = 13.4 Hz), 1.52 (1H, m), 1.50 (1H, m), 1.45 (1H, m), 1.43 (1H, m), 1.40 (1H, m), 1.33 (2H, m), 1.32 (3H, s), 1.20 (1H, td, *J* = 3.9, 12.9 Hz), 1.00 (3H, s), 0.98 (3H, d, *J* = 6.5 Hz), 0.90 (1H, m), 0.89 (3H, d, *J* = 6.8 Hz), 0.86 (1H, m), 0.82 (3H, d, *J* = 6.8 Hz), 0.77 (3H, d, *J* = 7.0 Hz), 0.72 (1H, dd, *J* = 10.2, 10.3 Hz); ¹³C NMR (CD₃OD, 150 MHz) δ 92.4 (CH), 82.7 (CH), 82.0 (d, *J* = 7.5 Hz, CH), 80.1 (CH), 78.2 (CH), 77.7 (CH), 76.2 (CH), 63.0 (CH), 58.9 (d, *J* = 7.5 Hz, CH), 54.4 (CH), 53.4 (d, *J* = 6.0 Hz, CH₃), 45.6 (CH), 45.3 (CH), 43.1 (C), 41.2 (CH₂), 40.0 (CH), 36.7 (C), 35.1 (CH₂), 34.8 (CH), 34.4 (CH), 28.4 (CH), 23.9 (CH₂), 22.0 (CH₃), 21.0 (CH₃), 20.0 (CH₂), 17.9 (CH₃), 17.7 (CH₃), 15.9 (CH₃), 10.8 (CH₃). HRESIMS calcd for C₂₉H₄₉O₁₂Na₃PS ([M+Na]⁺): 721.2375; found 721.2377.

¹H NMR (DMSO-*d*₆, 600 MHz) δ 5.68 (1H, s, broad), 5.08 (1H, s, broad), 4.72 (1H, s, broad), 4.61 (1H, s, broad), 4.08 (1H, d, *J* = 2.0 Hz), 3.89 (1H, s, broad), 3.79 (1H, s, broad), 3.53 (1H, d, *J* = 9.0 Hz), 3.31 (3H, d, *J* = 11.0 Hz), 3.26 (1H, dd, *J* = 9.0, 9.4 Hz), 3.13 (1H, s, broad), 2.14 (1H, ddd, *J* = 10.5, 10.5, 10.6 Hz), 2.03 (1H, m), 1.81 (1H, dd, *J* = 13.8, 13.8 Hz), 1.732 (1H, d, *J* = 12.0 Hz), 1.727 (1H, m), 1.68 (1H, dd, *J* = 13.0, 13.0 Hz), 1.58 (1H, d, *J* = 12.9 Hz), 1.36 (2H, m), 1.33 (1H, m), 1.27 (1H, m), 1.23 (1H, m) 1.23 (3H, s), 1.20 (1H, m), 1.12 (1H, dd, *J* = 12.9, 13.6 Hz), 1.10 (1H, dd, *J* = 13.0, 13.6 Hz), 0.91 (3H, d, *J* = 6.3 Hz), 0.86 (3H, s), 0.83 (3H,

d, $J = 7.0$ Hz), 0.78 (1H, dd, $J = 11.2, 12.0$ Hz), 0.76 (1H, m) 0.70 (3H, d, $J = 5.9$ Hz), 0.69 (3H, d, $J = 5.7$ Hz), 0.60 (1H, dd, $J = 10.1, 10.3$ Hz); ^{13}C NMR (DMSO- d_6 , 150 MHz) δ 92.5 (CH), 80.4 (CH), 78.6 (CH), 78.5 (d, $J = 13.5$ Hz, CH), 77.2 (CH), 74.3 (CH), 73.6 (CH), 61.0 (CH), 56.5 (d, $J = 6.0$ Hz, CH), 52.4 (CH), 51.0 (d, $J = 6.0$ Hz, CH₃), 44.2 (CH), 43.4 (CH), 41.2 (C), 38.9 (CH₂), 38.6 (CH₂), 35.2 (C), 33.5 (CH₂), 32.7 (CH), 32.5 (CH), 26.3 (CH), 22.4 (CH₂), 21.3 (CH₃), 20.3 (CH₃), 18.3 (CH₂), 17.0 (CH₃), 16.7 (CH₃), 15.2 (CH₃), 10.1 (CH₃).

^1H NMR (D₂O, 600 MHz) δ 4.64 (1H, s, broad), 4.40 (1H, d, $J = 2.6$ Hz), 4.15 (1H, s, broad), 4.06 (1H, s, broad), 3.95 (1H, dd, $J = 4.0, 10.1$ Hz), 3.62 (3H, d, $J = 10.9$ Hz), 3.54 (1H, dd, $J = 8.9, 9.1$ Hz), 3.45 (1H, dd, $J = 3.8, 10.6$ Hz), 2.21 (1H, ddd, $J = 10.6, 10.6, 10.7$ Hz), 2.07 (1H, dd, $J = 14.3, 14.3$ Hz), 2.00 (1H, m), 1.88 (1H, m), 1.87 (1H, m), 1.86 (1H, m), 1.77 (1H, d, $J = 13.4$ Hz), 1.54 (1H, m), 1.54 (1H, m), 1.51 (1H, m), 1.49 (1H, m), 1.42 (1H, m), 1.42 (1H, m), 1.27 (1H, m), 1.25 (3H, s), 1.21 (1H, dd, $J = 4.1, 12.7$ Hz), 0.99 (1H, m), 0.97 (3H, d, $J = 6.3$ Hz), 0.95 (3H, s), 0.88 (3H, d, $J = 6.9$ Hz), 0.88 (1H, m), 0.80 (3H, d, $J = 6.9$ Hz), 0.79 (1H, m), 0.75 (3H, d, $J = 6.9$ Hz); ^{13}C NMR (D₂O, 150 MHz) δ 91.2 (CH), 83.5 (CH), 82.0 (d, $J = 7.5$ Hz, CH), 79.0 (CH), 78.5 (CH), 77.1 (CH), 75.3 (CH), 61.9 (CH), 57.6 (d, $J = 9.0$ Hz, CH), 54.0 (d, $J = 6.0$ Hz, CH₃), 53.1 (CH), 44.6 (CH), 44.4 (CH), 42.6 (C), 40.1 (CH₂), 39.6 (CH₂), 36.5 (C), 34.2 (CH₂), 34.1 (CH), 33.4 (CH), 27.9 (CH), 23.4 (CH₂), 21.7 (CH₃), 20.5 (CH₃), 19.4 (CH₂), 17.5 (CH₃), 17.2 (CH₃), 15.4 (CH₃), 10.6 (CH₃).

^{31}P NMR (CD₃OD, 81 MHz) δ 0.84 (1P, s).

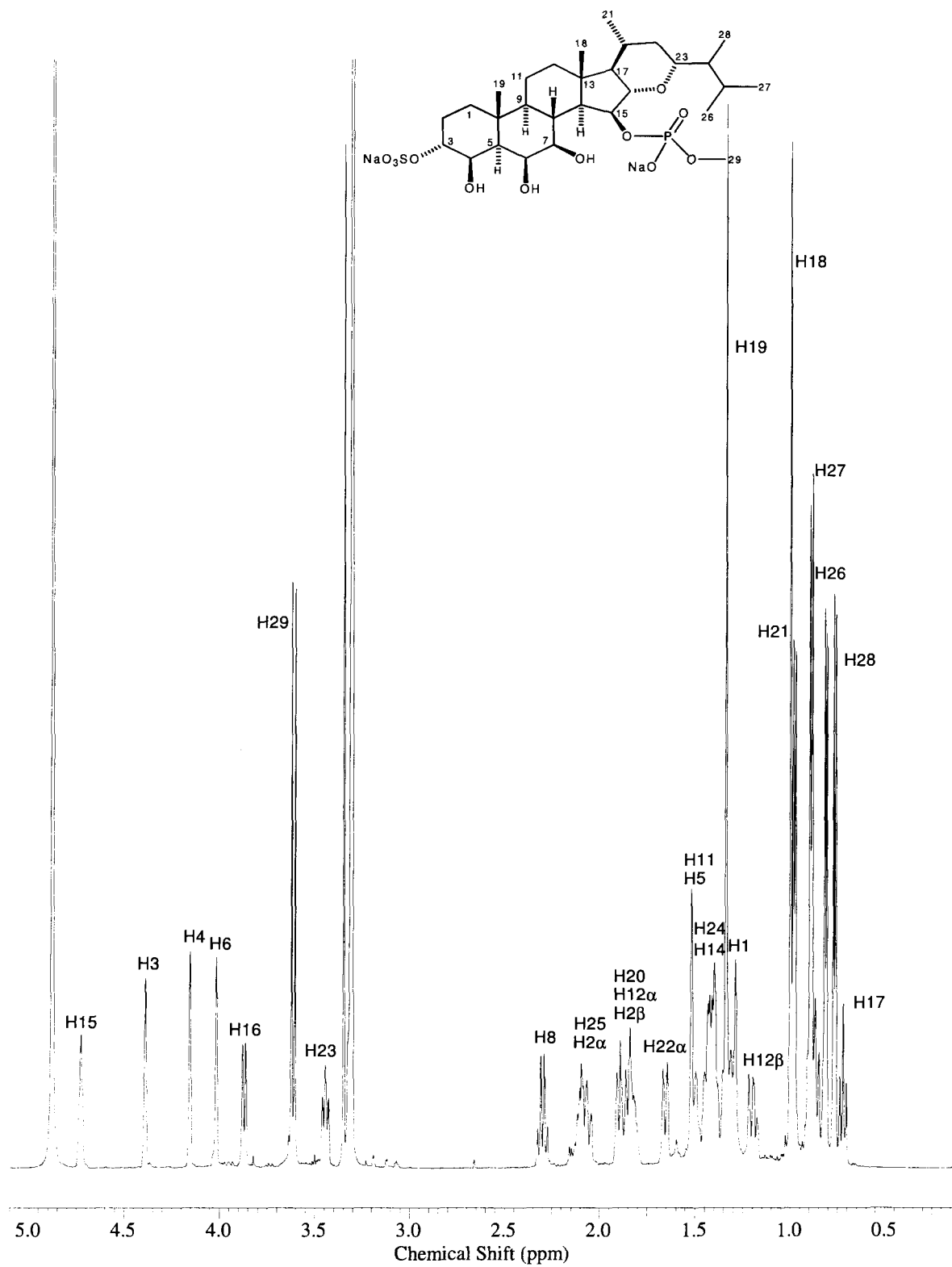


Figure 5.20. ¹H-NMR spectrum of haplosamate A (47) (recorded in CD₃OD at 600 MHz).

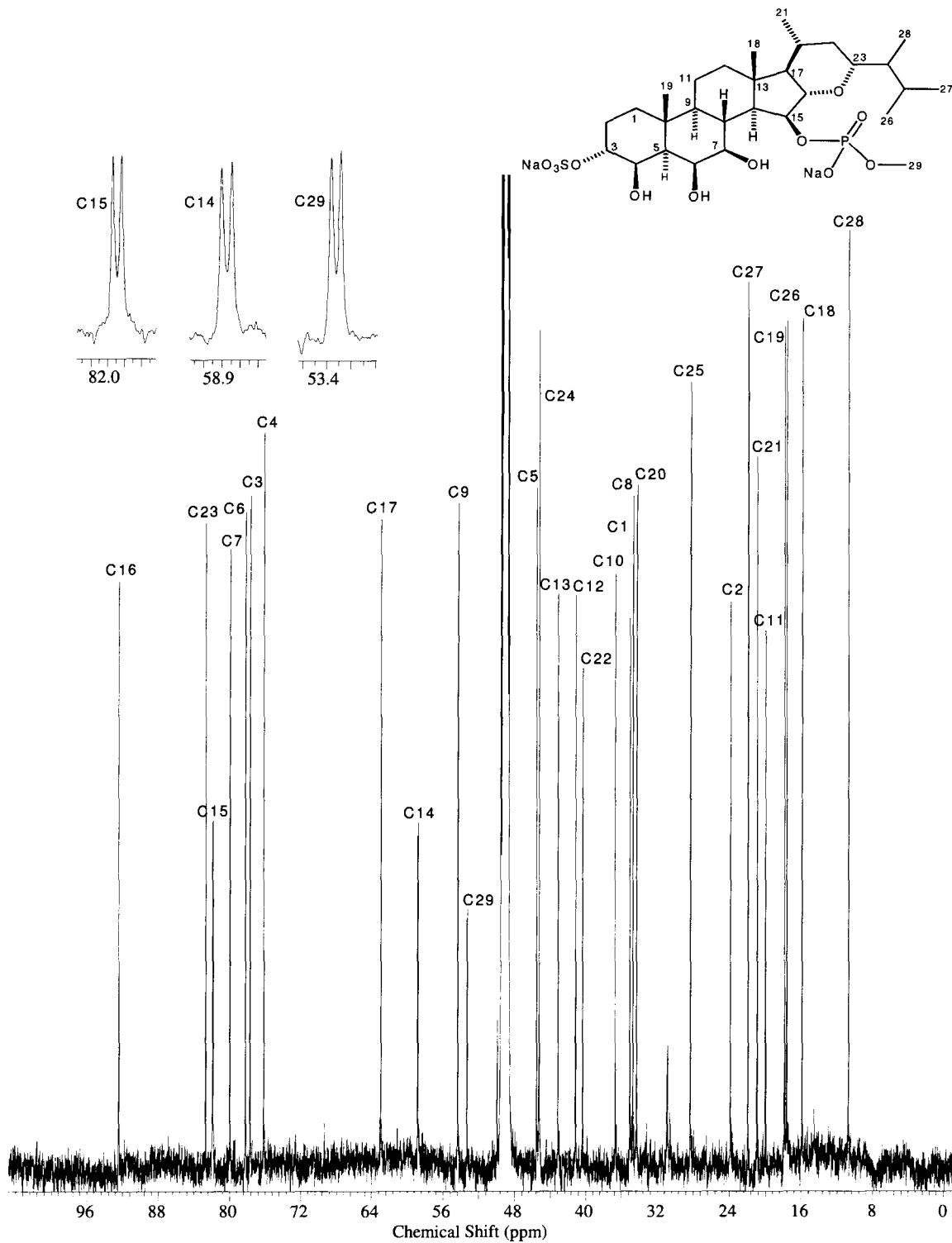
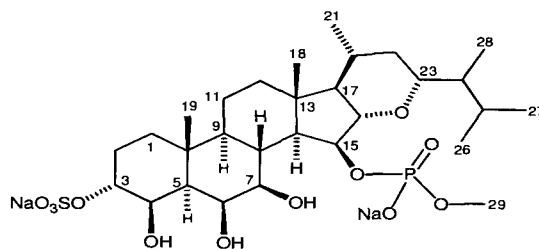
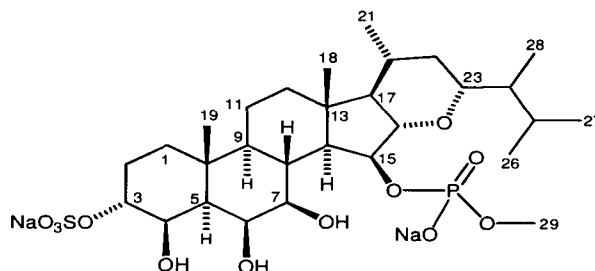


Figure 5.21. ^{13}C -NMR spectrum of haplosamate A (47) (recorded in CD_3OD at 150 MHz).

Table 5.7. NMR data for haplosamate A (**47**) (recorded in DMSO- d_6).

Carbon No	^{13}C δ (ppm) ^a	^1H δ (ppm) (mult, J (Hz)) ^{b,c}	HMBC ^b (H \rightarrow C)
1	33.5	H α 1.23 (m) H β 1.12 (dd, $J = 12.9, 13.6$ Hz)	C2, C10, C19,
2	22.4	H α 1.81 (dd, $J = 13.8, 13.8$ Hz) H β 1.68 (dd, $J = 13.0, 13.0$ Hz)	C4, C10
3	73.6	4.08 (d, $J = 2.0$ Hz)	C1, C4, C5
4	74.3	3.89 (s, broad) OH 5.08 (s, broad)	C2, C3, C10
5	44.2	1.27 (m)	C4, C6, C7, C9, C10, C19
6	77.2	3.79 (s, broad) OH 4.72 (s, broad)	C10
7	78.6	3.13 (s, broad) OH 5.68 (s, broad)	C9
8	32.7	2.14 (ddd, $J = 10.5, 10.5, 10.6$ Hz)	C7, C9, C10, C14
9	52.4	0.76 (m)	C8, C11
10	35.2		
11	18.3	1.36 (m)	C12
12	38.9	H α 1.73 (d, $J = 12.0$ Hz) H β 1.10 (dd, $J = 13.0, 13.6$ Hz)	C9, C11, C13, C14, C17, C18
13	41.2		
14	56.5	1.20 (m)	C7, C8, C12, C13, C17, C18
15	78.5	4.61 (s, broad)	C13, C16
16	92.5	3.53 (d, $J = 9.0$ Hz)	C15, C17, C20, C23
17	61.0	0.60 (dd, $J = 10.1, 10.3$ Hz)	C12, C13, C14, C16, C18, C20
18	15.2	0.86 (s)	C12, C13, C14, C17
19	17.0	1.23 (s)	C1, C2, C4, C5, C10
20	32.5	1.73 (m)	C13
21	20.3	0.91 (d, $J = 6.3$ Hz)	C13, C17, C20, C22, C23
22	38.6	H α 1.58 (d, $J = 12.9$ Hz) H β 0.78 (dd, $J = 11.2, 12.0$ Hz)	C17, C20, C23, C24
23	80.4	3.26 (dd, $J = 9.0, 9.4$ Hz)	C24, C28
24	43.4	1.33 (m)	C22, C23, C25, C26, C27, C28
25	26.3	2.03 (m)	C24, C26, C27, C28
26	21.3	0.83 (d, $J = 7.0$ Hz)	C24, C25, C27
27	16.7	0.70 (d, $J = 5.9$ Hz)	C24, C26
28	10.1	0.69 (d, $J = 5.7$ Hz)	C23, C25
29	51.0	3.31 (d, $J = 11.0$ Hz)	

^a Recorded at 150 MHz. ^b Recorded at 600 MHz. ^c According to HMQC recorded at 600 MHz.

Table 5.8. NMR data for haplosamate A (**47**) (recorded in DMSO-*d*₆).

Proton No	¹ H δ (ppm) (mult, <i>J</i> (Hz)) ^a	COSY ^a	NOESY ^a
1α	1.23 (m)	H2α, H2β	
1β	1.12 (dd, <i>J</i> = 12.9, 13.6 Hz)	H2α	
2α	1.81 (dd, <i>J</i> = 13.8, 13.8 Hz)	H1α, H1β, H3	H19
2β	1.68 (dd, <i>J</i> = 13.0, 13.0 Hz)	H1α, H3, H4, H5	
3	4.08 (d, <i>J</i> = 2.0 Hz)	H2α, H2β, H4	
4	3.89 (s, broad)	H2β, H3, 4OH, H5	
4OH	5.08 (s, broad)	H4	
5	1.27 (m)	H4, H6	
6	3.79 (s, broad)	H5, 6OH	
6OH	4.72 (s, broad)	H6	
7	3.13 (s, broad)	H6, H8	
7OH	5.68 (s, broad)		
8	2.14 (ddd, <i>J</i> = 10.5, 10.5, 10.6 Hz)	H7, H9, H14	H11, H18, H19
9	0.76 (m)	H8	
11	1.36 (m)	H9, H12α, H12β	H8
12α	1.73 (d, <i>J</i> = 12.0 Hz)	H11, H12β	H18
12β	1.10 (dd, <i>J</i> = 13.0, 13.6 Hz)	H11, H12α	
14	1.20 (m)	H8, H15	H15, H17
15	4.61 (s, broad)	H14, H16	H14
16	3.53 (d, <i>J</i> = 9.0 Hz)	H15, H17	
17	0.60 (dd, <i>J</i> = 10.1, 10.3 Hz)	H16, H20	H14, H22β
18	0.86 (s)		H8, H12α
19	1.23 (s)		H2α, H8
20	1.73 (m)	H17, H21, H22	
21	0.91 (d, <i>J</i> = 6.3 Hz)	H20	
22α	1.58 (d, <i>J</i> = 12.9 Hz)	H22β, H23	
22β	0.78 (dd, <i>J</i> = 11.2, 12.0 Hz)	H20, H22α, H23	H17
23	3.26 (dd, <i>J</i> = 9.0, 9.4 Hz)	H22α, H22β, H24	
24	1.33 (m)	H23, H25, H27	
25	2.03 (m)	H24, H26, H28	
26	0.83 (d, <i>J</i> = 7.0 Hz)	H25	
27	0.70 (d, <i>J</i> = 5.9 Hz)	H24	
28	0.69 (d, <i>J</i> = 5.7 Hz)	H25	
29	3.31 (d, <i>J</i> = 11.0 Hz)	P	

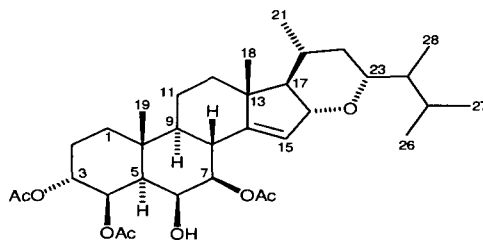
^a Recorded at 600 MHz.

Acetylation procedure

A solution of haplosamate A (0.0074, 0.0106 mmol) was dissolved in CH₃OH (5 mL) and refluxed for 2 h in the presence of HCl (2 mL, 4 mmol, 2M). After solvent evaporation, the obtained residue was dissolved in pyridine (2 mL, 24.8 mmol) and treated with acetic anhydride (3 mL, 31.7 mmol). Upon stirring overnight at 25°C, the solvent was concentrated *in vacuo* and the resulting solid purified using normal phase column chromatography (20 g, EtOAc/hexanes 3:7) to afford two different acetylated compounds: haplosamate A 3,4,7-(**60**) (0.0029 g, 0.0049 mmol, 46%) and 3,6,7-(**61**) triacetates (0.0031 g, 0.0052 mmol, 49%).

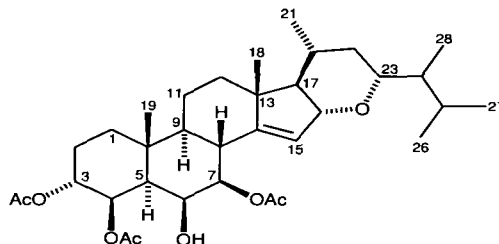
Haplosamate A 3,4,7-triacetate (**60**): for a summary of ¹H and ¹³C NMR assignments based on HMQC and HMBC data, see Tables 5.6, 5.9 and 5.10. ¹H NMR (C₆D₆, 600 MHz) δ 5.64 (1H, s, broad), 5.47 (1H, s, broad), 5.12 (1H, dd, *J* = 1.3, 2.8 Hz), 4.93 (1H, dd, *J* = 3.3, 10.8), 4.43 (1H, s, broad), 4.13 (1H, dd, *J* = 2.2, 7.1 Hz), 3.38 (1H, m), 2.63 (1H, dd, *J* = 11.3, 11.3 Hz), 2.16 (1H, m), 1.94 (1H, ddd, *J* = 3.0, 14.4, 14.6 Hz), 1.76 (3H, s), 1.74 (1H, m), 1.72 (1H, m), 1.66 (3H, s), 1.66 (1H, m), 1.63 (1H, m), 1.54 (1H, m), 1.54 (1H, m), 1.42 (3H, s), 1.38 (3H, s), 1.34 (1H, m), 1.31 (2H, m), 1.23 (1H, dd, *J* = 8.0, 9.4 Hz), 1.16 (1H, ddd, *J* = 3.9, 14.1, 14.6 Hz), 1.13 (1H, ddd, *J* = 3.3, 13.6, 14.1 Hz), 0.99 (1H, ddd, *J* = 1.2, 11.6 Hz), 0.94 (3H, d, *J* = 6.9 Hz), 0.90 (3H, s), 0.90 (3H, d, *J* = 6.9 Hz), 0.88 (3H, d, *J* = 7.2 Hz), 0.87 (3H, d, *J* = 6.6 Hz), 0.65 (1H, ddd, *J* = 2.5, 11.9, 11.9 Hz); ¹³C NMR (C₆D₆, 150 MHz) δ 169.9 (C), 169.9 (C), 169.2 (C), 151.0 (C), 123.9 (CH), 86.6 (CH), 80.7 (CH), 76.3 (CH), 73.2 (CH), 72.0 (CH), 70.5 (CH), 65.9 (CH), 53.3 (CH), 46.3 (C), 44.7 (CH), 44.0 (CH), 42.3 (CH₂), 39.9 (CH₂), 36.6 (CH), 36.0 (C), 34.8 (CH₂), 32.0 (CH), 28.2 (CH), 23.1 (CH₂), 22.1 (CH₃), 22.0 (CH₂), 21.5 (CH₃), 21.0 (CH₃), 20.9 (CH₃), 20.8 (CH₃), 18.4 (CH₃), 17.9 (CH₃), 17.1 (CH₃), 11.3 (CH₃). HRESIMS calcd for C₃₄H₅₂O₈Na ([M+Na]⁺): 611.3560; found 611.3558.

Haplosamate A 3,6,7-triacetate (**61**): for a summary of ^1H and ^{13}C NMR assignments based on HMQC and HMBC data, see Tables 5.6, 5.11 and 5.12. ^1H NMR (C_6D_6 , 600 MHz) δ 5.83 (1H, d, $J = 2.4$ Hz), 5.72 (1H, s, broad), 5.06 (1H, dd, $J = 3.8, 11.0$), 4.77 (1H, d, $J = 2.5$ Hz), 4.12 (1H, dd, $J = 2.5, 9.4$ Hz), 3.51 (1H, m), 3.37 (1H, ddd, $J = 2.2, 7.2, 9.3$ Hz), 2.65 (1H, dd, $J = 11.3, 11.3$ Hz), 2.17 (1H, m), 1.73 (1H, dd, $J = 3.1, 3.6$ Hz), 1.54 (1H, m), 1.40 (1H, m) 1.31 (1H, m), 1.31 (1H, m), 1.96 (1H, dddd, $J = 3.1, 3.3, 14.3, 14.4$ Hz), 1.76 (3H, s), 1.72 (3H, s), 1.67 (3H, s), 1.66 (1H, m), 1.62 (1H, m), 1.54 (1H, m), 1.42 (1H, m), 1.33 (3H, s), 1.23 (1H, dd, $J = 9.7, 10.8$ Hz), 1.17 (1H, ddd, $J = 3.3, 13.0, 13.3$ Hz), 1.11 (1H, ddd, $J = 3.3, 13.8, 13.8$ Hz), 0.98 (1H, dd, $J = 11.6, 12.0$ Hz), 0.95 (3H, d, $J = 6.7$ Hz), 0.90 (3H, s), 0.89 (3H, d, $J = 6.4$ Hz), 0.88 (3H, d, $J = 6.4$ Hz), 0.87 (3H, d, $J = 6.4$ Hz), 0.68 (3H, ddd, $J = 2.2, 11.6, 11.6$ Hz); ^{13}C NMR (C_6D_6 , 150 MHz) δ 170.6 (C), 170.2 (C), 169.4 (C), 150.7 (C), 124.3 (CH), 86.5 (CH), 80.7 (CH), 73.8 (CH), 73.3 (CH), 72.8 (CH), 72.6 (CH), 65.8 (CH), 53.3 (CH), 46.3 (C), 44.7 (CH), 43.3 (CH), 42.3 (CH_2), 39.4 (CH_2), 37.2 (CH), 36.2 (C), 35.1 (CH_2), 32.0 (CH), 28.2 (CH), 22.2 (CH_2), 22.1 (CH_3), 21.8 (CH_2), 21.4 (CH_3), 21.2 (CH_3), 21.0 (CH_3), 20.8 (CH_3), 18.3 (CH_3), 18.0 (CH_3), 17.1 (CH_3), 11.3 (CH_3). HRESIMS calcd for $\text{C}_{34}\text{H}_{52}\text{O}_8\text{Na}$ ($[\text{M}+\text{Na}]^+$): 611.3560; found 611.3564.

Table 5.9. NMR data for haplosamate A 3,4,7-triacetate derivative (**60**) (recorded in C₆D₆).

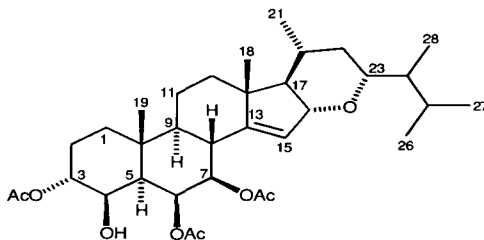
Carbon No	¹³ C δ (ppm) ^a	¹ H δ (ppm) (mult, J (Hz)) ^{b,c}	HMBC ^b (H→C)
1	34.8	Hβ 1.13 (ddd, J = 3.3, 13.6, 14.1 Hz) Hα 1.34 (m)	C3, C9, C10
2	23.1	Hα 1.94 (ddd, J = 3.0, 14.4, 14.6 Hz) Hβ 1.72 (m)	
3	70.5	5.12 (dd, J = 1.3, 2.8 Hz)	C1, C4, C5, C29
4	73.2	5.47 (s, broad)	C2, C3, C10, C31/C33
5	44.0	1.54 (m)	C4, C6, C9, C10
6	72.0	4.43 (s, broad)	C5, C7, C10
7	76.3	4.93 (dd, J = 3.3, 10.8)	C6, C8, C14, C31/C33
8	36.5	2.63 (dd, J = 11.3, 11.3 Hz)	C14, C15
9	53.3	0.65 (ddd, J = 2.5, 11.9, 11.9 Hz)	C19
10	36.0		
11	22.0	1.31 (m)	C8, C9, C10, C12
12	42.3	Hα 1.74 (m) Hβ 1.16 (ddd, J = 3.9, 14.1, 14.6 Hz)	C9, C11, C13, C14
13	46.3		
14	151.0		
15	123.9	5.64 (s, broad)	C8, C13, C14, C16, C17
16	86.6	4.13 (dd, J = 2.2, 7.1 Hz)	C14, C15, C20, C23
17	65.9	1.23 (dd, J = 8.0, 9.4 Hz)	C8, C12, C13, C16, C18, C20, C22
18	17.1	0.90 (s)	C12, C13
19	18.0	1.38 (s)	C1, C5, C9, C10
20	32.0	1.63 (m)	C22, C23, C25, C28
21	20.8	0.90 (d, J = 6.9 Hz)	C17, C20, C22
22	39.3	Hα 1.54 (m) Hβ 0.99 (ddd, J = 1.2, 11.6 Hz)	C21
23	80.7	3.38 (m)	C16, C24, C28
24	44.7	1.66 (m)	
25	28.2	2.16 (m)	C23, C24, C26, C27, C28
26	18.4	0.87 (d, J = 6.6 Hz)	C24, C25, C27
27	22.1	0.94 (d, J = 6.9 Hz)	C24, C25, C26
28	11.3	0.88 (d, J = 7.2 Hz)	C23, C27
29	169.2		
30	21.0	1.66 (s)	C29
31	169.9		
32 ^d	21.5	1.76 (s)	C31/C33
33	169.9		
34 ^d	20.9	1.42 (s)	C31/C33

^aRecorded at 150 MHz. ^bRecorded at 600 MHz. ^cAccording to HMQC recorded at 600 MHz. ^dInterchangeable.

Table 5.10. NMR data for haplosamate A 3,4,7-triacetate derivative (**60**) (recorded in C₆D₆).

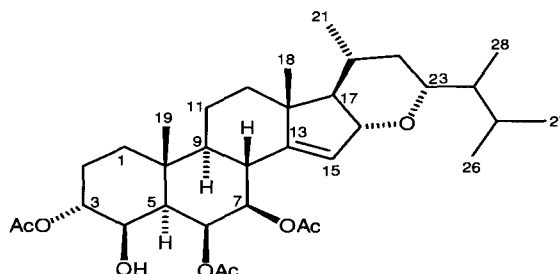
Proton No	¹ H δ (ppm) (mult, J (Hz)) ^a	COSY ^a	NOESY ^a
1 α	1.34 (m)	H1 β , H2 α	
1 β	1.13 (ddd, J = 3.3, 13.6, 14.1 Hz)	H1 α , H2 α , H2 β	
2 α	1.94 (ddd, J = 3.0, 14.4, 14.6 Hz)	H1 α , H1 β , H2 β , H3	H19
2 β	1.72 (m)	H1 β , H2 α , H3, H4	
3	5.12 (dd, J = 1.3, 2.8 Hz)	H2 α , H2 β , H4	
4	5.47 (s, broad)	H2 β , H3, H5	H6
5	1.54 (m)	H4, H6	H7
6	4.43 (s, broad)	H5, H7	H4
7	4.93 (dd, J = 3.3, 10.8)	H6, H8	H5
8	2.63 (dd, J = 11.3, 11.3 Hz)	H7, H9, H15, H16	H18, H19
9	0.65 (ddd, J = 2.5, 11.9, 11.9 Hz)	H8, H11	H12 β
11	1.31 (m)	H9	
12 α	1.74 (m)	H12 β	
12 β	1.16 (ddd, J = 3.9, 14.1, 14.6 Hz)	H12 α	H9
15	5.64 (s, broad)	H8, H16	
16	4.13 (dd, J = 2.2, 7.1 Hz)	H8, H15, H17	H23, H28
17	1.23 (dd, J = 8.0, 9.4 Hz)	H16, H20	
18	0.90 (s)		H8
19	1.38 (s)		H2 α , H8
20	1.63 (m)	H17, H21, H22 β	
21	0.90 (d, J = 6.9 Hz)	H20	
22 α	1.54 (m)	H23, H22 β	
22 β	0.99 (ddd, J = 1.2, 11.6 Hz)	H20, H23	
23	3.38 (m)	H22 α , H22 β , H24	H16, 28
24	1.66 (m)	H23, H25, H28	
25	2.16 (m)	H24, H26, H27	
26	0.87 (d, J = 6.6 Hz)	H25	
27	0.94 (d, J = 6.9 Hz)	H25	
28	0.88 (d, J = 7.2 Hz)	H24	H16, H23
30	1.66 (s)		
32 ^b	1.76 (s)		
34 ^b	1.42 (s)		

^aRecorded at 600 MHz.

Table 5.11. NMR data for haplosamate A 3,6,7-triacetate derivative (**61**) (recorded in C₆D₆).

Carbon No	¹³ C δ (ppm) ^a	¹ H δ (ppm) (mult, <i>J</i> (Hz)) ^{b,c}	HMBC ^b (H→C)
1	35.1	H α 1.11 (ddd, <i>J</i> = 3.3, 13.8, 13.8 Hz) H β 1.31 (m)	C3, C5
2	22.5	H α 1.96 (dddd, <i>J</i> = 3.1, 3.3, 14.3, 14.4 Hz) H β 1.54 (m)	
3	72.8	4.77 (d, <i>J</i> = 2.5 Hz)	C1
4	73.3	3.51 (m)	
5	43.3	1.42 (m)	C7, C9, C10, C19
6	72.6	5.83 (d, <i>J</i> = 2.4 Hz)	C5, C7, C8, C31
7	73.8	5.06 (dd, <i>J</i> = 3.8, 11.0)	C6, C8, C14, C33
8	36.2	2.65 (dd, <i>J</i> = 11.3, 11.3 Hz)	C7, C9, C14
9	53.3	0.68 (ddd, <i>J</i> = 2.2, 11.6, 11.6 Hz)	C5, C8, C10, C19
10	37.2		
11	21.8	1.40 (m), 1.31 (m)	
12	42.3	H α 1.73 (dd, <i>J</i> = 3.1, 3.6 Hz) H β 1.17 (ddd, <i>J</i> = 3.3, 13.0, 13.3 Hz)	C9, C11, C17
13	46.3		
14	150.9		
15	124.3	5.72 (s, broad)	C8, C13, C14, C16, C17
16	86.5	4.12 (dd, <i>J</i> = 2.5, 9.4 Hz)	C14, C15, C20, C23
17	65.8	1.23 (dd, <i>J</i> = 9.7, 10.8 Hz)	C12, C13, C16, C18, C20, C21, C22
18	17.1	0.90 (s)	C10, C12, C14, C17
19	18.0	1.33 (s)	C1, C5, C9, C10
20	32.0	1.62 (m)	C17, C22
21	20.8	0.89 (d, <i>J</i> = 6.4 Hz)	C20, C22, C23
22	39.4	H α 1.54 (m) H β 0.98 (dd, <i>J</i> = 11.6, 12.0 Hz)	C13, C20, C23
23	80.7	3.37 (ddd, <i>J</i> = 2.2, 7.2, 9.3 Hz)	C16, C24, C25, C28
24	44.7	1.66 (m)	C22, C23, C25, C26, C28
25	28.2	2.17 (m)	C23, C24, C26, C27, C28
26	18.3	0.87 (d, <i>J</i> = 6.4 Hz)	C24, C25, C27
27	22.1	0.95 (d, <i>J</i> = 6.7 Hz)	C24, C25, C26
28	11.3	0.88 (d, <i>J</i> = 6.4 Hz)	C23, C25
29	169.4		
30	21.2	1.72 (s)	C29
31	170.6		
32	21.4	1.76 (s)	C31
33	170.2		
34	21.0	1.67 (s)	C33

^aRecorded at 150 MHz. ^bRecorded at 600 MHz. ^cAccording to HMQC recorded at 600 MHz.

Table 5.12. NMR data for haplosamate A 3,6,7-triacetate derivative (**61**) (recorded in C₆D₆).

Proton No	¹ H δ (ppm) (mult, J (Hz)) ^a	COSY ^a	NOESY ^a
1α	1.31 (m)	H1β, H2α, H2β	
1β	1.11 (ddd, J = 3.3, 13.8, 13.8 Hz)	H1α, H2α, H2β	H9
2α	1.96 (dddd, J = 3.1, 3.3, 14.3, 14.4 Hz)	H1α, H1β, H3, H2β	H19
2β	1.54 (m)	H1α, H1β, H3, H2α	
3	4.77 (d, J = 2.5 Hz)	H1, H4α, H4β	
4	3.51 (m)	H3, H5	H6
5	1.42 (m)	H4, H6	H1, H6, H7, H9
6	5.83 (d, J = 2.4 Hz)	H5, H7	H1, H5, H7
7	5.06 (dd, J = 3.8, 11.0)	H6, H8	H5, H6, H9, H15
8	2.65 (dd, J = 11.3, 11.3 Hz)	H7, H9, H15	H18, H19
9	0.68 (ddd, J = 2.2, 11.6, 11.6 Hz)	H8, H11	H1β, H5, H7, H12β
11	1.40 (m), 1.31 (m)	H9, H12α	
12α	1.73 (dd, J = 3.1, 3.6 Hz)	H11, H12β	H18
12β	1.17 (ddd, J = 3.3, 13.0, 13.3 Hz)	H12α	H9
15	5.72 (s, broad)	H8	H7
16	4.12 (dd, J = 2.5, 9.4 Hz)	H17	H18, H23
17	1.23 (dd, J = 9.7, 10.8 Hz)	H16, H20	
18	0.90 (s)		H8, H12α, H16
19	1.33 (s)		H2α, H8
20	1.62 (m)	H17, H21	H23
21	0.89 (d, J = 6.4 Hz)	H20	
22α	1.54 (m)	H23, H22β	H23
22β	0.98 (dd, J = 11.6, 12.0 Hz)	H23, H22α	
23	3.37 (ddd, J = 2.2, 7.2, 9.3 Hz)	H22α, H22β, H24	H16, H20, H22α, H28
24	1.66 (m)	H23, H28	
25	2.17 (m)	H26, H27	
26	0.87 (d, J = 6.4 Hz)	H25	
27	0.95 (d, J = 6.7 Hz)	H25	
28	0.88 (d, J = 6.4 Hz)	H24	H23
30	1.72 (s)		
32	1.76 (s)		
34	1.67 (s)		

^aRecorded at 600 MHz.

Saturation transfer double-difference (STDD) NMR sample preparation

CB1 or CB2 cell lines were grown to confluency in T75 cell culture flasks and harvested by centrifugation at 500 g. The cell pellet was resuspended in 10 mL of a deuterated phosphate-buffered modified saline (PMS), prepared in D₂O (99.9%) using 11 mM phosphate (pH 6.2), 40 mM NaCl, 40 mM KCl and 80 mM sucrose. All preparations were done at room temperature. The suspension was centrifuged at 500 g for 10 min, the supernatant discarded, and the pellet resuspended in 5 mL of PMS. This wash was repeated two more times and after the last centrifugation, cell pellets were resuspended in 1.0 ml aliquots of PMS buffer which provided a cell concentration of approximately 5×10^6 cells/mL. Typical of GPCR expressing cell lines is a receptor density of about 10^6 per cell,⁴⁶⁹ which gives a total concentration of 5×10^{13} receptors/mL.

The NMR samples for each receptor were prepared in pairs of tubes, by previously adding haplosamate A (1.7 mg, 2.0 μ mol) to only one NMR tube, and splitting the above suspension into both tubes (total volume of each tube: 1.0 mL). This is equivalent to an approximate 24000-fold excess ligand/receptor.

Saturation transfer double-difference (STDD) NMR measurements

STD NMR spectra were recorded according to the procedure described by Claasen, Axmann, Meinecke and Meyer.⁴⁶⁹ All measurements were made at 298 K with a spectral width of 10 ppm on a Bruker Avance 600 MHz spectrometer, equipped with a 5 mm inverse double-resonance cryoprobe. Selective saturation of the protein was achieved by a train of Gaussian pulses of 50 ms length, truncated at 1% and separated by 1 ms delay. A total of 40 selective

pulses were applied, leading to a saturation train of 2.04 s. The on-resonance irradiation of the protein was performed at -1.1 ppm, while the off-resonance irradiation was set at 114 ppm, where no protein signals were present. The total number of scans was 64, 256 or 512, preceded by 8 dummy scans. The spectra were subtracted internally by phase cycling after every scan using different memory buffers for on- and off-resonance. A second manual subtraction of the STD spectrum for cells+receptor from the STD spectrum for cells+receptor+(47) sample, afforded a double-difference saturation transfer (STDD) spectrum. Spectra processing was performed on Silicon Graphics Octane workstations using XWinnmr 3.1 software (Bruker). Dr. Wolfgang Bermel from Bruker Analytik (Germany) kindly provided the automation routine commonly used for the additional difference in STDD.

Group epitope mapping analysis

The group epitope mapping was accomplished by referencing the STDD integrals for the individual protons to the strongest STD signal in each spectrum, which was assigned as 100%.

Table 5.13. Group epitope mapping (GEM) analysis for CB1/CB2 and haplosamate A (relative to H18/H21 at 0.96 ppm).

N	Proton	δ (ppm)	CB1 STD (%)	CB2 STD (%)
1	H28	0.75	76	49
2	H27	0.80	72	59
3	H26	0.88	91	76
4	H18, H21	0.95, 0.97	100	100
5	H22 β , H19, H1 α	1.21, 1.25, 1.27	59	39
6	H11, H24	1.420, 1.423	30	-
7	H14, H1 β , H5, H11	1.49, 1.51, 1.5421, 1.5422	37	-
8	H2 β , H22 α , H20	1.86, 1.87, 1.88	37	26
9	H6	4.15	21	50

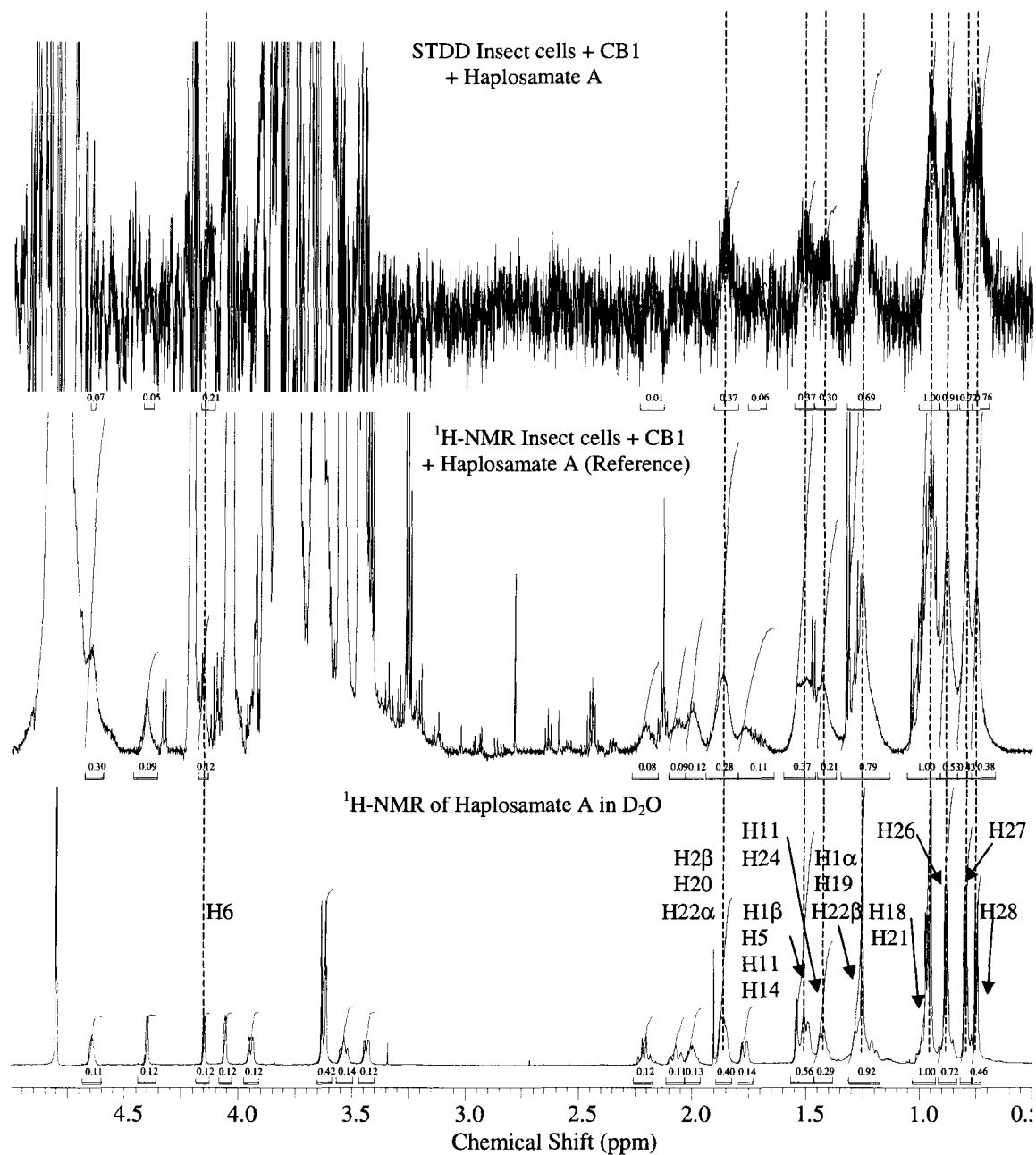


Figure 5.22. Integration of proton signals for the STD percentage measurement in a suspension of the cannabinol human receptor CB1 supported in insect cells and haplosamate A (47) (relative to H18/H21 at 0.96 ppm).

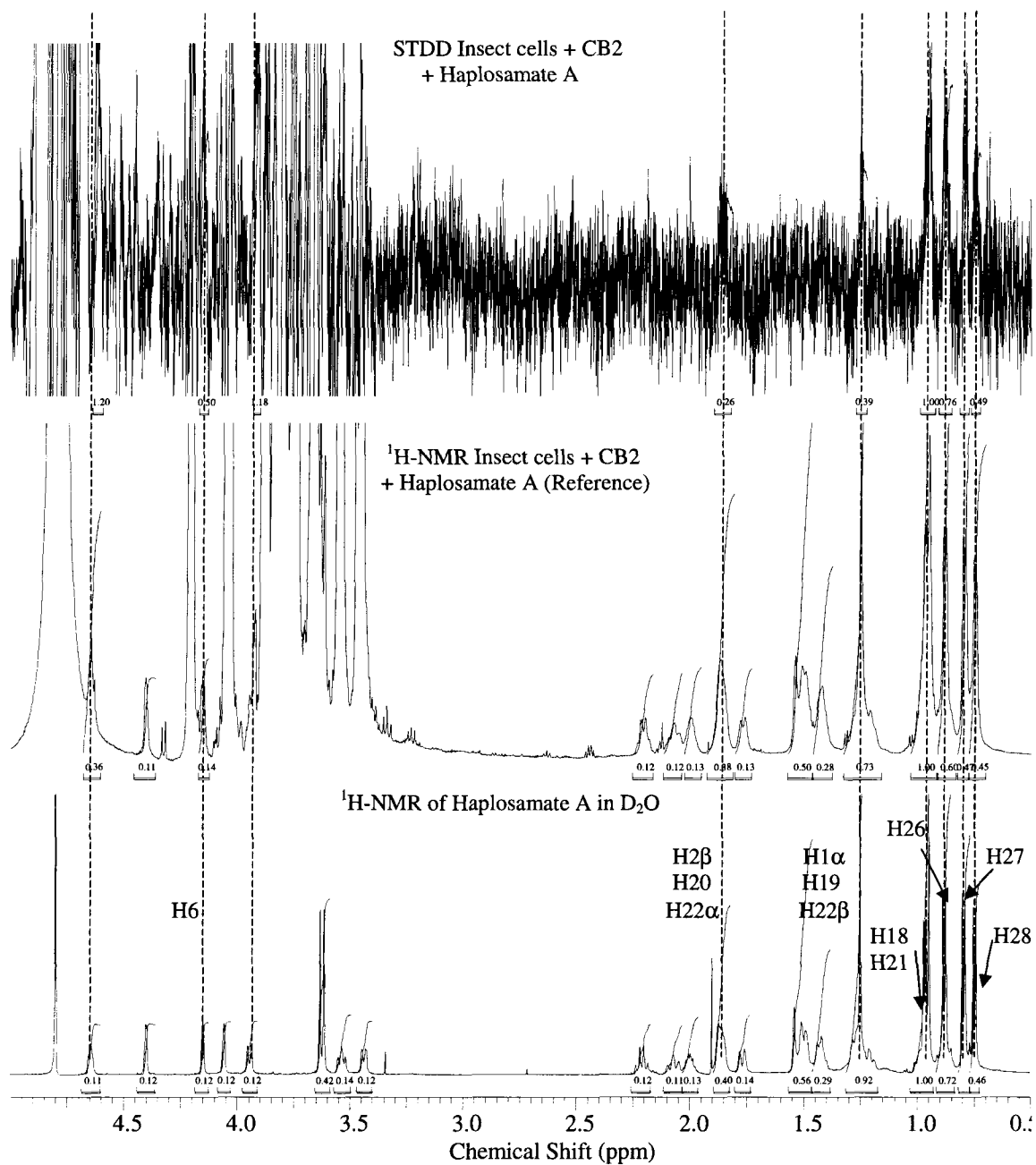


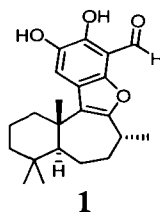
Figure 5.23. Integration of proton signals for the STD percentage measurement in a suspension of the cannabinol human receptor CB2 supported in insect cells and haplosamate A (47) (relative to H18/H21 at 0.96 ppm).

6. Synthesis of Liphagal Analogues

6.1. Liphagal, a selective PI3K α inhibitor

The phosphatidylinositol-3-kinase (PI3K) signaling pathway plays a central role in regulating cell proliferation and survival, adhesion, membrane trafficking, movement, differentiation, glucose transport, neurite outgrowth, as well as superoxide production.⁴⁷¹⁻⁴⁷⁴ There are several closely related PI3K isoforms exhibiting different biological activities,^{471,474-476} and over the past five years a growing appreciation of the therapeutic potential of PI3K inhibitors has encouraged significant efforts within the pharmaceutical industry to identify new inhibitory compounds with enhanced potency, selectivity and pharmacological properties.^{471,477} Such drugs are destined for the treatment of inflammatory and autoimmune disorders as well as cancer and cardiovascular diseases.^{472,475,478}

When a library of marine invertebrate extracts was screened as part of a program designed to find new isoform-selective PI3K inhibitors, the meroterpenoid liphagal (**1**) was identified via bioassay-guided fractionation of extracts from the sponge *Aka coralliphaga* collected in Dominica.⁴⁷² Liphagal (**1**), which has an unprecedented carbon skeleton, inhibited PI3K α with an IC₅₀ of 100 nM and approximately a 10-fold selectivity compared to PI3K γ in a fluorescent polarization enzyme bioassay.⁴⁷²



Liphagal (**1**) provided one more chemotype⁴⁷⁵ for the development of new synthetic PI3K inhibitors useful as biological tools and potential drug candidates.

6.2. The phosphatidylinositol-3-kinase (PI3K) signaling pathway

The term PI3K is applied to a large family of lipid signaling kinases that catalyze the phosphorylation of phosphatidylinositol-4,5-bisphosphate (PI-4,5-P₂ **2**) giving rise to the second messenger phosphatidylinositol-3,4,5-trisphosphate (PI-3,4,5-P₃ **3**).^{471,475,478} Although undetectable in resting cells, this compound is synthesized by PI3K's in response to a wide array of extracellular stimuli,^{472,474} and provides a critical signal for a downstream cascade of events that control diverse cellular processes (see Section 6.1 and Figure 6.1).^{471,472}

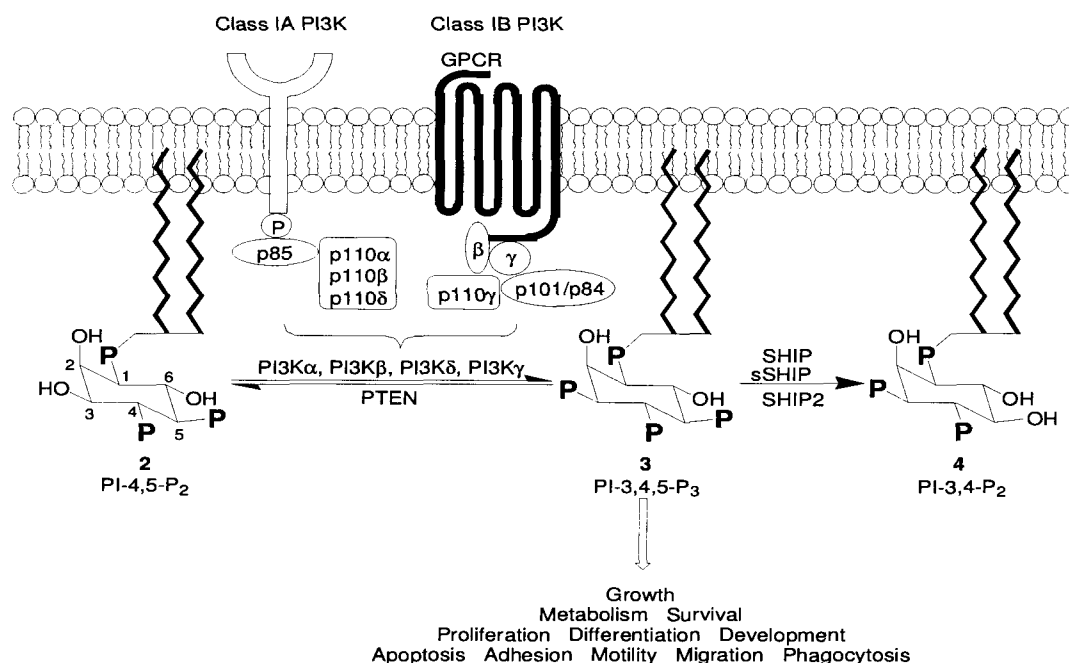


Figure 6.1. Enzymatic synthesis and degradation of PI-3,4,5-P₃ (**3**) during the first steps of the PI3K signaling pathway.^{473,476}

In order to terminate PI3K signaling and ensure a tight regulation, cells degrade PI-3,4,5-P₃ (**3**) back to PI-4,5-P₂ (**2**) via PTEN (a 3'-phosphatase termed phosphatase and tensin

homology deleted on chromosome ten), or to phosphatidylinositol-3,4-bisphosphate (PI-3,4-P₂ **4**) through at least three phosphatases: SHIP, sSHIP and SHIP2 (Src homology 2-containing inositol 5-phosphatases).^{471,479,480} Found only in blood cells, SHIP is a negative regulator of mast cell and macrophage activation, osteoclast formation and resorptive function.^{479,481} Its product PI-3,4-P₂ (**4**) can also mediate PI3K-dependent responses.⁴⁷¹

Table 6.1. Organization of the PI3K's family.^{471,475}

Class	Catalytic subunit	Adaptor/Binding partner	Distribution
IA	p110 α	p85 α , p50 α , p55 α	Broad
	p110 β	p85 β	Broad
	p110 δ	p55 α	Leukocytes
IB	p110 γ	p101/p84	Leukocytes
II ^a	PI3K-C2 $\alpha/\beta/\gamma$	Clathrin ^b	Broad ^c
III	PI3K	p150	Broad

^aThree isoforms, γ is liver specific. ^bA protein involved in endocytosis. ^cResistant to wortmannin.

Different types of PI3K's have been identified and grouped into three classes according to their primary and secondary structures, mode of regulation and substrate specificity (Table 6.1).^{471,475,478,480} Class I PI3K's have been the most extensively studied, and consist of two subgroups of heterodimeric proteins (Figure 6.1).⁴⁷⁸ The class IA members are composed of a catalytic 110 kDa subunit exhibiting three known isoforms (p110 α , p110 β , p110 δ), and a tightly associated 85 kDa regulatory subunit that controls their expression, activation and subcellular localization (five isoforms: p85 α , p85 β , p55 γ , p55 α and p50 α).^{471,480} They are often activated by growth factor and cytokine receptors through a tyrosine-kinase-dependent mechanism, and their main role seems to be the direction of energy into cell growth and proliferation.^{476,478} Unlike the omnipresent PI3K α and PI3K β isoforms, PI3K δ is predominantly expressed in the

haematopoietic (blood) system and possesses important roles in T and B-cell signaling, the neutrophil oxidative burst, and mast-cell-mediated allergic responses.^{475,478}

The only class IB isoform described so far, PI3K γ , possesses its 110 kDa-catalytic subunit associated with one of two regulatory subunits, p101 and p84 (Figure 6.1).^{475,482} PI3K γ is mostly activated by seven-transmembrane-spanning G-protein-coupled receptors (GPCR's) through direct interaction with the G protein $\beta\gamma$ -subunits.^{475,478,480} Like PI3K δ , it is also highly expressed in blood cells and controls processes in inflammation and allergy.^{476,478} The PI3K family is completed by the class II C2-domain-containing PI3K's and the class III phosphatidylinositol-specific 3-kinases (Table 6.1), of which little is known.^{476,482}

The differential tissue distribution of PI3K isoforms is a key factor in the distinct biological functions of PI3Ks.⁴⁷⁸ Complete genetic inactivation of the omnipresent PI3K α or PI3K β resulted in embryonic lethality, attributing essential and non-redundant roles to these isoforms.^{475,478} Therefore, from a drug development perspective pharmacological inhibition of PI3K α and PI3K β activities is likely to be associated with significant toxicity.⁴⁷⁷ By contrast, PI3K δ and PI3K γ expression is mainly restricted to the haematopoietic system, and mutant mice deprived of their expression or function, either by deletion of the whole gene (p110 δ and p110 γ -knockout mice) or by mutation of the kinase domain (p110 δ and p110 γ kinase-inactive knock-in mice), are viable, fertile and apparently healthy with a normal life span.^{475,476,478,483} Thus, both PI3K δ and PI3K γ isoforms represent promising therapeutic targets to intervene signaling pathways involved in inflammatory and auto immune diseases^{473,476,478,483,484} such as rheumatoid arthritis, systemic lupus erythematosus (SLE), multiple sclerosis, asthma, chronic obstructive pulmonary disease, and psoriasis.

Recent interest in PI3K signaling has also been fuelled by evidence that the PI3K pathway is among the most commonly activated signaling pathways in cancer.^{477,480} For instance,

the PI3K α isoform was found to be activated by mutation in colon, gastric and breast carcinomas,⁴⁷⁶ and is likely to be the most commonly mutated kinase in the human genome.⁴⁷⁷ The presence of PI3K β mutations in colon cancer and its role in metastasis of a prostate mouse model was recently demonstrated.⁴⁷⁶ An increase of PI-3,4,5-P₃ (**3**) has also proved to promote tumor progression in mutant mice lacking functional PTEN, a well-characterized tumor suppressor frequently inactivated in human cancer by mutation, gene deletion or epigenetic silencing.^{471,476,480} There is also evidence that SHIP acts as a tumor suppressor in both acute myelogenous leukemia (AML)⁴⁸⁵ and chronic myelogenous leukemia (CML).⁴⁸⁶ Furthermore, many tyrosine kinases that activate PI3K are themselves the target of mutations or amplification in cancer. Together, these observations clearly reveal a connection of genetic alterations in cancer that stimulate PI3K signaling, suggesting that PI3K activation is likely to be an essential step in tumorigenesis.^{476,480}

Such an impressive variety of potential therapeutic applications has led some authors to compare a pure hypothetical isoform-selective PI3K inhibitor with classical cyclooxygenase-inhibitor drugs like aspirin.⁴⁷⁵

6.3. First generation PI3K inhibitors

The early availability of PI3K inhibitors played an essential role in understanding PI3K signaling processes.^{472,477} The fungal natural product wortmannin (**5**),⁴⁸⁷⁻⁴⁸⁹ isolated from *Penicillium wortmanni*, was originally described as a potent inhibitor of the respiratory burst in neutrophils and monocytes,^{477,490} and later shown to target PI3K's via nucleophilic attack of Lys833 (p110 α within the ATP-binding site) at the highly electrophilic C20 position of the furan ring yielding an enamine (Figure 6.2).^{471,477} The concentration of wortmannin (**5**) required for

PI3K inhibition ranges between 1-100 nM.⁴⁷¹ Equivalent nucleophilic residues can be found in all PI3 and protein kinases, and probably account for the poor selectivity of **5**.^{473,476,478}

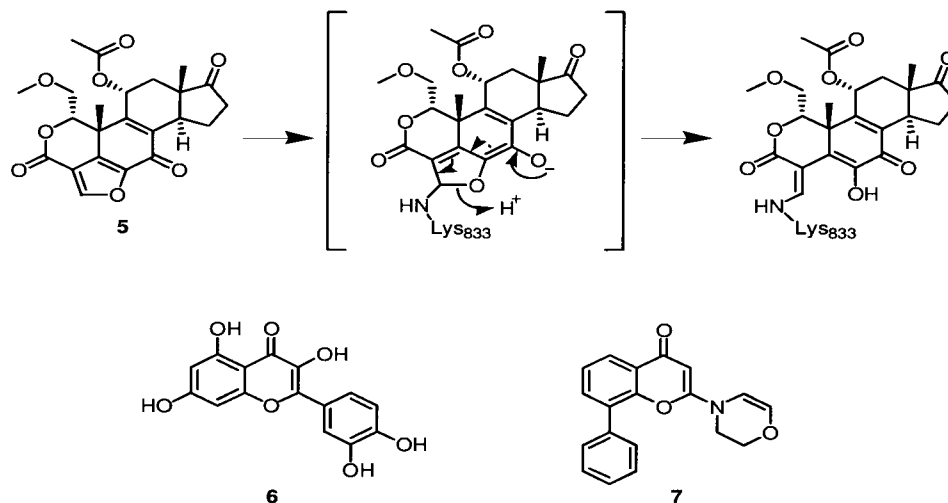


Figure 6.2. First generation PI3K inhibitors.

The widely distributed flavonoid quercetin (**6**)⁴⁹¹⁻⁴⁹⁴ showed inhibition of PI3K with an IC_{50} of 3.8 μ M, but also exhibited poor selectivity by acting on PI4K's as well as several tyrosine and serine/threonine kinases.^{471,477} This compound was used as a template for SAR studies, from which the synthetic inhibitor LY294002 (**7**) (IC_{50} 100 μ M) was identified.^{494,495} Unlike quercetin (**6**), LY294002 (**7**) had no detectable effect on other ATP-requiring enzymes.⁴⁷¹ Both compounds are competitive and inhibit PI3K's in a reversible fashion at the ATP binding site.^{477,494}

Wortmannin (**5**) and LY294002 (**7**) have been extensively used for more than a decade to analyze PI3K-driven pathways.^{477,478,480} These molecules, however, do not exhibit any degree of selectivity for individual PI3K isoforms and moreover, they have been shown to also block class II and class III PI3Ks, as well as other closely related enzymes such as mammalian target of

rapamycin (MTOR), and unrelated enzymes such as casein kinase 2 (CK2), myosin light chain kinase (MLCK) and polo-like kinase (PLK).^{471,474,478,480}

6.4. Isoform-selective second generation inhibitors

Although the multiple roles of PI3K's initially raised concerns about potential target-related toxicity and unwanted side effects, the benign phenotypes of the PI3K δ and PI3K γ mutant mice (knock-out and knock-in), as well as their confined expression pattern (blood cells) gained interest from pharmaceutical companies to pursue the development of orally active and selective small-molecule inhibitors of PI3K.^{475,477,496} As a result, over the past five years there has been a rapid increase in patenting activity disclosing new isoform-selective PI3K-inhibitor chemotypes, for the treatment of various human diseases including inflammatory autoimmune conditions (rheumatoid arthritis, SLE and psoriasis), allergic diseases (asthma), and cardiovascular disorders (thrombosis, atherosclerosis, cardiac hypertrophy).^{473-475,478,483} In 2006 alone, eight different lead compounds (including liphagal **1**) entered the patent literature.⁴⁷⁵

From a structural viewpoint, all PI3K inhibitors available to date can be classified in two groups: derivatives of LY294002 (arylmorpholine compounds) and non-related structures.^{474,475} The available co-crystal structure of PI3K γ with LY294002 (**7**) provided unique and valuable insights into the general binding mode and key interactions involved in PI3K γ binding (Figure 6.3).^{471,475,477} The oxygen in the morpholino ring forms a hydrogen bond with Val-882, whereas another hydrogen bridge links the chromone keto-oxygen and Lys-833. The first interaction is shared by all PI3K inhibitors and ATP, and a clamp of approximately 8 Å spanned between these two oxygen atoms is known to be essential for PI3K binding, making it a common motif throughout many chemotypes of PI3K inhibitors (Figure 6.3).⁴⁷⁷

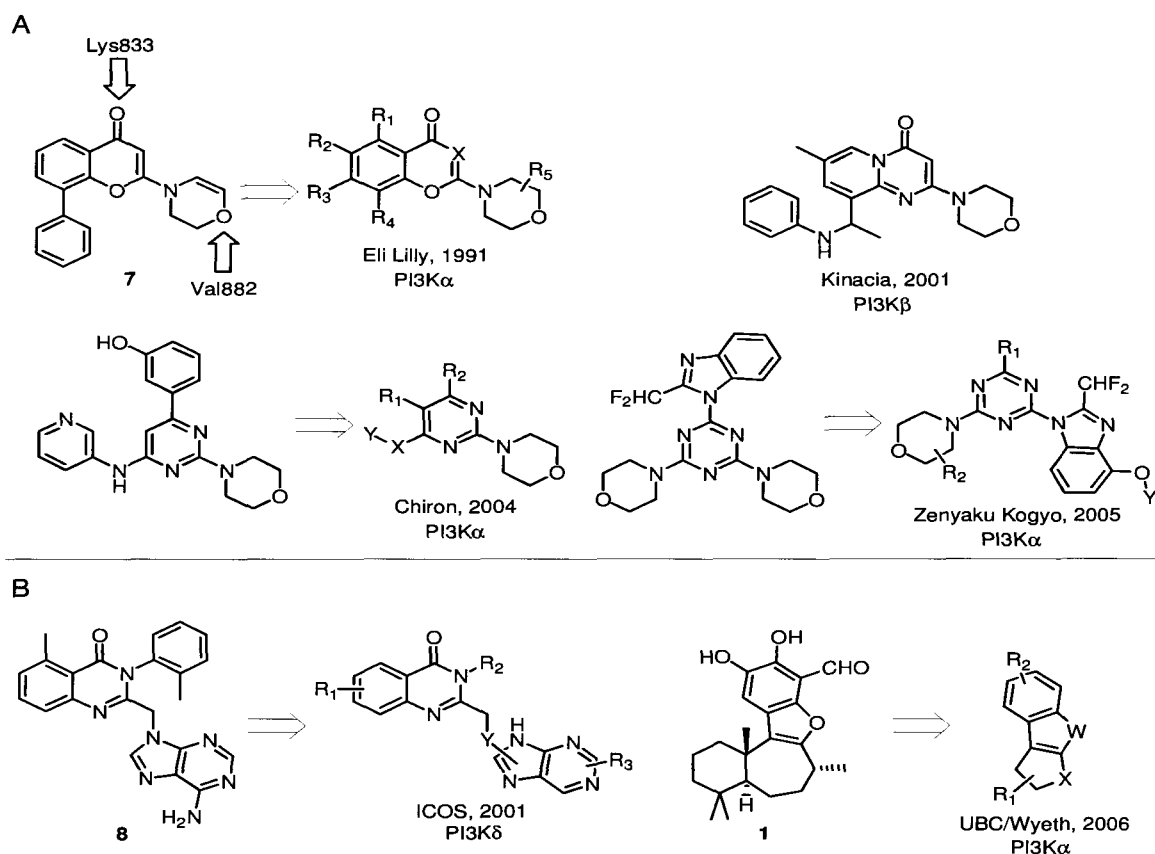
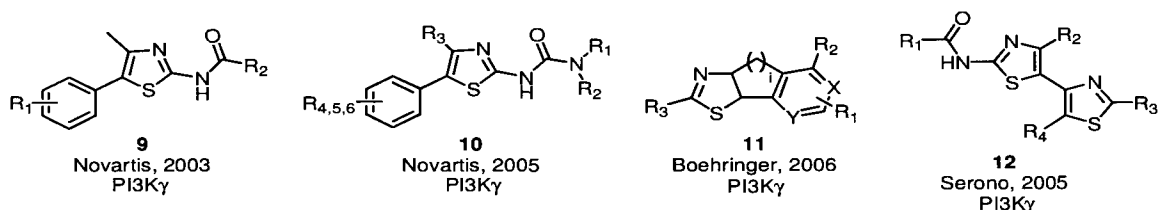
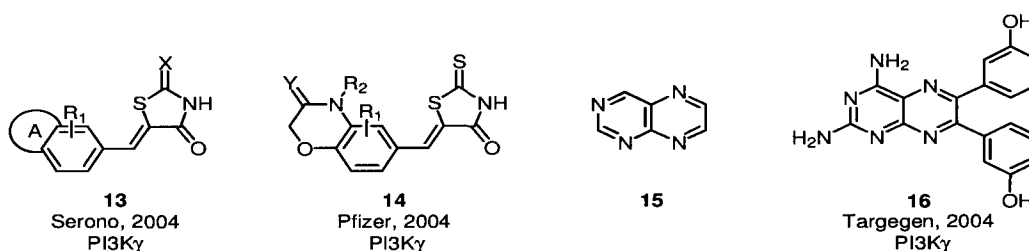


Figure 6.3. Some PI3K-inhibitory chemotypes: A) arylmorpholine and B) non-related structures.

The quinazolinone purine IC87114 (**8**) patented by ICOS 2001 is one of the most remarkable isoform-selective inhibitors described to date.^{474,477,497} The compound exhibited nanomolar inhibition of PI3K δ and a 100-1000-fold selectivity against the other class I PI3K's.⁴⁹⁷ In the following years, a series of aminothiazoles (**9-11**)^{498,499} and amino-bis-thiazoles (**12**)⁵⁰⁰ have been disclosed by Novartis, Boehringer and Serono, with a primary focus on respiratory diseases. Their linked aromatic and heteroaromatic cycles have been found to interact with the inositol binding site of PI3K γ .⁴⁷⁵



Almost simultaneously, Pfizer and Serono presented in 2004 thiazolidinediones derivatives (**13** and **14**)^{501,502} for the treatment of rheumatoid disease. In these compounds, the slightly acidic imide-NH of the thiazolidinedione motif was shown to bind PI3K γ .⁴⁷⁵ A third class of inhibitors is based on the alkaloid pteridine (**15**),⁵⁰³ and the lead compound of the series, TG100-115 (**16**),⁵⁰⁴ is currently in preclinical development for acute myocardial infarction.



Another structurally unrelated class of PI3K inhibitors was released by Bayer in 2004, and consists of imidazo[1,2-c]quinazolines (**17**)⁵⁰⁵ claiming a broad coverage of inflammatory and immunoregulatory disorders.

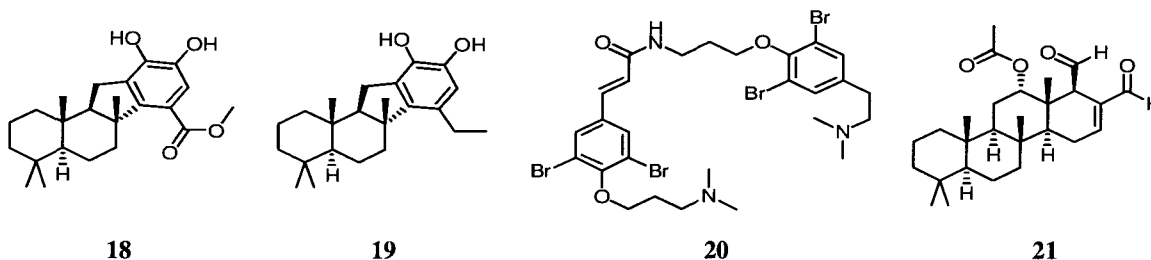


In general, all these molecules are reversible inhibitors that bind the ATP-binding pocket of PI3K and exhibit nanomolar affinity for their primary target.⁴⁷⁷ While no absolute preference

between PI3K isoforms has been achieved, some of them present a remarkable ~100-fold selectivity.⁴⁷⁵ Co-crystal structures for some of these inhibitors and p110 γ are also available.^{496,506}

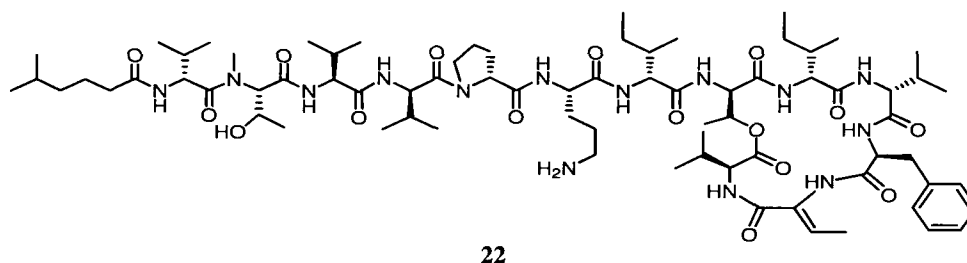
6.5. Marine natural products and the PI3K signaling pathway

A year before the reported isolation of liphagal (**1**) in 2006, the Andersen research group published the isolation and synthesis of another inositolphosphatase-active meroterpenoid. Identified from the sponge *Dactylospongia elegans* collected in Papua New Guinea, pelorol (**18**)^{479,507,508} exhibited selective *in vitro* activation of SHIP, whereas its C20 methyl analogue (**19**) showed promising *in vivo* activity in two mouse models of inflammation, confirming SHIP-activators as a new class of anti-inflammatory agents.⁴⁷⁹

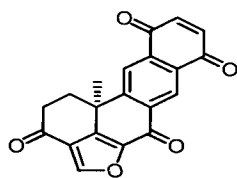


Also in 2005, Clardy and coworkers⁵⁰⁹ isolated a previously unreported bromotyrosine derivative from the sponge *Psammaphysilla* sp., collected in the Indian Ocean. Named psammaphysene A (**20**), the compound was shown to compensate for loss of PTEN (PTEN deficiencies have been observed in several human malignancies, Section 6.2) by relocalizing the transcription factor FOXO1a, one of its downstream targets. In another example, Xie and researchers⁵¹⁰ demonstrated that scalaradial (**21**),^{511,512} isolated from the sponge *Cacospongia*

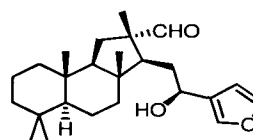
sp., binds to epidermal growth factor receptors (EGFR) and inhibits phosphorylation. EGFR's are one of the multiple activators of the PI3K signaling pathway.



Janmaat and colleagues⁵¹³ confirmed that inhibition of the PI3K pathway is an important determinant for the *in vitro* cytotoxic activity of kahalalide F (**22**), a known antitumor agent originally isolated from the Hawaiian marine mollusk *Elysia rufescens*⁵¹⁴⁻⁵¹⁶ and currently undergoing phase II clinical trials (Chapter 2, Section 2.1). Similarly, Ohizumi and his research group proposed the inhibition of PI3K activity as a mechanism for the observed halenaquinone⁵¹⁷⁻⁵¹⁹ (**23**)-induced apoptosis of nerve-growth factor PC12 cells.



23



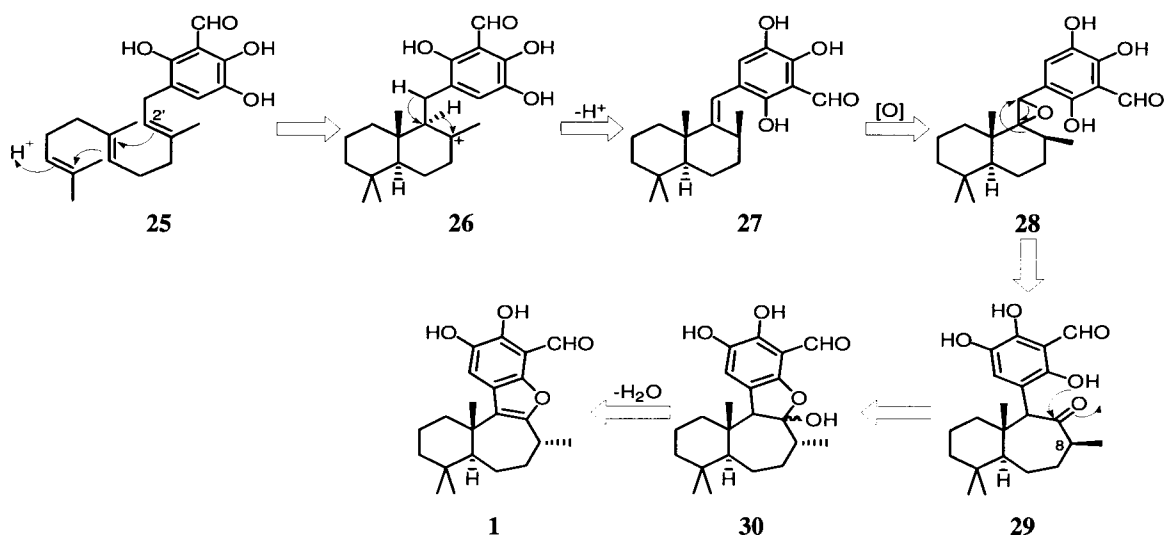
24

More recently in 2007, Sun and coworkers⁵²⁰ reported that hyrtiosal (**24**),^{521,522} isolated from the marine sponge *Hyrtios erectus*, is a noncompetitive inhibitor of protein tyrosine phosphatase 1B (PTP1B), a negative modulator of insulin signaling and one of the many downstream enzymes involved in the PI3K signaling pathway. Likewise, Kwon and Nam⁵²³ found that a PI3K-related insulin growth factor mediates apoptosis in gastric cancer cells when

they are treated with an unidentified polysaccharide extracted from the marine algae *Capsosiphon fulvescens*, commonly used as foodstuff in Korea.

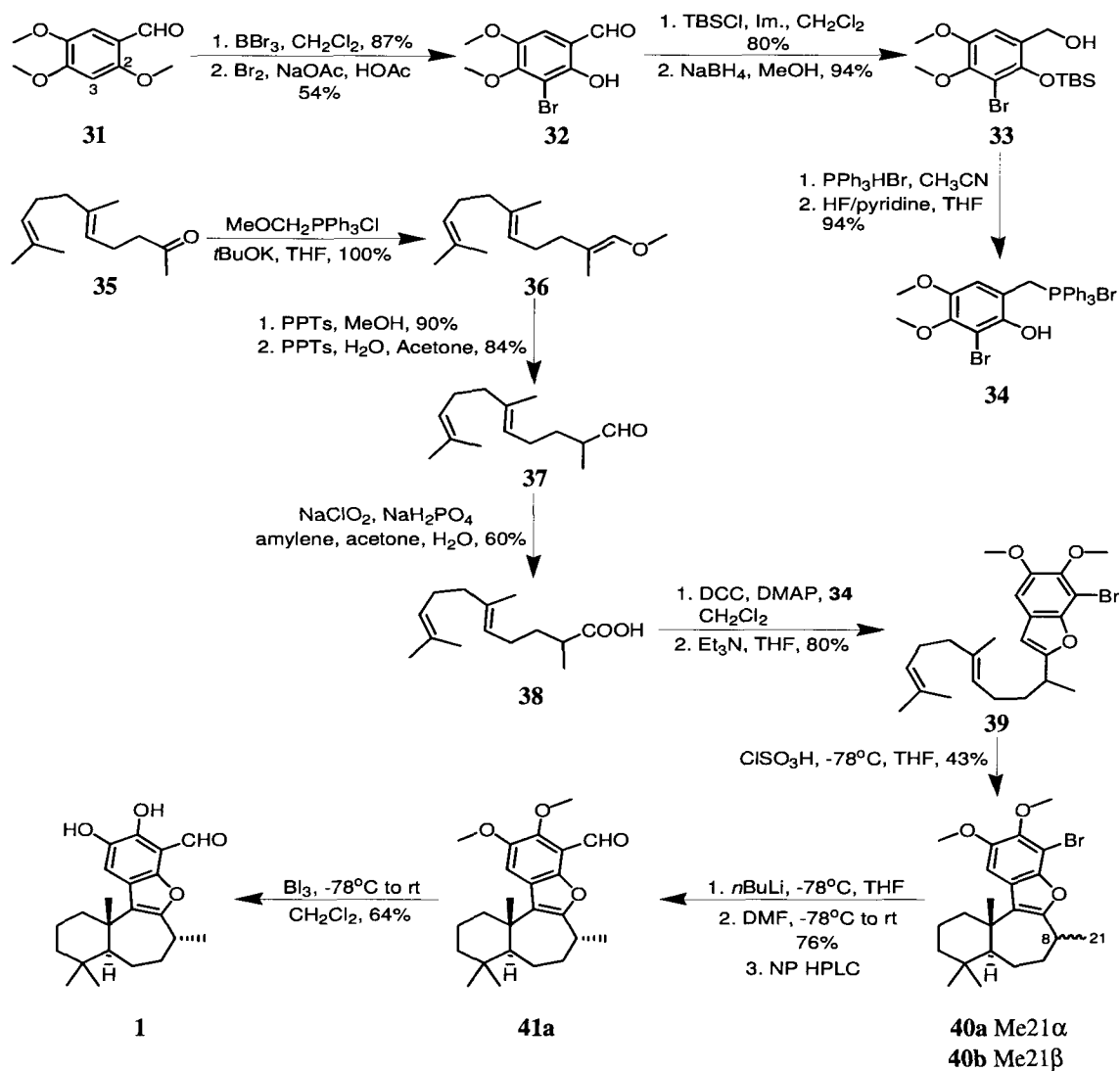
6.6. Biogenesis and synthetic preparations of liphagal

Liphagal (**1**) represented the first example of the “liphagane” meroterpenoid carbon skeleton.⁴⁷² Its biosynthesis may involve a proton initiated polyene cyclization, with C2' of farnesylated trihydroxybenzaldehyde (**25**) acting as a nucleophilic center, followed by two Wagner-Meerwein hydride shifts to produce siphonodictyal B (**27**) (Scheme 6.1).⁴⁷² This compound was first isolated in 1981 by Faulkner and coworkers^{524,525} from specimens of *Aka coralliphaga* collected in Belize.⁵²⁵ In 2003, Schmitz and his group⁵²⁶ found a sulfated version in *A. coralliphaga* sponges taken from the coasts of Micronesia, whereas more recently Kock and Assmann⁵²⁷ reisolated **27** from the same organism together with eleven previously unreported analogues, including several *ortho*-quinones with radical-scavenging properties.



Scheme 6.1. Proposed biogenesis of (+)-liphagal (**1**).⁴⁷²

Continuing from siphonodictyal B (**27**), a seven-membered ring could be generated via ring expansion of epoxide (**28**) to afford ketone (**29**), which undergoes epimerization at C8 and hemiketal formation to give **30**. In the last step, dehydration of **30** would yield liphagal (**1**).⁴⁷²

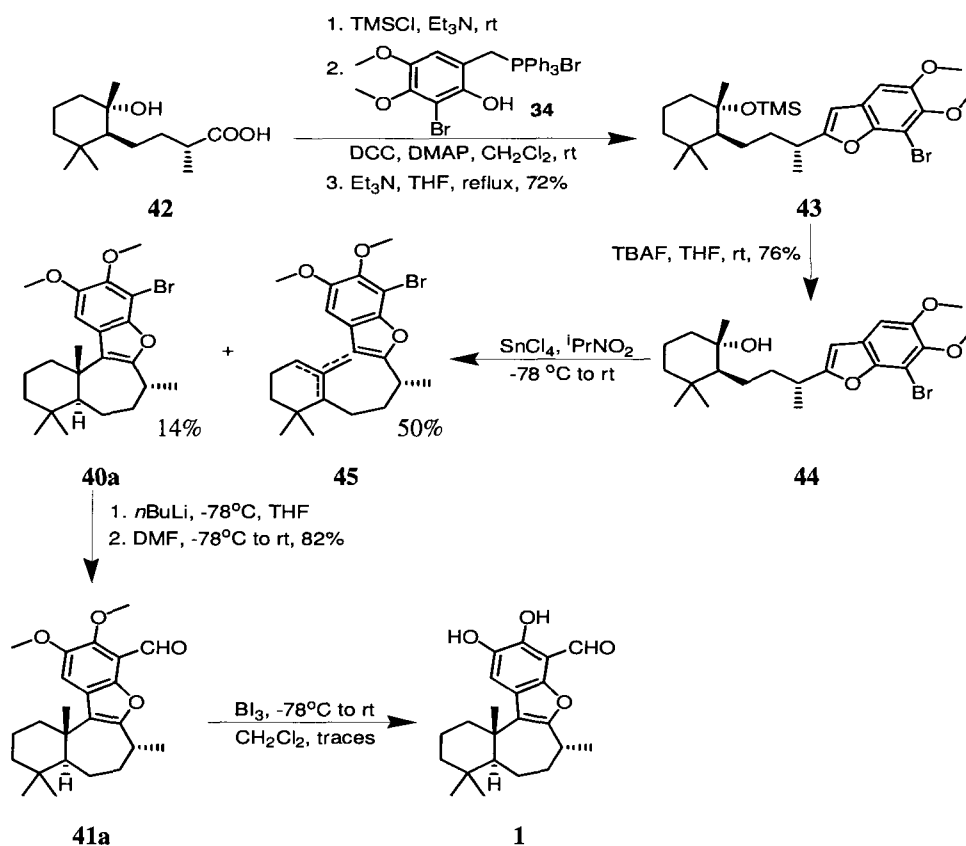


Scheme 6.2. Biomimetic synthesis of liphagal (**1**).⁴⁷² Only the natural enantiomeric configuration of **1** and its precursors is shown.

The structure of liphagal (**1**) was confirmed by synthesis. Using a biomimetic approach (Scheme 6.2), 2,4,5-trimethoxybenzaldehyde (**31**) was selectively demethylated at C2 with BBr_3 , and the resulting phenol was brominated at C3 to give **32**. Protection of this compound with TBSCl and reduction of the resulting aldehyde with sodium borohydride produced benzyl alcohol (**33**), which was treated with triphenylphosphine/HBr followed by removal of the TBS protecting group with HF/pyridine complex in THF to give phosphonium salt (**34**). Synthesis of the isoprenoid fragment started with a Wittig reaction on geranylacetone (**35**) to give enol ether (**36**). Hydrolysis of this intermediate formed aldehyde (**37**), which upon NaClO_2 oxidation yielded the corresponding acid (**38**). DCC-mediated coupling of **34** and **38**, followed by reflux with Et_3N in THF brought about an intramolecular Wittig reaction resulting in the formation of benzofuran (**39**).⁵²⁸

The key cyclization step proceeded with best results by treatment of **39** with chlorosulfonic acid at -78°C in nitropropane, affording a 2/5 mixture of the C8 epimers (**40a**) and (**40b**).⁵²⁹ The aldehyde functionality was introduced by halogen-lithium exchange followed by condensation with DMF and hydrolysis.⁵³⁰ After normal-phase HPLC separation, the desired compound (**41a**) was demethylated with BI_3 to yield liphagal (**1**).

Since the natural product possesses a dextrorotatory nature ($[\alpha]_{\text{D}}^{20} = +12.0^\circ$) and the previous synthesis leads to a racemic mixture of **1**, an enantioselective preparation was implemented using compound (**44**) as starting material in a Lewis acid-catalyzed cyclization step (Scheme 6.3).⁵³¹ This key precursor was obtained from the synthetically accessible (-)-(1'S,2'S,2R)-4-(2'-hydroxy-2',6',6'-trimethylcyclohexyl)-2-methylbutanoic acid (**42**)⁵³²⁻⁵³⁵ and phosphonium salt (**34**), as previously shown.



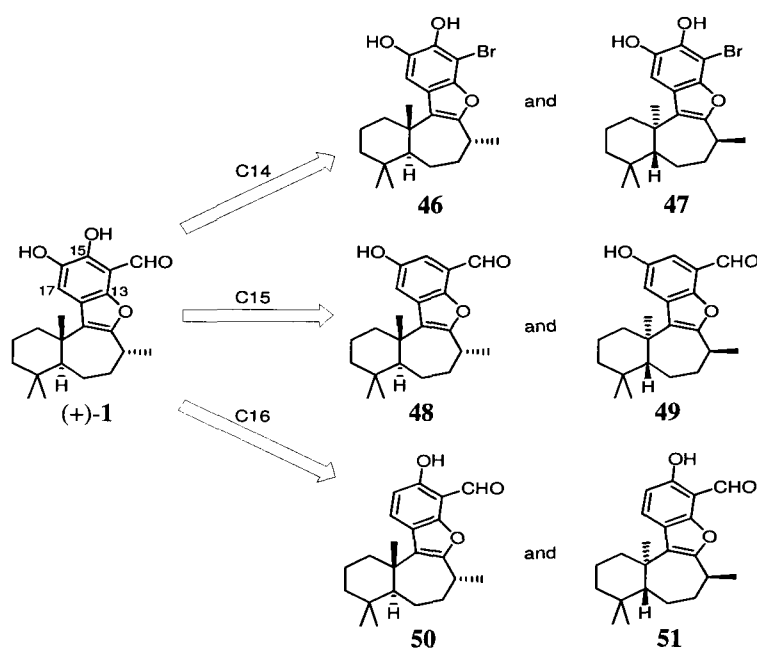
Scheme 6.3. Enantioselective synthesis of (+)-liphagal (**1**).⁵³¹

This enantioselective preparation afforded a highly unstable final product, only in enough quantities for its characterization as liphagal (**1**). Although new proton resonances could be detected in the ¹H-NMR spectrum of **1** in less than one hour, no degradation compounds were characterized. An important amount of intermediate (**44**) underwent dehydration and subsequent loss of chirality to give a mixture of benzofurans (**45**), which was transformed into racemic (**40a,b**) by treatment with chlorosulfonic acid in nitropropane at low temperature.

In order to carry out structure-activity relationship (SAR) studies and develop more stable isoform-selective PI3K inhibitors based on the new liphagane carbon skeleton, a compound optimization program was scheduled. This chapter summarizes the main findings obtained when a small library of liphagal analogues was prepared.

6.7. Preparation of liphagal analogues

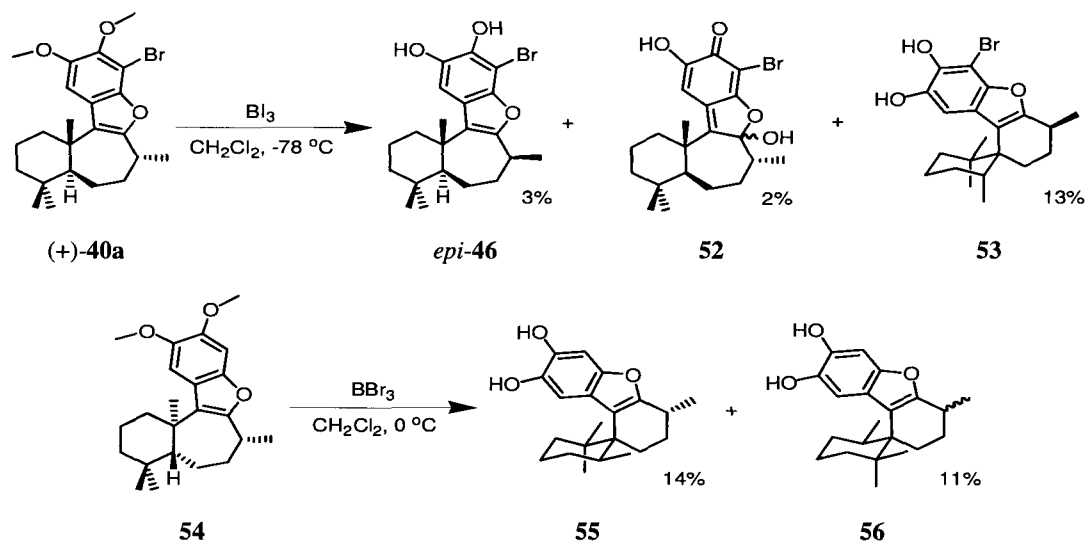
Our compound optimization program (Scheme 6.4) employed the enantioselective synthesis of liphagal (**1**) as a basis to generate a series of (+) and (-)-liphagane derivatives exhibiting a different substitution pattern in the aromatic portion, considered essential to bind PI3K α as well as to be the main source of instability.



Scheme 6.4. Planned sequential variation of functional groups in (+)-liphagal (**1**).

6.7.1. Variation at C14

Modification at C14 involved only demethylation of compound (**40a**). Additionally, the starting material was debrominated to examine whether the catechol is required for activity. However, BI₃ and BBr₃ mediated deprotections led to unexpected results (Scheme 6.5).



Scheme 6.5. Demethylations of (+)-40a and 54. Only one enantiomer is shown.

As expected, compound *epi*-(46) showed very similar NMR data (Figure 6.4, Table 6.2) when compared to that previously reported for starting material (+)-(40a).⁴⁷² The replacement of two sharp methyl singlets close to 4.0 ppm by two broad singlets at δ_{H} 4.73 and δ_{H} 4.85 typical for a catechol moiety, as well as a $[\text{M}-\text{H}]^-$ peak at m/z 405.1068 in agreement with the target formula $\text{C}_{21}\text{H}_{27}\text{O}_3\text{Br}$ (calculated for $\text{C}_{21}\text{H}_{26}\text{O}_3^{79}\text{Br}$: 405.1065), confirmed the expected double demethylation. Additionally, the very diagnostic methine H8 (δ_{H} 2.97, δ_{C} 31.6) displayed a more complicated coupling pattern and upfield chemical shift than expected, indicating epimerization at C8.

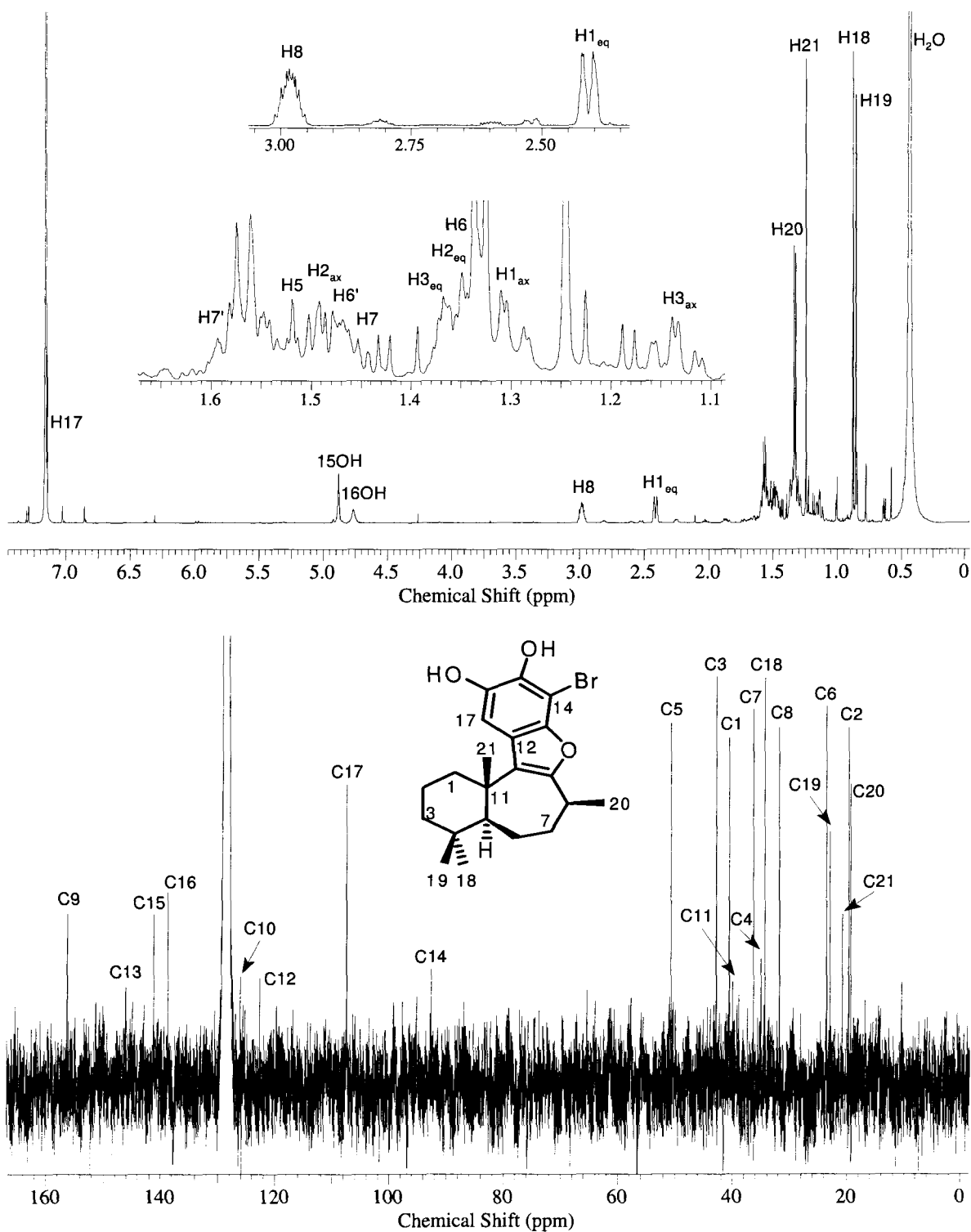
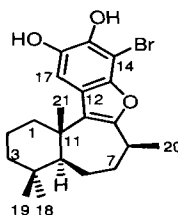


Figure 6.4. ^1H and ^{13}C -NMR spectra of (+)-8-*epi*-desformyl-14-bromoliphagane (**46**) (recorded in C_6D_6 at 600 and 150 MHz respectively).

Table 6.2. NMR data for (+)-8-*epi*-desformyl-14-bromoliphagane (**46**) (recorded in C₆D₆).

Carbon No	¹³ C δ (ppm) ^a	¹ H δ (ppm) (mult, J (Hz)) ^{b,c}	HMBC ^b (H→C)
1	40.5	H _{ax} 1.31 (m), H _{eq} 2.42 (m)	C10
2	19.5	H _{eq} 1.360 (m), H _{ax} 1.52 (qt, J = 3.2, 13.9 Hz)	
3	42.7	H _{ax} 1.15 (td, J = 3.4, 13.3 Hz), H _{eq} 1.37 (m)	
4	34.9		
5	50.5	1.56 (m)	C6, C19, C21
6	23.4	1.362 (m), 1.49 (m)	
7	36.2	1.47 (m), 1.60 (m)	
8	31.6	2.97 (m)	
9	156.1		
10	125.9		
11	39.9		
12	122.5		
13	146.0		
14	92.5		
15	141.0	OH 4.85 (s, broad)	
16	138.5	OH 4.73 (s, broad)	
17	107.3	7.14 (s)	C13, C15, C16
18	34.2	0.88 (s)	C3, C5, C19
19	22.8	0.86 (s)	C3, C4, C5
20	19.2	1.32 (d, J = 6.9 Hz)	C7, C8, C9
21	20.7	1.24 (s)	C1, C5, C10

^a Recorded at 150 MHz. ^b Recorded at 600 MHz. ^c According to HSQC recorded at 600 MHz.

This compound proved to be highly susceptible to the slightest presence of acid and O₂, and total degradation when dissolved in CDCl₃ occurred in less than five hours. With C₆D₆ as NMR solvent, **46** reacted slow enough to allow 2D NMR characterization. The main degradation product was identified as compound (**52**), also isolated from the initial reaction crude.

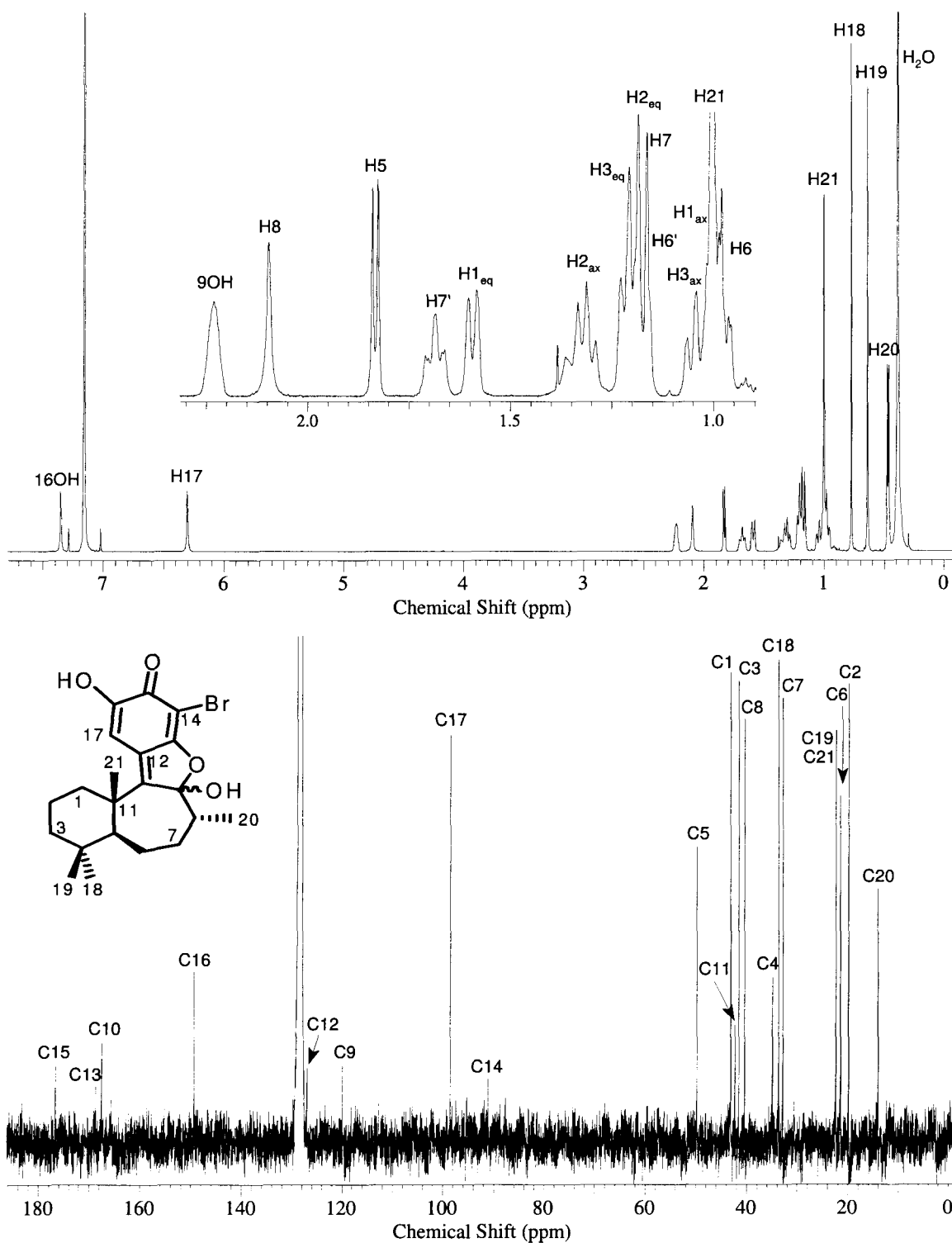
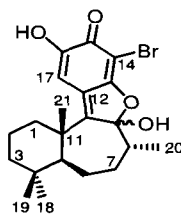


Figure 6.5. ^1H and ^{13}C -NMR spectra of (+)-14-bromo-9,16-dihydroxyliphagane quinone (**52**) (recorded in C_6D_6 at 600 and 150 MHz respectively).

Table 6.3. NMR data for (+)-14-bromo-9,16-dihydroxyliphagane quinone (**52**) (recorded in C_6D_6).

Carbon No	^{13}C δ (ppm) ^a	1H δ (ppm) (mult, J (Hz)) ^{b,c}	HMBC ^b (H→C)
1	43.1	H _{ax} 1.07 (m), H _{eq} 1.59 (m)	C3, C5
2	19.8	H _{eq} 1.21 (m), H _{ax} 1.33 (qt, $J = 2.9, 13.4$ Hz)	C3, C4, C5
3	41.5	H _{ax} 0.99 (td, $J = 2.5, 12.8$ Hz), H _{eq} 1.22 (m)	C1, C2, C5, C18, C19
4	34.9		
5	49.7	1.84 (d, $J = 8.4$ Hz)	C4, C6, C7, C10, C11, C18, C19
6	21.4	0.98 (m), 1.176 (m)	C4, C5, C7, C8, C11
7	32.8	1.179 (m), 1.71 (m)	C5, C9, C20
8	40.4	2.12 (m)	C9, C10
9	120.0	OH 2.24 (s, broad)	C8, C9
10	167.5		
11	42.3		
12	127.0		
13	168.3		
14	91.0		
15	176.6		
16	149.2	OH 7.36 (s)	C15, C16, C17
17	98.5	6.31 (s)	C12, C13, C15, C16
18	33.7	0.78 (s)	C2, C3, C4, C5, C19
19	22.3	0.64 (s)	C3, C4, C5, C18
20	14.0	0.47 (d, $J = 6.9$ Hz)	C7, C8, C9
21	22.3	1.01 (s)	C1, C5, C10

^a Recorded at 150 MHz. ^b Recorded at 600 MHz. ^c According to HSQC recorded at 600 MHz.

Besides possessing the diagnostic 1H -NMR methyl pattern for the liphagane skeleton inverted (d→s→s→s in Figure 6.5, compare with Figure 6.4: s→s→s→d), compound (**52**) exhibited a characteristic quinone carbonyl C15 (δ_C 176.6) and two broad singlets typical for OH

protons involved in hydrogen bonding, one of which (δ_{H} 7.36) must be located *ortho* to C15. The second (δ_{H} 2.24) was unambiguously placed at C9 (δ_{C} 120.0), a vinylic hemiketal carbon. This assignment was supported by HMBC correlations (Table 6.3, Figure 6.6). HRESIMS gave a $[\text{M}+\text{H}]^+$ peak at 423.1160 that corresponded to the molecular formula $\text{C}_{21}\text{H}_{27}\text{O}_4\text{Br}$ (calculated for $\text{C}_{21}\text{H}_{28}\text{O}_4^{79}\text{Br}$: 423.1171), confirming the presence of an extra oxygen. The new hydroxyl at C9 explains the high shielding effect experienced by H20 (δ_{H} 0.47, δ_{C} 14.0).

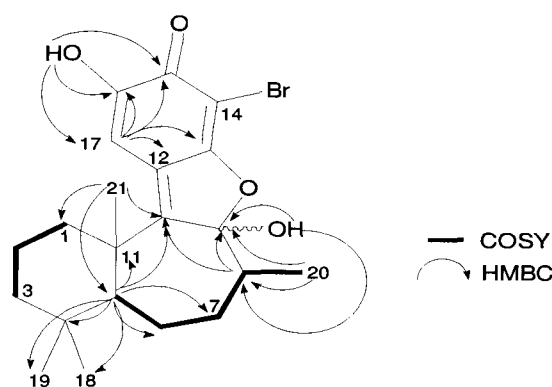


Figure 6.6. Representative HMBC (H→C) and COSY correlations for **52**.

The NMR data for a third reaction product (Figure 6.7, Table 6.4) revealed a compound that had undergone complete rearrangement of the liphagane skeleton, clearly indicated by a new methyl doublet replacing a singlet as the most shielded resonance in the ^1H -NMR (δ_{H} 0.85, δ_{C} 17.0). Although demethylation took place (broad singlets at 5.10 and 5.35 ppm), and the expected molecular formula $\text{C}_{21}\text{H}_{27}\text{O}_3\text{Br}$ was confirmed by HRESIMS (calculated for $\text{C}_{21}\text{H}_{27}\text{O}_3\text{Na}^{79}\text{Br}$ 429.1041; found 429.1050), 2D NMR analysis showed that ring contraction proceeded to yield spiro-compound (**53**) as the major reaction product. Unlike *epi-46*, **52** and their corresponding unnatural enantiomers, **53** exhibited a flat circular dichroism curve, implying that its formation may have involved ring opening and closing processes through a carbocation intermediate.

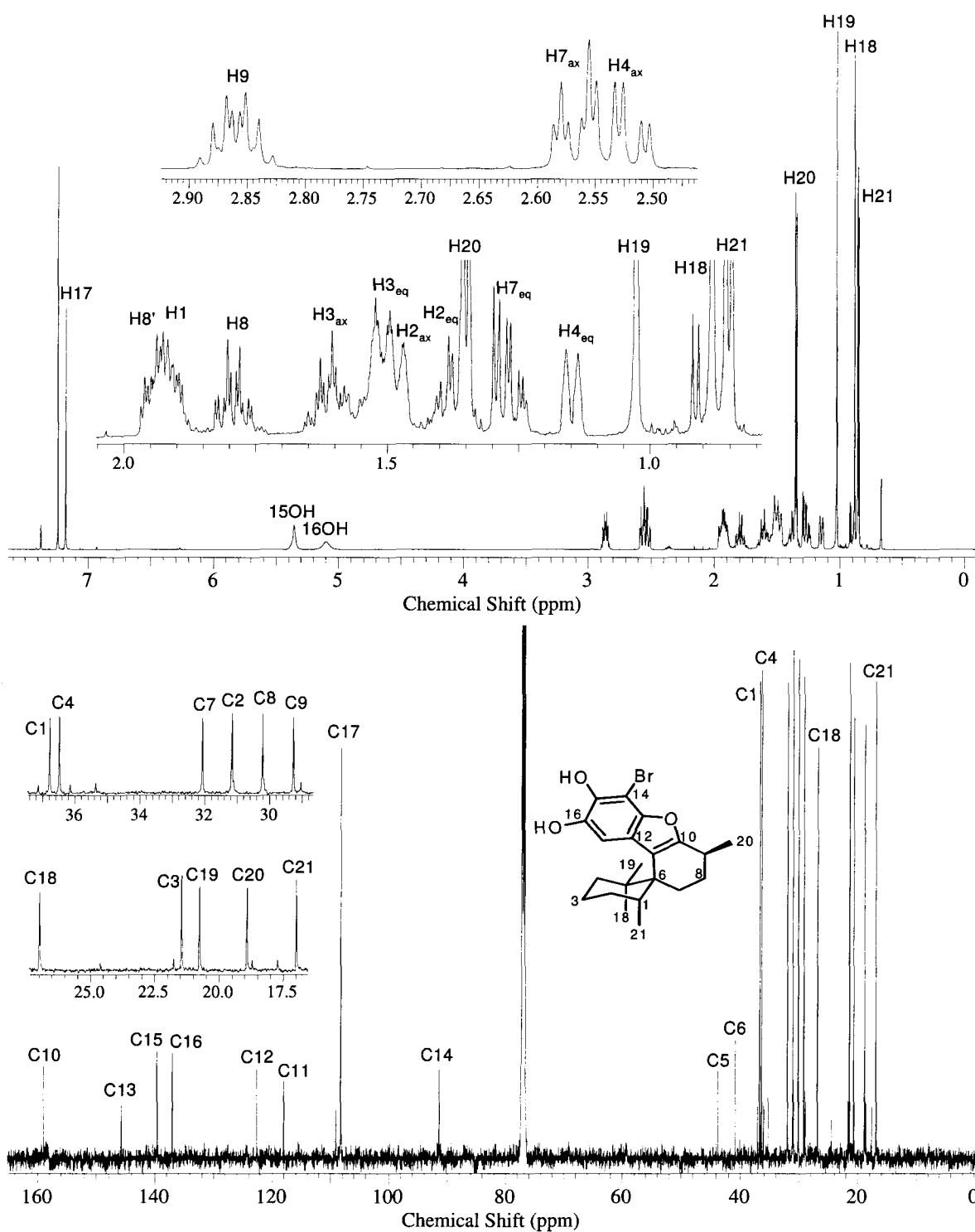
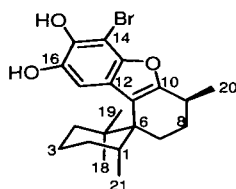


Figure 6.7. ^1H and ^{13}C -NMR spectra of (\pm) -desformyl-14-bromospiroliphagal (**53**) (recorded in CDCl_3 at 600 and 150 MHz respectively).

Table 6.4. NMR data for (\pm)-desformyl-14-bromospiroliphagal (**53**) (recorded in CDCl₃).

Carbon No	¹³ C δ (ppm) ^a	¹ H δ (ppm) (mult, <i>J</i> (Hz)) ^{b,c}	HMBC ^b (H→C)
1	36.8	1.91 (m)	C2, C3, C6, C21
2	31.2	H _{eq} 1.36 (m), H _{ax} 1.48 (m)	C3, C4, C21
3	21.4	H _{eq} 1.50 (m), H _{ax} 1.61 (qt, <i>J</i> = 4.4, 17.8 Hz)	C2
4	36.5	H _{eq} 1.15 (m), H _{ax} 2.51 (td, <i>J</i> = 4.2, 13.7 Hz)	C2, C3, C5, C7
5	43.8		
6	40.9		
7	32.1	H _{eq} 1.27 (m), H _{ax} 2.57 (dt, <i>J</i> = 3.7, 14.3 Hz)	C1, C5, C6, C8, C9, C11
8	30.2	H _{eq} 1.80 (m), H _{ax} 1.94 (m)	C5, C7, C9, C10, C20
9	29.3	2.86 (m)	C8, C10, C11, C20
10	159.1		
11	118.1		
12	122.7		
13	145.8		
14	91.5		
15	139.6	OH 5.35 (s, broad)	C14, C15, C16
16	137.1	OH 5.10 (s, broad)	C17
17	108.3	7.18 (s)	C11, C13, C14, C15, C16
18	27.0	0.88 (s)	C4, C5, C6, C19
19	20.7	1.03 (s)	C4, C5, C6, C18
20	18.9	1.35 (d, <i>J</i> = 6.8 Hz)	C8, C9, C10
21	17.0	0.85 (d, <i>J</i> = 6.8 Hz)	C1, C2, C6

^a Recorded at 150 MHz. ^b Recorded at 600 MHz. ^c According to HSQC recorded at 600 MHz.

The newly formed methyl doublet, assigned as H21, its α -methine H1 (δ_{H} 1.91, δ_{C} 36.8), as well as methyls H18 (δ_{H} 0.88, δ_{C} 27.0) and H19 (δ_{H} 1.03, δ_{C} 20.7), all presented a long-range HMBC correlation (among others, Table 6.4, Figure 6.8) with the quaternary spiro-carbon C6

(δ_C 40.9), absent in the starting material. This centre divides COSY correlations (Figure 6.8, Table 6.14, experimental section) in two groups, for each of the two six-membered rings constituting **53**. Similarly, methylene H7 (δ_H 1.27/2.57, δ_C 32.1) located in ring B displayed informative HMBC cross-peaks with all carbons two or three bonds apart, including C6, C1 and quaternary C5 (δ_C 43.8) in ring A.

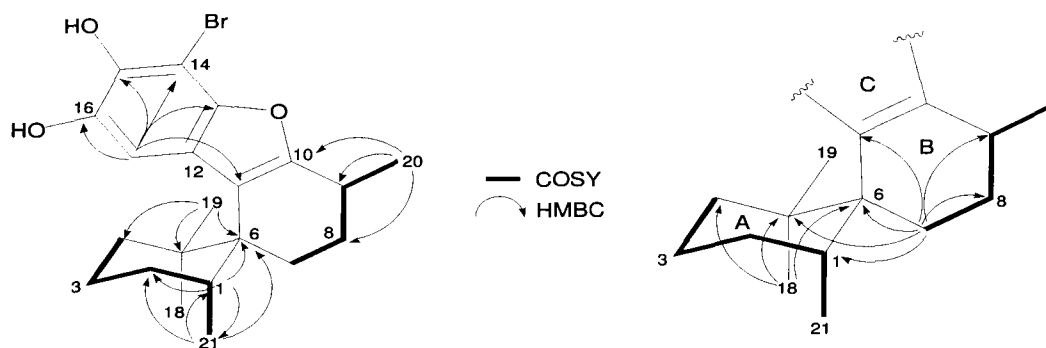
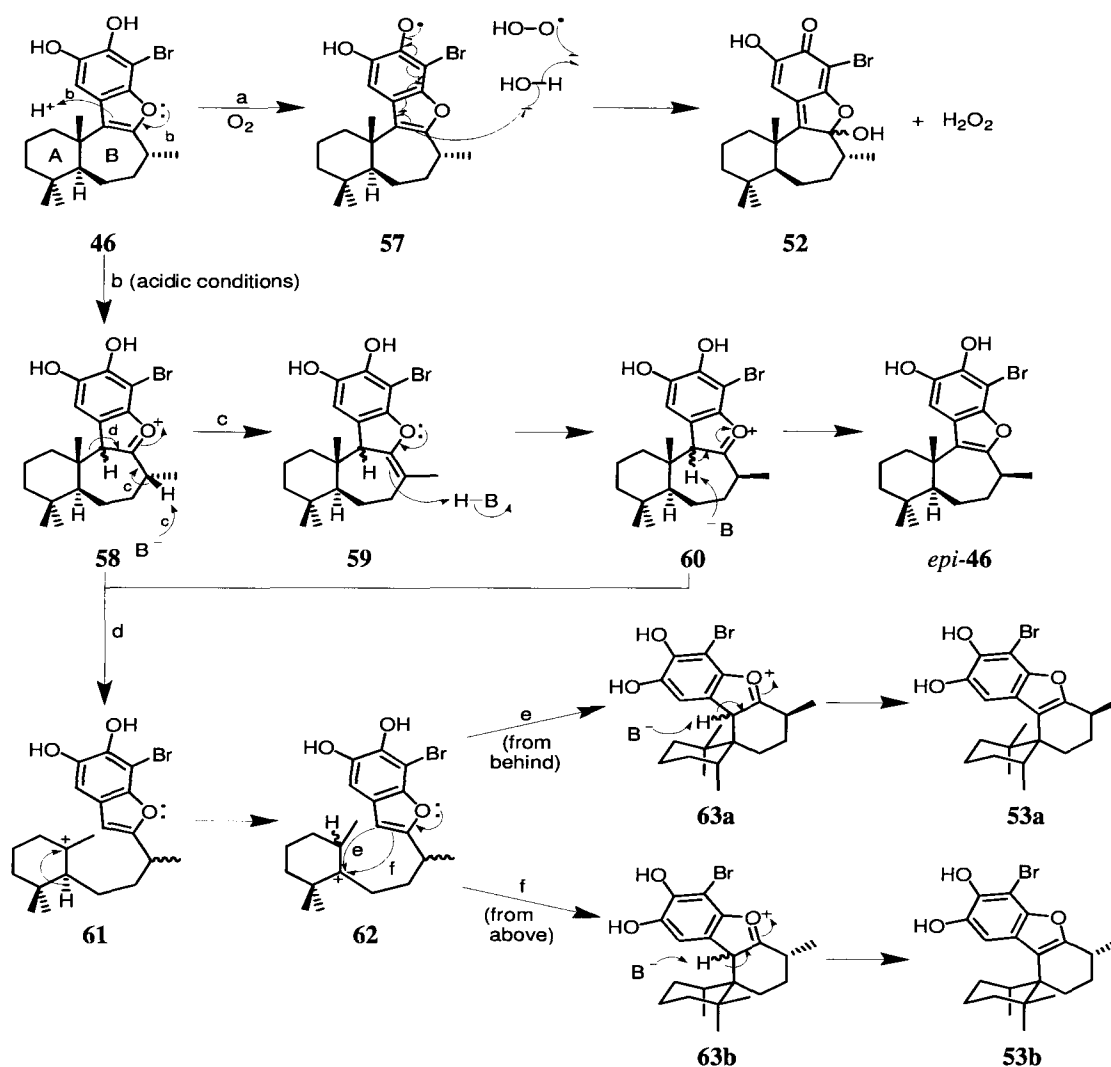


Figure 6.8. Representative HMBC (H→C) and COSY correlations for **53**.

All three deprotection products displayed a slightly yellow-green coloration that intensified with time. The effect was particularly dramatic for *epi*-**46** and **53**. According to Scheme 6.6, an O₂-mediated radical oxidative process in **46** could form **52** even in the absence of catalytic amounts of acid (route a, as when dissolved in C₆D₆). Work-up conditions generate small amounts of HI, that may catalyze epimerization at C8 to give *epi*-**46** (routes b and c), or ring contraction via carbocation intermediates (route d). An acid-promoted opening of the seven-membered B-ring of **58** would generate carbocation (**61**). Since formation of six-membered rings is favored (6-exo-trig),^{536,537} **61** might rearrange to **62** and undergo nucleophilic attack from both possible directions (behind and above the plane), yielding racemic spiro-compound (**53**). This mechanism explains the loss of optical activity via racemization observed for **53** recovered when

(+)-**40a** (having the ring junction configuration as in liphagal) and (-)-**40a** were separately treated with BI_3 .



Scheme 6.6. Proposed mechanisms for the formation of *epi*-**46**, **52** and **53a,b**.

When the same deprotection was repeated employing **54** and BBr_3 ,^{538,539} only two C9 diastereoisomeric and optically inactive spiro-compounds (**55**) and (**56**) were identified from the reaction crude (Figures 6.9, 6.18 and 6.19, Tables 6.16-6.19).

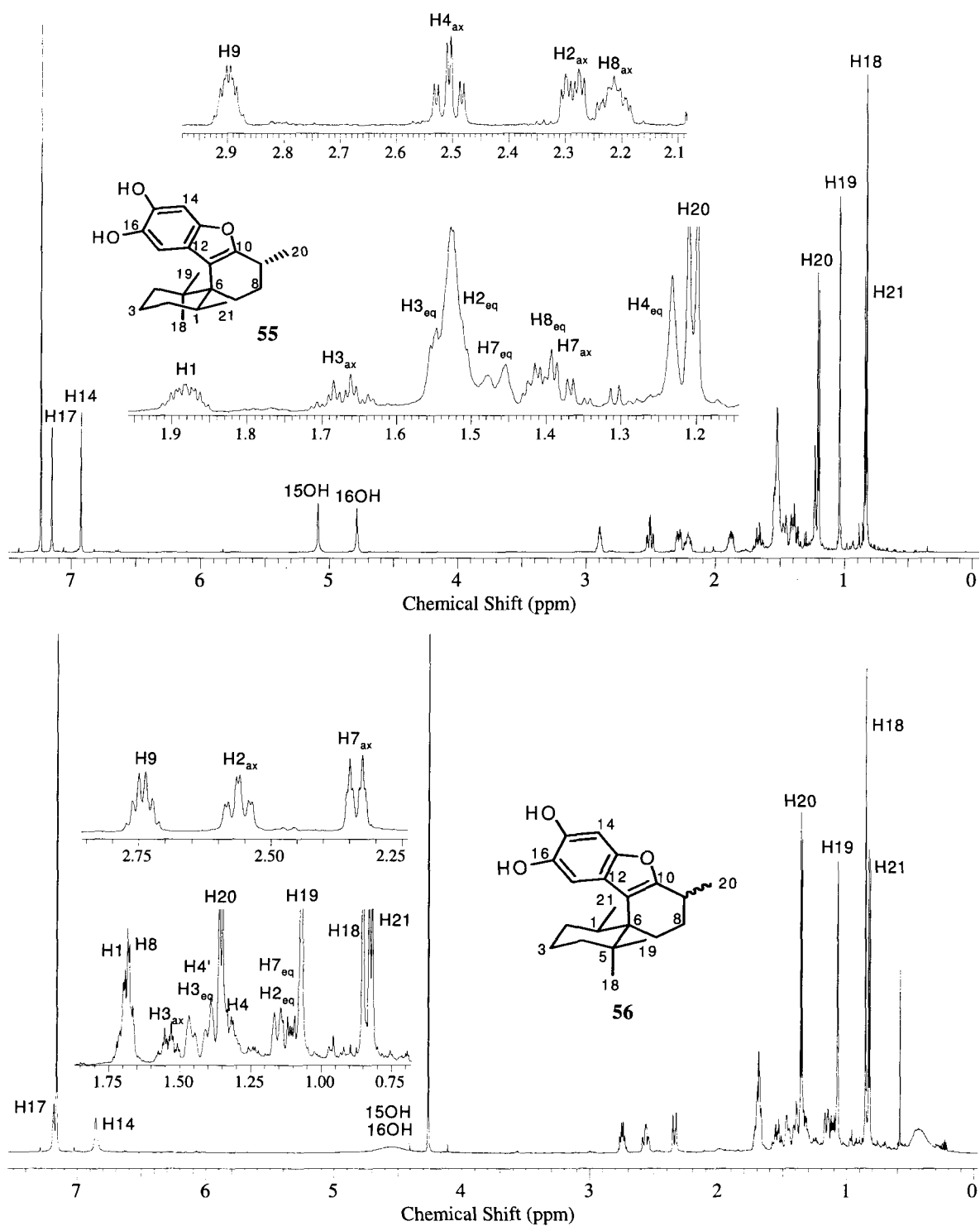
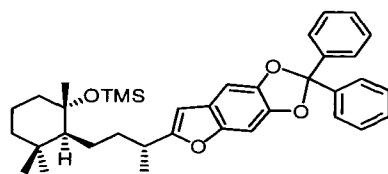


Figure 6.9. ¹H-NMR spectra of (±)-desformylspiroliphagal A (**55**) and B (**56**) (recorded in CDCl₃ and C₆D₆ respectively at 600 MHz).

Thus, in addition to racemization (both materials were also optically inactive), epimerization at C9 played a role during the formation of these compounds. t ROESY data for **56** (Table 6.19, experimental section) did not allow an unambiguous stereochemical assignment at C9, but the compound must have the same configuration as **55** in order to be its diastereoisomer. From this reaction, no products with the desired liphagane skeleton were detected. Higher temperatures and longer reaction times (both required to observe R_f changes when the deprotection was followed by TLC) favored carbocation formation and their rearranged products, together with epimerization at C9.

Evidently, both standard demethylation procedures proceeded with a high degree of rearrangements and side reactions that account for extremely low yields, and reflect the already established instability associated with the liphagane skeleton. Product isolation and purification was only possible after multiple column chromatography steps of reaction crudes, followed by HPLC. The amounts of polar degradation products separated during these refinement procedures were quite important, and displayed intense yellow to orange colorations as well as very complicated $^1\text{H-NMR}$ spectra.

Such clear incompatibility between standard demethylation reagents and our liphagane derivatives led us to evaluate other possible protecting groups for catechols. Considering the SnCl_4 mediated cyclization as the most unfriendly step, silicon-based reagents were discarded due to their intolerance toward Lewis acid conditions.⁵⁴⁰ Dichlorodiphenylmethane is widely used for protection of both 1,2-diols and catechols,⁵⁴⁰ and allowed the preparation of **64** and its enantiomer with acceptable yields (Experimental section).⁵⁴¹⁻⁵⁴³ However, upon SnCl_4 treatment neither cyclization products nor starting materials were detected in reaction crudes.

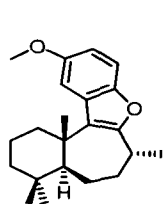


64

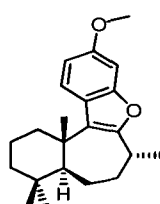
6.7.2. Variations at C15 and C16

As previously experienced, catechols are highly susceptible to oxidation and produce hydroxyquinones even under neutral conditions when exposed to atmospheric O₂. Their redox properties make these compounds useful in several biological settings.⁵⁴⁴ However, the instability associated with such a motif is not ideal for the further development and optimization of liphagal-inspired PI3K inhibitors. From a synthetic viewpoint, catechols represent an intractable functionality, and as 2-aminoimidazoles (Chapter 4) are usually deprotected in the last reaction step.^{472,479,541-543}

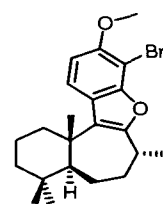
In order to confirm whether both hydroxyls at C15 and C16 are required for PI3K activity, monophenolic analogues (**65**)-(**67**) were prepared as natural (shown) and unnatural enantiomeric pairs, starting from (-) and (+)-(1*S*,2*S*,2*R*)-4-(2'-hydroxy-2',6',6'-trimethylcyclohexyl)-2-methylbutanoic acid (**42**) (15% and 18% respectively, 11 steps), as well as several phosphonium salts analogous to **34**, according to Scheme 6.3 and requiring only minor modifications to the liphagal synthetic procedures already reviewed (Experimental section).^{472,531}



65



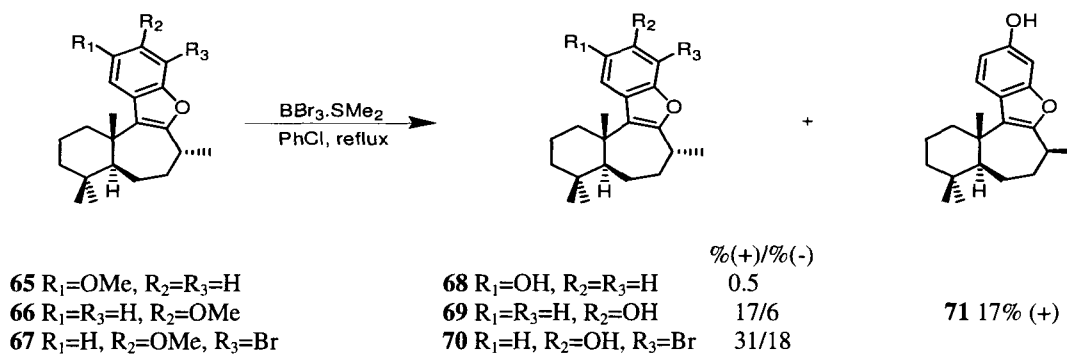
66



67

Efforts to formylate **67** via lithium-mediated C14 alkylation proceeded in very low yields (9-19%), giving mostly debromination product. A similar result was obtained with Weinreb amide as an electrophile. Anhydrous conditions are always a challenge and although measures were taken to eliminate water (THF was freshly distilled from Na/benzophenone, dry DMF was treated with activated molecular sieves, N₂ atmosphere), it is still possible that traces of water may have accounted for the low extent of formylation, especially when working on small scale (0.012-0.16 mmol). Friedel-Craft electrophilic substitution of the debrominated material may be another methodology to functionalize C14, but was not attempted due to the high risk of skeleton rearrangements under Lewis acid conditions, and an expected low regioselectivity.

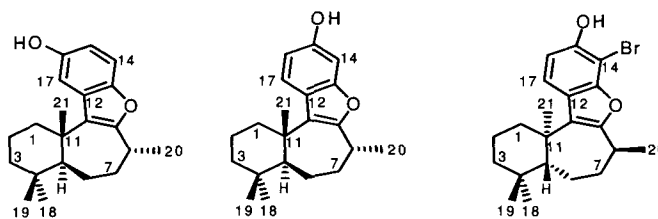
Therefore, it was decided to directly deprotect **67** and its debrominated analogue. A survey of demethylation methods led to BBr₃.SMe₂ as deprotecting reagent.^{545,546} Although some C8 epimerization was still detected, this compound definitely provided the best results, completely eliminating rearranged products (at least the ones that can be isolated) and improving reaction yields (up to 31%, Scheme 6.7). It has been suggested that an equilibrium is established between dimethyl sulfide and the aryl methyl ether starting material (both acting as Lewis bases), leading to an exceedingly mild BBr₃ release.⁵⁴⁵



Scheme 6.7. Final deprotection step in the synthesis of monophenolic liphagal derivatives.

Compounds (**68**)-(70) constitute good examples of aromatic ring activation by electron-donating substituents. As seen in Table 6.5, they shared quite similar ^{13}C -NMR data assigned to the invariable terpenoid portion (entries 1-11, 18-21). Presence of oxygen, whether from the hydroxyl or furan functionalities, is always evidenced by chemical shifts between 152.1-158.2 ppm, with the exception of C13 (δ 149.6) in **68**. A shielding effect is appreciated in this case, as well as for C12 in **69** and **70** (δ 122.8/123.6 respectively, compared with δ 130.1 in **68**), all *para* to the hydroxyl substituent. Activation of the *ortho* position is evidenced by >10 ppm differences at C14 (for **69**) and C17 (for **68**). The presence of a bulky bromine in **70** slightly shields C14 and its neighboring carbons when compared with **69**. In the case of hydroxyl, its strong electron-donating resonance effect outweighs a weaker electron withdrawing inductive effect.⁵⁴⁴ The opposite is true for halogens, but although weak, the ^{13}C -NMR data suggest donation of electronic density. Figure 6.10 shows ^{13}C -NMR spectra for **68** and **69**.

Similarly, ^1H -NMR data (Table 6.6) reflects shielding of protons *ortho* to the hydroxyl group when compared to the *meta*-positioned one (6.45/7.01 vs 7.17 for **68**, 6.55/6.71 vs 7.42 for **69**). The weak electron-donating effect of bromine additionally protects H17 (δ 7.23) in **70**. Multiplicity differences among aromatic spin systems clearly differentiate isomers **68** and **69** (Figure 6.11). In the case of **68**, H14 (δ 7.17) and H15 (δ 6.45) are vicinal and share a coupling constant of around $^3J = 8.7$ Hz. The additional doublet in H15 originates from a second long distance coupling with H17 (δ 7.01), hence the lower value of $^4J = 2.5$ Hz. For **69**, the situation is reversed: H14 (6.71) couples through four bonds with H16 (δ 6.55), which in turn is also coupled to its neighbor H17 (δ 7.42). Coupling constant values are comparable with those of **68**.

Table 6.5. ^{13}C -NMR assignments for (+)-16-hydroxyliphagane (**68**), (+)-15-hydroxyliphagane (**69**), and (+)-14-bromo-15-hydroxyliphagane (**70**) (recorded in C_6D_6).

C No	68	69 $^{13}\text{C } \delta$ (ppm) ^a	70
1	40.6	40.9	40.8
2	19.5	19.5	19.4
3	42.6	42.6	42.5
4	35.2	35.2	35.2
5	54.0	54.3	54.0
6	24.8	24.8	24.6
7	35.5	35.7	35.4
8	34.4	34.3	34.1
9	158.2	155.9	157.0
10	126.0	125.9	126.8
11	40.2	40.2	40.2
12	130.1	122.8	123.6
13	149.6	155.6	152.1
14	111.5	98.3	92.7
15	111.8	153.6	150.3
16	151.4	111.0	111.0
17	108.8	123.4	122.6
18	33.8	33.8	33.7
19	22.5	22.5	22.4
20	22.0	22.2	22.0
21	20.5	20.8	20.7

^aRecorded at 150 MHz.

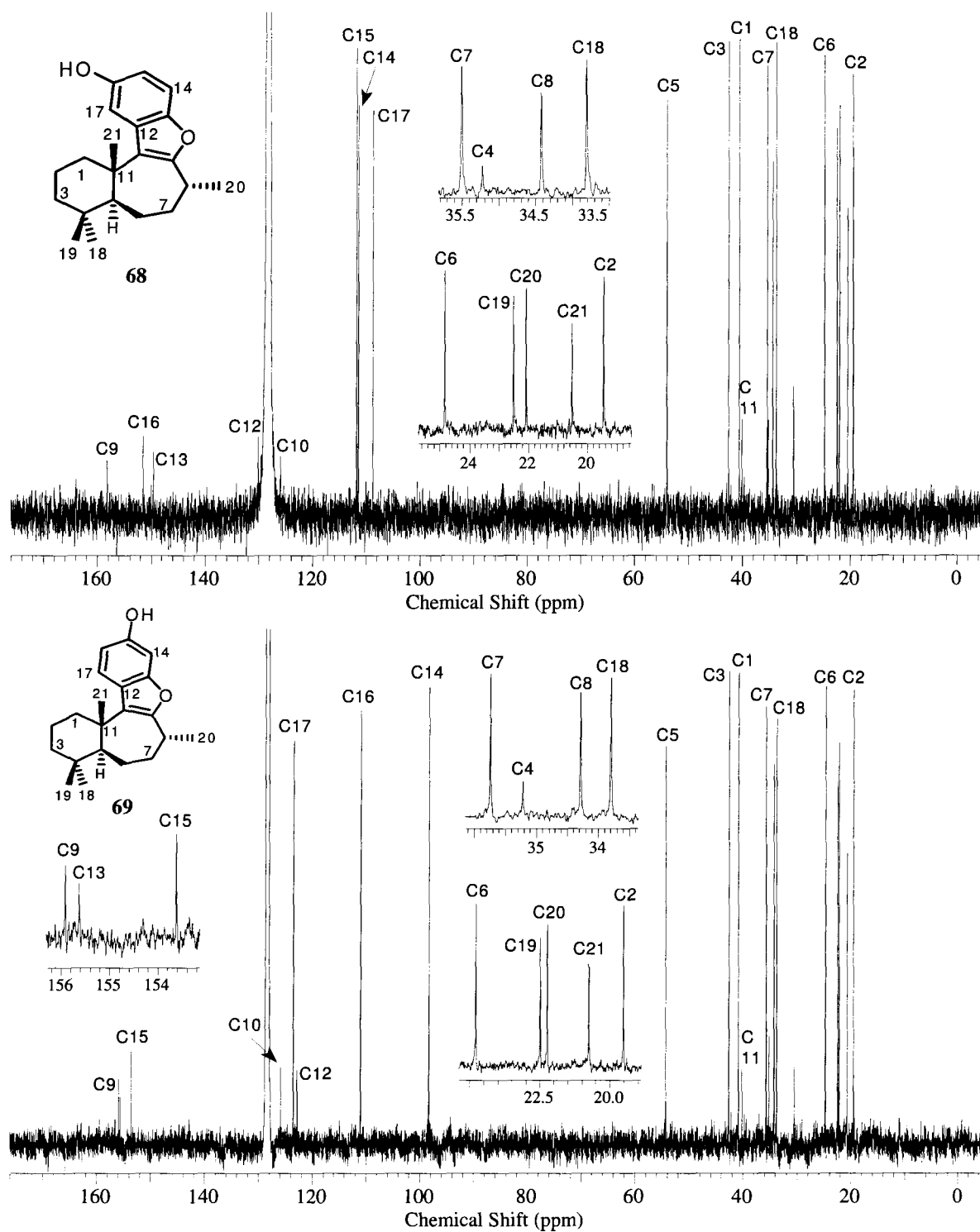
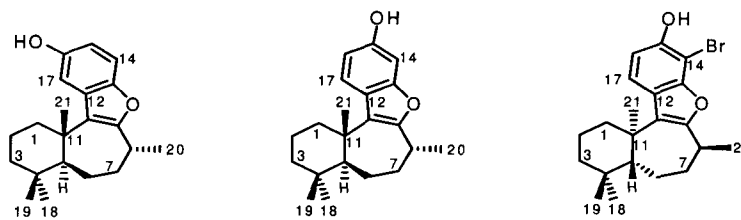


Figure 6.10. ^{13}C -NMR spectra of (+)-16-hydroxyliphagane (**68**) and (+)-15-hydroxyliphagane (**69**) (recorded in C_6D_6 at 150 MHz).

Table 6.6. ^1H -NMR assignments for (+)-16-hydroxyliphagane (**68**), (+)-15-hydroxyliphagane (**69**), and (+)-14-bromo-15-hydroxyliphagane (**70**) (recorded in C_6D_6).

Proton No	68	69	70
	^1H δ (ppm) (mult, J (Hz)) ^{a,b}		
1 _{ax}	1.50 (m)	1.50 (m)	1.40 (m)
1 _{eq}	2.57 (m)	2.56 (m)	2.42 (m)
2 _{eq}	1.42 (m)	1.40 (m)	1.38 (m)
2 _{ax}	1.63 (qt, 2.8, 13.3)	1.59 (qt, 2.8, 13.4)	1.56 (qt, 3.3, 13.7)
3 _{ax}	1.14 (td, 3.6, 13.3)	1.14 (td, 3.4, 13.2)	1.11 (td, 3.2, 13.3)
3 _{eq}	1.36 (m)	1.36 (m)	1.35 (m)
5	1.52 (m)	1.52 (m)	1.46 (dd, 2.3, 8.5)
6	1.43 (m), 1.66 (m)	1.44 (m), 1.65 (m)	1.37 (m), 1.62 (m)
7	1.32 (m), 1.90 (m)	1.33 (m), 1.93 (m)	1.27 (m), 1.85 (m)
8	3.09 (m)	3.11 (m)	3.01 (m)
14	7.17 (d, 8.6)	6.71 (d, 2.2)	-
15	6.45 (dd, 2.5, 8.8)	OH 3.84 (s)	OH 5.07 (s)
16	OH 3.73 (s)	6.55 (dd, 2.3, 8.5)	6.82 (d, 8.6)
17	7.01 (d, 2.5)	7.42 (d, 8.6)	7.23 (d, 8.6)
18	0.90 (s)	0.90 (s)	0.87 (s)
19	0.88 (s)	0.87 (s)	0.85 (s)
20	1.40 (d, 7.2)	1.42 (d, 7.1)	1.36 (d, 7.1)
21	1.29 (s)	1.30 (s)	1.22 (s)

^a Recorded at 600 MHz. ^b According to HSQC recorded at 600 MHz.

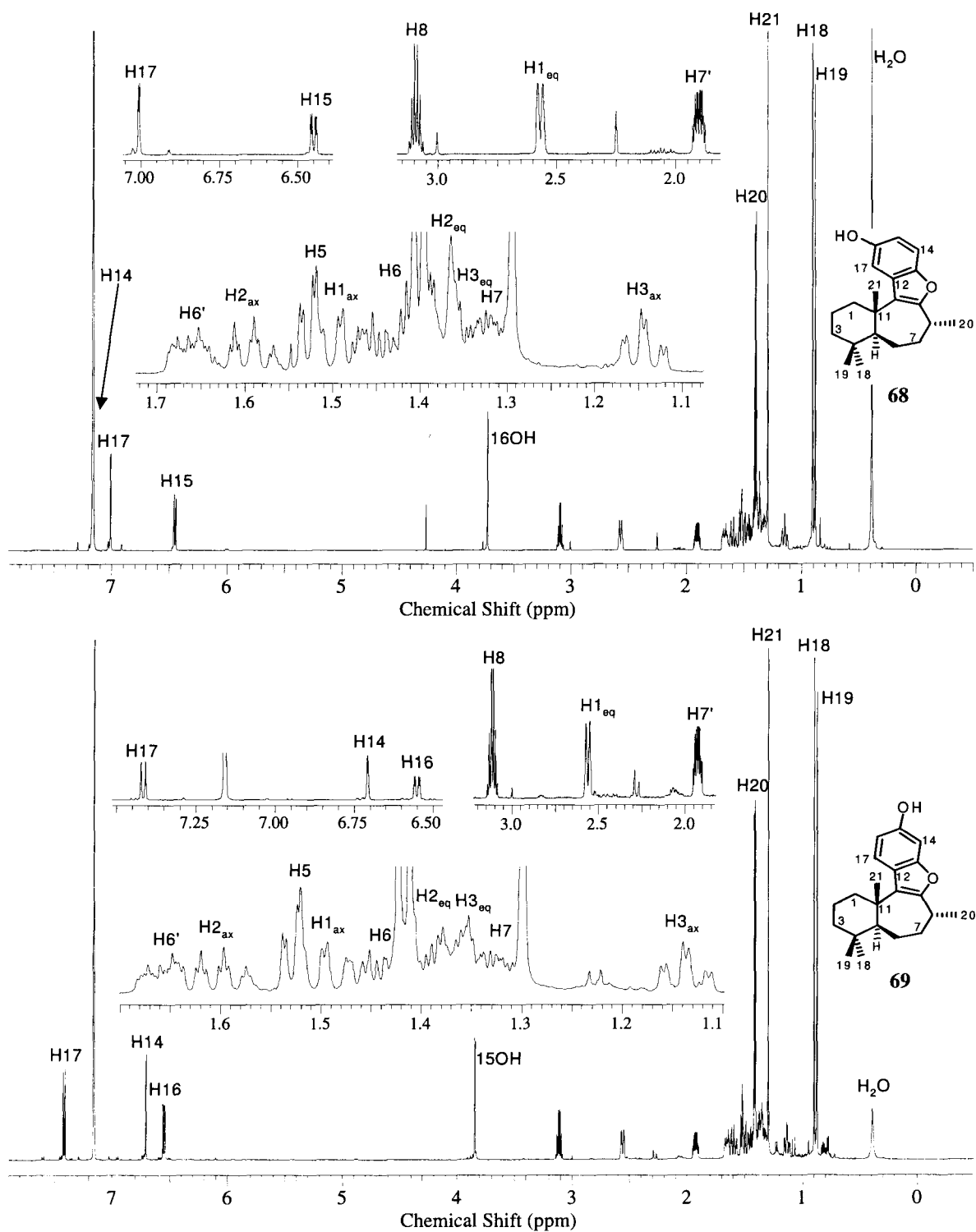


Figure 6.11. $^1\text{H-NMR}$ spectra of (+)-16-hydroxyliphagane (**68**) and (+)-15-hydroxyliphagane (**69**) (recorded in C_6D_6 at 600 MHz).

Proton assignments in the aromatic portion of both isomers were also confirmed by HMBC cross-peaks (Figure 6.12, Tables 6.22-6.25), particularly those corresponding to protons of the hydroxyl functionalities.

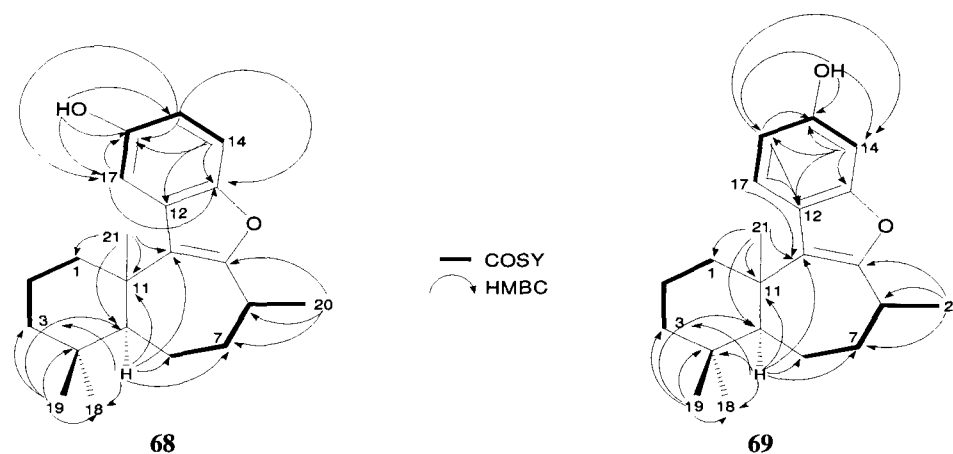
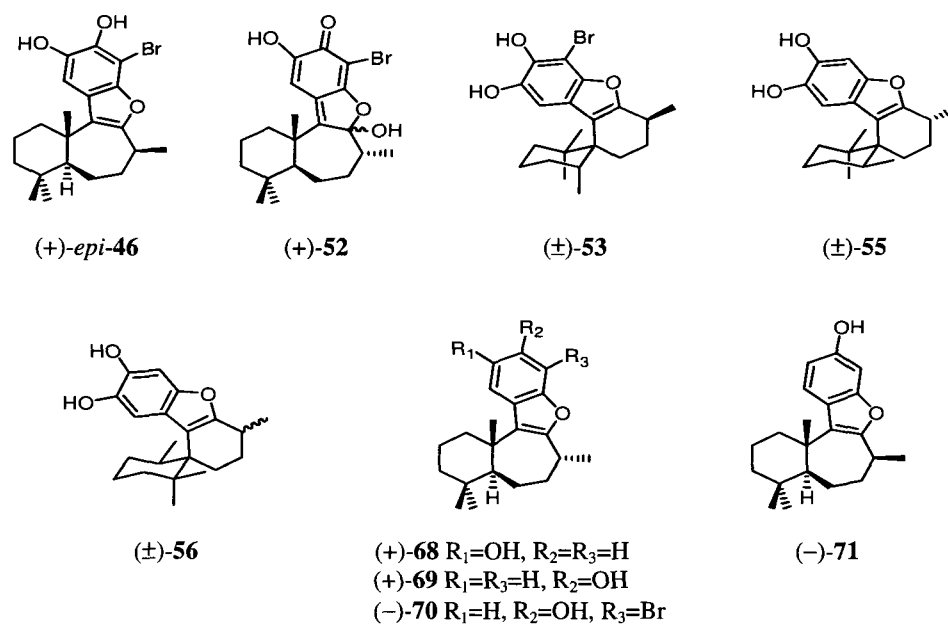


Figure 6.3. Key HMBC (H→C) and COSY correlations for **68** and **69**.

Compounds (**68**)-(71) showed more stability toward air and acidic conditions than their catechol counterparts. Although their color in solution tended to intensify with time, the effect was not as dramatic as observed with (+) and (-)-*epi-46*, allowing simple $[\alpha]_D$ measurements instead of the much safer circular dichroism (done under N_2). With such small amounts of materials, accurate magnitudes for specific rotation values cannot be expected, therefore only direction of rotation was considered to designate each enantiomer. The main mechanism of racemization involves carbocation formation and ring contraction, as proven by compounds (**53**), (**55**) and (**56**). Epimerization at C8 is also possible (as in *epi-46* and **71**), but all side products derived from both processes were separated during purification. Therefore, even if the rigid *trans* ring junction characteristic of these liphagane derivatives underwent some racemization during

the different synthetic steps, there is confidence that a high degree of enantioselectivity was achieved. Table 6.7 summarizes all the optical activity data acquired for these compounds.

Table 6.7. Optical activity measurements for liphagal (**1**) and its synthetic analogues.



N	Compound	Natural ^a	Unnatural
		$\Delta\epsilon$ (c MeCN) or $[\alpha]_D$ (c MeOH) at 20°C	
1	<i>epi</i> - 46	+0.078 (0.22) ^b	-0.11 (0.32) ^b
2	52	+0.26 (0.08) ^b	-0.28 (0.16) ^b
3	53		
4	55	Racemic ^b	
5	56		
6	68	+4.7 (0.2)	N.D.
7	69	+8.8 (0.2)	-11.3 (0.2)
8	70	-6.1 (0.2)	+16.4 (0.4)
9	71	-10.7 (0.4)	N.D.
10	Liphagal 1 ⁴⁷²	+12.0	N.D.

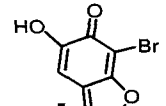
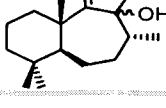
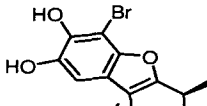

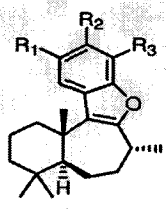
^aAs in (+)-liphagal (**1**). ^bAccording to CD. N.D.: no data available.

6.8. Biological evaluation of the new synthetic liphagane derivatives

The inhibitory activity of these compounds was assessed against two PI3K isoforms, using a fluorescent polarization assay that employs human PI3K expressed in SF9 insect cells.⁴⁷²

Table 6.8 shows the IC₅₀ values measured for both isoforms.

Table 6.8. Inhibition of PI3K α and PI3K γ by liphagal, LY294002, wortmannin, and several new liphagane derivatives.

N	Compound ^a	Notes ^b	α IC ₅₀ (μ M)	γ IC ₅₀ (μ M)			
1		N, (+)-52	3.3	>10			
2		U, (-)-52	5.2	>10			
3		N, (\pm)-53	0.695	5.3			
4		U, (\pm)-53	0.488	3.9			
			R₁	R₂	R₃		
5		N, 67	H	OCH ₃	Br	>10	>10
6		N, (+)- 68	OH	H	H	7.2	1.9
7		N, (+)- 69	H	OH	H	3.4	6.0
8		N, (+)- 69	H	OH	H	>10	>10
9		U, (-)- 69	H	OH	H	>10	9.0
10		N, (-)- 70	H	OH	Br	10.2	5.7
11		U, (+)- 70	H	OH	Br	5.6	3.4
12		N, C8- <i>epi</i> , (-)- 71	H	OH	H	2.2	2.2
13	Liphagal ⁴⁷²	N, (+)- 1	OH	OH	CHO	0.10	~1
14	Wortmannin (5) ⁴⁷²					0.012	N.D.
15	LY294002 (7) ⁴⁷²					0.55	N.D.

^aStructure for the naturally occurring ring junction (as in liphagal) is given. ^bN: natural; U: unnatural.

In general, all synthetic analogues were less biologically active than the natural product, inhibiting only in the micromolar range. The most active spiro compound, (\pm)-**53** (entries 3 and 4) exhibited PI3K α inhibitory activity in the same range as LY294002 (**7**). These compounds were prepared from enantiomeric starting materials and submitted for bioassay separately, although theoretically they are the same racemate. As expected, the difference in inhibition is not significant. Such a high activity suggests that the terpenoid substructure in liphagal and its analogues may not play a crucial role during binding, and correlates with previous considerations regarding the aromatic portion as the one in direct contact with the ATP binding site in PI3K.

Compounds (+) and (-)-**52** (entries 1 and 2), together with (\pm)-**53** displayed selectivity towards PI3K α . Such preference is reversed with the absence of one hydroxyl group, according to monophenolic compounds (**68**)-(70) (entries 6-11). There is no clear selectivity between enantiomeric pairs, although the unnatural monophenolic analogues (**69**) and (**70**) showed slightly higher potency (entries 9 and 11). Likewise, the presence of bromine replacing CHO as an electron withdrawing group seemed to be completely irrelevant. At least one hydroxyl group is required for activity, since methylated intermediate (**67**) was completely inactive (entry 5). No data was acquired for the extremely unstable *epi*-(**46**) enantiomeric pair, since the material was already degraded by the time it reached the biological screening stage.

Some inconsistency in IC₅₀ data is seen with (+)-**69** and its epimer (-)-**71** (entries 7-9 and 12). These analogues were evaluated at different time: a first run included only (+)-**69** and (-)-**71** (entries 7 and 12), whereas (+)-**69** and (-)-**69** were measured six months later (entries 8 and 9). This suggests that more reliable biological data can be derived from compounds examined at the same time.

Besides direct PI3K inhibition measurements, a secondary cell-based bioassay provided further evidence of PI3K signaling intervention for **68** and **69**, both in their (+)-natural

configuration. Figure 6.13 shows how liphagal (**1**) and LY292004 (**7**), at concentrations 5 and 3 $\mu\text{g}/\text{mL}$ respectively, are unable to inhibit the IgE-stimulated influx of extracellular calcium in bone marrow-derived mast cells.⁴⁸¹ Immunoglobulin E (IgE) is an antibody only found in mammals that binds mast cells and elicits an acute inflammatory response against invading bacteria and helminthic parasites.⁵⁴⁷ Unfortunately, this inflammatory response can also be detrimental and leads to allergic reactions and inflammatory disorders such as asthma, arthritis and multiple sclerosis.^{547,548} However, treatment with **68** and **69**, starting at 5 $\mu\text{g}/\text{mL}$, clearly inhibits the measured phenotypic response (calcium flux). The effect is more dramatic for **68**, and such selectivity between constitutional isomers suggests that a hydroxyl substituent at C16 may be a determinant for enhanced PI3K inhibition. Additional biological data is still being collected.

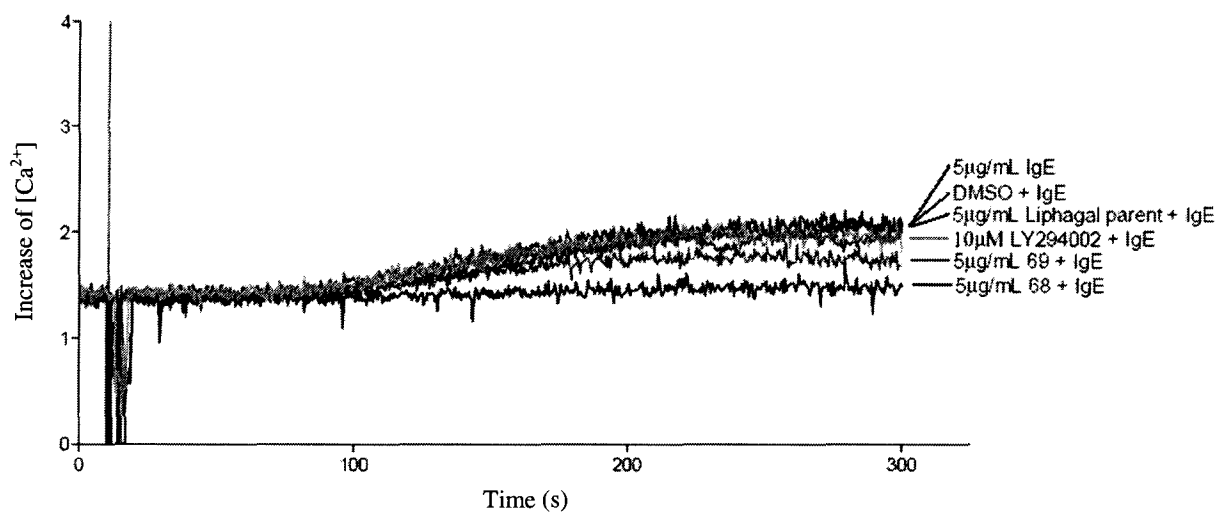


Figure 6.13. IgE-induced calcium influx in bone marrow-derived mast cells treated with DMSO (control), liphagal (**1**), LY294002 (**7**), **68** and **69**.

6.9. Conclusions and future directions

As part of an optimization program intended to develop more stable and isoform-selective PI3K inhibitors based on the new carbocyclic skeleton of liphagal (**1**), a small library of analogues was prepared according to the already designed enantioselective synthesis of **1**.^{472,531} The first group of compounds exhibited in the terpenoid fragment a typical *trans* ring junction and epimerization at C8 (*epi*-**46**, **52**), as well as a spiro carbon backbone produced by skeleton rearrangement, presumably through a carbocation mechanism (**53**, **55** and **56**). In the aromatic portion, the C14 aldehyde was also exchanged for bromine or proton (Figure 6.14).

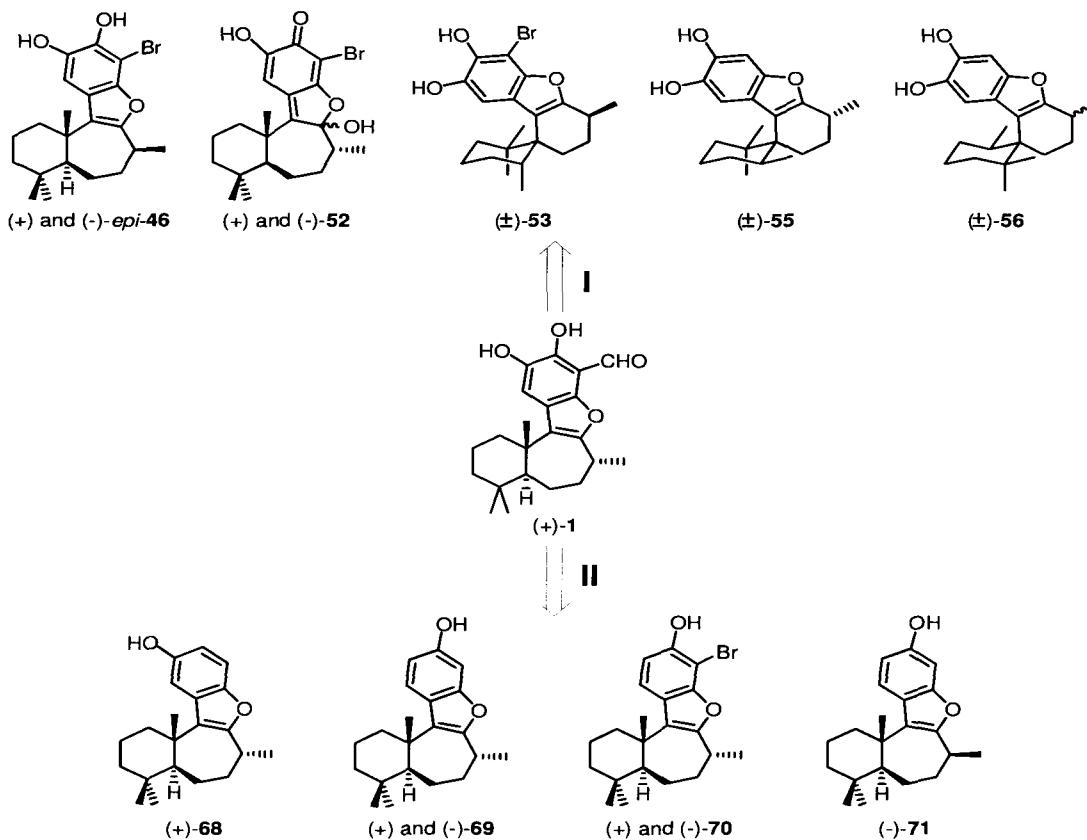


Figure 6.14. New synthetic liphagal-based PI3K inhibitors.

A second group of analogues preserved the terpenoid fragment, with variations only at C8 or in the positioning of aromatic substituents (**68-71**). Two main obstacles were faced during our synthesis of liphagal analogues. First, upon bromine-lithium exchange, attempts to functionalize C14 in the aromatic part of monophenolic methyl ethers (such as **67**), either with DMF or Weinreb amide, generated mostly debrominated material accompanied by only traces of desired product (9-19%). Although measures were taken to eliminate traces of water, a lack of true anhydrous conditions is always possible especially when working on small scales (0.012-0.16 mmol).

Secondly, standard demethylation procedures using BBr_3 or BI_3 were incompatible with the liphagane carbon skeleton, and generated significant amounts of polar degradation products separated via repetitive column chromatography and HPLC. This factor accounted for the extreme low yields obtained and reflects the clear instability associated with the tetracyclic liphagal backbone. A survey of demethylation procedures led to use of $\text{BBr}_3 \cdot \text{SMe}_2$ as deprotecting reagent,^{545,546} which provided the best conditions minimizing rearranged products and slightly improving reaction yields.

Regarding biological activity, all synthetic analogues exhibited micromolar inhibition of $\text{PI3K}\alpha$ and $\text{PI3K}\gamma$ and thus, are less active than the parent natural product. The most active compound showed inhibitory activity in the same range as LY294002 (**7**), and its spiral skeleton supports an accumulating amount of evidence designating the aromatic portion as that one directly involved in binding to PI3K 's. Further proof for this consideration includes the apparent lack of selectivity between enantiomeric pairs.

Compounds bearing a catechol motif tend to inhibit isoform $\text{PI3K}\alpha$ more effectively than monophenolic analogues, which in turn displayed selectivity towards $\text{PI3K}\gamma$. No clear preference was observed when bromine was introduced in the aromatic ring. Furthermore, the general lower

activity of all these analogues suggests that an efficient electron withdrawing group at C14 is capable of increasing activity to the nanomolar level. The presence of at least one hydroxyl group was confirmed to be essential for inhibition.

Additional evidence of PI3K signaling intervention was obtained when IgE-stimulated influx of extracellular calcium in bone marrow-derived mast cells was inhibited by analogues (68) and (69), suggesting a possible role as anti-inflammatory agents. The favored C16-hydroxylated isomer (68) was confirmed to inhibit calcium influx starting at 5 $\mu\text{g/mL}$, unlike the known PI3K inhibitors liphagal (1) and LY292004 (7).

The formation of *ortho*-hydroxyquinone (52), from the highly instable *epi*-(46) even under neutral conditions, confers a particular reactivity to C9 in the furan substructure. This side reaction provides support (in analogy to Scheme 6.6) for a possible binding mechanism between liphagal (1) and hydroxylated residues of PI3K's (such as serine for instance). Noteworthy, 1 and wortmannin (5) share the same substructure, and an equivalent position in the furan of 5 was shown long ago to bind covalently with Lys residues of p110 α within the ATP-binding site (Figure 6.2).^{471,477}

Several improvements are required in the enantioselective synthesis of liphagal (Scheme 6.3), particularly involving the low yielding demethylation step. This problem may be addressed by finding a more suitable protecting group for the catechol motif, capable of surviving SnCl₄ reaction conditions but labile enough to be safely removed from the unstable liphagane skeleton. Replacement of the currently used methyl ethers with benzyl ethers may be one possibility, since they can be later removed by mild hydrogenolysis. Furthermore, in order to improve yields and minimize debromination, the formylating step should be run at the highest scale possible (at least 1.0 mmol), and under the most strict anhydrous conditions.

Future preparations of liphagal-based PI3K inhibitors may focus efforts in modifying its aromatic substructure (attached to the furan ring). Although accessible, synthesis of the *trans*-fused terpenoic bicyclic system is time consuming and involves a highly toxic Barton-McCombie dehydroxylation protocol. In addition to evidence indicating its irrelevance in binding to PI3K's, this ring system is unstable as seen by formation of spiro-compounds and frequent C8 epimerization. More biological testing is required to determine whether it plays a role in PI3K isoform selectivity.

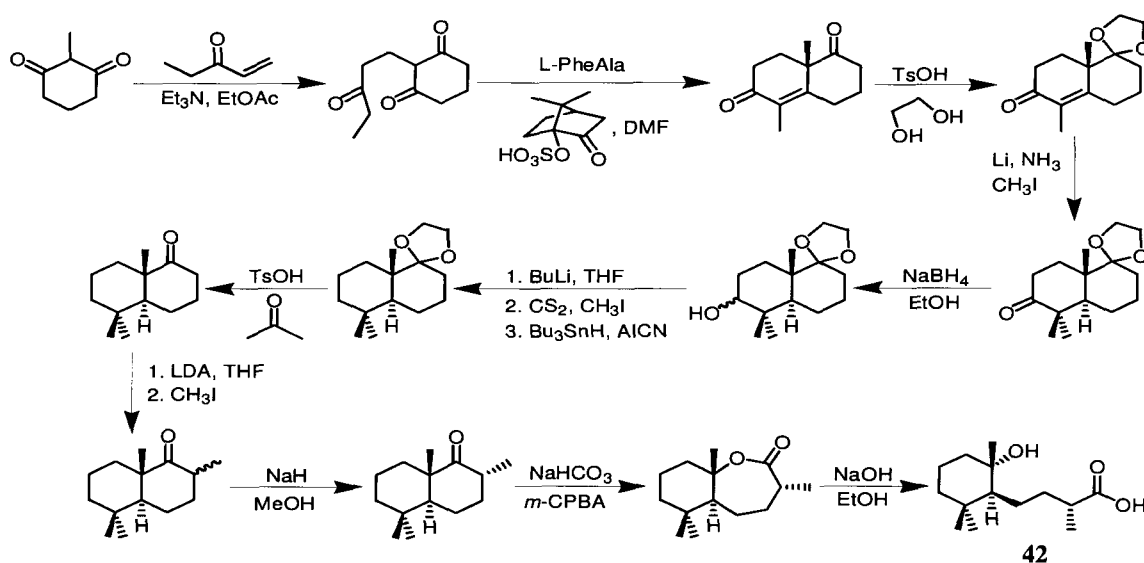
The present work points out two key requirements in the aromatic portion to achieve nanomolar PI3K inhibition: at least one hydroxyl group and a C=O electron-withdrawing substituent. By using methyl ketone as the latter one, the resulting analogue would definitely be more stable to oxidation and acidic conditions.

6.10. Experimental

General experimental procedures

For general experimental procedures see Section 2.6.

Preparation of (-) and (+)-(1'S,2'S,2R)-4-(2'-hydroxy-2',6',6'-trimethylcyclohexyl)-2-methylbutanoic acid (**42**)

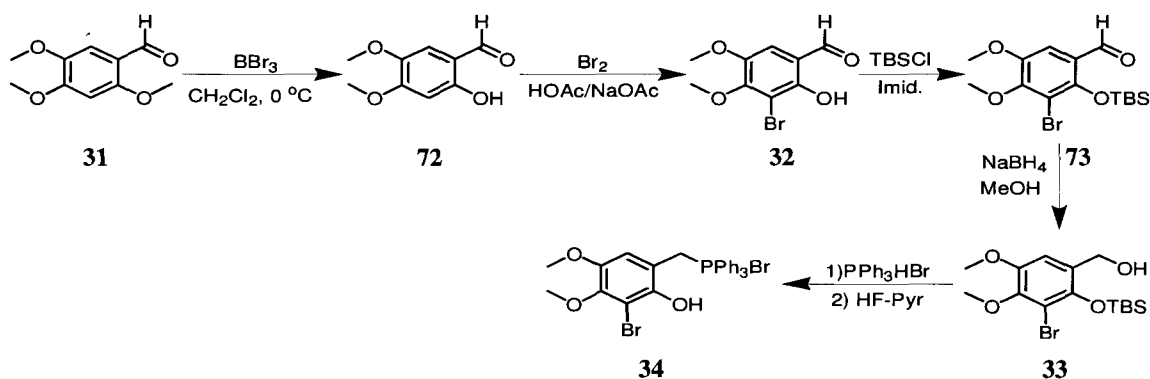


Both chiral acids were synthesized according to literature procedures.^{532,533,535} Once the corresponding (-) and (+)-Wieland-Miescher ketones had been prepared, Birch reduction, Barton-McCombie's radical protocol and an improved solventless Baeyer-Villiger oxidation⁵³⁴ afforded in a total of 11 steps the natural (-)-enantiomer (**42**) (15% overall yield), and its unnatural (+)-enantiomer (18% overall yield), as colorless oils.

(-)-(1'S,2'S,2R)-4-(2'-Hydroxy-2',6',6'-trimethylcyclohexyl)-2-methylbutanoic acid (**42**): ¹H NMR (CDCl₃, 300 MHz) δ 6.37 (2H, s, broad), 2.39 (1H, m), 1.85 (1H, m), 1.69 (1H, m), 1.60-

1.24 (7H, m), 1.23-1.04 (2H, m), 1.15 (3H, d, $J = 7.0$ Hz), 1.12 (3H, s), 0.88 (3H, s), 0.75 (3H, s); ^{13}C NMR (CDCl_3 , 75 MHz) δ 182.0 (C), 74.8 (C), 57.1 (CH), 42.8 (CH_2), 41.3 (CH_2), 40.0 (CH), 36.5 (CH_2), 35.4 (C), 32.7 (CH_3), 23.8 (CH_2), 23.1 (CH_3), 21.2 (CH_3), 20.3 (CH_2), 17.0 (CH_3). HRESIMS calcd for $\text{C}_{14}\text{H}_{26}\text{O}_3\text{Na}$ ($[\text{M}+\text{Na}]^+$): 265.1780; found 265.1781.

Preparation of [3-bromo-2-hydroxy-4,5-dimethoxyphenyl]-methyltriphenylphosphonium bromide (34)



To a solution of 2,4,5-trimethoxybenzaldehyde (11.8 g, 60 mmol) in CH_2Cl_2 (250 mL) at 0°C , was added BBr_3 (60 mL, 60 mmol, BBr_3 1.0 M in CH_2Cl_2), and the resulting dark mixture was stirred at room temperature for 16 hours. Water (250 mL) was then added and the mixture stirred for 30 minutes. The aqueous phase was extracted with CH_2Cl_2 , washed with $\text{Na}_2\text{S}_2\text{O}_3$, and dried over MgSO_4 . After filtration and solvent evaporation *in vacuo*, silica gel column chromatography of the residue (100% CH_2Cl_2) afforded phenol (**72**) (9.4 g, 86%) as a pale yellow solid.

To a solution of phenol (**72**) (9.4 g, 51 mmol) and NaOAc (6.4 g, 78 mmol) in HOAc (300 mL), was added slowly at room temperature bromine (4.7 mL, 94 mmol), and the resulting yellow solution was stirred for 2 hours. After solvent removal under vacuum, the residue was poured into an aqueous solution of NaHCO_3 . The aqueous phase was extracted with EtOAc and

the organic layer dried over Na_2SO_4 , filtered and evaporated under reduced pressure. TLC analysis for the yellow solid residue showed only desired product (**32**) (10.9 g, 82%).

Bromophenol (**32**) (10.9 g, 41.9 mmol), TBSCl (12.6 g, 84 mmol) and imidazole (12 g, 168 mmol), were stirred in CH_2Cl_2 (300 mL) at room temperature for 15 hours. The organic phase was diluted with CH_2Cl_2 , extracted with aqueous HCl 1.0 M, and washed with brine; to be then dried (Na_2SO_4), filtered and evaporated under reduced pressure. Silica gel chromatography of the residue (100 % CH_2Cl_2) afforded (**73**) (15.1 g, 96%) as a brown solid.

In the next reaction, aldehyde (**73**) (13.4 g, 36 mmol) in MeOH (200 mL), was treated with NaBH_4 (1.65 g, 43.5 mmol) at 0°C . After stirring for 30 minutes, aqueous NH_4Cl was added and the resulting mixture stirred for another 30 minutes. MeOH was evaporated under reduced pressure and the aqueous phase was extracted with EtOAc. Drying treatment with Na_2SO_4 , followed by filtration and solvent evaporation, provided pure (**33**) (11.2 g, 83%) as a white solid.

Finally, a solution of alcohol (**33**) (7.0 g, 18.5 mmol) and PPh_3HBr (6.4 g, 18.5 mmol) in acetonitrile (90 mL) was refluxed for 2 hours. After solvent removal under reduced pressure, the residue was dissolved in THF (90 mL) and HF/pyridine (3 mL) was added at room temperature, with formation of a precipitate. After additional stirring for 1 hour, the precipitate was filtered off and washed with Et_2O , yielding the phosphonium salt (**34**) (7.5 g, 80%) as a white powder.

2-Hydroxy-4,5-dimethoxybenzaldehyde (**72**): ^1H NMR (CDCl_3 , 400 MHz) δ 11.37 (1H, s, broad), 9.68 (1H, s), 6.88 (1H, s), 6.45 (1H, s), 3.91 (3H, s), 3.85 (3H, s); ^{13}C NMR (CDCl_3 , 100 MHz) δ 194.0 (C), 159.3 (2C), 157.2 (C), 142.9 (C), 113.2 (CH), 100.1 (CH), 56.4 (CH_3), 56.3 (CH_3). HRESIMS calcd for $\text{C}_9\text{H}_{11}\text{O}_4$ ($[\text{M}+\text{H}]^+$): 183.0657; found 183.0654.

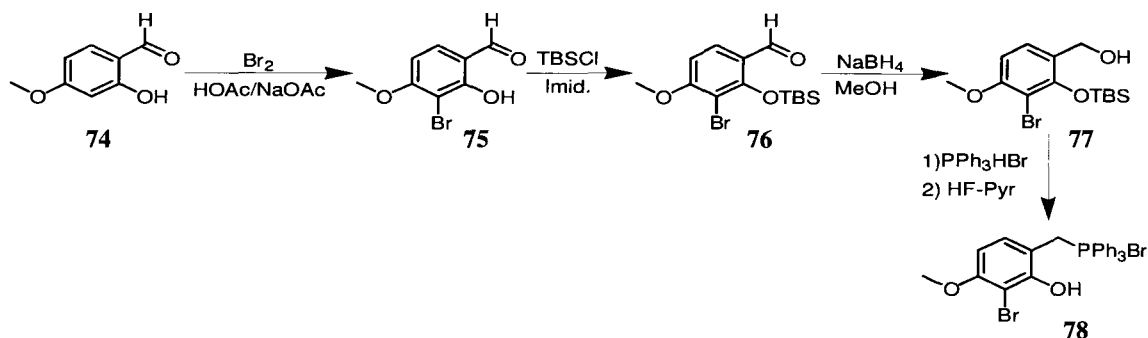
3-Bromo-2-hydroxy-4,5-dimethoxybenzaldehyde (**32**): ^1H NMR (CDCl_3 , 400 MHz) δ 11.54 (1H, s), 9.73 (1H, s), 7.00 (1H, s), 3.97 (3H, s), 3.86 (3H, s); ^{13}C NMR (CDCl_3 , 100 MHz) δ 194.4 (CH), 154.8 (C), 154.7 (C), 146.8 (C), 115.7 (C), 114.7 (CH), 106.9 (C), 61.0 (CH_3), 56.7 (CH_3). HRESIMS calcd for $\text{C}_9\text{H}_8\text{O}_4^{79}\text{Br}$ ($[\text{M}-\text{H}]^-$): 258.9606; found 258.9607.

3-Bromo-2-(*tert*-butyldimethylsilyloxy)-4,5-dimethoxybenzaldehyde (**73**): ^1H NMR (CDCl_3 , 400 MHz) δ 10.17 (1H, s), 7.29 (1H, s), 3.92 (3H, s), 3.86 (3H, s), 1.05 (9H, s), 0.21 (6H, s); ^{13}C NMR (CDCl_3 , 100 MHz) δ 188.6 (CH), 151.5 (C), 148.6 (2C), 123.8 (C), 112.9 (C), 108.7 (CH), 60.7 (CH_3), 56.2 (CH_3), 25.9 (3 CH_3), 18.7 (C), -3.47 (2 CH_3). HRESIMS calcd for $\text{C}_{15}\text{H}_{24}\text{O}_4\text{Si}^{79}\text{Br}$ ($[\text{M}+\text{H}]^+$): 375.0627; found 375.0624.

[3-Bromo-2-(*tert*-butyldimethylsilyloxy)-4,5-dimethoxyphenyl]-methanol (**33**): ^1H NMR (CDCl_3 , 600 MHz) δ 6.93 (1H, s), 4.64 (2H, s), 3.83 (3H, s), 3.81 (3H, s), 1.02 (9H, s), 0.24 (6H, s); ^{13}C NMR (CDCl_3 , 150 MHz) δ 148.2 (C), 146.5 (C), 144.2 (C), 127.8 (C), 112.1 (C), 111.4 (CH), 61.2 (CH_3), 60.5 (CH_3), 56.4 (CH_2), 26.2 (3 CH_3), 18.8 (C), -2.84 (2 CH_3). HRESIMS calcd for $\text{C}_{15}\text{H}_{25}\text{O}_4\text{NaSi}^{79}\text{Br}$ ($[\text{M}+\text{Na}]^+$): 399.0603; found 399.0602.

[3-Bromo-2-hydroxy-4,5-dimethoxyphenyl]-methyltriphenylphosphonium bromide (**34**): ^1H NMR (CDCl_3 , 400 MHz) δ 7.79-7.65 (9H, m), 7.63-7.55 (6H, m), 6.88 (1H, d, $J = 2.2$ Hz), 6.36 (1H, s, broad), 5.37 (2H, d, $J = 13.7$ Hz), 3.75 (3H, s), 3.49 (3H, s); ^{13}C NMR (CDCl_3 , 100 MHz) δ 146.8 (C), 146.3 (C), 146.1 (C), 144.1 (C), 142.2 (C), 140.5 (C), 134.89 (CH), 134.86 (2CH), 134.5 (3CH), 134.4 (3CH), 130.0 (3CH), 129.9 (3CH), 127.4 (C), 117.8 (CH, d, $J = 84.6$ Hz), 115.2 (C), 60.6 (CH_3), 56.5 (CH_3), 26.6 (CH_2 , d, $J = 63.0$ Hz); ^{31}P NMR (CDCl_3 , 81 MHz) δ 25.0 (1P, s). HRESIMS calcd for $\text{C}_{27}\text{H}_{25}\text{O}_3\text{P}^{79}\text{Br}$ ($[\text{M}+\text{H}]^+$): 507.0725; found 507.0728.

Preparation of (3-bromo-2-hydroxy-4-methoxyphenyl)-methyltriphenylphosphonium bromide (79)



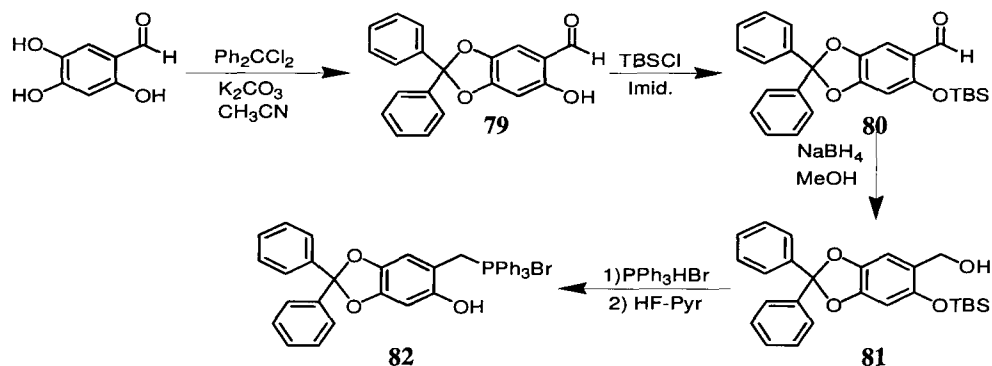
3-Bromo-2-hydroxy-4-methoxybenzaldehyde (**75**) (1.39 g, 46%) was prepared as stated for the synthesis of (**34**), from 2-hydroxy-4-methoxybenzaldehyde (2.0 g, 13.1 mmol) and Br_2 (0.70 mL, 13.1 mmol), using NaOAc (1.62 g, 19.7 mmol) and HOAc (76 mL) as solvent media. Following this reaction, 3-bromo-2-(*tert*-butyldimethylsilyloxy)-4-methoxybenzaldehyde (**76**) (1.55 g, 80%) was synthesized using (**75**) (1.3 g, 5.6 mmol), TBSCl (1.7 g, 11.2 mmol) and imidazole (1.5 g, 22.4 mmol). In the next step, [3-bromo-2-(*tert*-butyldimethylsilyloxy)-4-methoxyphenyl]-methanol (**77**) (1.41 g, 93 %) was obtained by reacting (**76**) (1.50 g, 4.3 mmol) and NaBH_4 (0.2 g, 5.2 mmol) in MeOH (25 mL). The final phosphonium salt (**78**) (1.29 g, 67%) was prepared from (**77**) (1.4 g, 4.0 mmol), PPh_3HBr (1.4 g, 4.0 mmol) and HF/pyridine (0.6 mL), as in the synthesis of (**34**).

3-Bromo-2-hydroxy-4-methoxybenzaldehyde (**75**): $^1\text{H NMR}$ (CDCl_3 , 400 MHz) δ 11.90 (1H, s), 9.69 (1H, s), 7.49 (1H, d, $J = 8.7$ Hz), 6.60 (1H, d, $J = 8.5$ Hz), 3.97 (3H, s); $^{13}\text{C NMR}$ (CDCl_3 , 100 MHz) δ 194.2 (CH), 162.7 (C), 160.1 (C), 134.5 (CH), 116.1 (C), 103.7 (CH), 99.6 (C), 56.8 (CH₃). HRESIMS calcd for $\text{C}_8\text{H}_7\text{O}_3\text{Na}^{79}\text{Br}$ ($[\text{M}+\text{Na}]^+$): 252.9476; found 252.9473.

3-Bromo-2-(*tert*-butyldimethylsilyloxy)-4-methoxybenzaldehyde (**76**): ^1H NMR (CDCl_3 , 400 MHz) δ 10.13 (1H, s), 7.77 (1H, d, $J = 8.9$ Hz), 6.66 (1H, d, $J = 8.7$ Hz), 3.93 (3H, s), 1.04 (9H, s), 0.22 (6H, s); ^{13}C NMR (CDCl_3 , 100 MHz) δ 188.3 (CH), 162.2 (C), 157.3 (C), 128.5 (CH), 123.0 (C), 105.7 (CH), 105.6 (C), 56.7 (CH_3), 25.9 (3CH_3), 18.7 (C), -3.33 (2CH_3). HRESIMS calcd for $\text{C}_{14}\text{H}_{21}\text{O}_3\text{Na}^{28}\text{Si}^{79}\text{Br}$ ($[\text{M}+\text{Na}]^+$): 367.0341; found 367.0332.

[3-Bromo-2-(*tert*-butyldimethylsilyloxy)-4-methoxyphenyl]-methanol (**77**): ^1H NMR (CDCl_3 , 400 MHz) δ 7.25 (1H, d, $J = 8.5$ Hz), 6.57 (1H, d, $J = 8.7$ Hz), 4.62 (1H, d, $J = 5.2$ Hz), 3.86 (3H, s), 1.03 (9H, s), 0.27 (6H, s); ^{13}C NMR (CDCl_3 , 100 MHz) δ 156.8 (C), 151.6 (C), 128.0 (CH), 125.8 (C), 105.1 (CH), 102.7 (C), 61.3 (CH_2), 56.4 (CH_3), 26.2 (3CH_3), 18.9 (C), -2.67 (2CH_3). HRESIMS calcd for $\text{C}_{14}\text{H}_{23}\text{O}_3\text{Na}^{28}\text{Si}^{79}\text{Br}$ ($[\text{M}+\text{Na}]^+$): 369.0498; found 369.0506.

(3-Bromo-2-hydroxy-4-methoxyphenyl)-methyltriphenylphosphonium bromide (**78**): ^1H NMR (CDCl_3 , 400 MHz) δ 7.71 (3H, m), 7.62-7.48 (12H, m), 6.94 (1H, dd, $J = 2.8, 8.6$ Hz), 6.24 (1H, d, $J = 8.7$ Hz), 4.96 (2H, d, $J = 13.1$ Hz), 3.72 (3H, s); ^{13}C NMR (CDCl_3 , 100 MHz) δ 156.8 (C), 152.5 (C), 146.8 (C), 140.3 (2C), 135.0 (2CH), 134.0 (3CH), 133.9 (3CH), 131.0 (C), 130.1 (3CH), 129.9 (3CH), 127.6 (CH), 117.5 (CH, d, $J = 85.1$ Hz), 107.1 (C), 104.0 (CH), 56.3 (CH_3), 25.7 (CH_2 , d, $J = 48.5$ Hz); ^{31}P NMR (CDCl_3 , 81 MHz) δ 22.4 (1P, s). HRESIMS calcd for $\text{C}_{26}\text{H}_{23}\text{O}_2^{31}\text{P}^{79}\text{Br}$ ($[\text{M}+\text{H}]^+$): 477.0619; found 477.0610.

Preparation of [6-hydroxy-2,2-diphenylbenzo[1,3]dioxol-5-yl]-methyltriphenylphosphonium bromide (**82**)

A slurry of the highly insoluble 2,4,5-trihydroxybenzaldehyde (1 g, 6.5 mmol), K_2CO_3 (2.7 g, 19.5 mmol), and Ph_2CCl_2 (1.6 mL, 8.4 mmol) in acetonitrile (30 mL), was stirred for 24 h. After filtration, the solvent was evaporated and the resulting residue poured into a silica gel column. Elution with a gradient mixture of EtOAc/hexanes (0 to 10%) provided desired (**79**) (0.098 g, 5%) as a gray solid.

The protected aldehyde (**79**) (0.09 g, 0.28 mmol) was dissolved in CH_2Cl_2 (20 mL), and treated with imidazole (0.077 g, 1.13 mmol) followed by TBSCl (0.085 g, 0.56 mmol). After stirring for 2 days, H_2O was added and CH_2Cl_2 extractions performed. The organic layer was dried over Na_2SO_4 and evaporated under reduced pressure. Silica gel chromatography of the resulting residue provided (**80**) (0.033 g, 27%) as a white solid.

Product (**80**) (0.033 g, 0.077 mmol) was dissolved in CH_3OH (10 mL) and treated at 0°C with NaBH_4 (0.0035 g, 0.092 mmol). After stirring for 30 minutes, aqueous NH_4Cl was added and the crude was stirred for another 30 minutes. EtOAc extractions, followed by Na_2SO_4 treatment, filtration and solvent evaporation, afforded alcohol (**81**) (0.030 g, 89%) as a white solid.

In the last reaction, (**81**) (0.030 g, 0.076 mmol) and PPh₃HBr (0.026 g, 0.076 mmol) in acetonitrile (5 mL) were refluxed for 2 h. The solvent was evaporated under reduce pressure, and the resulting solid residue was dissolved in THF (5 mL), to be then treated with HF/pyridine (1 mL). After 1 h, the precipitate was filtrated off and washed with Et₂O, to provide (**82**) (0.029 g, 59%) as a white powder.

6-Hydroxy-2,2-diphenylbenzo[1,3]dioxole-5-carbaldehyde (**79**): ¹H NMR (CDCl₃, 400 MHz) δ 11.84 (1H, s), 9.61 (1H, s), 7.67-7.55 (4H, m), 7.49-7.35 (6H, s), 6.92 (1H, s), 6.58 (1H, s); ¹³C NMR (CDCl₃, 100 MHz) δ 193.6 (CH), 161.4 (2C), 154.5 (C), 141.0 (C), 139.1 (2C), 129.4 (2CH), 128.3 (4CH), 126.12 (2CH), 126.09 (2CH), 109.6 (CH), 98.3 (CH) 89.9 (C). HRESIMS calcd for C₂₀H₁₄O₄Na ([M+Na]⁺): 341.0790; found 341.0798.

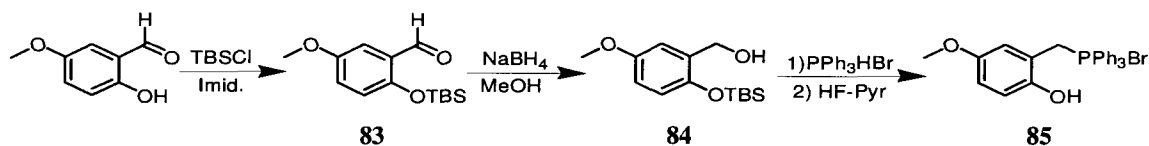
6-(*tert*-Butyldimethylsilyloxy)-2,2-diphenylbenzo[1,3]dioxole-5-carbaldehyde (**80**): ¹H NMR (CDCl₃, 600 MHz) δ 10.22 (1H, s), 7.55-7.51 (4H, m), 7.40-7.34 (6H, s), 7.27 (1H, s), 6.41 (1H, s), 0.98 (9H, s), 0.24 (6H, s); ¹³C NMR (CDCl₃, 150 MHz) δ 188.2 (CH), 156.9 (C), 153.4 (C), 142.6 (C), 139.4 (2C), 129.4 (2CH), 128.4 (4CH), 126.2 (4CH), 121.0 (C), 118.4 (C), 105.6 (CH), 101.2 (CH) 25.6 (3CH₃), 18.2 (C), -4.38 (2CH₃). HRESIMS calcd for C₂₆H₂₈O₄Na²⁸Si ([M+Na]⁺): 455.1655; found 455.1648.

[6-(*tert*-Butyldimethylsilyloxy)-2,2-diphenylbenzo[1,3]dioxol-5-yl]-methanol (**81**): ¹H NMR (CDCl₃, 600 MHz) δ 7.59-7.52 (4H, m), 7.40-7.30 (6H, s), 6.84 (1H, s), 6.44 (1H, s), 4.86 (1H, s), 4.54 (2H, s, broad), 0.99 (9H, s), 0.21 (6H, s); ¹³C NMR (CDCl₃, 150 MHz) δ 146.9 (C), 141.3 (C), 140.6 (C), 140.2 (C), 129.0 (2CH), 128.8 (C), 128.2 (2CH), 128.1 (2CH), 126.28 (2CH), 126.27 (2CH), 122.9 (C), 117.0 (C), 108.7 (CH), 101.0 (CH), 61.7 (CH₂), 25.7 (3CH₃),

18.1 (C), -4.26 (2CH₃). HRESIMS calcd for C₂₆H₃₀O₄Na²⁸Si ([M+Na]⁺): 457.1811; found 457.1814.

[6-Hydroxy-2,2-diphenylbenzo[1,3]dioxol-5-yl]-methyltriphenylphosphonium bromide (**82**): ¹H NMR (CD₃OD, 400 MHz) δ 7.67-7.55 (15H, m), 7.50-7.44 (4H, m), 7.42-7.34 (6H, s), 6.37 (1H, d, *J* = 2.2 Hz), 6.30 (1H, s), 4.67 (2H, d, *J* = 13.3 Hz); ¹³C NMR (CD₃OD, 100 MHz) δ 152.9 (C), 145.8 (C), 145.1 (C), 141.5 (C), 136.29 (C), 136.27 (C), 135.5 (3CH), 135.4 (3CH), 131.3 (3CH), 131.1 (3CH), 130.4 (2C), 129.5 (5CH), 128.0 (3CH), 127.4 (5CH), 119.9 (CH, d, *J* = 84.6 Hz), 111.5 (C), 106.2 (C), 98.8 (CH), 26.2 (CH₂, d, *J* = 48.8 Hz). HRESIMS calcd for C₃₈H₃₀O₃³¹P ([M+H]⁺): 565.1933; found 565.1922.

Synthesis of (2-hydroxy-5-methoxyphenyl)-methyltriphenylphosphonium bromide (**85**)



A solution of 2-hydroxy-5-methoxybenzaldehyde (1.52 g, 10.0 mmol), TBSCl (3.01 g, 20.0 mmol) and imidazole (2.01 g, 30.0 mmol) in CH₂Cl₂ (50 mL), were stirred at 25 °C for 16 h. The reaction mixture was washed with 1M HCl (30 mL) and saturated brine (20 mL), dried (Na₂SO₄) and concentrated. Silica gel column chromatography (5% EtOAc/hexanes) gave (**83**) as colorless oil (2.63 g, 99%).

Aldehyde (**83**) (1.0 g, 3.61 mmol) and NaBH₄ (142 mg, 3.75 mmol) were stirred in MeOH (20 mL) at room temperature for 1 h. Saturated NH₄Cl (10 mL) was added and the reaction mixture stirred for 30 minutes before being concentrated to an aqueous suspension. The aqueous phase was extracted with EtOAc, and the organic phases combined, dried (Na₂SO₄) and

concentrated. Silica gel column chromatography (10% EtOAc/hexanes) afforded (**84**) as a light yellow oil (0.97 g, 96%).

Protected alcohol (**84**) (1.54 g, 5.74 mmol) and PPh₃HBr (1.97 g, 5.74 mmol) were refluxed in CH₃CN (50 mL) for 2 h and the reaction cooled to room temperature. Volatiles were removed *in vacuo*, and the residue taken up in THF (100 mL) with HF/pyridine (1.0 mL) added dropwise. The resulting solution was stirred for 1 h at room temperature before being filtrated, and the precipitate washed with Et₂O to give desired (**85**) (2.62 g, 95%) as a white amorphous solid.

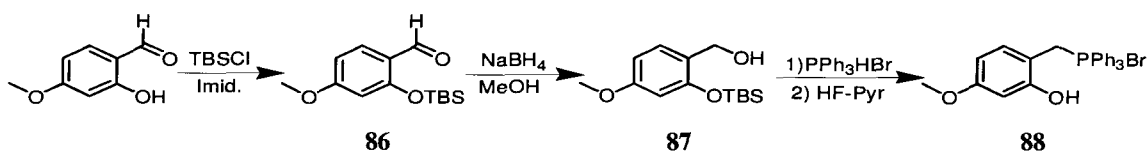
2-(*tert*-Butyldimethylsilanyloxy)-5-methoxybenzaldehyde (**83**): ¹H NMR (CDCl₃, 600 MHz) δ 10.42 (1H, s), 7.28 (1H, d, *J* = 3.1 Hz), 7.06 (1H, dd, *J* = 3.3, 8.8 Hz), 6.83 (1H, d, *J* = 9.1 Hz), 3.81 (3H, s), 1.02 (9H, s), 0.25 (6H, s); ¹³C NMR (CDCl₃, 150 MHz) δ 189.9 (CH), 154.0 (C), 153.3 (C), 127.1 (C), 123.9 (CH), 121.6 (CH), 109.5 (CH), 55.7 (CH₃), 25.7 (3CH₃), 18.3 (C), -4.4 (2CH₃). HRESIMS calcd for a C₁₄H₂₃O₃²⁸Si ([M+H]⁺): 267.1416; found 267.1412.

[2-(*tert*-Butyldimethylsilanyloxy)-5-methoxy-phenyl]-methanol (**84**): ¹H NMR (CDCl₃, 600 MHz) δ 6.90 (1H, d, *J* = 2.7 Hz), 6.74 (1H, d, *J* = 8.9 Hz), 6.71 (1H, dd, *J* = 2.8, 8.5 Hz), 4.65 (2H, s), 3.78 (3H, s), 2.23 (1H, s, broad), 1.02 (9H, s), 0.23 (6H, s); ¹³C NMR (CDCl₃, 150 MHz) δ 154.2 (C), 147.3 (C), 132.4 (C), 119.3 (CH), 114.2 (CH), 113.7 (CH), 62.2 (CH₂), 55.9 (CH₃), 26.0 (3CH₃), 18.4 (C), -4.0 (2CH₃). HRESIMS calcd for C₁₄H₂₄O₃Na²⁸Si ([M+Na]⁺): 291.1392; found 291.1395.

(2-Hydroxy-5-methoxyphenyl)-methyltriphenylphosphonium bromide (**85**): ¹H NMR (DMSO-*d*₆, 600 MHz) δ 9.32 (1H, s), 7.89 (3H, m), 7.72 (6H, m), 7.67 (6H, m), 6.71 (1H, dt, *J* = 2.5, 9.2

Hz), 6.66 (1H, d, $J = 9.1$ Hz), 6.33 (1H, t, $J = 2.6$ Hz), 4.86 (2H, d, $J = 15.1$ Hz), 3.38 (3H, s); ^{13}C NMR (DMSO- d_6 , 150 MHz) δ 151.6 (C), 149.8 (C), 134.90 (2C), 134.88 (C), 133.96 (5CH), 133.90 (4CH), 129.96 (3CH), 129.87 (3CH), 118.2 (CH, d, $J = 84.9$ Hz), 116.1 (CH), 115.7 (C), 114.0 (CH), 55.0 (CH_3), 23.6 (CH_2 , d, $J = 49.3$ Hz). HRESIMS calcd for $\text{C}_{26}\text{H}_{24}\text{O}_2\text{P}$ ($[\text{M}+\text{H}]^+$): 399.1514; found 399.1512.

Preparation of (2-hydroxy-4-methoxyphenyl)-methyltriphenylphosphonium bromide (**88**)



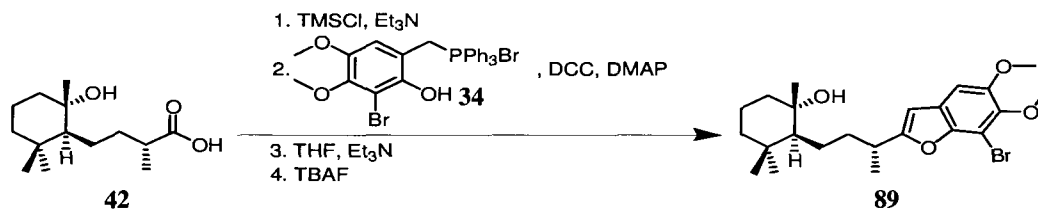
2-(*tert*-Butyldimethylsilyloxy)-4-methoxybenzaldehyde (**86**) (2.58 g, 97%) was prepared as before from 2-hydroxy-4-methoxybenzaldehyde (1.52 g, 10.0 mmol), TBSCl (3.01 g, 20.0 mmol) and imidazole (2.01 g, 30.0 mmol). In the next step, [2-(*tert*-butyldimethylsilyloxy)-4-methoxyphenyl]-methanol (**87**) (0.91 g, 90 %) was obtained by reacting (**86**) (1.00 g, 3.75 mmol) and NaBH_4 (142 mg, 3.75 mmol). The final (2-hydroxy-4-methoxyphenyl)-methyltriphenylphosphonium bromide (**88**) (1.50 g, 93%) was prepared from (**87**) (0.91 g, 3.39 mmol) and PPh_3HBr (1.16 g, 3.39 mmol), as previously stated for the synthesis of regioisomer compound (**85**).

2-(*tert*-Butyldimethylsilyloxy)-4-methoxybenzaldehyde (**86**): ^1H NMR (CDCl_3 , 600 MHz) δ 10.29 (1H, s), 7.77 (1H, d, $J = 8.8$ Hz), 6.57 (1H, dd, $J = 2.2, 8.8$ Hz), 6.33 (1H, d, $J = 2.2$ Hz), 3.82 (3H, s), 1.01 (9H, s), 0.28 (6H, s); ^{13}C NMR (CDCl_3 , 150 MHz) δ 188.7 (CH), 165.9 (C), 160.9 (C), 130.2 (CH), 121.6 (C), 108.0 (CH), 105.4 (CH), 55.7 (CH_3), 25.8 (3 CH_3), 18.5 (C), -4.2 (2 CH_3). HRESIMS calcd for $\text{C}_{14}\text{H}_{23}\text{O}_3^{28}\text{Si}$ ($[\text{M}+\text{H}]^+$): 267.1416; found 267.1410.

[2-(*tert*-Butyldimethylsilyloxy)-4-methoxyphenyl]-methanol (**87**): ^1H NMR (CDCl_3 , 600 MHz) δ 7.20 (1H, d, $J = 8.2$ Hz), 6.51 (1H, dd, $J = 2.2, 8.5$ Hz), 6.41 (1H, d, $J = 2.2$ Hz), 4.61 (2H, s), 3.78 (3H, s), 1.96 (1H, s, broad), 1.03 (9H, s), 0.28 (6H, s); ^{13}C NMR (CDCl_3 , 150 MHz) δ 160.4 (C), 154.8 (C), 130.1 (CH), 124.4 (C), 105.95 (CH), 105.81 (CH), 61.8 (CH_2), 55.5 (CH_3), 25.9 (3 CH_3), 18.4 (C), -4.0 (2 CH_3). HRESIMS calcd for $\text{C}_{14}\text{H}_{24}\text{O}_3\text{Na}^{28}\text{Si}$ ($[\text{M}+\text{Na}]^+$): 291.1392; found 291.1399.

(2-Hydroxy-4-methoxyphenyl)-methyltriphenylphosphonium bromide (**88**): ^1H NMR ($\text{DMSO}-d_6$, 600 MHz) δ 9.76 (1H, s), 7.88 (3H, m), 7.72 (6H, m), 7.64 (6H, m), 6.71 (1H, dd, $J = 8.4, 2.5$ Hz), 6.28 (1H, d, $J = 2.1$ Hz), 6.24 (1H, dd, $J = 2.3, 8.4$ Hz), 4.81 (2H, d, $J = 14.1$ Hz), 3.64 (3H, s); ^{13}C NMR ($\text{DMSO}-d_6$, 150 MHz) δ 160.4 (C), 157.0 (C), 134.84 (2C), 134.82 (C), 133.92 (5CH), 133.85 (4CH), 129.94 (3CH), 129.86 (3CH), 118.4 (CH, d, $J = 84.4$ Hz), 105.4 (C), 105.0 (CH), 101.1 (CH), 55.0 (CH_3), 22.8 (CH_2 , d, $J = 45.8$ Hz). HRESIMS calcd for $\text{C}_{26}\text{H}_{24}\text{O}_2\text{P}$ ($[\text{M}+\text{Na}]^+$): 399.1514; found 399.1520.

Preparation of (+) and (-)-2-[3-(7-bromo-5,6-dimethoxybenzofuran-2-yl)-butyl]-1,3,3-trimethylcyclohexanol (**89**)

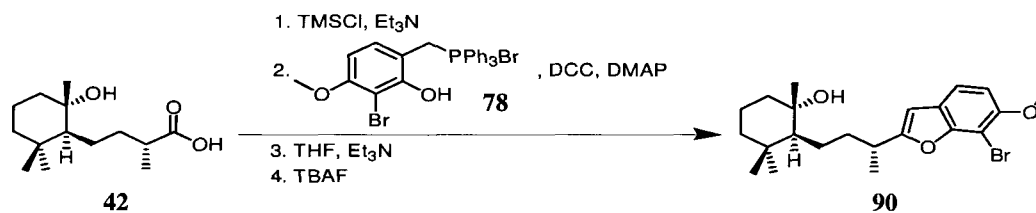


A solution of hydroxyacid (**42**) (unnatural: 0.86 g, 3.6 mmol; natural: 0.68 g, 2.8 mmol), Et₃N (3.01 mL, 21.6 mmol) and TMSCl (1.4 mL, 10.4 mmol) in CH_2Cl_2 (50 mL), was stirred at room temperature for 18 h. Water was added and CH_2Cl_2 extractions performed. The organic

extracts were combined, dried (Na_2SO_4) and concentrated *in vacuo*. This protected material (unnatural: 1.02 g, 3.23 mmol; natural: 0.78 g, 2.50 mmol) was dissolved in CH_2Cl_2 (50 mL), and stirred with phosphonium bromide (**34**) (2.46 g, 4.8 mmol), DCC (1.32 g, 6.4 mmol) and DMAP (73 mg, 0.6 mmol), at room temperature for 18 hours. After solvent removal under reduced pressure, the obtained residue was dissolved in THF (50 mL) and Et_3N (8.0 mL) was added. The resulting mixture was refluxed for 4 hours. Once at room temperature, silica was added and the THF was evaporated under reduced pressure. The resulting dried silica was poured into a silica gel column and eluted with 10% EtOAc/hexanes, to yield a silyl-protected benzofuran intermediate (unnatural: 1.10 g, 66%; natural: 0.56 g, 43%), which was then dissolved in CH_2Cl_2 and stirred in the presence of TBAF (2 mL) at 25 °C, until TLC showed the absence of starting material. The reaction crude was diluted with H_2O , and aqueous NaHCO_3 washings performed. After drying treatment (Na_2SO_4) and filtration, solvent removal *in vacuo* and silica gel column chromatography (50% EtOAc/hexanes) afforded desired compounds (**89**) (unnatural: 0.47 g, 49%; natural 0.30 g, 61%) as a colourless oil.

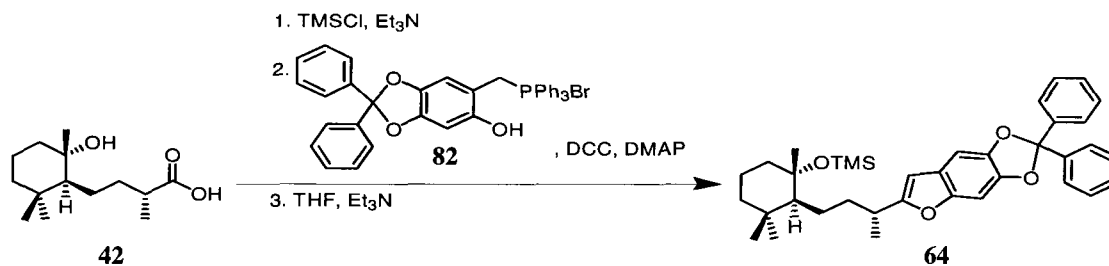
^1H NMR (CDCl_3 , 400 MHz) δ 6.87 (1H, s), 6.34 (1H, s), 3.83 (6H, s), 2.90 (1H, m), 1.98 (1H, m), 1.66 (1H, m), 1.62 (1H, dd, $J = 5.6, 5.9$ Hz), 1.48 (1H, m), 1.45 (1H, m), 1.33 (1H, dt, $J = 3.4, 13.4$ Hz), 1.31 (1H, m), 1.28 (3H, d, $J = 7.0$ Hz), 1.26 (1H, m), 1.25 (1H, m), 1.13 (1H, td, $J = 4.0, 12.8$ Hz), 1.08 (1H, m), 1.07 (3H, s), 0.87 (3H, s), 0.72 (3H, s); ^{13}C NMR (CDCl_3 , 100 MHz) δ 165.3 (C), 150.2 (C), 146.5 (C), 143.9 (C), 124.3 (C), 101.9 (CH), 101.2 (CH), 99.5 (C), 74.0 (C), 61.0 (CH_3), 57.1 (CH_3), 56.5 (CH), 43.3 (CH_2), 41.3 (CH_2), 38.3 (CH_2), 35.3 (C), 34.1 (CH_3), 32.7 (CH), 23.7 (CH_2), 23.2 (CH_3), 21.2 (CH_3), 20.3 (CH_2), 19.2 (CH_3). HRESIMS calcd for $\text{C}_{23}\text{H}_{33}\text{O}_4\text{Na}^{79}\text{Br}$ ($[\text{M}+\text{Na}]^+$): 475.1460; found 475.1468.

Preparation of (+) and (-)-2-[3-(7-bromo-6-methoxy-benzofuran-2-yl)-butyl]-1,3,3-trimethylcyclohexanol (**90**)



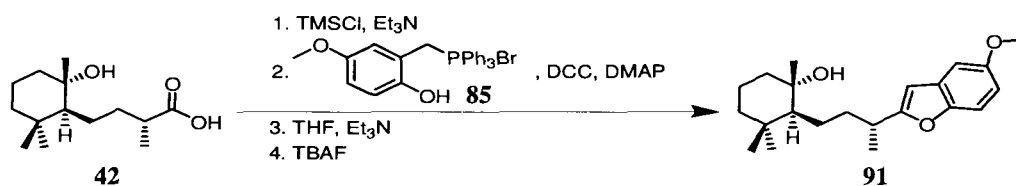
As in the previous procedure, a solution of hydroxyacid (**42**) (natural: 0.21 g, 0.9 mmol; unnatural: 0.24 g, 1.0 mmol), Et₃N (0.8 mL, 5.9 mmol) and TMSCl (0.4 mL, 3.0 mmol) in CH₂Cl₂ (30 mL), was stirred at room temperature for 18 h. After the usual work-up, the obtained protected material was dissolved in CH₂Cl₂ (30 mL), and stirred with phosphonium bromide (**78**) (1.24 g, 1.5 mmol), DCC (0.41 g, 2.0 mmol) and DMAP (20 mg, 0.16 mmol), at room temperature for 18 hours. After solvent removal under reduced pressure, the obtained residue was dissolved in THF (30 mL) and Et₃N (4.0 mL) was added. The resulting mixture was refluxed for 4 hours, whereupon silica gel column chromatography (20% EtOAc/hexanes) and TBAF silyl-deprotection as before, yielded alcohols (**90**) (natural: 0.13 g, 36%; unnatural: 0.17 g, 40%), as colourless oils. ¹H NMR (CDCl₃, 400 MHz) δ 7.29 (1H, d, *J* = 8.4 Hz), 6.80 (1H, d, *J* = 8.5 Hz), 6.37 (1H, d, *J* = 0.76 Hz), 3.90 (3H, s), 2.94 (1H, m), 2.01 (1H, m), 1.70 (1H, m), 1.65 (1H, dd, *J* = 5.3, 5.6 Hz), 1.51 (1H, m), 1.48 (1H, dd, *J* = 4.4, 7.0 Hz), 1.39 (1H, dt, *J* = 3.2, 12.8 Hz), 1.34 (1H, m), 1.31 (3H, d, *J* = 7.0 Hz), 1.29 (1H, m), 1.28 (1H, m), 1.17 (1H, td, *J* = 4.0, 12.6 Hz), 1.15 (1H, m), 1.10 (3H, s), 0.90 (3H, s), 0.74 (3H, s); ¹³C NMR (CDCl₃, 100 MHz) δ 164.5 (C), 153.2 (C), 152.8 (C), 123.6 (C), 118.6 (CH), 108.0 (CH), 100.8 (CH), 93.5 (C), 74.2 (C), 57.2 (CH₃), 43.4 (CH₂), 41.4 (CH₂), 38.3 (C), 35.4 (CH₂), 35.4 (CH), 34.1 (CH), 32.7 (CH₃), 23.7 (CH₂), 23.4 (CH₃), 21.3 (CH₃), 20.4 (CH₂), 19.2 (CH₃). HRESIMS calcd for C₂₂H₃₁O₃Na⁷⁹Br ([M+Na]⁺): 445.1354; found 445.1366.

Synthesis of (+) and (-)-2-[3-(2,2-diphenyl-1,3,5-trioxas-indacen-6-yl)-butyl]-1,3,3-trimethylcyclohexyloxy)-trimethylsilane (64)



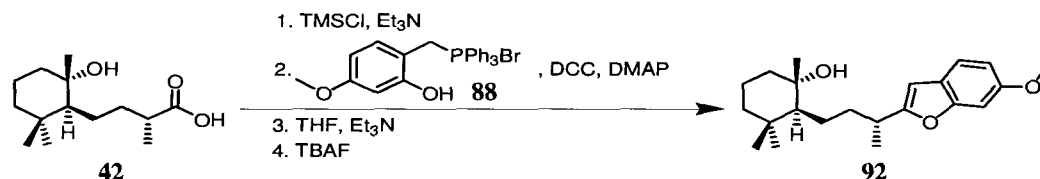
The title compounds (**64**) (natural: 0.0084 g, 72%; unnatural: 0.0034 g, 29%) were prepared in the same manner as intermediate (**89**), using hydroxyacid (**42**) (natural: 0.006 g, 0.02 mmol; unnatural: 0.006 g, 0.02 mmol), phosphonium bromide (**82**) (0.0125 g, 0.02 mmol), DCC (0.008 g, 0.038 mmol) and DMAP. ¹H NMR (CDCl₃, 400 MHz) δ 7.59-7.56 (4H, m), 7.38-7.28 (6H, m), 6.94 (1H, s), 6.89 (1H, s), 6.22 (1H, s), 2.80 (1H, m), 1.90 (1H, m), 1.88 (3H, m), 1.75 (1H, m), 1.73 (3H, m), 1.41 (1H, dd, $J = 12.2, 12.4$ Hz), 1.25 (3H, d, $J = 6.8$ Hz), 1.21 (1H, m), 1.19 (1H, m), 1.10 (3H, s), 0.85 (3H, s), 0.72 (3H, s), 0.042 (9H, s); ¹³C NMR (CDCl₃, 100 MHz) δ 163.6 (C), 150.5 (C), 149.5 (C), 144.6 (C), 143.7 (C), 140.43 (C), 140.41 (C), 129.0 (2CH), 128.2 (4CH), 126.4 (4CH), 122.0 (C), 100.7 (CH), 99.0 (CH), 93.4 (CH), 78.0 (C), 57.4 (CH), 43.3 (C), 38.6 (CH₂), 34.9 (CH₂), 34.3 (CH), 33.1 (CH₃), 25.4 (CH₂), 24.7 (CH₂), 24.0 (CH₃), 21.5 (CH₃), 20.5 (CH₂), 19.2 (CH₃), 2.84 (3CH₃).

Preparation of (-)-2-[3-(5-methoxybenzofuran-2-yl)-butyl]-1,3,3-trimethylcyclohexanol (91)



The title compound (0.133 g, 30%) was prepared as before, from (-)-hydroxyacid (**42**) (0.30 g, 1.31 mmol) and phosphonium salt (**85**) (0.942 g, 1.97 mmol). Colourless oil. $[\alpha]_D^{21} -28^\circ$ ($c = 0.24$, CHCl_3). $^1\text{H NMR}$ (CDCl_3 , 600 MHz) δ 7.30 (1H, d, $J = 8.9$ Hz), 6.97 (1H, d, $J = 2.7$ Hz), 6.80 (1H, dd, $J = 2.6, 8.8$ Hz), 6.35 (1H, s), 3.84 (3H, s), 2.92 (1H, m), 2.03 (1H, m), 1.74 (1H, m), 1.67 (1H, m), 1.54 – 1.36 (5H, m), 1.35 (1H, m), 1.33 (3H, d, $J = 7.0$ Hz), 1.20 (1H, td, $J = 3.7, 13.1$ Hz), 1.14 (1H, m), 1.12 (3H, s), 0.93 (3H, s), 0.78 (3H, s); $^{13}\text{C NMR}$ (CDCl_3 , 150 MHz) δ 165.2 (C), 155.9 (C), 149.7 (C), 129.7 (C), 111.5 (CH), 111.3 (CH), 103.4 (CH), 101.0 (CH), 74.5 (C), 57.6 (CH_3), 56.2 (CH), 43.6 (CH_2), 41.6 (C), 38.7 (CH_2), 35.7 (CH_2), 34.6 (CH), 33.0 (CH_3), 24.1 (CH_2), 23.6 (CH_3), 21.6 (CH_3), 20.7 (CH_2), 19.4 (CH_3). HRESIMS calcd for $\text{C}_{22}\text{H}_{32}\text{O}_3\text{Na}$ ($[\text{M}+\text{Na}]^+$): 367.2249; found 367.2251.

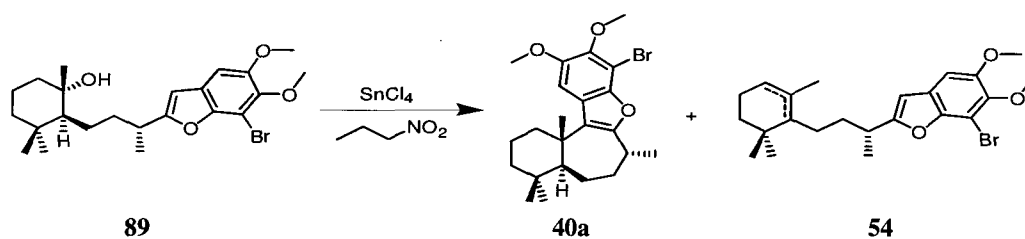
Preparation of (-)-2-[3-(6-methoxybenzofuran-2-yl)-butyl]-1,3,3-trimethylcyclohexanol (**92**)



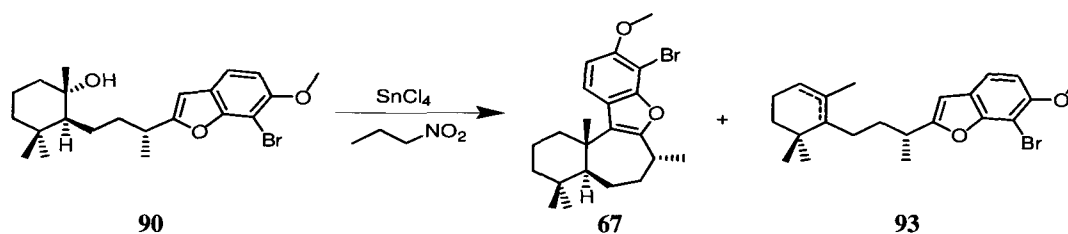
The title compound (0.177 g, 39%) was prepared using the previously reported methodology, from (-)-hydroxyacid (**42**) (0.30 g, 1.31 mmol) and phosphonium salt (**88**) (0.942 g, 1.97 mmol). Colourless oil. $[\alpha]_D^{21} -26^\circ$ ($c = 0.18$, CHCl_3). $^1\text{H NMR}$ (CDCl_3 , 600 MHz) δ 7.34 (1H, d, $J = 8.3$ Hz), 6.98 (1H, d, $J = 1.9$ Hz), 6.82 (1H, dd, $J = 2.2, 8.4$ Hz), 6.33 (1H, s), 3.85 (3H, s) 2.90 (1H, m), 2.02 (1H, m), 1.74 (1H, m), 1.68 (1H, m), 1.54 – 1.34 (5H, m), 1.32 (1H, m), 1.32 (3H, d, $J = 6.9$ Hz), 1.20 (1H, td, $J = 3.8, 13.2$ Hz), 1.14 (1H, m), 1.12 (3H, s), 0.93 (3H, s), 0.78 (3H, s); $^{13}\text{C NMR}$ (CDCl_3 , 150 MHz) δ 163.3 (C), 157.3 (C), 155.6 (C), 122.4 (C), 120.5 (CH), 111.2 (CH), 100.5 (CH), 96.0 (CH), 74.5 (C), 57.6 (CH_3), 56.0 (CH), 43.6 (CH_2),

41.7 (CH₂), 38.8 (CH₂), 35.7 (C), 34.5 (CH), 33.0 (CH₃), 24.1 (CH₂), 23.6 (CH₃), 21.6 (CH₃), 20.7 (CH₂), 19.4 (CH₃). HRESIMS calcd for C₂₂H₃₂O₃Na ([M+Na]⁺): 367.2249; found 367.2258.

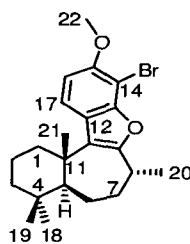
Preparation of (+) and (-)-desformyl-14-bromo-15,16-dimethoxylyphagal (**40a**)



To a solution of alcohol (**89**) (natural: 0.29 g, 0.65 mmol; unnatural: 0.46 g, 1.0 mmol) in 2-nitropropane (60 mL) at -78°C , was added SnCl₄ (0.6 mL, 5.0 mmol). After stirring for 20 minutes the mixture was slowly warmed to room temperature and water was then added. EtOAc extractions were performed and the organic phase was dried over Na₂SO₄, filtrated and evaporated under reduced pressure. Silica gel column chromatography (5% EtOAc/hexanes) of the residue afforded desired compound (**40a**) (natural: 0.074 g, 26%; unnatural: 0.12 g, 28%) as a colourless solid, and a slightly more polar fraction composed by a mixture of benzofurans (**54**) (around 0.080 mg). ¹H NMR (CDCl₃, 600 MHz) δ 7.11 (1H, s), 3.88 (3H, s), 3.86 (3H, s), 3.25 (1H, m), 2.55 (1H, m), 2.15 (1H, m), 1.83 (1H, m), 1.70 (1H, dt, $J = 3.1, 13.6$ Hz), 1.68 (1H, m), 1.58 (3H, m), 1.51 (1H, m), 1.49 (1H, m), 1.43 (3H, d, $J = 7.2$ Hz), 1.35 (3H, s), 1.23 (1H, td, $J = 3.3, 13.8$ Hz), 0.97 (3H, s), 0.93 (3H, s); ¹³C NMR (CDCl₃, 150 MHz) δ 158.0 (C), 149.0 (C), 146.0 (C), 144.0 (C), 126.0 (C), 124.1 (C), 105.3 (CH), 99.5 (C), 61.1 (CH₃), 57.3 (CH₃), 53.4 (CH), 41.9 (CH₂), 40.1 (CH₂), 38.9 (C), 36.0 (C), 34.8 (CH₂), 33.5 (CH₃), 33.3 (CH), 24.0 (CH₂), 22.02 (CH₃), 21.97 (CH₃), 20.0 (CH₃), 18.9 (CH₂). HRESIMS calcd for C₂₃H₃₂O₃⁷⁹Br ([M+H]⁺): 435.1535; found 435.1529.

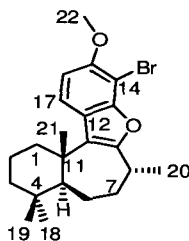
Preparation of (+) and (-)-14-bromo-15-methoxylyphagane (67)

To a solution of alcohol (**90**) (natural: 0.13 g, 0.31 mmol; unnatural: 0.17 g, 0.40 mmol) in 2-nitropropane (20 mL) at -78°C , was added SnCl_4 (0.22 mL, 1.9 mmol). After stirring for 20 minutes the mixture was slowly warmed to room temperature and water was then added. EtOAc extractions were performed and the organic phase was dried over Na_2SO_4 , filtrated and evaporated under reduced pressure. Silica gel column chromatography (5% EtOAc/hexanes) of the residue afforded (**67**) (natural: 0.073 g, 58%; unnatural: 0.062 g, 38%) as a colourless solid. For a summary of ^1H and ^{13}C NMR assignments, see Table 6.8. ^1H NMR (C_6D_6 , 600 MHz) δ 7.39 (1H, d, $J = 8.6$ Hz), 6.48 (1H, d, $J = 8.8$ Hz), 3.39 (3H, s), 3.06 (1H, m), 2.57 (1H, m), 1.86 (1H, m), 1.63 (1H, m), 1.61 (1H, m), 1.52 (1H, m), 1.44 (1H, m), 1.42 (1H, m), 1.38 (1H, m), 1.37 (3H, d, $J = 7.2$ Hz), 1.36 (1H, m), 1.31 (3H, s), 1.29 (1H, m), 1.13 (1H, td, $J = 3.6, 13.5$ Hz), 0.89 (3H, s), 0.88 (3H, s); ^{13}C NMR (C_6D_6 , 150 MHz) δ 157.6 (C), 154.1 (C), 153.4 (C), 126.5 (C), 124.5 (C), 121.8 (CH), 107.7 (CH), 94.8 (C), 57.0 (CH_3), 54.2 (CH), 42.7 (CH_2), 41.1 (CH_2), 40.5 (C), 35.5 (CH_2), 35.4 (C), 34.3 (CH), 33.6 (CH_3), 24.8 (CH_2), 22.6 (CH_3), 22.2 (CH_3), 20.9 (CH_3), 19.7 (CH_2). HRESIMS calcd for $\text{C}_{22}\text{H}_{29}\text{O}_2\text{Na}^{79}\text{Br}$ ($[\text{M}+\text{Na}]^+$): 427.1249; found 427.1254.

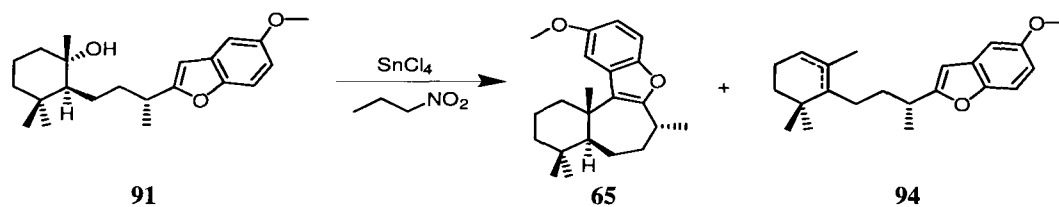
Table 6.9. NMR data for 14-bromo-15-methoxylyphagane (**67**) (recorded in C₆D₆).

Carbon No	¹³ C δ (ppm) ^a	¹ H δ (ppm) (mult, <i>J</i> (Hz)) ^{b,c}	HMBC ^b (H→C)
1	41.1	H _{ax} 1.44 (m), H _{eq} 2.57 (m)	C2, C3, C5, C11
2	19.7	H _{eq} 1.42 (m), H _{ax} 1.63 (m)	C4, C11
3	42.7	H _{ax} 1.13 (td, <i>J</i> = 3.6, 13.5 Hz), H _{eq} 1.36 (m)	C1, C2, C4, C18, C19
4	35.4		
5	54.2	1.52 (m)	C4, C10, C11, C18, C19, C21
6	24.8	1.38 (m), 1.61 (m)	C5, C8
7	35.5	1.29 (m), 1.86 (m)	C5, C6, C8, C9, C20
8	34.3	3.06 (m)	C6, C7, C9, C10, C20
9	157.6		
10	126.5		
11	40.5		
12	124.5		
13	154.1		
14	94.8		
15	153.4		
16	107.7	6.48 (d, <i>J</i> = 8.8 Hz)	C12, C14, C15
17	121.8	7.39 (d, <i>J</i> = 8.6 Hz)	C10, C12, C13, C14, C15, C16
18	33.6	0.89 (s)	C3, C4, C19
19	22.6	0.88 (s)	C5, C18
20	22.2	1.37 (d, <i>J</i> = 7.2 Hz)	C7, C8, C9
21	20.9	1.31 (s)	C5, C9, C10, C11
22	57.0	3.39 (s)	C15

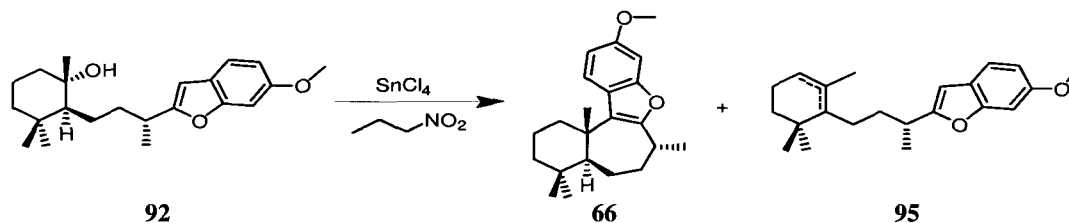
^aRecorded at 150 MHz. ^bRecorded at 600 MHz. ^cAccording to HSQC recorded at 600 MHz.

Table 6.10. NMR data for 14-bromo-15-methoxyliphagane (**67**) (recorded in C₆D₆).

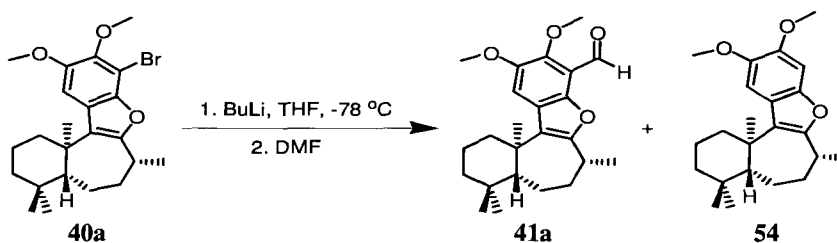
Proton No	¹ H δ (ppm) (mult, J (Hz)) ^a	COSY ^a
1 _{ax}	1.44 (m)	H1 _{eq}
1 _{eq}	2.57 (m)	H1 _{ax} , H2 _{ax} , H2 _{eq}
2 _{ax}	1.63 (m)	H1 _{eq} , H2 _{eq} , H3 _{ax}
2 _{eq}	1.42 (m)	H1 _{eq} , H2 _{ax}
3 _{ax}	1.13 (td, J = 3.6, 13.5 Hz)	H2 _{ax} , H3 _{eq}
3 _{eq}	1.36 (m)	H3 _{ax}
5	1.52 (m)	
6	1.38 (m), 1.61 (m)	H7, H8
7	1.29 (m), 1.86 (m)	H6
8	3.06 (m)	H7, H20
16	6.48 (d, J = 8.8 Hz)	H17
17	7.39 (d, J = 8.6 Hz)	H16
18	0.89 (s)	
19	0.88 (s)	
20	1.37 (d, J = 7.2 Hz)	H8
21	1.31 (s)	
22	3.39 (s)	

^aRecorded at 600 MHz.**Preparation of 16-methoxyliphagane (**65**)**

SnCl₄ (240 μL, 2.04 mmol) was added dropwise to a solution of starting material (**91**) (0.13 g, 0.38 mmol) in 2-nitropropane (30 mL) at -78°C. The usual work-up afforded a yellowish oil, which was used without any further purification in the following deprotection reaction.

Preparation of 15-methoxylyphagal (66)

SnCl₄ (240 μL, 2.04 mmol) was added dropwise to a solution of starting material (**92**) (0.18 g, 0.51 mmol) in 2-nitropropane (30 mL) at -78°C. The usual work-up afforded a yellowish oil, which was used without any further purification in the next step.

Formylation/debromination of (+) and (-)-desformyl-14-bromo-15,16-dimethoxylyphagal (40a)

To a solution of bromobenzofuran (**40a**) (natural: 4.4 mg, 0.012 mmol) in THF (5 mL) was added at -78°C *n*-BuLi (0.2 mL, 0.32 mmol, 1.6 M in hexanes). After stirring for 30 minutes, DMF (1 mL, 12.9 mmol) was added. The mixture was stirred for 1 hour and, after reaching room temperature, quenched with aqueous NH₄Cl. EtOAc extractions were performed and the organic extracts dried over Na₂SO₄, filtrated and evaporated under reduced pressure. Silica gel column chromatography (10% EtOAc/Hexanes) afforded dimethoxylyphagal (**41a**) (natural: 1.7 mg, 50%) and desformyl-14-bromo-15,16-dimethoxylyphagal (**54**) (natural: 2.2 mg, 56%).

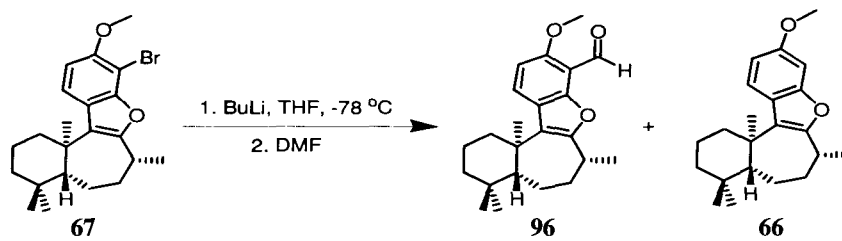
In another reaction, bromobenzofuran (**40a**) (unnatural: 24 mg, 0.055 mmol) in THF (5 mL) at -78 °C was treated with *n*-BuLi (0.041 mL, 0.066 mmol, 1.6 M). After stirring for 30

minutes, the cold bath was removed and the crude allowed reaching room temperature. Aqueous NH_4Cl was used to quench the reaction, followed by EtOAc extractions, Na_2SO_4 drying treatment and filtration. Solvent evaporation *in vacuo* provided desformyl-14-bromo-15,16-dimethoxylyphagal (**54**) (unnatural: 18.6 mg, 95%), as a colourless solid.

Dimethoxylyphagal (**41a**): ^1H NMR (CDCl_3 , 400 MHz) δ 10.54 (1H, s), 7.45 (1H, s), 3.95 (3H, s), 3.91 (3H, s), 3.28 (1H, m), 2.52 (1H, m), 2.14 (1H, m), 1.83 (1H, m), 1.70 (1H, m), 1.60-1.46 (5H, m), 1.44 (3H, d, $J = 7.2$ Hz), 1.35 (3H, s), 1.23 (2H, m), 0.96 (3H, s), 0.93 (3H, s). HRESIMS calcd for $\text{C}_{24}\text{H}_{33}\text{O}_4$ ($[\text{M}+\text{H}]^+$): 385.2379; found 385.2386.

Desformyl-14-bromo-15,16-dimethoxylyphagal (**54**): ^1H NMR (CDCl_3 , 400 MHz) δ 7.13 (1H, s), 6.91 (1H, s), 3.89 (3H, s), 3.87 (3H, s), 3.16 (1H, m), 2.57 (1H, m), 2.13 (1H, m), 1.82 (1H, m), 1.70 (2H, m), 1.57 (3H, m), 1.48 (1H, m), 1.44 (1H, m), 1.39 (3H, d, $J = 7.2$ Hz), 1.35 (3H, s), 1.24 (1H, td, $J = 3.1, 13.3$ Hz), 0.96 (3H, s), 0.93 (3H, s); ^{13}C NMR (CDCl_3 , 100 MHz) δ 155.8 (C), 148.4 (C), 146.8 (C), 144.8 (C), 125.3 (C), 120.3 (C), 105.5 (CH), 94.9 (CH), 57.0 (CH_3), 56.1 (CH_3), 53.6 (CH), 42.0 (CH_2), 40.2 (CH_2), 39.5 (C), 35.2 (CH_2), 34.8 (C), 33.6 (CH_3), 33.3 (CH), 24.3 (CH_2), 22.0 (CH_3), 21.9 (CH_3), 20.2 (CH_3), 18.9 (CH_2). HRESIMS calcd for $\text{C}_{23}\text{H}_{32}\text{O}_3\text{Na}$ ($[\text{M}+\text{Na}]^+$): 379.2249; found 379.2255.

Formylation/debromination of (+) and (-)-14-bromo-15-methoxylyphagane (**67**)

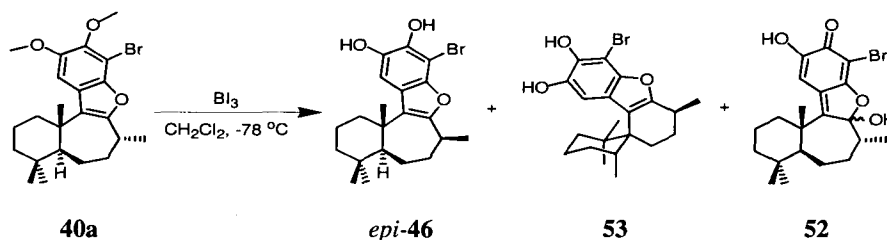


To a solution of bromobenzofuran (**67**) (natural: 66.3 mg, 0.16 mmol; unnatural: 53.0 mg, 0.13 mmol) in THF (10 mL) was added at -78°C *n*-BuLi (1.0 mL, 0.16 mmol, 0.16 M in hexanes). After stirring for 30 minutes, DMF (1.0 mL, 12.9 mmol) was added. The mixture was stirred for 1 hour and, after reaching room temperature, quenched with aqueous NH_4Cl . EtOAc extractions were performed and the organic extracts dried over Na_2SO_4 , filtrated and evaporated under reduced pressure. Silica gel column chromatography (10% EtOAc/Hexanes) afforded 14-formyl-15-methoxyliphagane (**96**) (natural: 5.1 mg, 9%; unnatural: 9.0 mg, 19%) and 15-methoxyliphagane (**66**) (natural: 17.9 mg, 34%; unnatural: 15.6 mg, 36%), which was used without any further purification in the next deprotection step.

14-Formyl-15-methoxyliphagane (**96**): ^1H NMR (CDCl_3 , 400 MHz) δ 10.59 (1H, s), 7.87 (1H, d, $J = 8.8$ Hz), 6.82 (1H, d, $J = 8.8$ Hz), 3.94 (3H, s), 3.25 (1H, m), 2.57 (1H, m), 2.18 (1H, m), 1.86 (1H, m), 1.73 (1H, m), 1.60-1.46 (5H, m), 1.45 (3H, d, $J = 7.2$ Hz), 1.37 (3H, s), 1.25 (2H, m), 0.96 (3H, s), 0.95 (3H, s). HRESIMS calcd for $\text{C}_{23}\text{H}_{30}\text{O}_3\text{Na}$ ($[\text{M}+\text{Na}]^+$): 377.2093; found 377.2096.

15-Methoxyliphagane (**66**): HRESIMS calcd for $\text{C}_{21}\text{H}_{27}\text{O}_3\text{Na}^{79}\text{Br}$ ($[\text{M}+\text{Na}]^+$): 429.1041; found 429.1050.

Deprotection of (+) and (-)-desformyl-14-bromo-15,16-dimethoxyliphagal (**40a**)



To a solution of (**40a**) (natural: 36 mg, 0.083 mmol; unnatural: 28 mg, 0.060 mmol) in CH_2Cl_2 (10 mL) at -78°C , was added BI_3 (0.33 mL, 0.33 mmol, 1 M in CH_2Cl_2). The resulting mixture was warmed to room temperature (2 h) and quenched with aqueous $\text{Na}_2\text{S}_2\text{O}_3$. The organic layer was separated and washed with HCl 0.1 M, followed by Na_2SO_4 addition, filtration and solvent evaporation. Silica gel column chromatography (30% EtOAc/Hexanes) provided one main fraction (one spot by TLC), which was additionally purified by reversed-phase HPLC (C18 Inertsil, 80% $\text{CH}_3\text{CN}/20\% \text{H}_2\text{O} + 0.05\% \text{TFA}$), to yield yellow fractions of 8-*epi*-desformyl-14-bromoliphagal (**46**) (natural: 1.1 mg, 3%; unnatural: 3.2 mg, 12%), (\pm)-14-bromospiroliphagane (**53**) (1.2 mg, 13%), and (-)-14-bromo-9,16-dihydroxyliphagane quinone (**52**) (natural: 0.8 mg, 2%; unnatural: 3.2 mg, 12%). Natural (**46**): CD (CH_3CN , c 0.22) λ 343.0 nm ($\Delta\epsilon$ +0.078), 297.0 (-0.042); (**52**): CD (CH_3CN , c 0.08) λ 351.0 nm ($\Delta\epsilon$ +0.26), 323.0 (-0.026). Unnatural (**46**): CD (CH_3CN , c 0.32) λ 343.0nm ($\Delta\epsilon$ -0.11), 297.0 (+0.084); (**52**): CD (CH_3CN , c 0.16) λ 353.0 nm ($\Delta\epsilon$ -0.28), 306.0 (+0.39)

(+)-8-*epi*-Desformyl-14-bromoliphagal (**46**): for a summary of ^1H and ^{13}C NMR assignments, see Tables 6.2 and 6.11-6.13. ^1H NMR (CDCl_3 , 600 MHz) δ 7.15 (1H, s), 5.33 (1H, s, broad), 5.10 (1H, s, broad), 3.27 (1H, m), 2.50 (1H, m), 1.87 (1H, m), 1.80 (1H, m), 1.74 (1H, dd, $J = 3.0, 9.4$ Hz), 1.68 (1H, m), 1.67 (1H, qt, $J = 3.0, 13.8$ Hz), 1.52 (1H, m), 1.49 (1H, m), 1.44 (1H, m), 1.361 (1H, m) 1.362 (3H, s), 1.360 (3H, d, $J = 6.7$ Hz), 1.21 (1H, td, $J = 3.5, 13.6$ Hz), 0.96 (3H, s), 0.93 (3H, s); ^{13}C NMR (CDCl_3 , 150 MHz) δ 155.8 (C), 145.0 (C), 139.6 (C), 137.2 (C), 125.4 (C), 121.8 (C), 106.5 (CH), 91.5 (C), 50.3 (CH), 42.0 (CH_2), 40.0 (CH_2), 39.4 (C), 35.8 (CH_2), 34.5 (C), 33.7 (CH_3), 31.1 (CH), 22.7 (CH_2), 22.3 (CH_3), 20.2 (CH_3), 18.8 (CH_2), 18.6 (CH_3). HRESIMS calcd for $\text{C}_{21}\text{H}_{26}\text{O}_3^{79}\text{Br}$ ($[\text{M}-\text{H}]^-$): 405.1065; found 405.1068.

^1H NMR (C_6D_6 , 600 MHz) δ 7.14 (1H, s), 4.85 (1H, s, broad), 4.73 (1H, s, broad), 2.97 (1H, m), 2.42 (1H, m), 1.60 (1H, m), 1.56 (1H, m), 1.52 (1H, qt, $J = 3.2, 13.9$ Hz), 1.49 (1H, m), 1.47 (1H, m), 1.37 (1H, m), 1.362 (1H, m), 1.360 (1H, m), 1.32 (3H, d, $J = 6.9$ Hz), 1.31 (1H, m), 1.24 (3H, s), 1.15 (1H, td, $J = 3.4, 13.3$ Hz), 0.88 (3H, s), 0.86 (3H, s); ^{13}C NMR (C_6D_6 , 600 MHz) δ 156.1 (C), 146.0 (C), 141.0 (C), 138.5 (C), 125.9 (C), 122.5 (C), 107.3 (CH), 92.5 (C), 50.5 (CH), 42.7 (CH_2), 40.5 (CH_2), 39.9 (C), 36.2 (CH_2), 34.9 (C), 34.2 (CH_3), 31.6 (CH), 23.4 (CH_2), 22.8 (CH_3), 20.7 (CH_3), 19.5 (CH_2), 19.2 (CH_3).

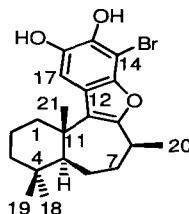
(\pm)-14-Bromospiroliphagane (**53**): for a summary of ^1H and ^{13}C NMR assignments, see Tables 6.4 and 6.14. ^1H NMR (CDCl_3 , 600 MHz) δ 7.18 (1H, s), 5.35 (1H, s, broad), 5.10 (1H, s, broad), 2.86 (1H, m), 2.57 (1H, dt, $J = 3.7, 14.3$ Hz), 2.51 (1H, td, $J = 4.2, 13.7$ Hz), 1.94 (1H, m), 1.91 (1H, m), 1.80 (1H, m), 1.61 (1H, qt, $J = 4.4, 17.8$ Hz), 1.50 (1H, m), 1.48 (1H, m), 1.36 (1H, m), 1.35 (3H, d, $J = 6.8$ Hz), 1.27 (1H, m), 1.15 (1H, m), 1.03 (3H, s), 0.88 (3H, s), 0.85 (3H, d, $J = 6.8$ Hz); ^{13}C NMR (CDCl_3 , 150 MHz) δ 159.1 (C), 145.8 (C), 139.6 (C), 137.1 (C), 122.7 (C), 118.1 (C), 108.3 (CH), 91.5 (C), 43.8 (C), 40.9 (C), 36.8 (CH), 36.5 (CH_2), 32.1 (CH_2), 31.2 (CH_2), 30.2 (CH_2), 29.3 (CH), 27.0 (CH_3), 21.4 (CH_2), 20.7 (CH_3), 18.9 (CH_3), 17.0 (CH_3). HRESIMS calcd for $\text{C}_{21}\text{H}_{27}\text{O}_3\text{Na}^{79}\text{Br}$ ($[\text{M}+\text{Na}]^+$): 429.1041; found 429.1050.

(-)-14-Bromo-9,16-dihydroxyliphagane quinone (**52**): for a summary of ^1H and ^{13}C NMR assignments, see Tables 6.4 and 6.15. ^1H NMR (C_6D_6 , 600 MHz) δ 7.36 (1H, s), 6.31 (1H, s), 2.24 (1H, s, broad), 2.22 (1H, m), 1.84 (1H, d, $J = 8.4$ Hz), 1.71 (1H, m), 1.59 (1H, m), 1.33 (1H, qt, $J = 2.9, 13.4$ Hz), 1.22 (1H, m), 1.21 (1H, m), 1.179 (1H, m), 1.176 (1H, m), 1.07 (1H, m), 1.01 (3H, s), 0.99 (1H, td, $J = 2.5, 12.8$ Hz), 0.98 (1H, m), 0.78 (3H, s), 0.64 (3H, s), 0.47 (3H, d, $J = 6.9$ Hz); ^{13}C NMR (C_6D_6 , 150 MHz) δ 176.6 (C), 168.3 (C), 167.5 (C), 149.2 (C), 127.0 (C),

120.0 (C), 98.5 (CH), 91.0 (C), 49.7 (CH), 43.1 (CH₂), 42.3 (C), 41.5 (CH₂), 40.4 (CH), 34.9 (C), 33.7 (CH₃), 32.8 (CH₂), 22.3 (CH₃), 22.3 (CH₃), 21.4 (CH₂), 19.8 (CH₂), 14.0 (CH₃).

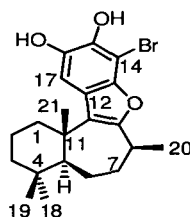
HRESIMS calcd for C₂₁H₂₈O₄⁷⁹Br ([M+H]⁺): 423.1171; found 423.1160.

Table 6.11. NMR data for (+)-8-epi-desformyl-14-bromoliphagal (**46**) (recorded in CDCl₃).



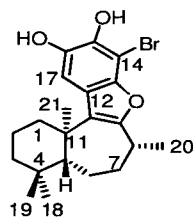
Carbon No	¹³ C δ (ppm) ^a	¹ H δ (ppm) (mult, J (Hz)) ^{b,c}	HMBC ^b (H→C)
1	40.0	H _{ax} 1.361 (m), H _{eq} 2.50 (m)	C2, C3, C5, C21
2	18.8	H _{eq} 1.49 (m), H _{ax} 1.67 (qt, J = 3.0, 13.8 Hz)	C4, C11
3	42.0	H _{ax} 1.21 (td, J = 3.5, 13.6 Hz), H _{eq} 1.44 (m)	C4, C18, C19
4	34.5		
5	50.3	1.74 (dd, J = 3.0, 9.4 Hz)	C4, C6, C7, C10, C11, C21
6	22.7	1.52 (m), 1.80 (m)	C4, C5, C7, C8, C11
7	35.8	1.68 (m), 1.87 (m)	C5, C6, C8, C9, C20
8	31.1	3.27 (m)	C6, C7, C9, C20
9	155.8		
10	125.4		
11	39.4		
12	121.8		
13	145.0		
14	91.5		
15	139.6	OH 5.33 (s, broad)	C14, C15, C16
16	137.2	OH 5.10 (s, broad)	C15, C16, C17
17	106.5	7.15 (s)	C10, C13, C14, C15, C16
18	33.7	0.96 (s)	C3, C4, C5, C19
19	22.3	0.93 (s)	C3, C5, C18
20	18.6	1.360 (d, J = 6.7 Hz)	C7, C8, C19
21	20.2	1.362 (s)	C5, C10, C11

^a Recorded at 150 MHz. ^b Recorded at 600 MHz. ^c According to HSQC recorded at 600 MHz.

Table 6.12. NMR data for (+)-8-*epi*-desformyl-14-bromoliphagal (**46**) (recorded in CDCl₃).

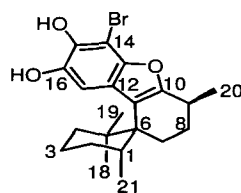
Proton No	¹ H δ (ppm) (mult, <i>J</i> (Hz)) ^a	COSY ^a
1 _{ax}	1.36 (m)	H1 _{eq} , H2 _{ax}
1 _{eq}	2.50 (m)	H1 _{ax} , H2 _{eq}
2 _{ax}	1.67 (qt, <i>J</i> = 3.0, 13.8 Hz)	H1 _{ax} , H2 _{eq} , H3 _{ax} , H3 _{eq}
2 _{eq}	1.49 (m)	H1 _{eq} , H2 _{ax}
3 _{ax}	1.21 (td, <i>J</i> = 3.5, 13.6 Hz)	H2 _{ax} , H3 _{eq}
3 _{eq}	1.44 (m)	H2 _{ax} , H3 _{ax}
5	1.74 (dd, <i>J</i> = 3.0, 9.4 Hz)	H6
6	1.52 (m), 1.80 (m)	H5, H7
7	1.68 (m), 1.87 (m)	H6, H8
8	3.27 (m)	H7, H20
15OH	5.33 (s, broad)	
16OH	5.10 (s, broad)	
17	7.15 (s)	
18	0.96 (s)	
19	0.93 (s)	
20	1.360 (d, <i>J</i> = 6.7 Hz)	H8
21	1.362 (s)	

^a Recorded at 600 MHz.

Table 6.13. NMR data for (-)-8-epi-desformyl-14-bromoliphagal (**46**) (recorded in C₆D₆).

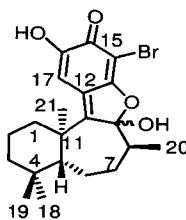
Proton No	¹ H δ (ppm) (mult, J (Hz)) ^a	COSY ^a
1 _{ax}	1.31 (m)	H1 _{eq}
1 _{eq}	2.42 (m)	H1 _{ax} , H2 _{ax}
2 _{ax}	1.360 (m)	H1 _{eq} , H2 _{eq} , H3 _{ax}
2 _{eq}	1.52 (qt, J = 3.2, 13.9 Hz)	H2 _{ax} , H3 _{ax}
3 _{ax}	1.15 (td, J = 3.4, 13.3 Hz)	H2 _{ax} , H2 _{eq}
3 _{eq}	1.37 (m)	
5	1.56 (m)	H6
6	1.362 (m), 1.49 (m)	H5, H7
7	1.47 (m), 1.60 (m)	H6, H8
8	2.97 (m)	H7, H20
15	OH 4.85 (s, broad)	
16	OH 4.73 (s, broad)	
17	7.14 (s)	
18	0.88 (s)	
19	0.86 (s)	
20	1.32 (d, J = 6.9 Hz)	H8
21	1.24 (s)	

^a Recorded at 600 MHz.

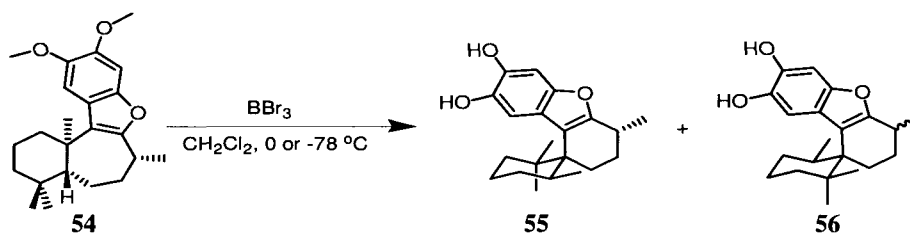
Table 6.14. NMR data for (\pm)-desformyl-14-bromospiroliphagane (**53**) (recorded in CDCl₃).

Proton No	¹ H δ (ppm) (mult, <i>J</i> (Hz)) ^a	COSY ^a	TROESY ^a
1	1.91 (m)	H2 _{eq} , H3 _{ax} , H21	H4 _{ax} , H20
2 _{eq}	1.36 (m)	H1	H18, H21
2 _{ax}	1.48 (m)	H3 _{eq}	H4 _{ax} , 15OH, 16OH, H19, H21
3 _{eq}	1.50 (m)	H2 _{ax} , H3 _{ax} , H4 _{eq}	
3 _{ax}	1.61 (qt, <i>J</i> = 4.4, 17.8 Hz)	H1, H3 _{eq} , H4 _{ax} , H4 _{eq}	
4 _{eq}	1.15 (m)	H4 _{ax} , H3 _{ax} , H3 _{eq}	
4 _{ax}	2.51 (td, <i>J</i> = 4.2, 13.7 Hz)	H3 _{ax} , H4 _{eq}	H1, H2 _{ax} , H17, H19
7 _{eq}	1.27 (m)	H7 _{ax} , H8 _{ax} , H8 _{eq}	
7 _{ax}	2.57 (dt, <i>J</i> = 3.7, 14.3 Hz)	H7 _{eq} , H8 _{ax}	H18
8 _{eq}	1.80 (m)	H7 _{eq} , H8 _{ax} , H9	H18, H20
8 _{ax}	1.94 (m)	H7 _{ax} , H7 _{eq} , H8 _{eq} , H9	H18
9	2.86 (m)	H8 _{eq} , H8 _{ax} , H20	
15OH	5.35 (s, broad)		H2 _{ax} , 16OH
16OH	5.10 (s, broad)		H2 _{ax} , 15OH
17	7.18 (s)		H4 _{ax} , H19
18	0.88 (s)		H2 _{eq} , H7 _{ax} , H8 _{ax} , H8 _{eq}
19	1.03 (s)		H2 _{ax} , H4 _{ax} , H17
20	1.35 (d, <i>J</i> = 6.8 Hz)	H9	H1, H8 _{eq}
21	0.85 (d, <i>J</i> = 6.8 Hz)	H1	H2 _{ax} , H2 _{eq}

^aRecorded at 600 MHz.

Table 6.15. NMR data for (-)-14-bromo-9,16-dihydroxyliphagane quinone (**52**) (recorded in C₆D₆).

Proton No	¹ H δ (ppm) (mult, J (Hz)) ^a	COSY ^a	TROESY ^a
1 _{ax}	1.07 (m)	H1 _{eq} , H2 _{ax}	
1 _{eq}	1.59 (m)	H1 _{ax} , H2 _{eq}	
2 _{ax}	1.33 (qt, J = 2.9, 13.4 Hz)	H1 _{ax} , H3 _{ax}	
2 _{eq}	1.21 (m)	H1 _{eq}	
3 _{ax}	0.99 (td, J = 2.5, 12.8 Hz)	H2 _{ax} , H3 _{eq}	
3 _{eq}	1.22 (m)	H3 _{ax}	
5	1.84 (d, J = 8.4 Hz)	H6	H18, H21
6	0.98 (m), 1.176 (m)	H5, H7	H18, H19, H21
7	1.179 (m), 1.71 (m)	H6, H8	H20, H21
8	2.22 (m)	H7, H20	
9OH	2.24 (s, broad)		
16OH	7.36 (s)		
17	6.31 (s)		
18	0.78 (s)		H6, H19
19	0.64 (s)		H6, H18, H21
20	0.47 (d, J = 6.9 Hz)	H8	H7, H21
21	1.01 (s)		H6, H7, H19, H20

^aRecorded at 600 MHz.Deprotection of desformyl-15,16-dimethoxyliphagal (**54**)

A solution of (**54**) (natural: 20 mg, 0.056 mmol; unnatural: 39 mg, 0.11 mmol) in CH₂Cl₂ (10 mL) at 0 °C, was treated with BBr₃ (0.84 mL, 0.84 mmol, 1 M in CH₂Cl₂). The resulting

mixture was stirred at room temperature for 4 h and quenched with aqueous $\text{Na}_2\text{S}_2\text{O}_3$. The organic layer was separated and washed with HCl 0.1 M, followed by Na_2SO_4 addition, filtration and solvent evaporation. Silica gel column chromatography (30% EtOAc/Hexanes) provided one main fraction (one spot by TLC), which was additionally purified by reversed-phase HPLC (C18 Inertsil, 75% $\text{CH}_3\text{CN}/25\%$ H_2O + 0.05% TFA), to afford (\pm)-desformylspiroliphagane A (**55**) (5.1 mg, 14%) and (\pm)-desformylspiroliphagane B (**56**) (4.1 mg, 11%).

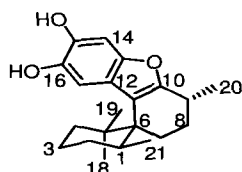
(\pm)-Desformylspiroliphagane A (**55**): for a summary of ^1H and ^{13}C NMR assignments, see Tables 6.16 and 6.17. ^1H NMR (CDCl_3 , 600 MHz) δ 7.15 (1H, s), 6.93 (1H, s), 5.09 (1H, s, broad), 4.79 (1H, s, broad), 2.89 (1H, m), 2.50 (1H, td, $J = 4.4, 13.6$ Hz), 2.28 (1H, ddd, $J = 4.1, 5.8, 14.3$ Hz), 2.20 (1H, m), 1.88 (1H, m), 1.67 (1H, qt, $J = 4.4, 17.9$ Hz), 1.54 (1H, m), 1.53 (1H, m), 1.47 (1H, m), 1.40 (1H, m), 1.38 (1H, dt, $J = 4.6, 12.9$ Hz), 1.22 (1H, m), 1.21 (3H, d, $J = 7.0$ Hz), 1.05 (3H, s), 0.84 (3H, d, $J = 7.2$ Hz), 0.83 (3H, s); ^{13}C NMR (CDCl_3 , 150 MHz) δ 159.0 (C), 149.1 (C), 140.5 (C), 138.8 (C), 122.2 (C), 116.9 (C), 109.3 (CH), 97.9 (CH), 43.7 (C), 41.5 (CH), 36.4 (C), 35.1 (CH_2), 30.9 (CH_2), 29.6 (CH_2), 28.4 (CH_2), 28.2 (CH), 26.0 (CH_3), 21.6 (CH_2), 20.6 (CH_3), 19.7 (CH_3), 16.8 (CH_3). HRESIMS calcd for $\text{C}_{21}\text{H}_{27}\text{O}_3$ ($[\text{M}+\text{H}]^+$): 327.1960; found 327.1953.

(\pm)-Desformylspiroliphagane B (**56**): for a summary of ^1H and ^{13}C NMR assignments, see Tables 6.18 and 6.19. ^1H NMR (C_6D_6 , 600 MHz) δ 7.18 (1H, s), 6.85 (1H, s), 4.55 (1H, s, broad), 4.55 (1H, s, broad), 2.74 (1H, m), 2.56 (1H, td, $J = 3.8, 14.1$ Hz), 2.34 (1H, dt, $J = 3.7, 14.3$ Hz), 1.70 (1H, m), 1.68 (2H, m), 1.54 (1H, qt, $J = 4.2, 13.3$ Hz), 1.45 (1H, m), 1.41 (1H, m), 1.36 (3H, d, $J = 6.9$ Hz), 1.32 (1H, m), 1.16 (1H, m), 1.11 (1H, m), 1.07 (3H, s), 0.85 (3H, s), 0.83 (3H, d, $J = 6.9$ Hz); ^{13}C NMR (C_6D_6 , 150 MHz) δ 158.7 (C), 150.2 (C), 141.8 (C), 140.8 (C), 123.1 (C),

117.9 (C), 110.1 (CH), 98.7 (CH), 44.2 (C), 41.7 (C), 37.5 (CH), 37.4 (CH₂), 33.0 (CH₂), 32.1 (CH₂), 31.2 (CH₂), 30.1 (CH), 27.7 (CH₃), 22.4 (CH₂), 21.4 (CH₃), 19.8 (CH₃), 17.8 (CH₃).

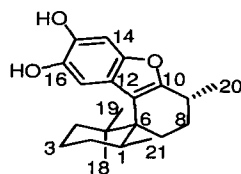
HRESIMS calcd for C₂₁H₂₇O₃ ([M-H]⁻): 327.1960; found 327.1969.

Table 6.16. NMR data for (±)-desformylspirolophane A (**55**) (recorded in CDCl₃).



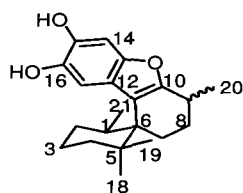
Carbon No	¹³ C δ (ppm) ^a	¹ H δ (ppm) (mult, J (Hz)) ^{b,c}	HMBC ^b (H→C)
1	41.5	1.88 (m)	C7, C21
2	28.4	H _{eq} 1.53 (m), H _{ax} 2.28 (ddd, J = 4.1, 5.8, 14.3 Hz)	C1, C4, C6, C7, C8, C11
3	21.6	H _{eq} 1.54 (m), H _{ax} 1.67 (qt, J = 4.4, 17.9 Hz)	C1, C4
4	35.1	H _{eq} 1.22 (m), H _{ax} 2.50 (td, J = 4.4, 13.6 Hz)	C2, C3, C6, C11
5	36.4		
6	43.7		
7	30.9	H _{ax} 1.38 (dt, J = 4.6, 12.9 Hz), H _{eq} 1.47 (m)	C1, C5, C21
8	29.6	H _{eq} 1.40 (m), H _{ax} 2.20 (m)	C6, C7, C9, C10, C20
9	28.2	2.89 (m)	C8, C20
10	159.0		
11	116.9		
12	122.2		
13	149.1		
14	97.9	6.93 (s)	C12, C13, C15, C16, C17
15	138.8	OH 5.09 (s, broad)	C14, C15, C16
16	140.5	OH 4.79 (s, broad)	C15, C16, C17
17	109.3	7.15 (s)	C11, C13, C14, C15, C16
18	26.0	0.83 (s)	C1, C5, C6, C7, C19
19	20.6	1.05 (s)	C1, C5, C6, C18
20	19.7	1.21 (d, J = 7.0 Hz)	C8, C9, C10
21	16.8	0.84 (d, J = 7.2 Hz)	C1, C5, C7

^a Recorded at 150 MHz. ^b Recorded at 600 MHz. ^c According to HSQC recorded at 600 MHz.

Table 6.17. NMR data for (\pm)-desformylspiroliphagane A (**55**) (recorded in CDCl₃).

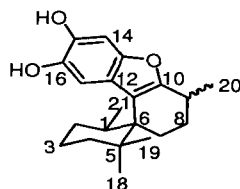
Proton No	¹ H δ (ppm) (mult, <i>J</i> (Hz)) ^a	COSY ^a	TROESY ^a
1	1.88 (m)	H7 _{ax} , H21	
2 _{eq}	1.53 (m)	H2 _{ax}	
2 _{ax}	2.28 (ddd, <i>J</i> = 4.1, 5.8, 14.3 Hz)	H2 _{eq} , H3 _{eq}	H21
3 _{eq}	1.54 (m)	H2 _{ax} , H3 _{ax} , H4 _{ax} , H4 _{eq}	
3 _{ax}	1.67 (qt, <i>J</i> = 4.4, 17.9 Hz)	H3 _{eq} , H4 _{ax} , H4 _{eq}	H8 _{eq}
4 _{eq}	1.22 (m)	H3 _{ax} , H3 _{eq} , H4 _{ax}	
4 _{ax}	2.50 (td, <i>J</i> = 4.4, 13.6 Hz)	H3 _{ax} , H3 _{eq} , H4 _{eq}	H19, H20, H21
7 _{ax}	1.38 (dt, <i>J</i> = 4.6, 12.9 Hz)	H1, H8 _{ax}	
7 _{eq}	1.47 (m)	H8 _{ax}	C18
8 _{eq}	1.40 (m)	H8 _{ax} , H9	H3 _{ax} , H18, H19
8 _{ax}	2.20 (m)	H7 _{ax} , H7 _{eq} , H8 _{eq} , H9	H21
9	2.89 (m)	H8 _{ax} , H8 _{eq} , H20	
14	6.93 (s)		
15OH	5.09 (s, broad)		16OH
16OH	4.79 (s, broad)		15OH
17	7.15 (s)		
18	0.83 (s)		H7 _{eq} , H8 _{eq}
19	1.05 (s)		H4 _{ax} , H8 _{eq}
20	1.21 (d, <i>J</i> = 7.0 Hz)	H9	H4 _{ax}
21	0.84 (d, <i>J</i> = 7.2 Hz)	H1	H2 _{ax} , H4 _{ax} , H8 _{ax}

^aRecorded at 600 MHz.

Table 6.18. NMR data for (\pm)-desformylspiroliphagane B (**56**) (recorded in C_6D_6).

Carbon No	^{13}C δ (ppm) ^a	1H δ (ppm) (mult, J (Hz)) ^{b,c}	HMBC ^b (H \rightarrow C)
1	37.5	1.70 (m)	C5, C21
2	37.4	H _{eq} 1.16 (m), H _{ax} 2.56 (td, $J = 3.8, 14.1$ Hz)	C3, C7, C6, C11
3	22.4	H _{eq} 1.45 (m), H _{ax} 1.54 (qt, $J = 4.2, 13.3$ Hz)	C2, C4, C6
4	32.1	1.32 (m), 1.41 (m)	C2
5	41.7		
6	44.2		
7	33.0	H _{eq} 1.11 (m) H _{ax} 2.34 (dt, $J = 3.7, 14.3$ Hz)	C1, C5, C6, C8, C9, C10, C11
8	31.2	1.68 (m)	C6, C7, C9, C10, C20
9	30.1	2.74 (m)	C8, C10, C11, C20
10	158.7		
11	117.9		
12	123.1		
13	150.2		
14	98.7	6.85 (s)	C12, C13, C15, C16
15	140.8	OH 4.55 (s, broad)	
16	141.8	OH 4.55 (s, broad)	
17	110.1	7.18 (s)	C11, C13, C15, C16
18	27.7	0.85 (s)	C1, C4, C5, C6, C19
19	21.4	1.07 (s)	C1, C5, C6, C18
20	19.8	1.36 (d, $J = 6.9$ Hz)	C8, C9, C10
21	17.8	0.83 (d, $J = 6.9$ Hz)	C2, C5, C7

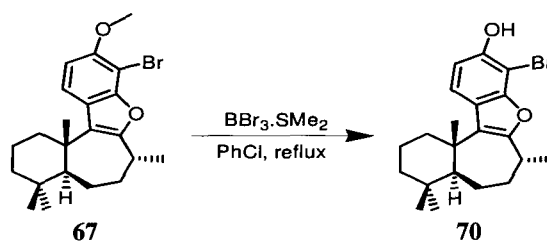
^aRecorded at 150 MHz. ^bRecorded at 600 MHz. ^cAccording to HSQC recorded at 600 MHz.

Table 6.19. NMR data for (\pm)-desformylspiroliphagane B (**56**) (recorded in C_6D_6).

Proton No	1H δ (ppm) (mult, J (Hz)) ^a	COSY ^a	TROESY ^a
1	1.70 (m)	H2 _{eq} , H21	H7 _{ax}
2 _{eq}	1.16 (m)	H1, H2 _{ax} , H3 _{ax} , H3 _{eq}	
2 _{ax}	2.56 (td, $J = 3.8, 14.1$ Hz)	H2 _{eq} , H3 _{ax} , H3 _{eq}	
3 _{eq}	1.45 (m)	H2 _{ax} , H2 _{eq} , H3 _{ax}	
3 _{ax}	1.54 (qt, $J = 4.2, 13.3$ Hz)	H2 _{ax} , H2 _{eq} , H3 _{eq} , H4	
4	1.32 (m), 1.41 (m)	H3 _{ax}	
7 _{eq}	1.11 (m)	H7 _{ax}	
7 _{ax}	2.34 (dt, $J = 3.7, 14.3$ Hz)	H7 _{eq} , H8	H1, H19
8	1.68 (m)	H7 _{ax} , H9	H18
9	2.74 (m)	H8, H20	
14	6.85 (s)		
15OH	4.55 (s, broad)		
16OH	4.55 (s, broad)		
17	7.18 (s)		
18	0.85 (s)		H8
19	1.07 (s)		H7 _{ax}
20	1.36 (d, $J = 6.9$ Hz)	H9	
21	0.83 (d, $J = 6.9$ Hz)	H1	

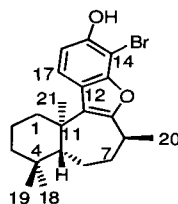
^aRecorded at 600 MHz.

Deprotection of (+) and (-)-14-bromo-15-methoxyliphagane (**67**)



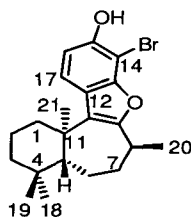
A solution of (**67**) (natural: 6.9 mg, 0.017 mmol; unnatural: 9.1 mg, 0.022 mmol) and $BBr_3 \cdot SMe_2$ (26 mg, 0.081 mmol) was refluxed in chlorobenzene, until TLC analysis showed absence of starting material (around 18 h). Once at room temperature, H_2O was added and the

crude was stirred for 30 minutes. The aqueous layer was extracted with EtOAc, dried (Na_2SO_4) and concentrated *in vacuo*. Silica gel column chromatography (20% EtOAc/hexanes) yielded one main fraction containing the desired product, which was additionally purified by reversed-phase HPLC (80% $\text{CH}_3\text{CN}/20\% \text{H}_2\text{O} + 0.05\% \text{TFA}$), to afford natural (-)-14-bromo-15-methoxyliphagane (**70**) (1.2 mg, 18%) and its unnatural (+)-enantiomer (2.7 mg, 31%), as pale yellow oils. UV (MeOH) λ_{max} (log ϵ) 262 nm (3.33). Natural: $[\alpha]_{\text{D}}^{20} -6.1$ (c 0.2, MeOH); unnatural: $[\alpha]_{\text{D}}^{20} +16.4$ (c 0.4, MeOH). For a summary of ^1H and ^{13}C NMR assignments, see Tables 6.5, 6.6, 6.20 and 6.21. ^1H NMR (C_6D_6 , 600 MHz) δ 7.23 (1H, d, $J = 8.6$ Hz), 6.82 (1H, d, $J = 8.6$ Hz), 5.07 (1H, s), 3.04 (1H, m), 2.42 (1H, m), 1.85 (1H, m), 1.62 (1H, m), 1.56 (1H, qt, $J = 3.3, 13.7$ Hz), 1.46 (1H, dd, $J = 2.3, 8.5$ Hz), 1.40 (1H, m), 1.38 (1H, m), 1.37 (1H, m), 1.36 (3H, d, $J = 7.1$ Hz), 1.35 (1H, m), 1.27 (1H, m), 1.22 (3H, s), 1.11 (1H, td, $J = 3.2, 13.3$ Hz), 0.87 (3H, s), 0.85 (3H, s); ^{13}C NMR (C_6D_6 , 150 MHz) δ 157.0 (C), 152.1 (C), 150.3 (C), 126.8 (C), 123.6 (C), 122.6 (CH), 111.0 (CH), 92.7 (C), 54.0 (CH), 42.5 (CH_2), 40.8 (CH_2), 40.2 (C), 35.4 (CH_2), 35.2 (C), 34.1 (CH), 33.7 (CH_3), 24.6 (CH_2), 22.4 (CH_3), 22.0 (CH_3), 20.7 (CH_3), 19.4 (CH_2). HRESIMS calcd for $\text{C}_{21}\text{H}_{26}\text{O}_2^{79}\text{Br}$ ($[\text{M}-\text{H}]^-$): 389.1116; found 389.1119.

Table 6.20. NMR data for (+)-14-bromo-15-hydroxyliphagane (70) (recorded in C₆D₆).

Carbon No	¹³ C δ (ppm) ^a	¹ H δ (ppm) (mult, <i>J</i> (Hz)) ^{b,c}	HMBC ^b (H→C)
1	40.8	H _{ax} 1.40 (m), H _{eq} 2.42 (m)	C2, C3, C5, C21
2	19.4	H _{eq} 1.38 (m), H _{ax} 1.56 (qt, <i>J</i> = 3.3, 13.7 Hz)	C5
3	42.5	H _{ax} 1.11 (td, <i>J</i> = 3.2, 13.3 Hz), H _{eq} 1.35 (m)	C1, C2, C5
4	35.2		
5	54.0	1.46 (dd, <i>J</i> = 2.3, 8.5 Hz)	C1, C4, C6, C10, C18, C19, C21
6	24.6	1.37 (m), 1.62 (m)	C4, C5, C8, C11
7	35.4	1.27 (m), 1.85 (m)	C5, C6, C8, C9, C20
8	34.1	3.04 (m)	C9, C10
9	157.0		
10	126.8		
11	40.2		
12	123.6		
13	152.1		
14	92.7		
15	150.3	OH 5.07 (s)	C14, C15, C16
16	111.0	6.82 (d, <i>J</i> = 8.6 Hz)	C12, C14, C15
17	122.6	7.23 (d, <i>J</i> = 8.6 Hz)	C10, C12, C13, C14, C15
18	33.7	0.87 (s)	C3, C4, C5, C19
19	22.4	0.85 (s)	C3, C4, C5, C18
20	22.0	1.36 (d, <i>J</i> = 7.1 Hz)	C7, C8, C9
21	20.7	1.22 (s)	C1, C5, C10, C11

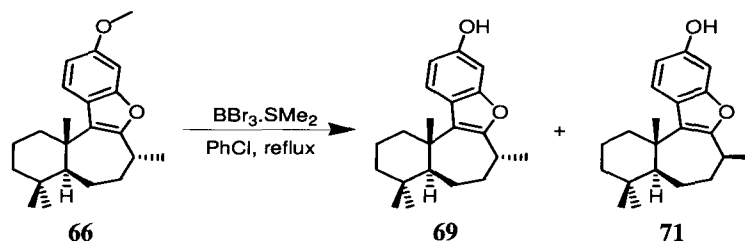
^a Recorded at 150 MHz. ^b Recorded at 600 MHz. ^c According to HSQC recorded at 600 MHz.

Table 6.21. NMR data for (+)-14-bromo-15-hydroxyliphagane (**70**) (recorded in C₆D₆).

Proton No	¹ H δ (ppm) (mult, J (Hz)) ^a	COSY ^a	TROESY ^a
1 _{ax}	1.40 (m)	H1 _{eq}	
1 _{eq}	2.42 (m)	H1 _{ax} , H2 _{eq}	H20, H21
2 _{ax}	1.56 (qt, J = 3.3, 13.7 Hz)	H3 _{ax} , H3 _{eq}	
2 _{eq}	1.38 (m)	H1 _{eq}	
3 _{ax}	1.11 (td, J = 3.2, 13.3 Hz)	H2 _{ax} , H3 _{eq}	H19
3 _{eq}	1.35 (m)	H2 _{ax} , H3 _{ax}	
5	1.46 (dd, J = 2.3, 8.5 Hz)		H19
6	1.37 (m), 1.62 (m)	H7	H19
7	1.27 (m), 1.85 (m)	H6, H8	H21
8	3.04 (m)	H7, H20	
15OH	5.07 (s)		
16	6.82 (d, J = 8.6 Hz)	H17	
17	7.23 (d, J = 8.6 Hz)	H16	
18	0.87 (s)		H21
19	0.85 (s)		H3 _{ax} , H5, H6
20	1.36 (d, J = 7.1 Hz)	H8	H1 _{eq}
21	1.22 (s)		H1 _{eq} , H7, H18

^aRecorded at 600 MHz.

Deprotection of (+) and (-)-15-methoxyliphagane (**66**)



The impure cyclization/debromination product (**66**) (natural: 5.5 mg, 0.017 mmol; unnatural: 8.1 mg, 0.025 mmol) and BBr₃·SMe₂ (60 mg, 0.19 mmol) were refluxed in chlorobenzene, until TLC analysis showed absence of starting material (around 18 h). Once at

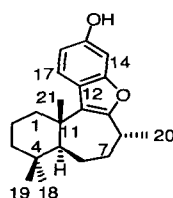
room temperature, H₂O was added and the crude was stirred for 30 minutes. The aqueous layer was extracted with EtOAc, dried (Na₂SO₄) and concentrated *in vacuo*. Silica gel column chromatography (10% EtOAc/hexanes) yielded one main fraction containing the desired product, which was additionally purified by reversed-phase HPLC (70% CH₃CN/30% H₂O + 0.05% TFA), to afford (+)-15-hydroxylyphagane (**69**) (0.9 mg, 17%) and (-)-8-*epi*-15-hydroxylyphagane (**71**) (0.9 mg, 17%) from the natural starting material; and unnatural (-)-15-hydroxylyphagane (**69**) (0.5 mg, 6%), all as pale yellow oils. (**69**): UV (MeOH) λ_{\max} (log ϵ) 245 nm (2.84); (**71**): UV (MeOH) λ_{\max} (log ϵ) 244 nm (3.42). Natural (**69**): $[\alpha]_{\text{D}}^{20}$ +8.8 (c 0.2, MeOH); (**71**): $[\alpha]_{\text{D}}^{20}$ -10.7 (c 0.4, MeOH). Unnatural (**69**): $[\alpha]_{\text{D}}^{20}$ -11.3 (c 0.2, MeOH).

(+)-15-Hydroxylyphagane (**69**): for a summary of ¹H and ¹³C NMR assignments, see Tables 6.5, 6.6, 6.22 and 6.23. ¹H NMR (C₆D₆, 600 MHz) δ 7.42 (1H, d, *J* = 8.6 Hz), 6.71 (1H, d, *J* = 2.2 Hz), 6.55 (1H, dd, *J* = 2.3, 8.5 Hz), 3.84 (1H, s), 3.11 (1H, m), 2.56 (1H, m), 1.93 (1H, m), 1.65 (1H, m), 1.59 (1H, qt, *J* = 2.8, 13.4 Hz), 1.52 (1H, m), 1.50 (1H, m), 1.44 (1H, m), 1.42 (3H, d, *J* = 7.1 Hz), 1.40 (1H, m), 1.36 (1H, m), 1.33 (1H, m), 1.30 (3H, s), 1.14 (1H, td, *J* = 3.4, 13.2 Hz), 0.90 (3H, s), 0.87 (3H, s); ¹³C NMR (C₆D₆, 150 MHz) δ 155.9 (C), 155.6 (C), 153.6 (C), 125.9 (C), 123.4 (CH), 122.8 (C), 111.0 (CH), 98.3 (CH), 54.3 (CH), 42.6 (CH₂), 40.9 (CH₂), 40.2 (C), 35.7 (CH₂), 35.2 (C), 34.3 (CH), 33.8 (CH₃), 24.8 (CH₂), 22.5 (CH₃), 22.2 (CH₃), 20.8 (CH₃), 19.5 (CH₂). HREIMS calcd for C₂₁H₂₈O₂ (M⁺): 312.20893; found 312.20798.

(-)-8-*epi*-15-Hydroxylyphagane (**71**): ¹H NMR (C₆D₆, 600 MHz) δ 7.36 (1H, d, *J* = 8.6 Hz), 6.74 (1H, d, *J* = 2.3 Hz), 6.54 (1H, dd, *J* = 2.3, 8.6 Hz), 3.84 (1H, s), 3.07 (1H, m), 2.56 (1H, m), 1.70-1.52 (7H, m), 1.42 (1H, dd, *J* = 3.4, 6.5 Hz), 1.40 (1H, m), 1.35 (3H, d, *J* = 7.1 Hz), 1.34 (3H, s), 1.15 (1H, td, *J* = 3.7, 13.4 Hz), 0.91 (3H, s), 0.90 (3H, s); ¹³C NMR (C₆D₆, 150 MHz) δ

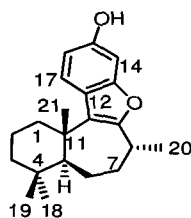
155.5 (C), 155.0 (C), 153.5 (C), 125.2 (C), 123.1 (CH), 122.9 (C), 111.1 (CH), 98.5 (CH), 50.9 (CH), 42.8 (CH₂), 40.8 (CH₂), 39.9 (C), 36.5 (CH₂), 35.0 (C), 34.2 (CH), 31.7 (CH₃), 23.5 (CH₂), 22.9 (CH₃), 21.0 (CH₃), 19.63 (CH₃), 19.60 (CH₂). HREIMS calcd for C₂₁H₂₈O₂ (M⁺): 312.20893; found 312.20954.

Table 6.22. NMR data for (+)-15-hydroxyliphagane (**69**) (recorded in C₆D₆).



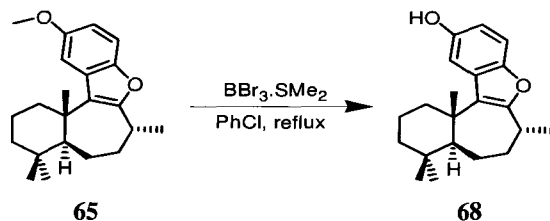
Carbon No	¹³ C δ (ppm) ^a	¹ H δ (ppm) (mult, J (Hz)) ^{b,c}	HMBC ^b (H→C)
1	40.9	H _{ax} 1.50 (m), H _{eq} 2.56 (m)	C2, C3, C5, C11
2	19.5	H _{eq} 1.40 (m), H _{ax} 1.59 (qt, J = 2.8, 13.4 Hz)	C1
3	42.6	H _{ax} 1.14 (td, J = 3.4, 13.2 Hz), H _{eq} 1.36 (m)	C1, C2, C4, C18, C19
4	35.2		
5	54.3	1.52 (m)	C2, C3, C4, C6, C7, C10, C11, C18, C19, C21
6	24.8	1.44 (m), 1.65 (m)	C4, C5, C11
7	35.7	1.33 (m), 1.93 (m)	C5, C6, C8, C9, C20
8	34.3	3.11 (m)	C6, C7, C9, C10, C20
9	155.9		
10	125.9		
11	40.2		
12	122.8		
13	155.6		
14	98.3	6.71 (d, J = 2.2 Hz)	C12, C13, C15, C16
15	153.6	OH 3.84 (s)	C14, C15, C16
16	111.0	6.55 (dd, J = 2.3, 8.5 Hz)	C12, C14, C15
17	123.4	7.42 (d, J = 8.6 Hz)	C10, C12, C13, C14, C15
18	33.8	0.90 (s)	C2, C3, C4, C5, C19, C21
19	22.5	0.87 (s)	C3, C4, C5, C18
20	22.2	1.42 (d, J = 7.1 Hz)	C7, C8, C9, C11
21	20.8	1.30 (s)	C1, C5, C10, C11

^a Recorded at 150 MHz. ^b Recorded at 600 MHz. ^c According to HSQC recorded at 600 MHz.

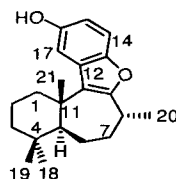
Table 6.23. NMR data for (+)-15-hydroxyliphagane (**69**) (recorded in C₆D₆).

Proton No	¹ H δ (ppm) (mult, J (Hz)) ^a	COSY ^a	TROESY ^a
1 _{ax}	1.50 (m)	H1 _{eq}	
1 _{eq}	2.56 (m)	H1 _{ax} , H2 _{ax}	H5, H21
2 _{eq}	1.40 (m)	H2 _{ax}	
2 _{ax}	1.59 (qt, J = 2.8, 13.4 Hz)	H1 _{eq} , H2 _{eq} , H3 _{ax}	
3 _{ax}	1.14 (td, J = 3.4, 13.2 Hz)	H2 _{ax} , H3 _{eq}	H6, H19
3 _{eq}	1.36 (m)	H3 _{ax}	H19
5	1.52 (m)		H1 _{eq} , H18
6	1.44 (m), 1.65 (m)	H7	H3 _{ax} , H18
7	1.33 (m), 1.93 (m)	H6, H8	
8	3.11 (m)	H7, H20	
14	6.71 (d, J = 2.2 Hz)		
15OH	3.84 (s)		
16	6.55 (dd, J = 2.3, 8.5 Hz)	H17	
17	7.42 (d, J = 8.6 Hz)	H16	
18	0.90 (s)		H5, H6
19	0.87 (s)		H3 _{ax} , H3 _{eq} , H21
20	1.42 (d, J = 7.1 Hz)	H8	
21	1.30 (s)		H1 _{eq} , H19

^aRecorded at 600 MHz.

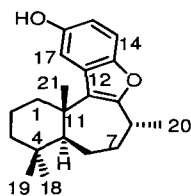
Deprotection of (+)-16-methoxylyphagane (65)

The resulting cyclization mixture (**65**) was dissolved in chlorobenzene (10 mL) and refluxed in the presence of $\text{BBr}_3 \cdot \text{SMe}_2$ (90 mg, 0.29 mmol), until TLC analysis showed absence of starting material (around 12 h). Work-up as stated in the previous experimental procedure, followed by silica gel column chromatography (10% EtOAc/hexanes) and reversed-phase HPLC (85% $\text{CH}_3\text{CN}/15\% \text{H}_2\text{O} + 0.05\% \text{TFA}$), yielded desired (+)-16-hydroxylyphagane (**68**) as a pale yellow oil (0.6 mg, 0.5% from acyclic **91**). $[\alpha]_{\text{D}}^{20} +4.7$ (*c* 0.2, MeOH); UV (MeOH) λ_{max} (log ϵ) 297 nm (3.82). For a summary of ^1H and ^{13}C NMR assignments, see Tables 6.5, 6.6, 6.24 and 6.25. ^1H NMR (C_6D_6 , 600 MHz) δ 7.17 (1H, d, $J = 8.6$ Hz), 7.01 (1H, d, $J = 2.5$ Hz), 6.45 (1H, dd, $J = 2.5, 8.8$ Hz), 3.73 (1H, s), 3.09 (1H, m), 2.57 (1H, m), 1.90 (1H, m), 1.66 (1H, m), 1.63 (1H, qt, $J = 2.8, 13.3$ Hz), 1.52 (1H, m), 1.50 (1H, m), 1.43 (1H, m), 1.42 (1H, m), 1.40 (3H, d, $J = 7.2$ Hz), 1.36 (1H, m), 1.32 (1H, m), 1.29 (3H, s), 1.14 (1H, td, $J = 3.6, 13.3$ Hz), 0.90 (3H, s), 0.88 (3H, s); ^{13}C NMR (C_6D_6 , 150 MHz) δ 158.2 (C), 151.4 (C), 149.6 (C), 130.1 (C), 126.0 (C), 111.8 (CH), 111.5 (CH), 108.8 (CH), 54.0 (CH), 42.6 (CH_2), 40.6 (CH_2), 40.2 (C), 35.5 (CH_2), 35.2 (C), 34.4 (CH), 33.8 (CH_3), 24.8 (CH_2), 22.5 (CH_3), 22.0 (CH_3), 20.5 (CH_3), 19.5 (CH_2). HREIMS calcd for $\text{C}_{21}\text{H}_{28}\text{O}_2$ (M^+): 312.20893; found 312.20861.

Table 6.24. NMR data for (+)-16-hydroxyliphagane (**68**) (recorded in C₆D₆).

Carbon No	¹³ C δ (ppm) ^a	¹ H δ (ppm) (mult, <i>J</i> (Hz)) ^{b,c}	HMBC ^b (H→C)
1	40.6	H _{ax} 1.50 (m), H _{eq} 2.57 (m)	C2, C3, C5, C10
2	19.5	H _{eq} 1.42 (m), H _{ax} 1.63 (qt, <i>J</i> = 2.8, 13.3 Hz)	C1, C3
3	42.6	H _{ax} 1.14 (td, <i>J</i> = 3.6, 13.3 Hz), H _{eq} 1.36 (m)	C1, C2, C18, C19
4	35.2		
5	54.0	1.52 (m)	C3, C6, C7, C10, C11, C18, C19, C21
6	24.8	1.43 (m), 1.66 (m)	C5, C8, C11
7	35.5	1.32 (m), 1.90 (m)	C5, C6, C8, C9, C20
8	34.4	3.09 (m)	C6, C7, C9, C10, C20
9	158.2		
10	126.0		
11	40.2		
12	130.1		
13	149.6		
14	111.5	7.17 (d, <i>J</i> = 8.6 Hz)	C12, C13, C16, C17
15	111.8	6.45 (dd, <i>J</i> = 2.5, 8.8 Hz)	C13, C16, C17
16	151.4	OH 3.73 (s)	C15, C16, C17
17	108.8	7.01 (d, <i>J</i> = 2.5 Hz)	C13, C15, C16
18	33.8	0.90 (s)	C2, C3, C4, C5, C19
19	22.5	0.88 (s)	C3, C4, C5, C18
20	22.0	1.40 (d, <i>J</i> = 7.2 Hz)	C7, C8, C9, C11
21	20.5	1.29 (s)	C1, C5, C10, C11

^aRecorded at 150 MHz. ^bRecorded at 600 MHz. ^cAccording to HSQC recorded at 600 MHz.

Table 6.25. NMR data for (+)-16-hydroxyliphagane (**68**) (recorded in C₆D₆).

Proton No	¹ H δ (ppm) (mult, <i>J</i> (Hz)) ^a	COSY ^a	TROESY ^a
1 _{ax}	1.50 (m)	H1 _{eq}	
1 _{eq}	2.57 (m)	H1 _{ax} , H2 _{eq} , H2 _{ax}	
2 _{eq}	1.42 (m)	H1 _{eq} , H3 _{eq}	
2 _{ax}	1.63 (qt, <i>J</i> = 2.8, 13.3 Hz)	H1 _{eq} , H3 _{ax}	
3 _{ax}	1.14 (td, <i>J</i> = 3.6, 13.3 Hz)	H2 _{ax}	H18
3 _{eq}	1.36 (m)	H2 _{eq}	
5	1.52 (m)		H18
6	1.43 (m), 1.66 (m)	H7	H21
7	1.32 (m), 1.90 (m)	H6, H8	
8	3.09 (m)	H7, H20	
14	7.17 (d, <i>J</i> = 8.6 Hz)	H15	
15	6.45 (dd, <i>J</i> = 2.5, 8.8 Hz)	H14, H17	
16OH	3.73 (s)		
17	7.01 (d, <i>J</i> = 2.5 Hz)	H15	
18	0.90 (s)		H3 _{ax} , H5
19	0.88 (s)		H21
20	1.40 (d, <i>J</i> = 7.2 Hz)	H8	
21	1.29 (s)		H6, H19

^aRecorded at 600 MHz.

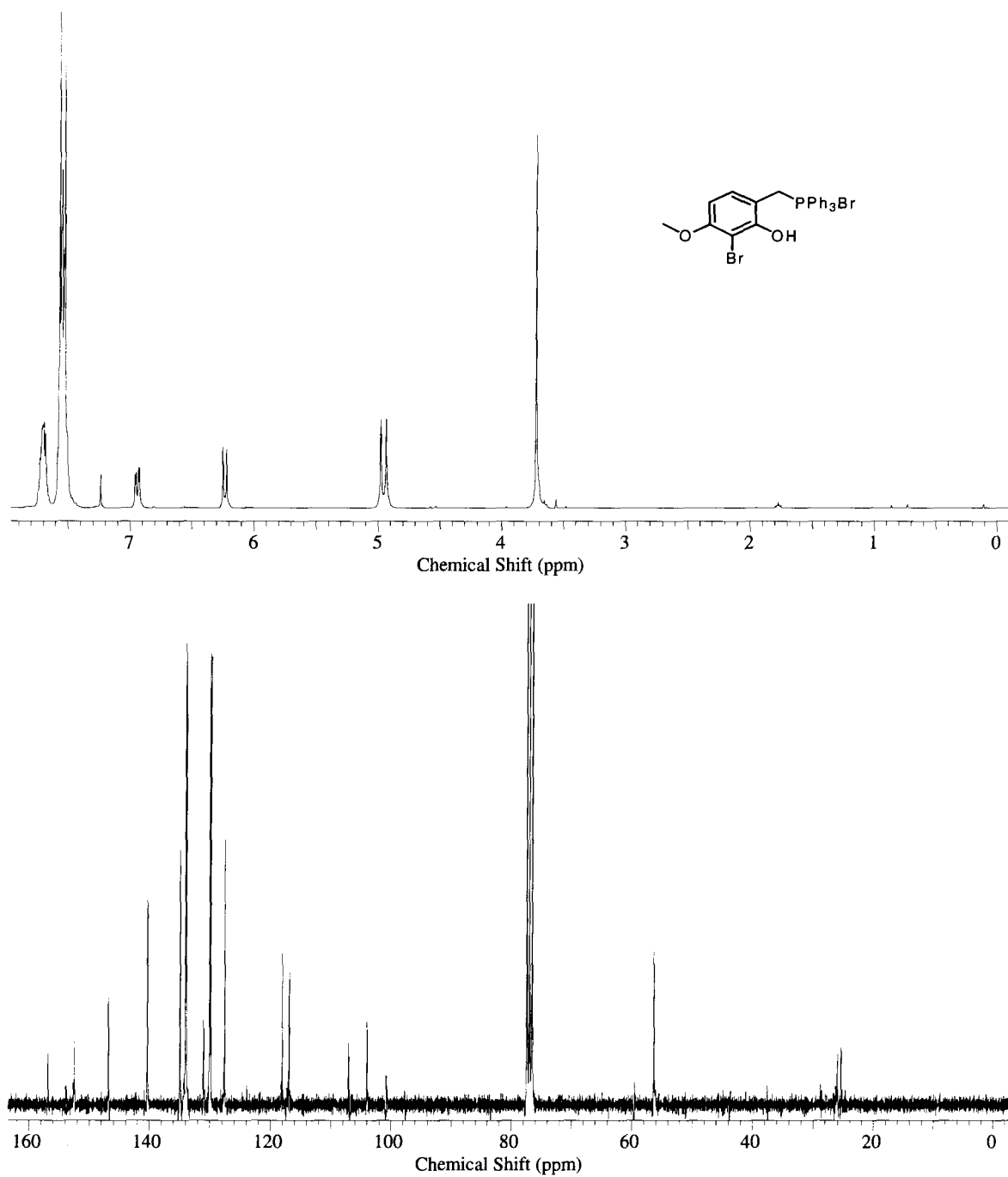


Figure 6.15. a) ¹H-NMR and b) ¹³C-NMR spectra of (2-hydroxy-4-methoxyphenyl)-methyltriphenylphosphonium bromide (**78**) (recorded in CDCl₃ at 300 and 75 MHz respectively).

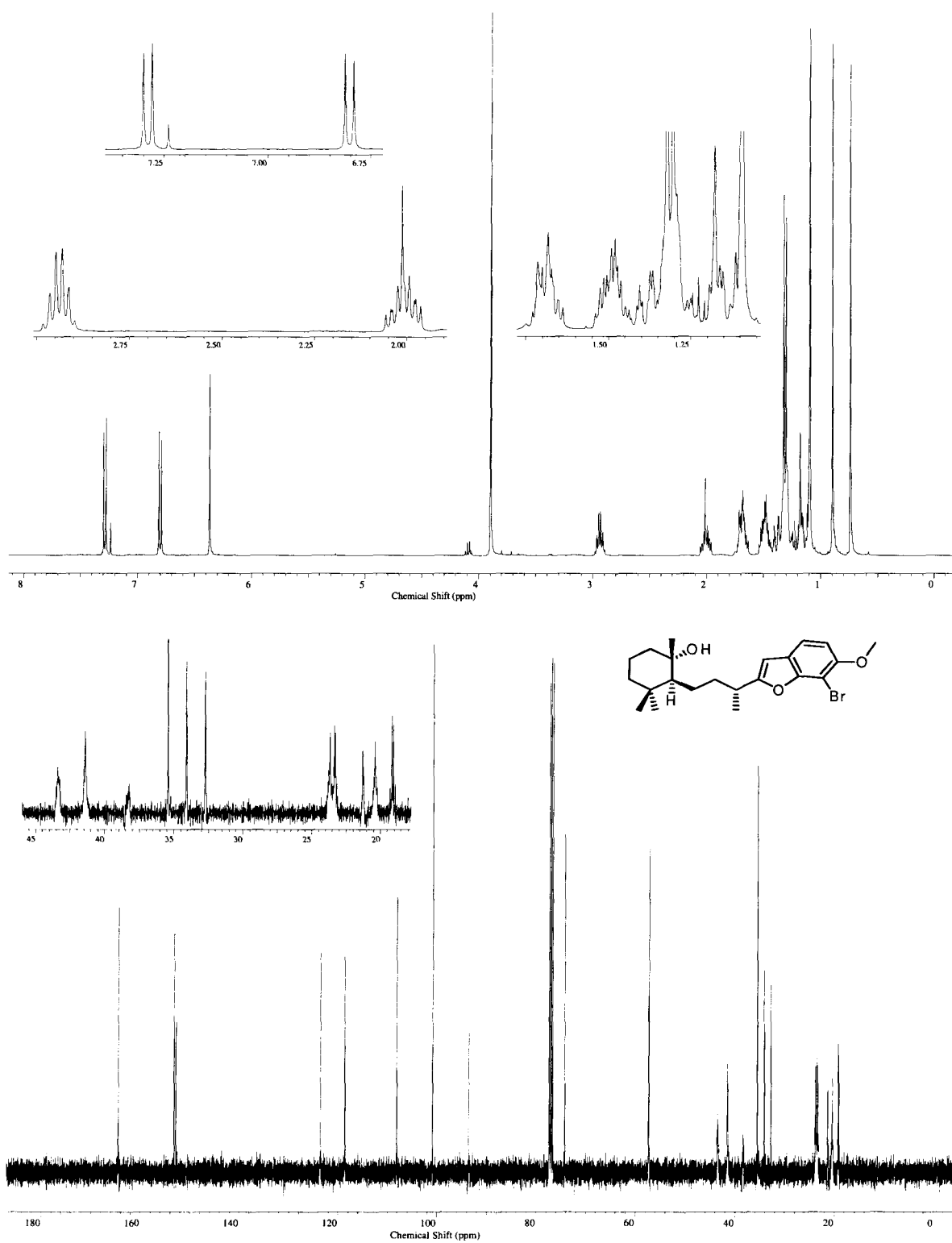


Figure 6.16. ^1H and ^{13}C -NMR spectra of 2-[3-(7-bromo-6-methoxy-benzofuran-2-yl)-butyl]-1,3,3-trimethylcyclohexanol (**90**) (recorded in CDCl_3 at 400 and 100 MHz respectively).

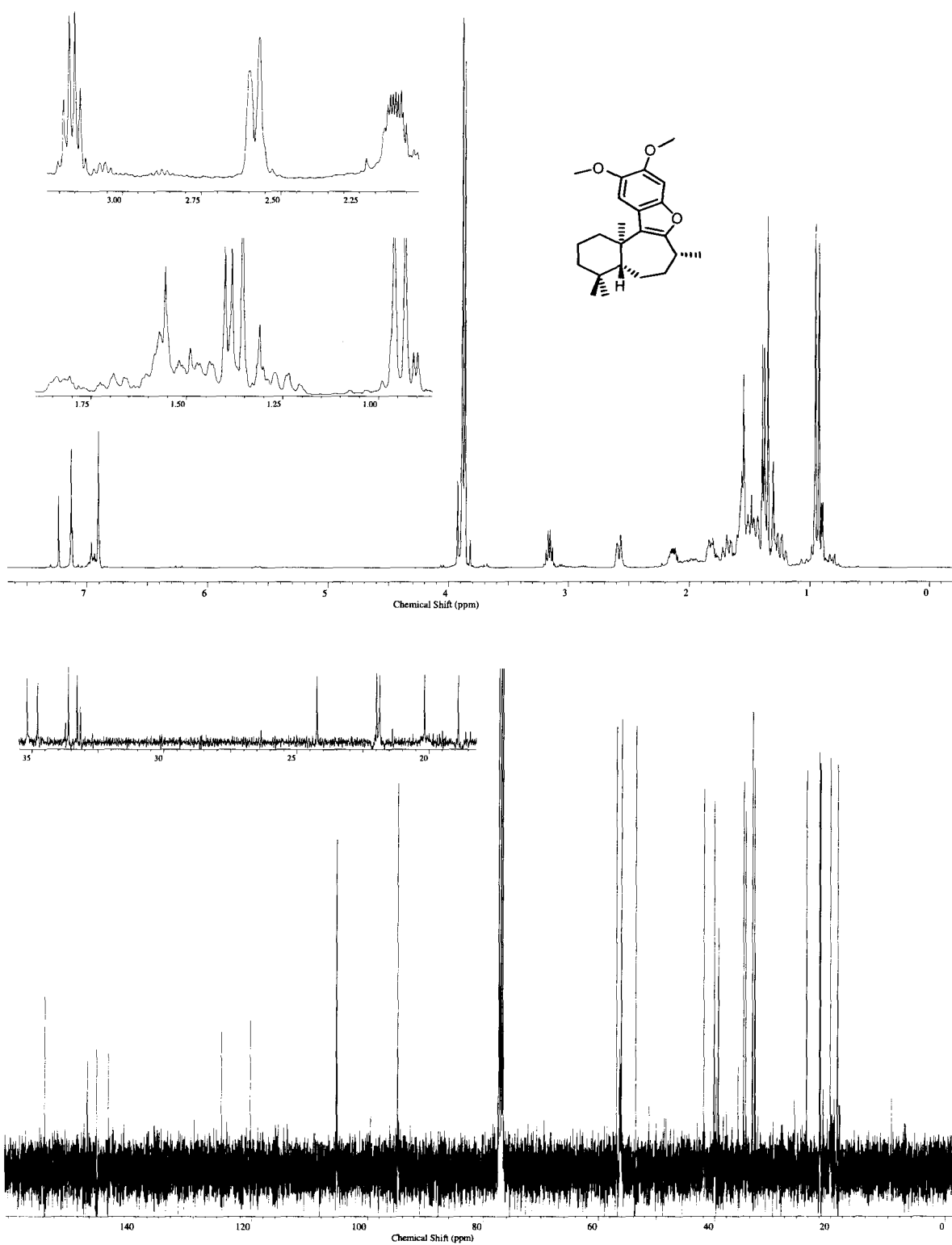


Figure 6.17. ^1H and ^{13}C -NMR spectra of desformyl-15,16-dimethoxyliphagal (**54**) (recorded in C_6D_6 at 400 and 100 MHz respectively).

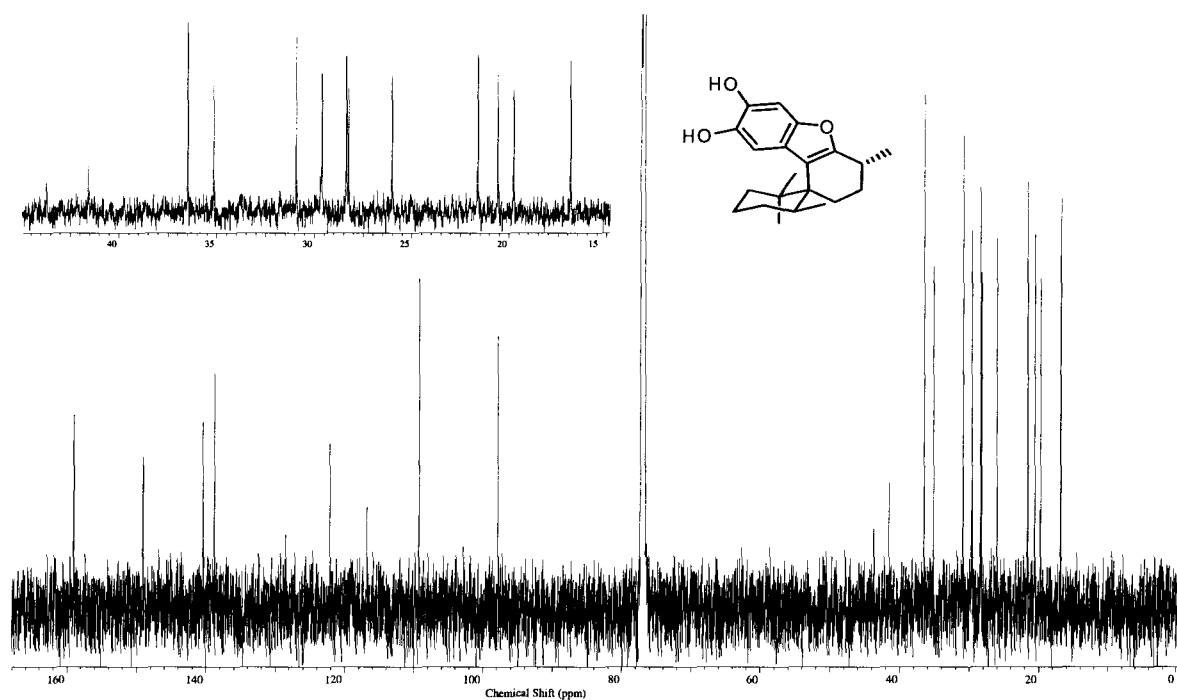


Figure 6.18. ^{13}C -NMR spectrum of (±)-desformylspiroliphagane A (**55**) (recorded in CDCl_3 at 150 MHz).

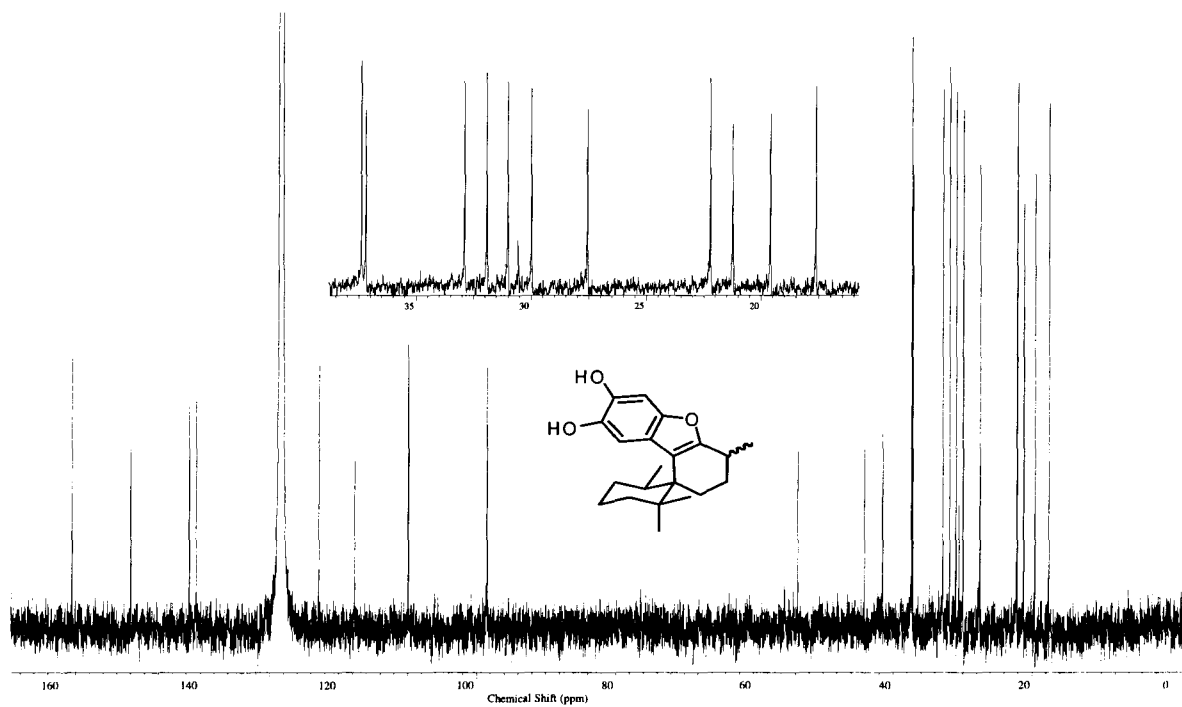


Figure 6.19. ^{13}C -NMR spectrum of (±)-desformylspiroliphagane B (**56**) (recorded in CDCl_3 at 150 MHz).

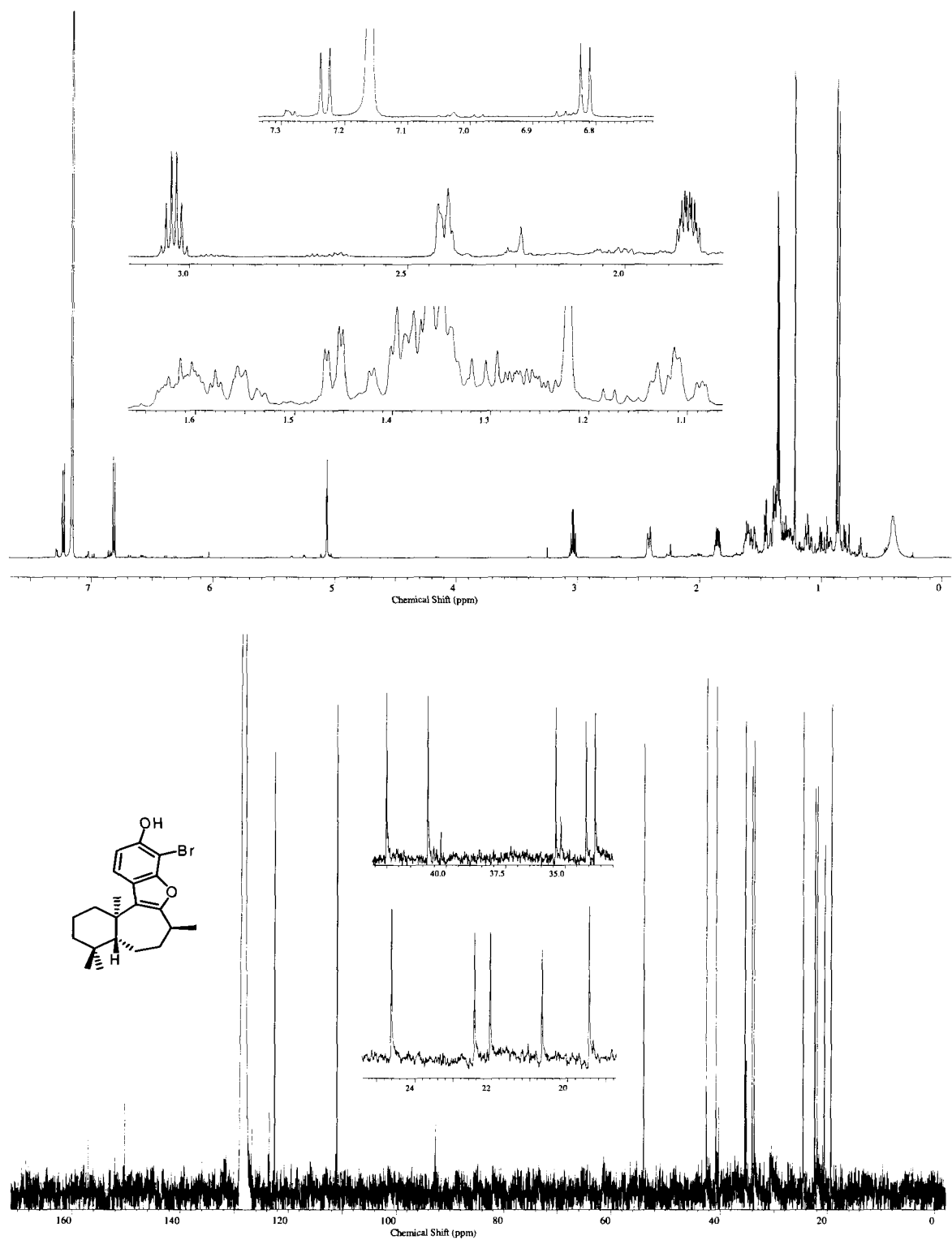


Figure 6.20. ^1H and ^{13}C -NMR spectra of (+)-14-bromo-15-hydroxyliphagane (**70**) (recorded in C_6D_6 at 600 and 150 MHz respectively).

7. References

- (1) Andersen, R. J.; Williams, D. E. *Chemistry of the Marine Environment*; The Royal Society of Chemistry: Cambridge, 2000, 55-76 pp.
- (2) Fenical, W. *Oceanography*. **2006**, *19*, 110-119.
- (3) Cans, R. *Nature*. **1997**, *388*, 334-337.
- (4) Rawat, D. S.; Joshi, M. C.; Joshi, P.; Atheaya, H. *Anti-Cancer Agents in Medicinal Chemistry*. **2006**, *6*, 33-40.
- (5) MarinLit database. Department of Chemistry, University of Canterbury: <http://www.chem.canterbury.ac.nz/marinlit/marinlit.shtml>, 2005.
- (6) Blunt, J. W.; Copp, B. R.; Munro, M. H. G.; Northcote, P. T.; Prinsep, M. R. *Nat. Prod. Rep.* **2005**, *22*, 15-61.
- (7) Simmons, T. L.; Andrianosolo, E.; McPhail, K.; Flatt, P.; Gerwick, W. H. *Mol. Cancer. Ther.* **2005**, *4*, 333-342.
- (8) Williams, D. H.; Stone, M. J.; Hauck, P. R.; Rahman, S. K. *J. Nat. Prod.* **1989**, *52*, 1189-1208.
- (9) Jacquot, D. E. N.; Lindel, T. *Curr. Org. Chem.* **2005**, *9*, 1551-1565.
- (10) Lindquist, N.; Lobkovski, E.; Clardy, J. *Tetrahedron Lett.* **1996**, *37*, 9131-9134.
- (11) Lindquist, N. *J. Nat. Prod.* **2002**, *65*, 681-684.
- (12) Lindquist, N.; Shigematsu, N.; Pannell, L. *J. Nat. Prod.* **2000**, *63*, 1290-1291.
- (13) Rezanka, T.; Hanus, L. O.; Dembitsky, V. M. *Tetrahedron*. **2004**, *60*, 12191-12199.
- (14) Barsby, T.; Kelly, M. T.; Gagne, S. M.; Andersen, R. J. *Org. Lett.* **2001**, *3*, 437-440.
- (15) Olivera, B. M.; Cruz, L. J.; Santos, V.; LeCheminant, G. W.; Griffin, D.; Zeikus, R.; McIntosh, J. M.; Galyean, R.; Varga, J.; Gray, W. R.; Rivier, J. *Biochem.* **1987**, *26*, 2086-2090.
- (16) Layer, R. T.; McIntosh, J. M. *Mar. Drugs*. **2006**, *4*, 119-142.
- (17) Lindquist, N. *Mar. Biol.* **1996**, *126*, 745-755.
- (18) Munro, M. H. G.; Blunt, J. W.; Dumdei, E. J.; Hickford, S. J. H.; Lill, R. E.; Li, S.; Battershill, C. N.; Duckworth, A. R. *J. Biotech.* **1999**, *70*, 15-25.
- (19) Blunt, J. W.; Copp, B. R.; Munro, M. H. G.; Northcote, P. T.; Prinsep, M. R. *Nat. Prod. Rep.* **2004**, *21*, 1-49.
- (20) Keyzers, R. A.; Davies-Coleman, M. T. *Chem. Soc. Rev.* **2005**, *34*, 355-365.
- (21) Dembitsky, V. M.; Glorizova, T. A.; Poroikov, V. V. *Mini-Rev. Med. Chem.* **2005**, *5*, 319-336.
- (22) Blunt, J. W.; Copp, B. R.; Hu, W. P.; Munro, M. H. G.; Northcote, P. T.; Prinsep, M. R. *Nat. Prod. Rep.* **2007**, *24*, 31-86.
- (23) Blunt, J. W.; Copp, B. R.; Munro, M. H. G.; Northcote, P. T.; Prinsep, M. R. *Nat. Prod. Rep.* **2006**, *23*, 26-78.
- (24) Piel, J.; Butzke, D.; Fusetani, N.; Hui, D.; Platzer, M.; Wen, G.; Matsunaga, S. *J. Nat. Prod.* **2005**, *68*, 472-479.
- (25) Fortman, J. L.; Sherman, D. H. *ChemBioChem.* **2005**, *6*, 960-978.
- (26) Bergmann, W.; Feeney, R. J. *J. Am. Chem. Soc.* **1950**, *72*, 2809-2814.
- (27) Bergmann, W.; Feeney, R. J. *J. Org. Chem.* **1951**, *16*, 981-987.
- (28) Nicholas, G. M.; Phillips, A. J. *Nat. Prod. Rep.* **2005**, *22*, 144-161.
- (29) Hassfeld, J.; Kalesse, M.; Stellfeld, T.; Christmann, M. *Adv. Biochem. Engin. Biotechnol.* **2005**, *97*, 133-203.
- (30) Ruckle, T.; Schwarz, M. K.; Rommel, C. *Nature*. **2006**, *5*, 903-918.

- (31) Blunt, J. W.; Copp, B. R.; Munro, M. H. G.; Northcote, P. T.; Prinsep, M. R. *Nat. Prod. Rep.* **2003**, *20*, 1-48.
- (32) Nicholas, G. M.; Phillips, A. J. *Nat. Prod. Rep.* **2006**, *23*, 79-99.
- (33) Morris, J. C.; Nicholas, G. M.; Phillips, A. J. *Nat. Prod. Rep.* **2007**, *24*, 87-108.
- (34) Hamada, Y.; Shioiri, T. *Chem. Rev.* **2005**, *105*, 4441-4482.
- (35) Inoue, M. *Chem. Rev.* **2005**, *105*, 4379-4405.
- (36) Nicolaou, K. C. *J. Org. Chem.* **2005**, *70*, 7007-7027.
- (37) Stanovnik, B.; Svete, J. *Mini-Rev. Org. Chem.* **2005**, *2*, 211-224.
- (38) Baran, P. S.; Maimone, T. J.; Richter, J. M. *Nature.* **2007**, *446*, 404-408.
- (39) Yeung, K. S.; Paterson, I. *Chem. Rev.* **2005**, *105*, 4237-4313.
- (40) Blunt, J. W.; Copp, B. R.; Munro, M. H. G.; Northcote, P. T.; Prinsep, M. R. *Nat. Prod. Rep.* **2004**, *21*, 1-49.
- (41) Blunt, J. W.; Copp, B. R.; Munro, M. H. G.; Northcote, P. T.; Prinsep, M. R. *Nat. Prod. Rep.* **2006**, *23*, 26-78.
- (42) Blunt, J. W.; Copp, B. R.; Hu, W.; Munro, M. H. G.; Northcote, P. T.; Prinsep, M. R. *Nat. Prod. Rep.* **2007**, *24*, 31-86.
- (43) Aneiros, A.; Garateix, A. *J. Chromatography B.* **2004**, *803*, 41-53.
- (44) Rawat, D. S.; Joshi, M. C.; Joshi, P.; Atheaya, H. *Anti-Cancer Agents in Medicinal Chemistry.* **2006**, *6*, 33-40.
- (45) Rinehart, K. L.; Lithgow-Bertelloni, A. M. *Chem. Abs.* 1991, *115*, 248086: G. B. Patent 22026, 1990.
- (46) Urdiales, J. L.; Morata, P.; Nunez-Castro, I.; Sanchez-Jimenez, F. *Cancer Lett.* **1996**, *102*, 31-40.
- (47) Pettit, G. R.; Kamano, Y.; Herald, C. L.; Fujii, Y.; Kizu, H.; Boyd, M. R.; Boettner, F. E.; Doubek, D. L.; Schmidt, J. M.; Chapuis, J. C.; Michel, C. *Tetrahedron.* **1993**, *49*, 9151-9170.
- (48) Pettit, G. R.; Kamano, Y.; Herald, C. L.; Tuinman, A. A.; Boettner, F. E.; Kizu, H.; Schmidt, J. M.; Baczynskyj, L.; Tomer, K. B.; Bontems, R. J. *J. Am. Chem. Soc.* **1987**, *109*, 6883-6890.
- (49) Ebbinghaus, S.; Hersh, E.; Cunningham, C. C.; O'Day, S.; McDermott, D.; Stephenson, J.; Richards, D. A.; Eckhart, J.; Haider, O. L.; Hammond, L. A. *J. Clin. Oncol.* **2004**, *22*, 7530-7536.
- (50) Kerbrat, P.; Dieras, V.; Pavlidis, N.; Ravaud, A.; Wanders, J.; Fumoleau, P. *Eur. J. Cancer.* **2003**, *39*, 317-325.
- (51) Talpir, R.; Benayahu, Y.; Kashman, Y.; Pannell, L.; Schleyer, M. *Tetrahedron Lett.* **1994**, *35*, 4453-4456.
- (52) Andersen, R. J.; Coleman, J. E.; Piers, E.; Wallace, D. J. *Tetrahedron Lett.* **1997**, *38*, 317-320.
- (53) Nieman, J. A.; Coleman, J. E.; Wallace, D. J.; Piers, E.; Lim, L. Y.; Roberge, M.; Andersen, R. J. *J. Nat. Prod.* **2003**, *66*, 183-187.
- (54) Hamann, M. T.; Scheuer, P. J. *J. Am. Chem. Soc.* **1993**, *115*, 5825-5829.
- (55) Goetz, G.; Nakao, Y.; Scheuer, P. J. *J. Nat. Prod.* **1997**, *60*, 562-566.
- (56) Horgen, F. D.; Santos, D. B.; Goetz, G.; Sakamoto, B.; Kan, Y.; Nagai, H.; Scheuer, P. J. *J. Nat. Prod.* **2000**, *63*, 152-155.
- (57) Coleman, J. E.; Silva, D.; Kong, F.; Andersen, R. J. *Tetrahedron.* **1995**, *39*, 10653-10662.
- (58) Anderson, H. J.; Coleman, J. E.; Andersen, R. J.; Roberge, M. *Cancer Chemother. Pharmacol.* **1997**, *39*, 223-226.
- (59) Bai, R.; Durso, N. A.; Sacket, D. L.; Hamel, E. *Biochem.* **1999**, *38*, 14302-14310.

- (60) Loganzo, F.; Discafani, C. M.; Annable, T.; Beyer, C.; Musto, S.; Hari, M.; Tan, X.; Hardy, C.; Hernandez, R.; Baxter, M.; Singanallore, T.; Khafizova, G.; Poruchynsky, M. S.; Fojo, T.; Nieman, J. A.; Ayrál-Kaloustian, S.; Zask, A.; Andersen, R. J.; Greenberger, L. M. *Cancer res.* **2003**, *63*, 1838-1845.
- (61) Gerard, J.; Haden, P.; Kelly, M. T.; Andersen, R. J. *Tetrahedron Lett.* **1996**, *37*, 7201-7204.
- (62) Gerard, J.; Haden, P.; Kelly, M. T.; Andersen, R. J. *J. Nat. Prod.* **1999**, *62*, 80-85.
- (63) Gerard, J.; Lloyd, R.; Barsby, T.; Haden, P.; Kelly, M. T.; Andersen, R. J. *J. Nat. Prod.* **1997**, *60*, 223-229.
- (64) Barsby, T.; Kelly, M. T.; Gagne, S. M.; Andersen, R. J. *Org. Lett.* **2001**, *3*, 437-440.
- (65) Barsby, T.; Kelly, M. T.; Andersen, R. J. *J. Nat. Prod.* **2002**, *65*, 1447-1451.
- (66) Ford, P. W.; Gustafson, K. R.; McKee, T. C.; Shigematsu, N.; Maurizi, L. K.; Pannell, L. K.; Williams, D. E.; Silva, E. D.; Lassota, P.; Allen, T. M.; Soest, R. V.; Andersen, R. J.; Boyd, M. R. *J. Am. Chem. Soc.* **1999**, *121*, 5899-5909.
- (67) Williams, D. E.; Austin, P.; Diaz-Marrero, A. R.; Soest, R. V.; Matainaho, T.; Roskelley, C. D.; Roberge, M.; Andersen, R. J. *Org. Lett.* **2005**, *7*, 4173-4176.
- (68) Barsby, T.; Warabi, K.; Sorensen, D.; Zimmerman, W. T.; Kelly, M. T.; Andersen, R. J. *J. Org. Chem.* **2006**, *71*, 6031-6037.
- (69) Desjardine, K.; Pereira, A.; Wright, H.; Matainaho, T.; Kelly, M. T.; Andersen, R. J. *J. Nat. Prod.* **2007**, *70*, submitted for publication.
- (70) Boman, H. G. *Annu. Rev. Immunol.* **1995**, *13*, 61-92.
- (71) Ganz, T.; Lehrer, R. I. *Pharmacol. Ther.* **1995**, *66*, 191-205.
- (72) Arima, K.; Kakikuma, A.; Tamura, G. *Biochem. Biophys. Res. Commun.* **1968**, *31*, 488-494.
- (73) Kakikuma, A.; Hori, M.; Isono, M.; Tamura, G.; Arima, K. *Agric. Biol. Chem.* **1969**, *33*, 971-997.
- (74) Nagai, S.; Okimura, K.; Kaizawa, N.; Ohki, K.; Kanatomo, S. *Chem. Pharm. Bull.* **1996**, *44*, 5-10.
- (75) Peypoux, F.; Bonmatin, J. M.; Wallach, J. *Appl. Microbiol. Biotechnol.* **1999**, *51*, 553-563.
- (76) Kim, P. I.; Bai, H.; Chae, H.; Chung, S.; Kim, Y.; Park, R.; Chi, Y. T. *J. Appl. Microbiol.* **2004**, *97*, 942-949.
- (77) Thaniyavarn, J.; Roongsawang, N.; Kameyama, T.; Haruki, M.; Imanaka, T.; Morikawa, M.; Kanaya, S. *Biosci. Biotechnol. Biochem.* **2003**, *67*, 1239-1244.
- (78) Kulper, I.; Lagendijk, E. L.; Pickford, R.; Derrick, J. P.; Lamers, G. E. M.; Thoamas-Oates, J. E.; Lugtemberg, B. J. J.; Bloemberg, G. V. *Mol. Microbiol.* **2004**, *51*, 97-113.
- (79) Kalinovskaya, N. I.; Kuznetsova, T. A.; Ivanova, E. P.; Romanenko, L. A.; Voinov, V. G.; Huth, F.; Laatsch, H. *Mar. Biotechnol.* **2002**, *4*, 179-188.
- (80) Grangemard, I.; Bonmatin, J. M.; Bernillon, J.; Das, B. C.; Peypoux, F. *J. Antibiotics.* **1999**, *52*, 363-373.
- (81) Naruse, N.; Tenmyo, O.; Kobaru, S.; Kamei, H.; Miyaki, T.; Konishi, M.; Oki, T. *J. Antibiotics.* **1990**, *43*, 267-280.
- (82) Peypoux, F.; Bonmatin, J. M.; Labbe, H.; Das, B. C.; Ptak, M.; Michel, G. *Eur. J. Biochem.* **1991**, *202*, 101-106.
- (83) Tsukagoshi, N.; Tamura, G.; Arima, K. *Biochim. Biophys. Acta.* **1970**, *196*, 204-210.
- (84) Kameda, Y.; Matsui, K.; Kato, H.; Yamada, T.; Sagai, H. *Chem. Pharm. Bull.* **1972**, *20*, 1551-1557.
- (85) Kracht, M.; Rokos, H.; Ozel, M.; Kowall, M.; Pauli, G.; Vater, J. *J. Antibiotics.* **1999**, *52*, 613-619.

- (86) Vollenbroich, D.; Ozel, M.; Vater, J.; Kamp, R. M.; Pauli, G. *Biologicals*. **1997**, *25*, 289-297.
- (87) Vollenbroich, D.; Pauli, G.; Ozel, M.; Vater, J. *Appl. Environ. Microbiol.* **1997**, *63*, 44-49.
- (88) Beven, L.; Wroblewski, H. *Res. Microbiol.* **1997**, *148*, 163-175.
- (89) Imai, Y.; Sugino, H.; Takinuma, A. *Takeda Kenkyusho Ho.* **1971**, *30*, 728-734.
- (90) Mereles, J. R.; Toguchi, A.; Harshey, R. M. *J. Bacteriol.* **2001**, *183*, 5848-5854.
- (91) Rodrigues, L.; Banar, I. M.; Texeira, J.; Oliveira, R. *J. Antimicrob. Chemother.* **2006**, *57*, 609-618.
- (92) Kalinovskaya, N. I.; Kuznetsova, T. A.; Rashkes, Y.; Mil'gron, Y.; Mil'gron, E.; Willis, R.; Wood, A.; Kurtz, H.; Carabedian, C.; Murphy, P.; Elyakov, G. *Russ. Chem. Bull.* **1995**, *44*, 951-955.
- (93) Coleman, J. E.; Soest, R. V.; Andersen, R. J. *J. Nat. Prod.* **1999**, *62*, 1137-1141.
- (94) Schmidt, E. W.; Obratsova, A. Y.; Davidson, S. K.; Faulkner, D. J.; Haygood, M. G. *Mar. Biol.* **2000**, *136*, 969-977.
- (95) De-Rosa, S.; Mitova, M.; Tommonaro, G. *Biomol. Engineering.* **2003**, *20*, 311-316.
- (96) Lehrer, R. I.; Tincu, J. A.; Taylor, S. W.; Menzel, L. P.; Waring, A. J. *Integr. Comp. Biol.* **2003**, *43*, 313-322.
- (97) Ovchinnikova, T. V.; Aleshina, G. M.; Balandin, S. V.; Krasnosdembskaya, A. D.; Markelov, M. L.; Frolova, E. I.; Leonova, Y. F.; Tagaev, A. A.; Krasnodembsky, E. G.; Kokryakov, V. N. *FEBS Lett.* **2004**, *577*, 209-214.
- (98) Trischman, J. A.; Tapiolas, D. M.; Jensen, P. R.; Dwight, R.; Fenical, W.; McKee, T. C.; Ireland, C. M.; Stout, T. J.; Clardy, J. *J. Am. Chem. Soc.* **1994**, *116*, 757-758.
- (99) Lu, P. J.; Wulf, G.; Zhen-Zhou, X.; Davies, P.; Ping-Lu, K. *Nature.* **1999**, *399*, 784-788.
- (100) Caceres, A.; Kosik, K. S. *Nature.* **1990**, *343*, 461-463.
- (101) Zhen-Zhou, X.; Lu, G.; Wulf, G.; Lu, P. J. *Cell. Mol. Life Sci.* **1999**, *56*, 788-806.
- (102) Gothel, S. F.; Marahiel, M. A. *Cell. Mol. Life Sci.* **1999**, *55*, 423-436.
- (103) Nelson, J. *Investigation into the biologically active metabolites of Coccoloba acuminata and Minuartia guianensis*. Masters Degree Thesis, University of British Columbia: Vancouver, 2002, pp 2-11.
- (104) Scherkenbeck, J.; Chen, H.; Haynes, R. K. *Eur. J. Org. Chem.* **2002**, 2350-2355.
- (105) Chen, H.; Haynes, R. K.; Scherkenbeck, J. *Eur. J. Org. Chem.* **2004**, 38-47.
- (106) Chen, H.; Guo, X. K.; Zhong, X. B. *Chinese J. Chem.* **2006**, *24*, 1411-1417.
- (107) Lipomi, D. J.; Langille, N. F.; Panek, J. S. *Org. Lett.* **2004**, *6*, 3533-3536.
- (108) Easwar, S.; Argade, N. P. *Tetrahedron Asymm.* **2003**, *14*, 333-337.
- (109) Anderson, G. W.; McGregor, A. C. *J. Am. Chem. Soc.* **1957**, *79*, 6180-6183.
- (110) Gibson, F. S.; Bergmeier, S. C.; Rapoport, H. *J. Org. Chem.* **1994**, *59*, 3216-3218.
- (111) Coste, J.; LeNguyen, D.; Castro, B. *Tetrahedron Lett.* **1990**, *31*, 205-208.
- (112) Okada, Y. *Curr. Org. Chem.* **2001**, *5*, 1-43.
- (113) May, J. P.; Fournier, P.; Pellicelli, J.; Patrick, B. O.; Perrin, D. *J. Org. Chem.* **2005**, *70*, 8424-8430.
- (114) *Sigma-Aldrich Advancing Science Catalogue: Ontario*, 2005, 1794.
- (115) Desai, J. D.; Banat, I. M. *Microbiol. Mol. Biol. Rev.* **1997**, *61*, 47-64.
- (116) Cooper, D. G.; Macdonald, C. R.; Duff, S. J. B.; Kosaric, N. *Appl. Environ. Microbiol.* **1981**, *42*, 408-412.
- (117) Youssef, N. H.; Duncan, K. E.; McInerney, M. J. *Appl. Environ. Microbiol.* **2005**, *71*, 7690-7695.
- (118) Morrison, J. D.; Ciardelli, T. L.; Husman, J. R. *Tetrahedron Lett.* **1976**, 1773-1776.

- (119) Nagai, S.; Okimura, K.; Kaizawa, N.; Ohki, K.; Kanatomo, S. *Chem. Pharm. Bull.* **1996**, *1*, 5-10.
- (120) Pagadoy, M.; Peypoux, F.; Wallach, J. *Int. J. Pep. Res. Ther.* **2005**, *11*, 195-202.
- (121) Stelakatos, G. C.; Paganou, A.; Zervas, L. *J. Chem. Soc. (C)*. **1966**, 1191-1199.
- (122) Greene, T. W.; Wuts, P. G. M. *Protecting groups in Organic Chemistry*; 3rd ed.; John Wiley & Sons: Toronto, 1999, 749 p.
- (123) Carpino, L.; Han, G. Y. *J. Org. Chem.* **1972**, *37*, 3404-3409.
- (124) Neises, B.; Andries, T.; Steglich, W. *J. Chem. Soc., Chem. Commun.* **1982**, 1132-1133.
- (125) Tarbell, D. S.; Yamamoto, Y.; Pope, B. M. *Proc. Nat. Acad. Sci. USA*. **1972**, *69*, 730-732.
- (126) Einhorn, J.; Einhorn, C.; Luche, J. L. *Synlett*. **1991**, *1*, 37-38.
- (127) Ponnusamy, E.; Fotadar, U.; Spisni, A.; Fiat, D. *Synthesis*. **1986**, *1*, 48-49.
- (128) *Evans Group pKa's Table*, 2007. Available at: http://daecr1.harvard.edu/pdf/evans_pKa_table.pdf.
- (129) *Bordwell pKa Table (Acidity in DMSO)*, 2007. Available at: <http://www.chem.wisc.edu/areas/reich/pkatable/index.htm>.
- (130) Hamada, Y.; Shiori, T. *Chem. Rev.* **2005**, *105*, 4441-4482.
- (131) Kopple, K. D. *J. Pharm. Sci.* **1972**, *61*, 1345-1356.
- (132) Mueller, A. J.; DuHadaway, J.; Donover, P. S.; Sutanto-Ward, E.; Prendergast, G. C. *Nat. Med.* **2005**, *11*, 312-319.
- (133) Uyttenhove, C.; Pilotte, L.; Theate, I.; Stroobant, V.; Colau, D.; Parmentier, N.; Boon, T.; Eyde, B. J. *Nat. Med.* **2003**, *9*, 1269-1274.
- (134) Brastianos, H. C.; Vottero, E.; Patrick, B. O.; Soest, R. V.; Matainaho, T.; Mauk, A. G.; Andersen, R. J. *J. Am. Chem. Soc.* **2006**, *128*, 16046-16047.
- (135) Mueller, A. J.; Prendergast, G. C. *Cancer Res.* **2005**, *65*, 8065-8068.
- (136) Munn, D. H.; Zhou, M.; Attwood, J. T.; Bondarev, I.; Conway, S.; Marshal, B.; Mellor, A. L. *Science*. **1998**, *281*, 1191-1193.
- (137) Mueller, A. J.; Malachowski, W. P.; Prendergast, G. C. *Expert Opin. Ther. Targets*. **2005**, *9*, 831-849.
- (138) Littlejohn, T. K.; Takikawa, O.; Skylas, D.; Jamie, J. F.; Walker, M. J.; Truscott, R. J. W. *Prot. Exp. Pur.* **2000**, *19*, 22-29.
- (139) Truscott, R. J. W. *Int. J. Biochem. Cell Biol.* **2003**, *35*, 1500-1504.
- (140) Takikawa, O.; Littlejohn, T. K.; Truscott, R. J. W. *Exp. Eye Res.* **2001**, *72*, 271-277.
- (141) Takikawa, O.; Yoshida, R.; Kido, R.; Hayaishi, O. *J. Biol. Chem.* **1986**, *261*, 3648-3653.
- (142) Ino, K.; Yoshida, N.; Kajiyama, H.; Shibata, K.; Yamamoto, E.; Kidokoro, K.; Takahashi, N.; Terauchi, M.; Nawa, A.; Nomura, S.; Nagasaka, T.; Takikawa, O.; Kikkawa, F. *Brit. J. Cancer*. **2006**, *95*, 1555-1561.
- (143) Malachowski, W. P.; Metz, R.; Prendergast, G. C.; Mueller, A. J. *Drugs of the Future*. **2005**, *30*, 897-909.
- (144) Yamamoto, S.; Hayaishi, O. *J. Biol. Chem.* **1967**, *242*, 5260-5266.
- (145) Zheng, X.; Koropatnick, J.; Li, M.; Zhang, K.; Ling, F.; Ren, X.; Hao, X.; Sun, H.; Vladau, C.; Franek, J. A.; Feng, B.; Urquhart, B. L.; Zhong, R.; Freeman, D. J.; Garcia, B.; Min, W. P. *J. Immunol.* **2006**, *177*, 5639-5646.
- (146) Hou, D. Y.; Mueller, A. J.; Sharma, M. D.; DuHadaway, J.; Banerjee, T.; Johnson, M.; Mellor, A. L.; Prendergast, G. C.; Munn, D. H. *Cancer Res.* **2007**, *67*, 792-801.
- (147) Mellor, A. L. *Biochem. Biophys. Comm.* **2005**, *338*, 20-24.
- (148) Vottero, E.; Balgi, A.; Woods, K.; Tugendreich, S.; Melese, T.; Andersen, R. J. *J. Biotechnol.* **2006**, *1*, 282-288.
- (149) Munn, D. H.; Mellor, A. L. *Trends Mol. Med.* **2004**, *10*, 15-18.

- (150) Munn, D. H.; Mellor, A. L. *Immunol. Rev.* **2006**, *213*, 146-158.
- (151) Okamoto, A.; Nikaido, T.; Ochiai, K.; Takakura, S.; Saito, M.; Aoki, Y.; Ishii, N.; Yanaihara, N.; Yamada, K.; Takikawa, O.; Kawaguchi, R.; Isonishi, S.; Tanaka, T.; Urashima, M. *Clin. Cancer. Res.* **2005**, *11*, 6030-6039.
- (152) Brandacher, G.; Perathoner, A.; Ladurner, R.; Schneeberger, S.; Obrist, P.; Winkler, C.; Werner, E. R.; Werner-Felmayer, G.; Weiss, H. G.; Gobel, G.; Margreiter, R.; Konigsrainer, A.; Fuchs, D.; Amberger, A. *Clin. Cancer. Res.* **2006**, *12*, 1144-1151.
- (153) Malina, H. Z.; Matin, X. D. *Graefe's Arch. Clin. Exp. Ophthalmol.* **1993**, *231*, 482-486.
- (154) Serbecic, N.; Beutelspacher, S. C. *Exp. Eye Res.* **2006**, *82*, 416-426.
- (155) Eguchi, N.; Watanabe, Y.; Kawanishi, K.; Hashimoto, Y.; Hayaishi, O. *Arch. Biochem. Biophys.* **1984**, *232*, 602-609.
- (156) Vottero, E. R. *Thesis Doctoral: Inhibitors of Human Indoleamine 2,3-Dioxygenase*; The University of British Columbia: Vancouver, 2006. 138 p.
- (157) Tenen, S. S.; Hirsch, J. D. *Nature.* **1980**, *288*, 609-610.
- (158) Takikawa, O.; Kuroiwa, T.; Yamazaki, F.; Kido, R. *J. Biol. Chem.* **1988**, *263*, 2041-2048.
- (159) Fahy, E.; Andersen, R. J.; Cun-heng, H.; Clardy, J. *J. Org. Chem.* **1985**, *50*, 1149-1150.
- (160) Blunt, J. W.; Copp, B. R.; Munro, M. H. G.; Northcote, P. T.; Prinsep, M. R. *Nat. Prod. Rep.* **2003**, *20*, 1-48.
- (161) Blunt, J. W.; Copp, B. R.; Munro, M. H. G.; Northcote, P. T.; Prinsep, M. R. *Nat. Prod. Rep.* **2004**, *21*, 1-49.
- (162) Blunt, J. W.; Copp, B. R.; Munro, M. H. G.; Northcote, P. T.; Prinsep, M. R. *Nat. Prod. Rep.* **2006**, *23*, 26-78.
- (163) Blunt, J. W.; Copp, B. R.; Hu, W.; Munro, M. H. G.; Northcote, P. T.; Prinsep, M. R. *Nat. Prod. Rep.* **2007**, *24*, 31-86.
- (164) Fahy, E.; Andersen, R. J. *J. Org. Chem.* **1986**, *51*, 57-61.
- (165) MarinLit database. Department of Chemistry, University of Canterbury: <http://www.chem.canterbury.ac.nz/marinlit/marinlit.shtml>, 2005.
- (166) Cimino, G.; DeRosa, S.; DeStefano, S.; Sodano, G. *Tetrahedron Lett.* **1980**, *21*, 3303-3304.
- (167) Fattorusso, E.; Lanzotti, V.; Magno, S.; Novellino, E. *Biochem. Syst. Ecol.* **1985**, *13*, 167.
- (168) Fattorusso, E.; Lanzotti, V.; Magno, S.; Novellino, E. *J. Org. Chem.* **1985**, *1985*.
- (169) Aiello, A.; Fattorusso, E.; Magno, S. *J. Nat. Prod.* **1987**, *50*, 191-194.
- (170) Aiello, A.; Fattorusso, E.; Magno, S.; Mayol, L. *Tetrahedron.* **1987**, *43*, 5929-5932.
- (171) Fusetani, N.; Yasukawa, K.; Matsunaga, S.; Hashimoto, K. *Comp. Biochem. Physiol.* **1986**, *83*, 511-513.
- (172) Seo, Y.; Cho, K. W.; Rho, J. R.; Shin, J. *Tetrahedron.* **1996**, *52*, 10583-10596.
- (173) Lindquist, N. *Mar. Biol.* **1996**, *126*, 745-755.
- (174) Lindquist, N.; Lobkovski, E.; Clardy, J. *Tetrahedron Lett.* **1996**, *37*, 9131-9134.
- (175) Lindquist, N. *J. Nat. Prod.* **2002**, *65*, 681-684.
- (176) Johnson, M. K.; Alexander, K. E.; Lindquist, N.; Loo, G. *Biochem. Pharmacol.* **1999**, *58*, 1313-1319.
- (177) Lindquist, N.; Shigematsu, N.; Pannell, L. *J. Nat. Prod.* **2000**, *63*, 1290-1291.
- (178) Rezanka, T.; Hanus, L. O.; Dembitsky, V. M. *Tetrahedron.* **2004**, *60*, 12191-12199.
- (179) Houssen, W. E.; Jaspars, M. *J. Nat. Prod.* **2005**, *68*, 453-455.
- (180) Fahy, E.; Andersen, R. J. *Can. J. Chem.* **1987**, *65*, 376-383.
- (181) Fahy, E.; Andersen, R. J. *J. Org. Chem.* **1986**, *51*, 5145-5148.
- (182) Pathirana, C.; Andersen, R. J.; Wright, J. L. C. *Can. J. Chem.* **1990**, *68*, 394-396.
- (183) Singh, H.; Moore, R. E.; Scheuer, P. J. *Experientia.* **1967**, *23*, 624-626.
- (184) Rideout, J. A.; Sutherland, M. D. *Aust. J. Chem.* **1985**, *38*, 793-808.

- (185) Kitahara, T.; Naganawa, H.; Okazaki, T.; Okami, Y.; Umezawa, H. *J. Antibiotics*. **1975**, *28*, 280.
- (186) Pinheiro, R. M.; MacQuhae, M. M.; Bettolo, G. B. M.; Monache, F. D. *Phytochemistry* **1984**, *23*, 1737-1740.
- (187) Monache, F. D.; MacQuhae, M. M.; Ferrari, F.; Bettolo, G. B. M. *Tetrahedron*. **1979**, *35*, 2143-2149.
- (188) Kitanaka, S.; Igarashi, H.; Takido, M. *Chem. Pharm. Bull.* **1985**, *33*, 971-974.
- (189) Kitanaka, S.; Takido, M. *Chem. Pharm. Bull.* **1990**, *38*, 1292-1294.
- (190) Dagne, E.; Van-Wyk, B. E.; Mueller, M.; Steglich, W. *Phytochemistry*. **1996**, *41*, 795-799.
- (191) Matsumoto, T.; Takeda, Y.; Soh, K.; Gotoh, H.; Imai, S. *Chem. Pharm. Bull.* **1996**, *44*, 1318-1325.
- (192) Brady, S. F.; Singh, M. P.; Janso, J. E.; Clardy, J. *Org. Lett.* **2000**, *2*, 4047-4049.
- (193) Austin, W. C. *An Annotated Checklist of Marine Invertebrates in the Cold Temperate Northeast Pacific*; Fotoprint Ltd: Victoria, 1985; Vol. 1, 350 p.
- (194) Retrieved from <http://en.wikipedia.org/wiki/Hydrozoa>. June 2007.
- (195) Chiou, T. J.; Chou, Y. T.; Tzeng, W. F. *Proc. Natl. Sci. Counc. Repub. China B.* **1998**, *22*, 13-21.
- (196) Chiou, T. J.; Tzeng, W. F. *Toxicol.* **2000**, *154*, 75-84.
- (197) Chiou, T. J.; Chu, S. T.; Tzeng, W. F. *Toxicol.* **2003**, *191*, 77-88.
- (198) Tetef, M.; Margolin, K.; Ahn, C.; Akman, S.; Chow, W.; Leong, L.; Morgan, R. J.; Raschko, J.; Somlo, G.; Doroshov, J. H. *Invest. New Drugs*. **1995**, *13*, 157-162.
- (199) Verrax, J.; Cadrobbi, J.; Marques, C.; Taper, H.; Habraken, Y.; Piette, J.; Calderon, P. B. *Apoptosis*. **2004**, *9*, 223-233.
- (200) Andersen, R. J.; Pereira, A.; Huang, X. H.; Mauk, G.; Vottero, E.; Roberge, M.; Balgi, A. *Indoleamine 2,3-dioxygenase (IDO) inhibitors, and their therapeutic use*. WO 2005-CA1087 20050713, Canada, 2006, 47 pp.
- (201) Koehn, F. E.; Carter, G. T. *Nat. Rev. Drug. Discov.* **2005**, *4*, 206-220.
- (202) Schiff, P. B.; Fant, J.; Horwitz, S. B. *Nature*. **1979**, *277*, 665-667.
- (203) Altmann, K. H.; Gertsch, J. *Nat. Prod. Rep.* **2007**, *24*, 327-357.
- (204) Blunt, J. W.; Copp, B. R.; Munro, M. H. G.; Northcote, P. T.; Prinsep, M. R. *Nat. Prod. Rep.* **2003**, *20*, 1-48.
- (205) Blunt, J. W.; Copp, B. R.; Munro, M. H. G.; Northcote, P. T.; Prinsep, M. R. *Nat. Prod. Rep.* **2004**, *21*, 1-49.
- (206) Blunt, J. W.; Copp, B. R.; Munro, M. H. G.; Northcote, P. T.; Prinsep, M. R. *Nat. Prod. Rep.* **2005**, *22*, 15-61.
- (207) Blunt, J. W.; Copp, B. R.; Munro, M. H. G.; Northcote, P. T.; Prinsep, M. R. *Nat. Prod. Rep.* **2006**, *23*, 26-78.
- (208) Blunt, J. W.; Copp, B. R.; Hu, W.; Munro, M. H. G.; Northcote, P. T.; Prinsep, M. R. *Nat. Prod. Rep.* **2007**, *24*, 31-86.
- (209) Jin, Z. *Nat. Prod. Rep.* **2005**, *22*, 196-229.
- (210) Manzo, E.; Soest, R. V.; Matainaho, L.; Roberge, M.; Andersen, R. J. *Org. Lett.* **2003**, *5*, 4591-4594.
- (211) Gunasekera, S. P.; Gunasekera, M.; Longley, R. E.; Schulte, G. K. *J. Org. Chem.* **1990**, *55*, 4912-4915.
- (212) Gunasekera, S. P.; Gunasekera, M.; Longley, R. E.; Schulte, G. K. *J. Org. Chem.* **1991**, *56*, 1346-1346.
- (213) Pettit, G. R.; Cichacz, Z. A.; Gao, F.; Boyd, M. R.; Schmidt, J. M. *J. Chem. Soc.; Chem. Comm.* **1994**, 1111-1112.

- (214) Lindel, T.; Jensen, P. R.; Fenical, W.; Long, B. H.; Cassaza, A. M.; Carboni, J. M.; Fairchild, C. R. *J. Am. Chem. Soc.* **1997**, *119*, 8744-8745.
- (215) Cinel, B.; Roberge, M.; Behrisch, H.; Ofwegen, L.; Castro, C. B.; Andersen, R. J. *Org. Lett.* **2000**, *2*, 257-260.
- (216) Britton, R.; Roberge, M.; Behrisch, H.; Andersen, R. J. *Tetrahedron Lett.* **2001**, *42*, 2953-2956.
- (217) Long, B. H.; Carboni, J. M.; Wasserman, J.; Cornell, L. A.; Cassaza, A. M.; Jensen, P. R.; Lindel, T.; Fenical, W.; Fairchild, C. R. *Cancer Res.* **1998**, *58*, 1111-1115.
- (218) D'Ambrosio, M.; Guerrero, A.; Pietra, F. *Helv. Chim. Acta.* **1987**, *70*, 2019-2027.
- (219) Hung, D. T.; Chen, J.; Schreiber, S. L. *Chem. Biol.* **1996**, *3*, 287-293.
- (220) Isbrucker, A.; Cummins, J.; Pomponi, S.; Longley, R. E.; Wright, A. E. *Biochem. Pharmacol.* **2003**, *66*, 75-82.
- (221) Quinoa, E.; Kakou, Y.; Crews, P. *J. Org. Chem.* **1988**, *53*, 3644-3646.
- (222) Corley, D. G.; Herb, R.; Moore, R. E.; Scheuer, P. J. *J. Org. Chem.* **1988**, *53*, 3644-3646.
- (223) Mooberry, S. L.; Tien, G.; Hernandez, A. H.; Pluburkan, A.; Davidson, B. S. *Cancer Res.* **1999**, *59*, 653-660.
- (224) Pryor, D. E.; O'Brate, A.; Bilcer, G.; Diaz, J. F.; Wang, Y.; Kabaki, M.; Jung, M. K.; Andreu, J. M.; Ghosh, A. K.; Giannakakou, P.; Hamel, E. *Biochemistry.* **2002**, *41*, 9109-9115.
- (225) West, L. Y.; Northcote, P. T.; Battershill, C. N. *J. Org. Chem.* **2000**, *65*, 445-449.
- (226) Hood, K. A.; West, L. M.; Rouwe, B.; Northcote, P. T.; Verridge, B.; Wakefield, S. J.; Miller, J. H. *Cancer Res.* **2002**, *62*, 3356-3360.
- (227) Gaitanos, T. N.; Buey, R. M.; Diaz, J. F.; Northcote, P. T.; Teesdale-Spittle, P.; Andreu, J. M.; Miller, J. H. *Cancer Res.* **2004**, *64*, 5063-5067.
- (228) Williams, D. E.; Sturgeon, C. M.; Roberge, M.; Andersen, R. J. *J. Am. Chem. Soc.* **2007**, *129*, 5822-5823.
- (229) Karjala, G.; Chan, Q.; Manzo, E.; Andersen, R. J.; Roberge, M. *Cancer Res.* **2005**, *65*, 3040-3043.
- (230) Roberge, M.; Cinel, B.; Anderson, H. J.; Lim, L.; Jiang, X.; Xu, L.; Bigg, C. M.; Kelly, M. T.; Andersen, R. J. *Cancer Res.* **2000**, *60*, 5052-5058.
- (231) Benharref, A.; Pais, M. *J. Nat. Prod.* **1996**, *59*, 177-180.
- (232) Litaudon, M.; Guyot, M. *Tetrahedron Lett.* **1986**, *27*, 4455-4456.
- (233) Thirionet, I.; Daloze, D.; Braeckman, J. C.; Willemsen, P. *Nat. Prod. Lett.* **1998**, *12*, 209-214.
- (234) Ciminiello, P.; Fattorusso, E.; Magno, S. *J. Nat. Prod.* **1994**, *57*, 1564-1569.
- (235) Ciminiello, P.; Fattorusso, E.; Magno, S. *J. Nat. Prod.* **1995**, *58*, 689-696.
- (236) Kobayashi, J.; Honma, K.; Sasaki, T.; Tsuda, M. *Chem. Pharm. Bull.* **1995**, *43*, 403-407.
- (237) Mierzwa, R.; King, A.; Conover, M. A.; Tozzi, S.; Puar, M. S.; Patel, M.; Coval, S. J. *J. Nat. Prod.* **1994**, *57*, 175-177.
- (238) Tabudravu, J. N.; Jaspars, M. *J. Nat. Prod.* **2002**, *65*, 1798-1801.
- (239) Tsuda, M.; Shigemori, H.; Ishibashi, M.; Kobayashi, J. *Tetrahedron Lett.* **1992**, *33*, 2597-2598.
- (240) Tsuda, M.; Shigemori, H.; Ishibashi, M.; Kobayashi, J. *J. Nat. Prod.* **1992**, *55*, 1325-1327.
- (241) Ishibashi, M.; Tsuda, M.; Ohizumi, Y.; Sasaki, T.; Kobayashi, J. *Experientia.* **1991**, *47*, 299-300.
- (242) Wu, H.; Nakamura, H.; Kobayashi, J.; Ohizumi, Y.; Hirata, Y. *Experientia.* **1986**, *42*, 855-856.
- (243) Kobayashi, J.; Honma, K.; Tsuda, M. *J. Nat. Prod.* **1995**, *58*, 467-470.

- (244) Wasserman, H. H.; Wang, J. *J. Org. Chem.* **1998**, *63*, 5581-5586.
- (245) Jin, Z. *Nat. Prod. Lett.* **2006**, *23*, 464-496.
- (246) Ahond, A.; Bedoya-Zurita, M.; Colin, M.; Fizames, C.; Laboute, P.; Lavelle, F.; Laurent, D.; Poupat, C.; Pusset, M.; Pusset, J.; Thoison, O.; Poitier, P. *C. R. Acad. Sci. Paris, serie II.* **1981**, *307*, 145-148.
- (247) Grube, A.; Kock, M. *Org. Lett.* **2006**, *8*, 4675-4678.
- (248) Grube, A.; Kock, M. *Angew. Chem. Int. Ed.* **2007**, *46*, 2320-2324.
- (249) Jacquot, D. E. N.; Lindel, T. *Curr. Org. Chem.* **2005**, *9*, 1551-1565.
- (250) O'Malley, D. P.; Li, K.; Maue, M.; Zografos, A. L.; Baran, P. S. *J. Am. Chem. Soc.* **2007**, *129*, 4762-4775.
- (251) Miyake, F. Y.; Yakushijin, K.; Horne, D. A. *Angew. Chem. Int. Ed.* **2005**, *44*, 3280-3282.
- (252) Bedoya-Zurita, M.; Ahond, A.; Poupat, C.; Poitier, P. *Tetrahedron.* **1989**, *45*, 6713-6720.
- (253) Commercon, A.; Gueremy, C. *Tetrahedron Lett.* **1991**, *32*, 1419-1422.
- (254) Olofson, A.; Yakushijin, K.; Horne, D. A. *J. Org. Chem.* **1997**, *62*, 7918-7919.
- (255) Marchais, S.; Mourabit, A. A.; Poupat, C.; Potier, P. *Tetrahedron Lett.* **1998**, *39*, 8085-8088.
- (256) Xu, Y. Z.; Yakushijin, K.; Horne, D. A. *Tetrahedron Lett.* **1994**, 6981-6984.
- (257) Lawson, A. *J. Chem. Soc.* **1956**, 307.
- (258) Storey, B. T.; Sullivan, W. W.; Moyer, C. L. *J. Org. Chem.* **1964**, *29*, 3118.
- (259) Lencini, G. C.; Lazzari, E. *J. Heterocycl. Chem.* **1966**, *3*, 152.
- (260) Cavalleri, B.; Ballota, R.; Lencini, G. C. *J. Heterocycl. Chem.* **1972**, *9*, 979.
- (261) Nishimura, T.; Kitajima, K. *J. Org. Chem.* **1976**, *41*, 1590-1593.
- (262) Nishimura, T.; Kitajima, K. *J. Org. Chem.* **1979**, *44*, 818-824.
- (263) Little, T. L.; Webber, S. E. *J. Org. Chem.* **1994**, *59*, 7299-7305.
- (264) Cima, F. D.; Cavazza, M.; Veracini, C. A.; Pietra, F. *Tetrahedron Lett.* **1975**, *48*, 4267-4268.
- (265) Imafuku, K.; Kikuchi, Y.; Yin, B. *Bull. Chem. Soc. Jpn.* **1987**, *60*, 185-191.
- (266) Cavazza, M.; Cabrino, R.; Cima, F. D.; Pietra, F. *J. Chem. Soc., Perkin Trans. 1.* **1978**, 609-612.
- (267) Birman, V. B.; Jiang, X. T. *Org. Lett.* **2004**, *6*, 2369-2371.
- (268) Baran, P. S.; O'Malley, D. P.; Zografos, A. L. *Angew. Chem. Int. Ed.* **2004**, *43*, 2674-2677.
- (269) Aberle, N. S.; Lessene, G.; Watson, K. G. *Org. Lett.* **2006**, *8*, 419-421.
- (270) Shengule, S. R.; Karuso, P. *Org. Lett.* **2006**, *8*, 4083-4084.
- (271) Olofson, A.; Yakushijin, K.; Horne, D. A. *J. Org. Chem.* **1998**, *63*, 1248-1253.
- (272) Illgen, K.; Nerdinger, S.; Behnke, D.; Friedrich, C. *Org. Lett.* **2005**, *7*, 2517-2518.
- (273) Fujiwara, N.; Fujita, H.; Iwai, K.; Kurimoto, A.; Murata, S.; Kawakami, H. *Bioorg. Med. Chem. Lett.* **2000**, *10*, 1317-1320.
- (274) Alvi, K. A.; Crews, P. *J. Nat. Prod.* **1991**, *54*, 1509-1515.
- (275) Ando, N.; Terashima, S. *Synlett.* **2006**, No 17, 2836-2840.
- (276) Martin, S. F.; Humphrey, J. M.; Ali, A.; Hillier, M. C. *J. Am. Chem. Soc.* **1999**, *121*, 866-867.
- (277) Nicolaou, K. C.; Montagnon, T.; Ulven, T.; Baran, P. S.; Zhong, Y. L.; Sarabia, F. *J. Am. Chem. Soc.* **2002**, *124*, 5718-5728.
- (278) Molina, P.; Frenesda, P. M.; Sanz, M. A. *J. Org. Chem.* **1999**, *64*, 2540-2544.
- (279) Aboud-Jneid, R.; Ghoulemi, S.; Martin, M. T.; Dau, E. T. H.; Travert, N.; Mourabit, A. *Org. Lett.* **2004**, *6*, 3933-3936.
- (280) Wright, A. E.; Chiles, S. A.; Cross, S. S. *J. Nat. Prod.* **1991**, *54*, 1684-1686.

- (281) Schroif-Gregoire, C.; Travert, N.; Zaparucha, A.; Mourabit, A. A. *Org. Lett.* **2006**, *8*, 2961-2964.
- (282) Nagai, W.; Kirk, K. L.; Cohen, L. A. *J. Org. Chem.* **1973**, *38*, 1971-1974.
- (283) Kirk, K. L. *J. Org. Chem.* **1978**, *43*, 4381-4383.
- (284) Daninos-Zhegal, S.; Mourabit, A. A.; Ahond, A.; Poupat, C.; Poitier, P. *Tetrahedron.* **1997**, *53*, 7605.
- (285) Carver, D. S.; Lindell, S. D.; Saville-Stones, E. A. *Tetrahedron.* **1997**, *53*, 14481-14496.
- (286) Jain, R.; Avramovitch, B.; Cohen, L. A. *Tetrahedron.* **1998**, *54*, 3235-3242.
- (287) Lindel, T.; Hoffmann, H. *Tetrahedron Lett.* **1997**, *38*, 8935.
- (288) Berree, F.; LeBleis, P. G.; Carboni, B. *Tetrahedron Lett.* **2002**, *43*, 4935-4938.
- (289) Lindel, T.; Hochgurtel, M. *J. Org. Chem.* **2000**, *65*, 2806-2809.
- (290) Ohta, S.; Tsuno, N.; Nakamura, S.; Taguchi, N.; Yamashita, M.; Kawasaki, I.; Fujieda, M. *Heterocycles.* **2000**, *53*, 1939.
- (291) Meketa, M. L.; Weinreb, S. M. *Org. Lett.* **2006**, *8*, 1443-1446.
- (292) Meketa, M. L.; Weinreb, S. M. *Org. Lett.* **2007**, *9*, 853-855.
- (293) Baran, P. S.; Shenvi, R. A. *J. Am. Chem. Soc.* **2006**, *128*, 14028-14029.
- (294) Nakamura, S.; Kawasaki, I.; Kunimura, M.; Matsui, M.; Noma, Y.; Yamashita, M.; Ohta, S. *J. Chem. Soc.; Perkin Trans. 1.* **2002**, 1061-1066.
- (295) Wang, X.; Porco, J. A. *J. Org. Chem.* **2001**, *66*, 8215-8221.
- (296) Moody, K.; Thompson, R. H.; Fattorusso, E.; Minale, L.; Sodano, G. *J. Chem. Soc.; Perkin Trans. 1.* **1972**, 18-24.
- (297) Haasbroek, P. P.; Oliver, D. W.; Carpy, A. J. M. *J. Chem. Crystallogr.* **1998**, *28*, 193-196.
- (298) *Bordwell pKa Table (Acidity in DMSO)*, 2007. Available at: <http://www.chem.wisc.edu/areas/reich/pkatable/index.htm>.
- (299) *Evans Group pKa's Table*, 2007. Available at: http://daecr1.harvard.edu/pdf/evans_pKa_table.pdf.
- (300) Bates, G. S.; Ramaswamy, S. *Can. J. Chem.* **1980**, *58*, 716-728.
- (301) Juaristi, E.; Tapia, J.; Mendez, R. *Tetrahedron.* **1986**, *42*, 1253-1264.
- (302) Coste, J.; LeNguyen, D.; Castro, B. *Tetrahedron Letters* **1990**, *31*, 205-208.
- (303) Hong, B. C.; Shin, H. F. *J. Chem. Soc., Chem. Commun.* **1999**, *29*, 3097-3106.
- (304) Takagi, H.; Hayashi, T.; Mizutani, T.; Masuda, H.; Ogoshi, H. *J. Chem. Soc., Perkin Trans. 1.* **1999**, 1885-1892.
- (305) Galvez, N.; Moreno-Manas, M.; Sebastian, R. M.; Vallribera, A. *Tetrahedron.* **1996**, *52*, 1609-1616.
- (306) Meyers, A. I.; Hutchings, R. H. *Tetrahedron.* **1993**, *49*, 1807-1820.
- (307) Chandrasekhar, S.; Gopalaiah, K. *Tetrahedron Lett.* **2003**, *44*, 7437-7439.
- (308) Stevenson, R. *J. Am. Chem. Soc.* **1963**, *28*, 188-190.
- (309) Tamiya, J.; Sorensen, E. J. *Tetrahedron.* **2003**, *59*, 6921-6932.
- (310) Ghiaci, M.; Imanzadeh, G. H. *Synth. Commun.* **1998**, *28*, 2275-2280.
- (311) Anilkumar, R.; Chandrasekhar, S. *Tetrahedron Lett.* **2000**, *41*, 5427-5429.
- (312) Tamura, Y.; Kita, Y.; Matsutaka, Y.; Terashima, M. *Chem. Pharm. Bull.* **1971**, *19*, 523-528.
- (313) Tamura, Y.; Kita, Y.; Terashima, M. *Chem. Pharm. Bull.* **1971**, *19*, 529-534.
- (314) Price, J. A. *J. Am. Chem. Soc.* **1955**, *77*, 5436-5437.
- (315) Fox, G. J.; Hallas, G.; Hepworth, J. D.; Paskins, K. N. *Org. Synth.* **1976**, *55*, 20-28.
- (316) Campos, K. R.; Lee, S.; Journet, M.; Kowal, J. J.; Cai, D.; Larsen, R. D.; Reider, P. J. *Tetrahedron Lett.* **2002**, *43*, 6957-6959.
- (317) Brummond, K. M.; Gesenberg, K. D. *Tetrahedron Lett.* **1999**, *40*, 2231-2234.

- (318) Kinder, F. R.; Wattanasin, S.; Versace, R. W.; Blair, K. W.; Bontempo, J.; Green, M. A.; Lu, Y. J.; Marepalli, H. R.; Phillips, P. E.; Roche, D.; Tran, L. D.; Wang, R.; Waykole, L.; Xu, D. D.; Zabludoff, S. *J. Org. Chem.* **2001**, *66*, 2118-2122.
- (319) Beak, P.; Meyers, A. *Acc. Chem. Res.* **1986**, *19*, 356-363.
- (320) Clark, R. D.; Jahangir, A. *Org. React.* **1995**, *47*, 1-314.
- (321) Collum, D. B. *Acc. Chem. Res.* **1993**, *26*, 227-234.
- (322) Koser, G. F.; Relenyi, A. G.; Kalos, A. N.; Rebrovic, L.; Wettach, R. H. *J. Org. Chem.* **1982**, *47*, 2487-2489.
- (323) Moriarty, R. M.; Prakash, O. *Acc. Chem. Res.* **1986**, *19*, 244-250.
- (324) Koser, G. F.; Wettach, R. H. *J. Org. Chem.* **1977**, *42*, 1476-1478.
- (325) Stang, P. J.; Zhdankin, V. V. *Chem. Rev.* **1996**, *96*, 1123-1178.
- (326) Moriarty, R. M.; Gupta, S. C.; Hu, H.; Berenschot, D. R.; White, K. B. *J. Am. Chem. Soc.* **1981**, *103*, 686-688.
- (327) Paquette, L. A.; Nakatani, S.; Zydowski, T. M.; Edmondson, S. D.; Sun, L. Q.; Skerlj, R. *J. Org. Chem.* **1999**, *64*, 3244-3254.
- (328) Lessene, G.; Tripoli, R.; Cazeau, P.; Biran, C.; Bordeau, M. *Tetrahedron Lett.* **1999**, *40*, 4037-4040.
- (329) Molander, G. A.; Bessieres, B.; Eastwood, P. R.; Noll, B. C. *J. Org. Chem.* **1999**, *64*, 4124-4129.
- (330) Montana, A. M.; Garcia, F.; Grima, P. M. *Tetrahedron.* **1999**, *55*, 5483-5504.
- (331) Hudrlik, P. F.; Abdallah, Y. M.; Kulkarni, A. K.; Hudrlik, A. M. *J. Org. Chem.* **1992**, *57*, 6552-6555.
- (332) Yamazaki, S.; Yanase, Y.; Yamamoto, K. *J. Chem. Soc.; Perkin Trans. 1.* **2000**, 1991-1996.
- (333) Hudrlik, P. F.; Abdallah, Y. M.; Hudrlik, A. M. *Tetrahedron Lett.* **1992**, *33*, 6743-6746.
- (334) Damrauer, R. *Organometallics.* **1985**, *4*, 1779-1784.
- (335) Aprahamian, S. L.; Shechter, H. *Tetrahedron Lett.* **1990**, *31*, 1089-1093.
- (336) Talami, S.; Stirling, C. J. M. *Can. J. Chem.* **1999**, *77*, 1105-1107.
- (337) Pezacki, J. P.; Loncke, P. G.; Ross, J. P.; Warkentin, J.; Gadosy, T. A. *Org. Lett.* **2000**, *2*, 2733-2736.
- (338) Hijji, Y. M.; Hudrlik, P. F.; Hudrlik, A. M. *J. Chem. Soc.; Chem. Comm.* **1998**, 1213-1214.
- (339) Turnbull, K.; Krein, D. M. *Synth. Commun.* **2003**, *33*, 2061-2067.
- (340) Antonioletti, R.; Bovicelli, P.; Malancona, S. *Tetrahedron.* **2002**, *58*, 589-596.
- (341) Rao, A. V. R.; Chakraborty, T. K.; Reddy, K. L. *Tetrahedron Lett.* **1990**, *31*, 1439-1442.
- (342) Moriarty, R. M.; Khosrowshahi, J. S. *Tetrahedron Lett.* **1986**, *27*, 2809-2812.
- (343) Saito, M.; Kayama, Y.; Watanabe, T.; Fukushima, H.; Hara, T. *J. Med. Chem.* **1980**, *23*, 1364-1372.
- (344) Goksu, S.; Secen, H.; Sutbeyaz, Y. *Synthesis.* **2002**, *16*, 2373-2378.
- (345) Minisci, F.; Galli, R.; Cecere, M. *Gazz. Chim. Ital.* **1964**, *94*, 67-90.
- (346) Fristad, W. E.; Brandvold, T. A.; Peterson, J. R.; Thompson, S. R. *J. Org. Chem.* **1985**, *50*, 3647-3649.
- (347) Bernatowicz, M. S.; Wu, Y.; Matsueda, G. R. *J. Org. Chem.* **1992**, *57*, 2497-2502.
- (348) Chung, R.; Yu, E.; Incarvito, C. D.; Austin, D. J. *Org. Lett.* **2004**, *6*, 3881-3884.
- (349) Jung, S. H.; Kohn, H. *Tetrahedron Lett.* **1984**, *25*, 399-402.
- (350) Jung, S. H.; Kohn, H. *J. Am. Chem. Soc.* **1985**, *107*, 2931-2943.
- (351) Patai, S. *The Chemistry of Amidines and Imidates*; John Wiley & Sons: London, 1975; Vol. 1, 283-348.

- (352) Patai, S.; Rappoport, Z. *The Chemistry of Amidines and Imidates*; John Wiley & Sons: Chichester, 1991; Vol. 2, 485-526 p.
- (353) Bose, A. K.; Greer, F.; Gots, J. S.; Price, C. C. *J. Am. Chem. Soc.* **1959**, *24*, 1309-1313.
- (354) Nicolaou, K. C.; Zhong, Y. L.; Baran, P. S. *J. Am. Chem. Soc.* **2000**, *122*, 7596-7597.
- (355) Nicolaou, K. C.; Mathison, C. J. N.; Montagnon, T. *J. Am. Chem. Soc.* **2004**, *126*, 5192-5201.
- (356) Nicolaou, K. C.; Montagnon, T.; Baran, P. S.; Zhong, Y. L. *J. Am. Chem. Soc.* **2002**, *124*, 2245-2258.
- (357) Sergeev, S. A.; Hesse, M. *Helv. Chim. Acta.* **2003**, *86*, 750-755.
- (358) Ragendra, G.; Miller, M. J. *J. Org. Chem.* **1987**, *52*, 4471-4477.
- (359) Domingo, L. R.; Gil, S.; Parra, M.; Saez, J. A.; Torres, M. *Tetrahedron.* **2003**, *59*, 6233-6239.
- (360) Chae, J.; Buchwald, S. L. *J. Org. Chem.* **2004**, *69*, 3336-3339.
- (361) Khan, K. M.; Hayat, S.; Ullah, Z.; Rahman, A.; Choudhary, M. I.; Maharvi, G. M.; Bayer, E. *Synth. Commun.* **2003**, *33*, 3435-3453.
- (362) Teichgraber, J.; Holzgrabe, U. *Tetrahedron.* **2003**, *59*, 8697-8703.
- (363) Gracias, V.; Gasielki, A. F.; Djuric, S. W. *Org. Lett.* **2005**, *7*, 3183-3186.
- (364) Chen, Y.; Dias, H. V. R.; Lovely, C. J. *Tetrahedron Lett.* **2003**, *44*, 1379-1382.
- (365) Fustero, S.; Bartolome, A.; Sanz-Cervera, J. F.; Sanchez-Rosello, M.; Garcia-Soler, J.; Ramirez, C.; Simon-Fuentes, A. *Org. Lett.* **2003**, *5*, 2523-2526.
- (366) Wipf, P.; Rector, S. R.; Takahashi, H. *J. Am. Chem. Soc.* **2002**, *124*, 14848-14849.
- (367) Furstner, A.; Thiel, O. R. *J. Org. Chem.* **2000**, *65*, 1738-1742.
- (368) Deiters, A.; Martin, S. F. *Chem. Rev.* **2004**, *104*, 2199-2238.
- (369) Chochrek, P.; Wicha, J. *Org. Lett.* **2006**, *8*, 2551-2553.
- (370) Martin, J. D.; Perez, C.; Ravelo, J. L. *J. Am. Chem. Soc.* **1985**, *107*, 516-618.
- (371) Chen, K. X.; Njoroge, G.; Prongay, A.; Pichardo, J.; Madison, V.; Girijavallabhan, V. *Bioorg. Med. Chem. Lett.* **2005**, *15*, 4475-4478.
- (372) Somers, P. K.; Wandless, T. J.; Schreiber, S. L. *J. Am. Chem. Soc.* **1991**, *113*, 8045-8056.
- (373) Dess, D. B.; Martin, J. C. *J. Am. Chem. Soc.* **1991**, *113*, 7277-7287.
- (374) Kohn, H.; Jung, S. H. *J. Am. Chem. Soc.* **1983**, *105*, 4106-4108.
- (375) Frigerio, M.; Santagostino, M.; Sputore, S.; Palmisano, G. *J. Org. Chem.* **1995**, *60*, 7272-7276.
- (376) Chaudhari, S. S. *Synlett.* **2000**, 278.
- (377) Frigerio, M.; Santagostino, M.; Sputore, S. *J. Org. Chem.* **1999**, *64*, 4537-4538.
- (378) Frigerio, M.; Santagostino, M. *Tetrahedron Lett.* **1994**, *35*, 8019-8022.
- (379) Sivasubramanian, S.; Aravind, S.; Kumarasingh, L. T.; Arumugam, N. *J. Org. Chem.* **1986**, *51*, 1986-1987.
- (380) Magnus, P.; Lacour, J. *J. Am. Chem. Soc.* **1992**, *114*.
- (381) Nicolaou, K. C.; Vega, J. A.; Vassilikogiannakis, G. *Angew. Chem. Int. Ed.* **2001**, *40*, 4441-4445.
- (382) Zhang, C.; Yang, R.; Chen, L.; Zhong, B.; Yun, L.; Wang, H. *J. Label. Compd. Radiopharm.* **2004**, *47*, 583-590.
- (383) Haldar, P.; Guin, J.; Ray, J. K. *Tetrahedron Lett.* **2005**, *46*, 1071-1074.
- (384) Kotha, S.; Ghosh, A. K. *Tetrahedron Lett.* **2004**, *45*, 2931-2934.
- (385) Card, P. J. *J. Org. Chem.* **1982**, *47*, 2169-2173.
- (386) Hattori, T.; Date, M.; Sakurai, K.; Morohashi, N.; Kosugi, H.; Miyano, S. *Tetrahedron Lett.* **2001**, *42*, 8035-8038.
- (387) Piers, E.; Britton, R.; Andersen, R. J. *J. Org. Chem.* **2000**, *65*, 530-535.
- (388) Furstner, A.; Domostoj, M. M.; Scheiper, B. *J. Am. Chem. Soc.* **2005**, *127*, 11620-11621.

- (389) Rosenthal, D.; Grabowich, P.; Sabo, E. F.; Fried, J. *J. Am. Chem. Soc.* **1963**, *85*, 3971-3979.
- (390) Mekouar, K.; Genisson, Y.; Leue, S.; Greene, A. E. *J. Org. Chem.* **2000**, *65*, 5212-5215.
- (391) Lipshutz, B. H.; Hagen, W. *Tetrahedron Lett.* **1992**, *33*, 5865-5868.
- (392) Jain, R.; Cohen, L. A. *Tetrahedron.* **1996**, *52*, 5363-5379.
- (393) Turner, R. M.; Lindell, S. D. *J. Org. Chem.* **1991**, *56*, 5739-5740.
- (394) Katritzky, A. R.; Slawinski, J. J.; Brunner, F. J. *Chem. Soc.; Perkin Trans. 1.* **1989**, 1139-1145.
- (395) Griffith, R. K.; DiPietro, R. A. *Synth. Commun.* **1986**, *16*, 1761-1770.
- (396) Felder, C. C.; Glass, M. *Annu. Rev. Pharmacol. Toxicol.* **1998**, *38*, 179-200.
- (397) Lambert, D. M.; Fowler, C. J. *J. Med. Chem.* **2005**, *48*, 5059-5087.
- (398) Marzo, V. D.; Petrocellis, L. D. *Annu. Rev. Med.* **2006**, *57*, 553-574.
- (399) Pacher, P.; Batkai, S.; Kunos, G. *Pharmacol. Rev.* **2006**, *58*, 389-462.
- (400) Stott, C. G.; Guy, G. W. *Euphytica.* **2004**, *140*, 83-93.
- (401) O'Shaughnessy, W. B. *On the preparations of the Indian Hemp, or Gunjah (Cannabis indica): the effects on the animal system in health, and their utility in the treatment of Tetanus and other convulsive diseases*; Transactions of the Medical and Physical Society of Bengal 1838-1840: Calcutta, 1840.
- (402) Health Canada. Health Canada's marihuana supply. Ottawa, Ont: Health Canada; 2005 [cited 2005 Oct 1]. Available from: http://www.hc-sc.gc.ca/dhp-mps/marihuana/supply-approvis/index_e.html.
- (403) Gaoni, Y.; Mecholaum, R. *J. Am. Chem. Soc.* **1971**, *93*, 217-224.
- (404) Mecholaum, R.; Gaoni, Y. *Forstschritte der Chemie Organischer Naturstoffe* **1967**, *25*, 175-213.
- (405) Mecholaum, R.; Gaoni, Y. *Tetrahedron Lett.* **1967**, *8*, 1109-1111.
- (406) ElSohly, M. A.; Slade, D. *Life Sciences.* **2005**, *78*, 539-548.
- (407) Court of Appeals for Ontario. R. v Parker. Toronto, Ont: Court of Appeals for Ontario; 2000 [cited 2006 February 1]. Available from: http://www.ontariocourts.on.ca/decisions/OntarioCourtsSearch_VOpenFile.cfm?serverFilePath=d%3A%5Cusers%5Contario%20courts%5Cwww%5Cdecisions%5C2000%5Cjuly%5Cparker%2Ehtm.
- (408) Marihuana Medical Access Regulations (2001). Canada Gazette, Part II (reference July 4, 2001-SOR 2001-227). [cited 2005 Oct 1]. Available from: <http://www.hc-sc.gc.ca>. Available from: http://www.hc-sc.gc.ca/dhp-mps/alt_formats/hecs-sesc/pdf/marihuana/marihuana-reg_e.pdf
- (409) *Information for Health Care Professionals*; Health Canada: Ottawa, 2003.
- (410) Petrzilka, T.; Haefliger, W.; Sikemeier, C. *Helv. Chim. Ac.* **1969**, *52*, 1102-1134.
- (411) Howlett, A. C.; Barth, F.; Bonner, T. I.; Cabral, G.; Casellas, P.; Devane, W. A.; Felder, C. C.; Herkenham, M.; Mackie, K.; Martin, B. R.; Mecholaum, R.; Pertwee, R. G. *Pharmacol. Rev.* **2002**, *54*, 161-202.
- (412) From: Wikipedia, The Free Encyclopedia. 2007. <http://en.wikipedia.org>.
- (413) Begg, M.; Pacher, P.; Batkai, S.; Osei-Hyaiman, D. *Pharmacol. Ther.* **2005**, *106*, 133-145.
- (414) Pertwee, R. G. *Curr. Neuropharmacol.* **2004**, *2*, 9-29.
- (415) Devane, W. A.; Hanus, L.; Breuer, A.; Pertwee, R. G.; L A Stevenson; Griffin, G.; Gibson, D.; Mandelbaum, A.; Etinger, A.; Mechoulam, R. *Science.* **1992**, *258*, 1946-1949.
- (416) Gonsiorek, W.; Lunn, C.; Fan, X.; Narula, S.; Lundell, D.; Hipkin, W. *Mol. Pharmacol.* **2000**, *57*, 1045-1050.

- (417) Mecholaum, R.; Shabat, S. B.; Hanus, L.; Ligumsky, M.; Kaminski, N. E.; Schatz, A. R.; Gopher, A.; Almong, A.; Martin, B. R.; Compton, D. R.; Pertwee, R. G.; Griffin, G. *Biochem. Pharmacol.* **1995**, *50*, 83-90.
- (418) Guzman, M. *Nature Cancer.* **2003**, *3*, 745-755.
- (419) Demuth, D. G.; Molleman, A. *Life Sciences.* **2006**, *78*, 549-563.
- (420) Piomelli, D. *Neuropharmacol.* **2004**, *47*, 359-367.
- (421) Novak, J.; Salemink, C. A. *J. Chem. Soc. Perkin Trans. I.* **1983**, 2867-2871.
- (422) Razdan, R. K.; Handrick, R. *J. Am. Chem. Soc.* **1970**, *92*, 6061-6062.
- (423) Razdan, R. K.; Pars, H. G.; Granchelli, F. E. *J. Am. Chem. Soc.* **1968**, *11*, 377-378.
- (424) Childers, W. E.; Pinnick, H. W. *J. Org. Chem.* **1984**, *49*, 5277-5279.
- (425) Gill, E. W. *J. Chem. Soc. (C).* **1971**, 579-582.
- (426) Marriott, K. S. C.; Huffman, J. W.; Wiley, J. L.; Martin, B. R. *Bioorg. Med. Chem.* **2006**, *14*, 2386-2397.
- (427) Mecholaum, R.; Gaoni, Y. *J. Am. Chem. Soc.* **1965**, *87*, 3273-3275.
- (428) Mukhopadhyay, S.; Howlett, A. C. *Mol. Pharmacol.* **2005**, *67*, 2016-2024.
- (429) Portier, M.; Carmona, M. R.; Pecceu, F.; Combes, T.; Poinot-Chazel, C.; Calandra, B.; Barth, F.; Fur, G.; Casellas, P. *J. Pharmacol. Exp. Ther.* **1999**, *288*, 582-589.
- (430) Jay, J. E.; Watson, S. J.; Benson, J. A. *Medicinal Marijuana*; National Academy Press.: Washigton, D.C., 1999.
- (431) Martin, B. R. *Pharmacol. Rev.* **1986**, *38*, 45-74.
- (432) Knight, P. J. K.; Pfeifer, T. A.; Grigliatti, T. A. *Anal. Biochem.* **2003**, *320*, 88-103.
- (433) Knight, J. C.; Grigliatti, T. A. *Arch. Insect Biochem. Physiol.* **2004**, *57*, 142-150.
- (434) Xu, W.; Filppula, S. A.; Mercier, R.; Yaddanapudi, S.; Pavlopoulos, S.; Cal, J.; Pierce, W. M.; Makriyannis, A. *J. Peptide Res.* **2005**, *66*, 138-150.
- (435) Swevers, L.; Morou, E.; Balatsos, N.; Iatrou, K.; Georgoussi, Z. *CMLS, Cell. Mol. Life. Sci.* **2005**, *62*, 919-930.
- (436) Kaul, P. N. *Pure & Appl. Chem.* **1982**, *54*, 1963-1972.
- (437) Qureshi, A.; Faulkner, D. J. *Tetrahedron.* **1999**, *55*, 8323-8330.
- (438) Fujita, M.; Nakao, Y.; Matsunaga, S.; Seiki, M.; Itoh, Y.; Soest, R. W. M. V.; Heubes, M.; Faulkner, D. J.; Fusetani, N. *Tetrahedron.* **2001**, *57*, 3885-3890.
- (439) Kornprobst, J. M.; Sallenave, C.; Barnathan, G. *Comp. Biochem. Physiol.* **1998**, *119B*, 1-51.
- (440) De-Riccardis, F.; Iorizzi, M.; Minale, L.; Riccio, R.; Debitus, C. *Tetrahedron Lett.* **1992**, *33*, 1097-1100.
- (441) De-Riccardis, F.; Minale, L.; Riccio, R.; Bruno, G.; Iorizzi, M.; Debitus, C. *Gazz. Chim. Italian.* **1993**, *123*, 79-86.
- (442) Alam, M.; Sanduja, R.; Hossain, M. B.; Helm, D. *J. Am. Chem. Soc.* **1982**, *104*, 5232-5234.
- (443) Abraham, S. P.; Hoang, T. D.; Alam, M.; Jones, E. B. G. *Pure & Appl. Chem.* **1994**, *66*, 2391-2394.
- (444) Kenji, G. M.; Nakajima, S.; Baba, N.; Iwasa, J. *Chem. Exp.* **1991**, *6*, 233-236.
- (445) Kenji, G. M.; Baba, N.; Iwasa, J. *Okayama Daigaku Nogabuku Gakujutsu Hokoku.* **1998**, *87*, 17-21.
- (446) Gu, J.; Li, W.; Kang, Y.; Su, B.; Fong, H. H. S.; Breemen, R. B.; Pezzuto, J. M.; Kinghorn, A. D. *Chem. Pharm. Bull.* **2003**, *51*, 530-539.
- (447) Su, B.; Gu, J.; Kang, Y. H.; Park, E. J.; Pezzuto, J. M.; Kinghorn, A. D. *Mini-Rev. Org. Chem.* **2004**, *1*, 115-123.
- (448) MarinLit database. Department of Chemistry, University of Canterbury: <http://www.chem.canterbury.ac.nz/marinlit/marinlit.shtml>, 2005.

- (449) Dr. Raymond J. Andersen, Department of Chemistry, UBC. Personal communication, 2006.
- (450) Carlini, E. A.; Santos, M. *Psychopharmacol.* **1970**, *18*, 82-93.
- (451) Gareau, Y.; Dufresne, C.; Gallant, M.; Rochette, C.; Sawyer, N.; Slipetz, D. M.; Tremblay, N.; Weech, P.; Metters, K.; Labelle, M. *Bioorg. Med. Chem. Lett.* **1996**, *6*, 189-194.
- (452) Mecholaum, R.; Lander, N.; Varkony, T. H.; Kimmel, I.; Becker, O.; Ben-Zvi, Z.; Edery, H.; Porath, G. *J. Med. Chem.* **1980**, *23*, 1068-1072.
- (453) Picone, R. P.; Fournier, D. J.; Makriyannis, A. *J. Peptide Res.* **2002**, *60*, 348-356.
- (454) Thomas, B. F.; Adams, I. B.; Mascarella, S. W.; Martin, B. R.; Razdan, R. K. *J. Med. Chem.* **1996**, *39*, 471-479.
- (455) Xie, X. Q.; Eissenstat, M.; Makriyannis, A. *Life Sciences.* **1995**, *56*, 1963-1970.
- (456) Mayer, M.; Meyer, B. *J. Am. Chem. Soc.* **2001**, *123*, 6108-6117.
- (457) Meinecke, R.; Meyer, B. *J. Med. Chem.* **2001**, *44*, 3059-3065.
- (458) Mayer, M.; Meyer, B. *Angew. Chem. Int. Ed.* **1999**, *38*, 1784-1788.
- (459) Meyer, B.; Weimar, T.; Peters, T. *Eur. J. Biochem.* **1997**, *246*, 705-709.
- (460) Shuker, S.; Hajduk, P. J.; Meadows, R. P.; Fesik, S. W. *Science.* **1996**, *274*, 1531-1534.
- (461) Chen, A.; Shapiro, M. J. *J. Am. Chem. Soc.* **1998**, *120*, 10258-10259.
- (462) Siriwardena, A. H.; Tian, F.; Noble, S.; Prestegard, J. H. *Angew. Chem. Int. Ed.* **2002**, *41*, 3454-3457.
- (463) Neffe, A. T.; Bilanz, M.; Meyer, B. *Org. Biomol. Chem.* **2006**, *4*, 3259-3267.
- (464) Murata, T.; Hemmi, H.; Nakamura, S.; Shimizu, K.; Suzuki, Y.; Yamaguchi, I. *FEBS J.* **2005**, *272*, 4938-4948.
- (465) Brecker, L.; Straganz, G. D.; Tyl, C. E.; Steiner, W.; Nidetzky, B. *J. Mol. Cat. B.* **2006**, *42*, 85-89.
- (466) Milton, M. J.; Williamson, R. T.; Koehn, F. E. *Bioorg. Med. Chem. Lett.* **2006**, *16*, 4279-4282.
- (467) Megy, S.; Bertho, G.; Gharbi-Benarous, J.; Baleux, F.; Benarous, R.; Girault, J. P. *FEBS Lett.* **2006**, *580*, 5411-5422.
- (468) Klein, J.; Meinecke, R.; Mayer, M.; Meyer, B. *J. Am. Chem. Soc.* **1999**, *121*, 5336-5337.
- (469) Claasen, B.; Axmann, M.; Meinecke, R.; Meyer, B. *J. Am. Chem. Soc.* **2005**, *127*, 916-919.
- (470) Turner, C. E.; ElSohly, M. A.; Boeren, E. G. *J. Nat. Prod.* **1980**, *43*, 169-234.
- (471) Ward, S.; Sotsios, Y.; Dowden, J.; Bruce, I.; Finan, P. *Chem. Biol.* **2003**, *10*, 207-213.
- (472) Marion, F.; Williams, D. E.; Patrick, B. O.; Hollander, I.; Mallon, R.; Kim, S. C.; Roll, D. M.; Feldberg, L.; Soest, R. V.; Andersen, R. J. *Org. Lett.* **2006**, *8*, 321-324.
- (473) Wymann, M. P.; Zvelebil, M.; Laffargue, M. *Trends Pharmacol. Sci.* **2003**, *24*, 366-376.
- (474) Ward, S.; Finan, P. *Curr. Opin. Pharmacol.* **2003**, *3*, 426-434.
- (475) Ruckle, T.; Schwarz, M. K.; Rommel, C. *Nature.* **2006**, *5*, 903-918.
- (476) Wymann, M. P.; Marone, R. *Curr. Opin. Cell Biol.* **2005**, *17*, 141-149.
- (477) Knight, Z. A.; Shokat, K. M. *Biochem. Soc. Trans.* **2007**, *35*, 245-249.
- (478) Rommel, C.; Camps, M.; Ji, H. *Nature Immunol.* **2007**, *7*, 191-201.
- (479) Yang, L.; Williams, D. E.; Mui, A.; Ong, C.; Krystal, G.; Soest, R. V.; Andersen, R. J. *Org. Lett.* **2005**, *7*, 1073-1076.
- (480) Lu, Y.; Wang, H.; Mills, G. B. *Rev. Clin. Exp. Hematol.* **2003**, *7*, 205-228.
- (481) Huber, M.; Helgason, C. D.; Damen, J. E.; Liu, L.; Humphries, R. K.; Krystal, G. *Proc. Natl. Acad. Sci.* **1998**, *95*, 11330-11335.
- (482) Sotsios, Y.; Ward, S. *Immunol. Rev.* **2000**, *177*, 217-235.

- (483) Barbier, D. F.; Bartolome, A.; Hernandez, C.; Flores, J. M.; Redondo, C.; Fernandez-Arias, C.; Camps, M.; Ruckle, T.; Schwarz, M. K.; Rodriguez, S.; Martinez, C.; Balomenos, D.; Rommel, C.; Carrera, A. C. *Nat. Med.* **2005**, *11*, 933-935.
- (484) Wymann, M. P.; Bjorklof, K.; Calvez, R.; Finan, P.; Thomas, M.; Trifilieff, A.; Barbier, M.; Altruda, F.; Hirsch, E.; Laffargue, M. *Biochem. Soc. Trans.* **2003**, *31*, 275-280.
- (485) Luo, J. M.; Yoshida, H.; Komura, S.; Ohishi, N.; Pan, L.; Shigeno, K.; Hanamura, I.; Miura, K.; Iida, S.; Ueda, R.; Naoe, T.; Akao, Y.; Ohno, R.; Ohnishi, K. *Leukemia*. **2003**, *2003*, 1-8.
- (486) Sattler, M.; Salgia, R.; Shrickhande, G.; Verma, S.; Rohrschneider, J. L.; Griffin, J. D. *Oncogene*. **1997**, *15*, 2379-2384.
- (487) MacMillan, J.; Vanstone, A. E.; Yeboah, S. K. *J. Chem. Soc., Chem. Comm.* **1968**, 613-614.
- (488) Petcher, T. J.; Weber, H. P.; Kis, Z. *J. Chem. Soc., Chem. Comm.* **1972**, 1061-1062.
- (489) Brian, P. W.; Curtis, P. J.; Hemming, H. G.; Norris, G. L. F. *Trans. Brit. Mycol. Soc.* **1957**, *40*, 366-371.
- (490) Nakanishi, S.; Kakita, S.; Takahashi, I.; Kawahara, K.; Tsukuda, E.; Sano, T.; Yamada, K.; Yoshida, M.; Kase, H.; Matsuda, Y.; Hashimoto, Y.; Nonomura, Y. *J. Biol. Chem.* **1992**, *267*, 2157-2163.
- (491) Kozo, H. *Yakugaku Zasshi*. **1933**, *53*, 1093-1098.
- (492) Marini-Bettolo, G. B.; Deulefeu, V.; Hug, E. *Gazzeta Chimica Italiana*. **1950**, *80*, 63-75.
- (493) Chimenti, F.; Cottaglia, F.; Bonsignore, L.; Casu, L.; Casu, M.; Floris, C.; Secci, D.; Bolasco, A.; Chimenti, P.; Granese, A.; Befani, O.; Turini, P.; Alcaro, S.; Ortuso, F.; Trombetta, G.; Loizzo, A.; Guarino, I. *J. Nat. Prod.* **2006**, *69*, 945-949.
- (494) Chen, X.; Garelick, M. G.; Wang, H.; Li, V.; Athos, J.; Storm, D. R. *Nat. Neurosci.* **2005**, *8*, 925-931.
- (495) Vlahos, C. J.; Matter, W. F.; Hui, K. Y.; Brown, R. F. *J. Biol. Chem.* **1994**, *269*, 5241-5248.
- (496) Camps, M.; Ruckle, T.; Ji, H.; Ardissonne, V.; Rintelen, F.; Shaw, J.; Chabert, C.; Gillieron, C.; Francon, B.; Martin, T.; Gretener, D.; Perrin, D.; Leroy, D.; Vitte, P. A.; Hirsch, E.; Wymann, M. P.; Cirillo, R.; Schwarz, M. K.; Rommel, C. *Nat. Med.* **2005**, *11*, 936-943.
- (497) Sadhu, C.; Masinovski, B.; Dick, K.; Sowell, C. G.; Staunton, D. E. *J. Immunol.* **2003**, *170*, 2647-2654.
- (498) Bruce, I.; Finan, P.; Leblanc, C.; McCarthy, C.; Whitehead, L.; Blair, N. E.; Bloomfield, G. C.; Hayler, J.; Kirman, L.; Oza, M. S.; Shukla, L. *5-Phenylthiazole derivatives and their use as phosphatidylinositol 3-kinase (PI3K) inhibitors for the treatment of allergic and inflammatory diseases*, 2003. PCT Int. Appl., WO03072557.
- (499) Breitfelder, S.; Maier, U.; Brandl, T.; Hoenke, C.; Grauert, M.; Pautsch, A.; Hoffmann, M.; Kalkbrenner, F.; Joergensen, A.; Schaenzle, G.; Peters, S.; Buettner, F.; Bauer, E. *Preparation of fused thiazoles such as pyrazolobenzothiazoles, thiazolocyclopentapyrazoles, thiazolocycloheptapyrazoles, thiazoloquinazolines, and naphthothiazoles as PI3 kinase inhibitors*, 2006. PCT Int. Appl., WO-06040279.
- (500) Quattropiani, A.; Rueckle, T.; Schwarz, M.; Dorbais, J.; Sauer, W.; Cleva, C.; Desforges, G. *Preparation of thiazole derivatives as modulators of the phosphoinositide 3-kinases (PI3Ks)*, 2005. PCT Int. Appl., WO-05068444.
- (501) Bravian, N. C.; Kolz, C. N.; Para, K. S.; Patt, W. C.; Visnick, M. *Preparation of benzoxazin-3-ones and derivatives as inhibitors of PI3K kinase for treating inflammations, cardiovascular diseases and cancer*, 2004. PCT Int. Appl., WO-04052373.

- (502) Ruckle, T.; Jiang, X.; Gaillard, P.; Church, D. D.; Valloton, T. *Preparation of azolidinone-vinyl fused-benzene derivatives for therapeutic uses as PI3 kinase inhibitors*, 2004. PCT Int. Appl., WO-04007491.
- (503) Zuleta, I. A.; Vitelli, M. L.; Baggio, R.; Garland, M. T.; Seldes, A. M.; Palermo, J. A. *Tetrahedron*. **2002**, *58*, 4481-4486.
- (504) Wrasidlo, W. *Preparation of vaculostatic agents and methods of use*, 2004. PCT Int. Appl., WO-04030635.
- (505) Shimada, M. *Preparation of azole-pyrimidine derivatives as PI3K inhibitors with therapeutic uses*, 2004. PCT Int. Appl., WO-04029055.
- (506) Knight, Z. A.; Gonzalez, B.; Feldman, M. E.; Zunder, E. R.; Goldenberg, D. D.; Williams, O.; Loewith, R.; Stokoe, D.; Balla, A.; Toth, B. *Cell*. **2006**, *125*, 733-747.
- (507) Kwak, J. H.; Schmitz, F. J.; Kelly, M. *J. Nat. Prod.* **2000**, *63*, 1153-1156.
- (508) Goclik, E.; Konig, G. M.; Wright, A. D.; Kaminsky, R. *J. Nat. Prod.* **2000**, *63*, 1150-1152.
- (509) Schroeder, F. C.; Kau, T. R.; Silver, P. A.; Clardy, J. *J. Nat. Prod.* **2005**, *68*, 574-576.
- (510) Xie, Y.; Liu, L.; Huang, X.; Guo, Y.; Luo, L. *J. Pharmacol. Exp. Ther.* **2005**, *314*, 1210-1217.
- (511) Crews, P.; Bescansa, P. *J. Nat. Prod.* **1986**, *49*, 1041-1052.
- (512) DeRosa, S.; Puliti, R.; Crispino, A.; DeGiulio, A. *J. Nat. Prod.* **1994**, *57*, 256-262.
- (513) Janmaat, M. L.; Rodriguez, J. A.; Jimeno, J.; Kruyt, F. A. E.; Giaccone, G. *Mol. Pharmacol.* **2005**, *68*, 502-510.
- (514) Hamann, M. T.; Scheuer, P. J. *J. Am. Chem. Soc.* **1993**, *115*, 5825-5829.
- (515) Goetz, G.; Nakao, Y.; Scheuer, P. J. *J. Nat. Prod.* **1997**, *60*, 562-566.
- (516) Horgen, F. D.; Santos, D. B.; Goetz, G.; Sakamoto, B.; Kan, Y.; Nagai, H.; Scheuer, P. J. *J. Nat. Prod.* **2000**, *63*, 152-155.
- (517) Roll, D. M.; Scheuer, P. J.; Matsumoto, G. K.; Clardy, J. *J. Am. Chem. Soc.* **1983**, *105*, 6177-6178.
- (518) Kobayashi, J.; Hirase, T.; Shigemori, H. *J. Nat. Prod.* **1992**, *55*, 994-998.
- (519) Schmitz, F. J.; Bloor, S. J. *J. Org. Chem.* **1988**, *53*, 3922-3925.
- (520) Sun, T.; Wang, Q.; Yu, Z.; Zhang, Y.; Guo, Y.; Chen, K.; Shen, X.; Jiang, H. *ChemBioChem*. **2007**, *8*, 187-193.
- (521) Iguchi, K.; Shimada, Y.; Yamada, Y. *J. Org. Chem.* **1991**, *57*, 522-524.
- (522) Lunardi, I.; Santiago, G. M. P.; Imamura, P. M. *Tetrahedron Lett.* **2002**, *43*, 3609-3611.
- (523) Kwon, M. J.; Nam, T. J. *Cell. Biol. Int.* **2007**, *31*, 768-775.
- (524) Sullivan, B. W.; Faulkner, J. *J. Org. Chem.* **1986**, *51*, 4568-4573.
- (525) Sullivan, B. W.; Djura, P.; McIntyre, D.; Faulkner, J. *Tetrahedron*. **1981**, *37*, 979-982.
- (526) Mukku, V. J. R. V.; Edrada, R. A.; Schmitz, F. J.; Shanks, M. K.; Chaudhuri, B.; Fabbro, D. *J. Nat. Prod.* **2003**, *66*, 686-689.
- (527) Grube, A.; Assmann, M.; Lichte, E.; Sasse, F.; Pawlik, J. R.; Kock, M. *J. Nat. Prod.* **2007**, *70*, 504-509.
- (528) Yuan, Y.; Men, H.; Lee, C. *J. Am. Chem. Soc.* **2004**, *126*, 14720-14721.
- (529) Kraus, G. A.; Nguyen, T.; Bae, J.; Hostetter, J.; Steadham, E. *Tetrahedron*. **2004**, *60*, 4223-4225.
- (530) Tanaka, H.; Hiroo, M.; Ichino, K.; Ito, K. *J. Chem. Soc., Chem. Comm.* **1988**, 749-751.
- (531) Marion, F.; Andersen, R. J. *Enantioselective synthesis of Liphagal*, 2005, unpublished material.
- (532) Hagiwara, H.; Nagatomo, H.; Shin-ichi, K.; Sakai, H.; Hoshi, T.; Suzuki, T.; Ando, M. *J. Chem. Soc., Perkin Trans. 1*. **1999**, 457-459.
- (533) Hagiwara, H.; Uda, H. *J. Org. Chem.* **1988**, *53*, 2308-2311.

- (534) Yakura, T.; Kitano, T.; Ikeda, M.; Uenishi, J. *Tetrahedron Lett.* **2002**, *43*, 6925-6927.
- (535) Ling, T.; Poupon, E.; Rueden, E. J.; Kim, S. H.; Theodorakis, E. A. *J. Am. Chem. Soc.* **2002**, *124*, 12261-12267.
- (536) Baldwin, J. E. *J. Chem. Soc., Chem. Comm.* **1976**, *384*, 734-736.
- (537) Baldwin, J. E.; Thomas, R. C.; Kruse, L. I.; Silberman, L. *J. Org. Chem.* **1997**, *42*, 3846-3852.
- (538) Weinstock, J.; Ladd, D. L.; Wilson, J. W.; Brush, C. K.; Yim, N. C. F.; Gallager, G.; McCarthy, M. E.; Silvestri, J.; Sarau, H. M.; Flaim, K. E.; Ackerman, D. M.; Setler, P. E.; Tobia, A. J.; Hahn, R. A. *J. Med. Chem.* **1986**, *29*, 2315-2325.
- (539) Ross, S. T.; Franz, R. G.; Gallager, G.; Brenner, M.; Wilson, J. W.; DeMarinis, R. M.; Hieble, J. P.; Sarau, H. M. *J. Med. Chem.* **1987**, *30*, 35-40.
- (540) Greene, T. W.; Wuts, P. G. M. *Protecting groups in Organic Chemistry*; 3rd ed.; John Wiley & Sons: Toronto, 1999, 749 p.
- (541) Alam, A.; Takagushi, Y.; Ito, H.; Yoshida, T.; Tsuboi, S. *Tetrahedron.* **2005**, *61*, 1909-1918.
- (542) Tanada, Y.; Mori, K. *Eur. J. Org. Chem.* **2001**, 1963-1966.
- (543) Cren-Olive, C.; Lebrum, S.; Rolando, C. *J. Chem. Soc., Perkin Trans. 1.* **2002**, 821-830.
- (544) McMurry, J. *Organic Chemistry*; 5th ed.; Brooks/Cole: Pacific Grove, USA, 1999, 593-689.
- (545) Williard, P. G.; Fryhle, C. B. *Tetrahedron Lett.* **1980**, *21*, 3731-3734.
- (546) Bonini, C.; Cristiani, G.; Funicello, M.; Viggiani, L. *Synth. Commun.* **2006**, *36*, 1983-1990.
- (547) Lam, V.; Kalesnikoff, J.; Lee, C. W. K.; Hernandez-Hansen, V.; Wilson, B. S.; Oliver, J. M.; Krystal, G. *Blood.* **2003**, *102*, 1405-1413.
- (548) Kim, C. H.; Hangoc, G.; Cooper, S.; Helgason, C. D.; Yew, S.; Humphries, R. K.; Krystal, G.; Broxmeyer, H. E. *J. Clin. Invest.* **1999**, *104*, 1751-1759.